

ADA 032883

AFAPL-TR-76-65
VOLUME IV

11

THE GENERATION AND RADIATION OF SUPERSONIC JET NOISE VOLUME IV SHOCK-ASSOCIATED NOISE DATA

LOCKHEED-GEORGIA COMPANY
MARIETTA, GEORGIA 30063

DDC
RECEIVED
DEC 7 1976
RESERVED

SEPTEMBER 1976

TECHNICAL REPORT AFAPL-TR-76-65
FINAL REPORT FOR PERIOD 6 NOVEMBER 1972 - 6 NOVEMBER 1975

Approved for public release; distribution unlimited

DEPARTMENT OF TRANSPORTATION
OFFICE OF NOISE ABATEMENT
WASHINGTON, D.C.

AIR FORCE AERO-PROPULSION LABORATORY
AIR FORCE WRIGHT AERONAUTICAL LABORATORIES
AIR FORCE SYSTEMS COMMAND
WRIGHT-PATTERSON AIR FORCE BASE, OHIO 45433

NOTICE

When Government drawings, specifications, or other data are used for any purpose other than in connection with a definitely related Government procurement operation, the United States Government thereby incurs no responsibility nor any obligation whatsoever; and the fact that the Government may have formulated, furnished, or in any way supplied the said drawings, specifications, or other data, is not to be regarded by implication or otherwise as in any manner licensing the holder or any other person or corporation, or conveying any rights or permission to manufacture, use, or sell any patented invention that may in any way be related thereto.

This final report was prepared by the Lockheed-Georgia Company, Marietta, Georgia, under Contract F33615-75-C-2032. The effort was sponsored by the Air Force Aero-Propulsion Laboratory, Air Force Systems Command, Wright-Patterson AFB, Ohio and the Department of Transportation under Project 3066, Task 14, and Work Unit 08 with Mr. Paul A. Shahady (AFAPL/TBC) as Project Engineer. Dr. Gordon Banerian was the Project Manager for the Department of Transportation. Dr. Harry E. Plumblee of Lockheed-Georgia was technically responsible for the work.

This report has been reviewed by the Information Office, ASD/OIP, and is releasable to the National Technical Information Service (NTIS). At NTIS, it will be available to the general public, including foreign nations.

This technical report has been reviewed and is approved for publication.

Paul A. Shahady
PAUL A. SHAHADY
Project Engineer
USAF

G. Banerian
DR. GORDON BANERIAN
Project Manager
Department of Transportation

FOR THE COMMANDER

Robert E. Henderson
ROBERT E. HENDERSON
Manager, Combustion Technical Area

ADMISSION FOR

WHITE SECTION

DEPT. SECTION

NTIS

7 C

CLASSIFIED

EXEMPTION

BY

CLASSIFICATION/AVAILABILITY CODES

DATE

FILE NO.

11

Copies of this report should not be returned unless return is required by security considerations, contractual obligations, or notice on a specific document.

UNCLASSIFIED

SECURITY CLASSIFICATION OF THIS PAGE (When Data Entered)

REPORT DOCUMENTATION PAGE		READ INSTRUCTIONS BEFORE COMPLETING FORM	
1. REPORT NUMBER AFAPL TR-76-65 -Vol-4	2. GOVT ACCESSION NO.	3. RECIPIENT'S CATALOG NUMBER	
4. TITLE (and Subtitle) THE GENERATION AND RADIATION OF SUPERSONIC JET NOISE. Volume IV, Shock-Associated Noise Data.		5. TYPE OF REPORT & PERIOD COVERED FINAL TECHNICAL REPORT 6 NOV 72 - 6 NOV 75	
6. AUTHOR(s) H. K. Tanna, P. D. Dean, and R. H. Burrin		7. PERFORMING ORG. REPORT NUMBER LG76ER0133-14-1	
9. PERFORMING ORGANIZATION NAME AND ADDRESS Lockheed-Georgia Company Marietta, Georgia		8. CONTRACT OR GRANT NUMBER(s) F33615-73-C-2032	
11. CONTROLLING OFFICE NAME AND ADDRESS Air Force Aero Propulsion Laboratory/TBC Wright-Patterson AFB, Ohio 45433		10. PROGRAM ELEMENT, PROJECT, TASK AREA & WORK UNIT NUMBERS PE 62203F, Project 3066 Task 14, Work Unit 08	
14. MONITORING AGENCY NAME & ADDRESS (if different from Controlling Office)		12. REPORT DATE 23 Jun 1976	
		13. NUMBER OF PAGES 412	
		15. SECURITY CLASS. (of this report) Unclassified	
15a. DECLASSIFICATION/DOWNGRADING SCHEDULE			
16. DISTRIBUTION STATEMENT (of this Report) Approved for Public Release; Distribution Unlimited.			
17. DISTRIBUTION STATEMENT (of the abstract entered in Block 20, if different from Report)			
18. SUPPLEMENTARY NOTES			
19. KEY WORDS (Continue on reverse side if necessary and identify by block number) Acoustics, Turbulence, Jet Noise, Laser Velocimetry, Supersonic Jets, Shock Noise			
20. ABSTRACT (Continue on reverse side if necessary and identify by block number) This report is published in four volumes. Volume I summarizes the work accomplished. Volume II contains a detailed discussion of work accomplished since the publication of the interim report, and all the major conclusions reached during the program. Volume III is a data report which presents a detailed compilation of the turbulent mixing noise 1/3-octave spectra. Volume IV (this volume) is another data report, and it contains the narrow-band spectra for broadband shock-associated noise.			

DD FORM 1 JAN 73 1473

EDITION OF 1 NOV 65 IS OBSOLETE

UNCLASSIFIED

SECURITY CLASSIFICATION OF THIS PAGE (When Data Entered)

PREFACE

This report was prepared by the Lockheed-Georgia Company, Marietta, Georgia, for the Air Force Aero Propulsion Laboratory, Wright-Patterson Air Force Base under Contract F33615-73-C-2032. The report covers work done in the period 6 November 1972 through 6 November 1975. The work described herein is part of the Air Force Aero Propulsion Laboratory's joint program with the Department of Transportation to define and control the noise emission of aircraft propulsion systems.

Mr. Paul Shahady was the Air Force Aero Propulsion Laboratory's Project Engineer. The program is being conducted under Project 3066, Task 14. Dr. Gordon Banerian was the Project Manager for the Department of Transportation. Lockheed's Program Manager was Harry E. Plumblee, Jr.

Major contributors to the work performed under this contract and presented in this report are: Robert H. Burrin, Peter D. Dean, Philip E. Doak, Michael J. Fisher, Sham S. Kapur, Jark C. Lau, Geoffrey M. Lilley, William T. Mayo, Donald M. Meadows, Christopher L. Morfey, Philip J. Morris, David M. Smith, H. K. "Bob" Tanna, Brian J. Tester, and M. Clay Whiffen.

The assistance of the following individuals is gratefully acknowledged: C. Benton Reid and L. V. Mazzarella, who operated the test facilities and data acquisition systems; C. R. Huie, who helped in the buildup and operation of the laser velocimeter; R. B. Harrison and C. T. Walker, who constructed and maintained the acoustic and flow facilities; J. P. McKenna, who kept up with the budget and other administrative details, and last, but certainly not least, most gracious appreciation is extended to Barbara C. Reagan for her superb typing of all manuscripts.

Gratitude is expressed to the University of Southampton for permitting Professor Philip E. Doak, Professor Geoffrey M. Lilley, Dr. Michael J. Fisher, and Dr. Christopher L. Morfey to participate in the performance of the research reported herein.

This report was submitted on 23 June 1976.

Publication of this report does not constitute Air Force approval of the report's findings or conclusions. It is published only for the exchange and stimulation of ideas.

SHOCK ASSOCIATED NOISE EXPERIMENTS

The characteristics of the sound field of shock-containing under-expanded jets are studied by measuring the noise from a two-inch diameter convergent nozzle over an extensive envelope of supercritical jet operating conditions. The measurements, which are accurate and comprehensive, were conducted in the Lockheed anechoic facility. The results are presented in this Volume in a systematic manner in the form of narrowband spectra. The details pertinent to the experimental program and the data presentation format are summarized below.

SCREECH SUPPRESSION

The total noise spectrum from an incorrectly expanded jet flow contains discrete components (or screech) in addition to the basic turbulent mixing noise and the broadband shock-associated noise. In order to study the trends and dependencies of the *broadband* component accurately, it is vital to keep the contamination by screech to a minimum in the experimental program. In the present experiments, screech suppression was successfully achieved by wrapping all surfaces surrounding the nozzle exit with sound absorbing material, and incorporating a small projection inside the nozzle lip. This projection interrupts the feedback loop between the first shock and the nozzle exit plane, which has been previously proposed and verified as the physical mechanism of screech generation. The detailed calibration tests, conducted prior to the main shock-associated noise experiments, established that all results are essentially uncontaminated by the presence of screech.

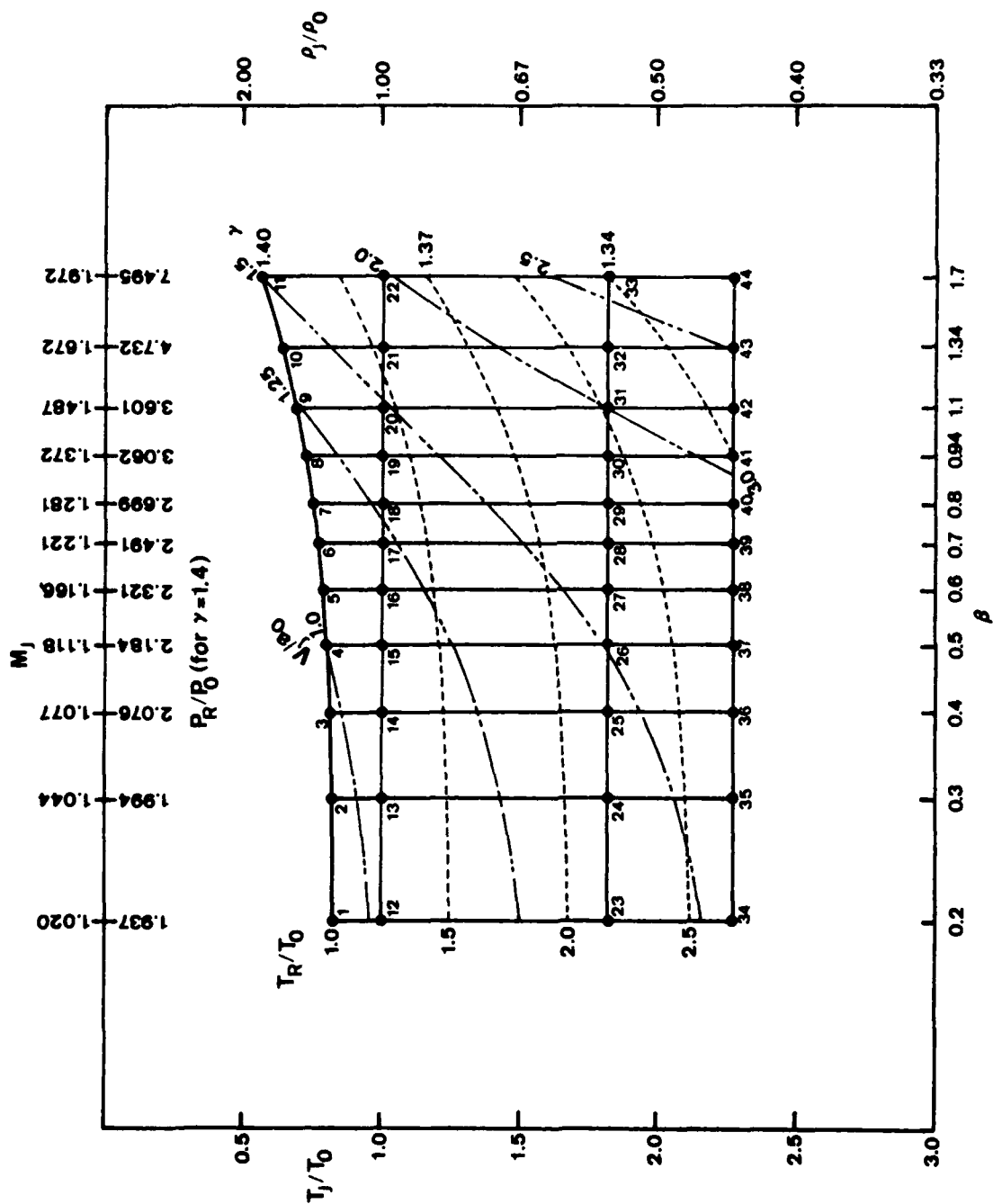
EXPERIMENTAL PROGRAM CHART

The jet operating conditions for the shock-associated noise experiments were chosen carefully to be compatible with the turbulent mixing noise experiments so that, whenever possible, the results from under-expanded (shock-containing) jets can be compared directly with the corresponding results from fully-expanded (shock-free) jets. The experimental program chart for shock-associated noise, somewhat similar to the experimental program chart for turbulent mixing noise (presented in Volume III), is shown on the following page. It contains all the information pertinent to the shock-associated noise test program.

The major difference between this chart and the previous chart for mixing noise experiments, arises from the observation that while the intensity of turbulent mixing noise (for a fixed measurement configuration) is essentially a function of jet exit velocity ratio [$I \propto (V_j/a_0)^8$], the intensity of *broadband* shock-associated noise is primarily a function of the nozzle operating pressure ratio, P_R/P_0 . For the latter, the measured intensity has been observed to vary according to

$$I \propto \beta^4, \quad \text{where} \quad \beta = (M_J^2 - 1)^{\frac{1}{2}}.$$

EXPERIMENTAL PROGRAM CHART SHOCK-ASSOCIATED NOISE



The experimental program has therefore been designed such that the jet operating conditions (T_R/T_O , P_R/P_O) chosen yield test points at reasonably spaced values of $\log_{10}\beta$.

The chart shows the values of β (and hence M_J and P_R/P_O) on the X-axis and the values of jet static temperature ratio T_J/T_O (assuming ideal expansion) on the Y-axis for the 44 test points that constitute the complete experimental program, covering a wide envelope of supercritical jet operating conditions of practical interest. By considering test points in each horizontal line, the jet efflux temperature is kept constant while varying the pressure ratio parameter β . Conversely, on each vertical line, a constant value of β is maintained while jet exit temperature is varied. Also shown on the chart are lines of constant total (or stagnation) temperature ratio, T_R/T_O , and constant jet exit velocity ratio, V_J/a_O . These two parameters have been calculated using the isentropic flow equations and therefore include the assumption that the jet flow is correctly expanded. The main reason for including these lines of constant T_R/T_O and constant V_J/a_O in the experimental program chart is to give an overall indication of the ranges of these parameters. But in addition, they serve to provide approximate values of these quantities for each test point, simply by a quick glance at the diagram.

The values of the parameter β were chosen such that in addition to obtaining reasonably spaced values of $\log_{10}\beta$, the twelve test points on the three vertical lines for $\beta = 0.94$, 1.34 , and 1.70 , are identical to the jet operating conditions used in the turbulent mixing noise tests for the three convergent-divergent nozzles (of nominal design Mach numbers 1.4 , 1.7 , and 2.0).

The values of the parameter T_J/T_O chosen for this test program are also identical to those utilized in the mixing noise tests. The four nominal values of T_J/T_O are

$$T_J/T_O = \text{unheated (i.e. } T_R/T_O = 1), 1.00, 1.82, \text{ and } 2.27.$$

For unheated tests (TP's 1 through 11), the contribution of the broadband shock-associated noise relative to the contribution from mixing noise (which, for fixed pressure ratio, increases with increasing temperature due to the increase in jet exit velocity) to the total sound field is at a maximum, and therefore the variation of shock-associated noise with P_R/P_O can be highlighted accurately. The test points (12 through 22) at isothermal jet operating conditions provide minimum effects of temperature, and hence form a base line for studying the effects of temperature on shock-associated noise. Finally, test points 23 through 44 provide data at high temperatures.

To summarize, the experimental program chart for shock-associated noise readily provides all the information relevant to this phase of the experimental program. Taken together with the results of the turbulent mixing noise experiments given in Volume III, it is possible to define accurately the jet operating conditions, the observer angles, and the frequencies over which the shock-associated noise dominates over the turbulent mixing noise from a jet exhaust.

MEASUREMENT AND DATA REDUCTION PROCEDURES

In the case of turbulent mixing noise from jet exhausts, the acoustic spectrum is broadband, and the time-averaged spectrum is smooth over the frequency range of interest. One-third octave analysis with sufficient time constant is therefore adequate for obtaining accurate frequency analysis of the sound field. However, when a convergent nozzle is operated at supercritical pressure ratios or when a convergent-divergent nozzle is operated at off-design (under-expanded or over-expanded jet flows) pressure ratios, the resulting acoustic spectrum contains a broadband shock-associated noise contribution and harmonics with well-defined peak frequencies, in addition to the basic mixing noise. (The discrete component, or "screech," is not discussed here since, as mentioned earlier, it has been suppressed in the present experiments.) The intensity, and more importantly, for frequency analysis considerations, the bandwidth of this shock-associated noise contribution varies with the nozzle operating conditions and the observer angle. One-third octave analysis is therefore not adequate for an accurate study of the measured shock-associated noise phenomena, although it is also true that whenever the bandwidth of the broadband peak is fairly large, one-third octave analysis provides all the necessary information in such cases. In view of this important consideration, the acoustic measurement and data reduction procedures that were adopted in the present shock-associated test program are as follows.

The signals from the twelve microphones were recorded simultaneously on a 14-channel Honeywell FM tape recorder at 120 inches per second (ips), and during the subsequent frequency analysis, the tape was played back at the reduced speed of 30 ips. For the present 2-inch diameter nozzle, the effective frequency range of interest is from 1 KHz to 40 KHz. With reduced tape speed, the spectra were therefore analyzed from 250 Hz to 10 KHz.

The analysis was conducted with a constant filter bandwidth, B , of 50 Hz, which is equivalent to an effective filter bandwidth of 200 Hz over the required frequency range.

The values of remaining analysis parameters were optimized with two considerations in mind: (i) the statistical accuracy of the data analysis, and (ii) the time taken to perform one spectrum analysis. The number of degrees of freedom, n , was set equal to 100. This means that the true mean-square value, with 98% confidence level, lies between 1.5 times observed mean-square value and 0.75 times observed mean-square value. Expressed in terms of the familiar decibel scale, the true mean-square value is within +1.76 dB and -1.25 dB of the observed mean-square value, with 98% confidence. Of course, the deviation between the true and observed mean-square values will be smaller if a less accurate confidence level is chosen.

Once the value for the number of degrees of freedom was selected, the values of the remaining analysis parameters followed automatically, according to standard statistical data analysis techniques.

The ideal time constant, RC , is $n/4B$, i.e. 0.5 second. However, in some preliminary data analysis exploration, it was found that a time constant of 1 second was more appropriate in the present (broadband) analysis. With this larger time constant, the spectrum from the X-Y plotter was easier to read

(i.e., it reduced the large pen movements that existed with a 0.5 second time constant), and hence, a time constant of one second was used in all frequency analysis.

The minimum tape loop length in seconds, T , is twice the ideal RC, which in this case corresponds to 1 second (or 30 inches in length). Since the analysis time would be relatively large, it was decided to make tape loops of approximately 120 inches in order to reduce tape wear.

The sweep rate, SR , must be less than $B/2T$, which in this case is a linear sweep rate of 25 cycles per second. This rate was used at all times.

It is interesting to note that the total analysis time is $A_t = [f(\max) - f(\min)]/SR$, which is approximately 6½ minutes per spectrum. During each narrow-band spectrum analysis, a simultaneous one-third octave band analysis was also conducted, which required no additional analysis time. The resulting one-third octave spectra were processed on the Univac 418 computer with the existing data reduction program, which incorporates the atmospheric attenuation corrections and computes the overall SPL for each spectrum.

DATA PRESENTATION

The nominal values of jet operating conditions defining the test points covering the entire experimental program are tabulated in detail, and the various parameters are defined in the list of symbols. It can be seen that for every test point number (TPN), there are two corresponding run numbers (RN); the first run number refers to measurements in the rear arc, whereas the second run number refers to measurements in the forward arc. Although, in the experimental program, the microphones were located at $7\frac{1}{2}^\circ$ intervals over the angular range from 15° to 150° to the downstream jet axis, the narrowband spectra given in this Volume are at 15° intervals, simply to reduce the size of the Volume. Each one of the four hundred spectra is identified by the code number that appears on the top right-hand corner. The identification is constructed as follows:

TPN/RN/R or F/ θ°

The first number gives the test point number (TPN), and the second number gives the run number (RN). This is followed by the letter R or F, which signifies that the measurements were conducted in the rear arc or the forward arc configuration, respectively. The last number gives the angular position of the microphone, referenced to the jet exhaust axis.

It should be noted that all data given here are for a two-inch diameter convergent nozzle with the measurement points at 72 diameters. For application to other measurement configurations, the normal scaling laws must be applied.

Finally, the reader is made aware of the point that due to the presence of the kaowool wrapping near the nozzle exit, there is no direct line of sight between the 150° microphone position and the nozzle lip. The spectra at this microphone angle are therefore likely to be affected (normally resulting into

slightly lower levels than expected), and should be treated with caution. No such problem exists, however, for results at angles smaller than approximately 135° .

SHOCK ASSOCIATED NOISE EXPERIMENTS

TEST POINT CONDITIONS
(NOMINAL)

LIST OF SYMBOLS

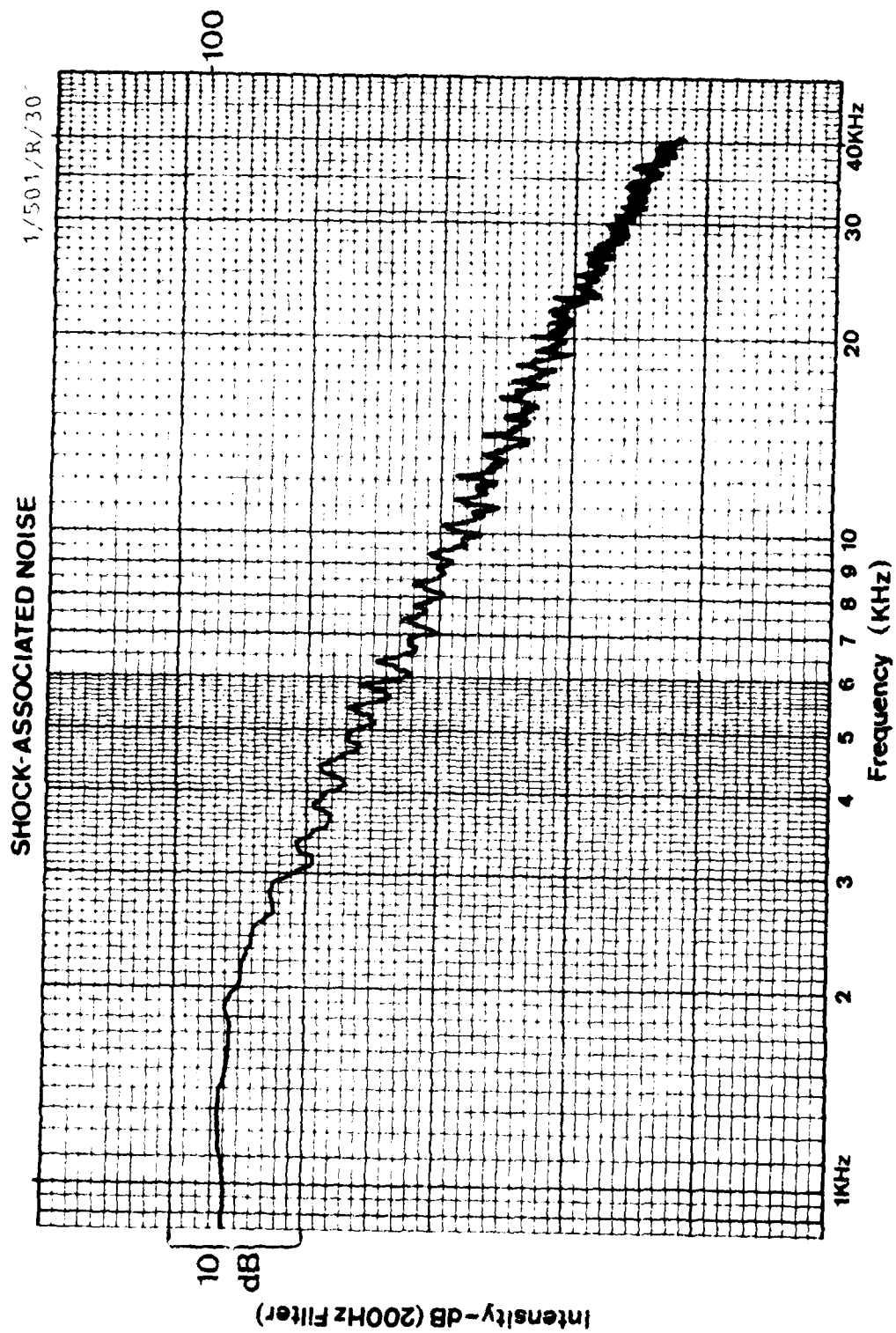
a_0	ambient speed of sound
a_j	speed of sound in jet flow at nozzle exit plane
D	jet nozzle diameter
M_j	jet Mach number, V_j/a_j
P_R/P_0	pressure ratio
R	microphone distance from nozzle exit plane
RN	run number
TPN	test point number
T_j/T_0	static (or jet exit) temperature ratio
T_R/T_0	stagnation (or total) temperature ratio
V_j/a_0	jet exit velocity ratio
γ	$= (M_j^2 - 1)^{\frac{1}{2}}$
γ	ratio of specific heats
θ	microphone angle relative to downstream jet axis

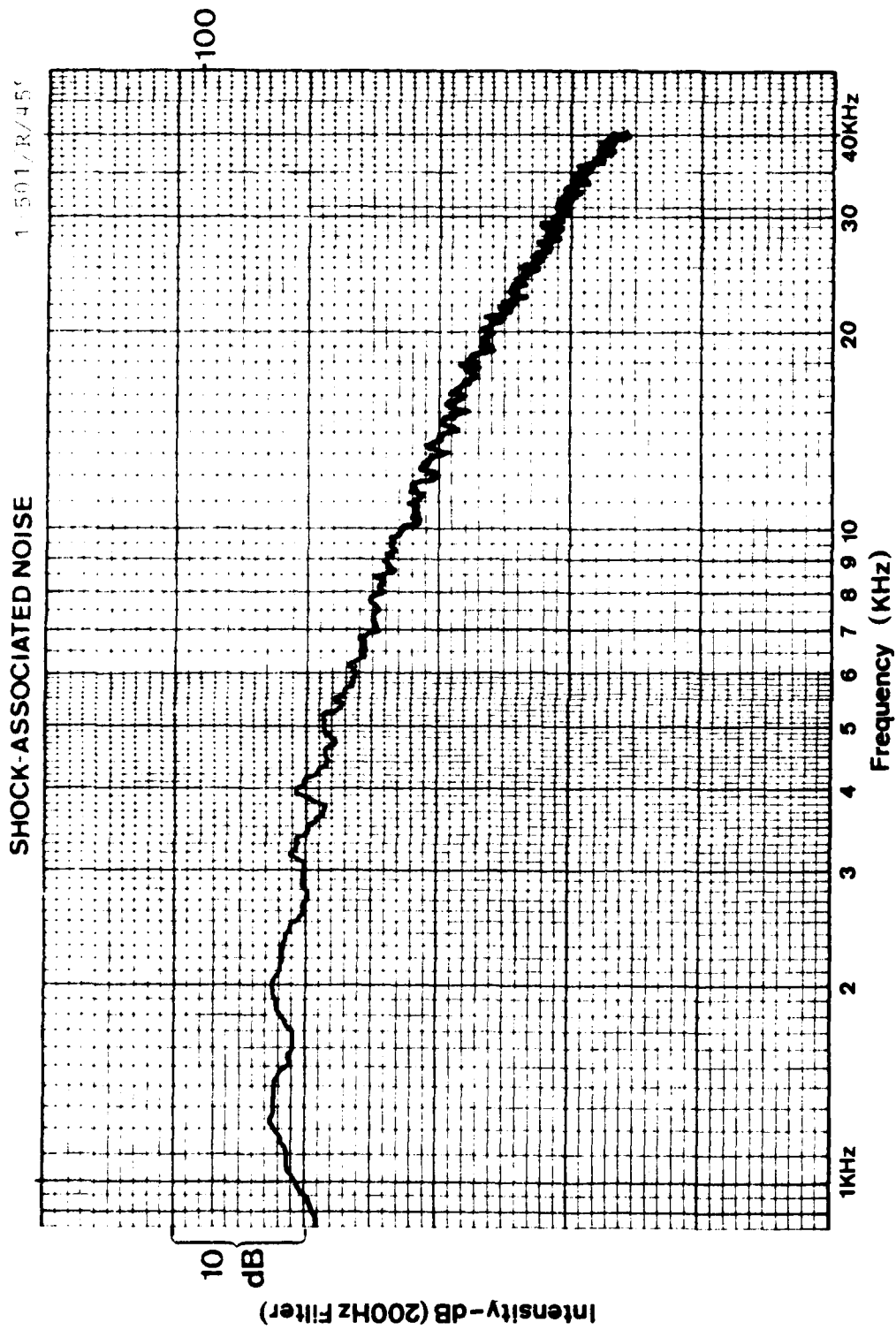
TPN	β	T_J/T_O	M_J	V_J/a_O	γ	P_R/P_O	T_R/T_O	REAR ARC		FORWARD ARC	
								RN	PAGE NO.	RN	PAGE NO.
1	0.20	0.828	1.020	0.928	1.40	1.937	1.000	501	13 - 17	545	18 - 22
2	0.30	0.821	1.044	0.946	1.40	1.994	1.000	502	23 - 27	546	28 - 32
3	0.40	0.812	1.077	0.970	1.40	2.076	1.000	503	33 - 37	547	38 - 42
4	0.50	0.800	1.118	1.000	1.40	2.184	1.000	504	43 - 47	548	48 - 52
5	0.60	0.786	1.166	1.034	1.40	2.321	1.000	505	53 - 57	549	58 - 62
6	0.70	0.700	1.221	1.071	1.40	2.491	1.000	506	63 - 67	550	68 - 72
7	0.80	0.753	1.281	1.111	1.40	2.699	1.000	507	73 - 77	551	78 - 82
8	0.94	0.726	1.372	1.170	1.40	3.062	1.000	508	83 - 87	552	88 - 92
9	1.10	0.693	1.487	1.238	1.40	3.601	1.000	509	93 - 97	553	98 - 102
10	1.34	0.641	1.672	1.339	1.40	4.732	1.000	510	103 - 107	554	108 - 112

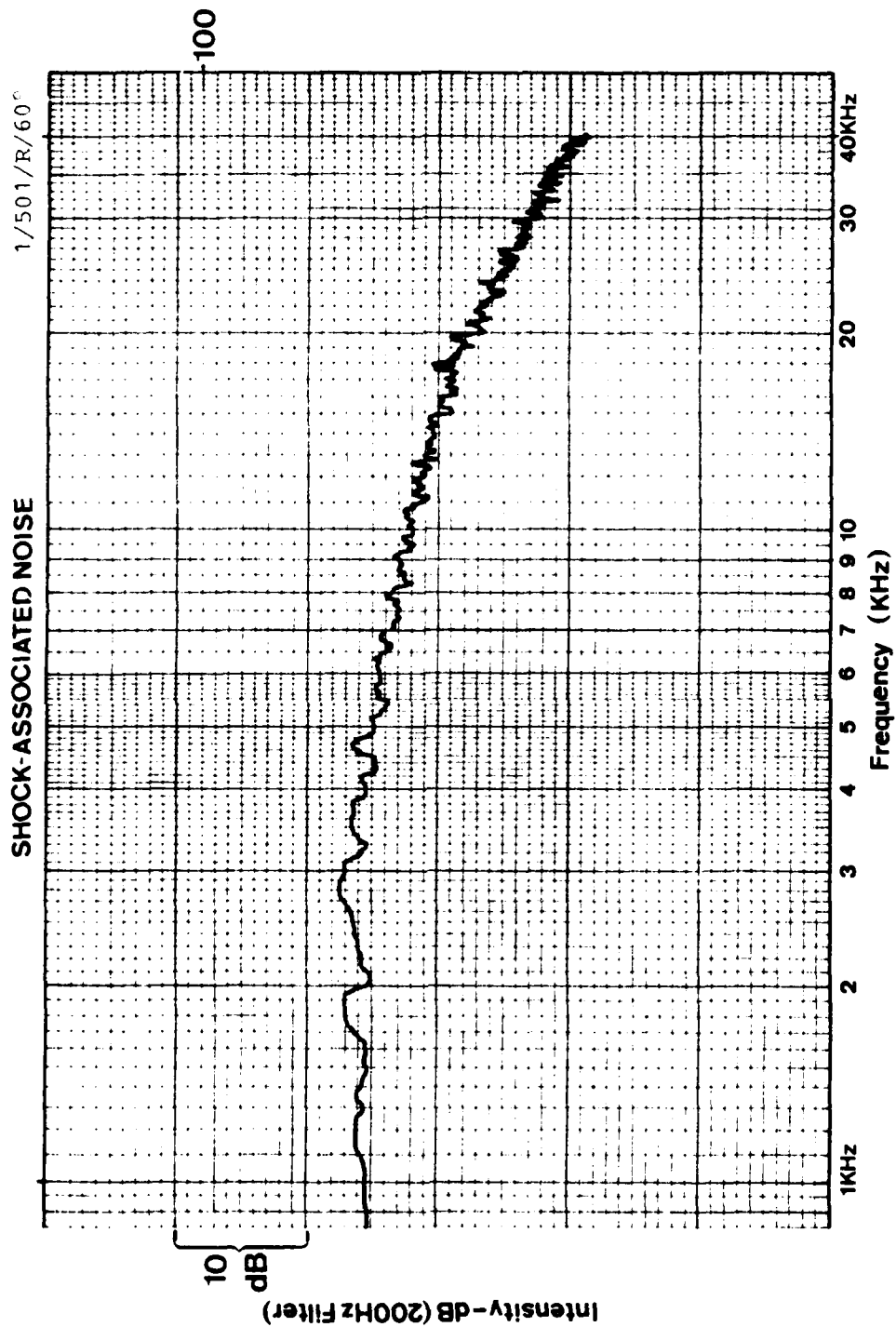
TPN	α	T_J/T_O	M_J	V_J/a_O	τ	P_R/P_O	T_R/T_O	REAR ARC		FORWARD ARC	
								RN	PAGE NO.	RN	PAGE NO.
12	0.20	1.000	1.020	1.020	1.40	1.937	1.208	543	113 - 117	556	118 - 122
13	0.30		1.044	1.044	1.40	1.994	1.218	542	123 - 127	557	128 - 132
14	0.40		1.077	1.077	1.40	2.076	1.232	541	133 - 137	558	138 - 142
15	0.50		1.118	1.118	1.40	2.184	1.250	540	143 - 147	559	148 - 152
16	0.60		1.166	1.166	1.39	2.313	1.265	539	153 - 157	560	158 - 162
17	0.70		1.221	1.221	1.39	2.482	1.291	538	163 - 167	561	168 - 172
18	0.80		1.281	1.281	1.39	2.688	1.320	537	173 - 177	562	178 - 182
19	0.94		1.372	1.372	1.39	3.050	1.367	536	183 - 187	563	188 - 192
20	1.10		1.487	1.487	1.39	3.586	1.431	535	193 - 197	564	198 - 202
21	1.34	1.000	1.672	1.672	1.39	4.715	1.545	534	203 - 207	565	208 - 212

TPN	β	T_J/T_O	M_J	V_J/a_O	γ	P_R/P_O	T_R/T_O	REAR ARC		FORWARD ARC	
								RN	PAGE NO.	RN	PAGE NO.
23	0.20	1.820	1.020	1.376	1.37	1.919	2.170	532	213 - 217	567	218 - 222
24	0.30		1.044	1.408	1.37	1.974	2.187	531	223 - 227	568	228 - 232
25	0.40		1.077	1.453	1.37	2.054	2.211	530	233 - 237	569	238 - 242
26	0.50		1.118	1.508	1.37	2.160	2.241	529	243 - 247	570	248 - 252
27	0.60		1.166	1.573	1.36	2.287	2.266	528	253 - 257	571	258 - 262
28	0.70		1.221	1.647	1.36	2.454	2.308	527	263 - 267	572	268 - 272
29	0.80		1.281	1.728	1.36	2.657	2.357	526	273 - 277	573	278 - 282
30	0.94		1.372	1.852	1.36	3.013	2.437	525	283 - 287	574	288 - 292
31	1.10		1.487	2.006	1.35	3.529	2.524	524	293 - 297	575	298 - 302
32	1.34	1.820	1.672	2.256	1.35	4.647	2.710	523	303 - 307	576	308 - 312

TPN	β	T_J/T_O	M_J	V_J/a_O	γ	P_R/P_O	T_R/T_O	REAR ARC		FORWARD ARC	
								RN	PAGE NO.	RN	PAGE NO.
34	0.20	2.270	1.020	1.536	1.35	1.906	2.683	512	313 - 317	578	318 - 322
35	0.30		1.044	1.573	1.35	1.961	2.703	513	323 - 327	579	328 - 332
36	0.40		1.077	1.623	1.35	2.040	2.731	514	333 - 337	580	338 - 342
37	0.50		1.118	1.684	1.35	2.145	2.767	515	343 - 347	581	348 - 352
38	0.60		1.166	1.757	1.35	2.278	2.810	516	353 - 357	582	358 - 362
39	0.70		1.221	1.839	1.34	2.435	2.845	517	363 - 367	583	368 - 372
40	0.80		1.281	1.929	1.34	2.636	2.903	518	373 - 377	584	378 - 382
41	0.94		1.372	2.068	1.34	2.989	2.997	519	383 - 387	585	388 - 392
42	1.10		1.487	2.240	1.34	3.515	3.123	520	393 - 397	586	398 - 402
43	1.34	2.270	1.672	2.519	1.33	4.612	3.317	521	403 - 407	587	408 - 412

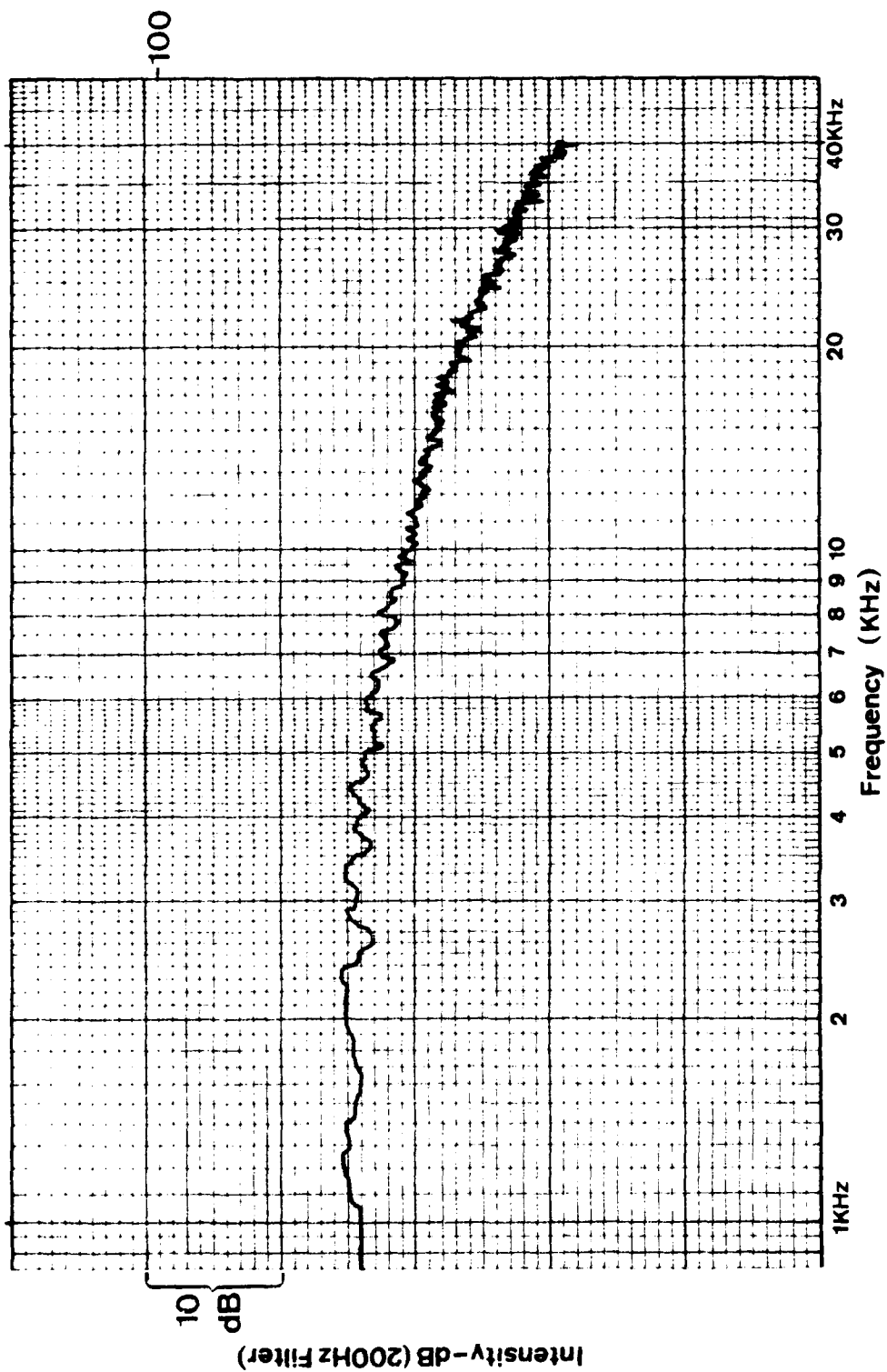


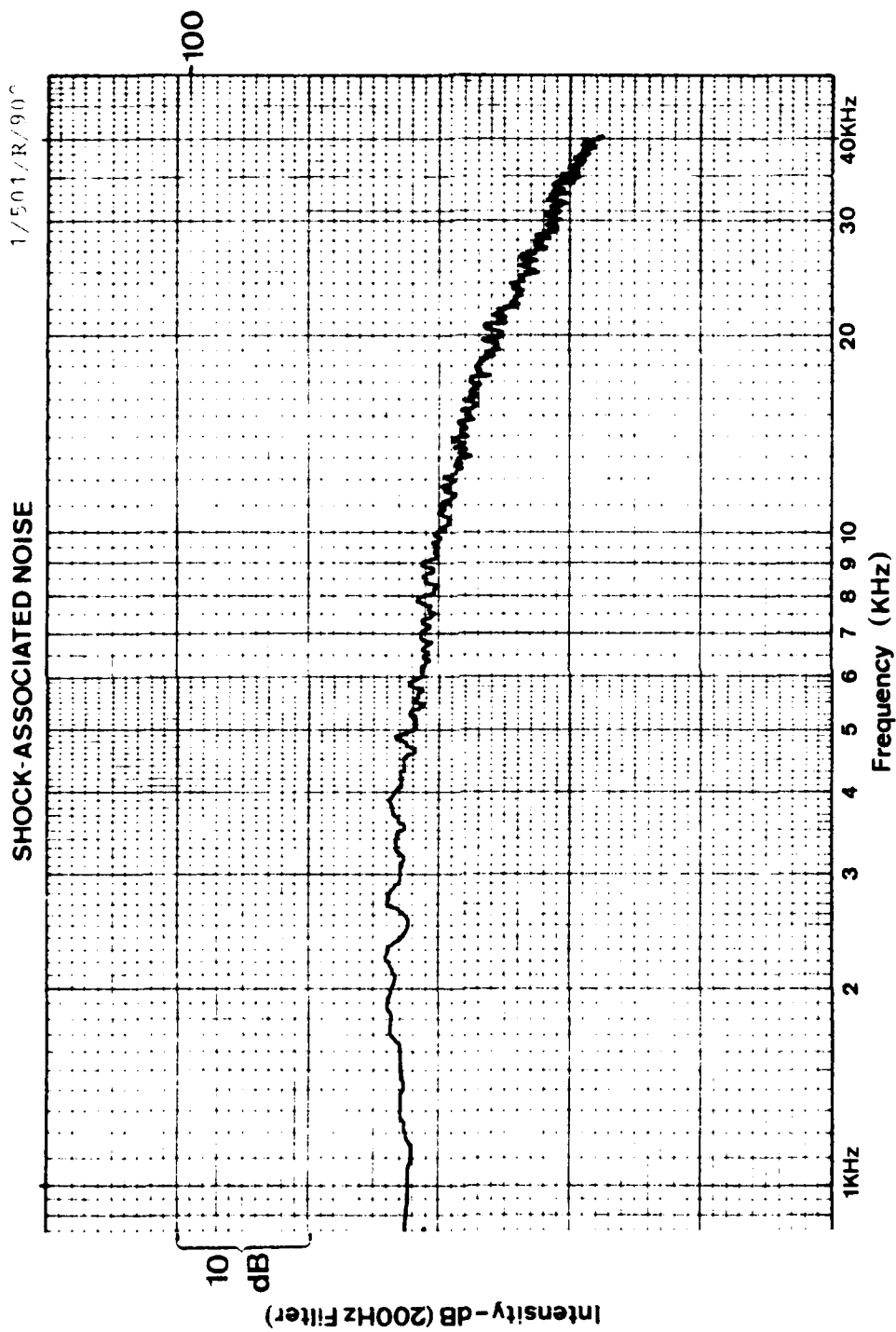


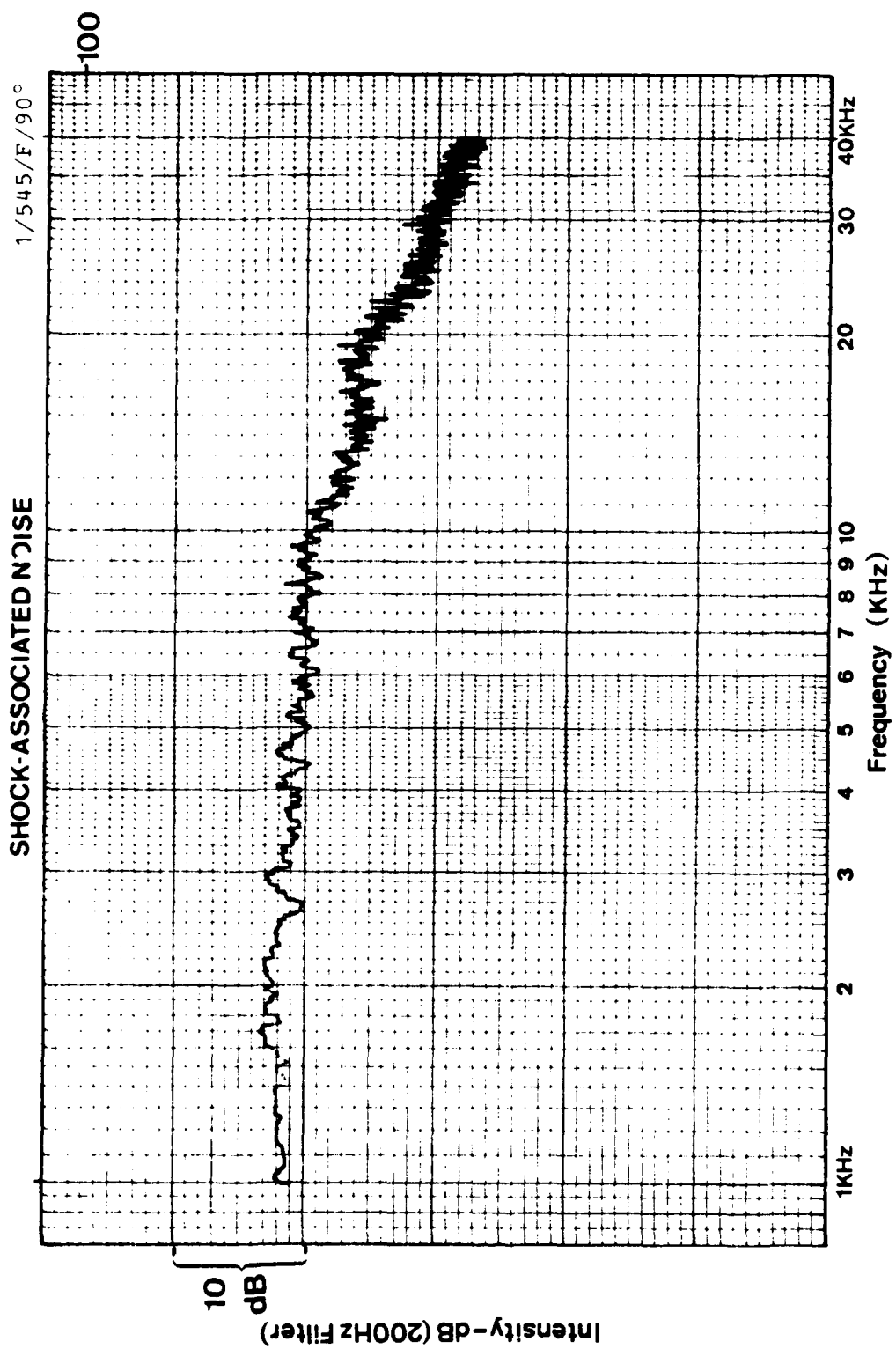


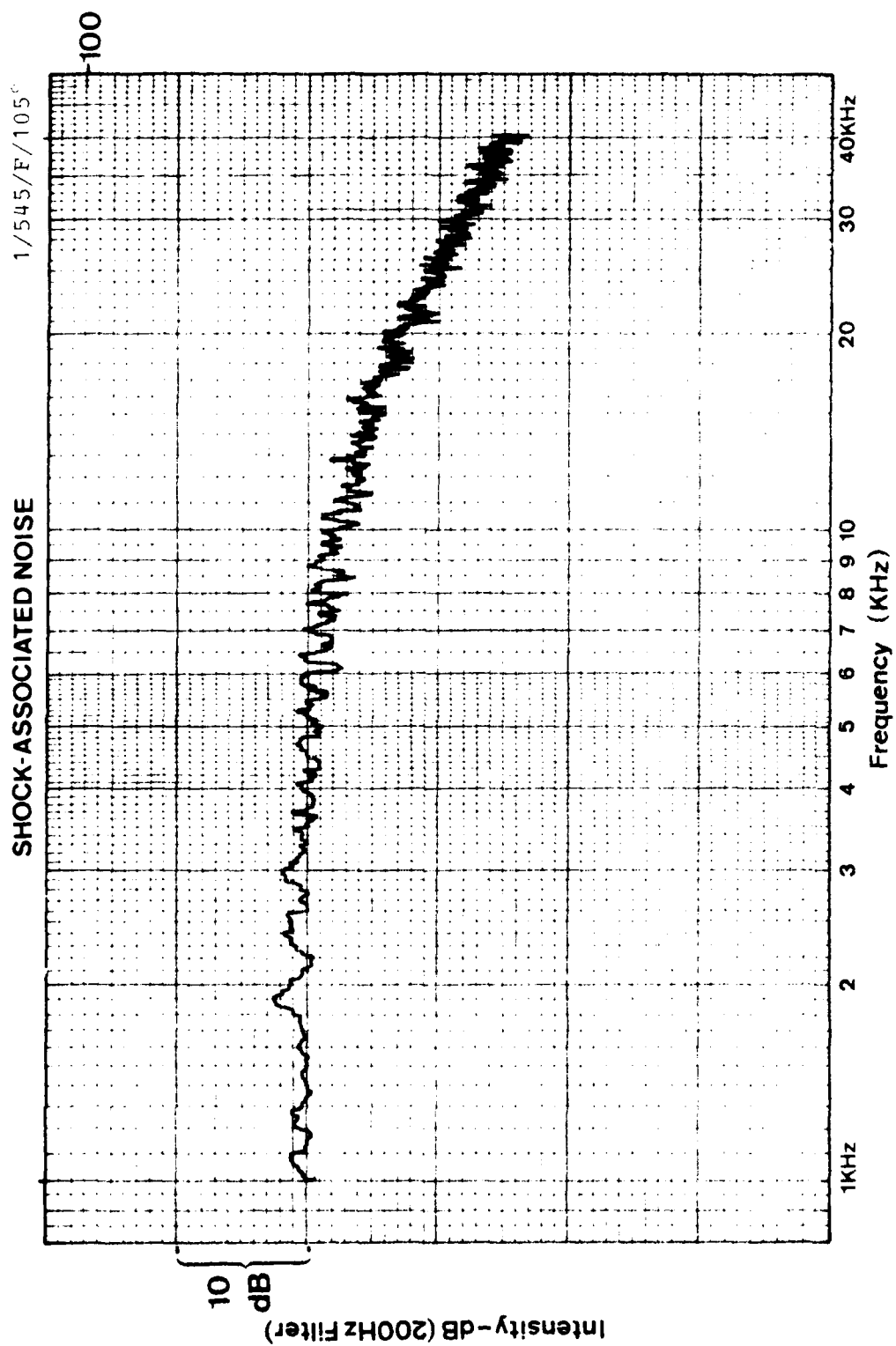
SHOCK-ASSOCIATED NOISE

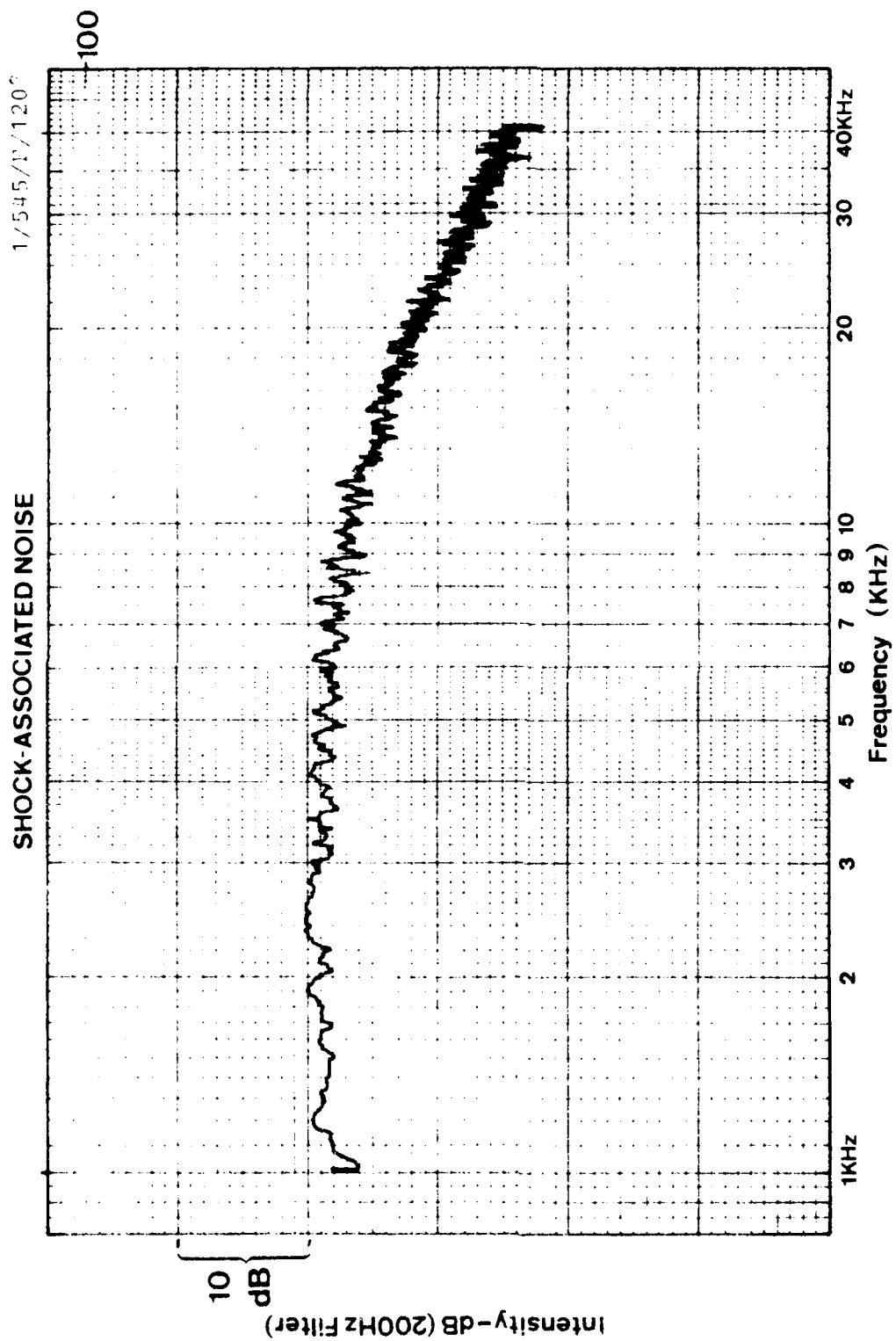
1/501/R/75

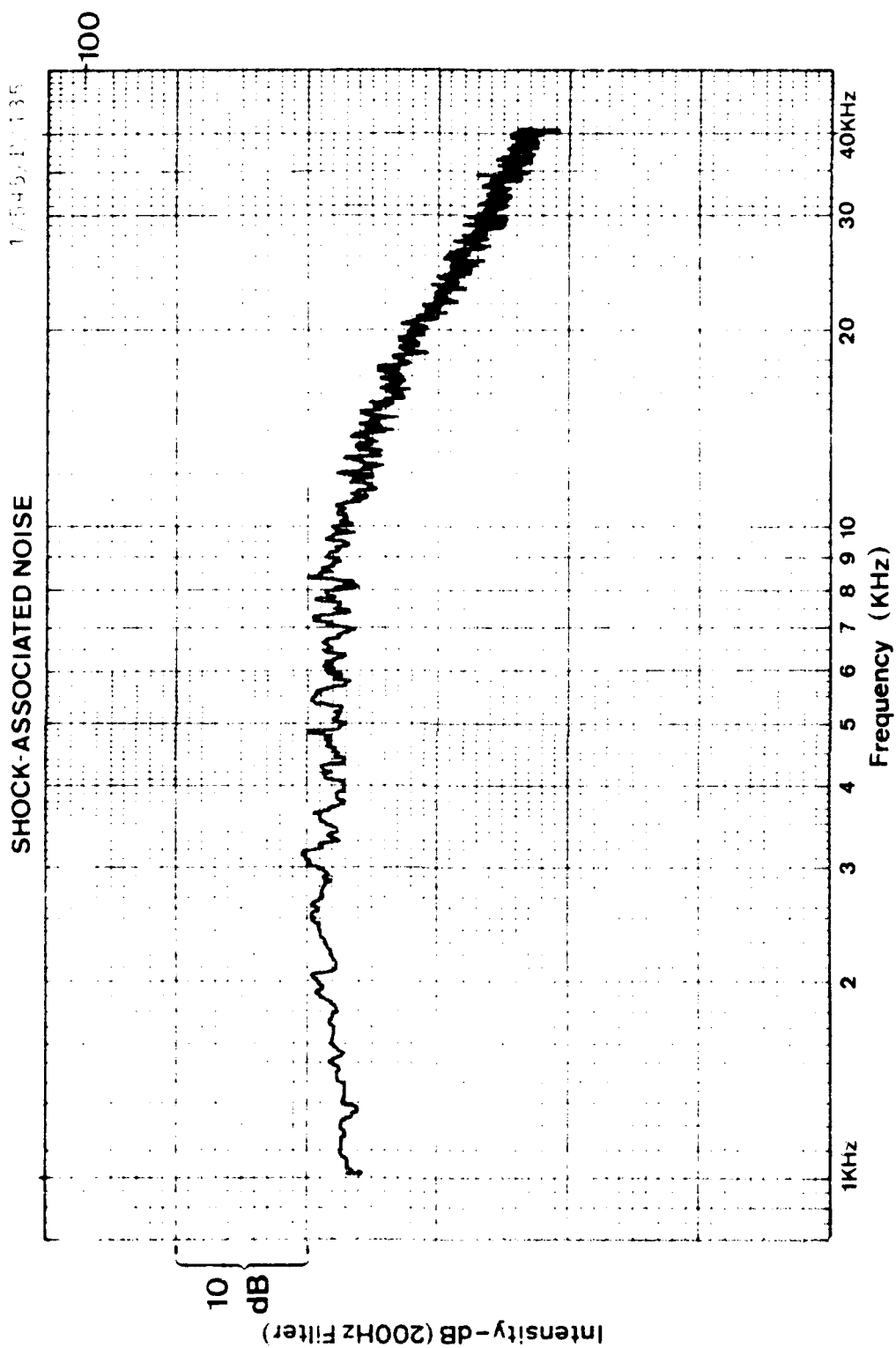


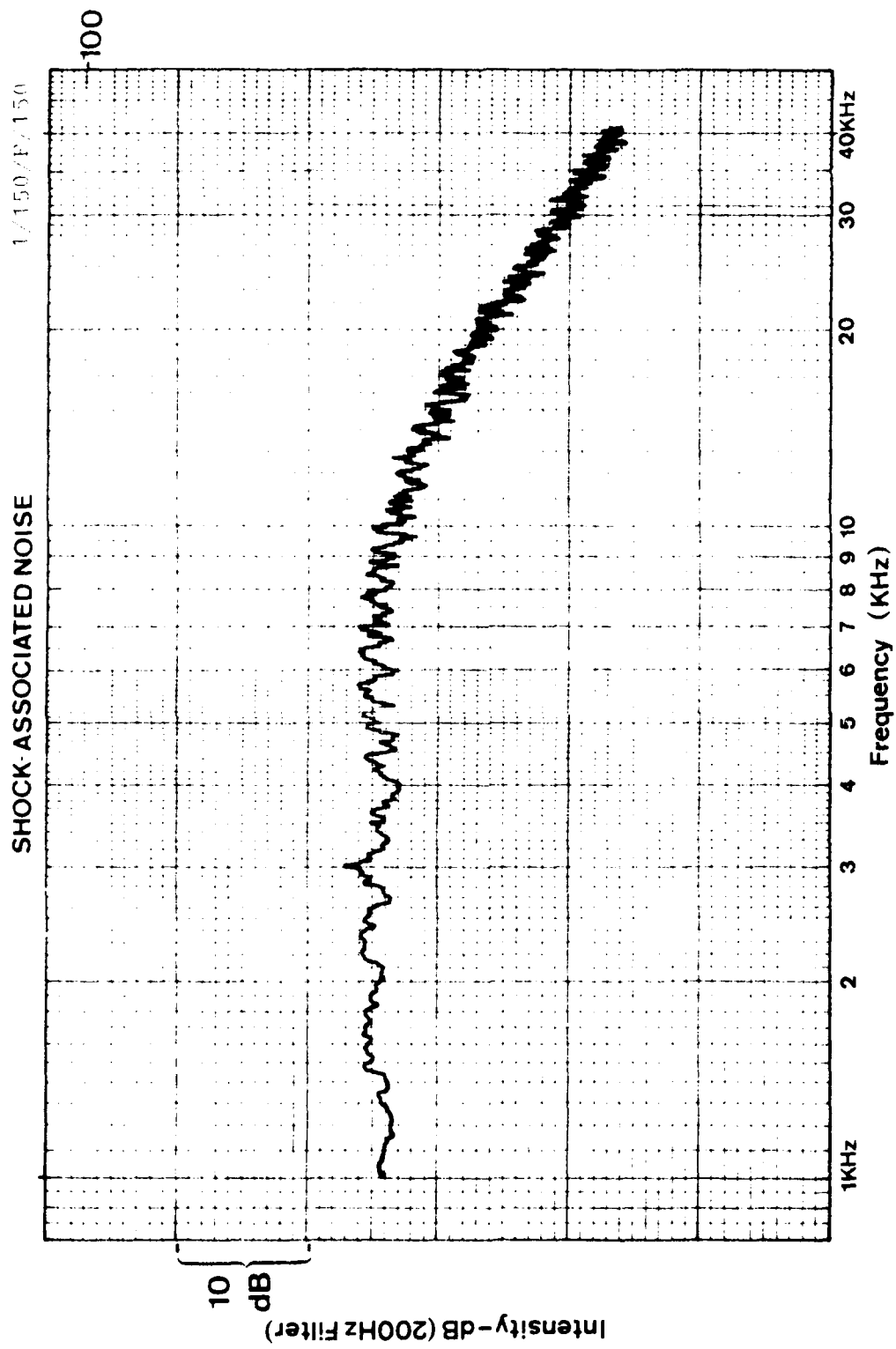


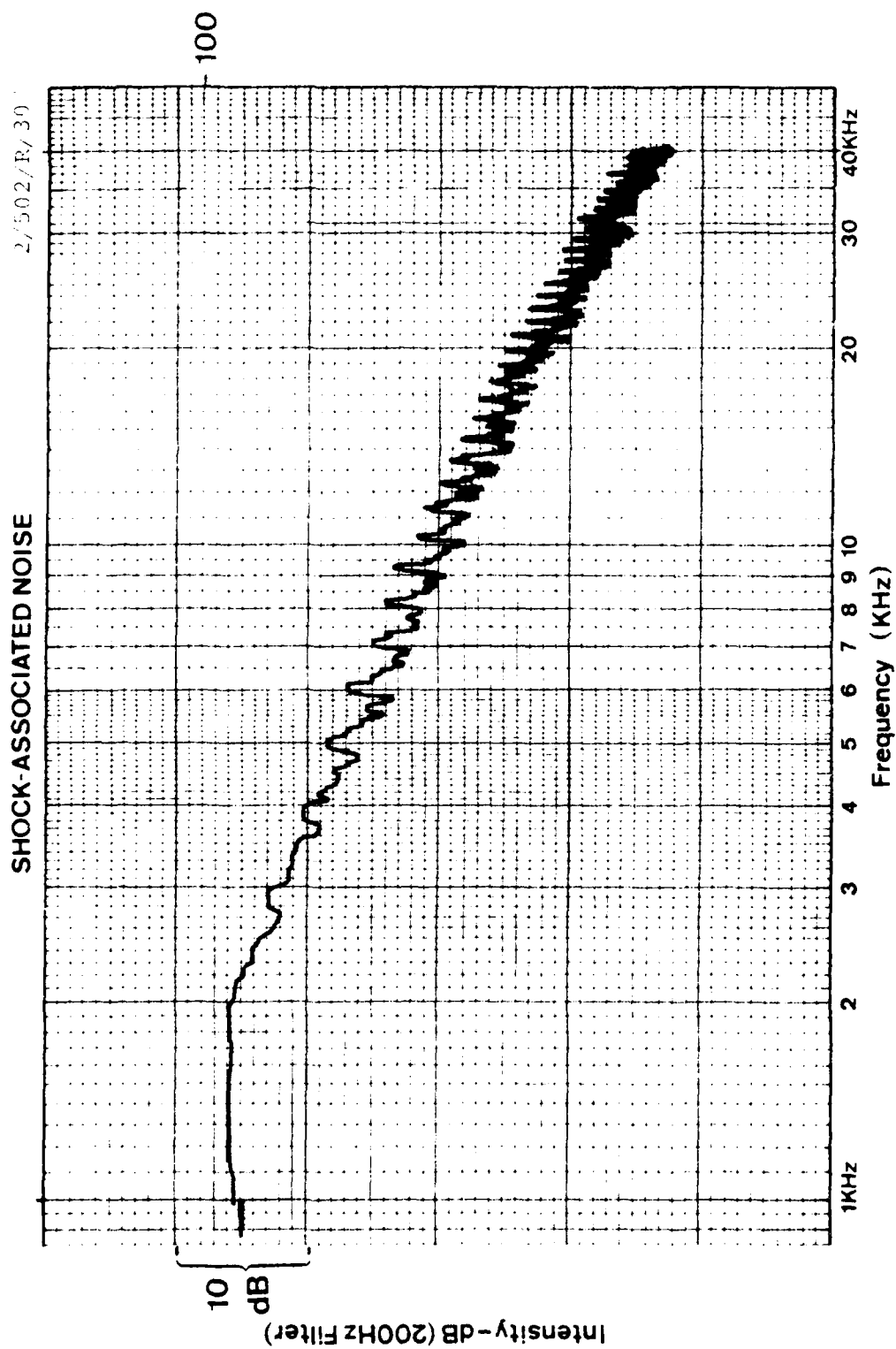


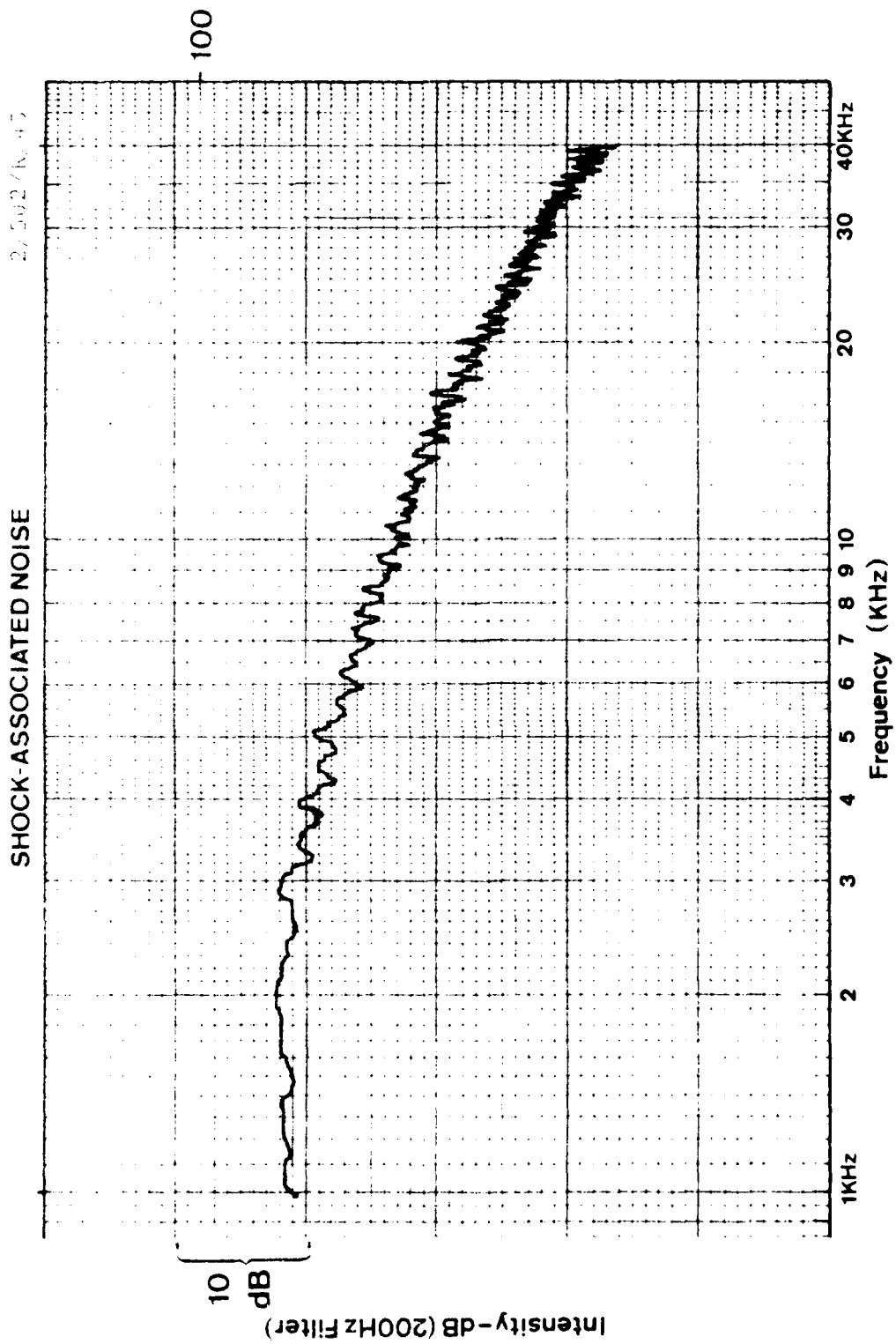


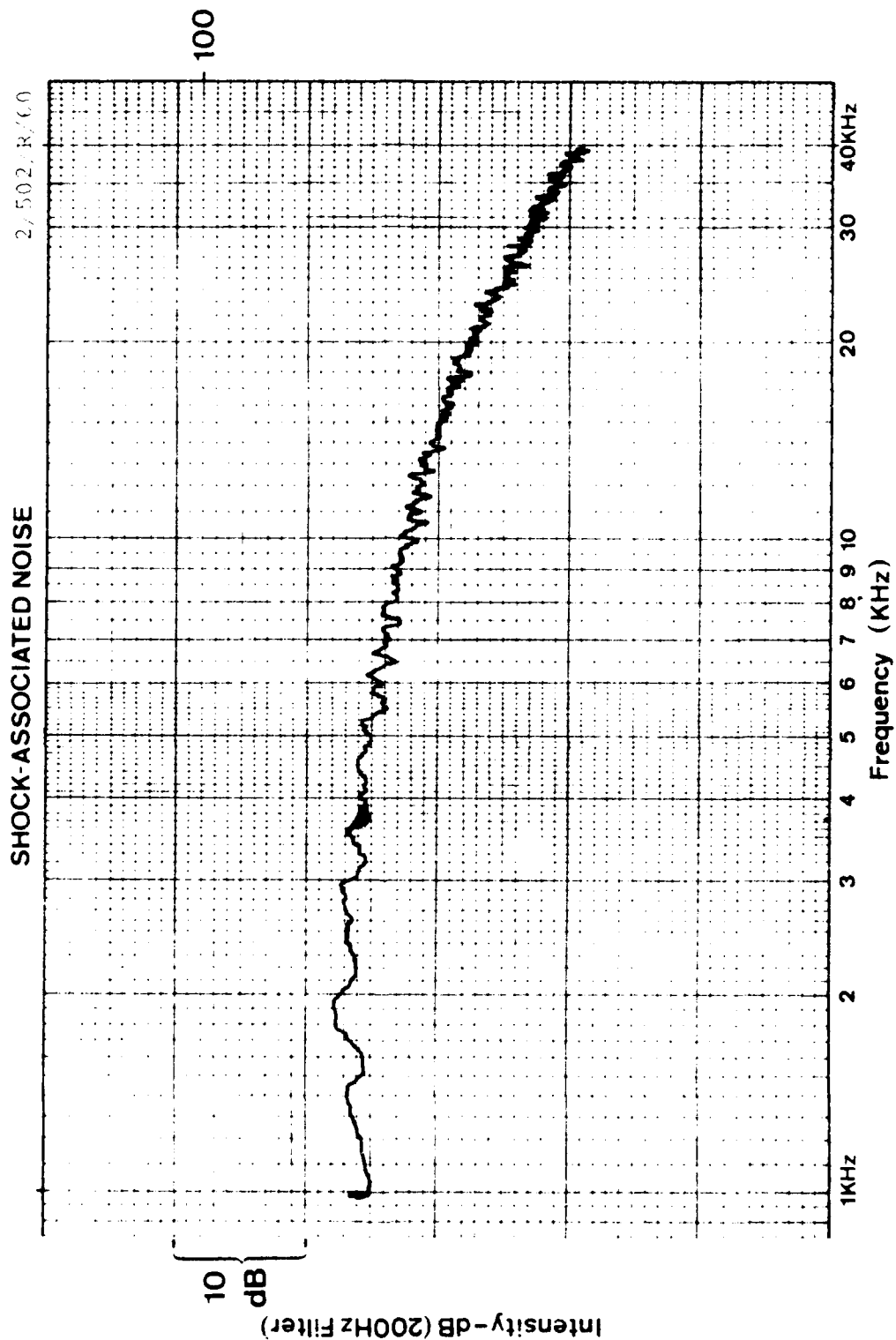






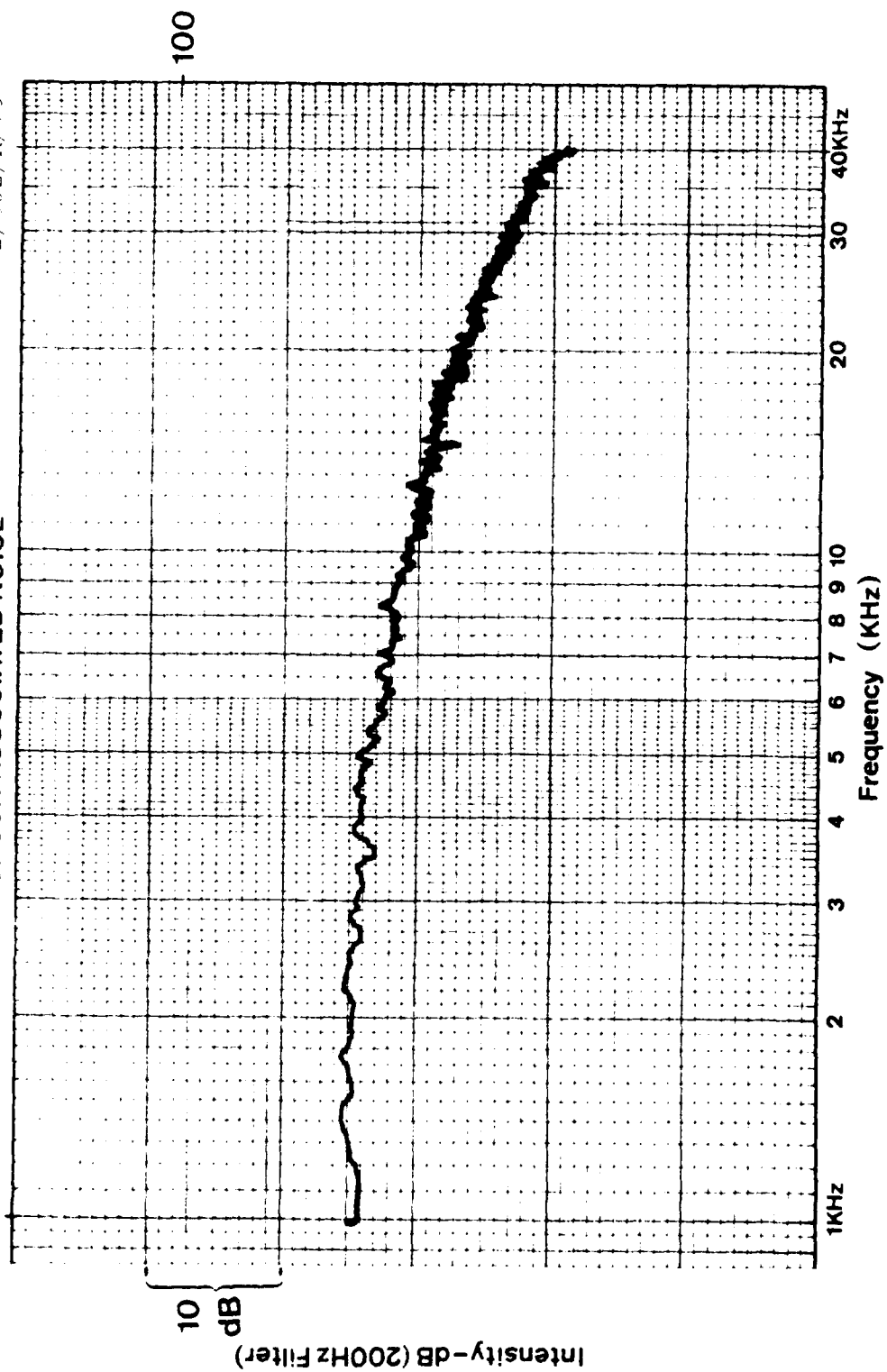


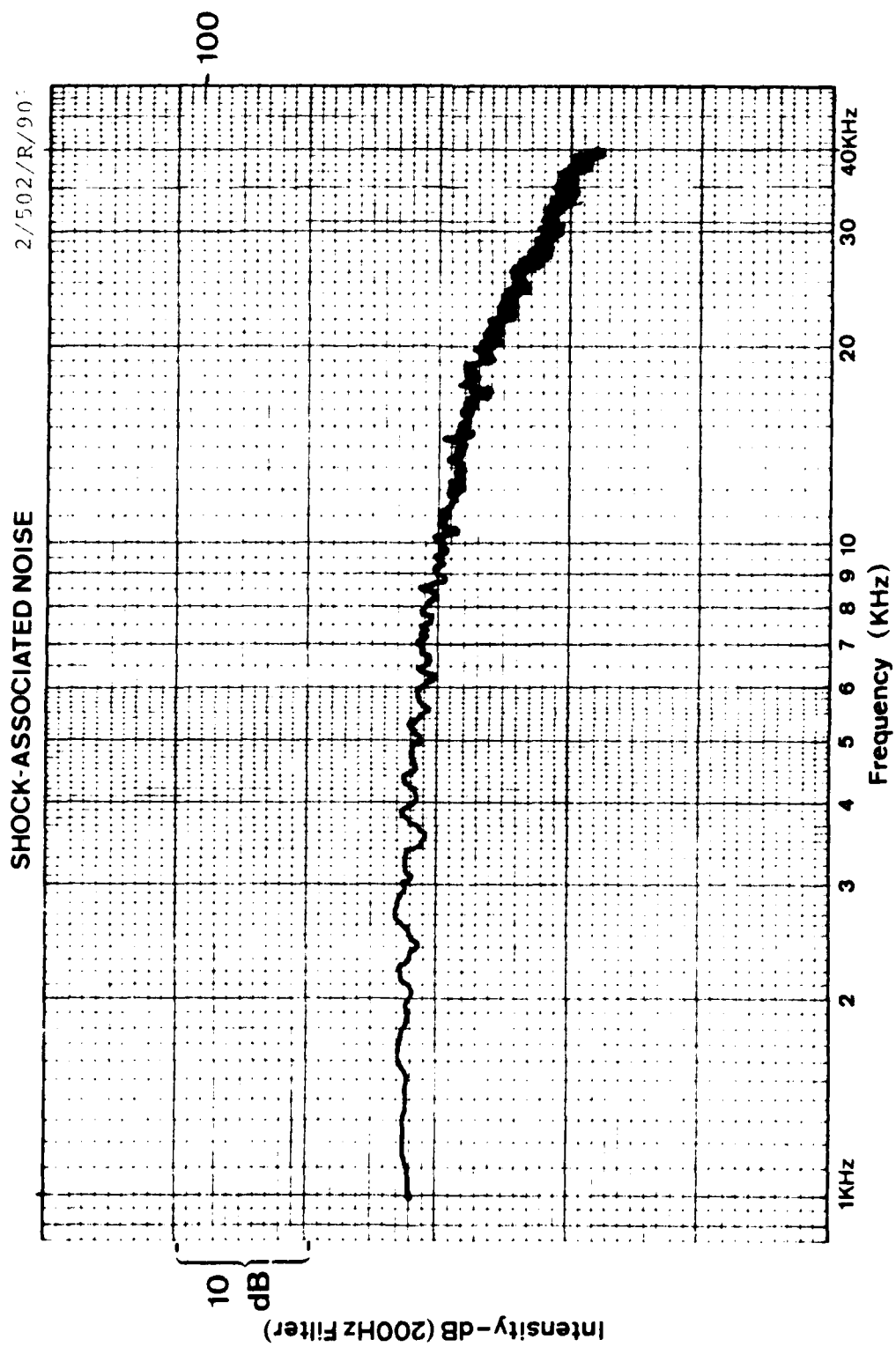


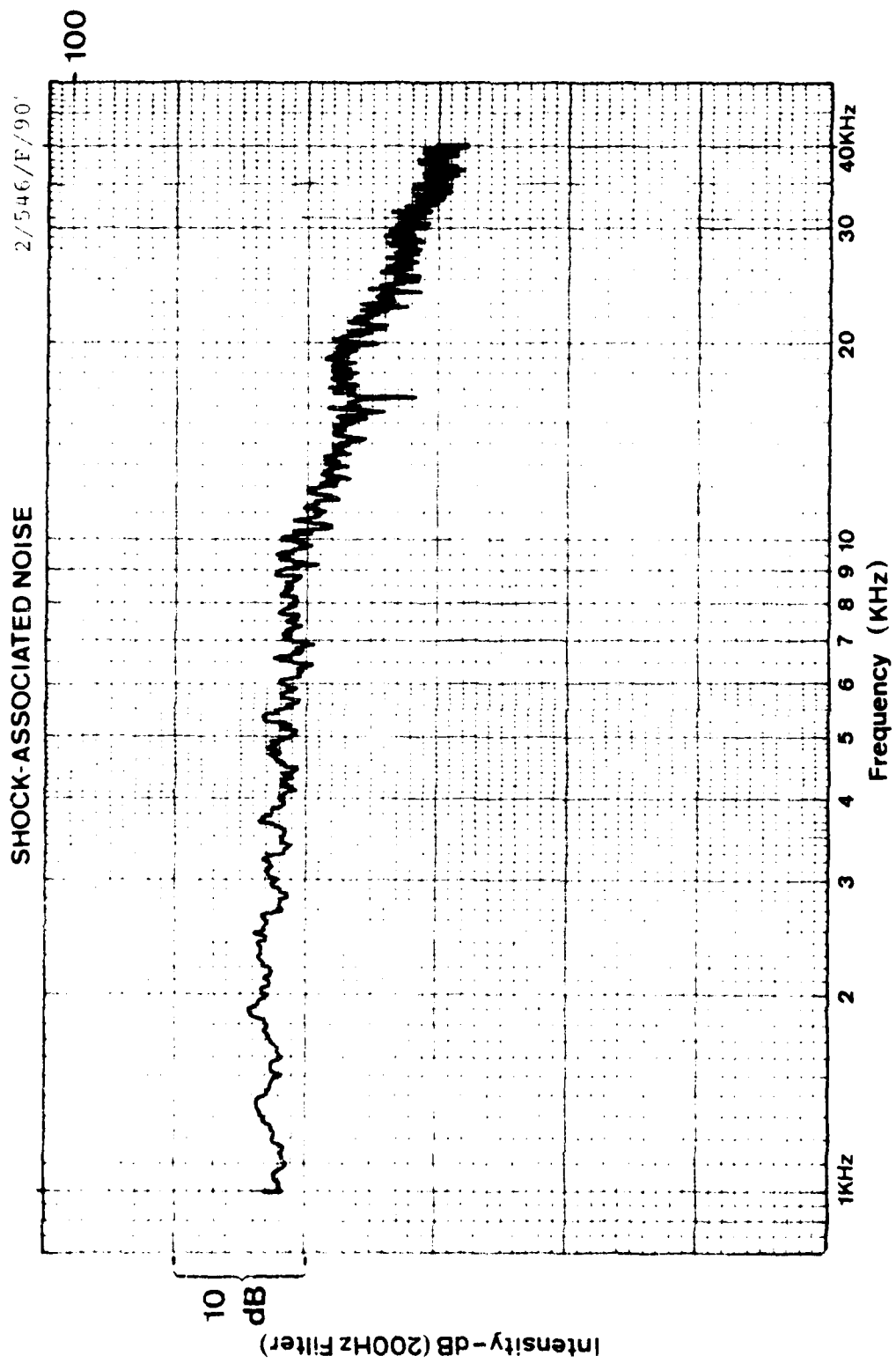


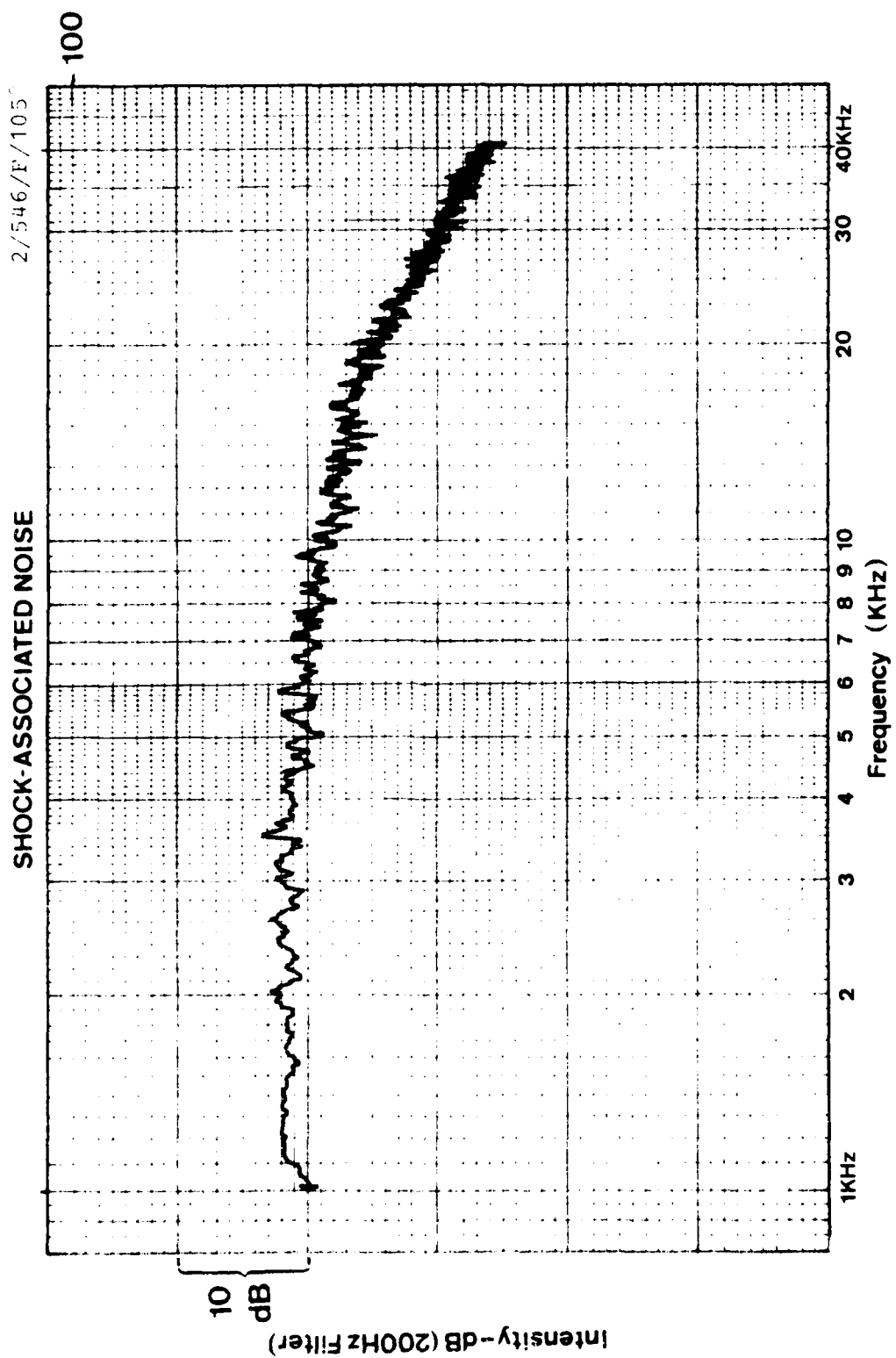
SHOCK-ASSOCIATED NOISE

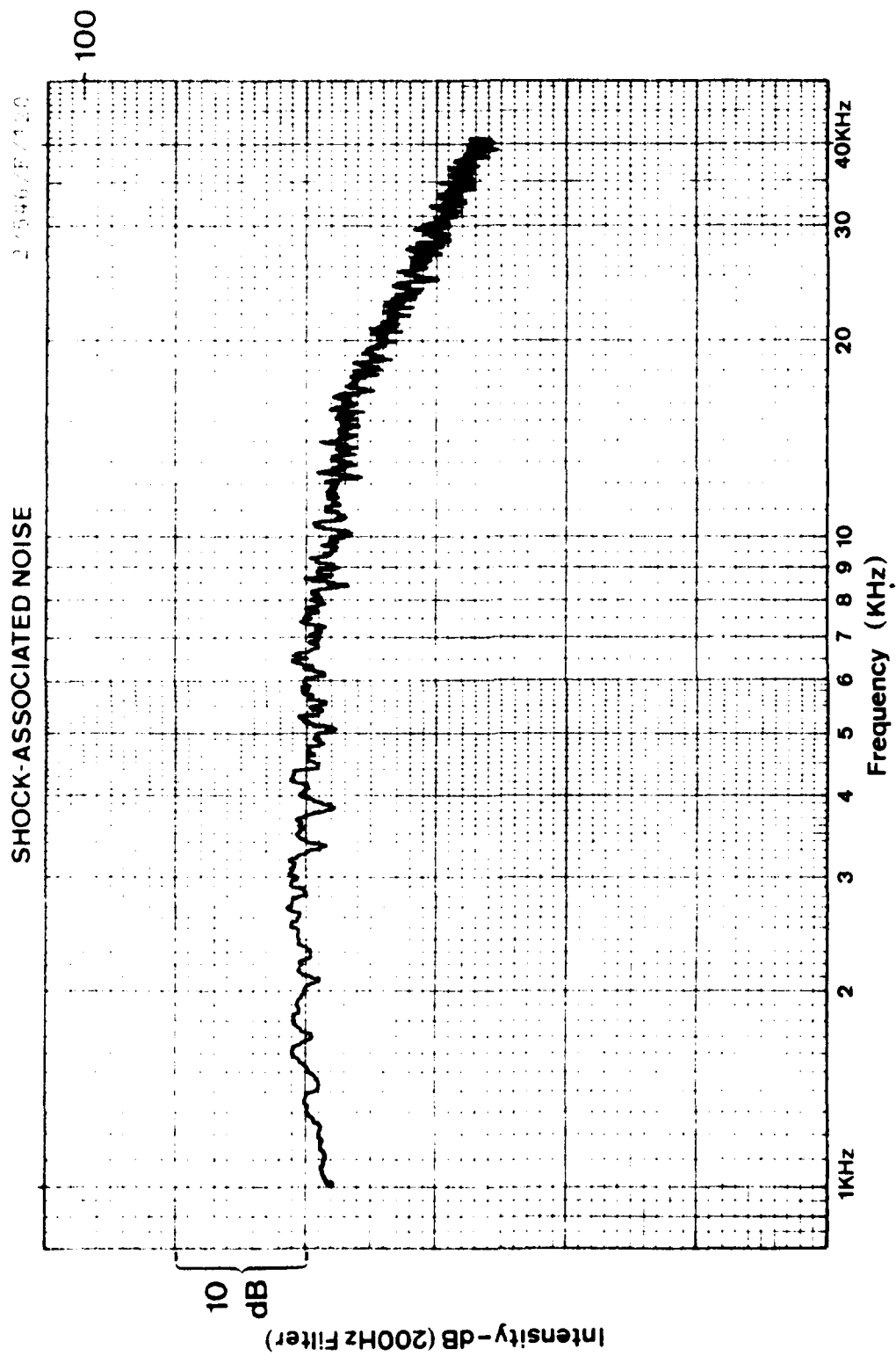
2/502/R/75

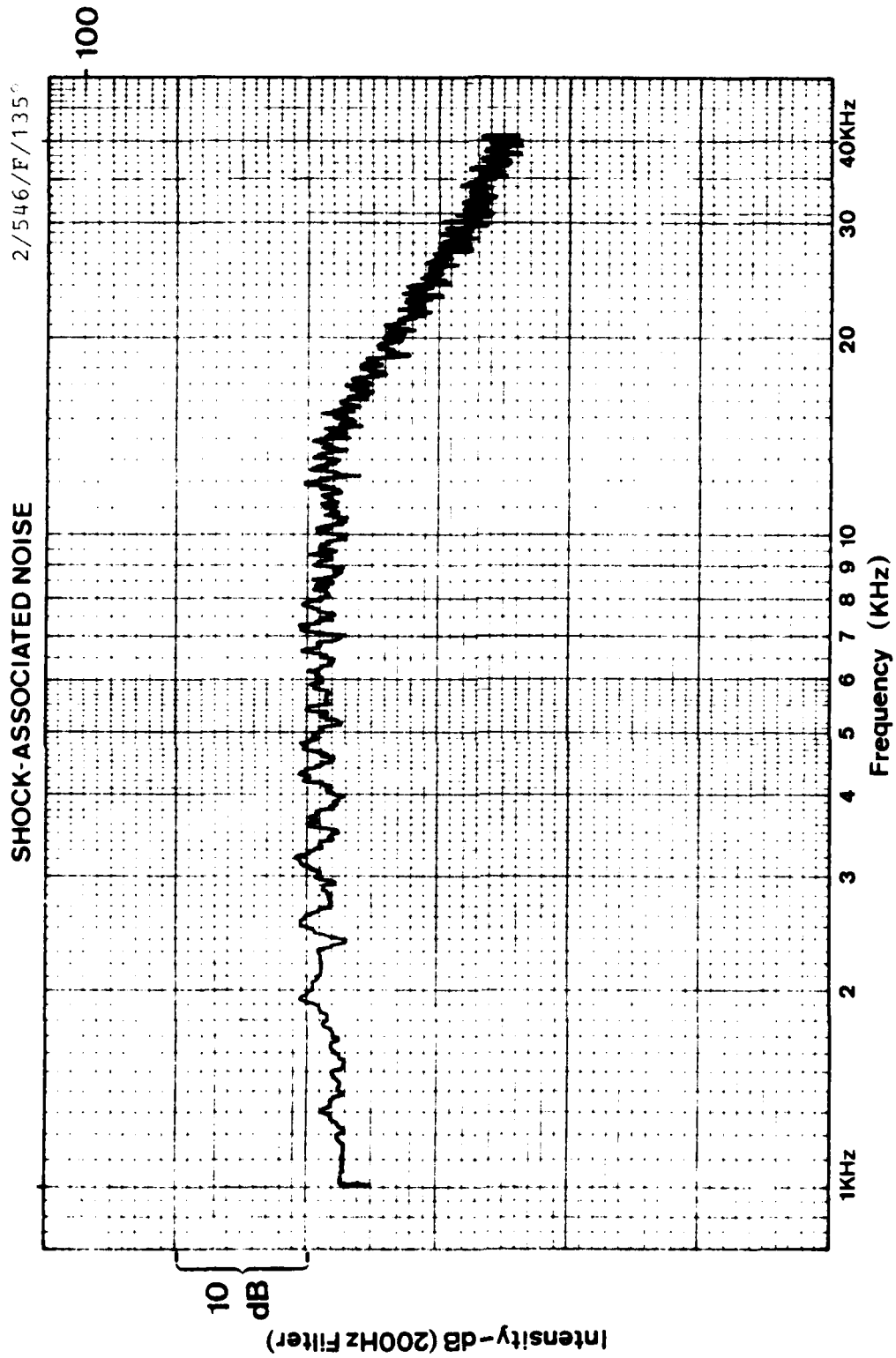


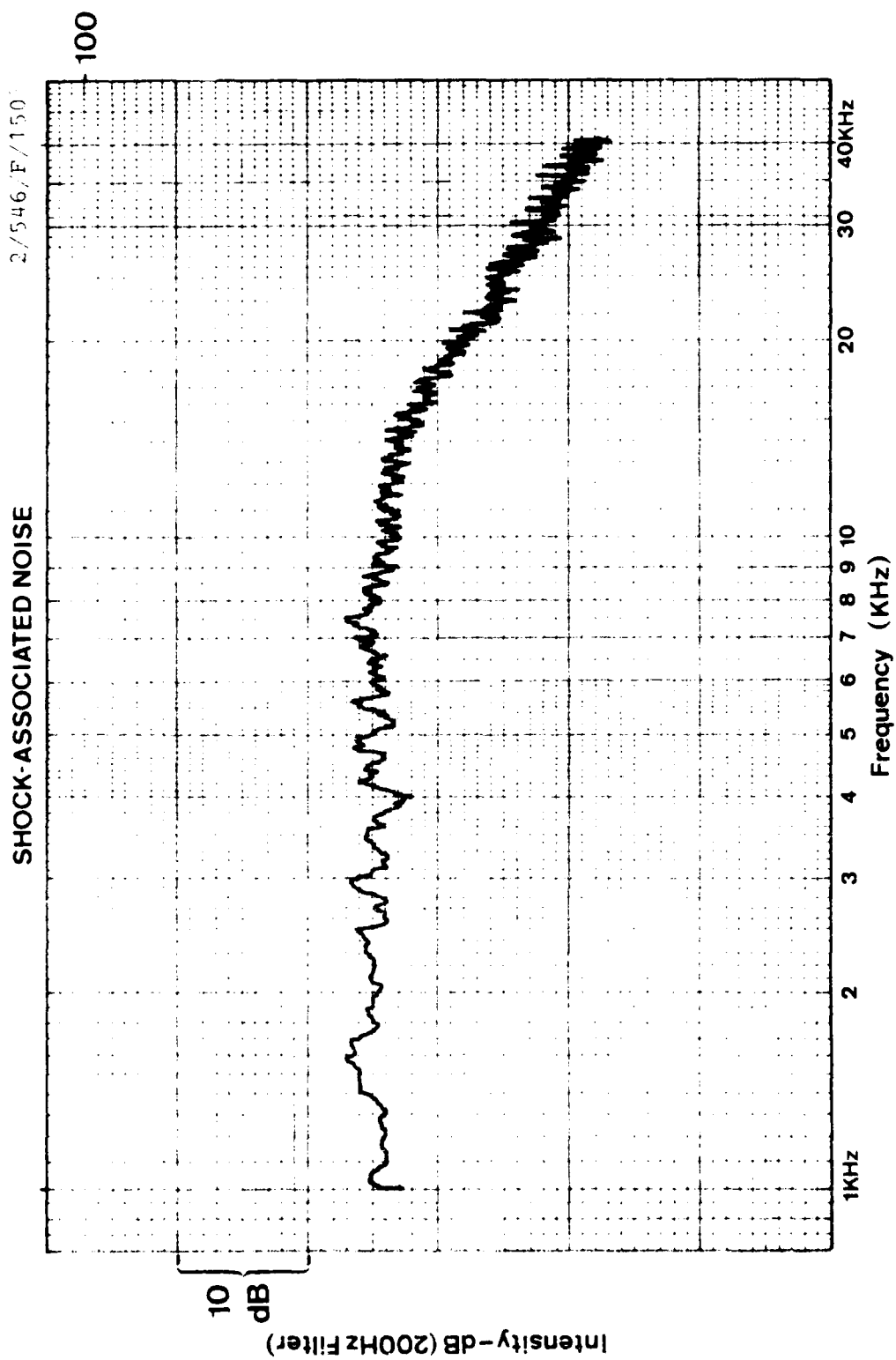


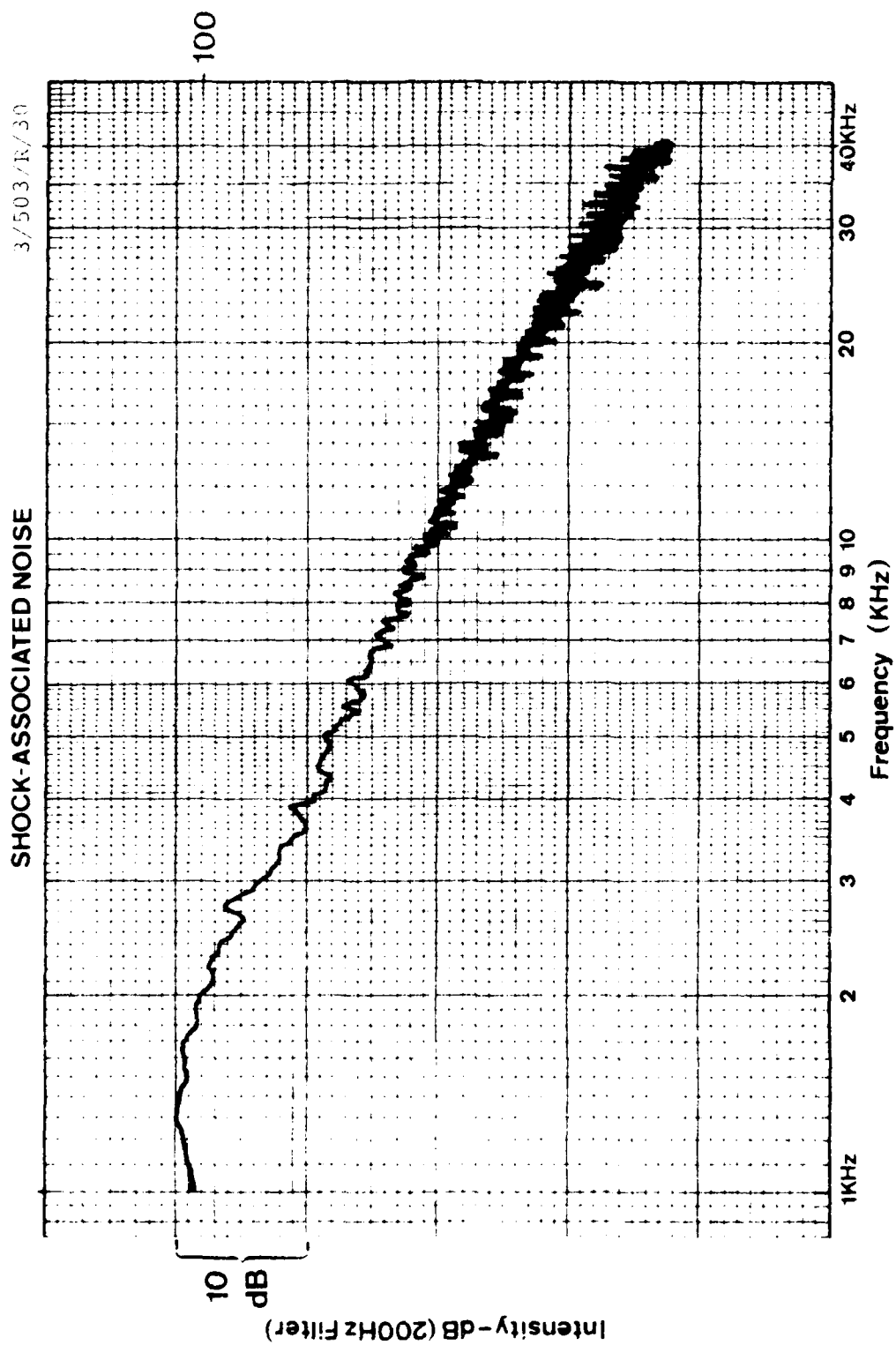


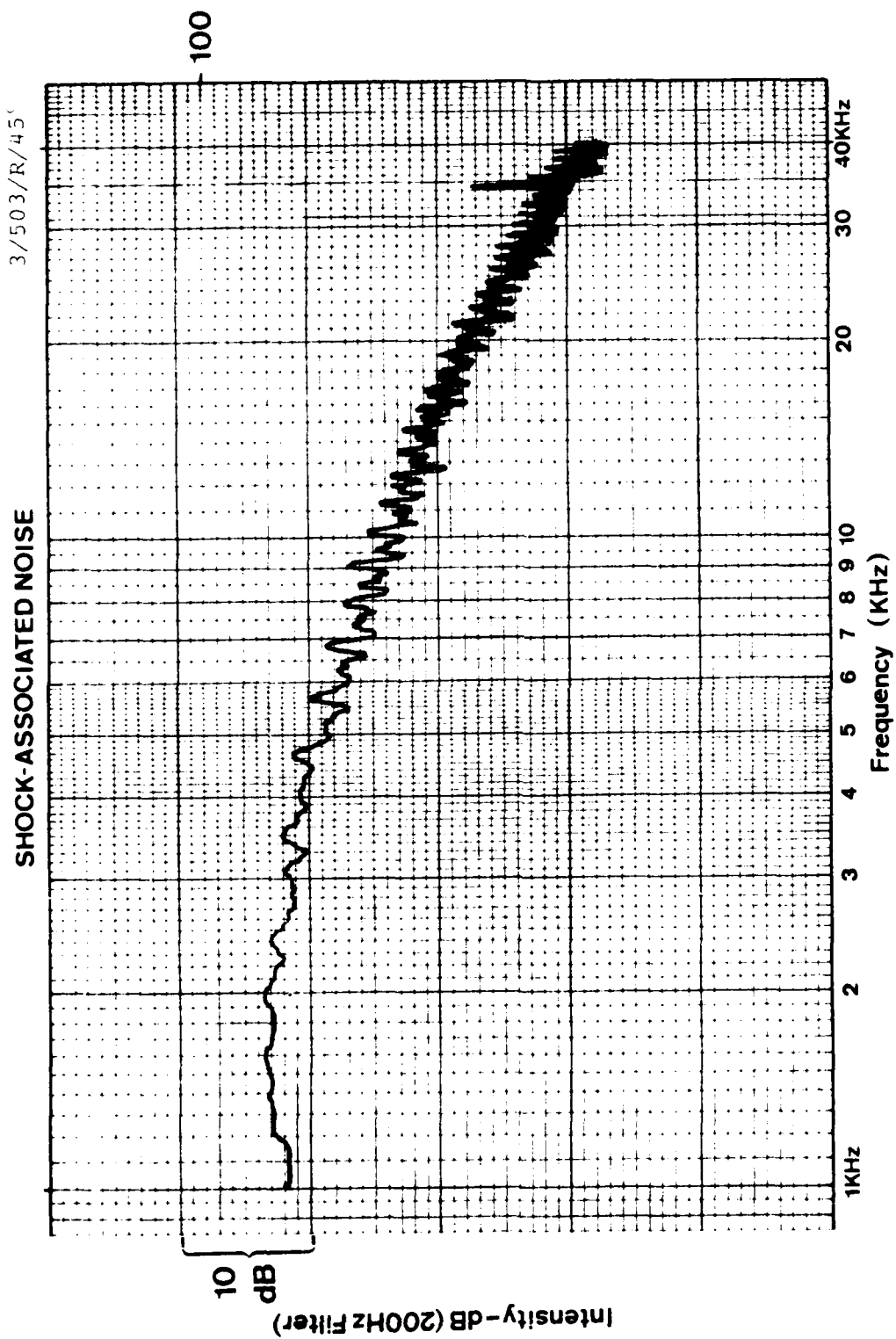


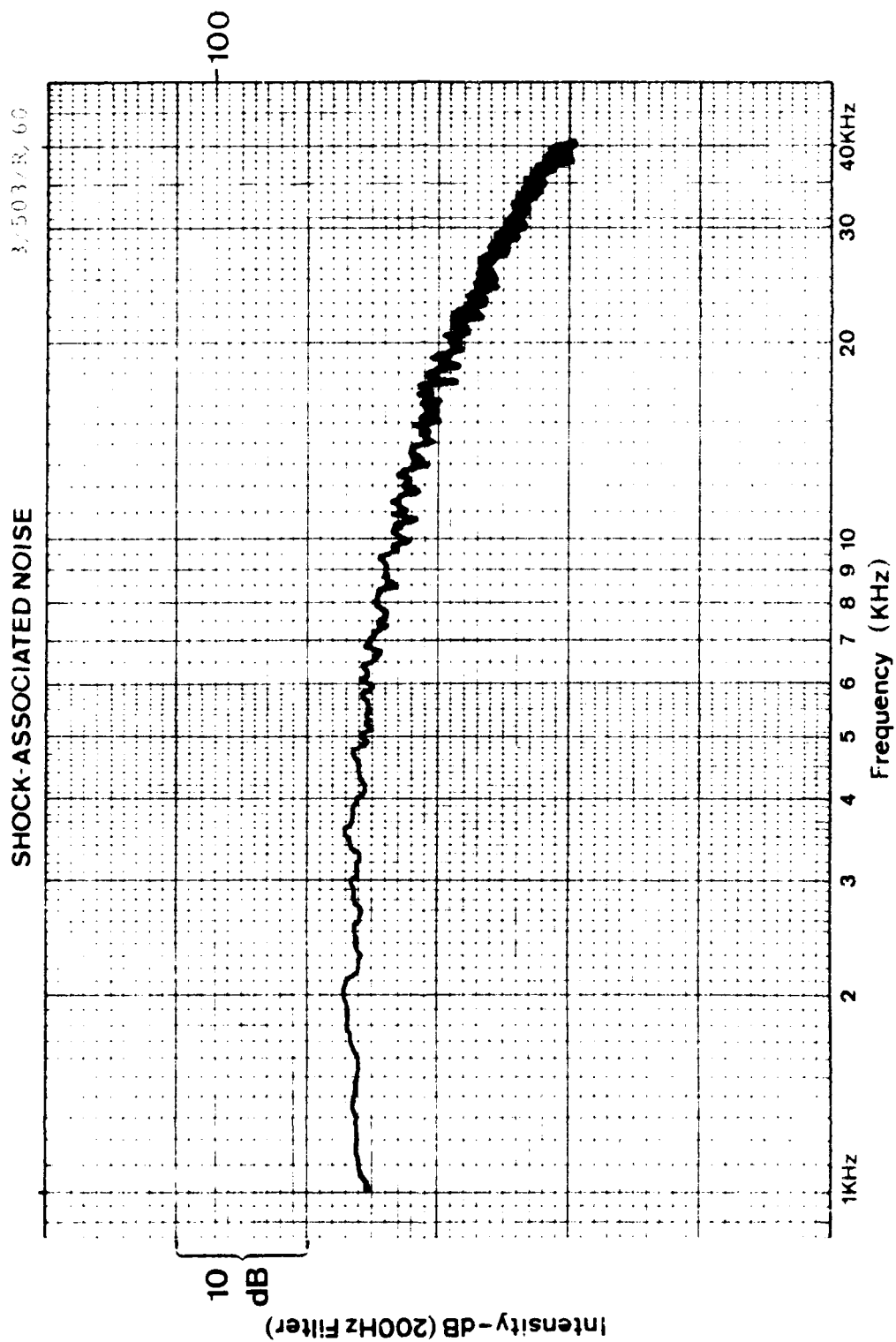


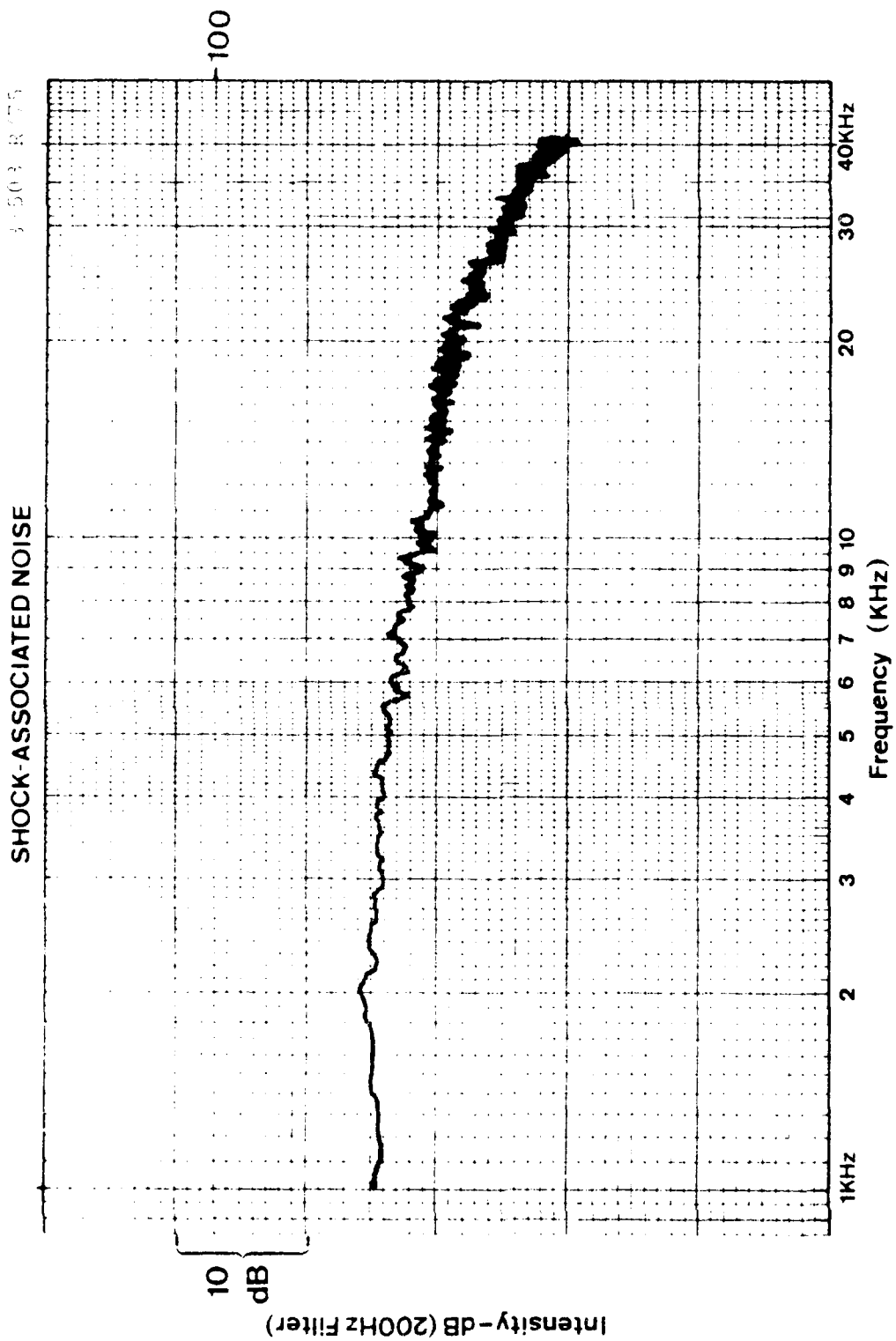












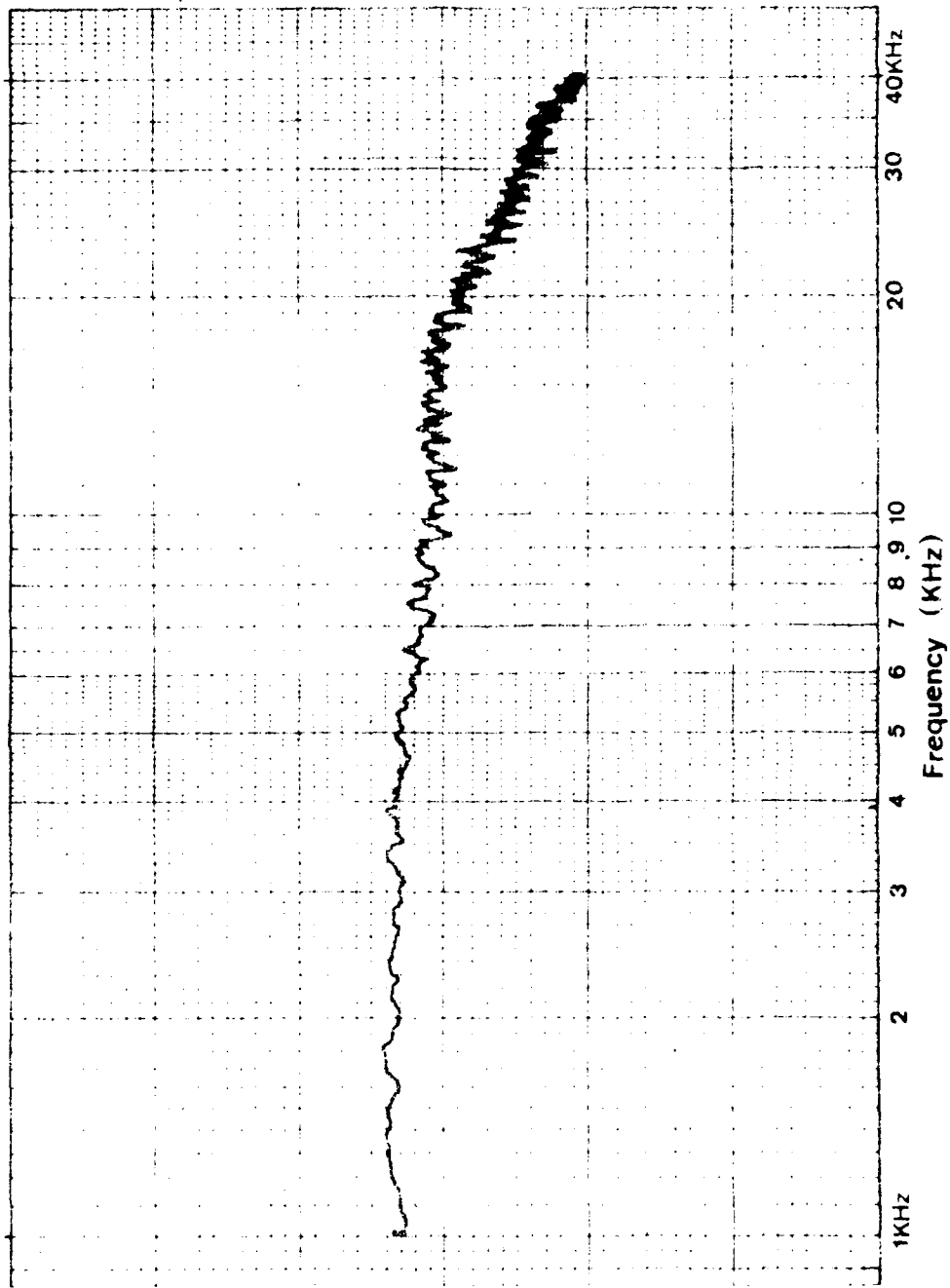
SHOCK-ASSOCIATED NOISE

3-75003-10-10

-100

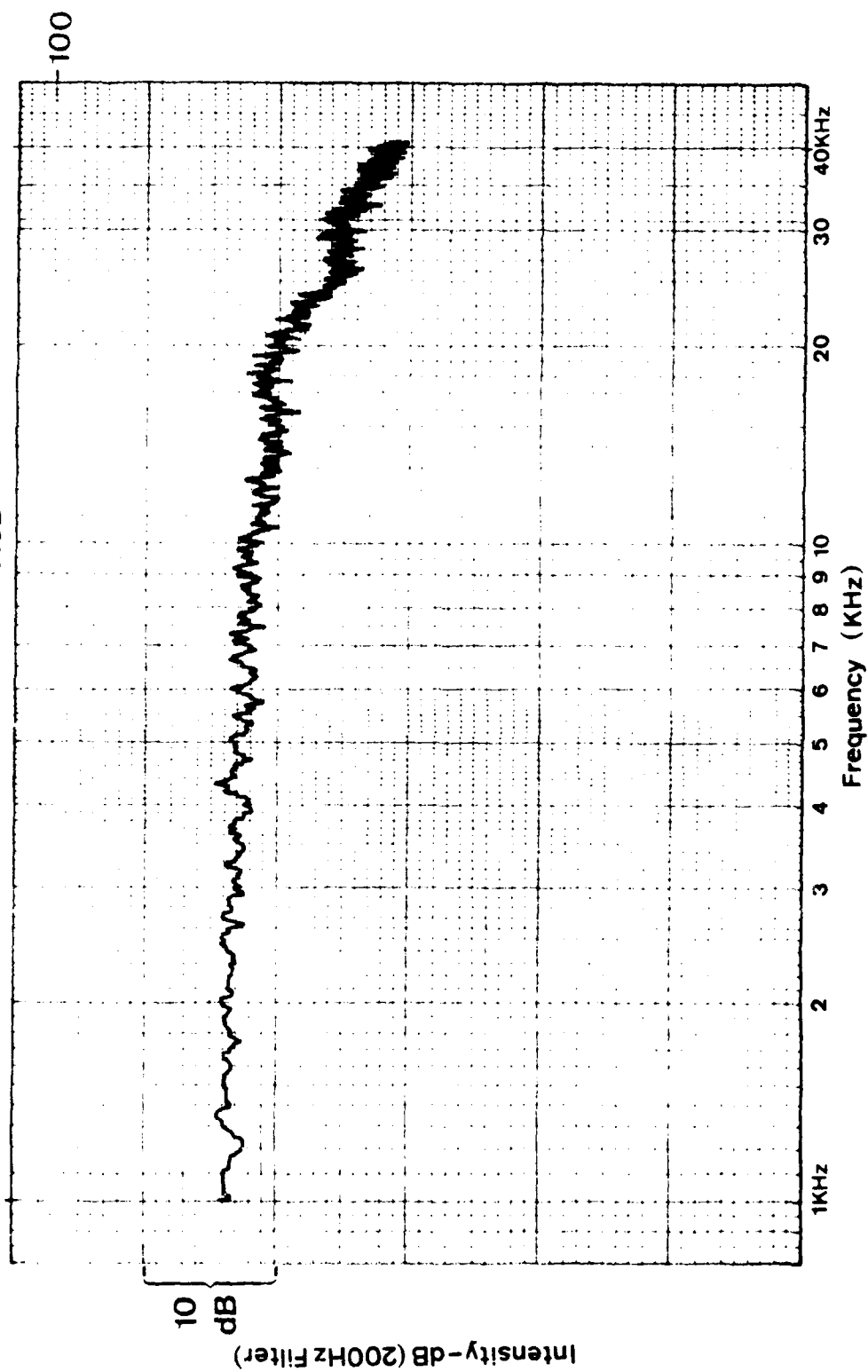
10
dB

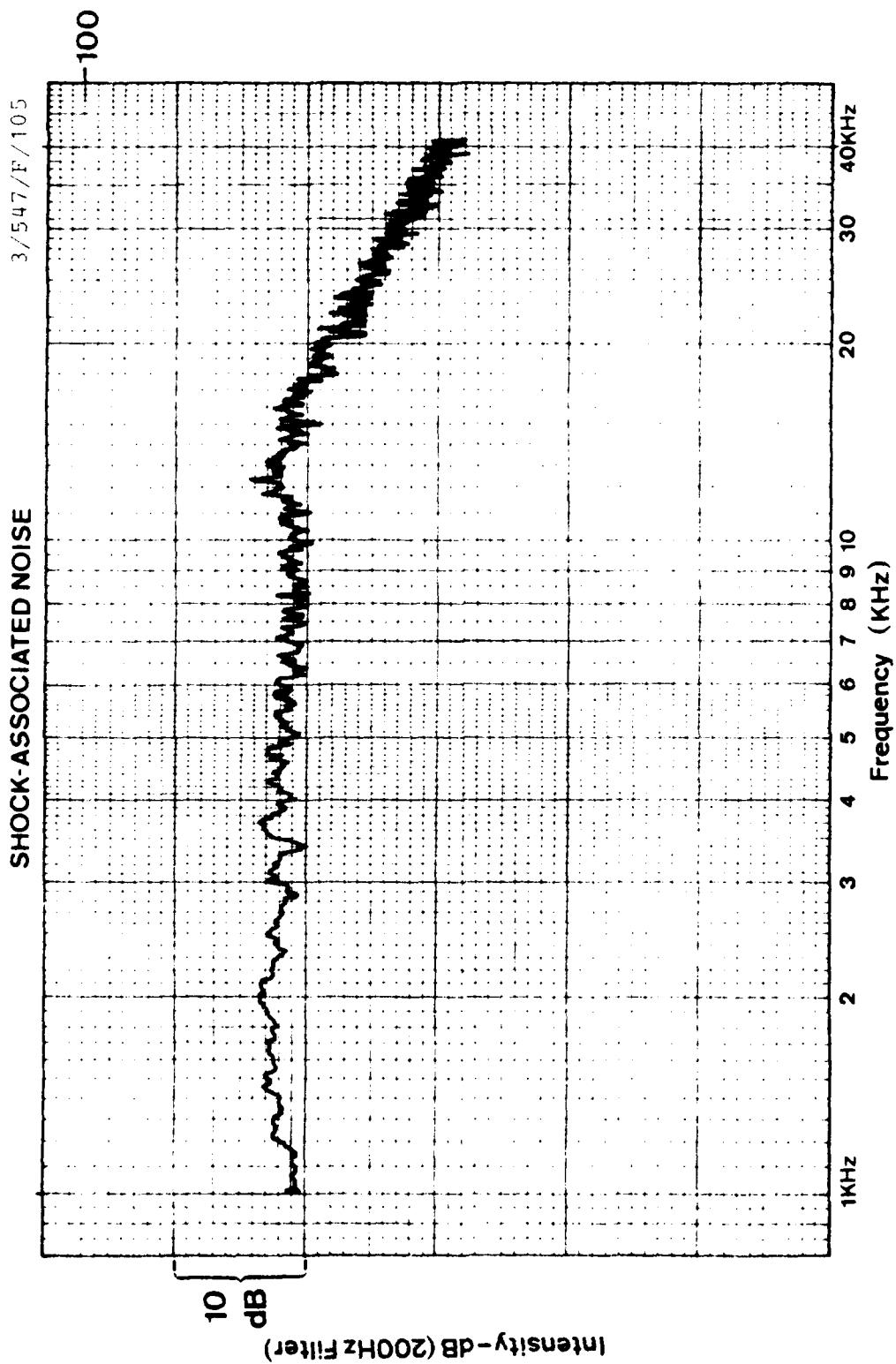
Intensity - dB (200Hz Filter)

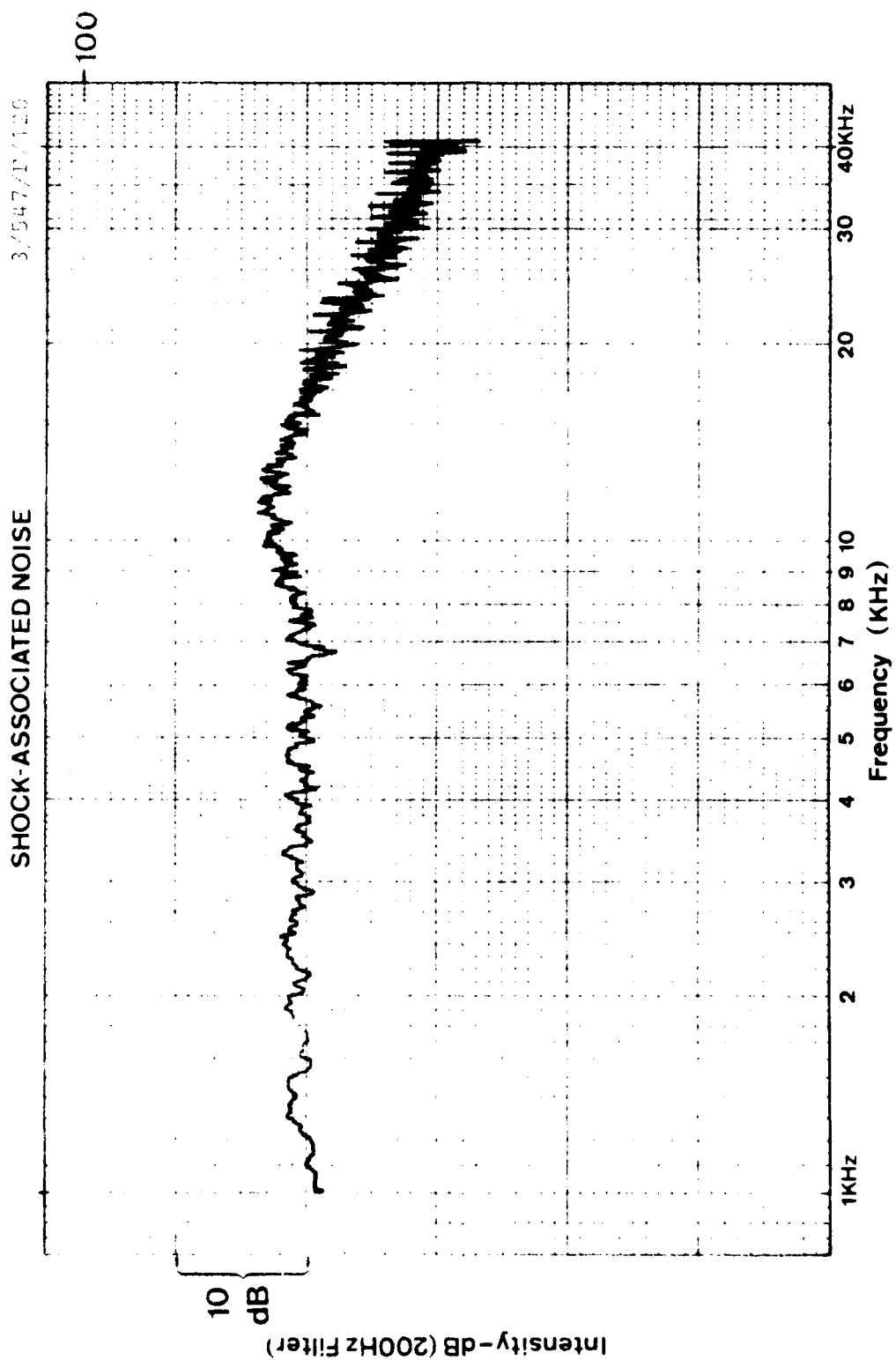


SHOCK-ASSOCIATED NOISE

3/547/P. 93

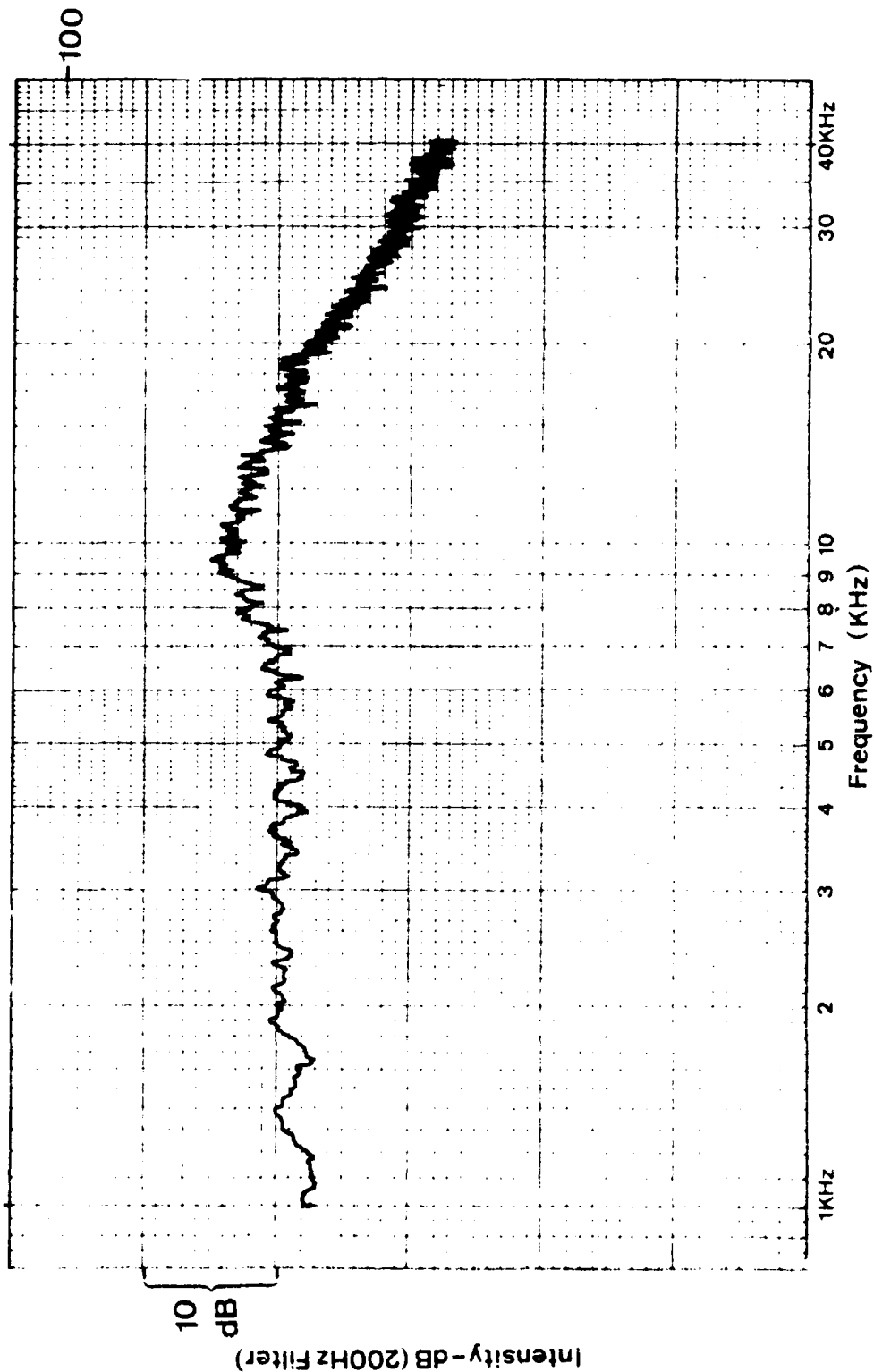


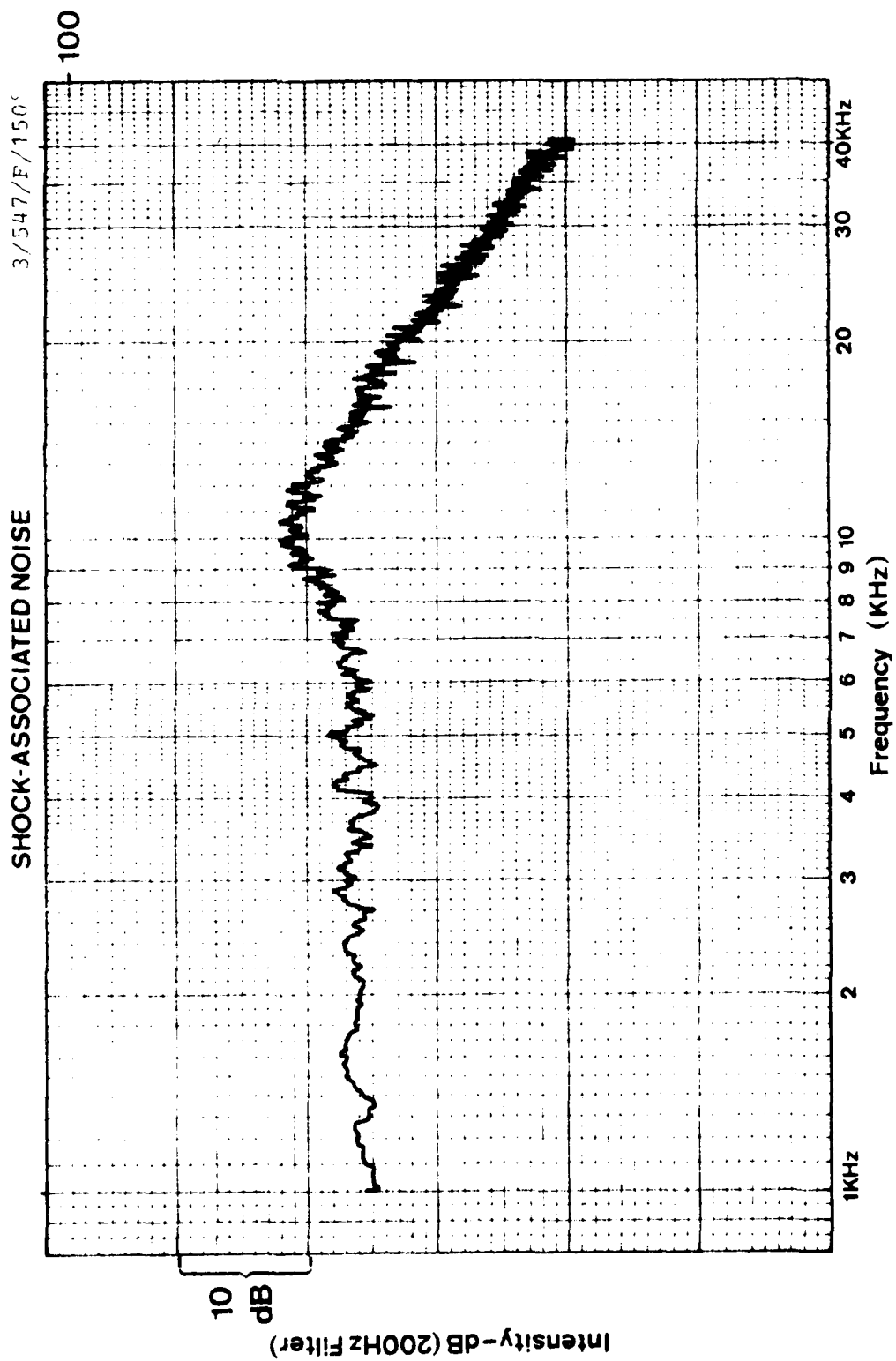




SHOCK-ASSOCIATED NOISE

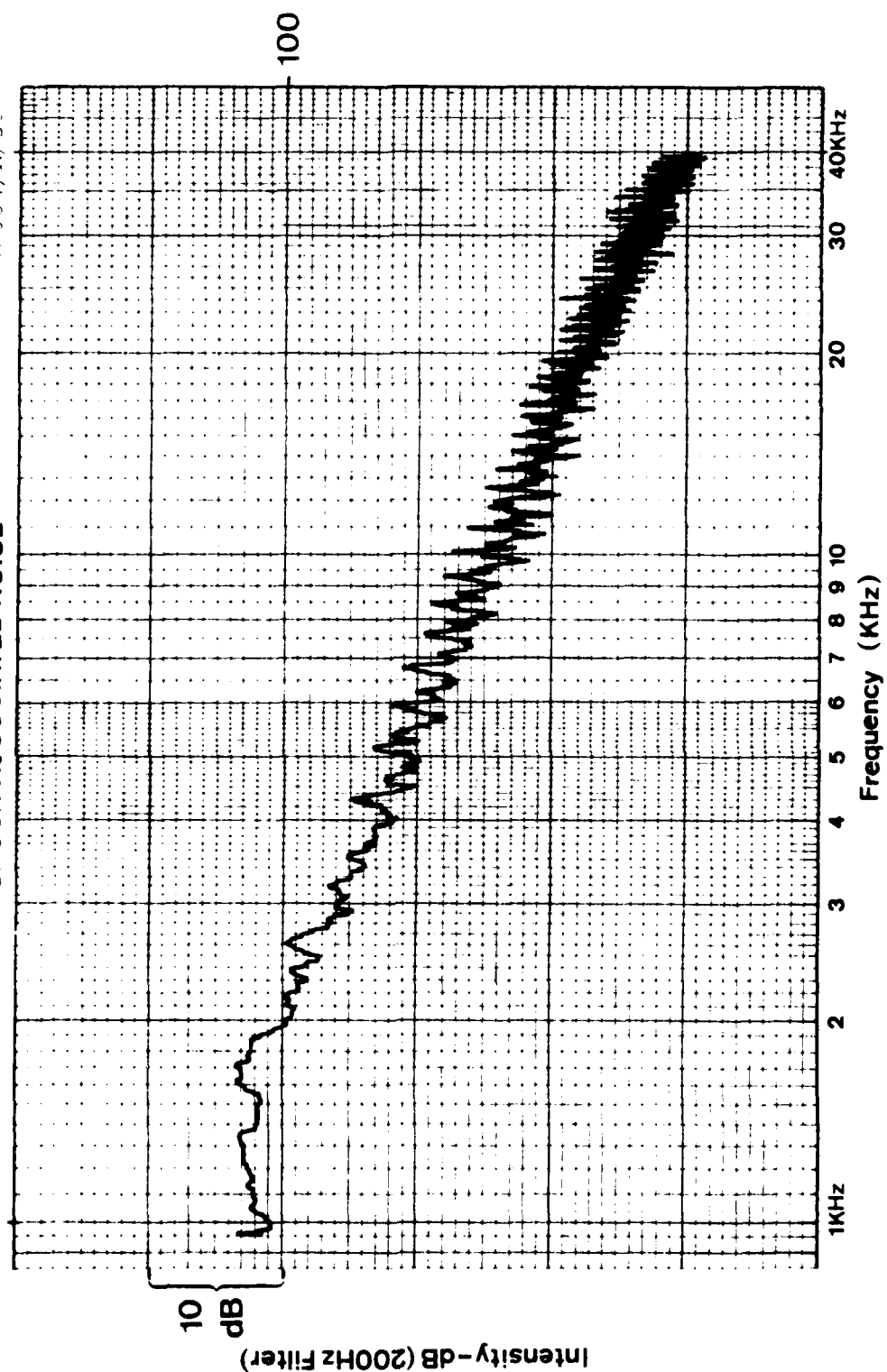
3/547/F/135'





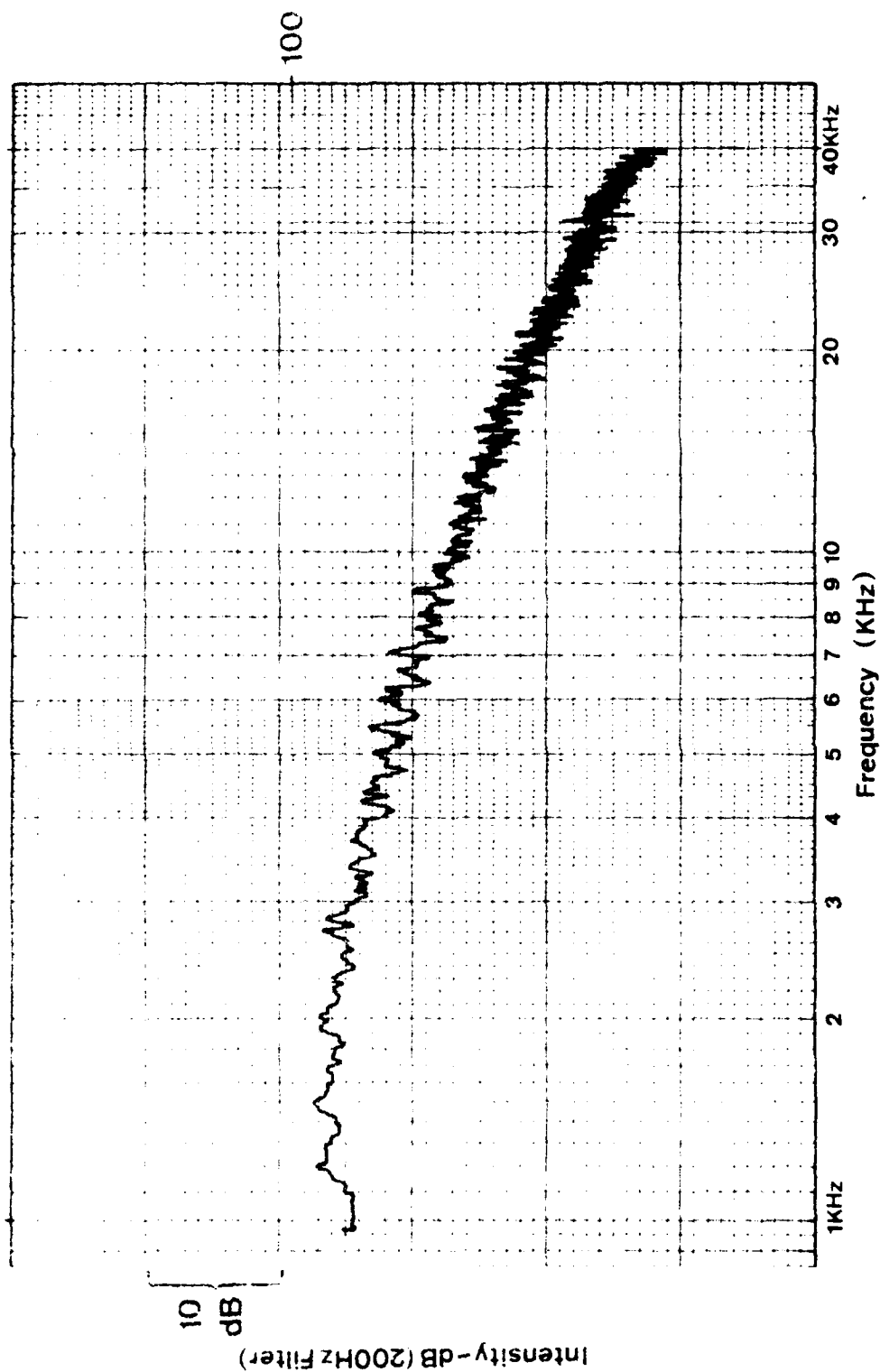
SHOCK-ASSOCIATED NOISE

47504/R/39



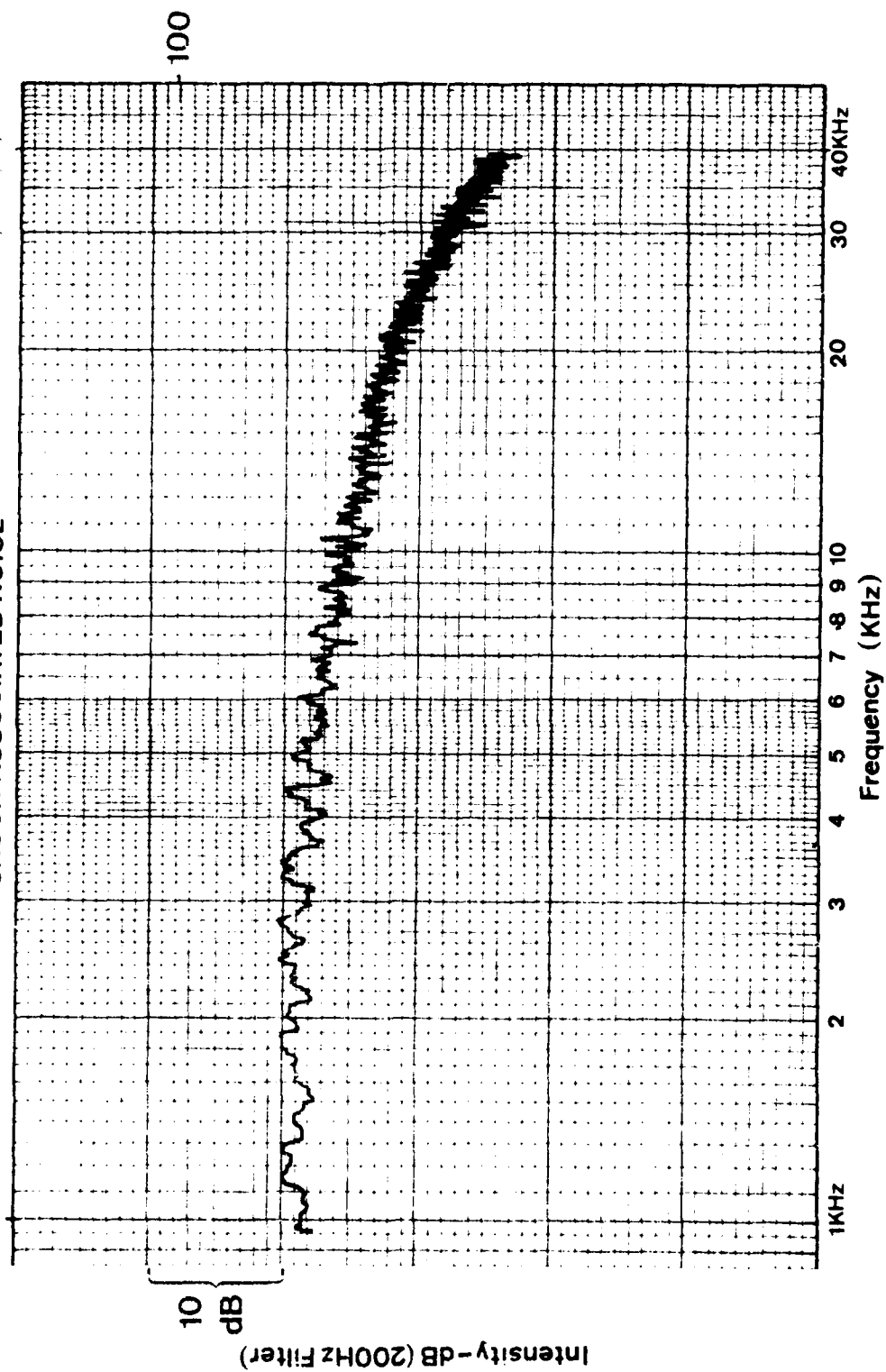
SHOCK-ASSOCIATED NOISE

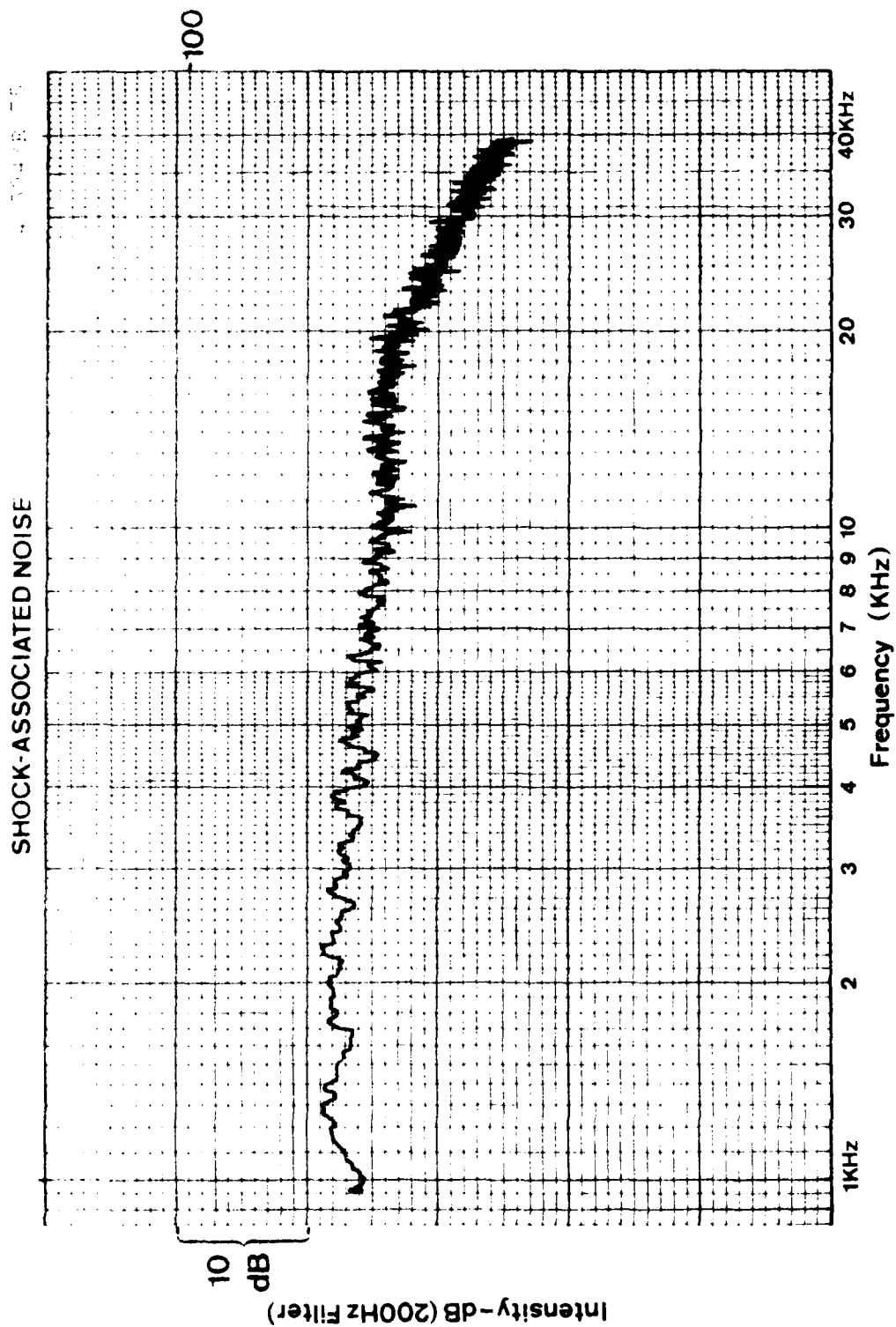
4.50-8.00

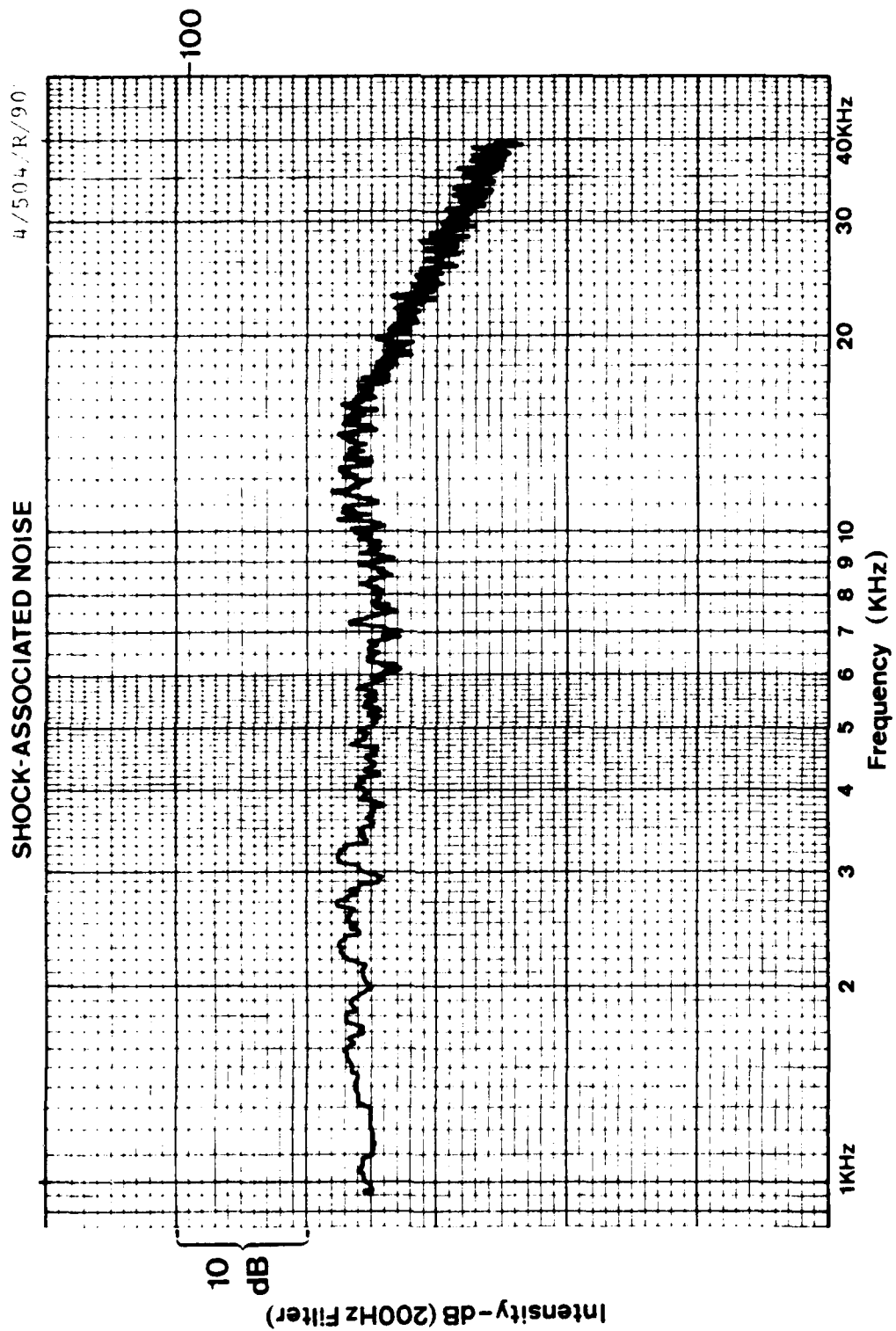


SHOCK-ASSOCIATED NOISE

4/504/R/60

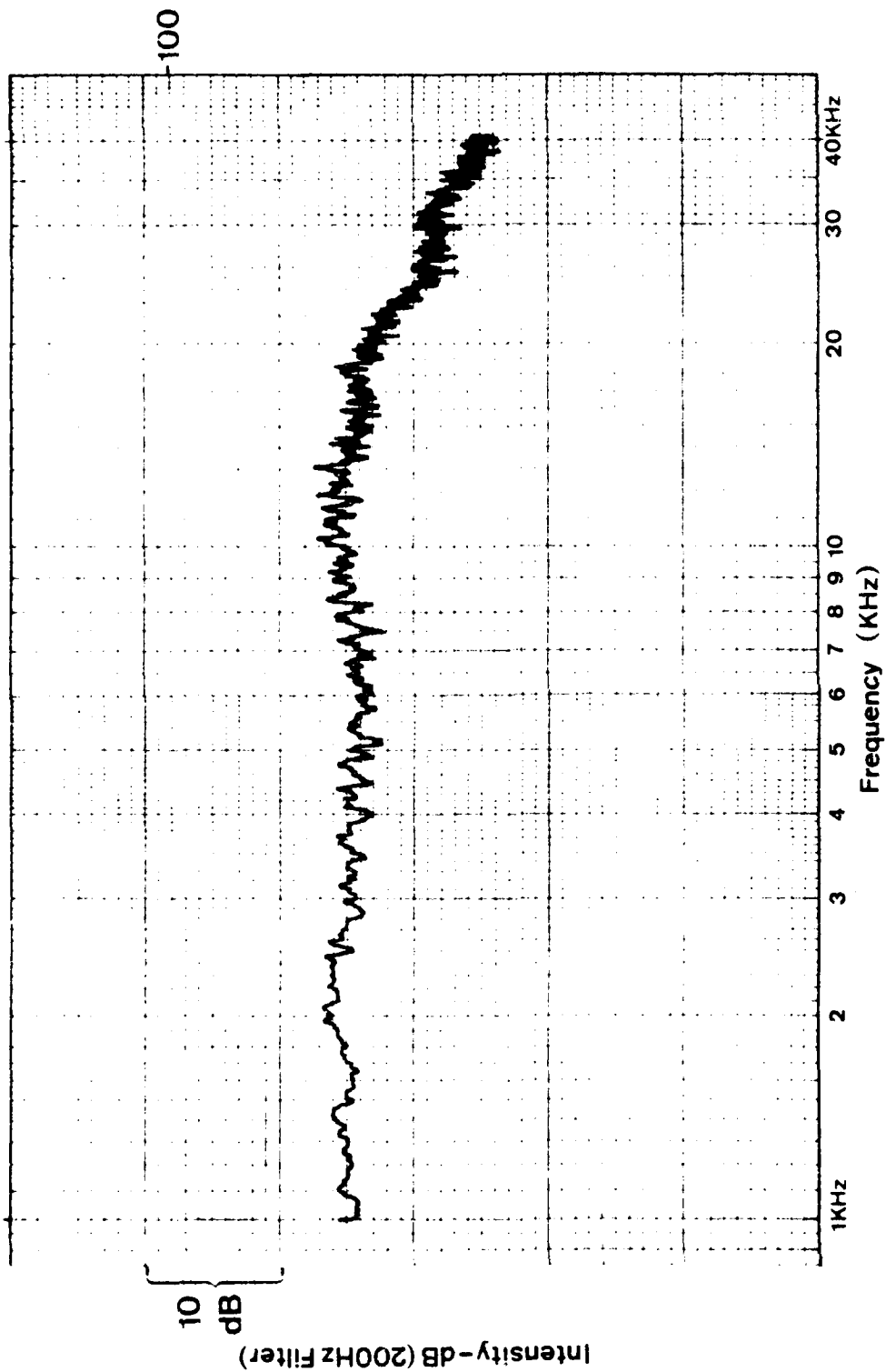


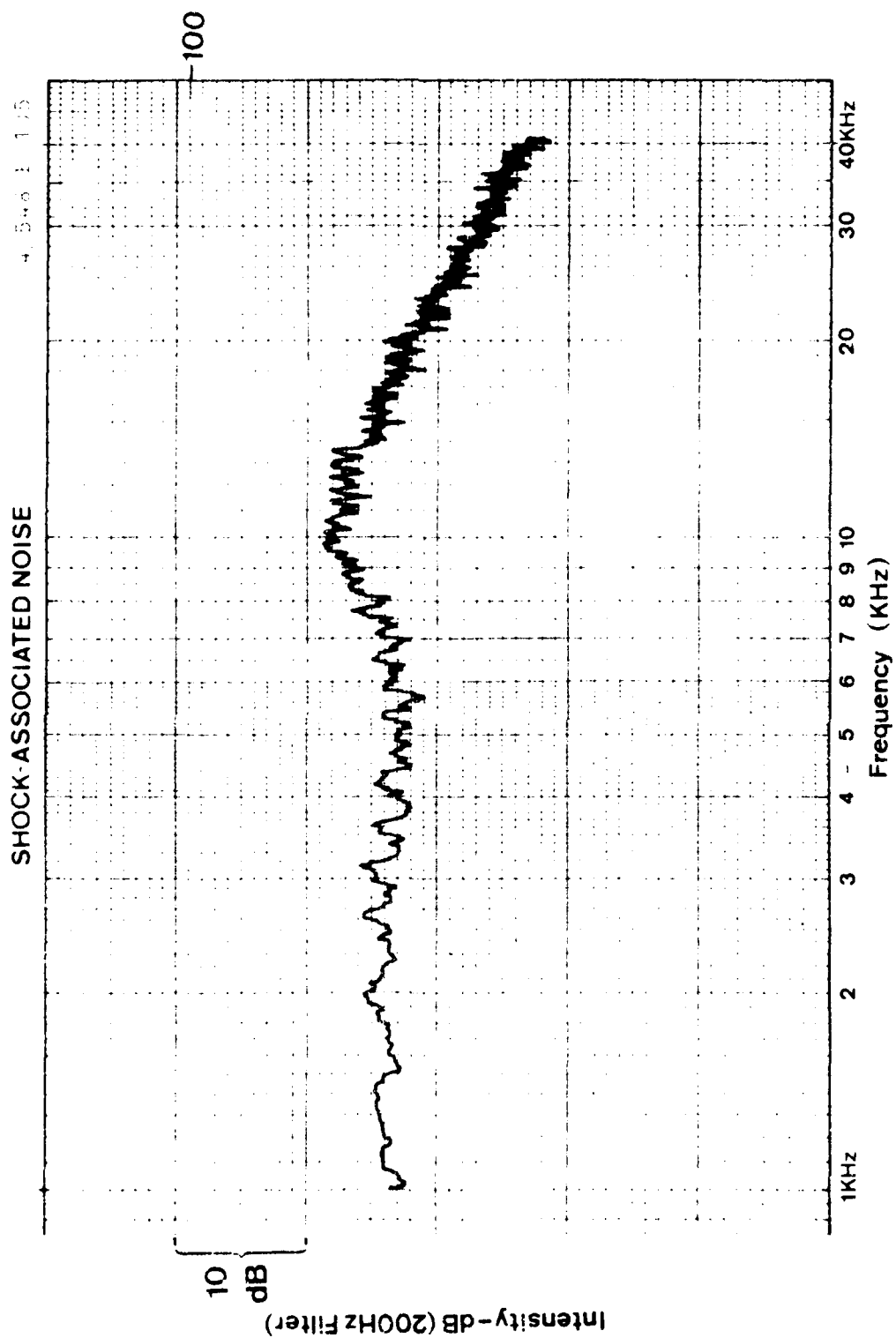


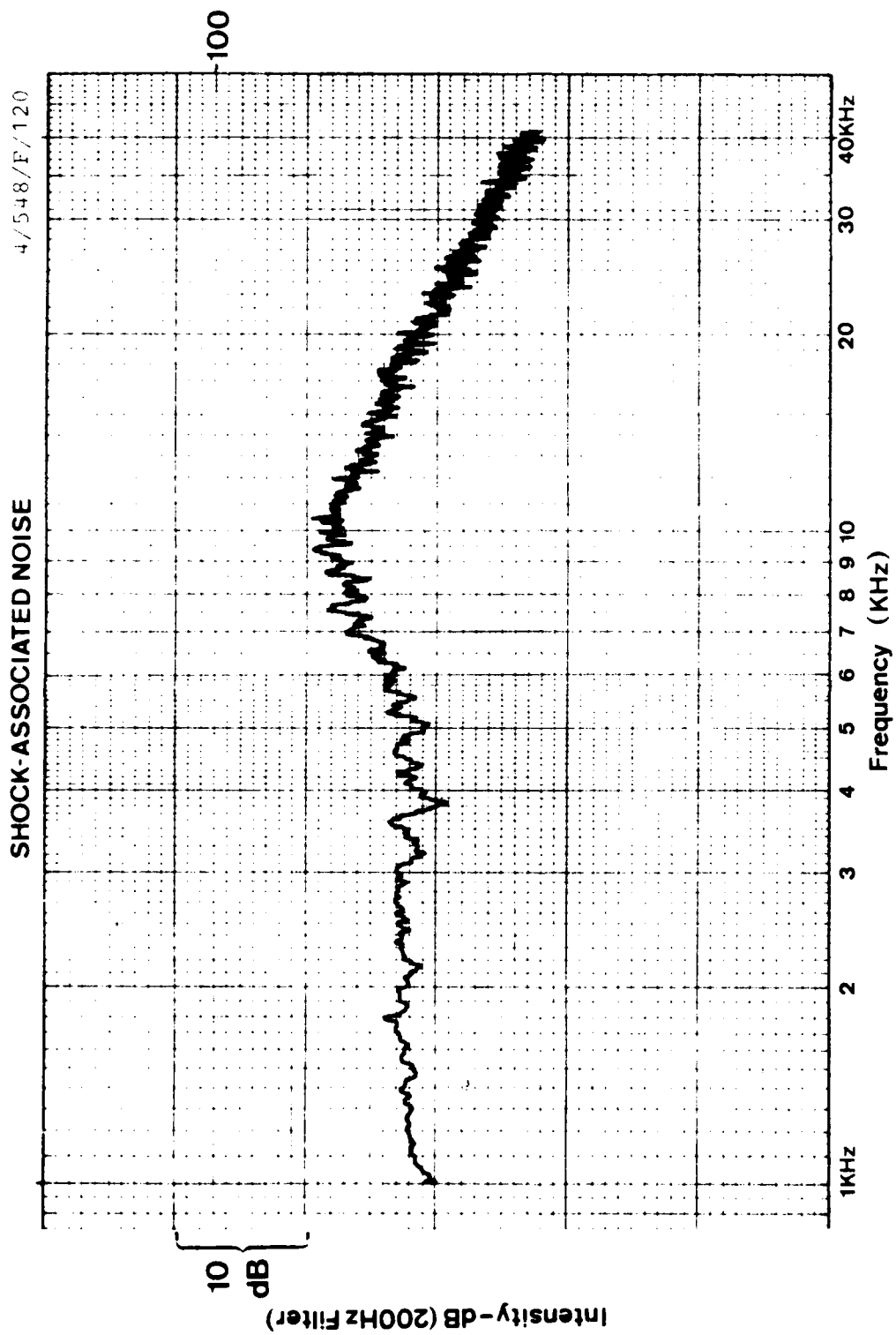


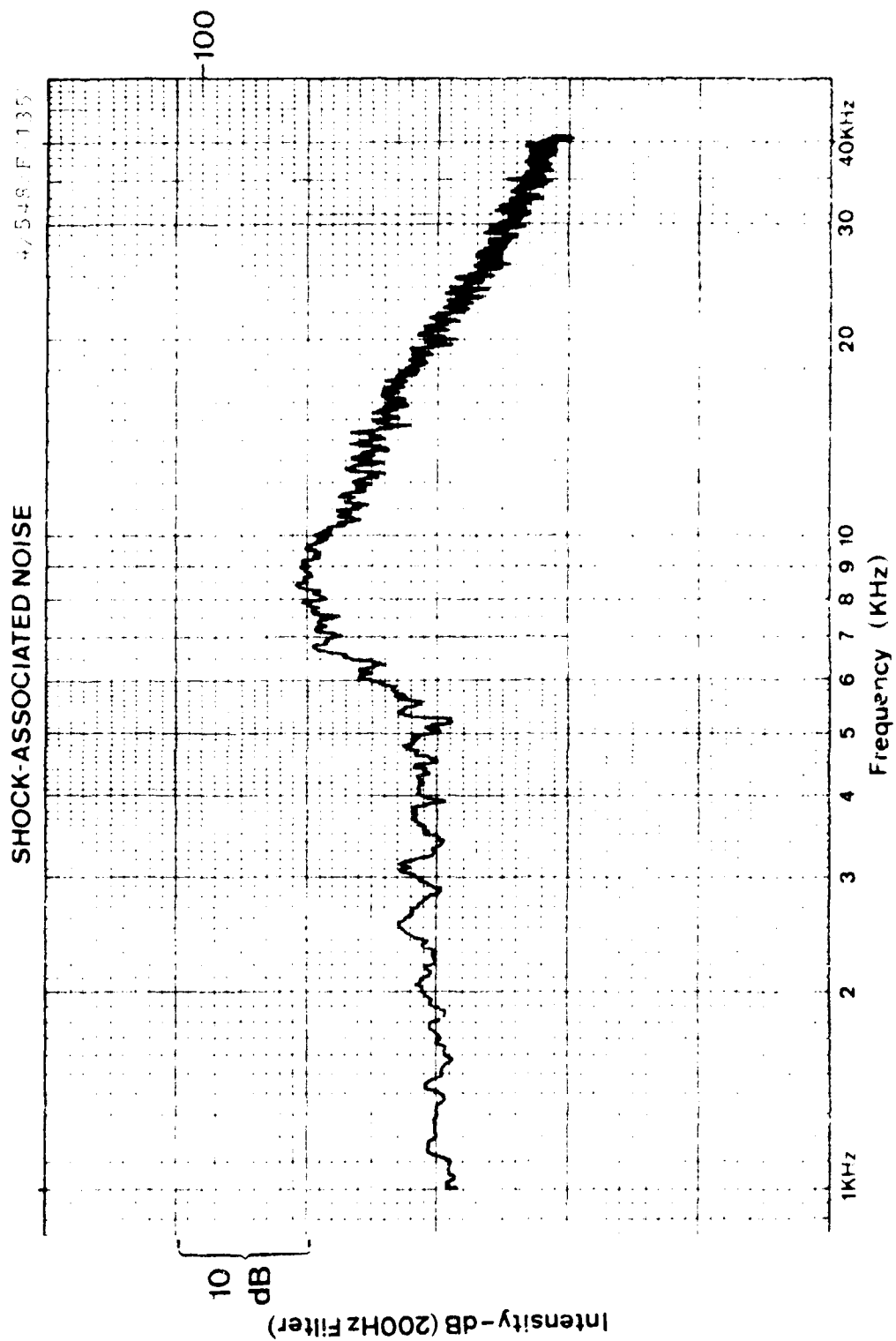
SHOCK-ASSOCIATED NOISE

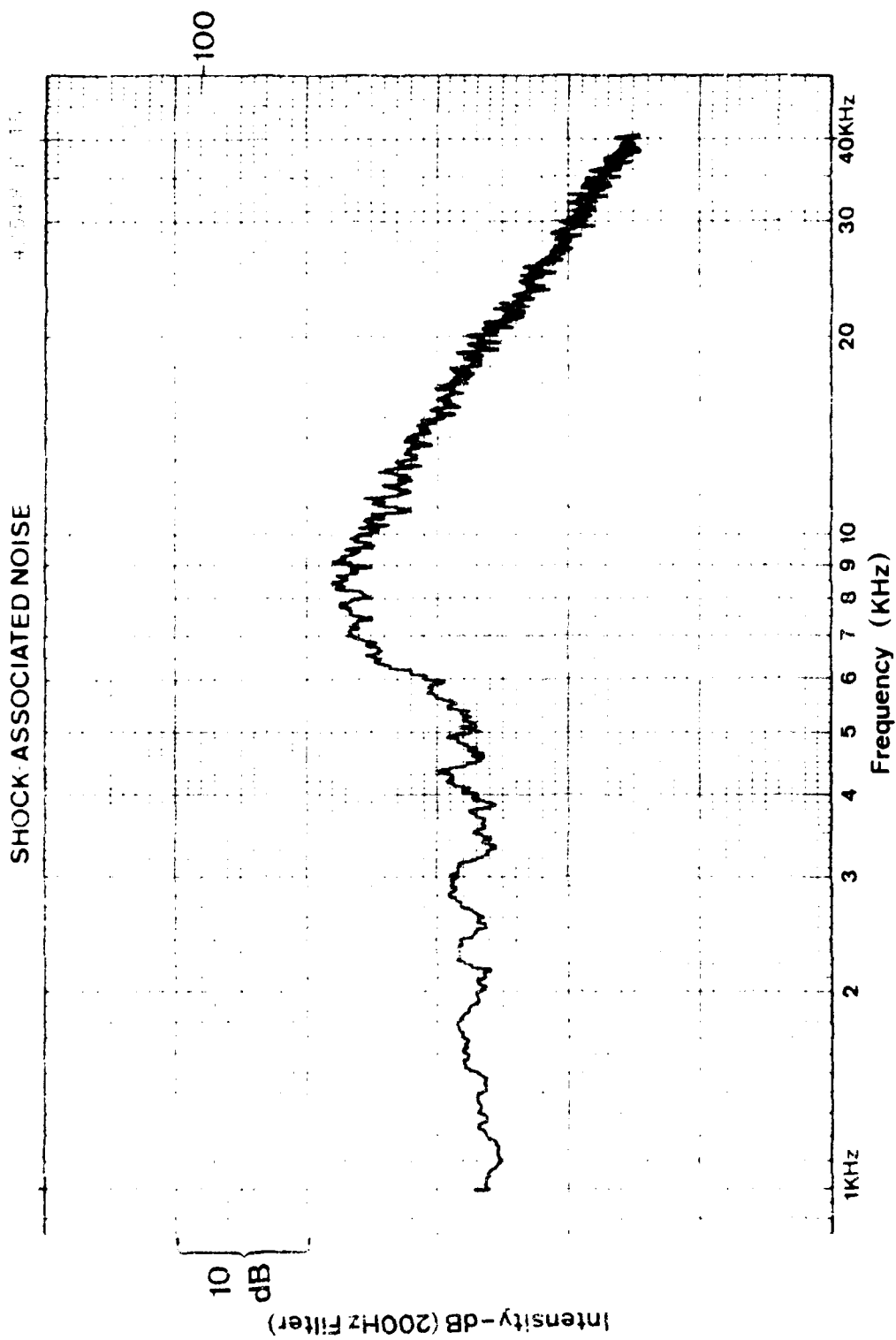
548 P 90





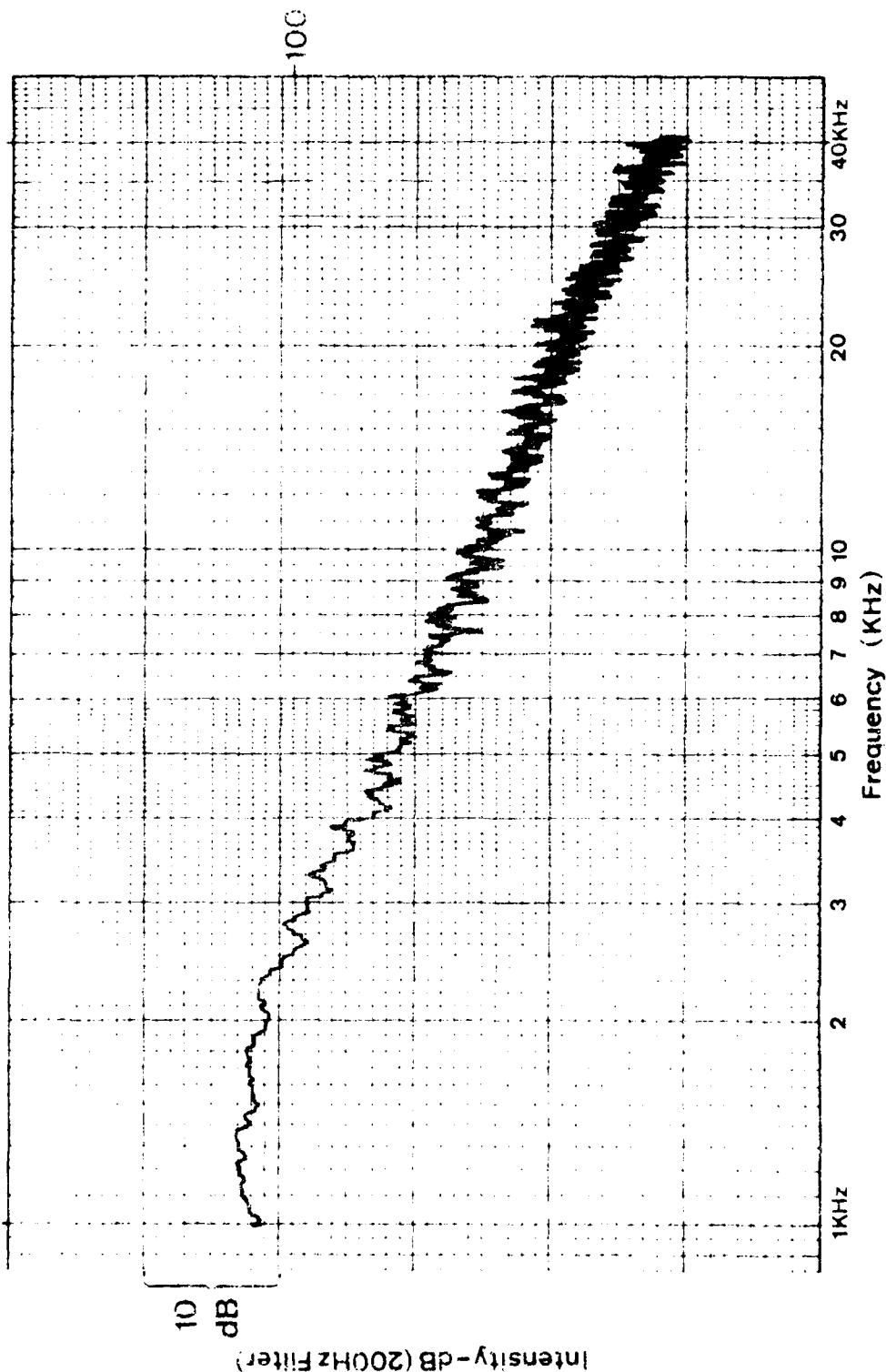






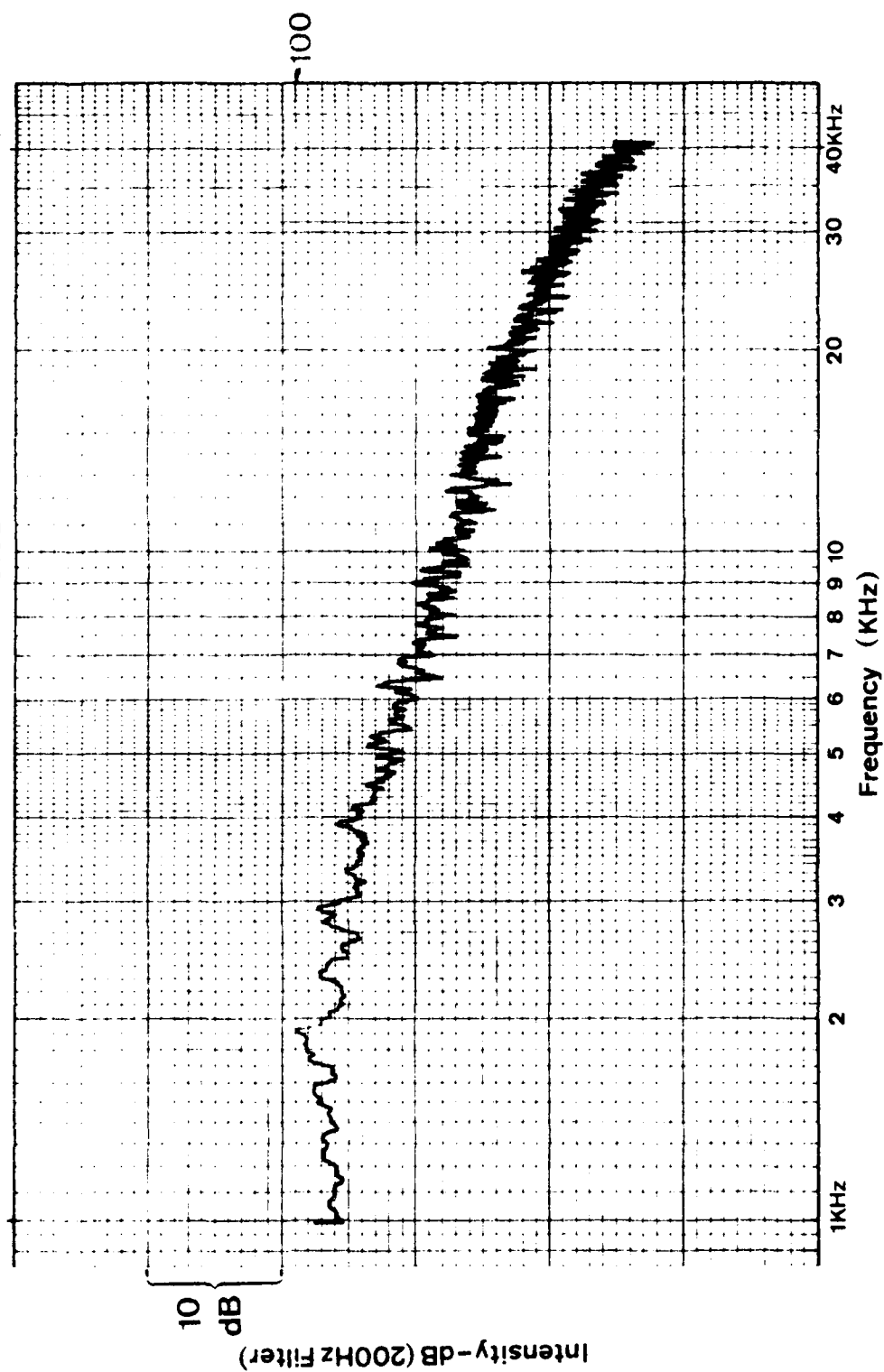
SHOCK-ASSOCIATED NOISE

5,000 R 50



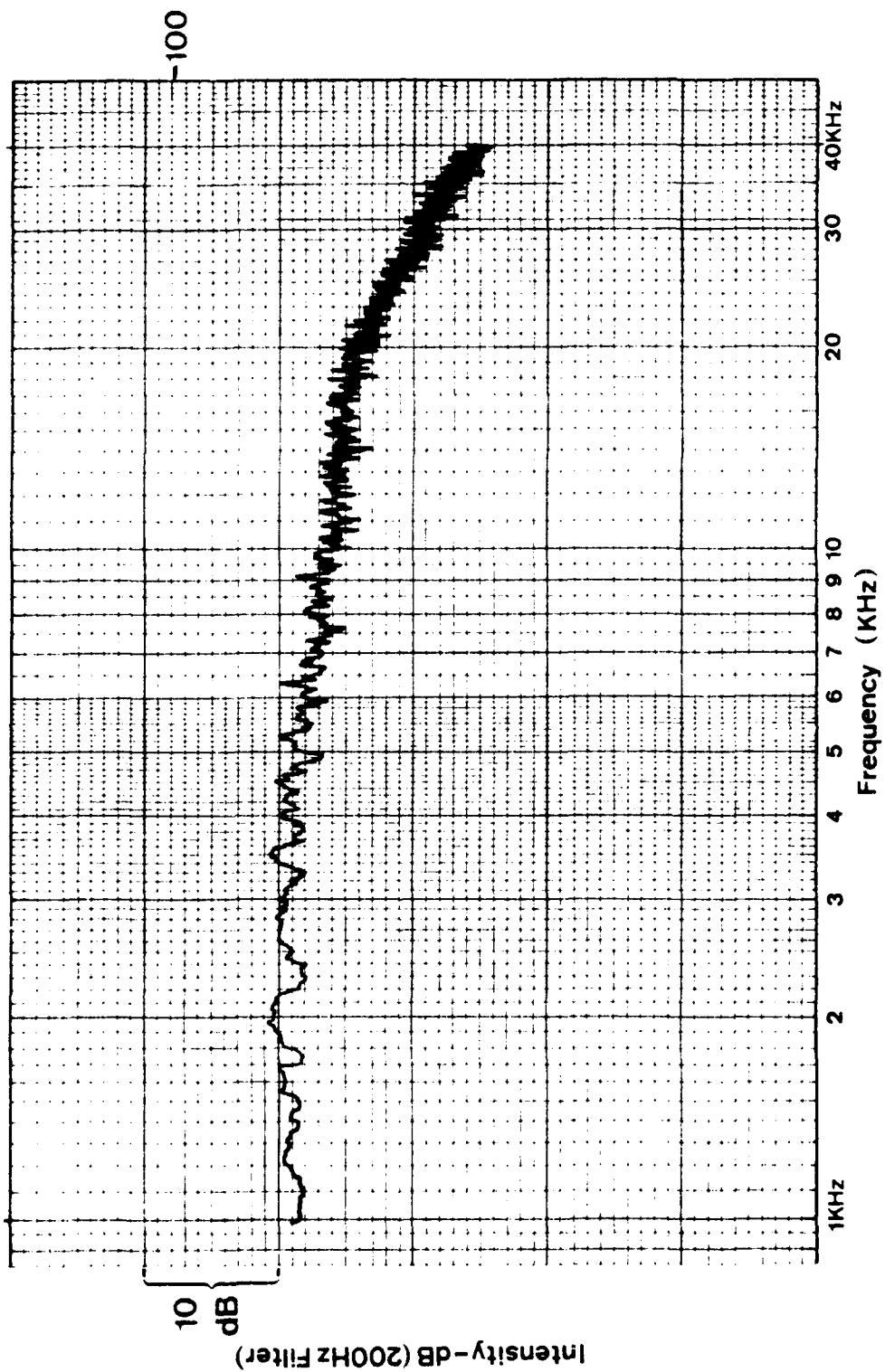
SHOCK-ASSOCIATED NOISE

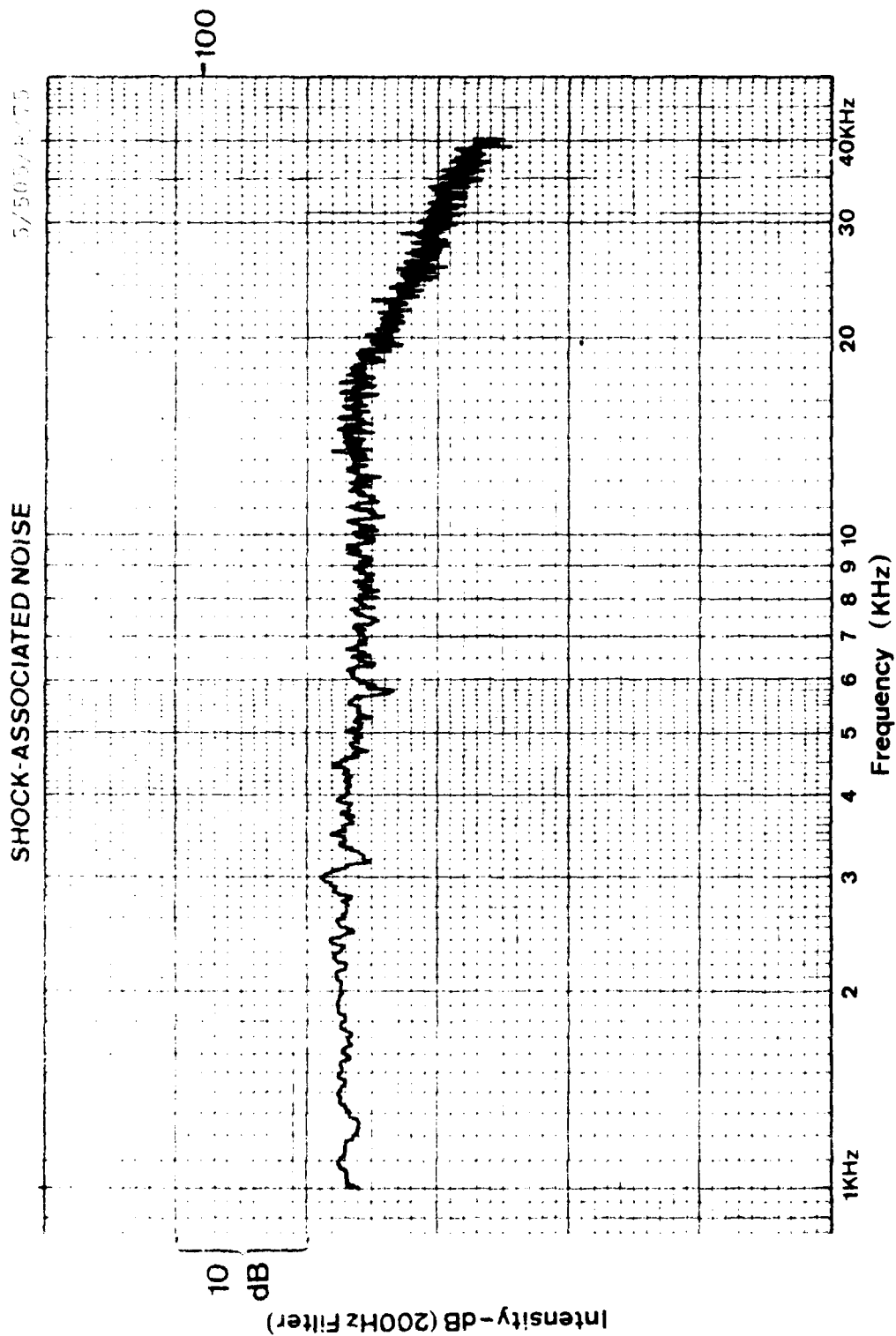
5/505/R/45



SHOCK-ASSOCIATED NOISE

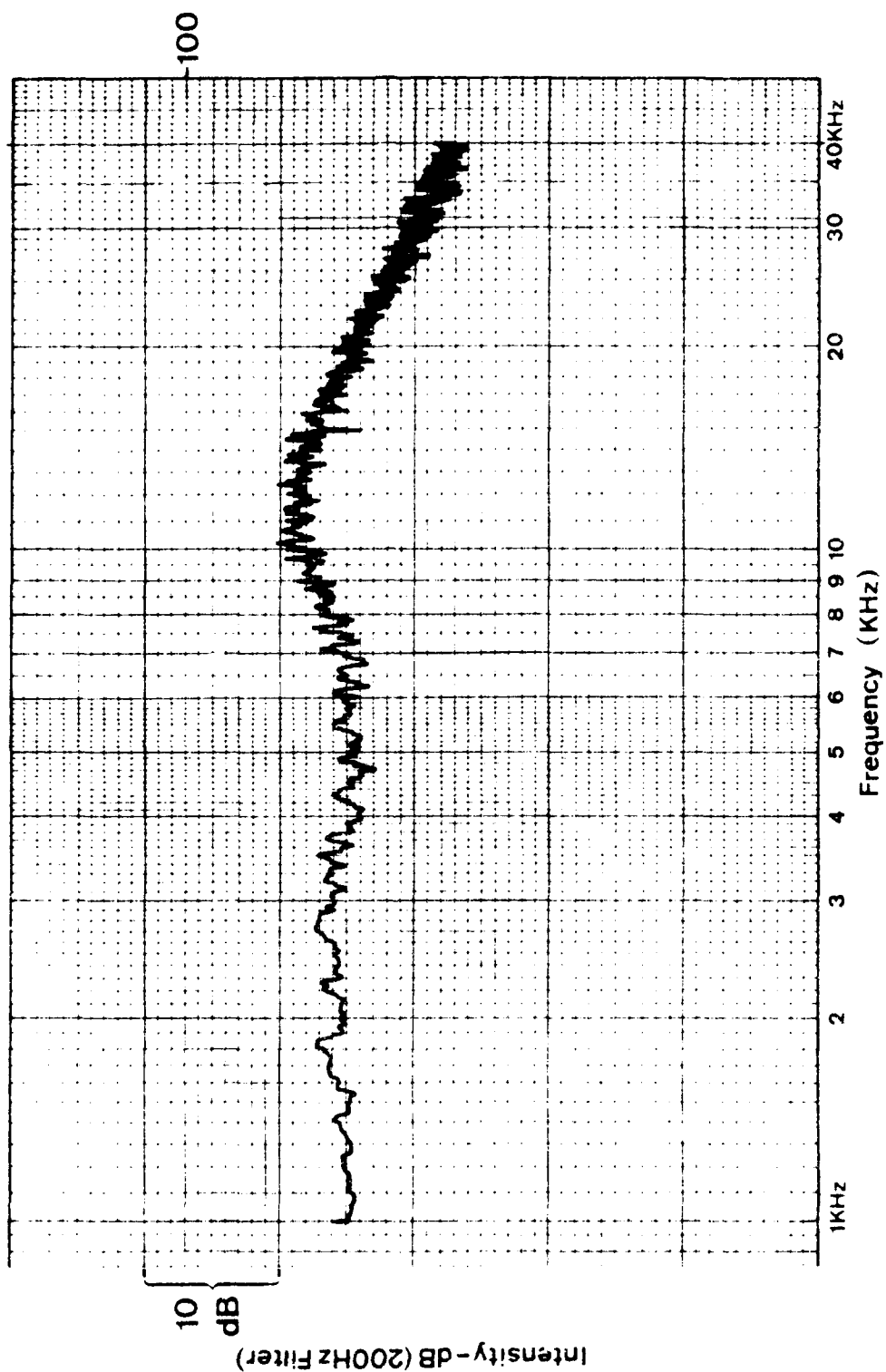
5/505/R/60





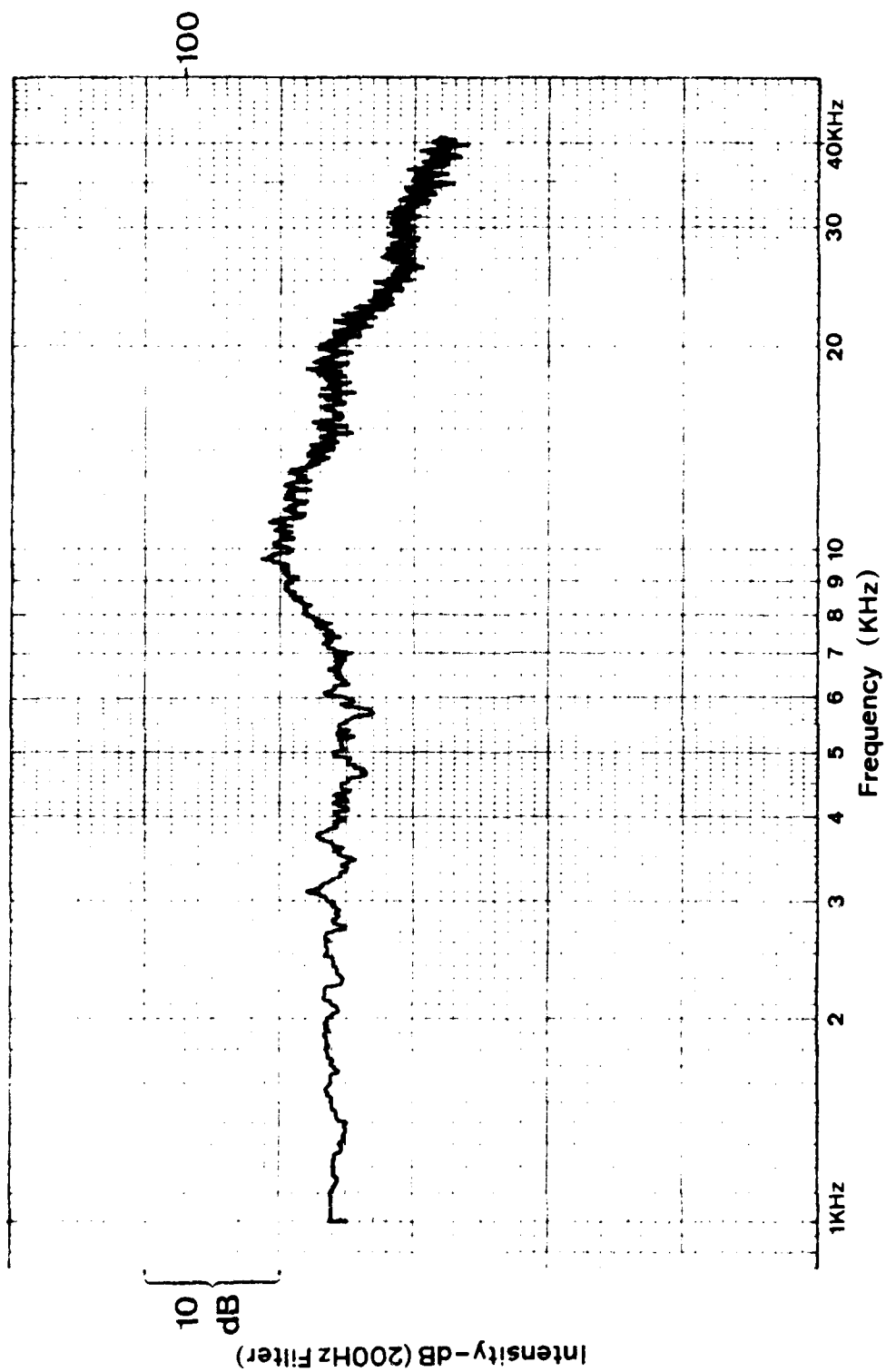
SHOCK-ASSOCIATED NOISE

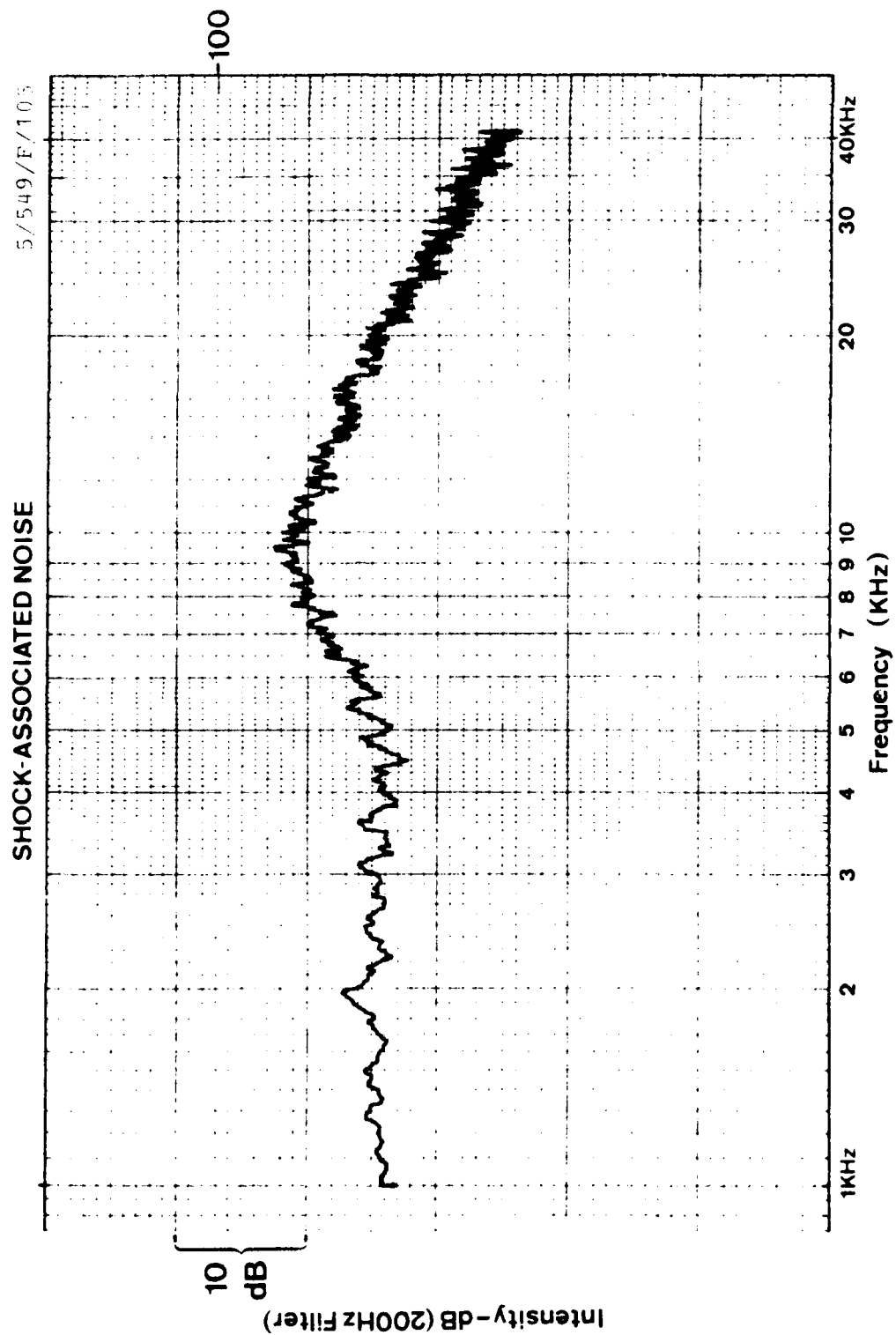
5/505/R/90



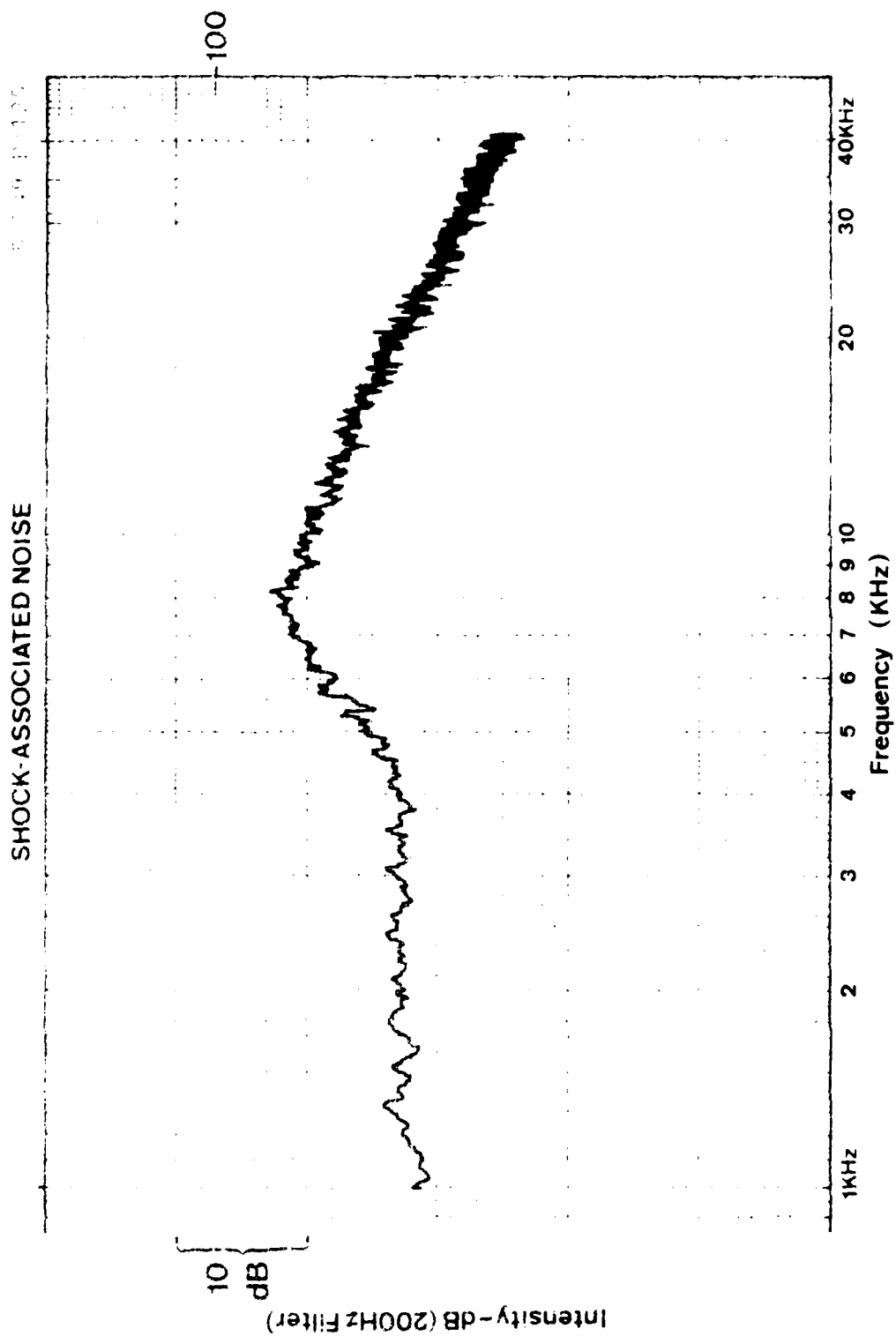
SHOCK-ASSOCIATED NOISE

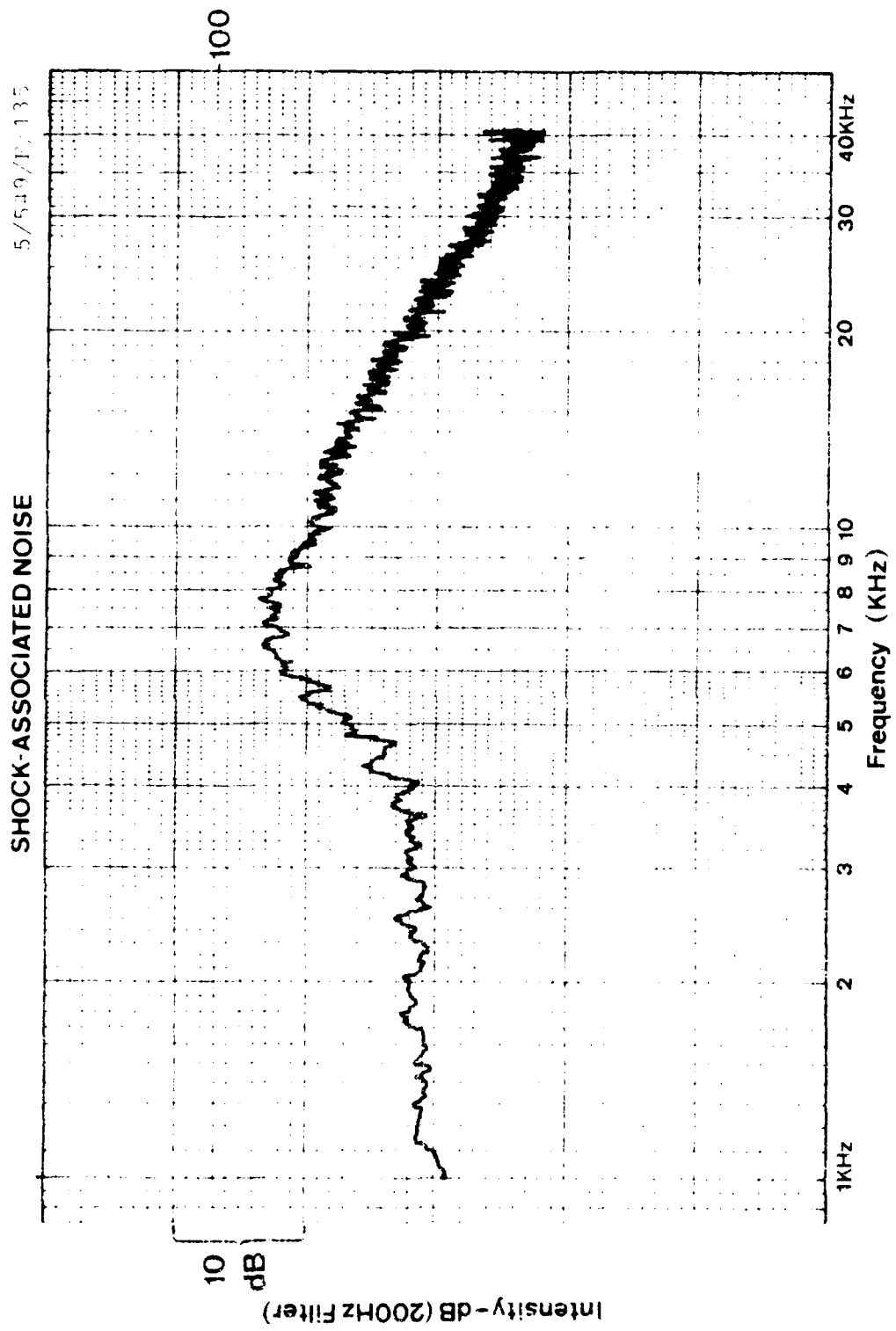
5/5+9/F/90



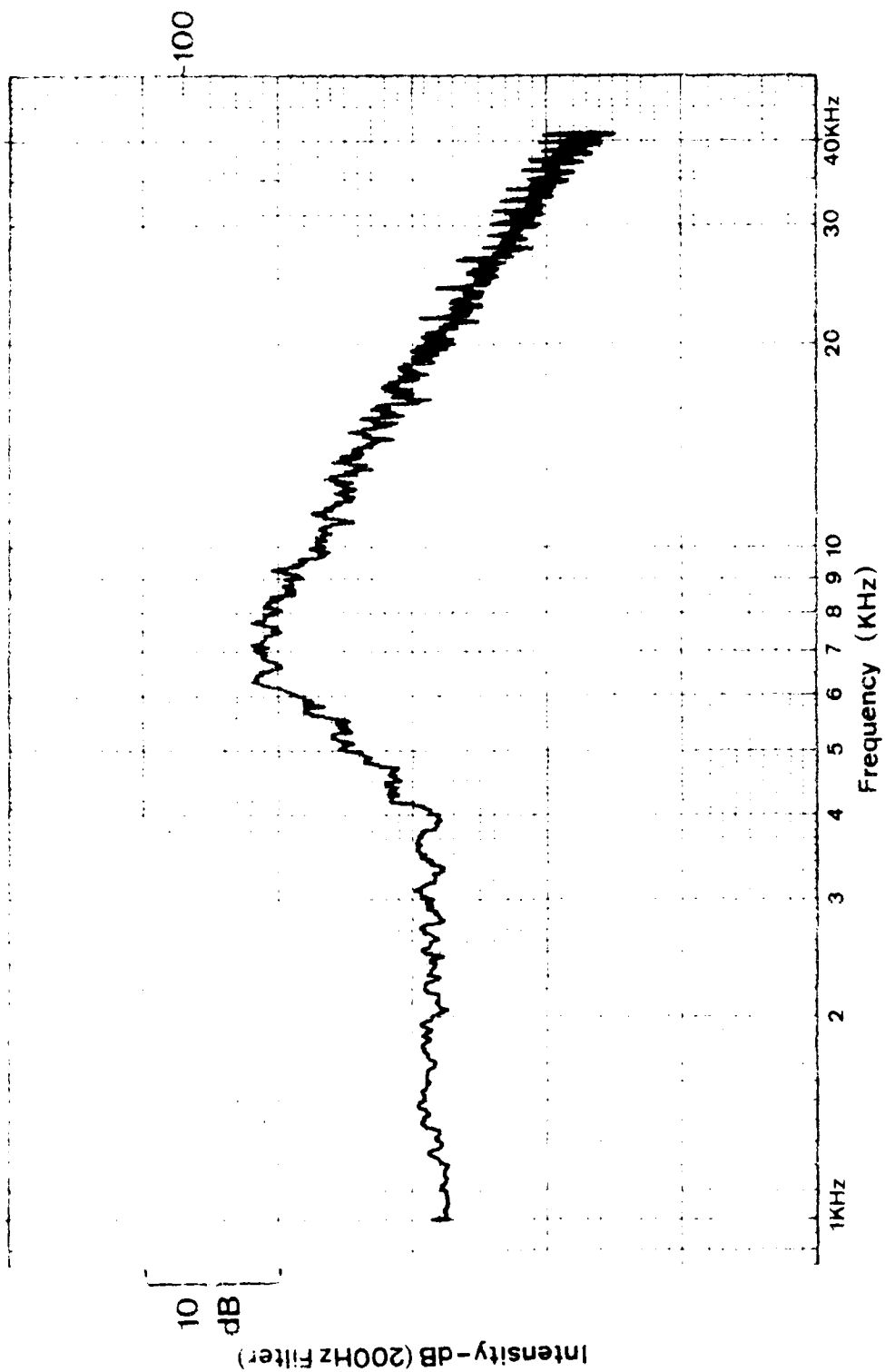


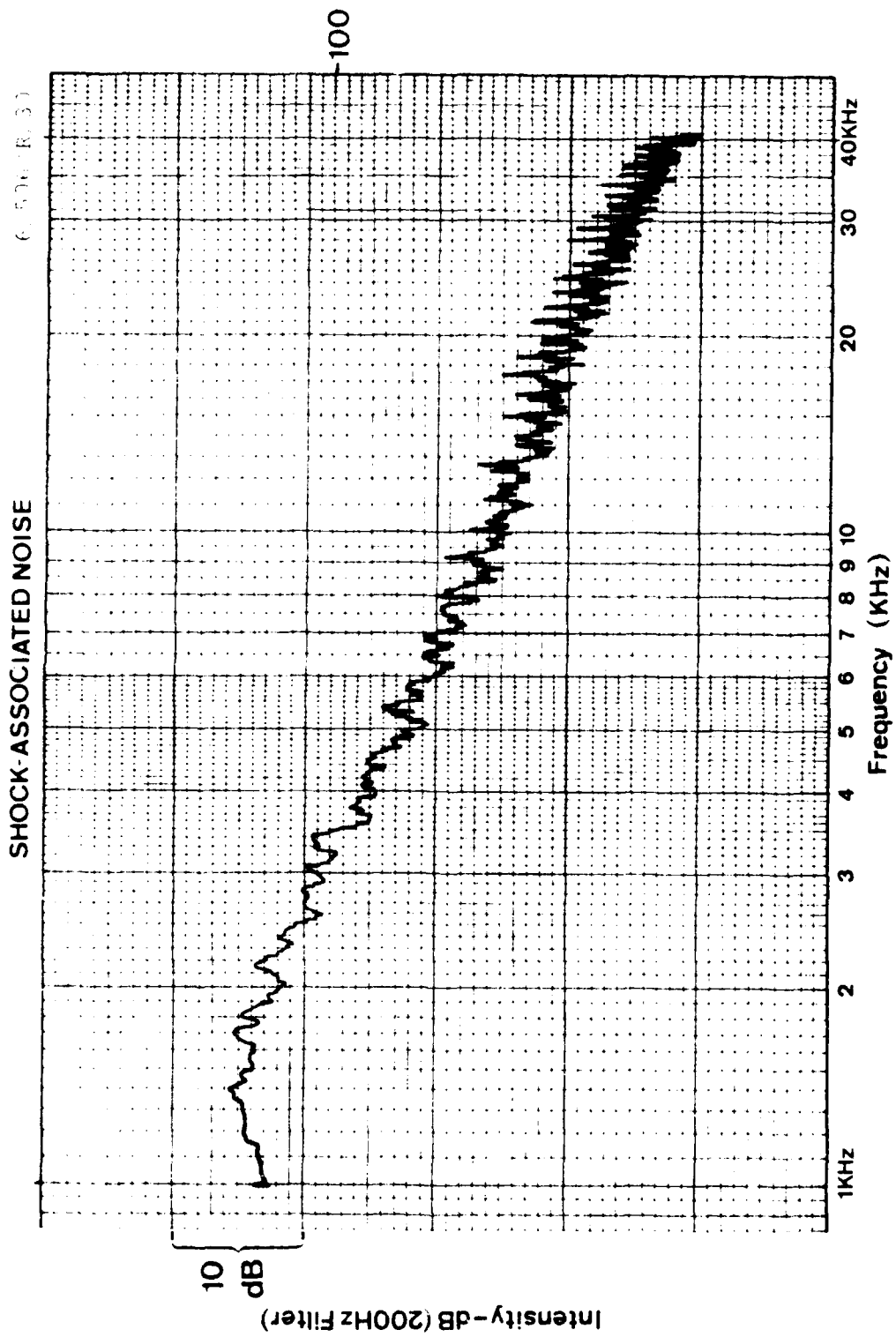
SHOCK-ASSOCIATED NOISE



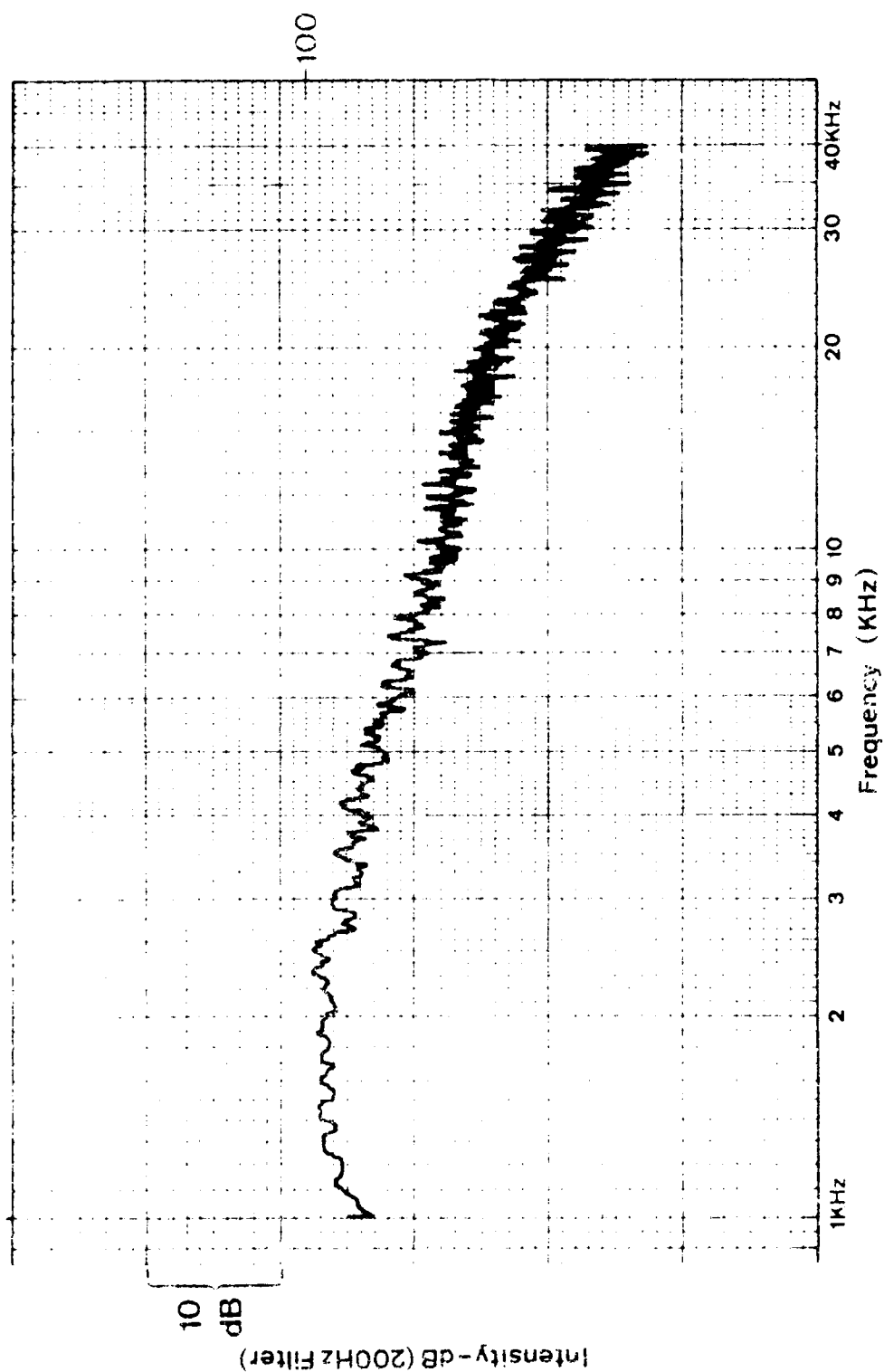


SHOCK ASSOCIATED NOISE

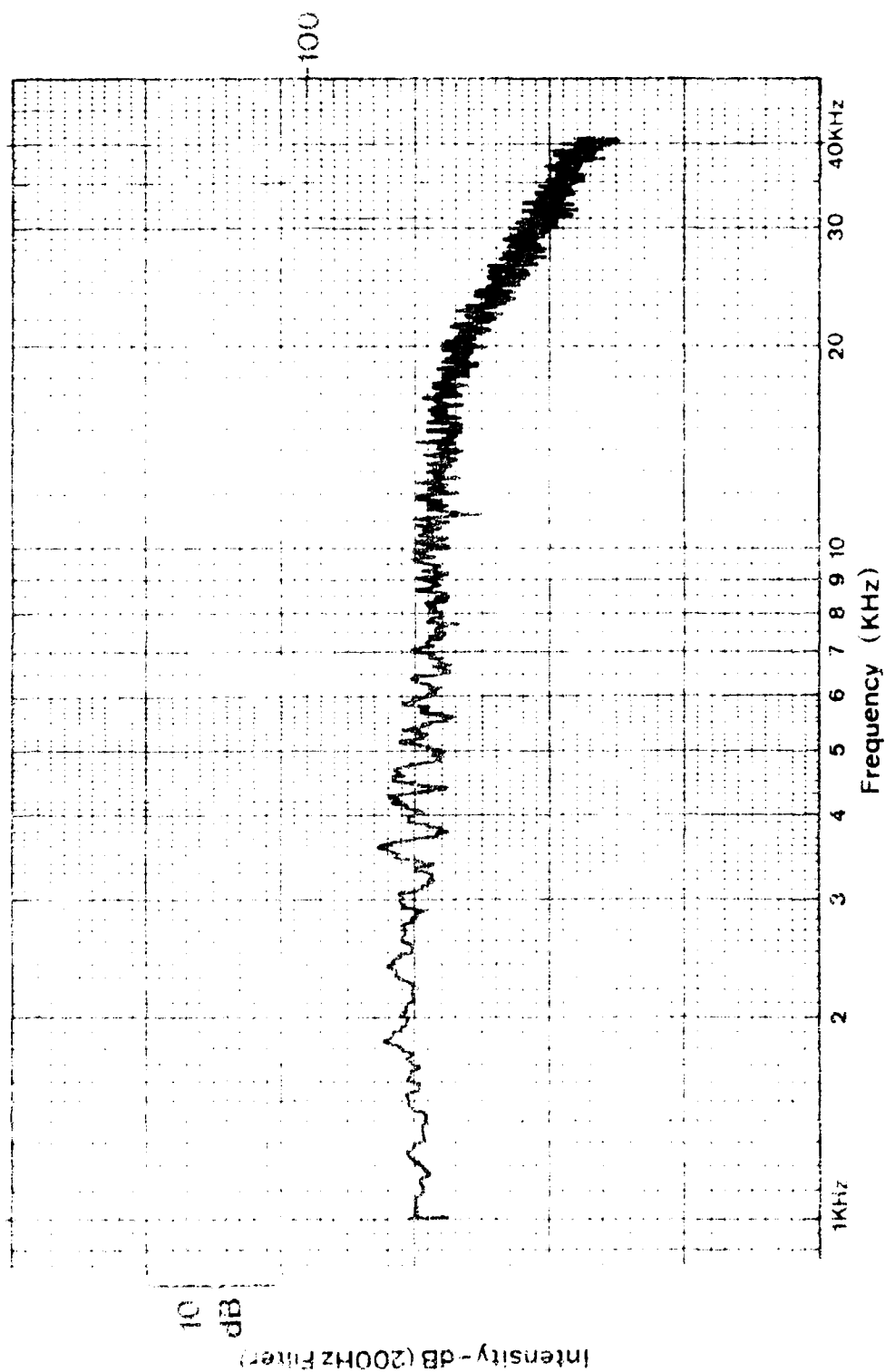


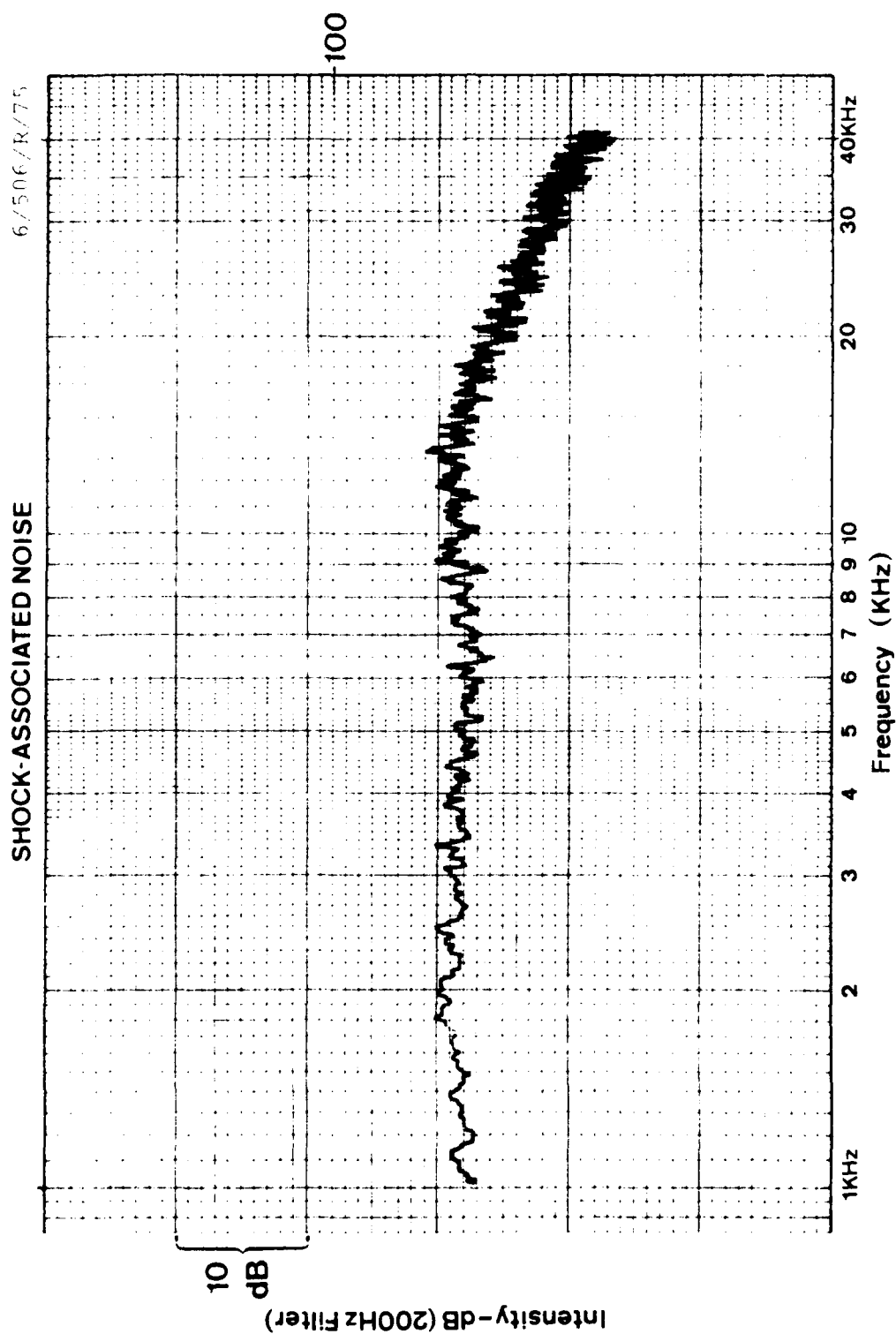


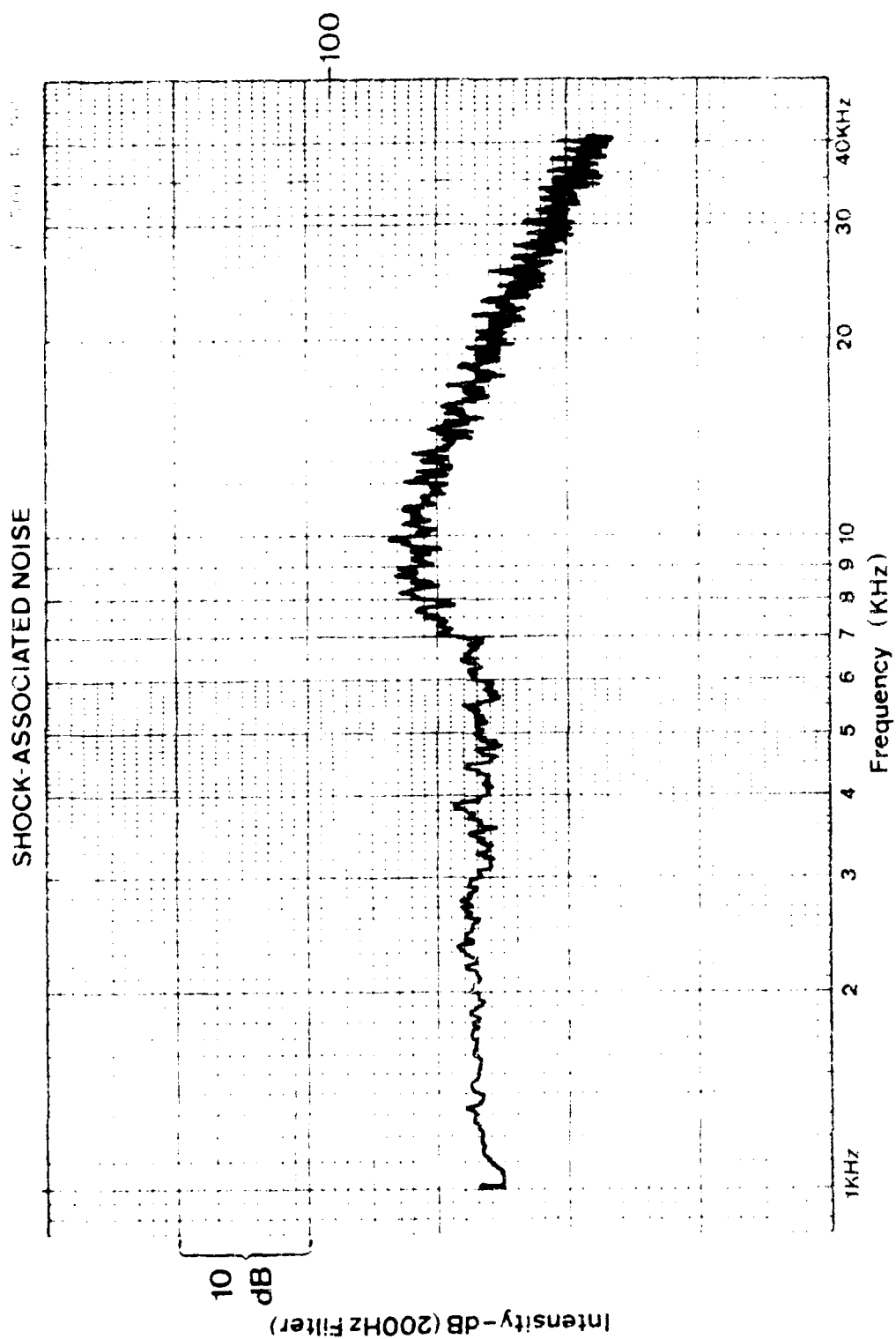
SHOCK-ASSOCIATED NOISE

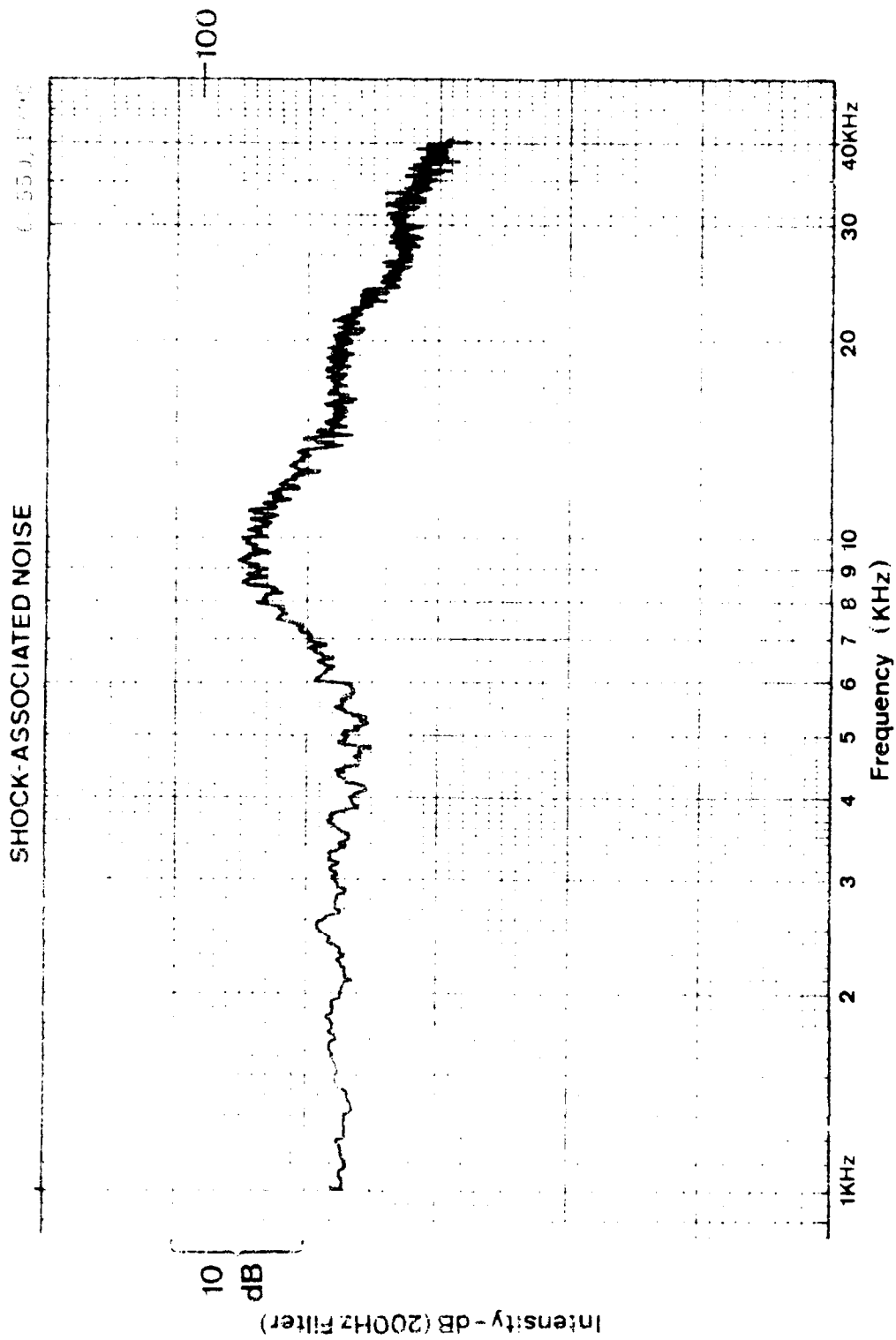


SHOCK ASSOCIATED NOISE



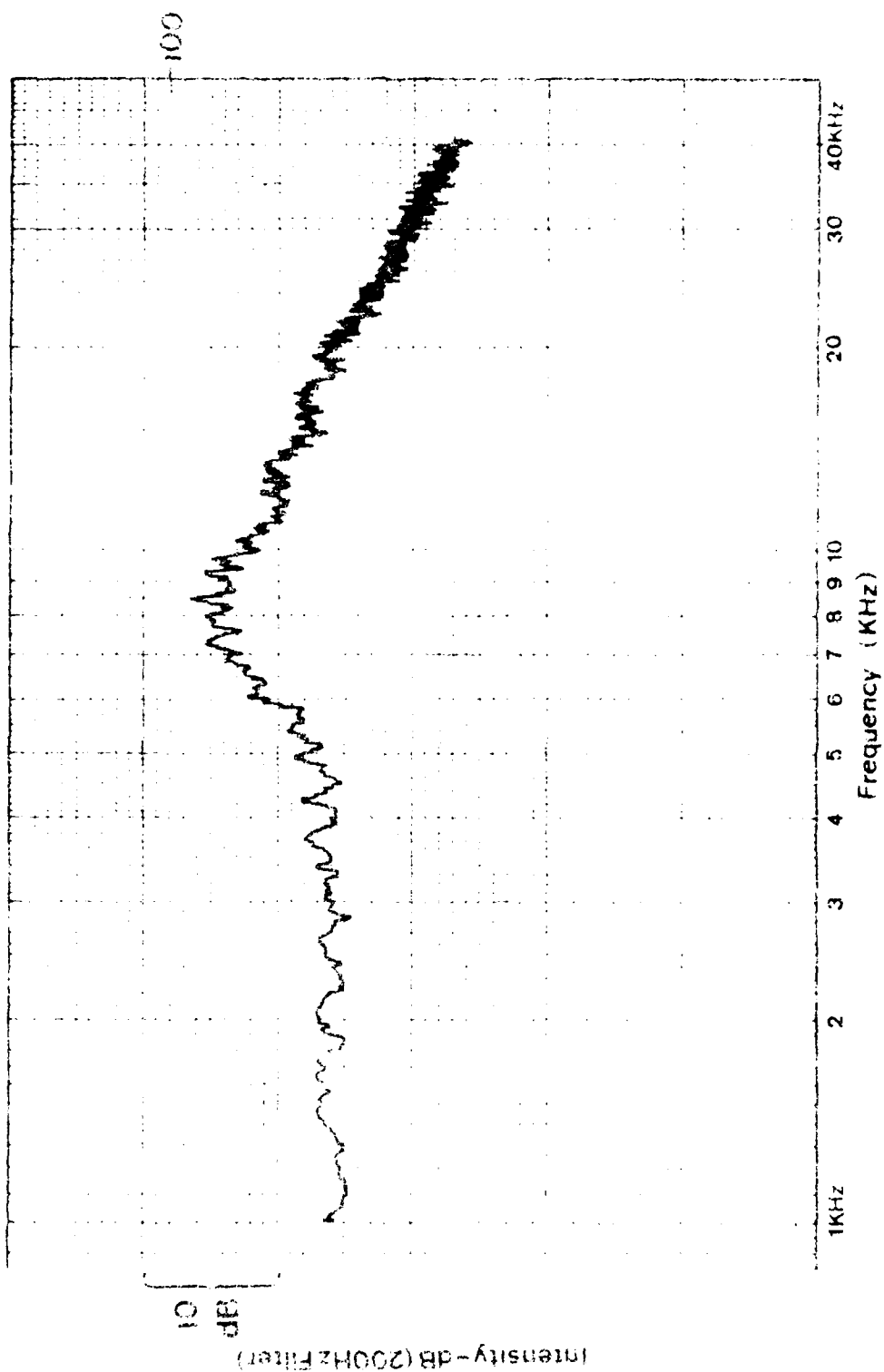


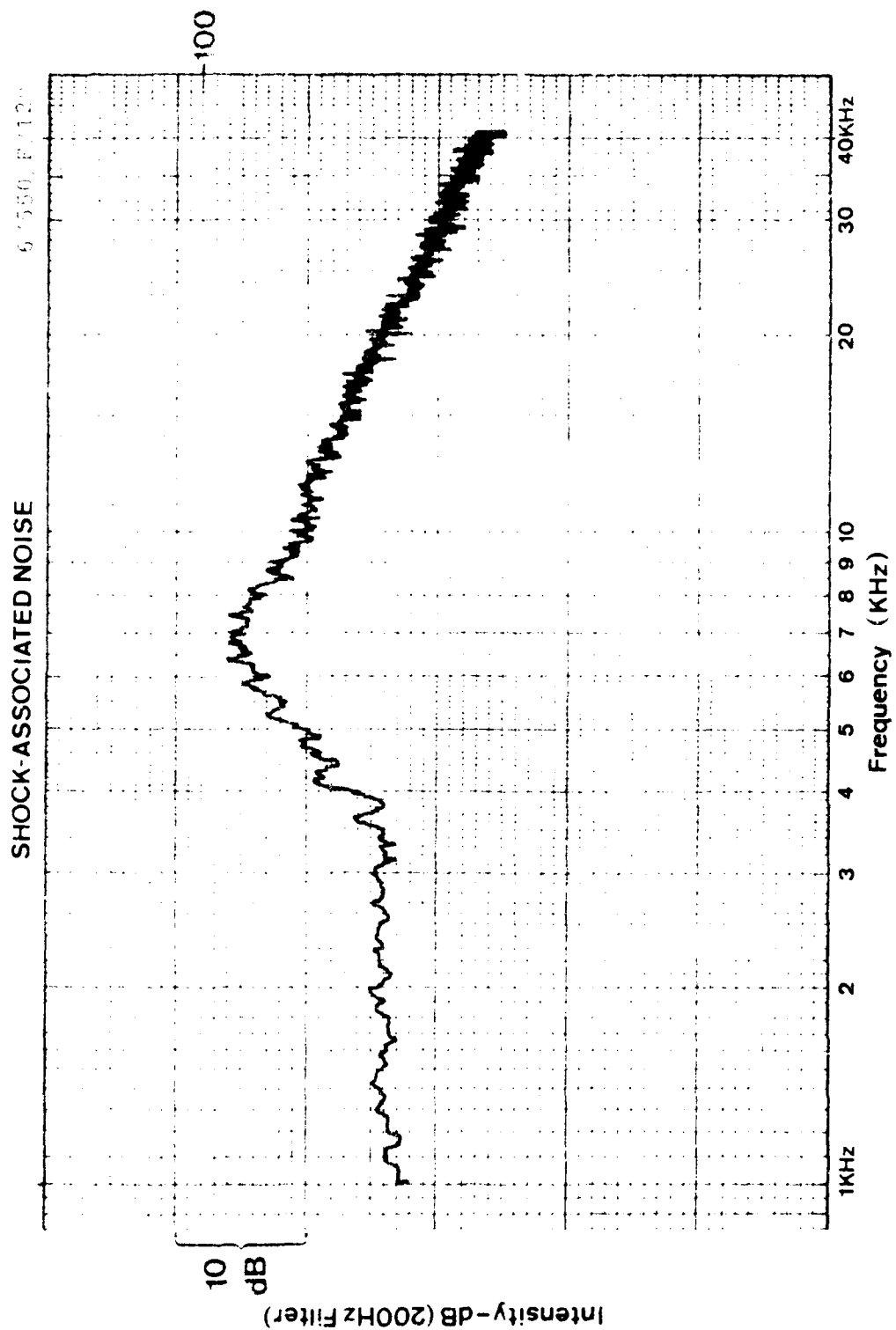


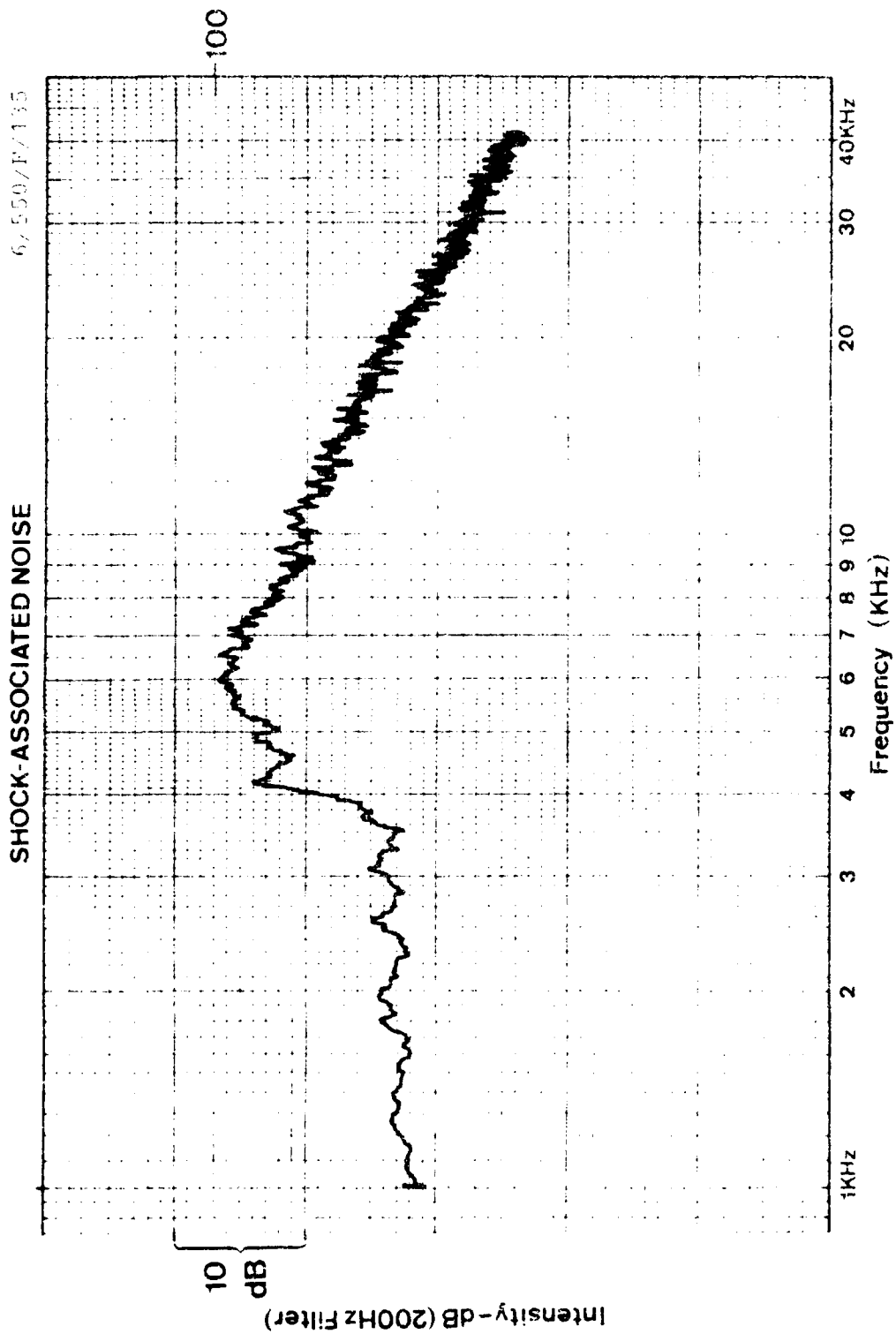


SHOCK-ASSOCIATED NOISE

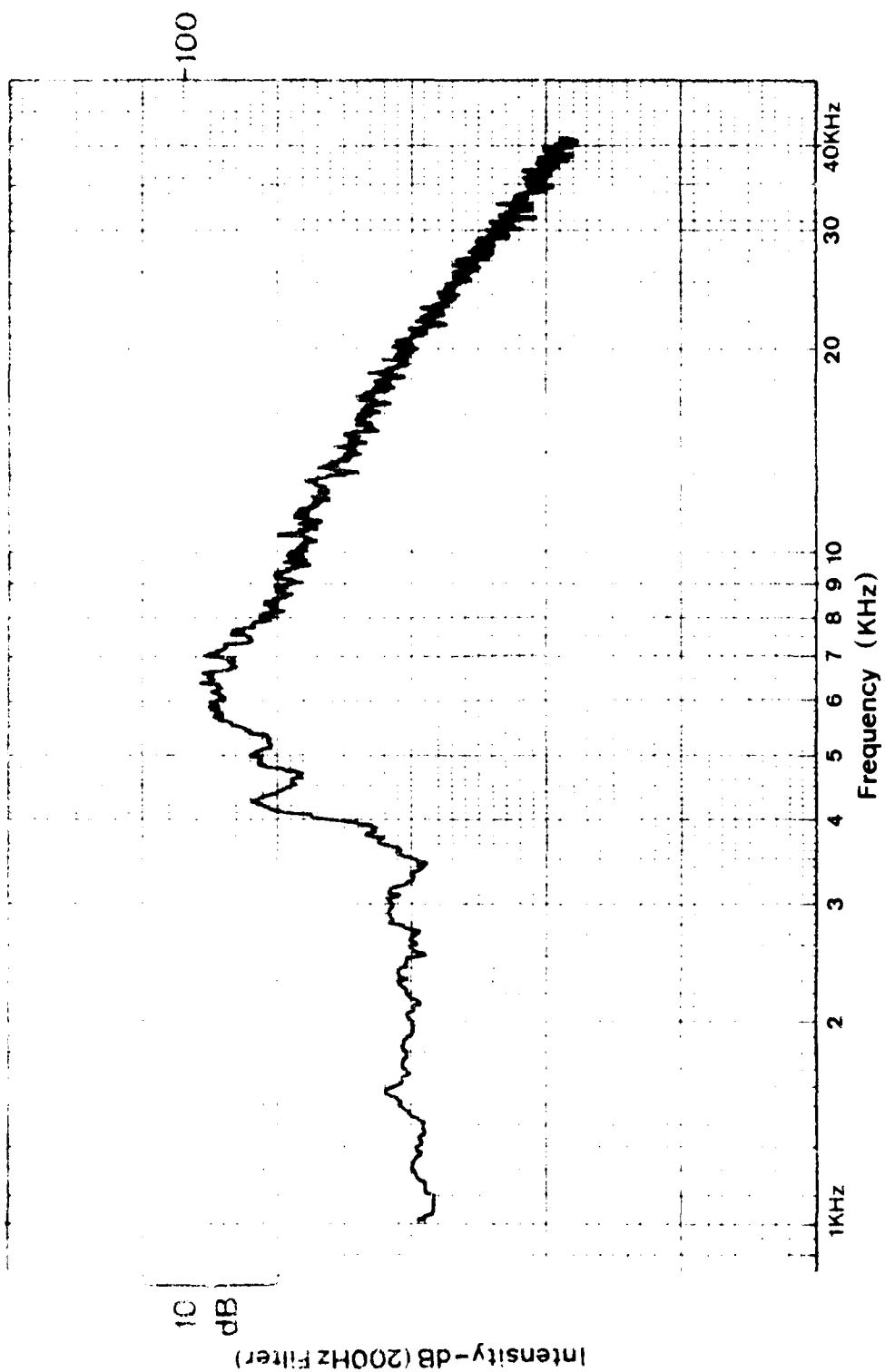
60550 P. 117





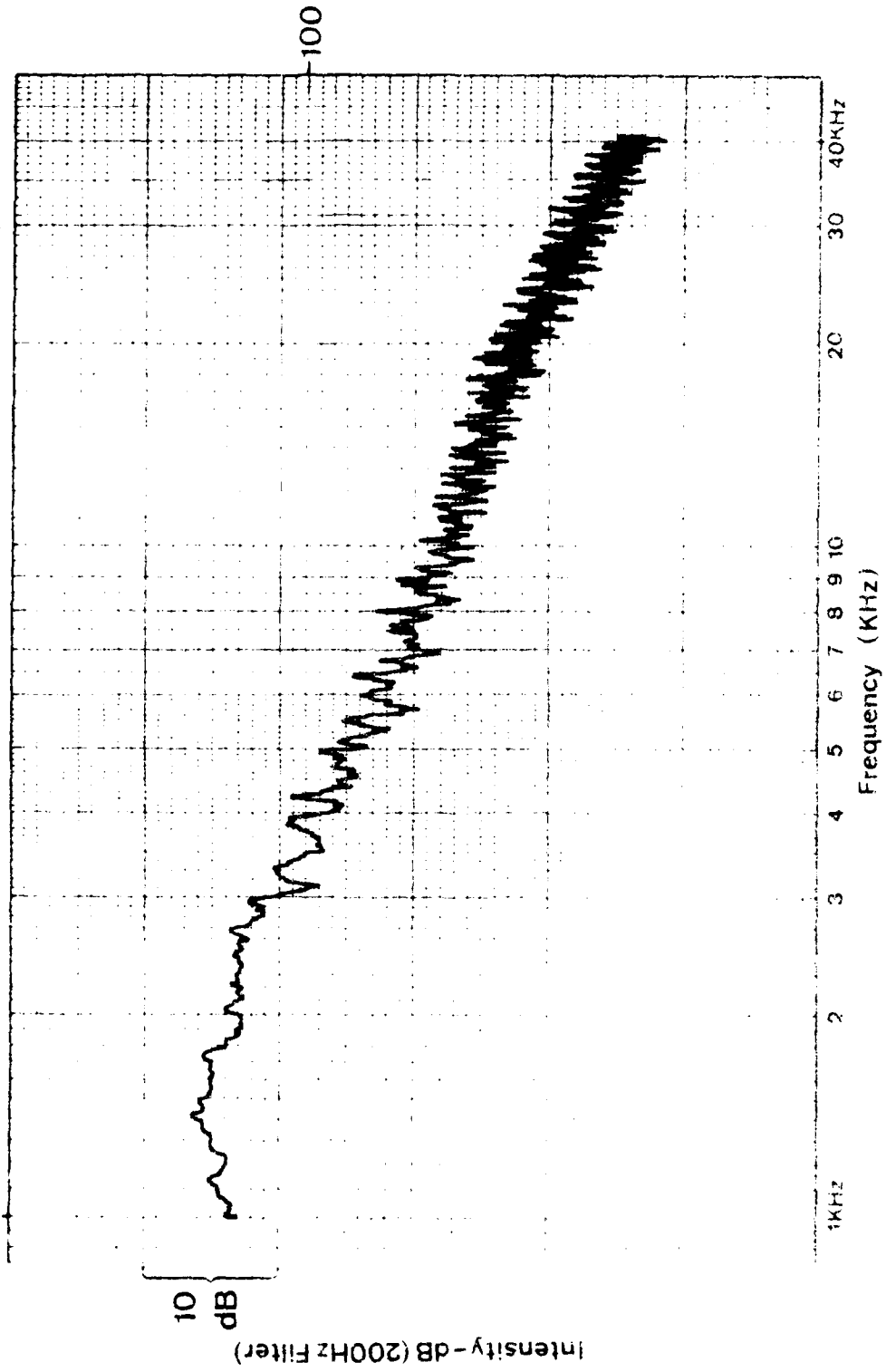


SHOCK-ASSOCIATED NOISE

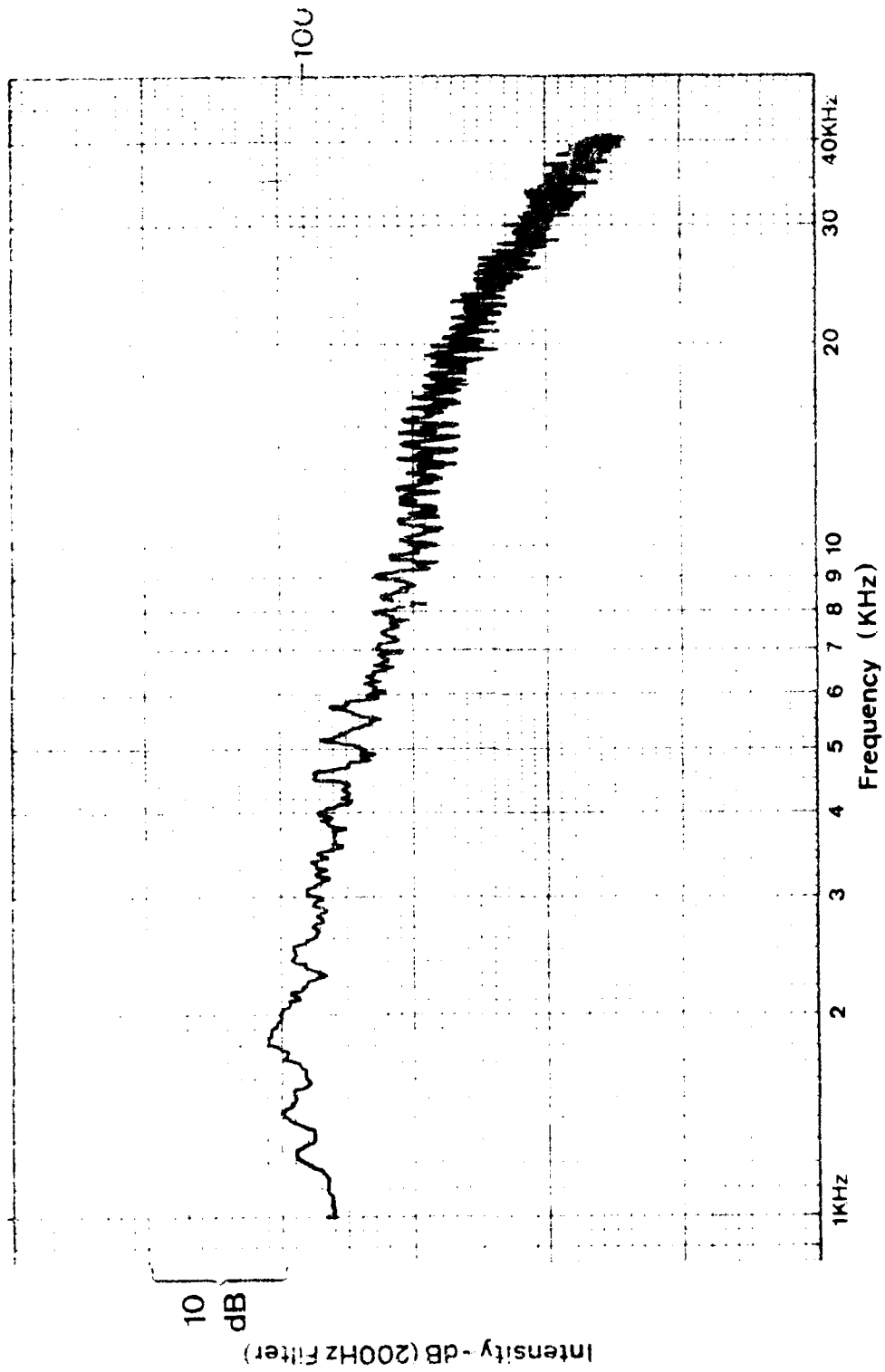


SHOCK-ASSOCIATED NOISE

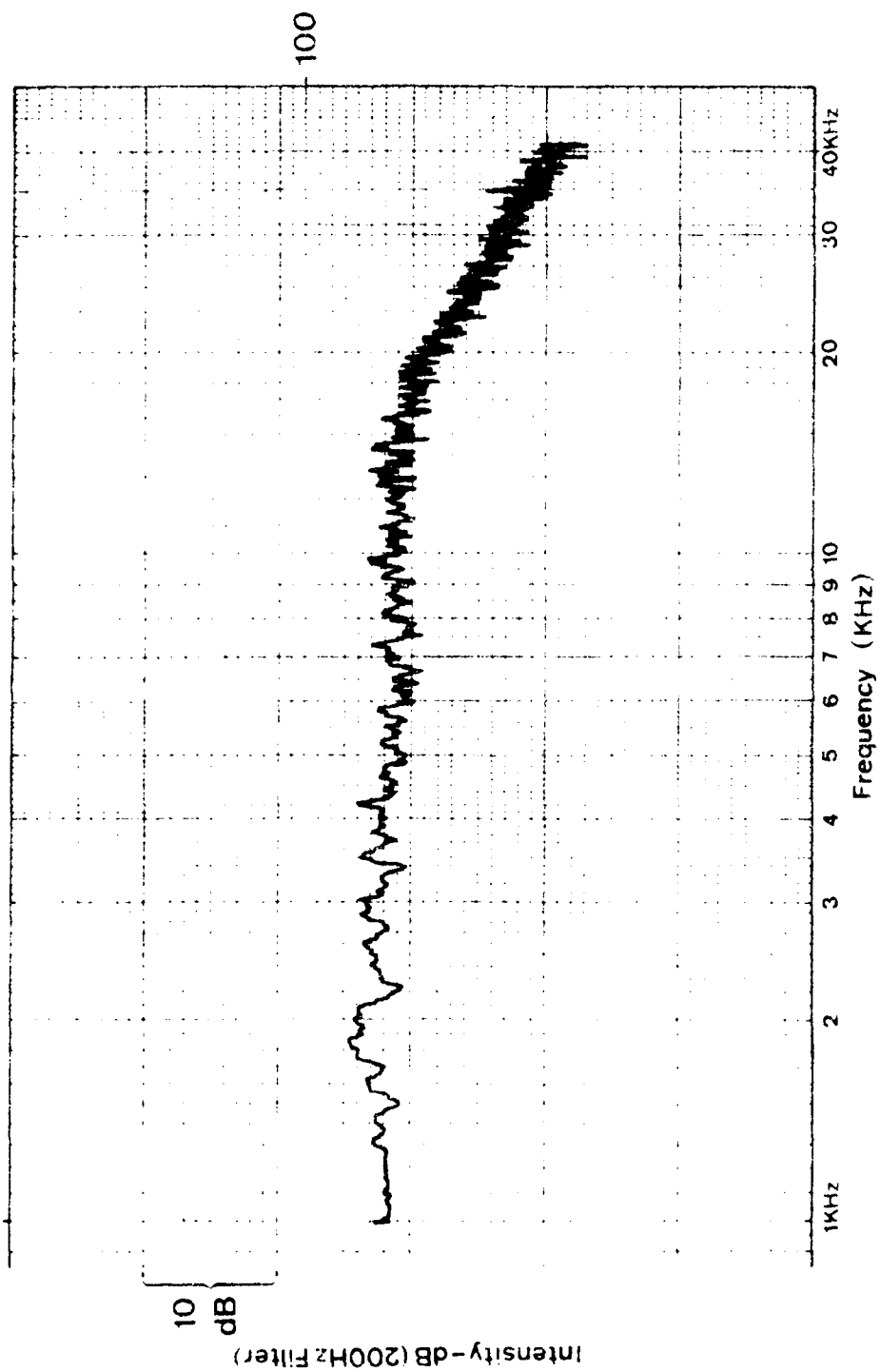
7/507/R. 30



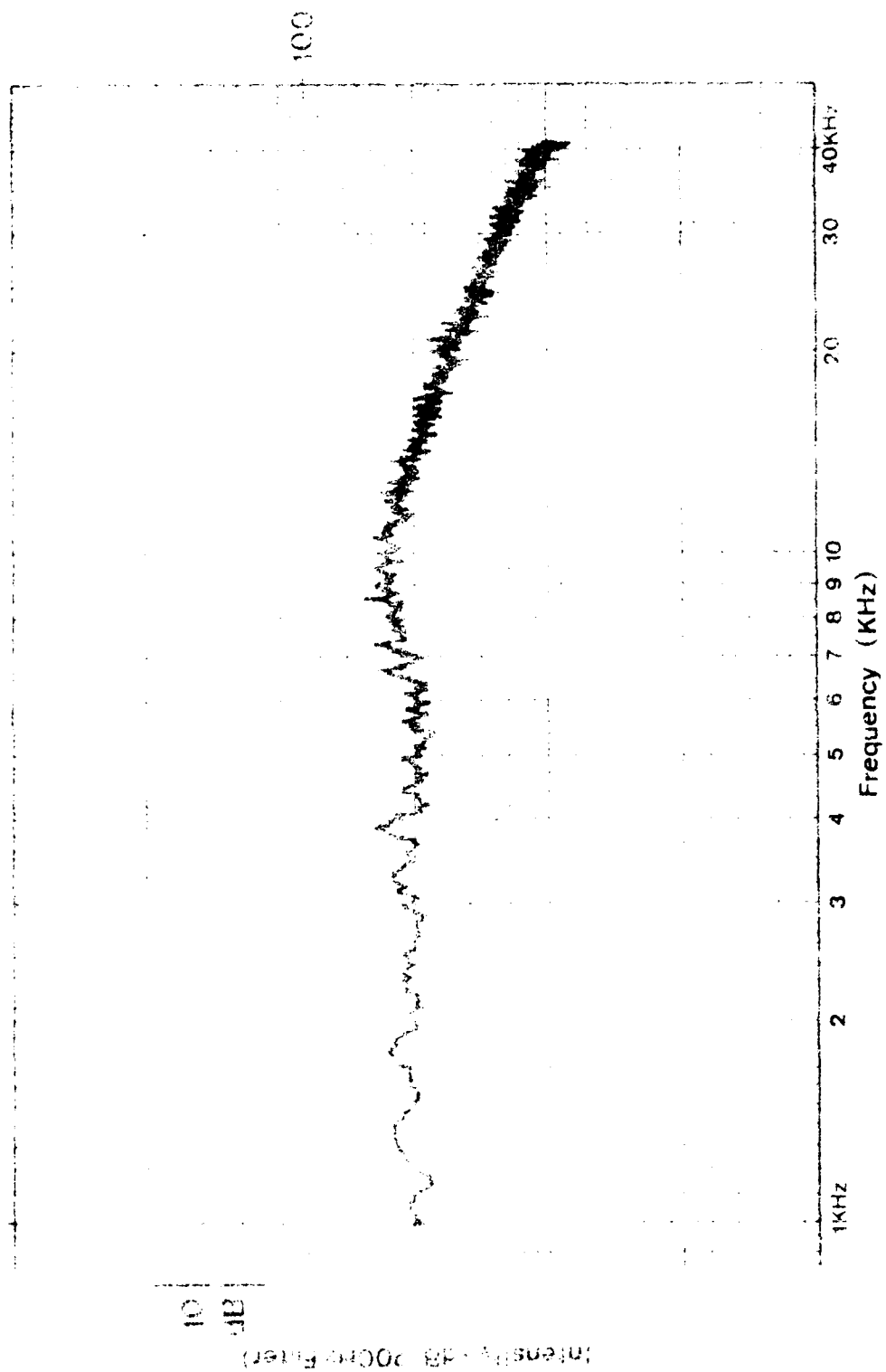
SHOCK-ASSOCIATED NOISE



SHOCK ASSOCIATED NOISE

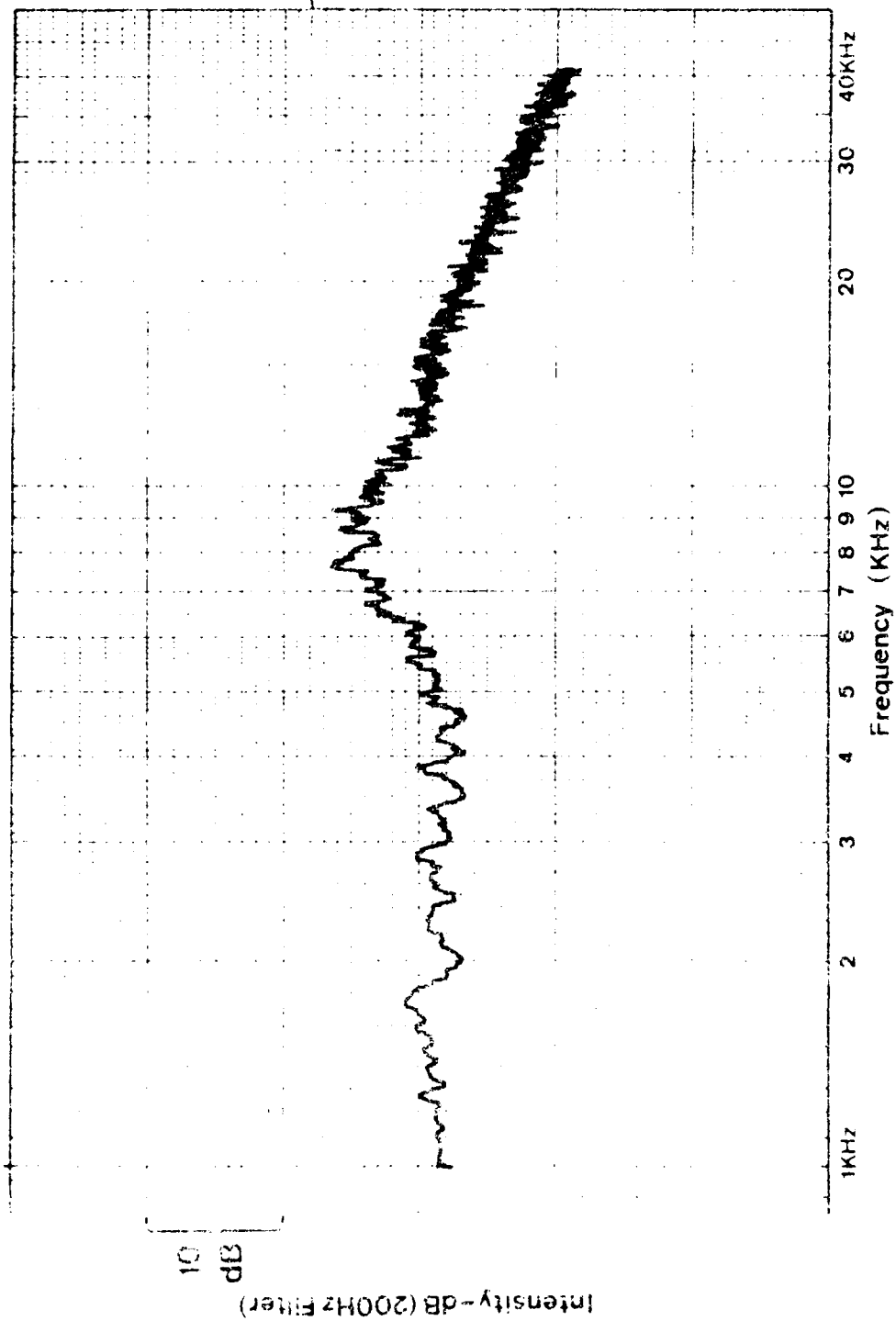


SHOCK ASSOCIATED NOISE

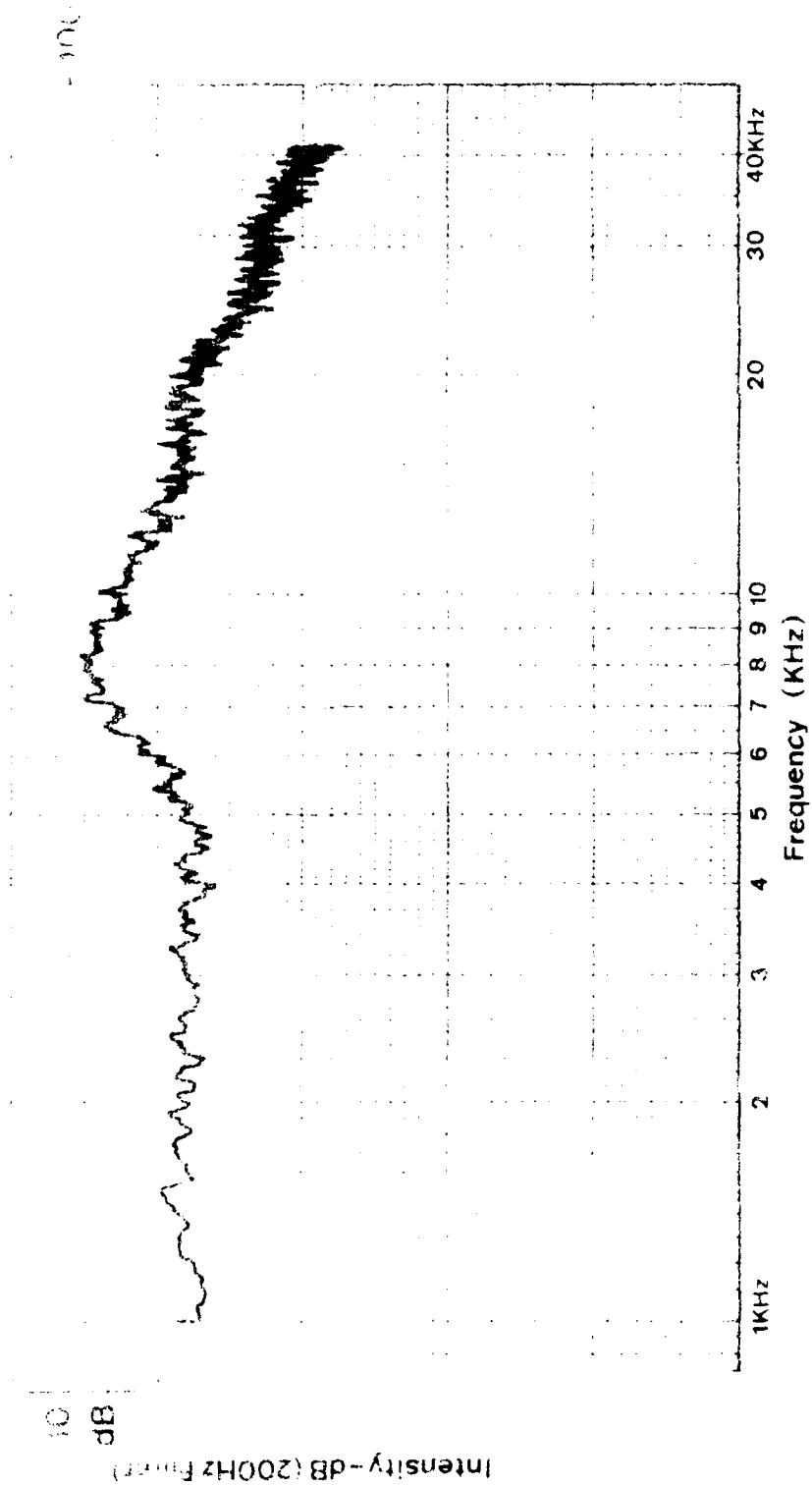


SHOCK-ASSOCIATED NOISE

12 SEP 68 R 001

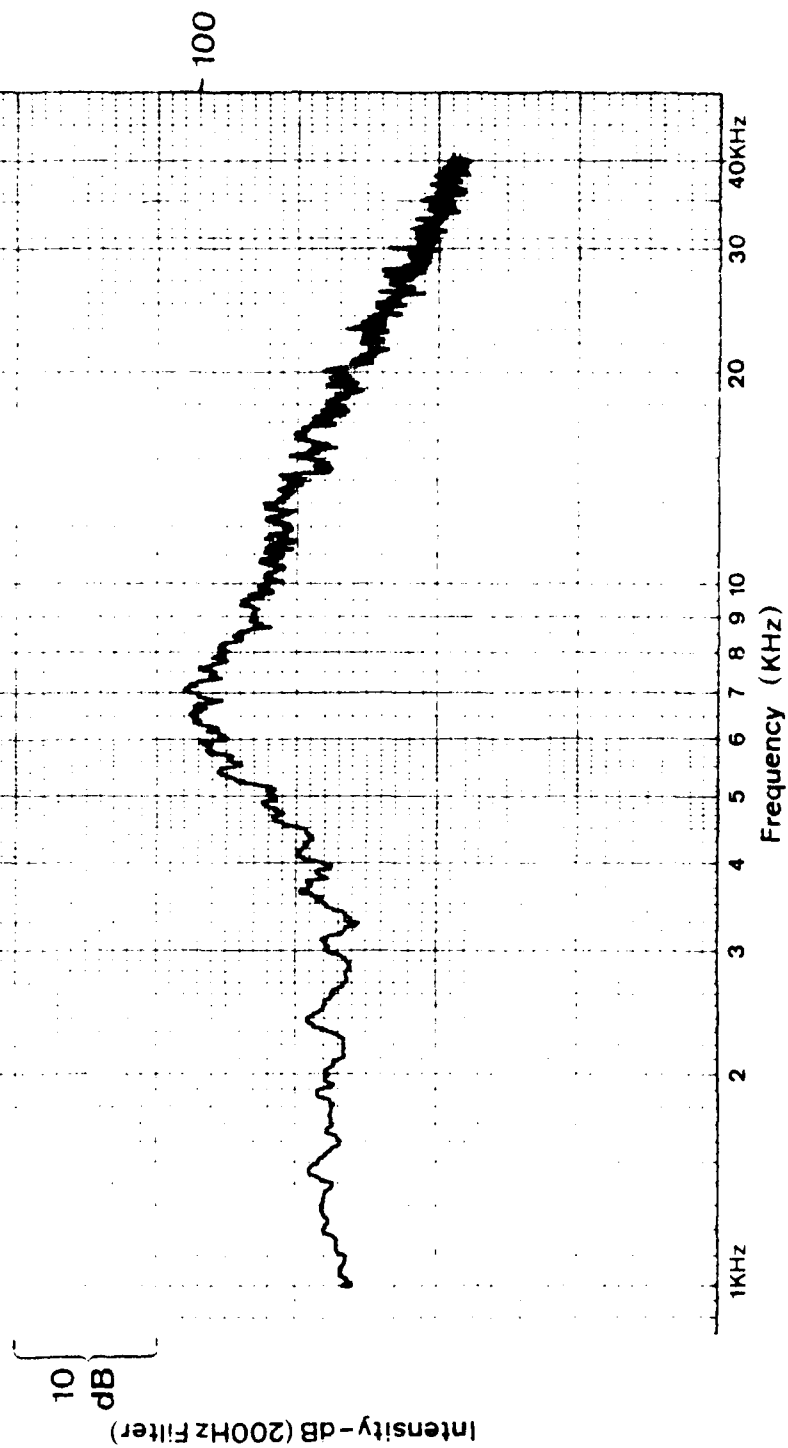


BLOCK ASSOCIATED NOISE



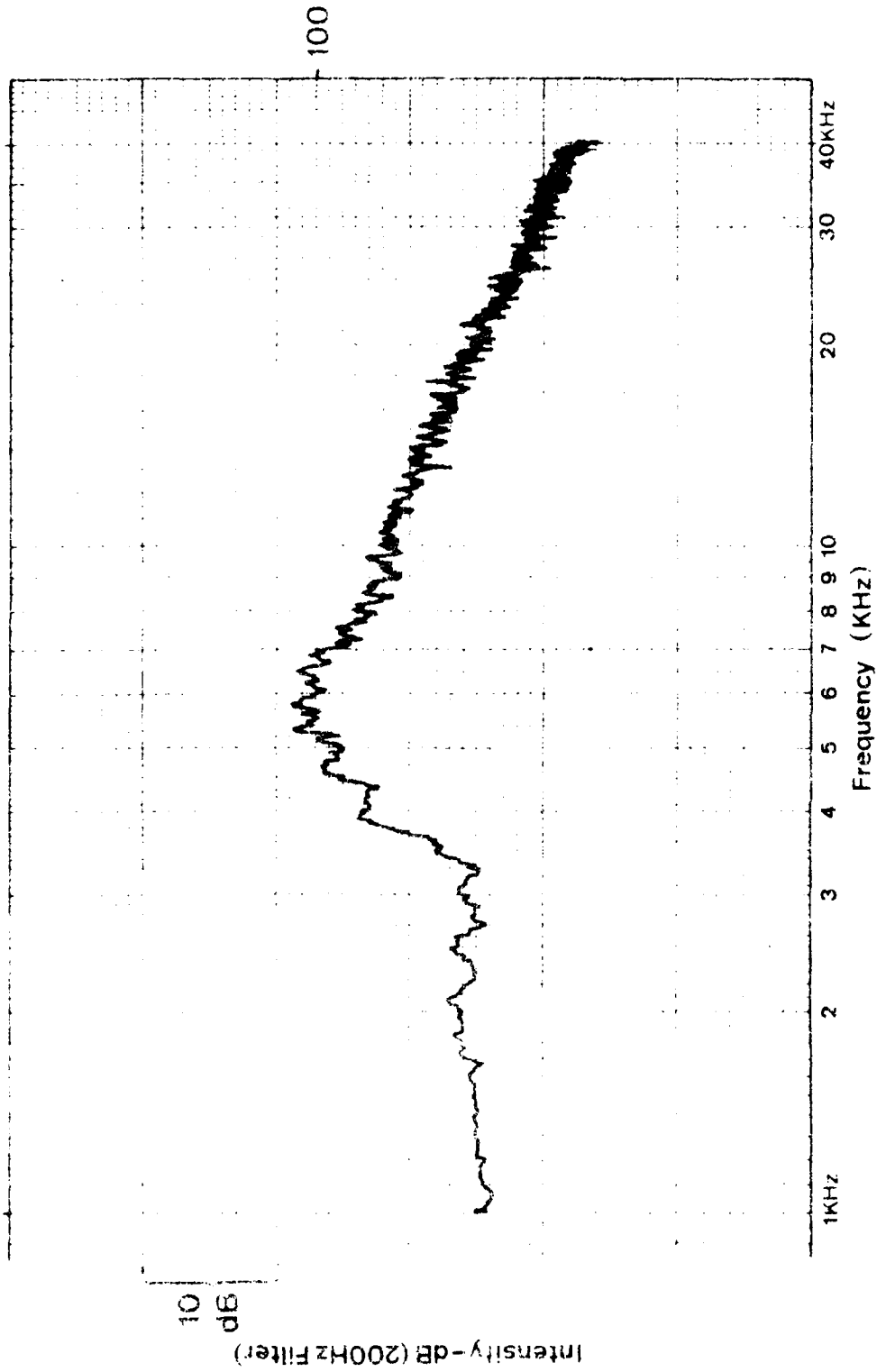
SHOCK-ASSOCIATED NOISE

7.551/P.105



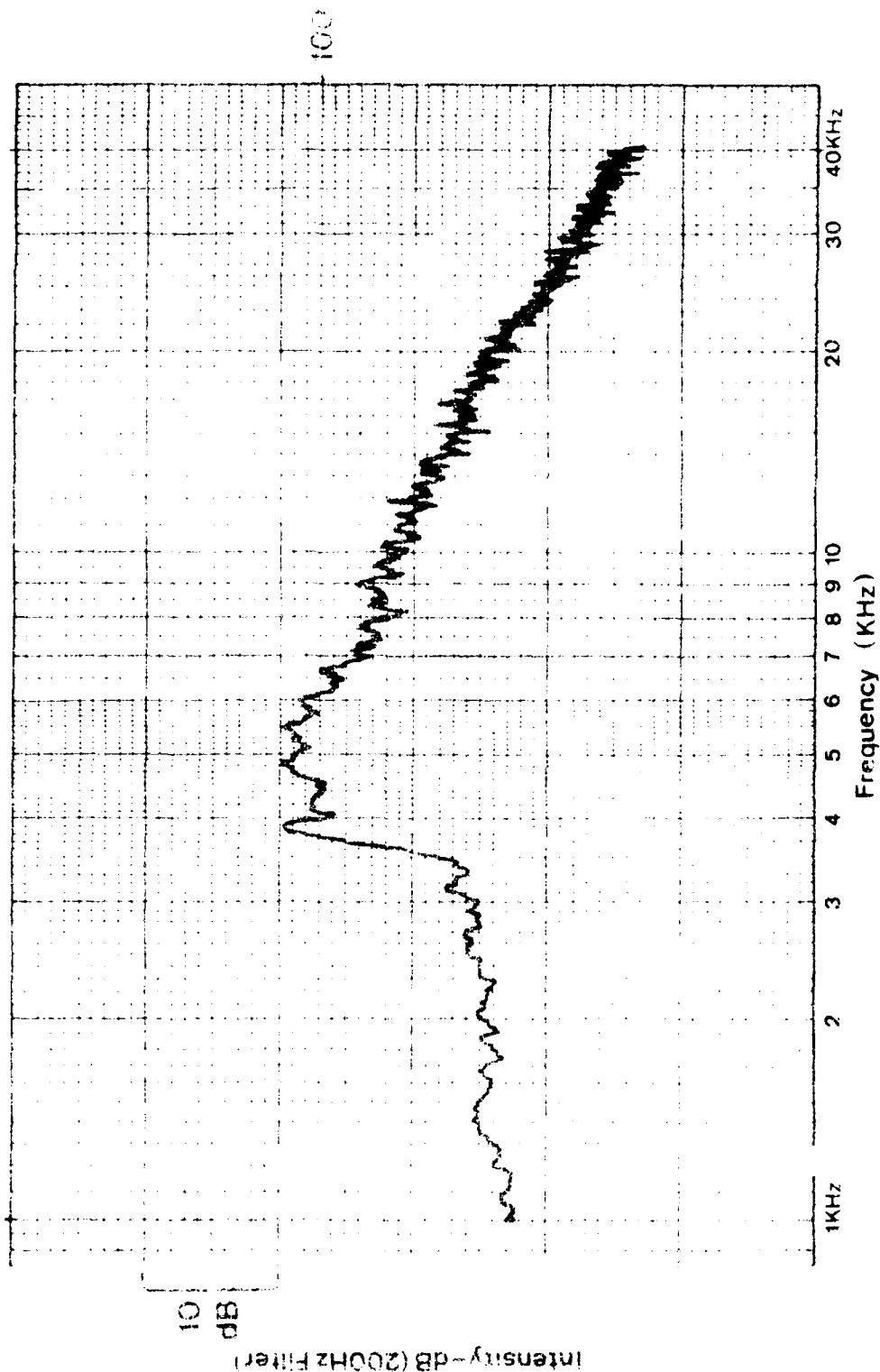
SHOCK-ASSOCIATED NOISE

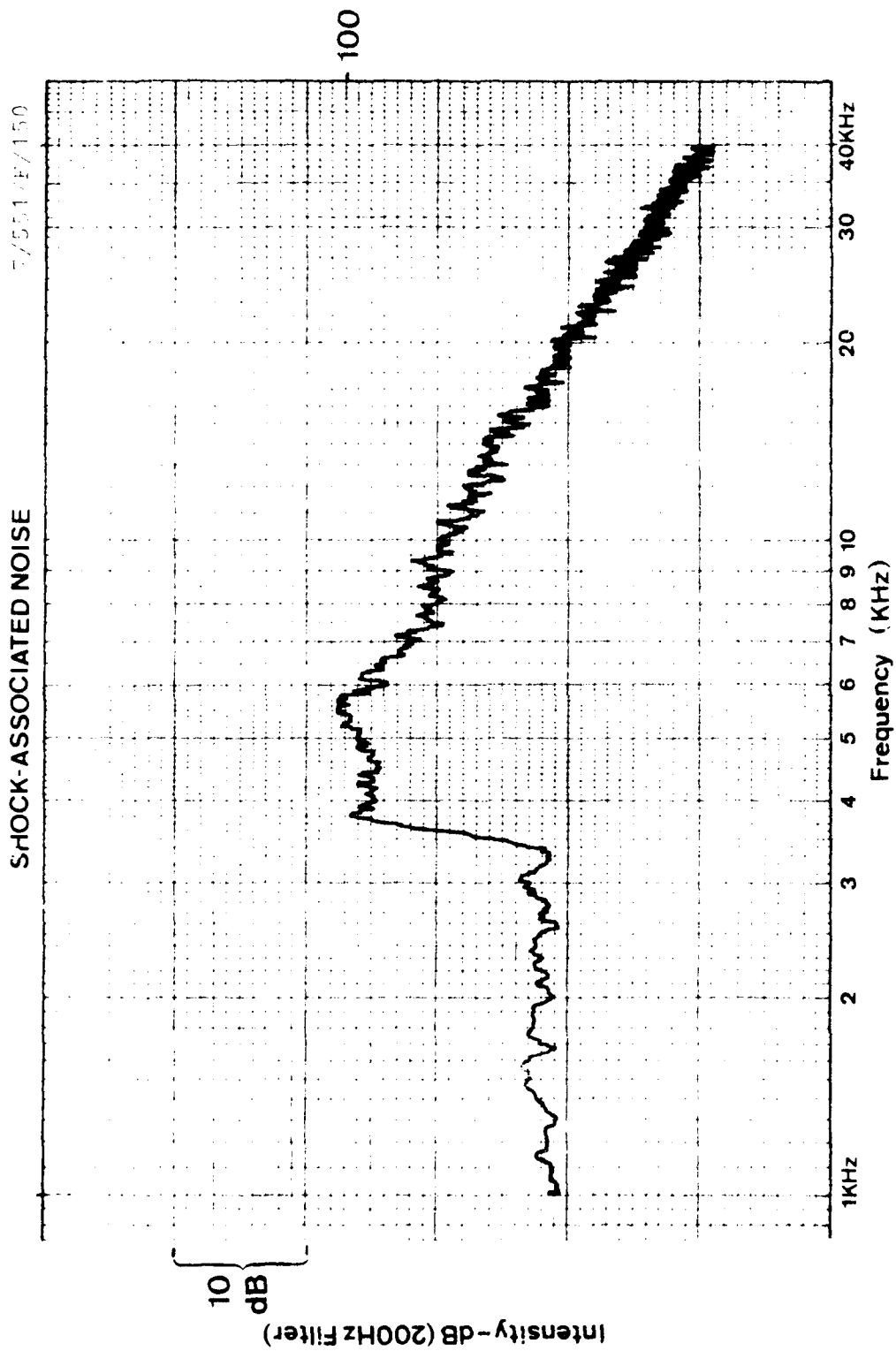
7/551 128



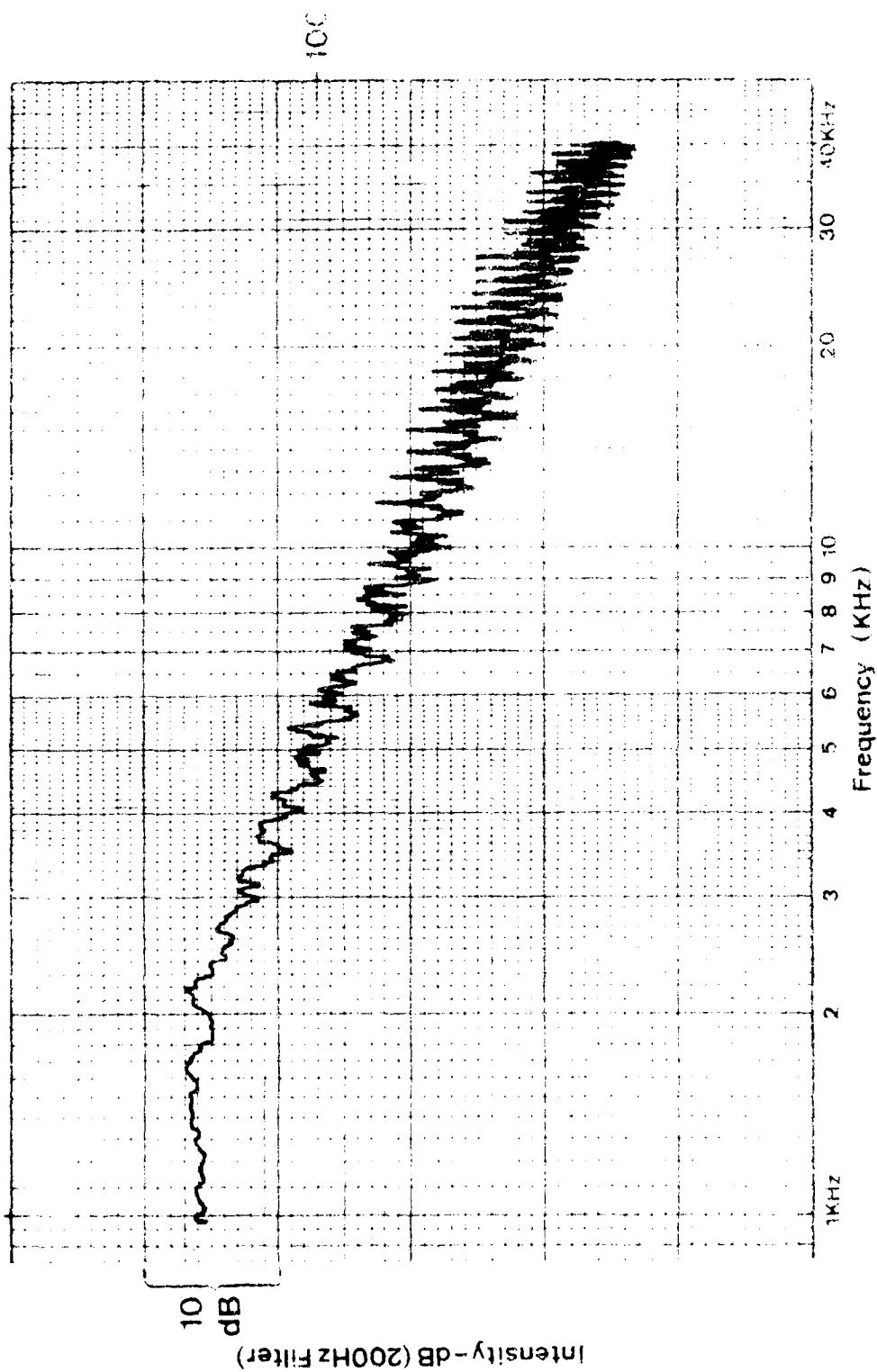
SHOCK ASSOCIATED NOISE

7/551, IV/133





SHOCK-ASSOCIATED NOISE

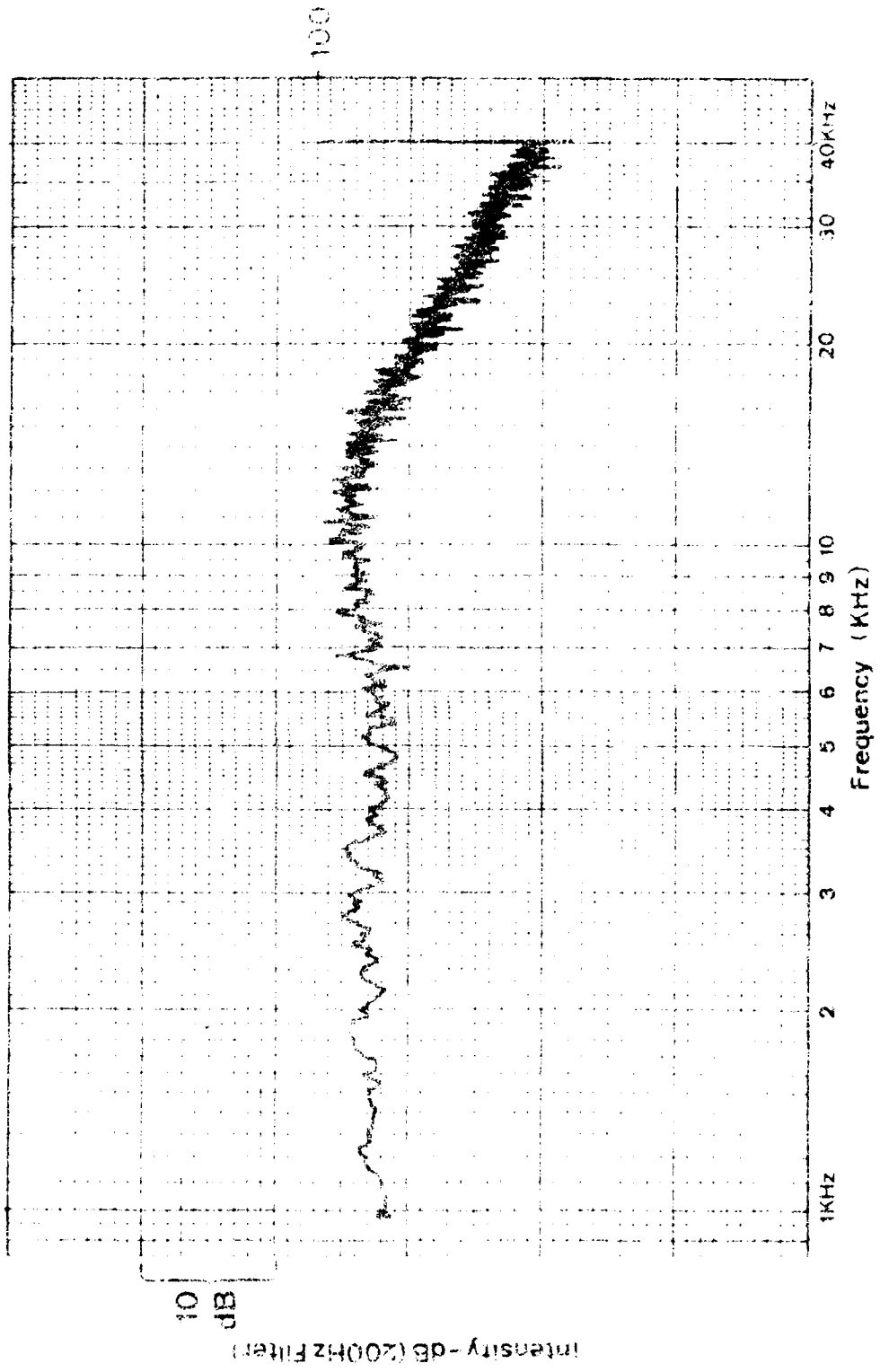


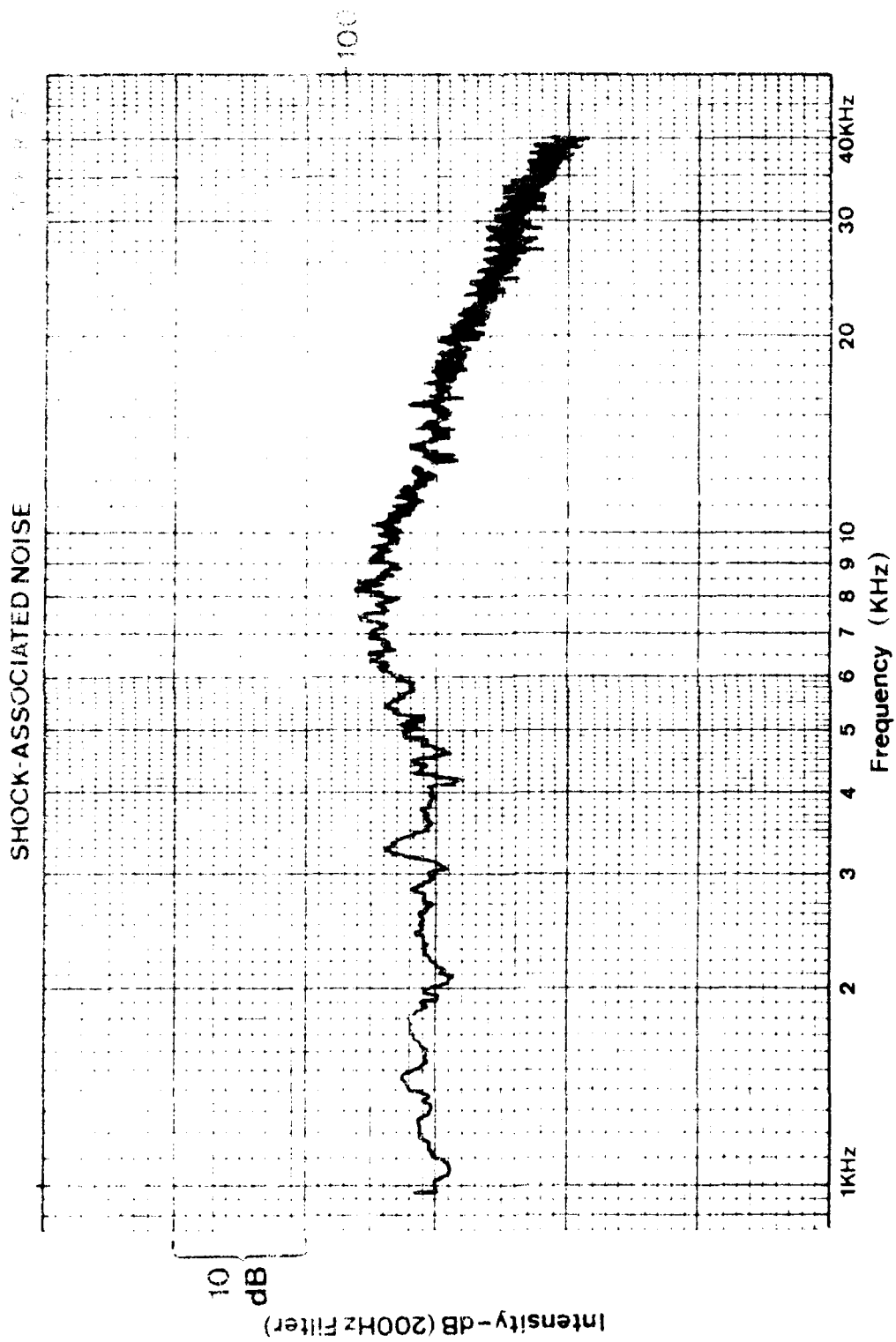
100



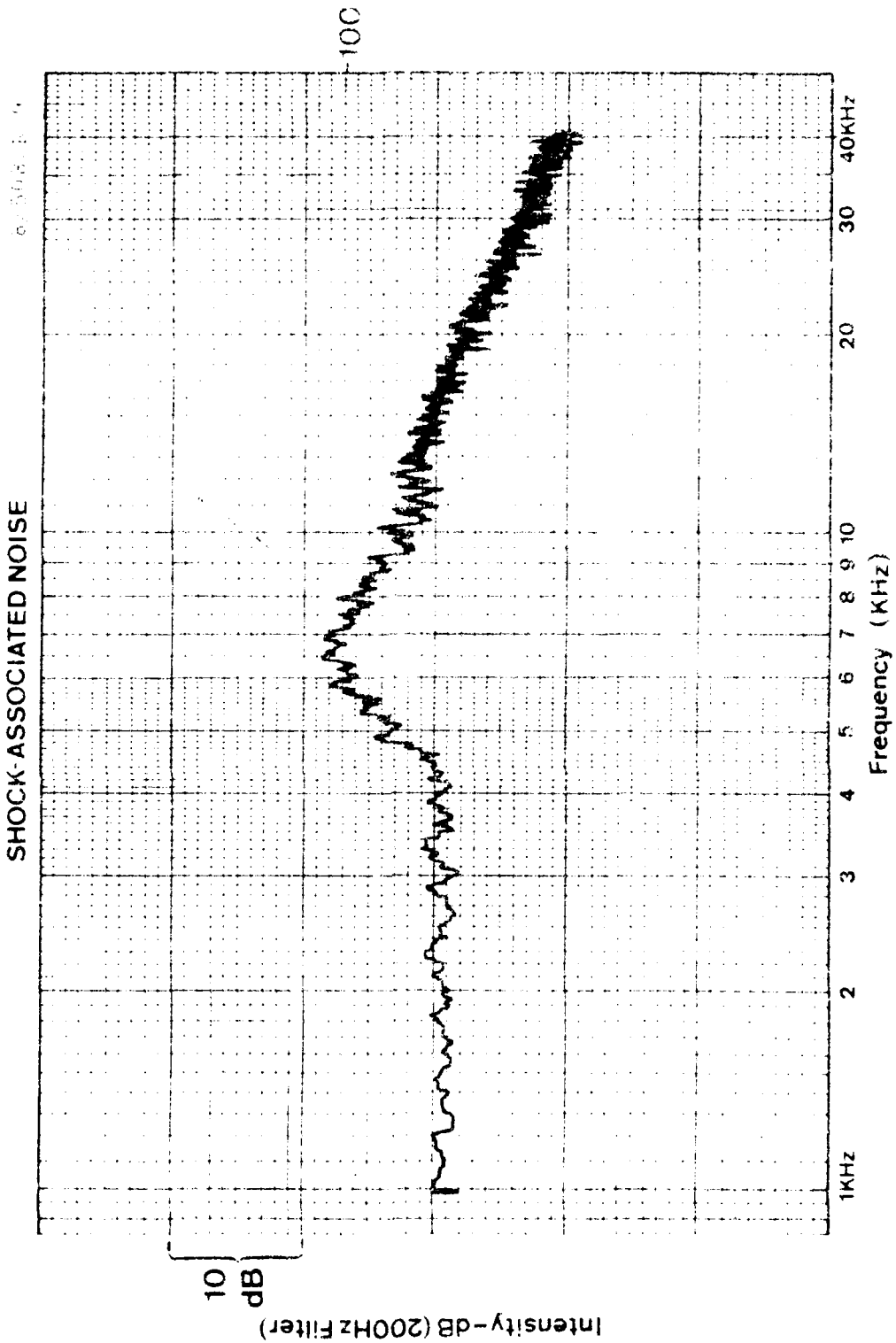
Intensity - dB (200Hz Filter)

SHOCK ASSOCIATED NOISE

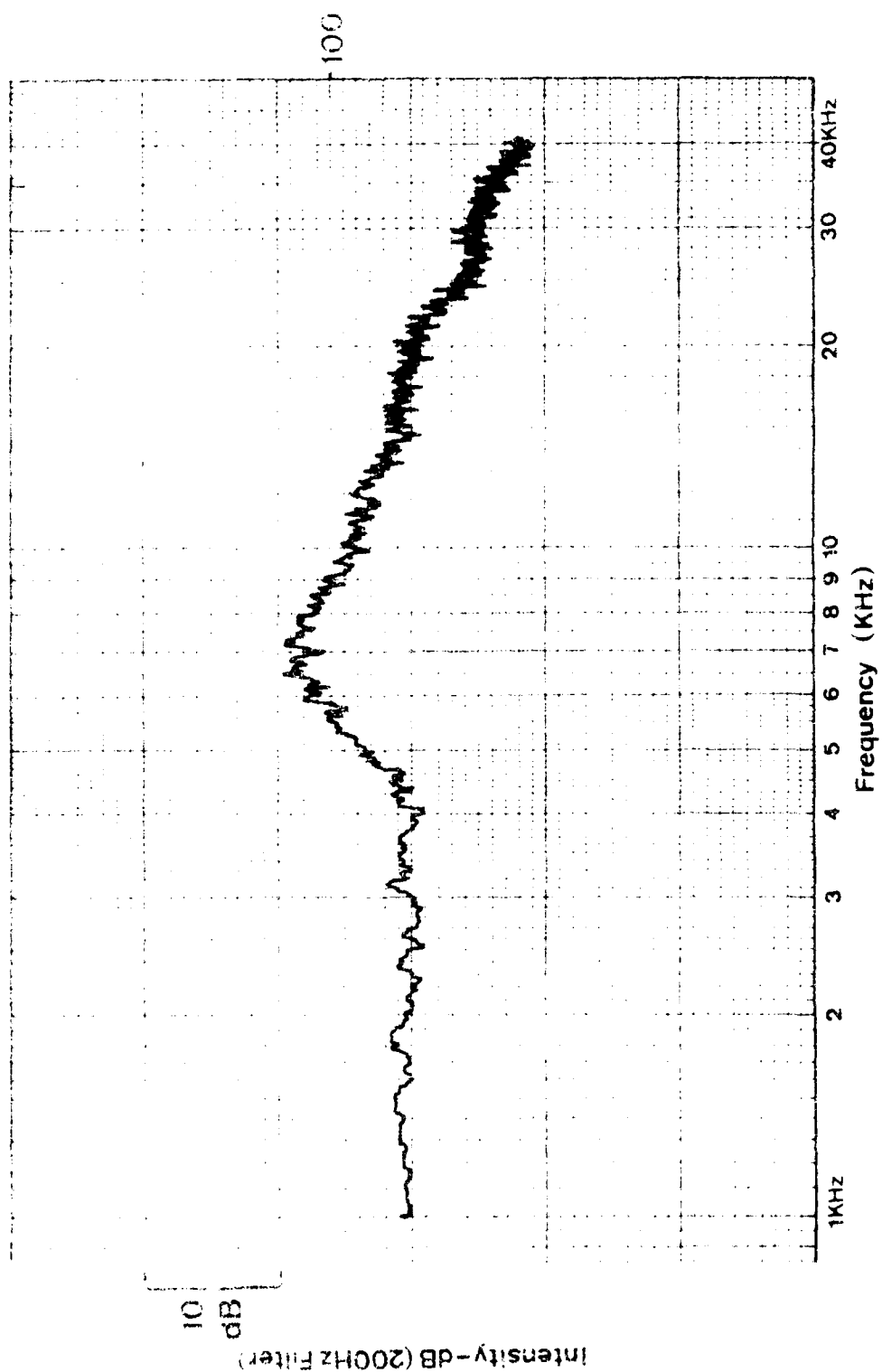




SHOCK-ASSOCIATED NOISE

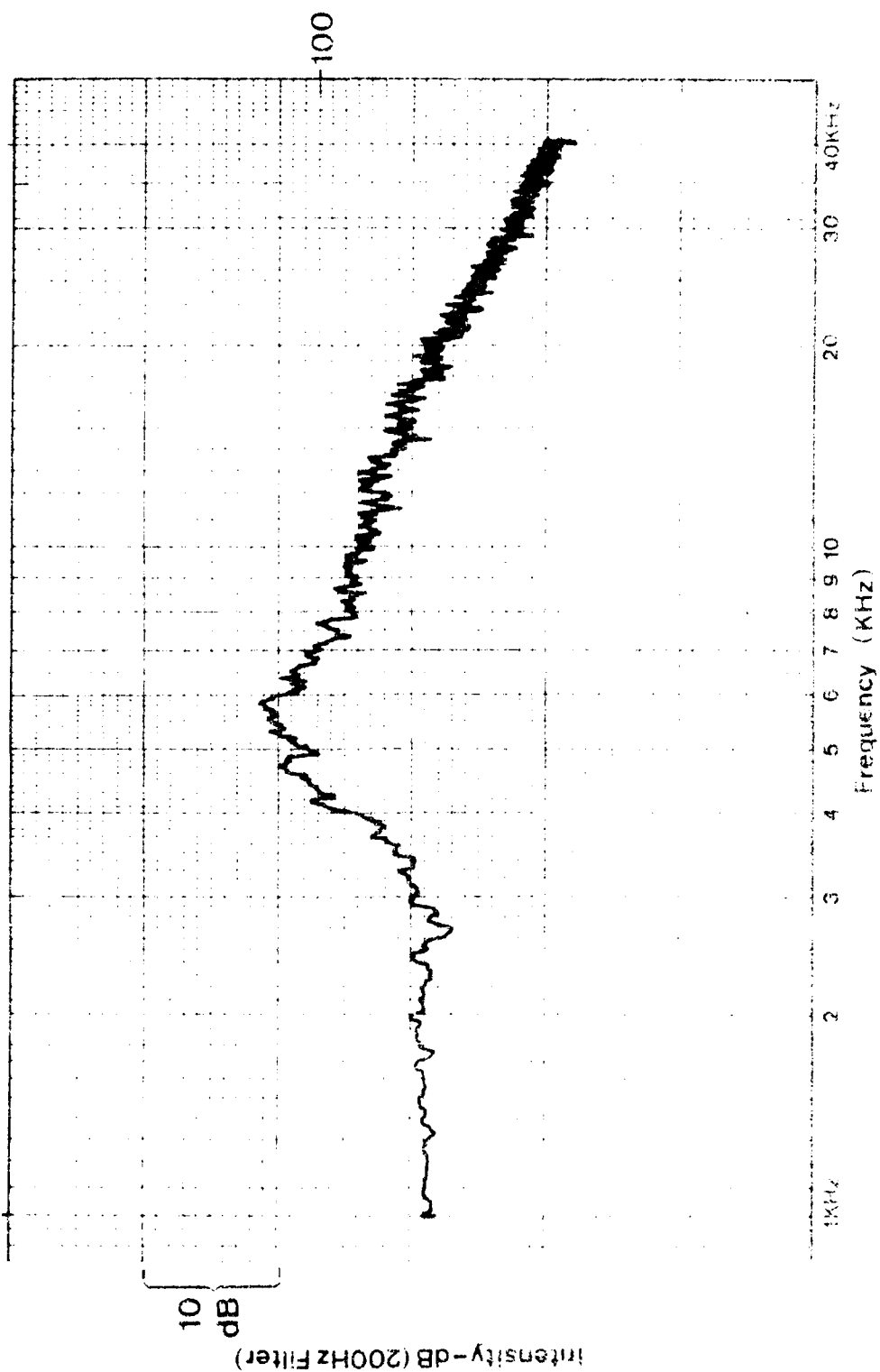


SHOCK ASSOCIATED NOISE

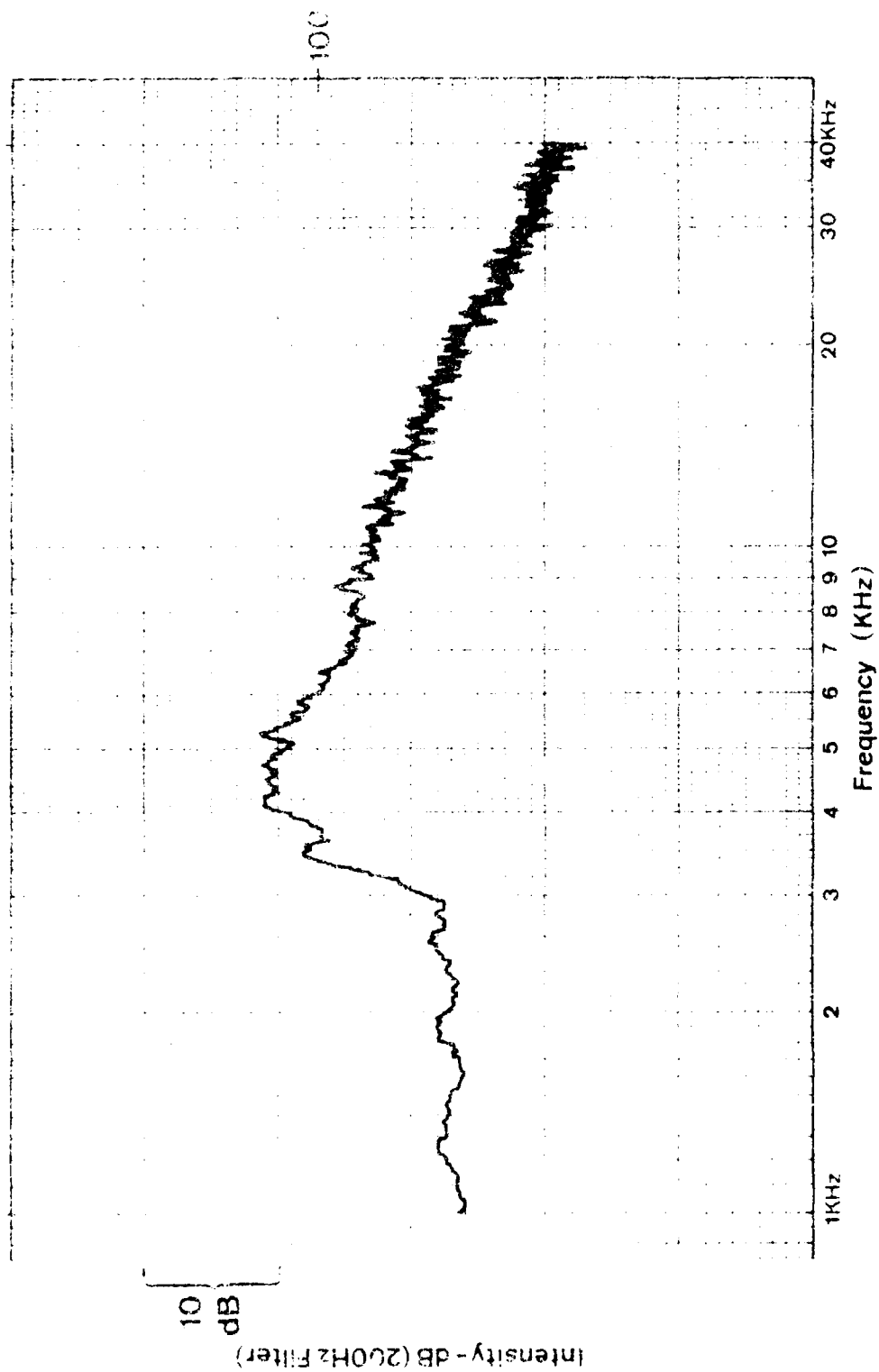


SHOCK-ASSOCIATED NOISE

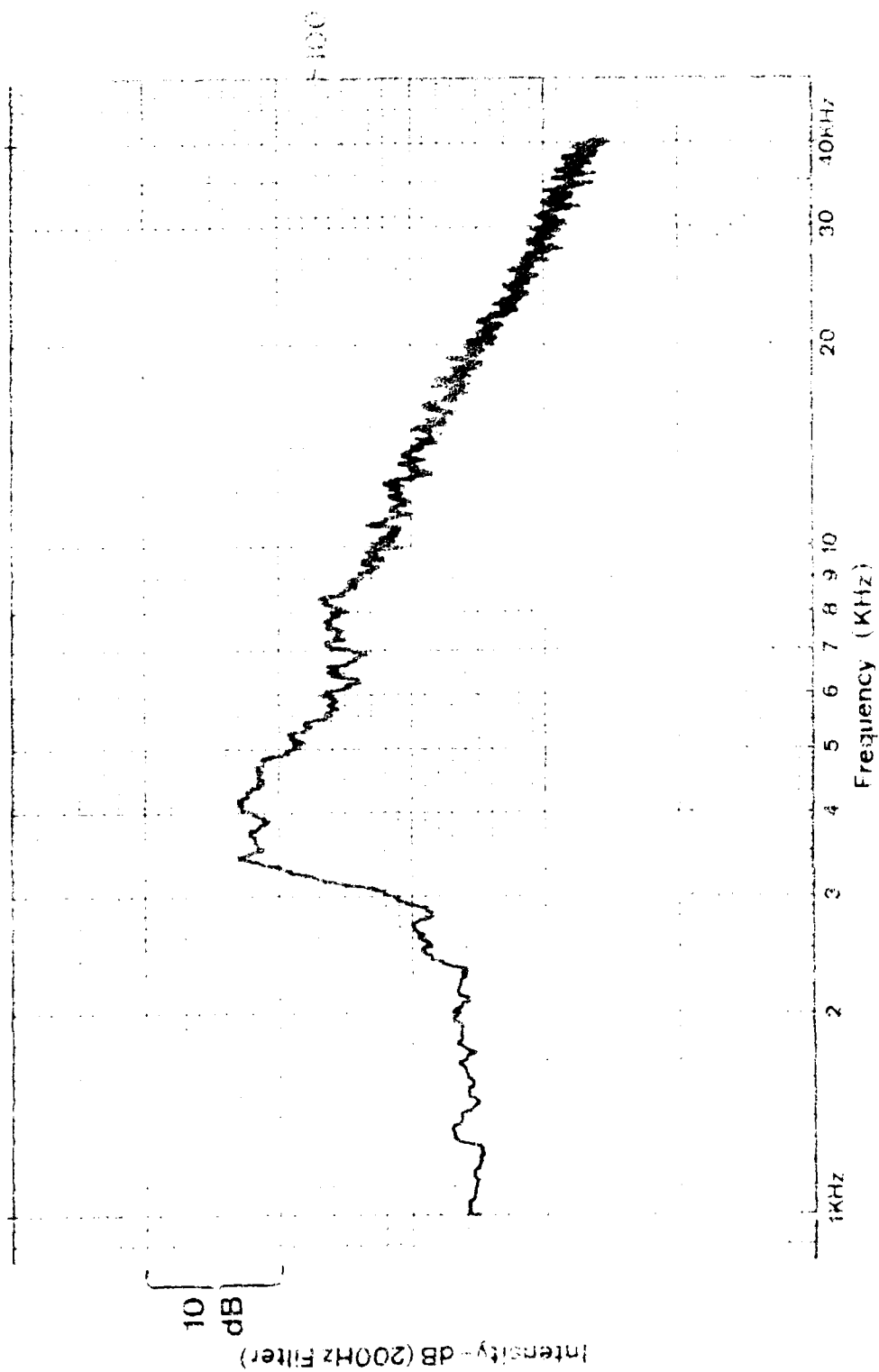
8/552 P4105



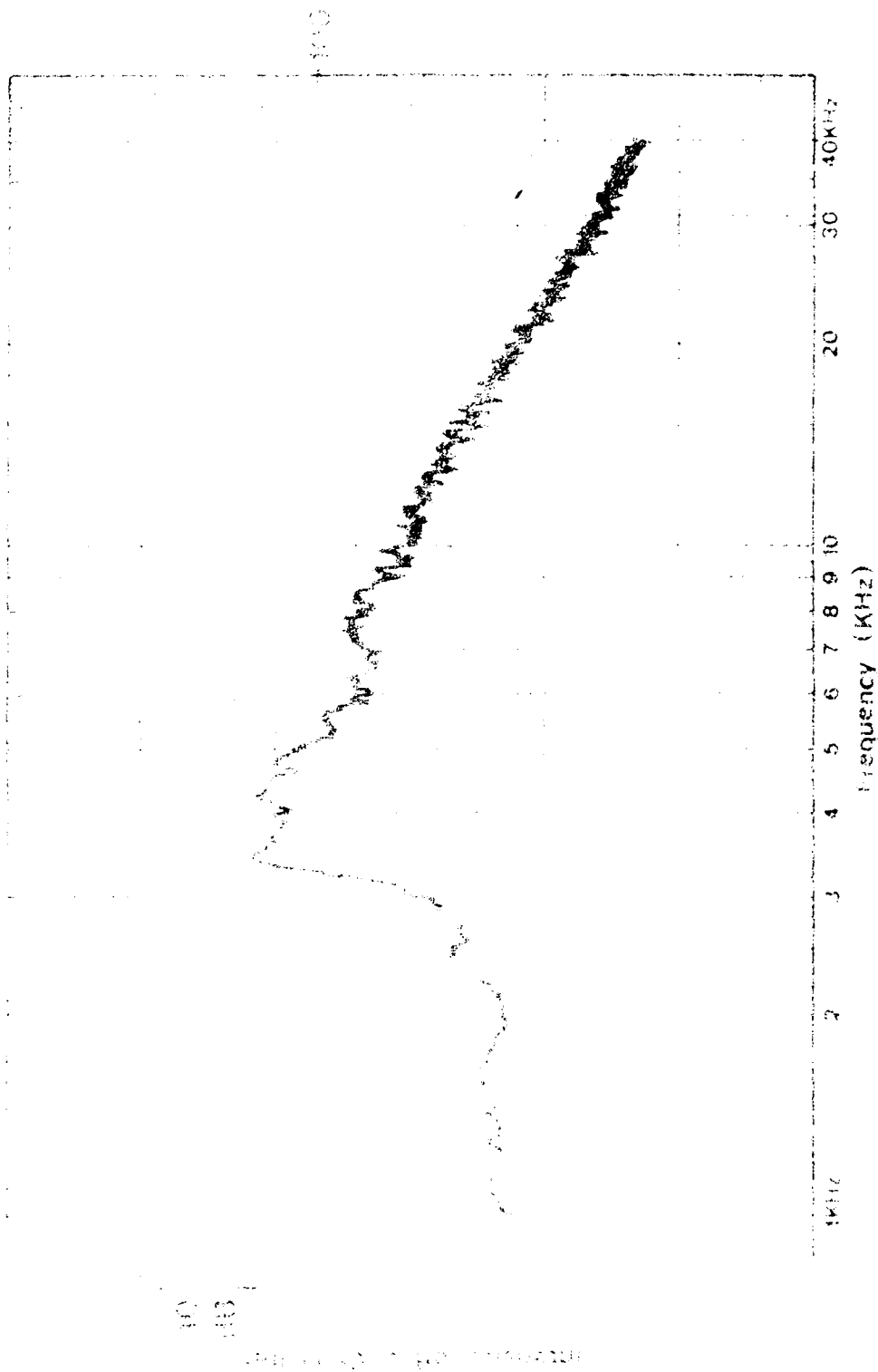
SHOCK ASSOCIATED NOISE

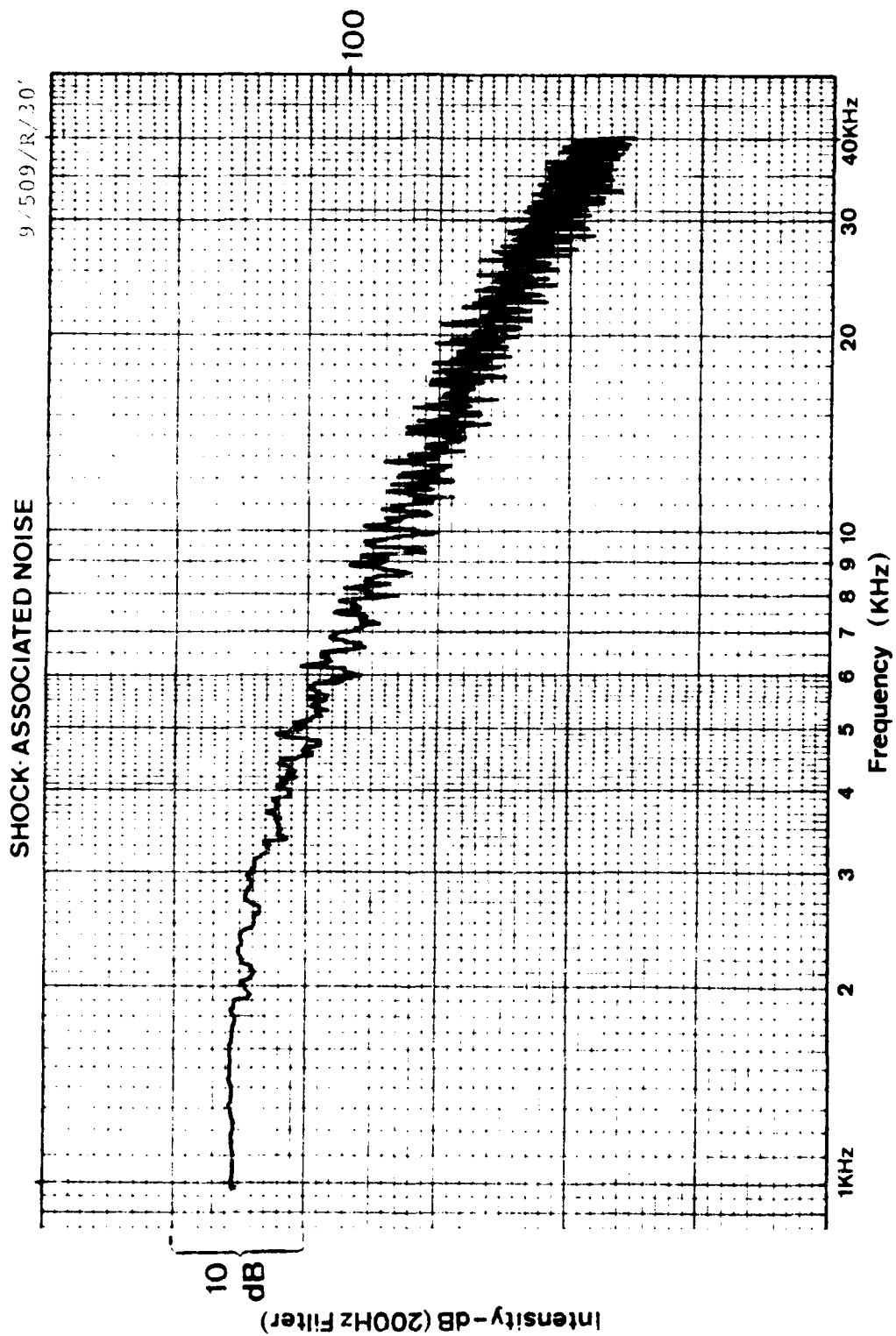


SHOCK-ASSOCIATED NOISE

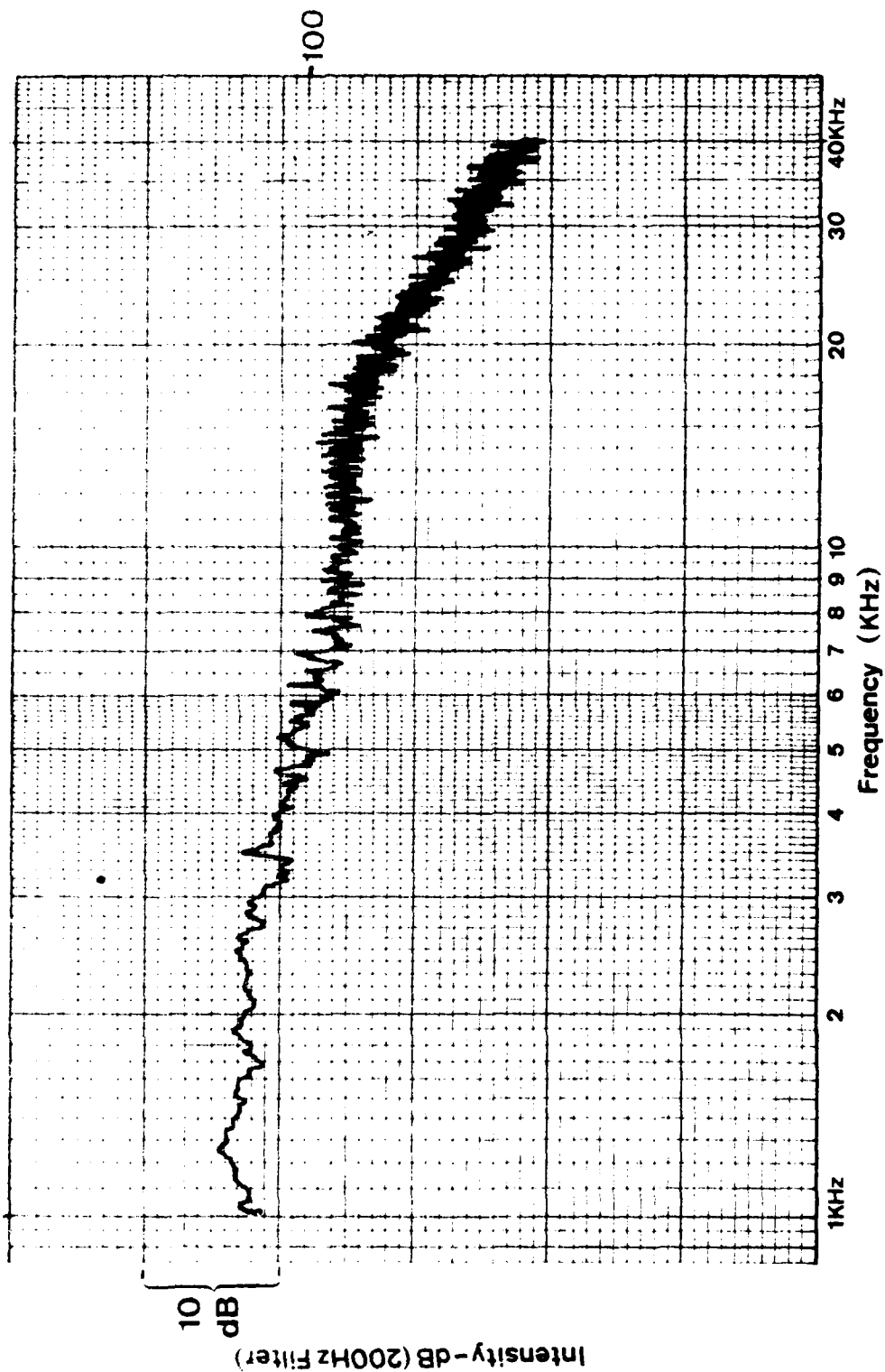


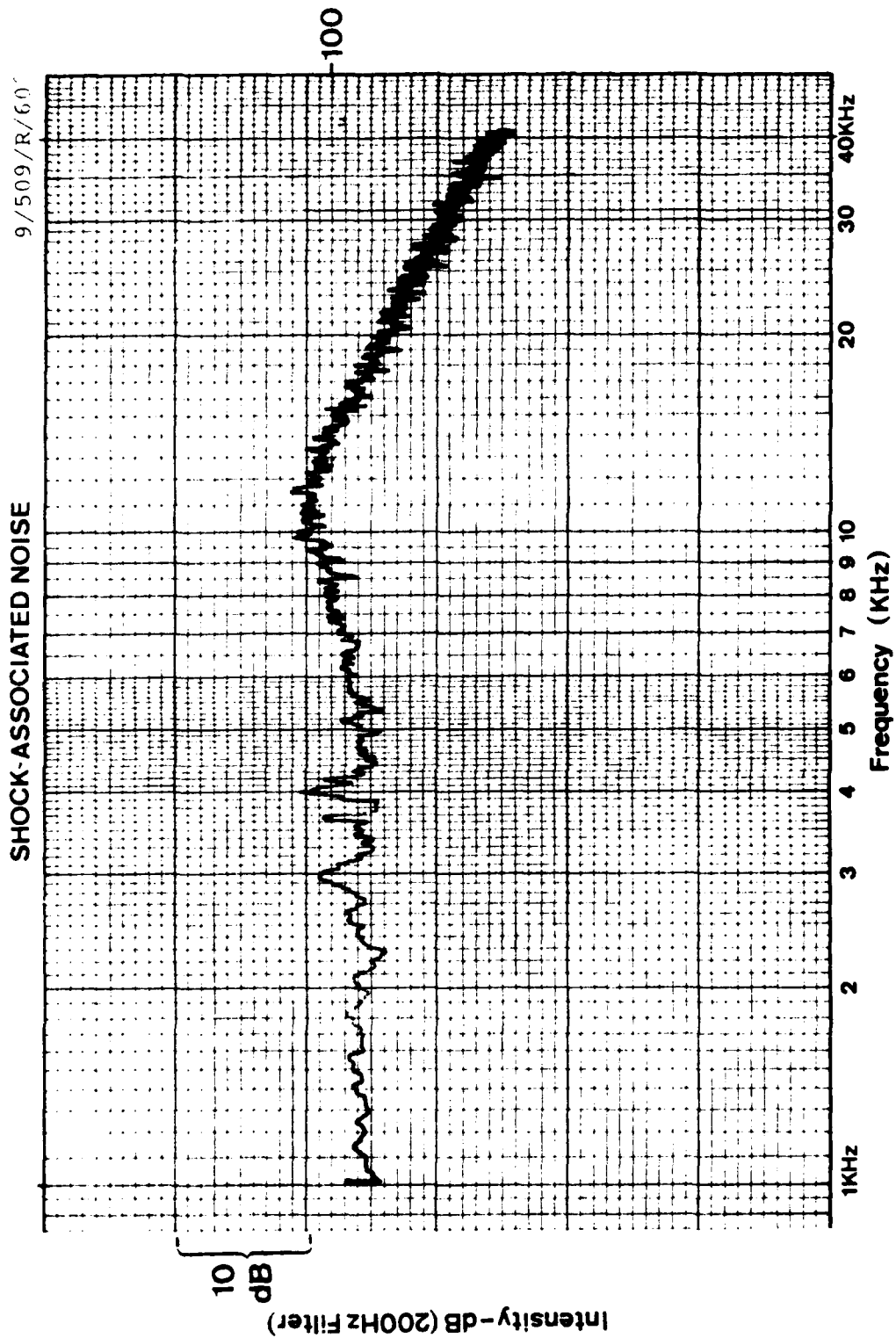
SPECTRUM ASSOCIATED NOISE

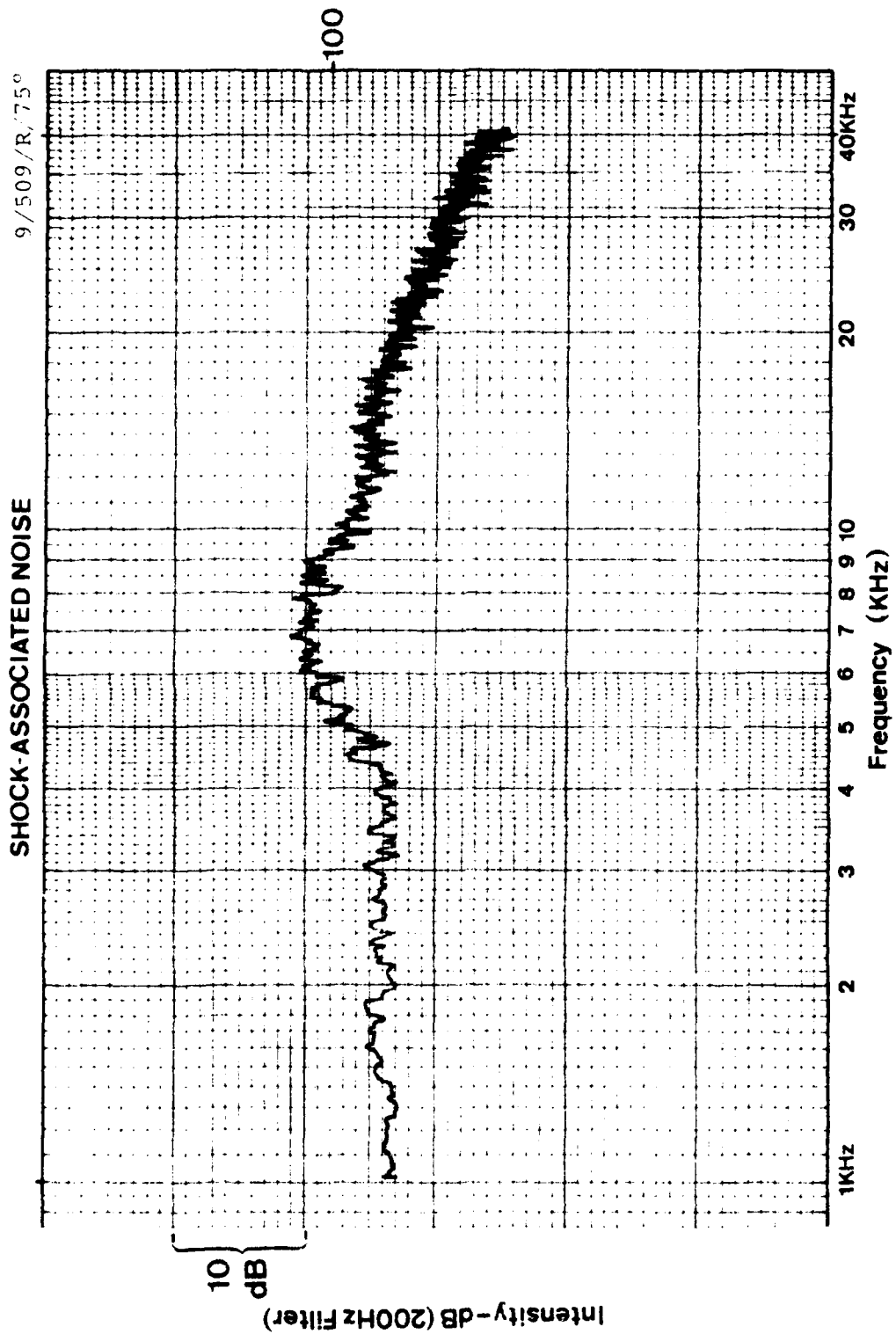


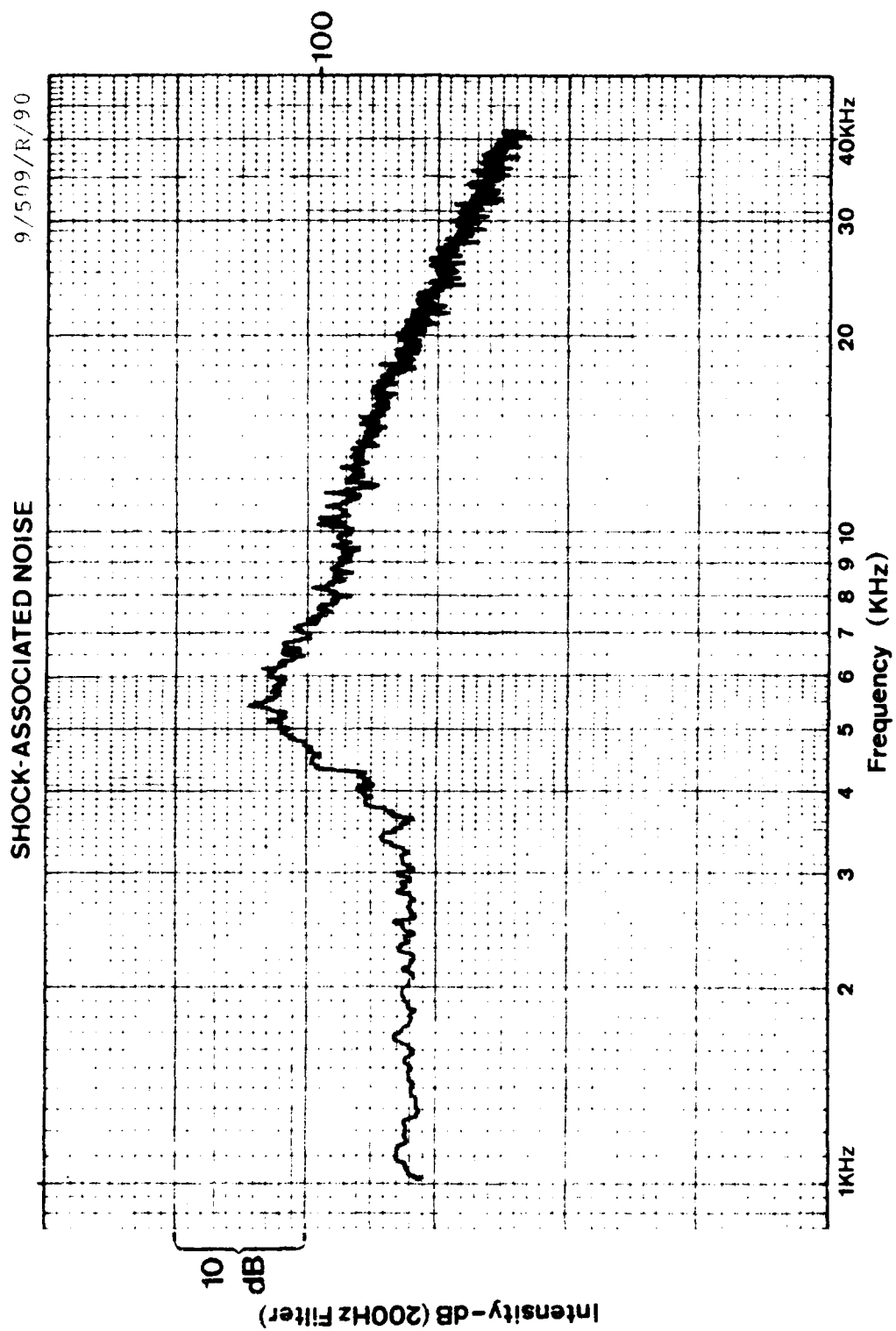


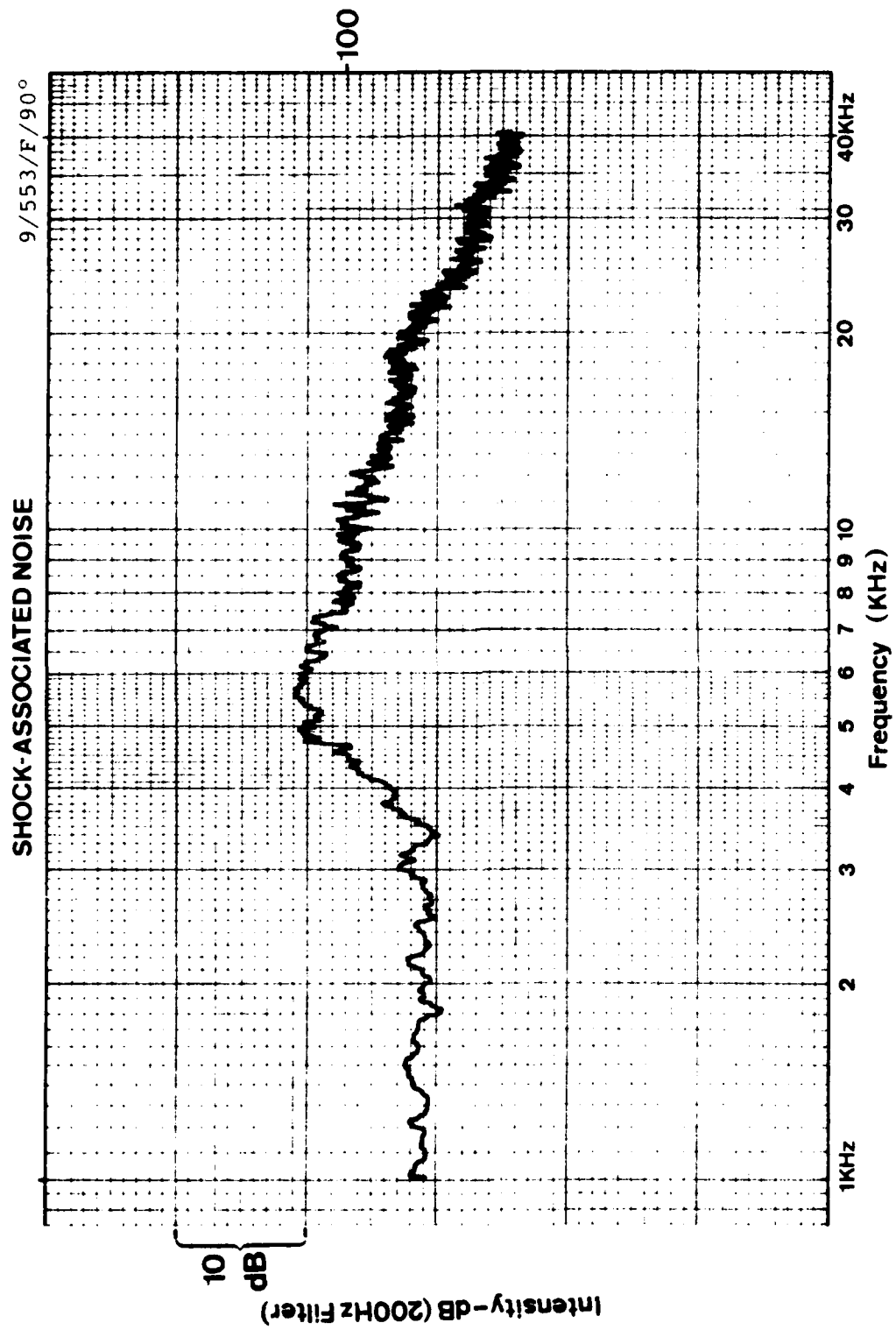
SHOCK-ASSOCIATED NOISE

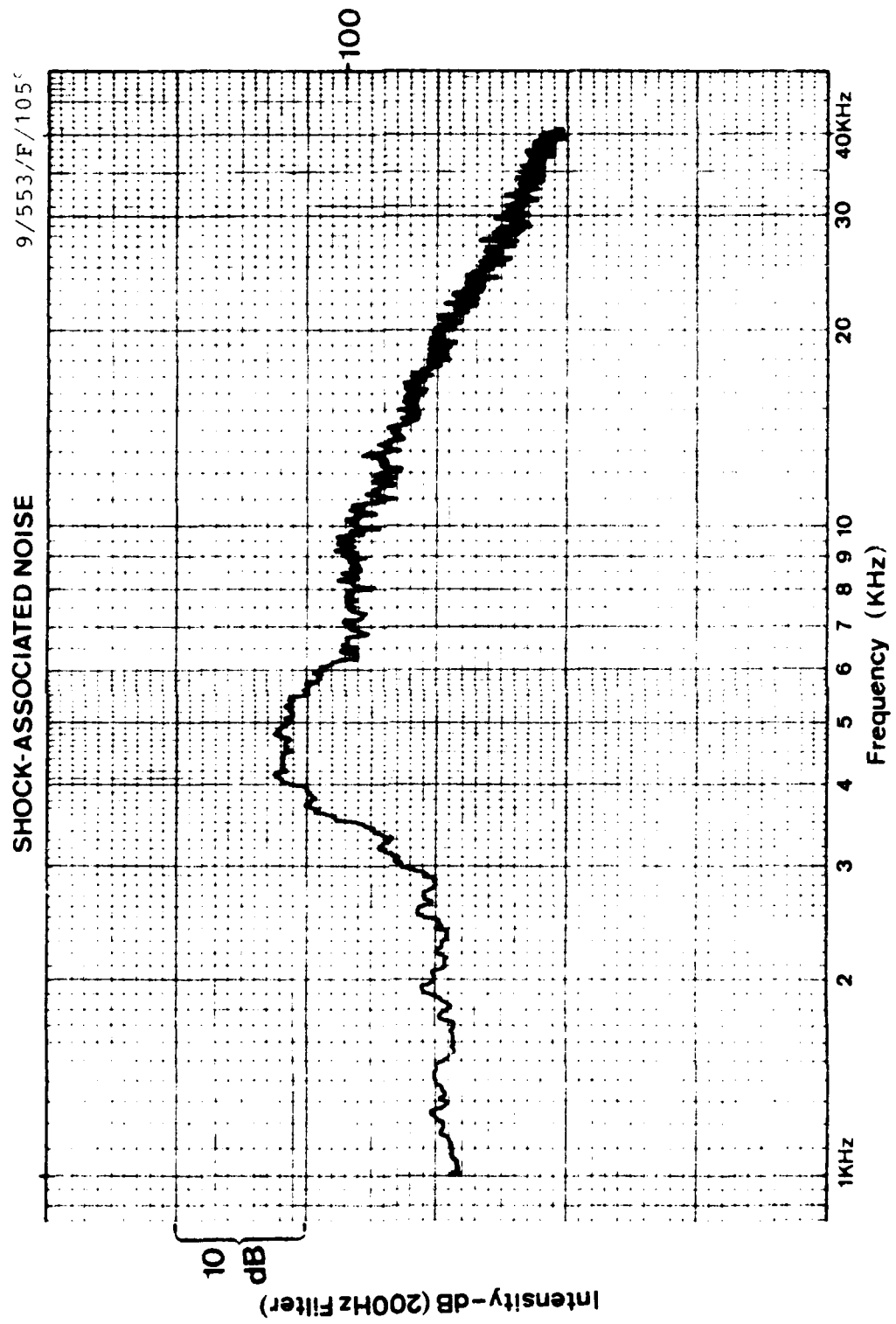


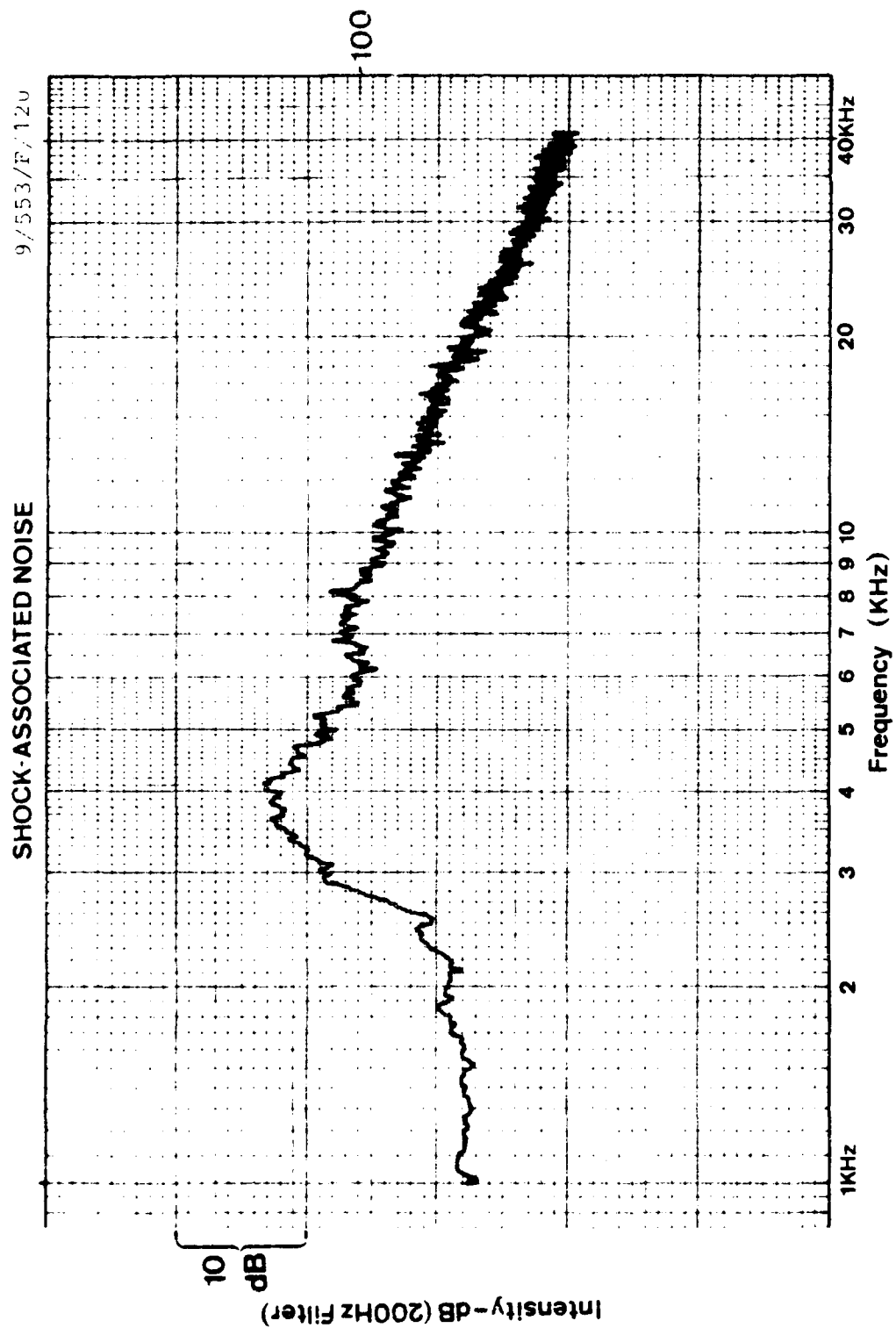


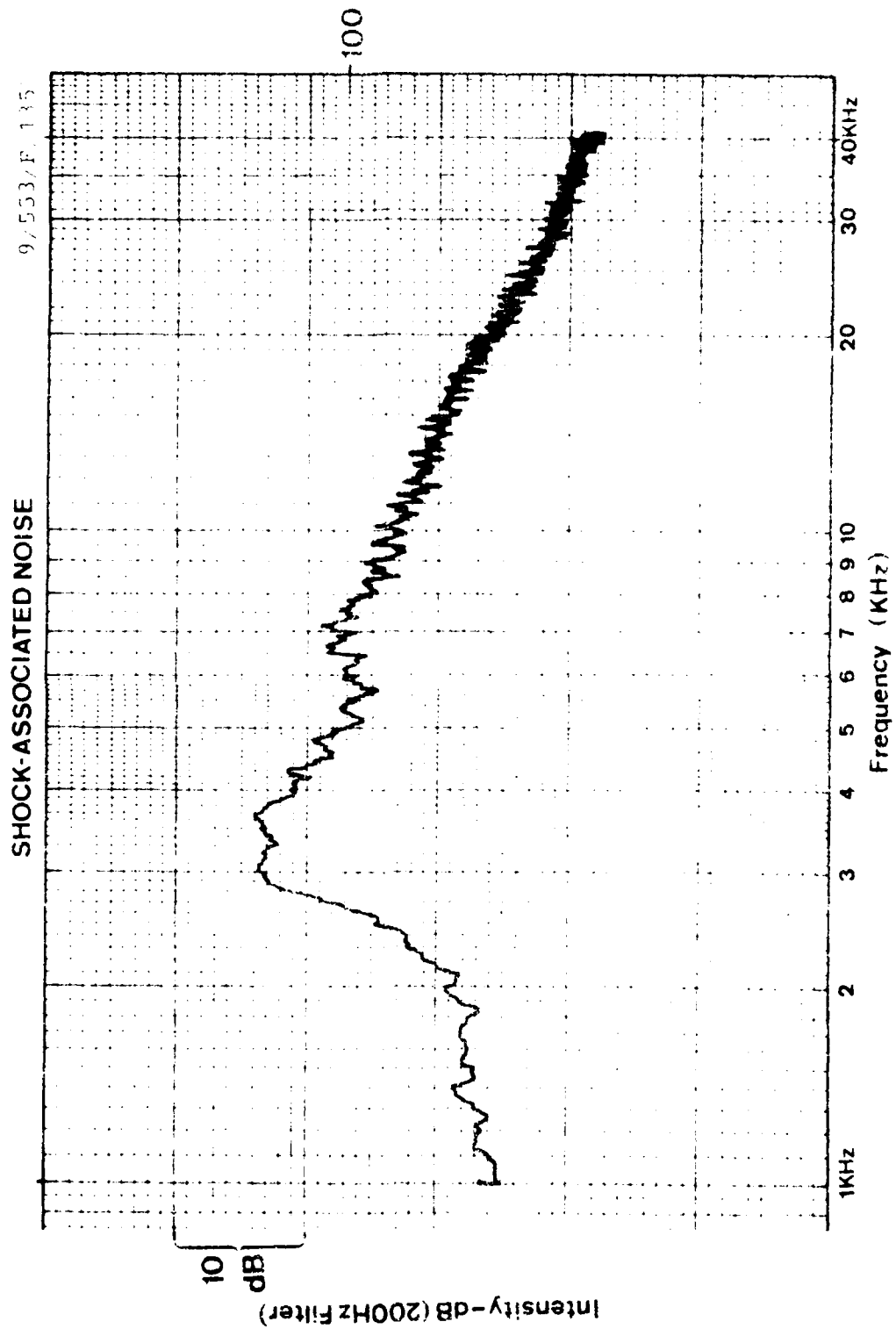


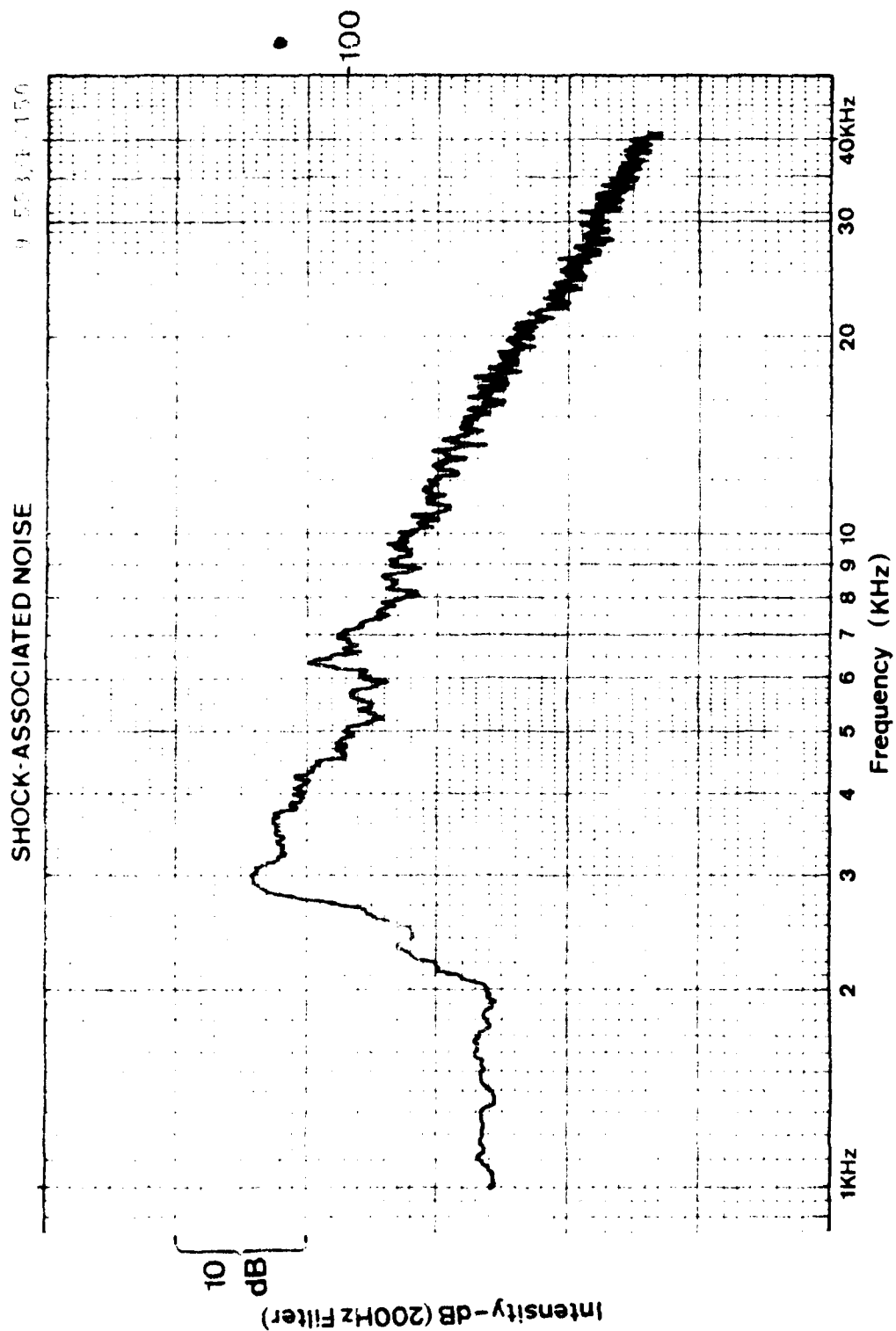


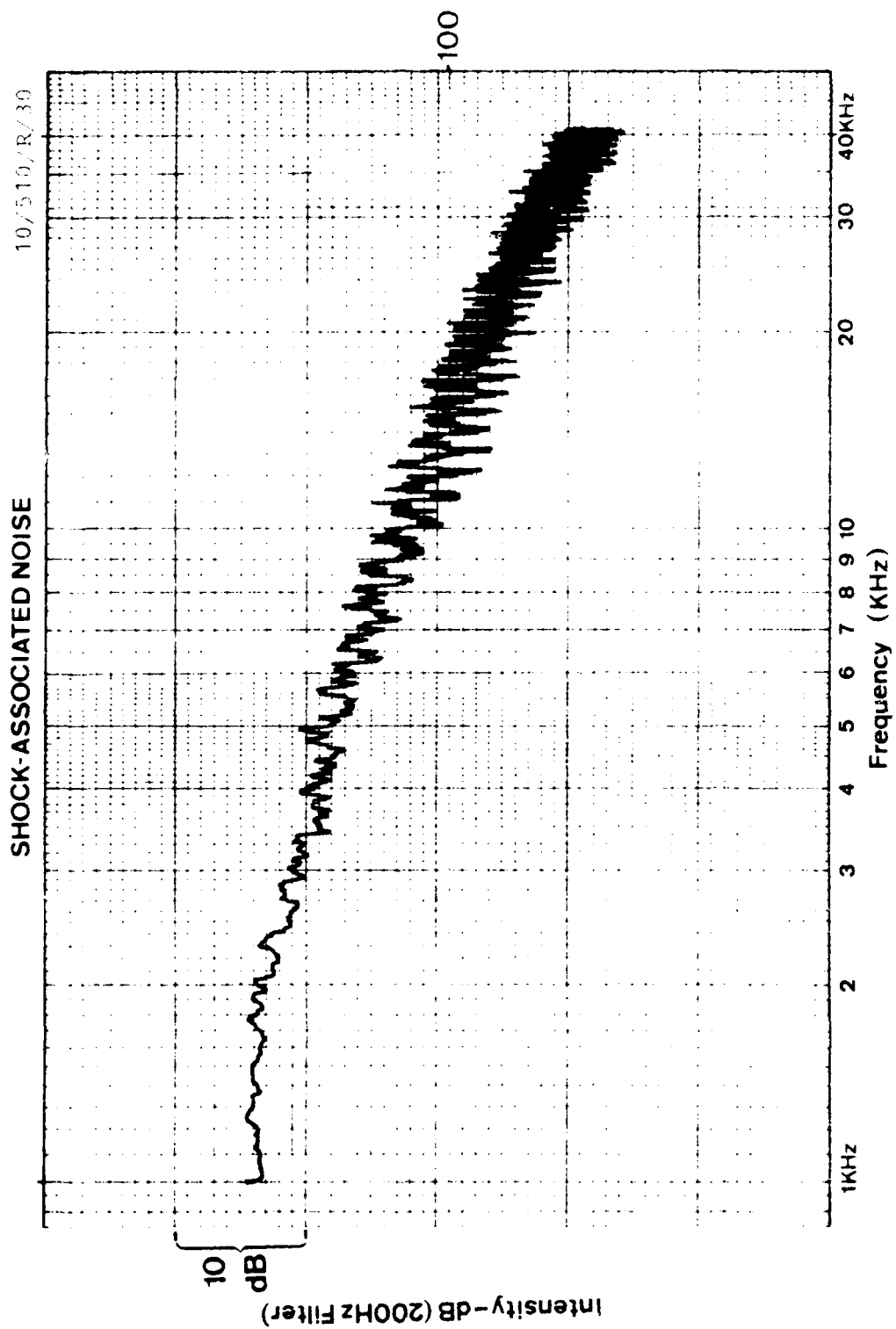


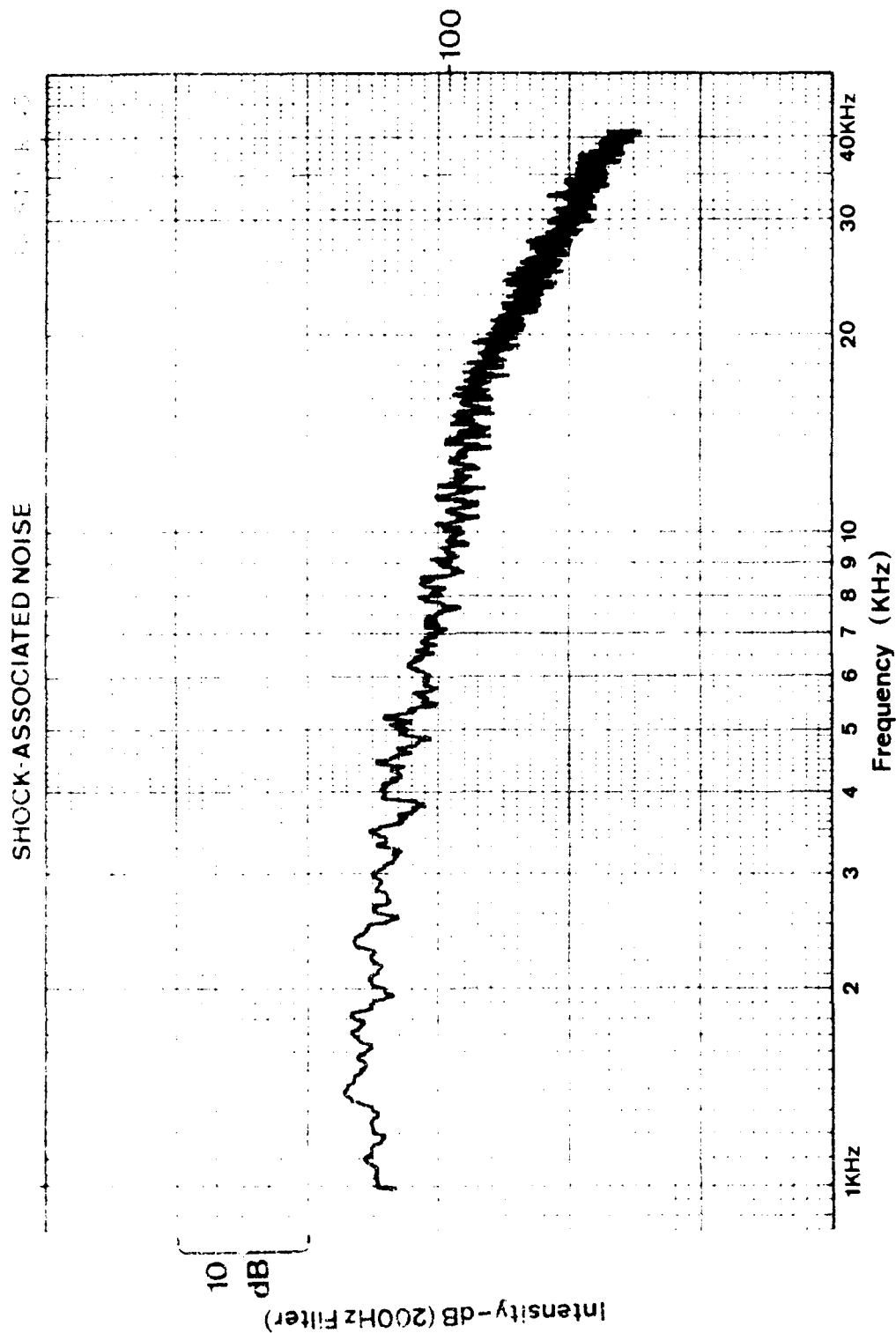


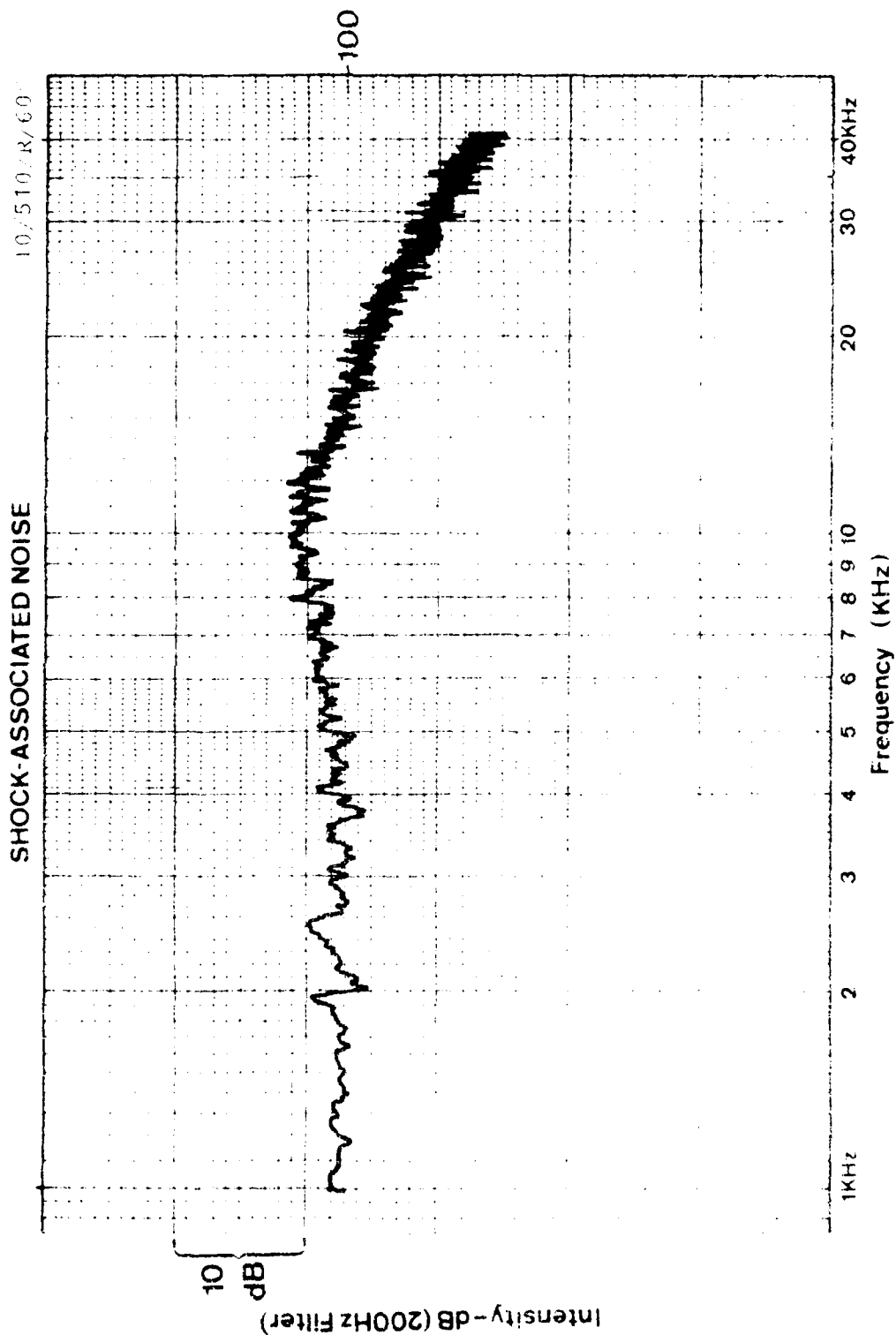


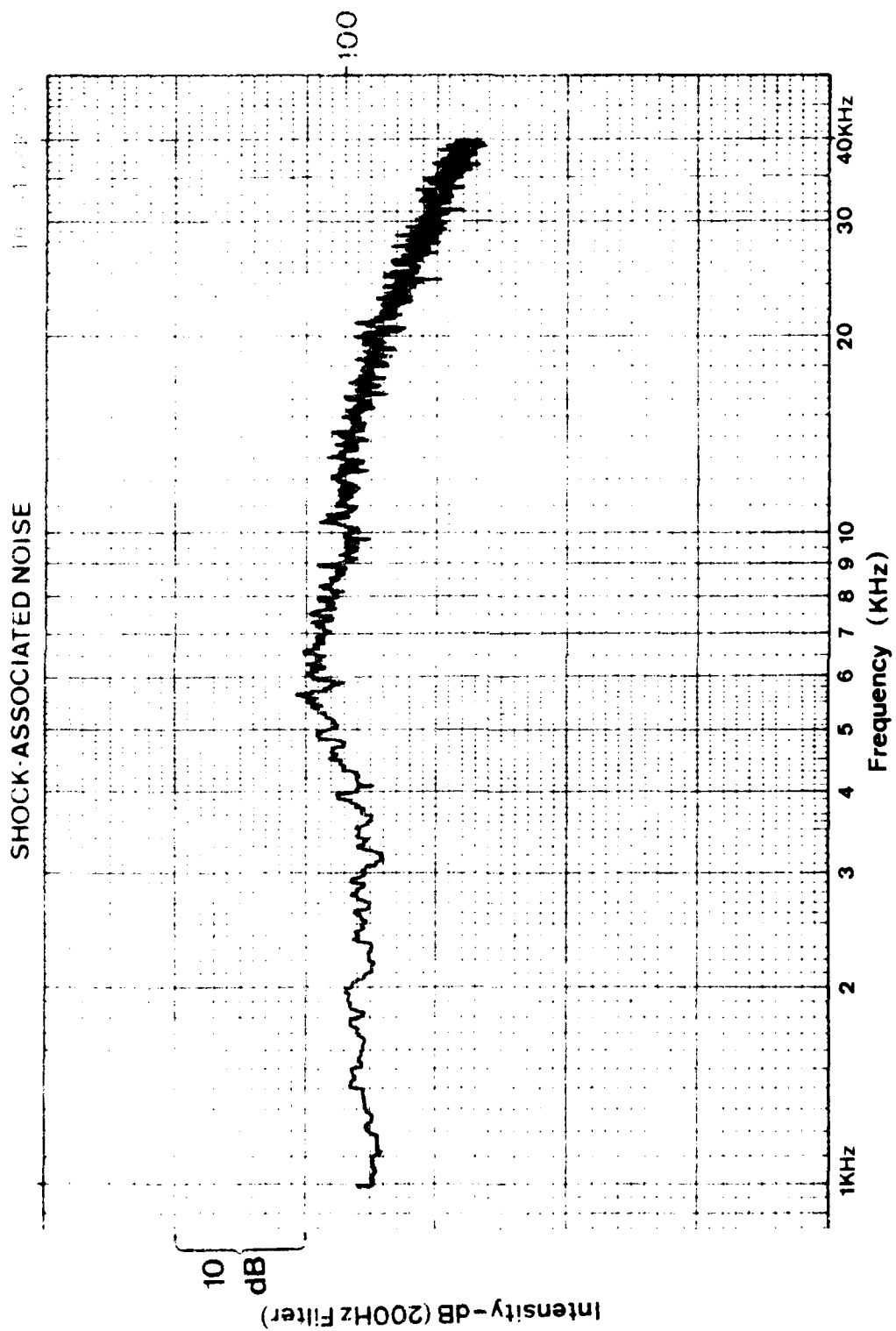


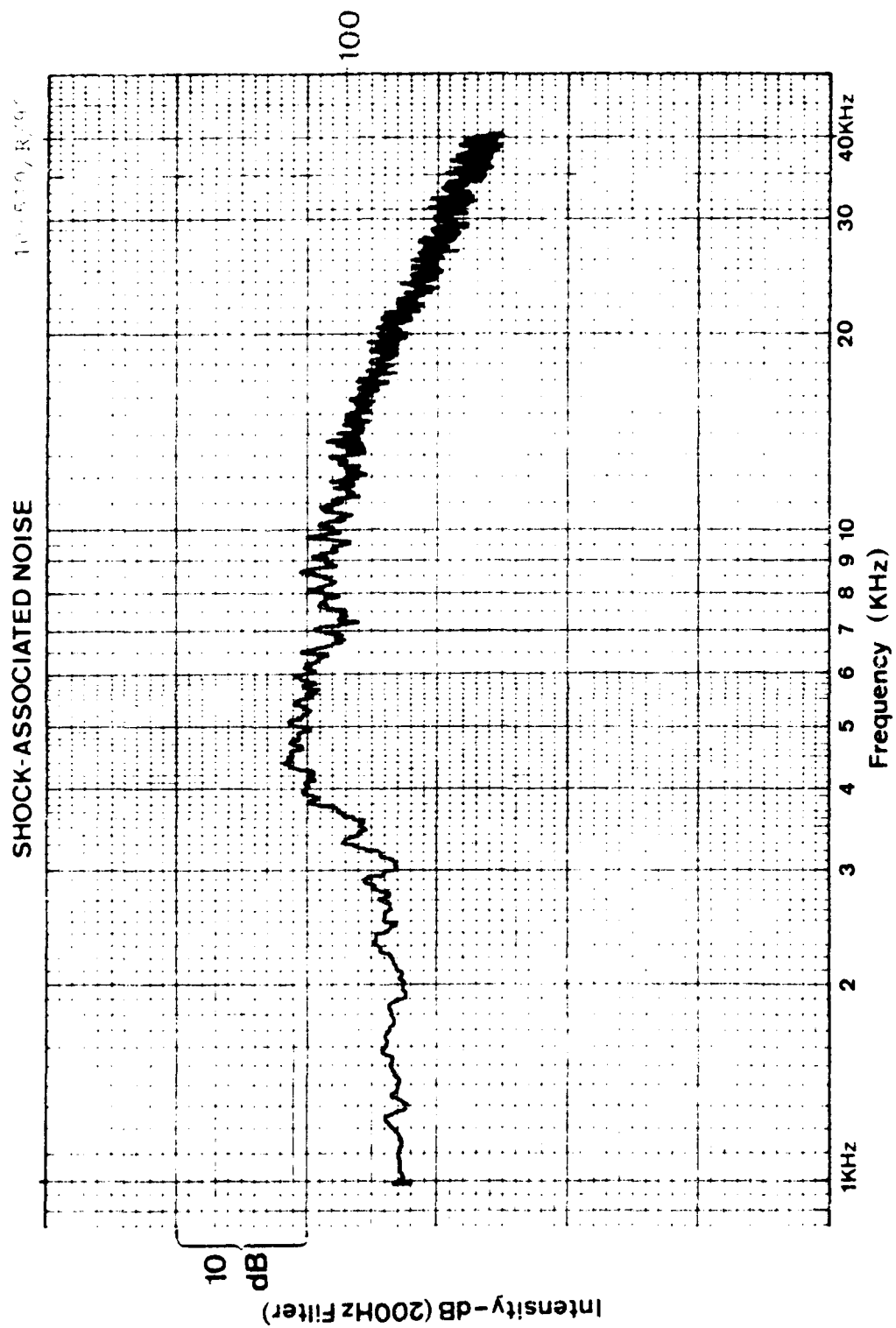


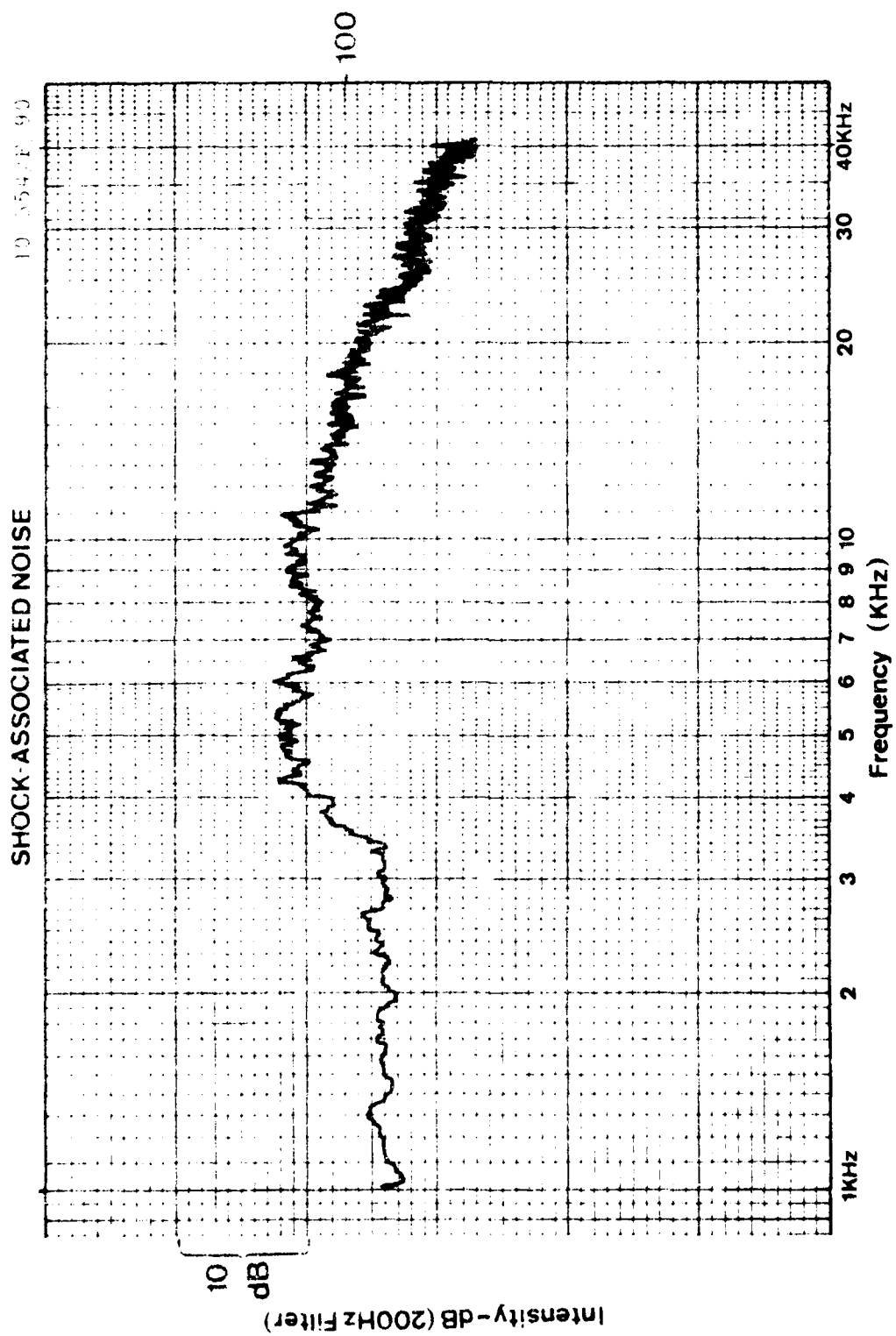


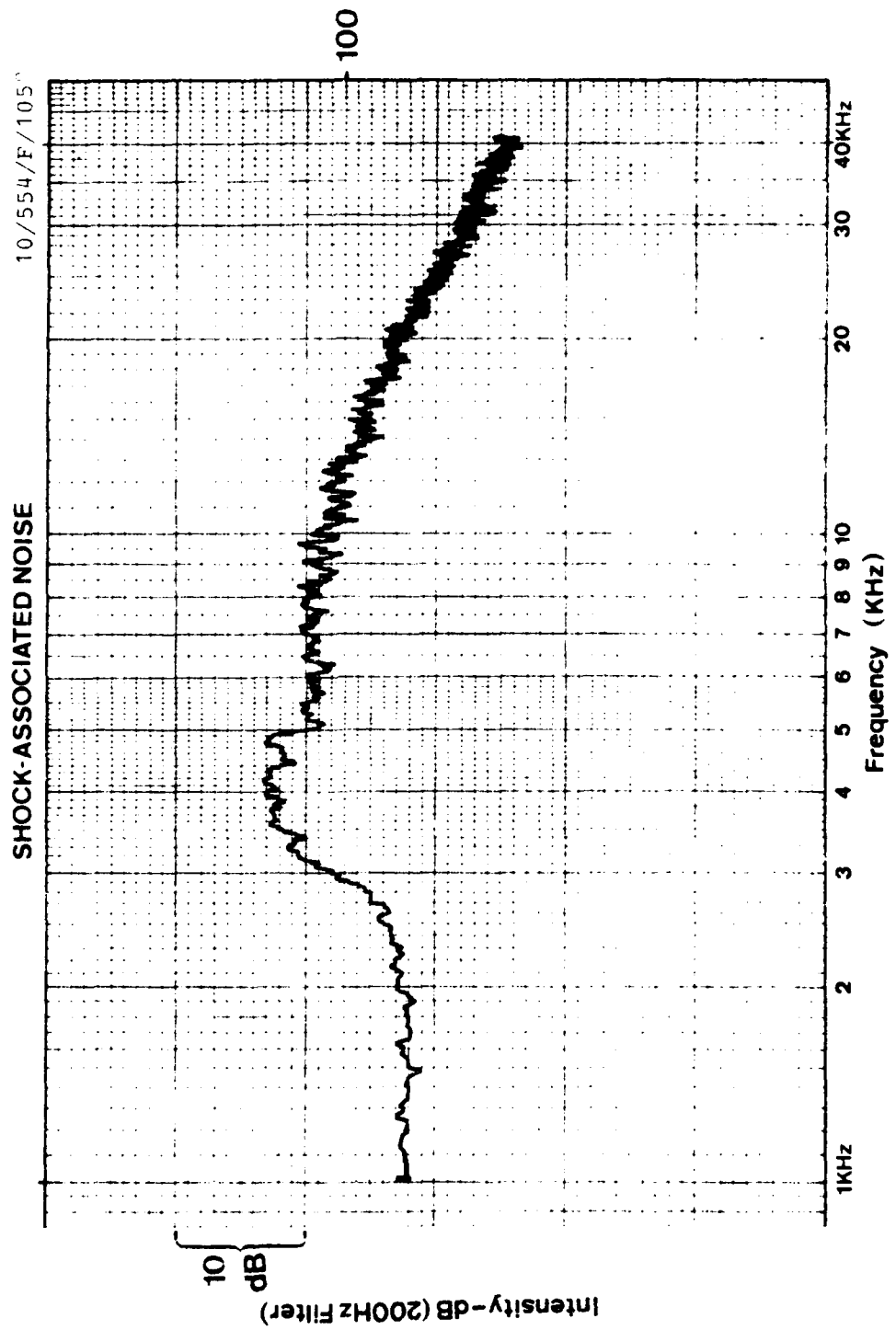


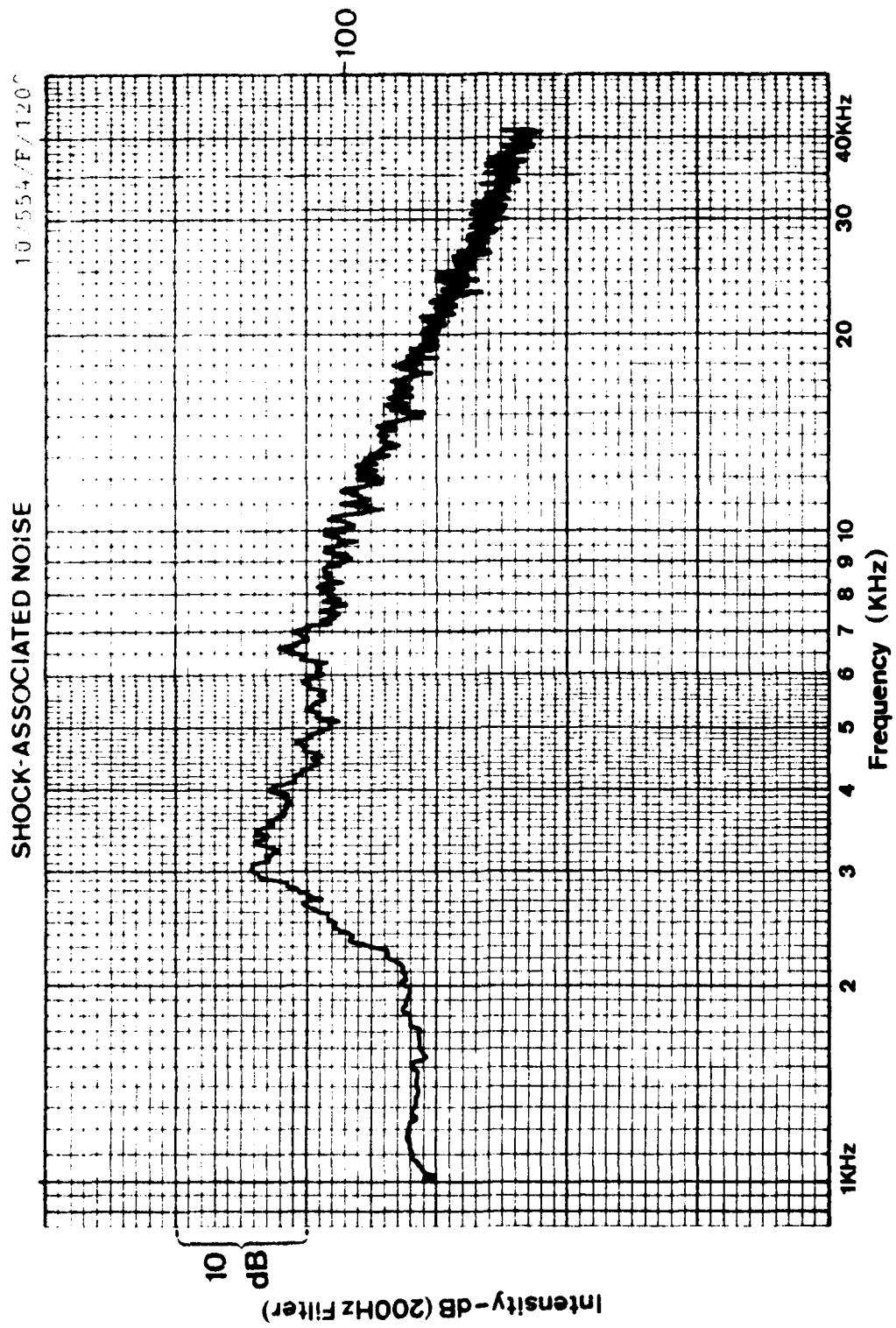


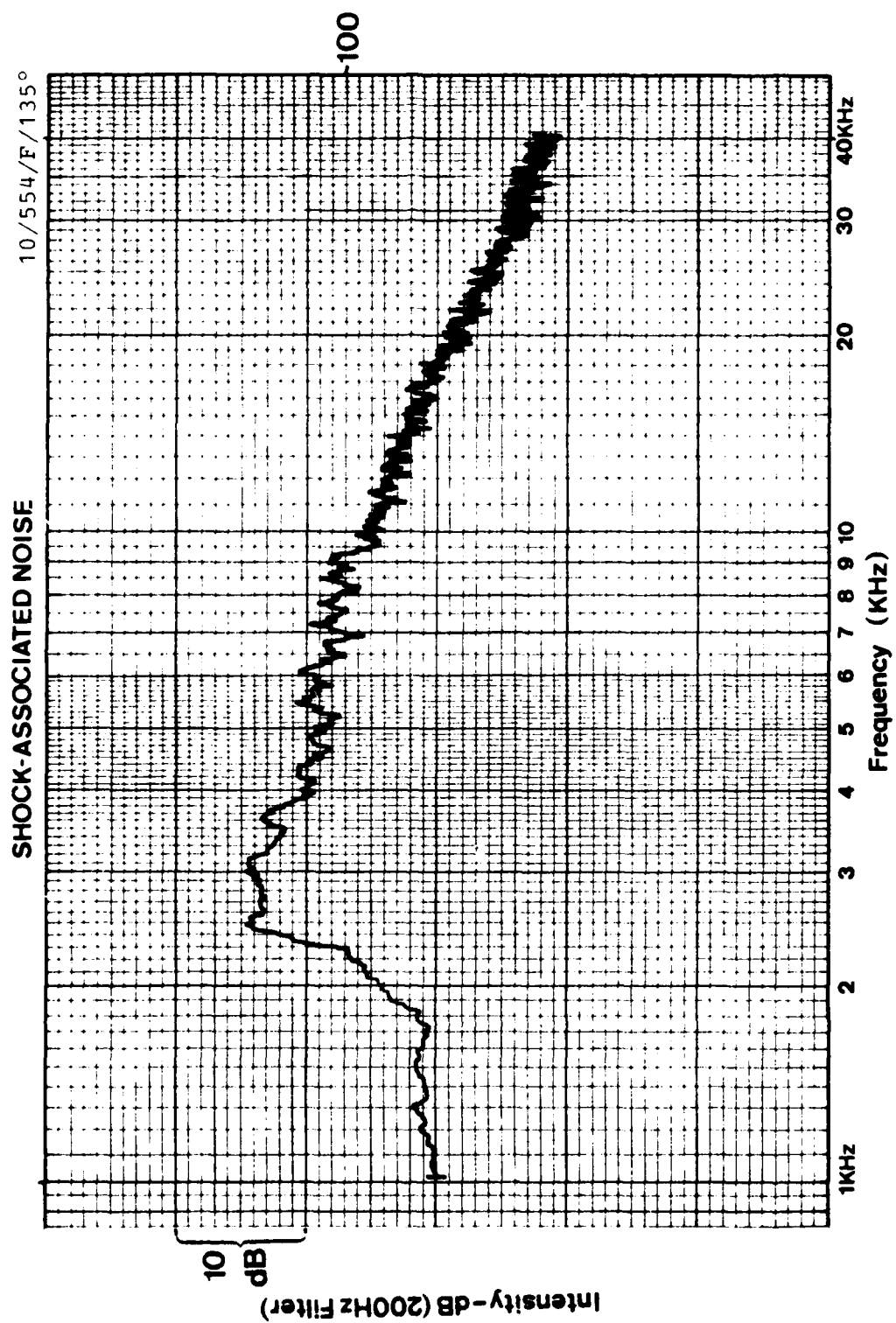


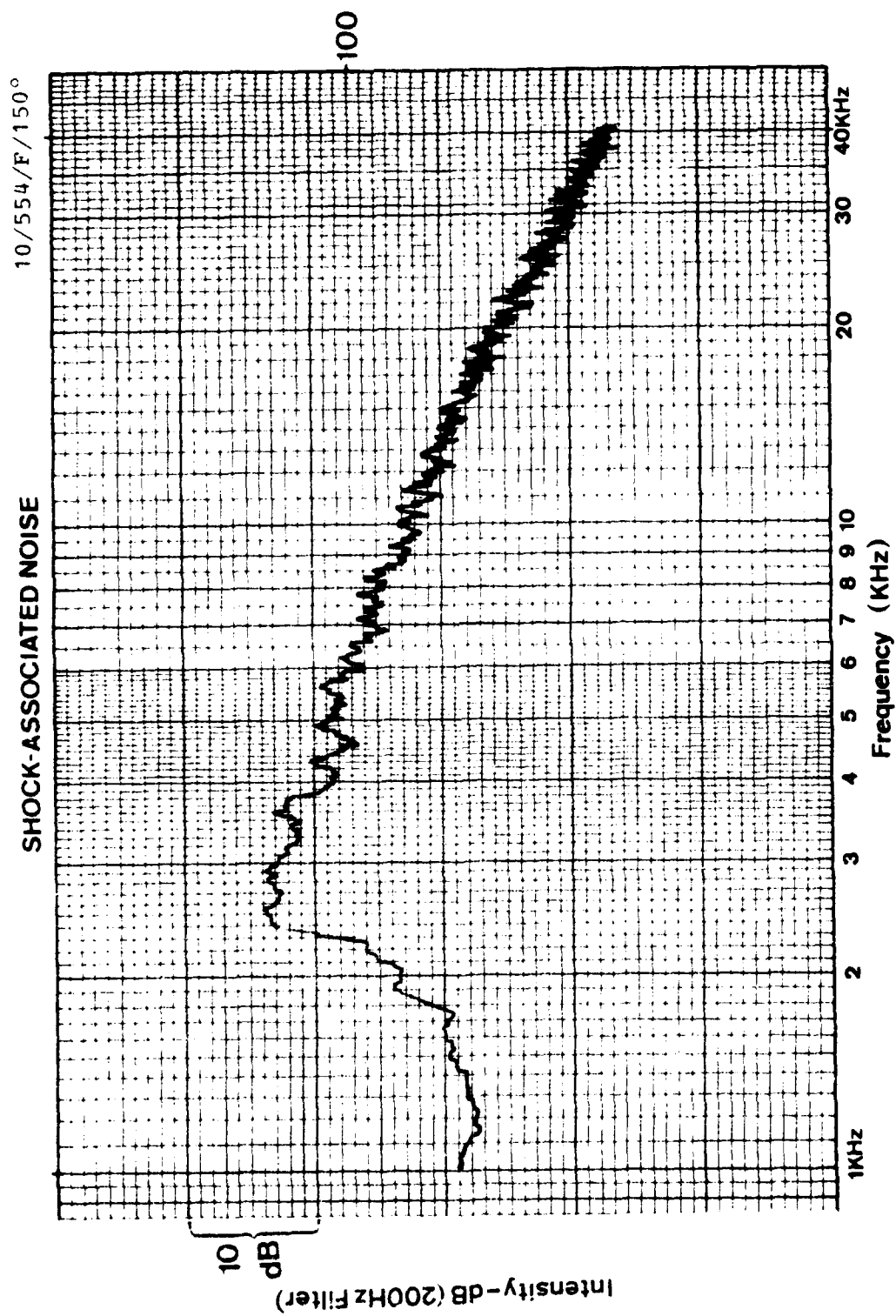


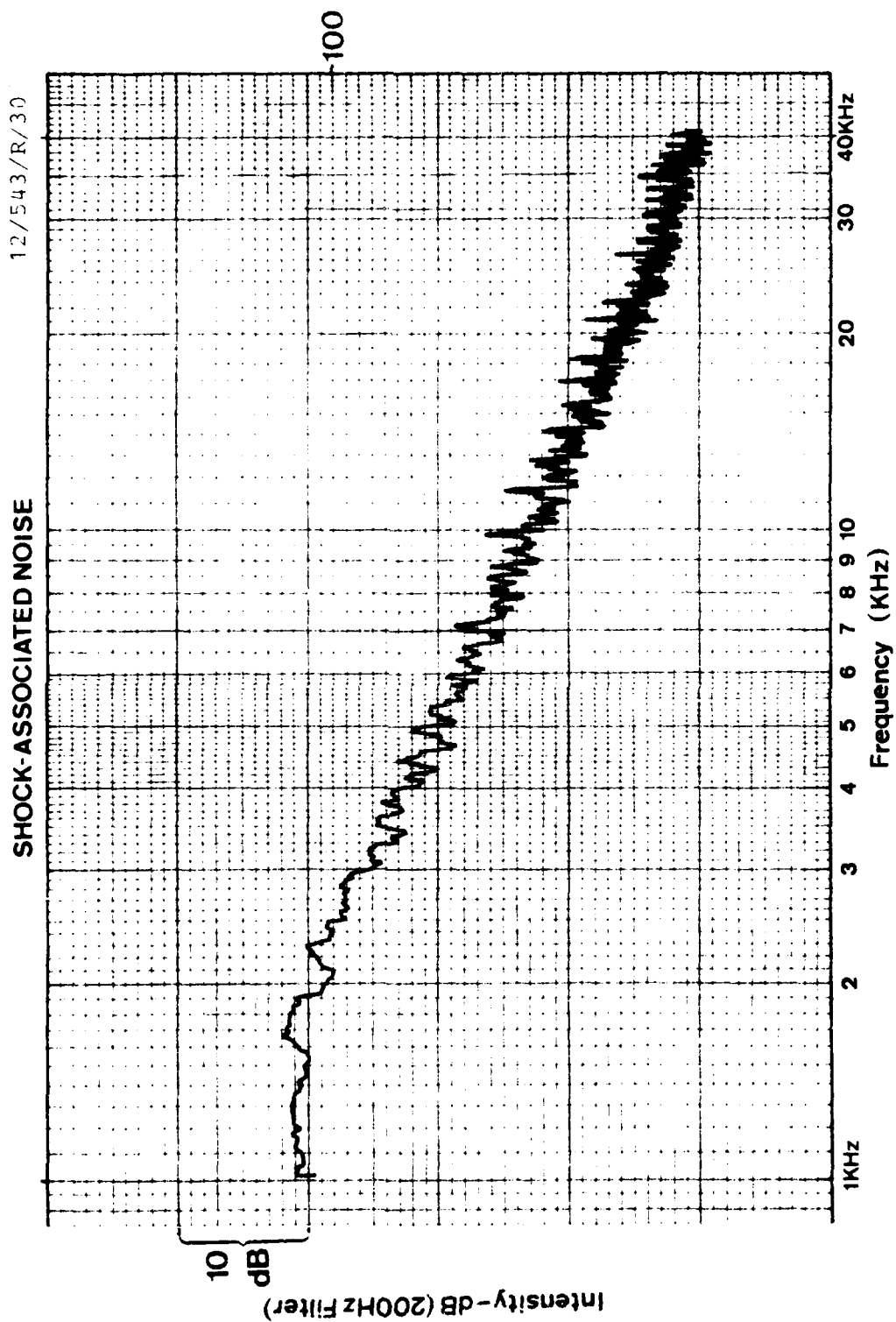


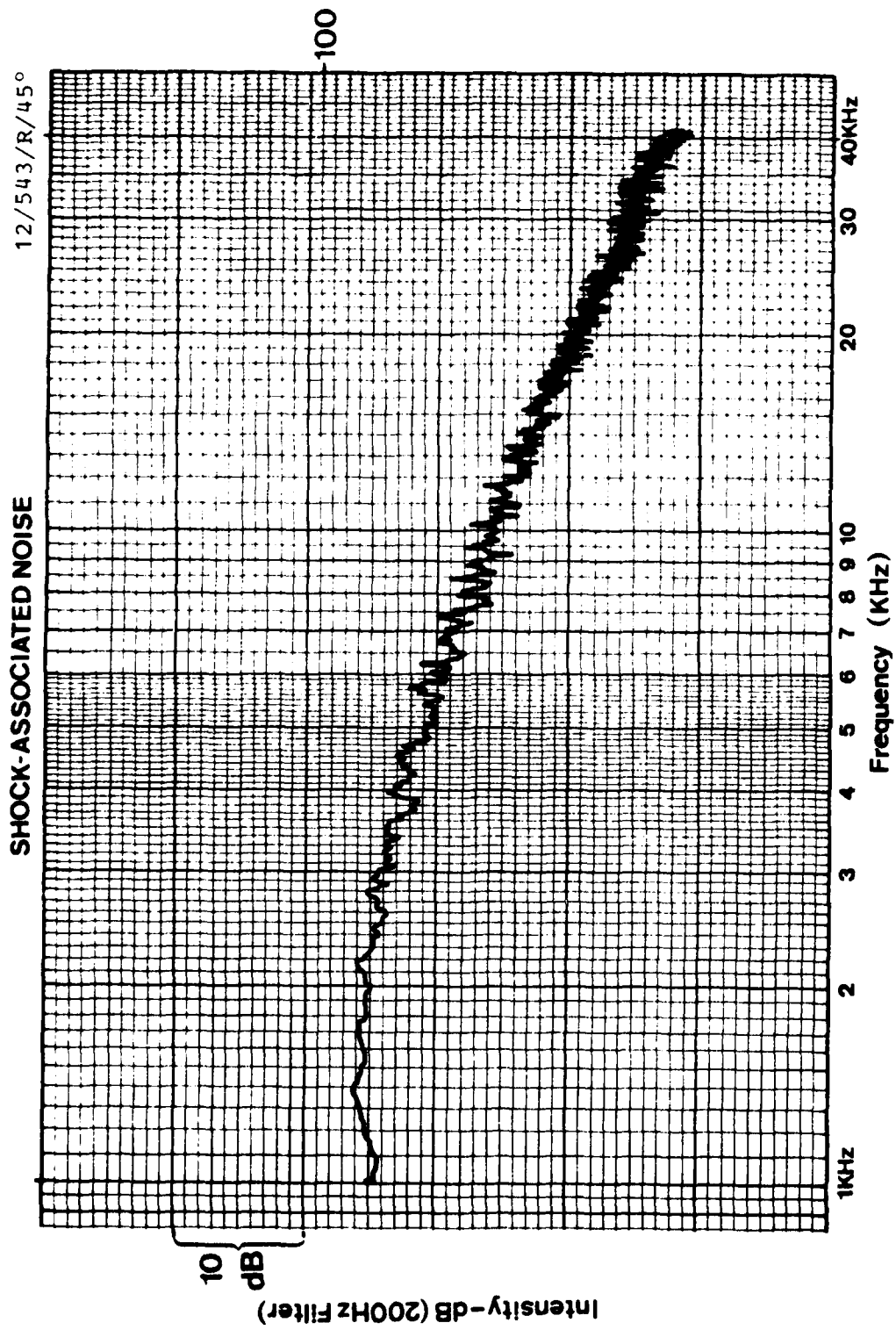


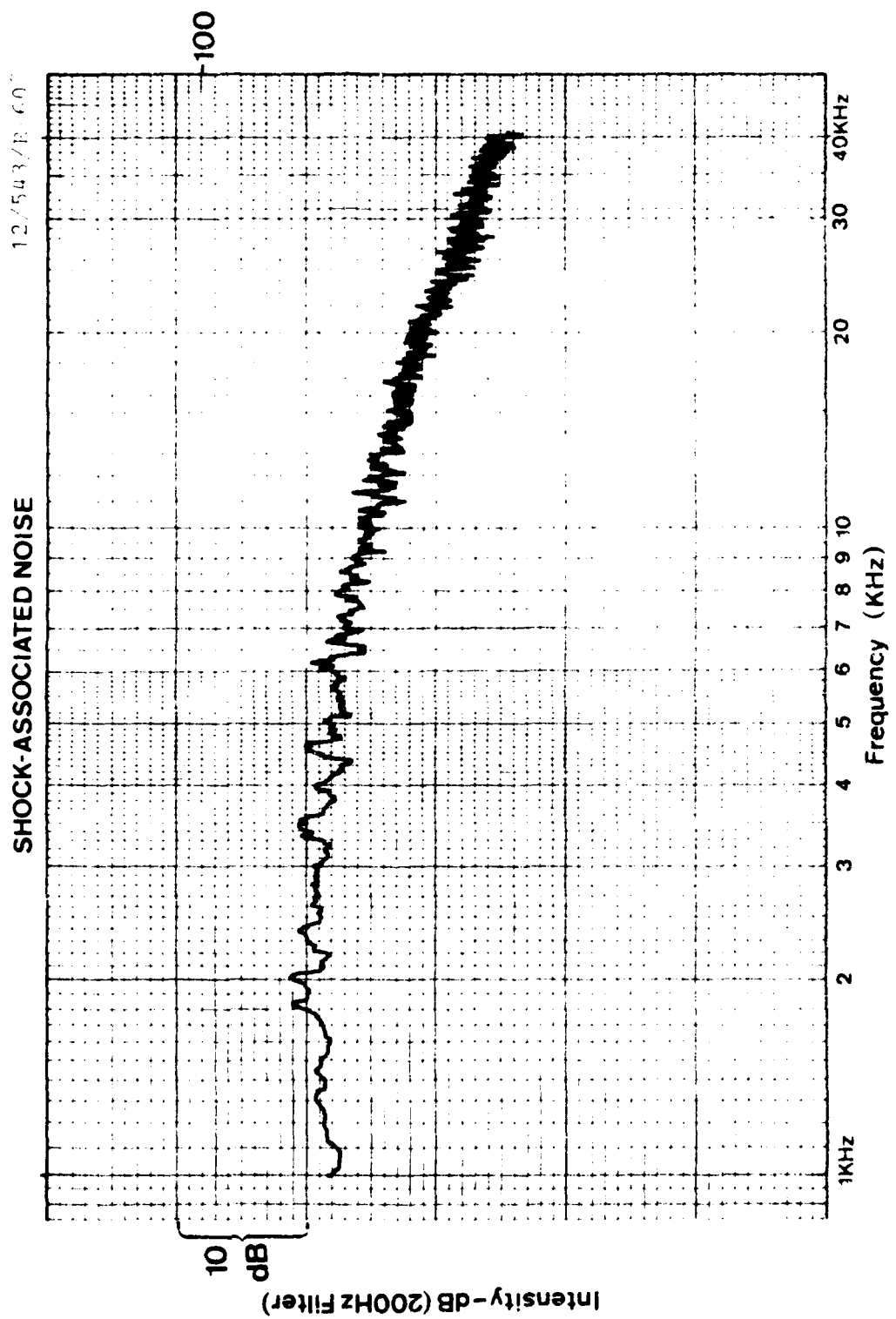


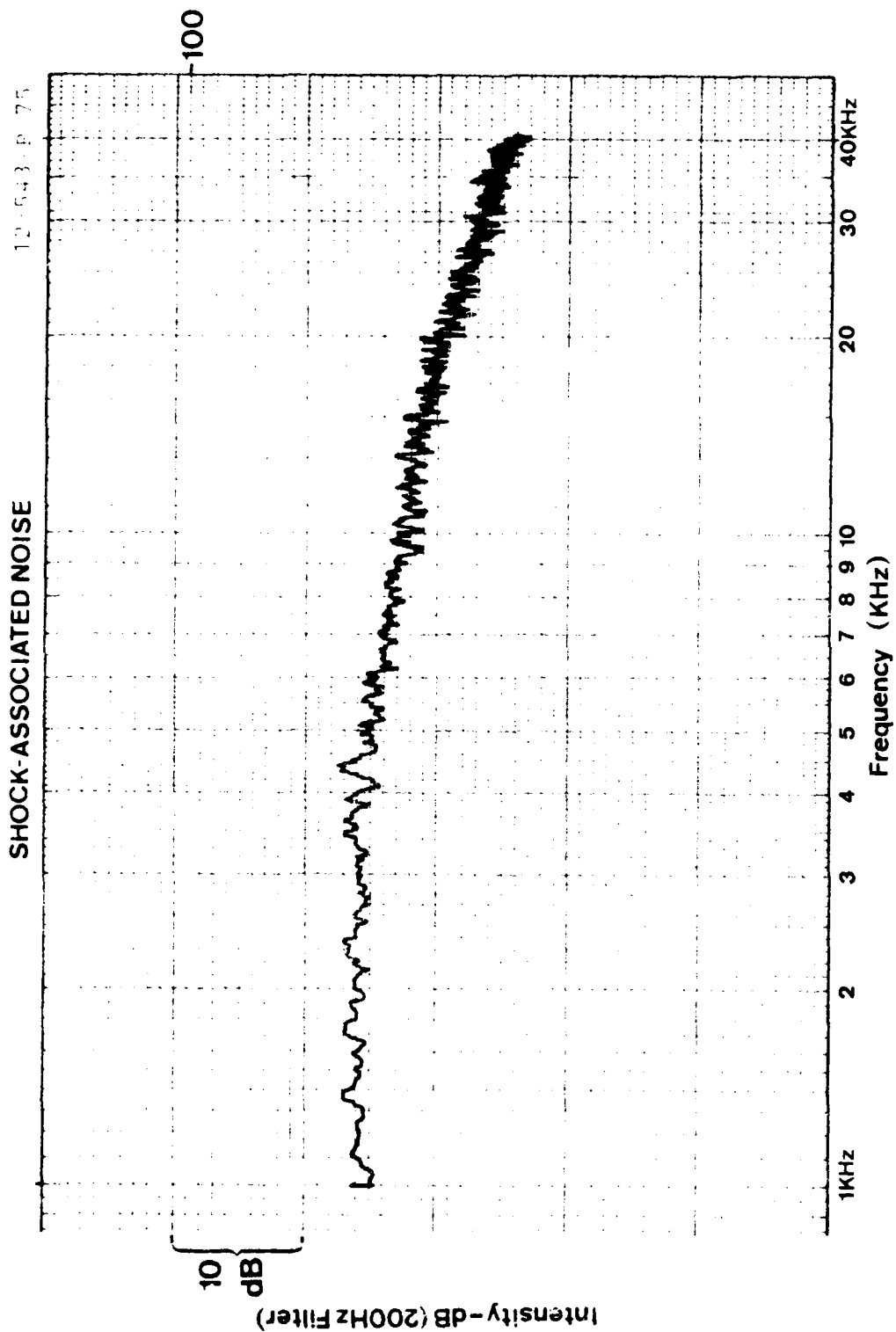


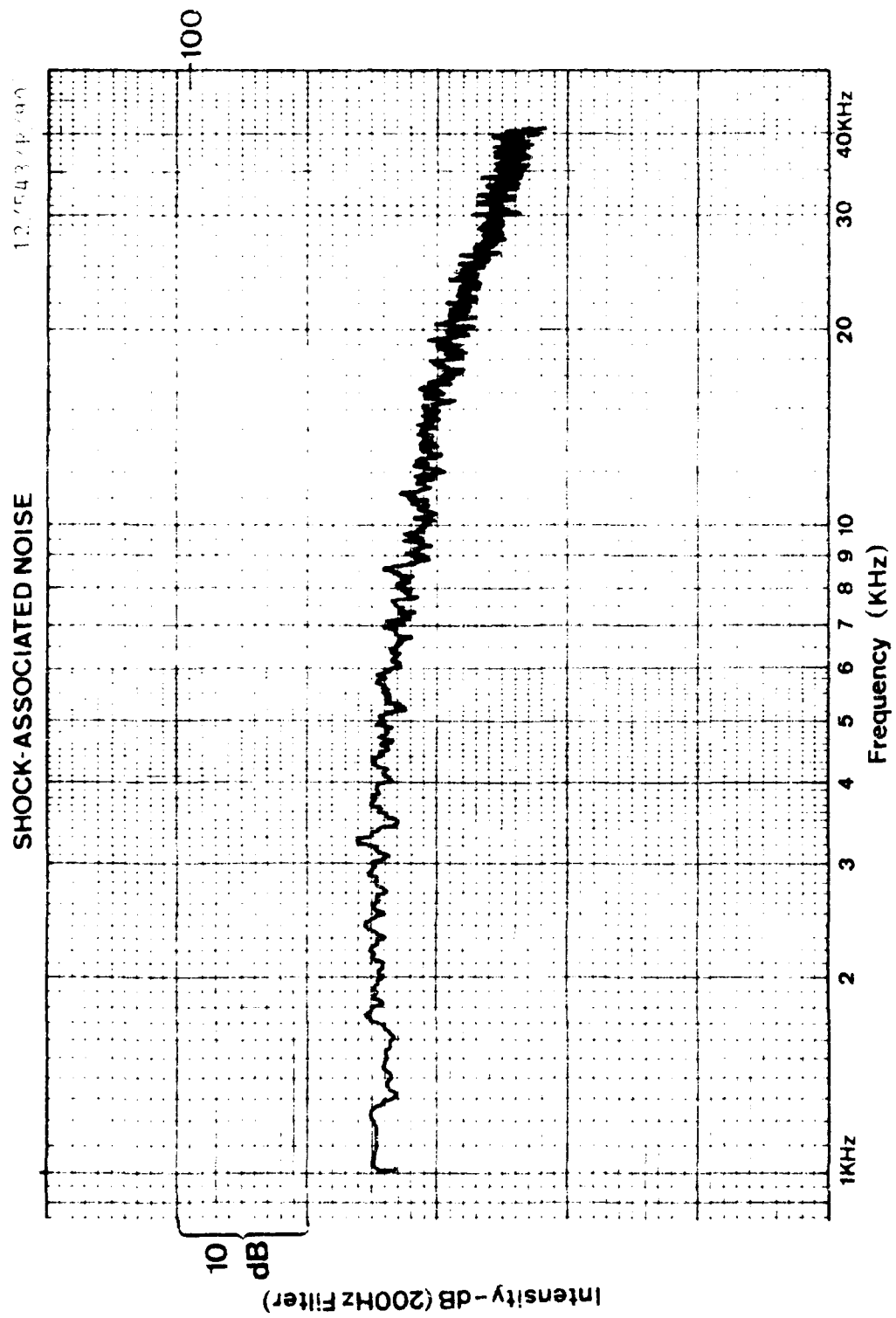


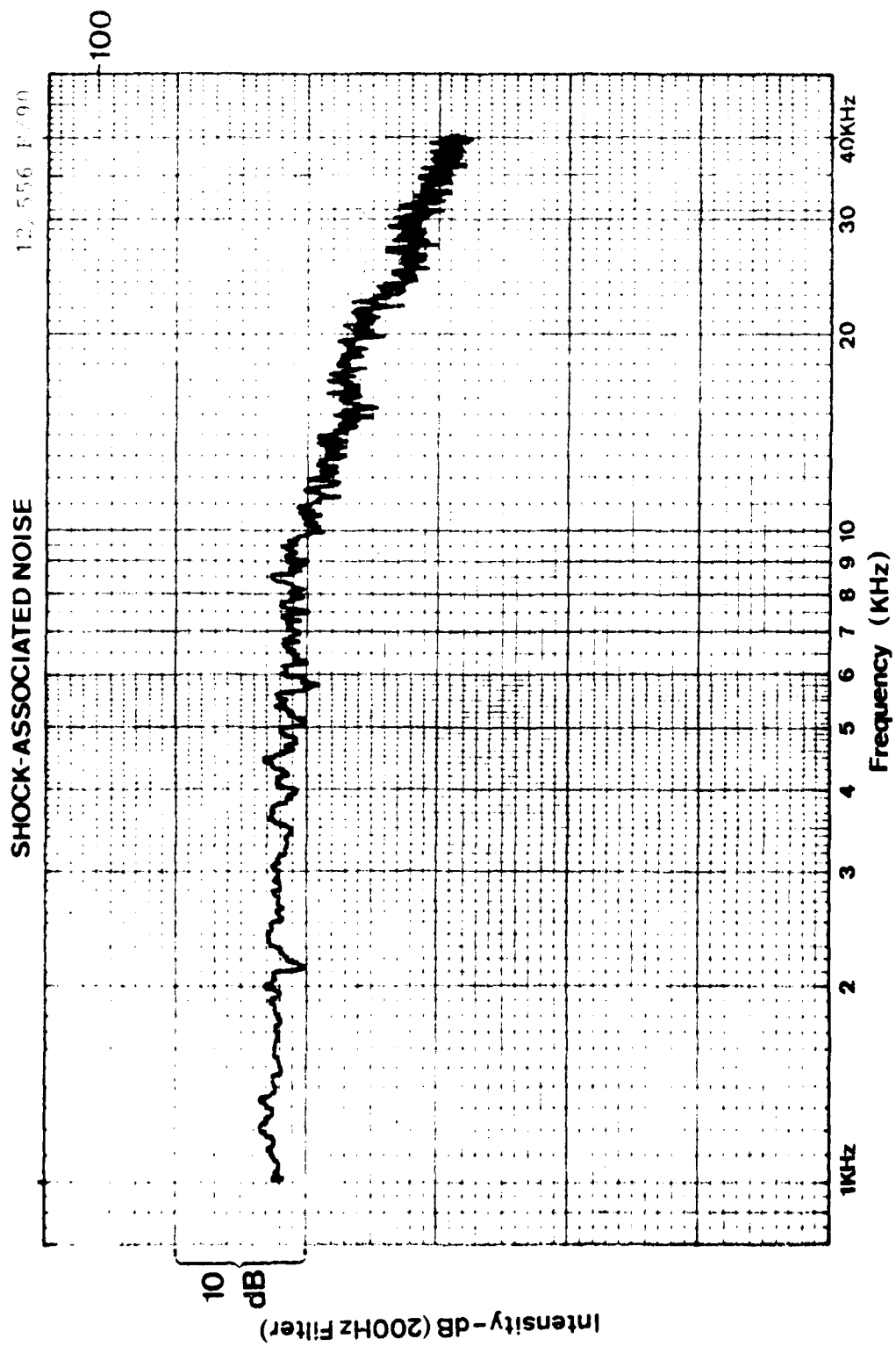


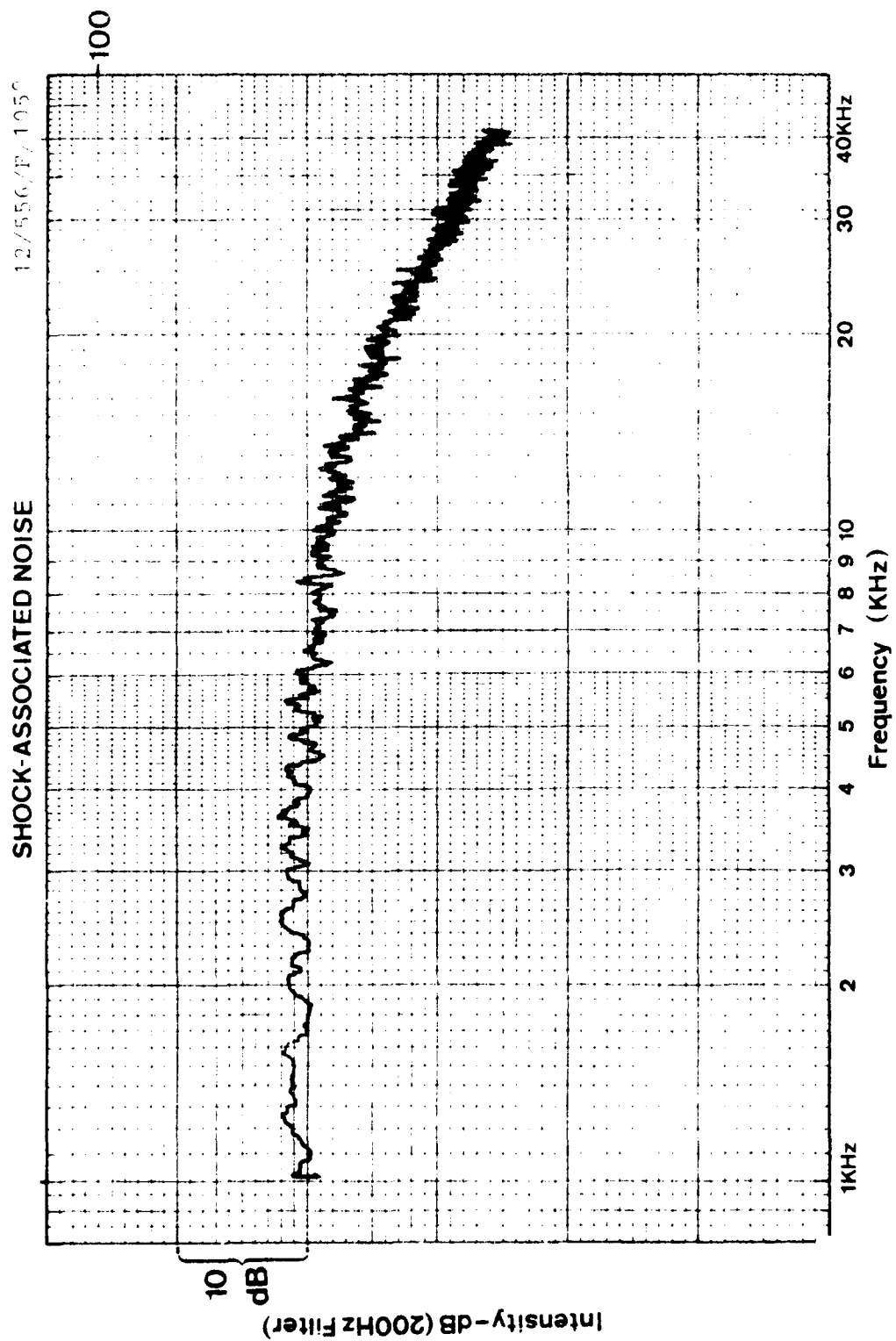


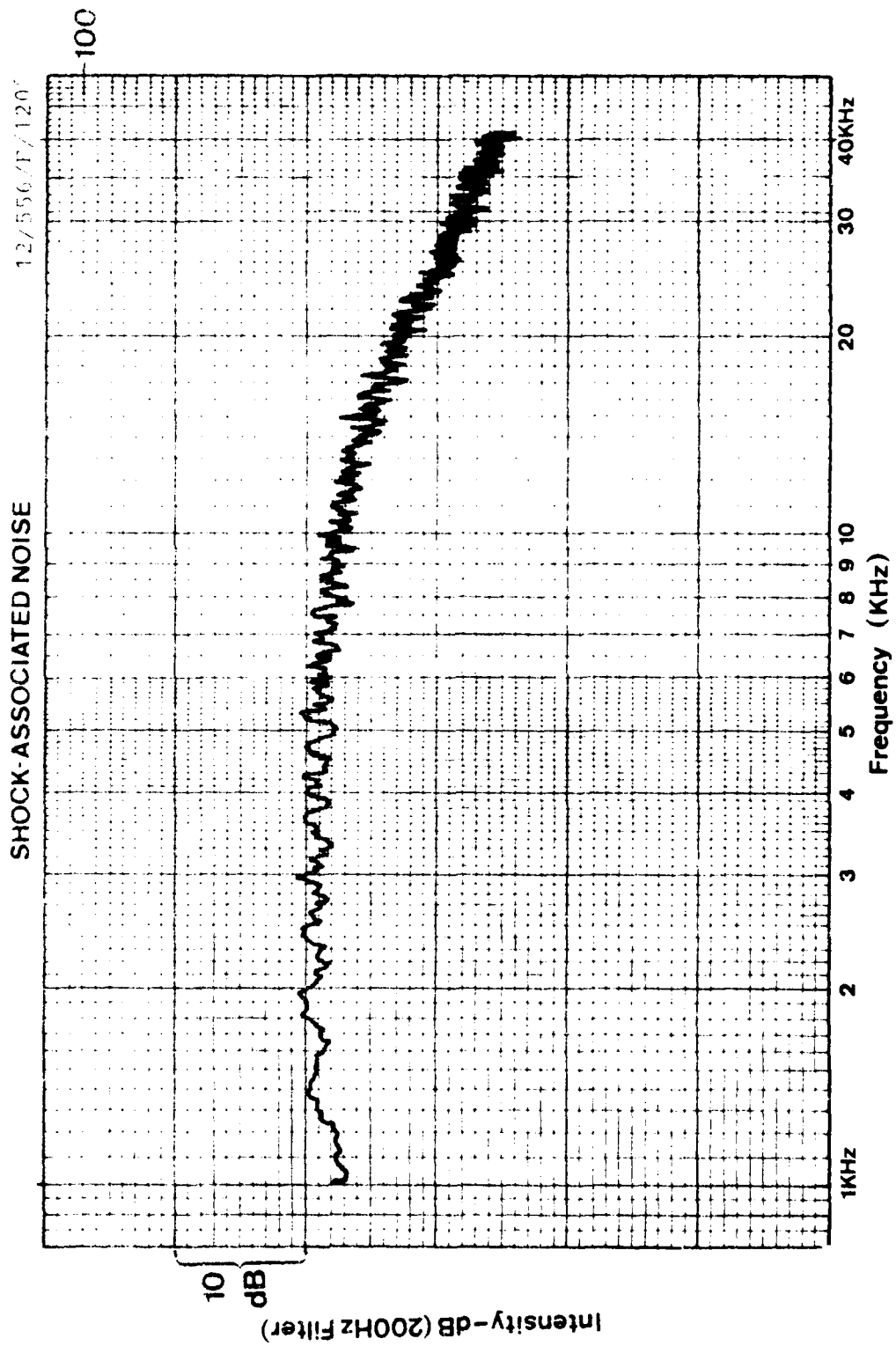


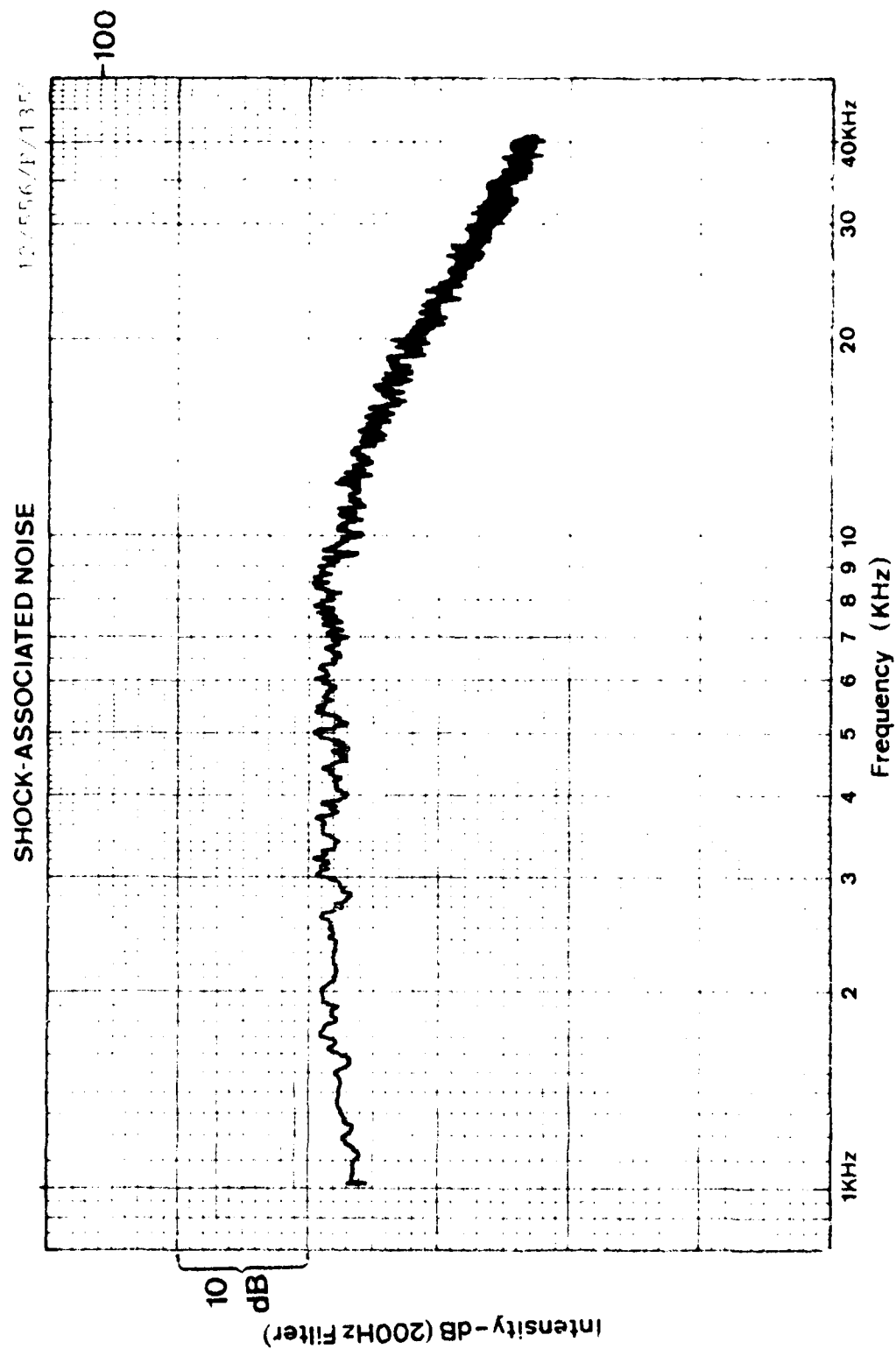


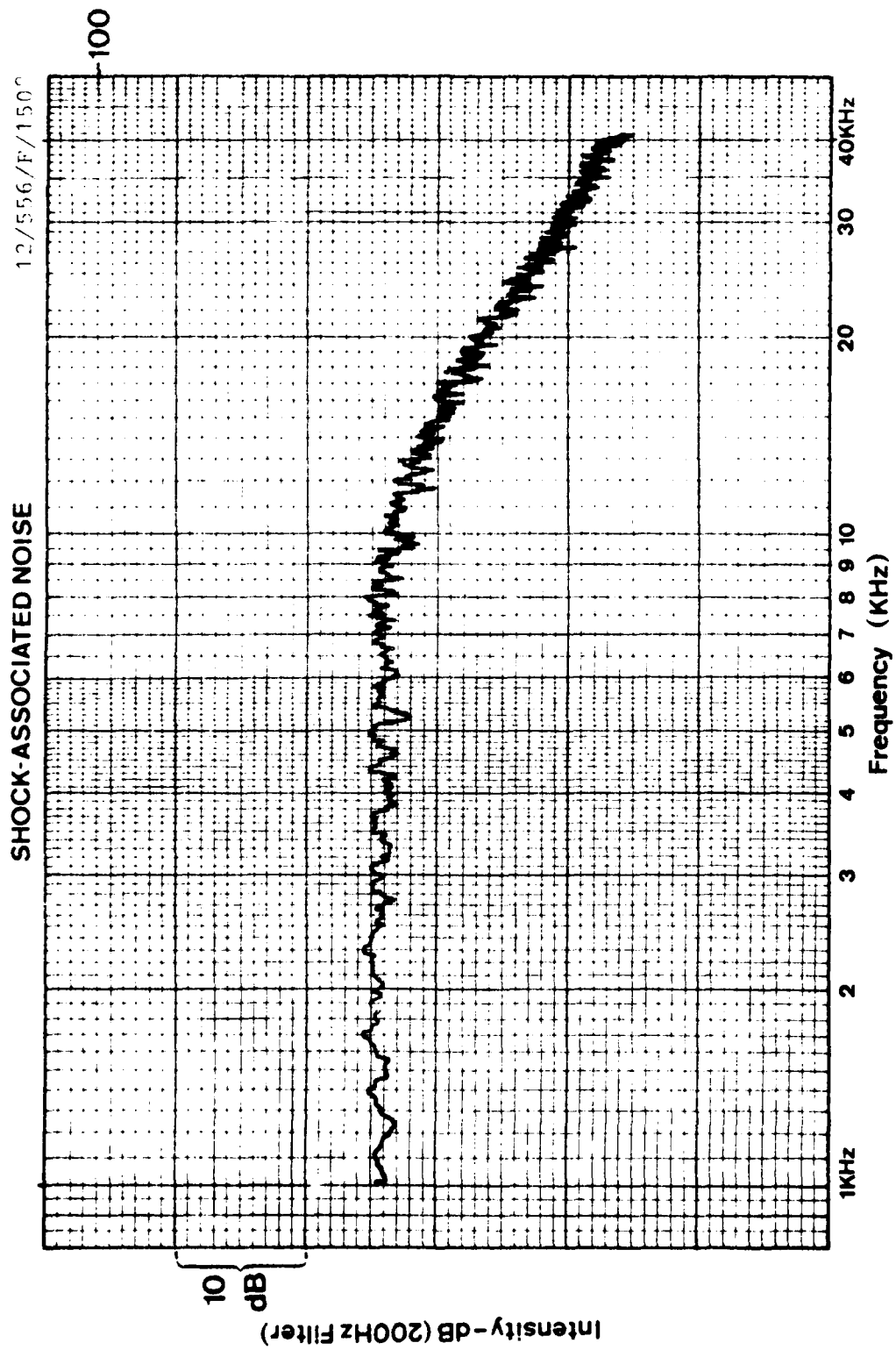


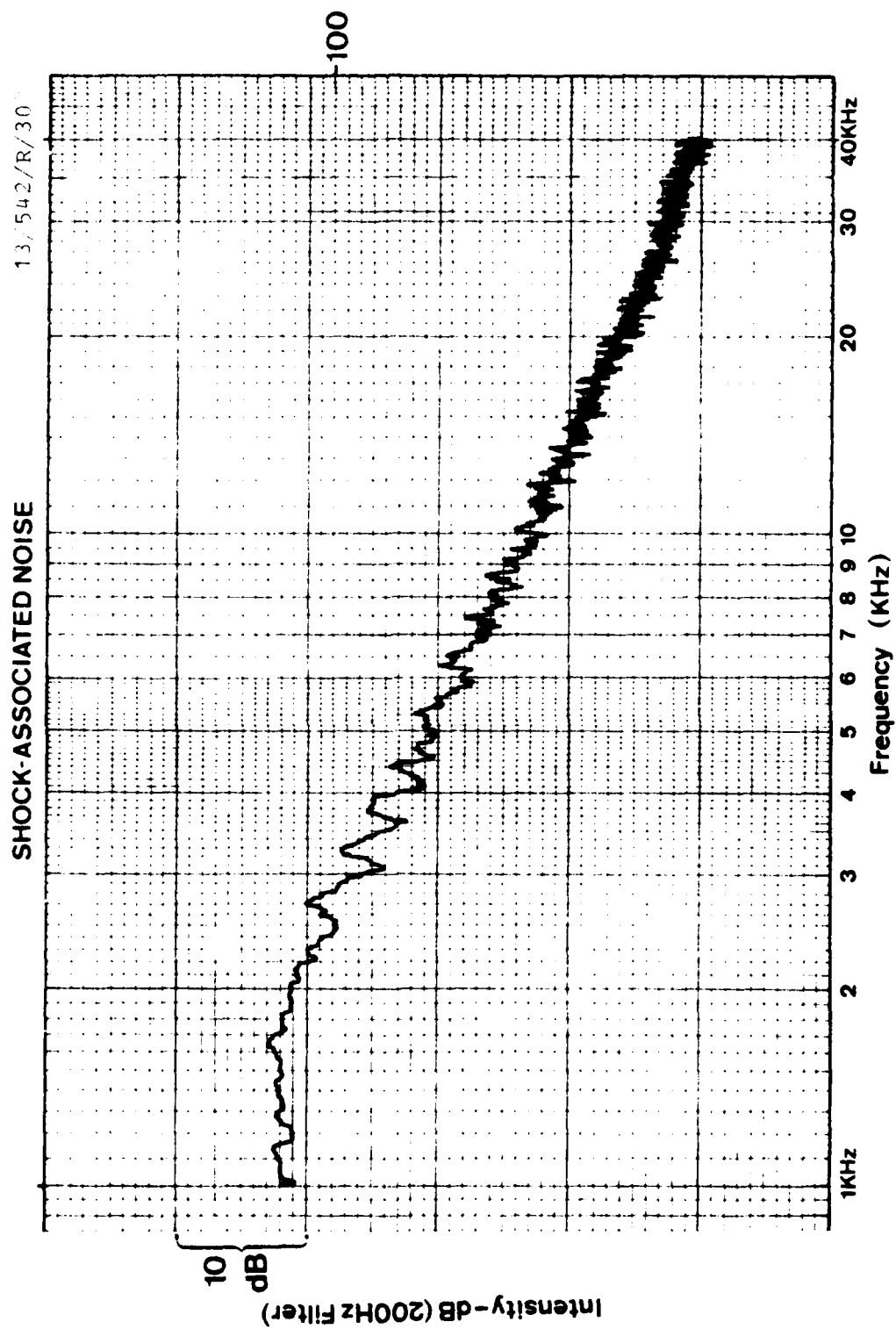


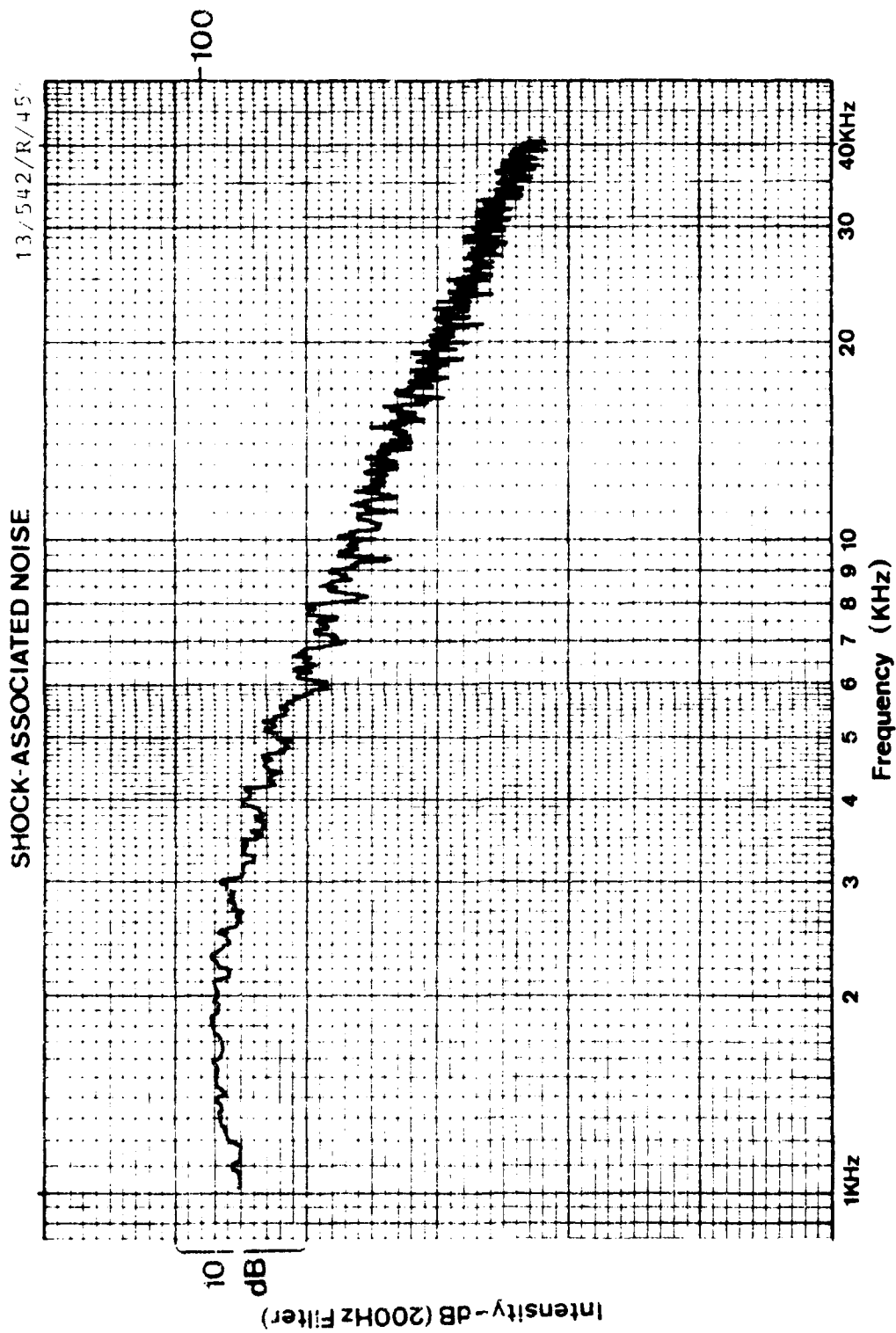


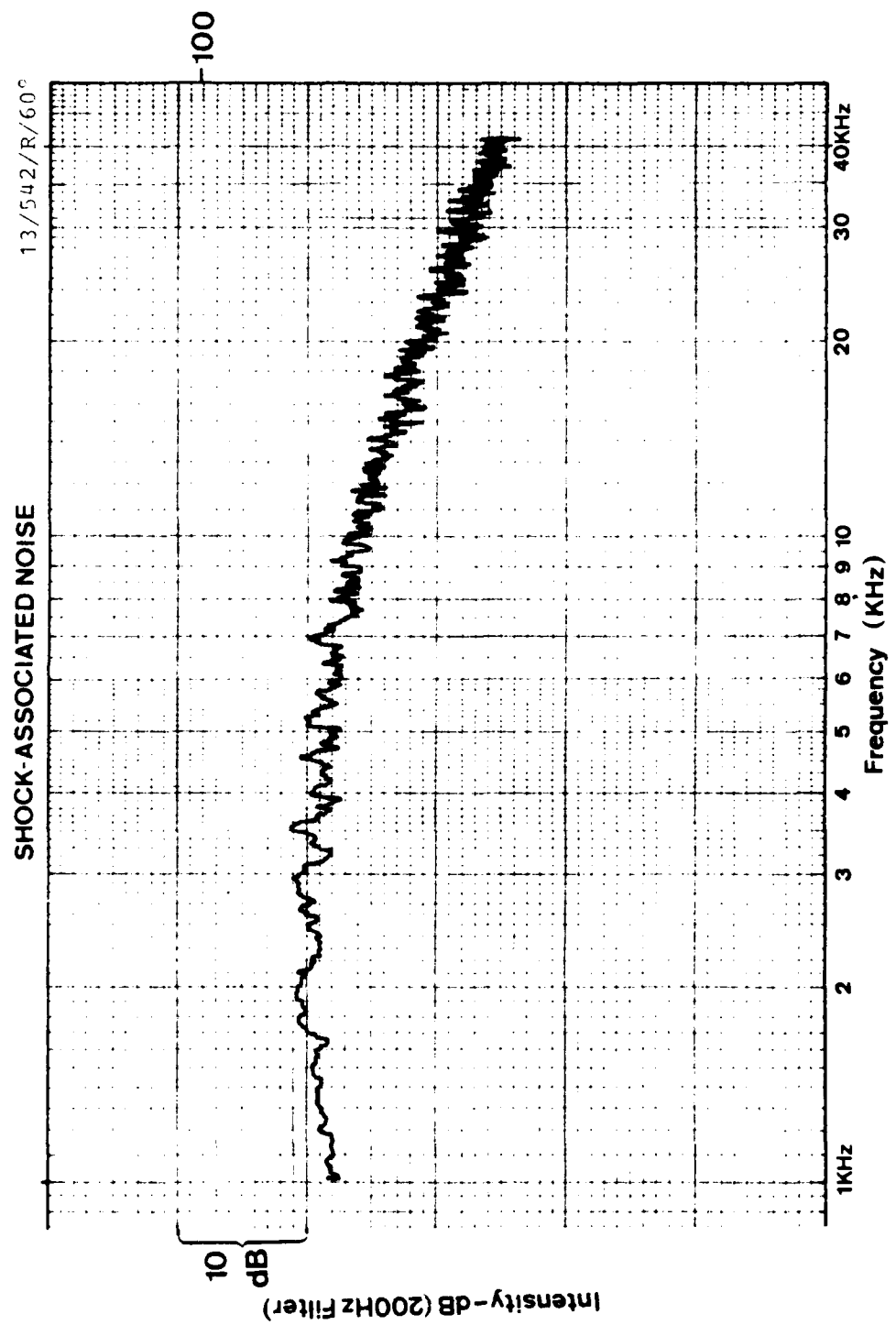


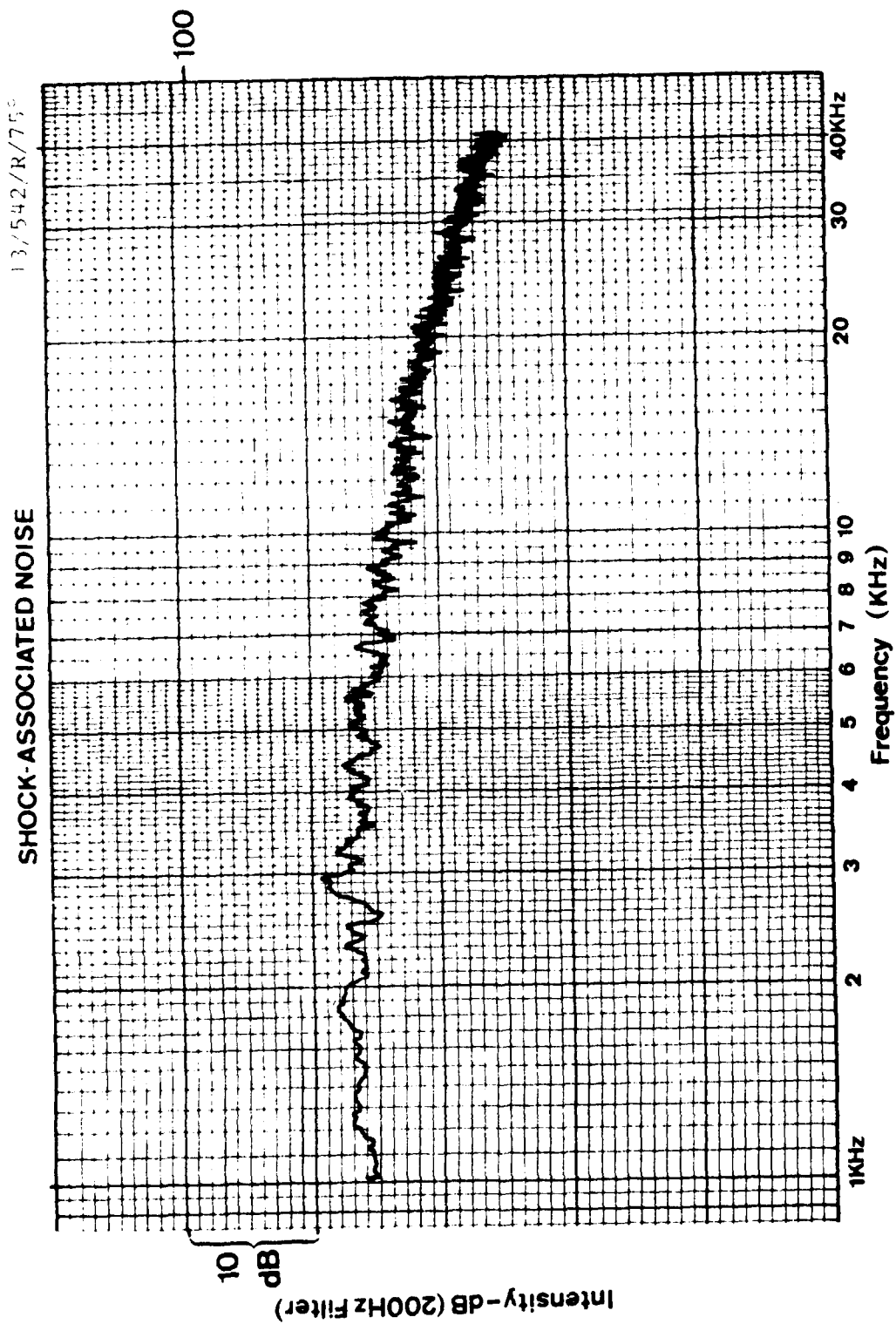


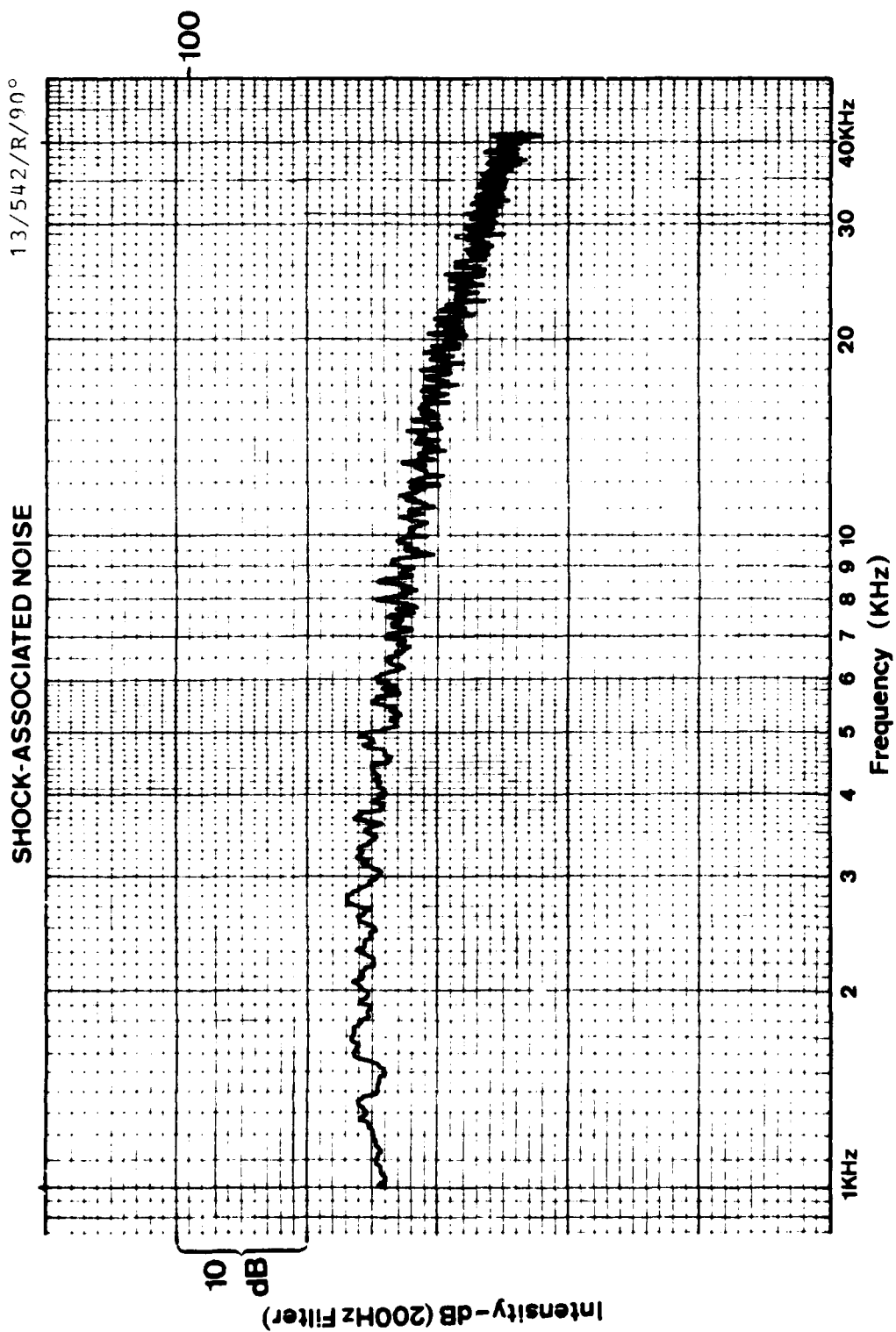


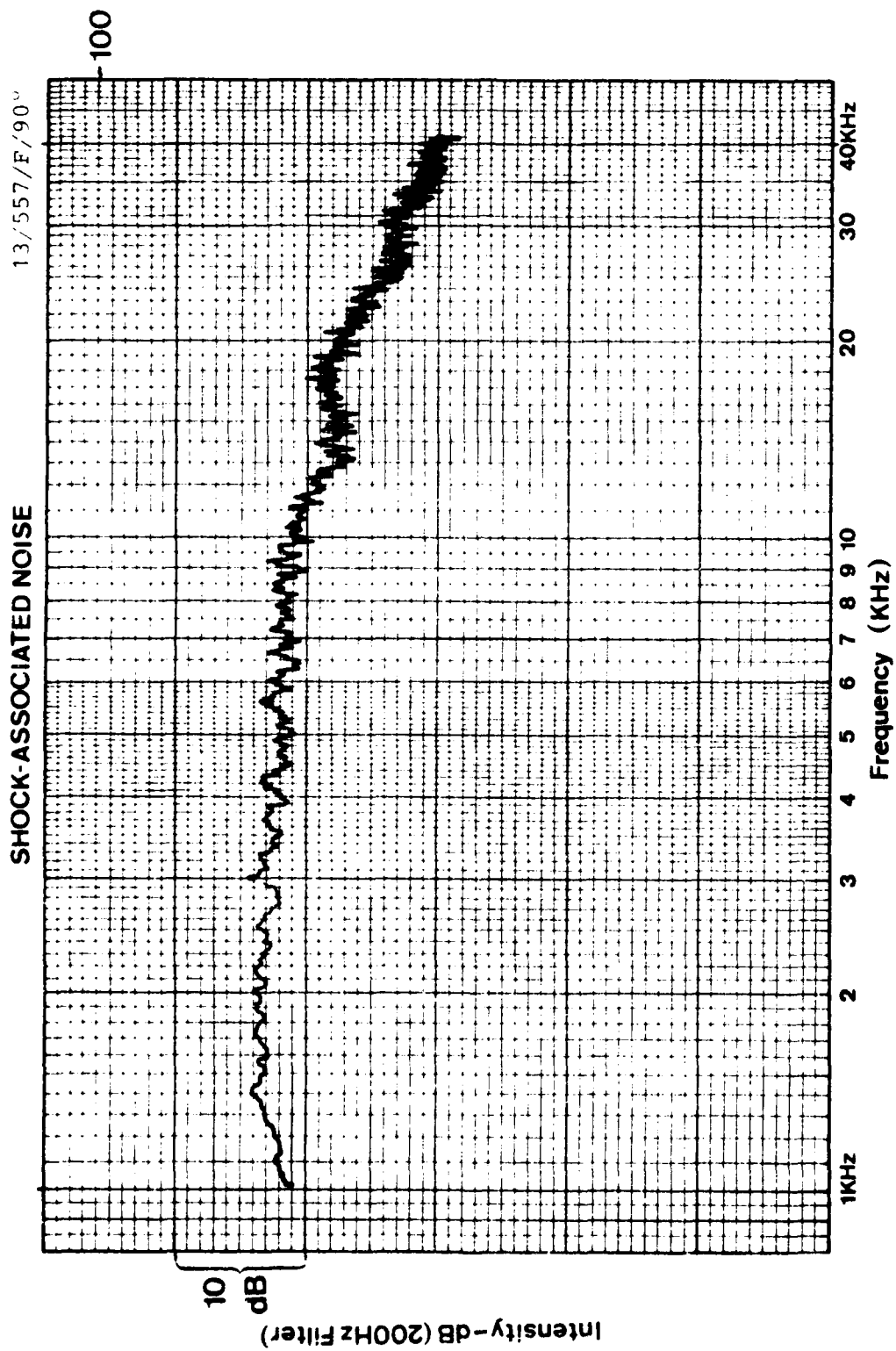


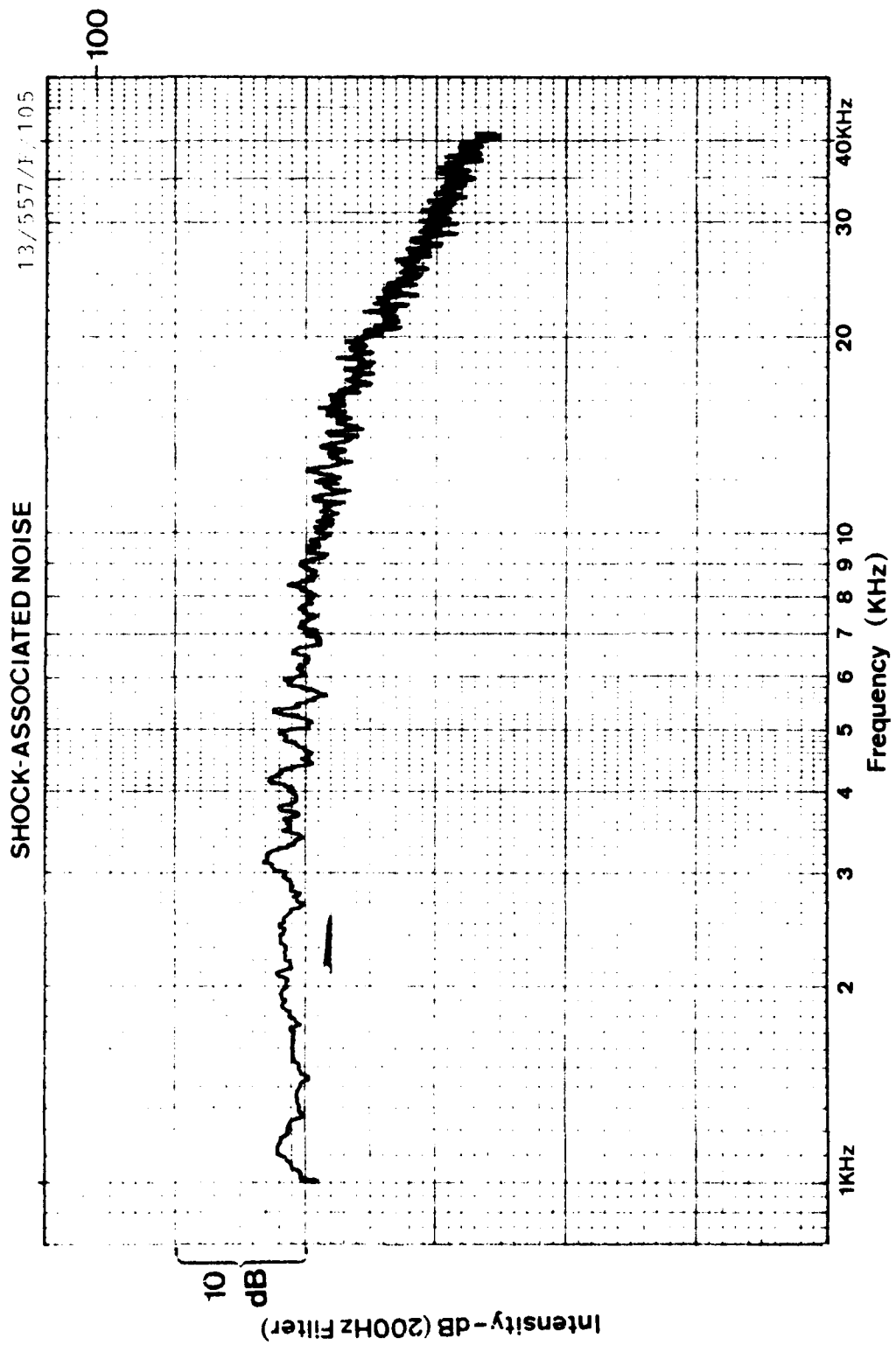


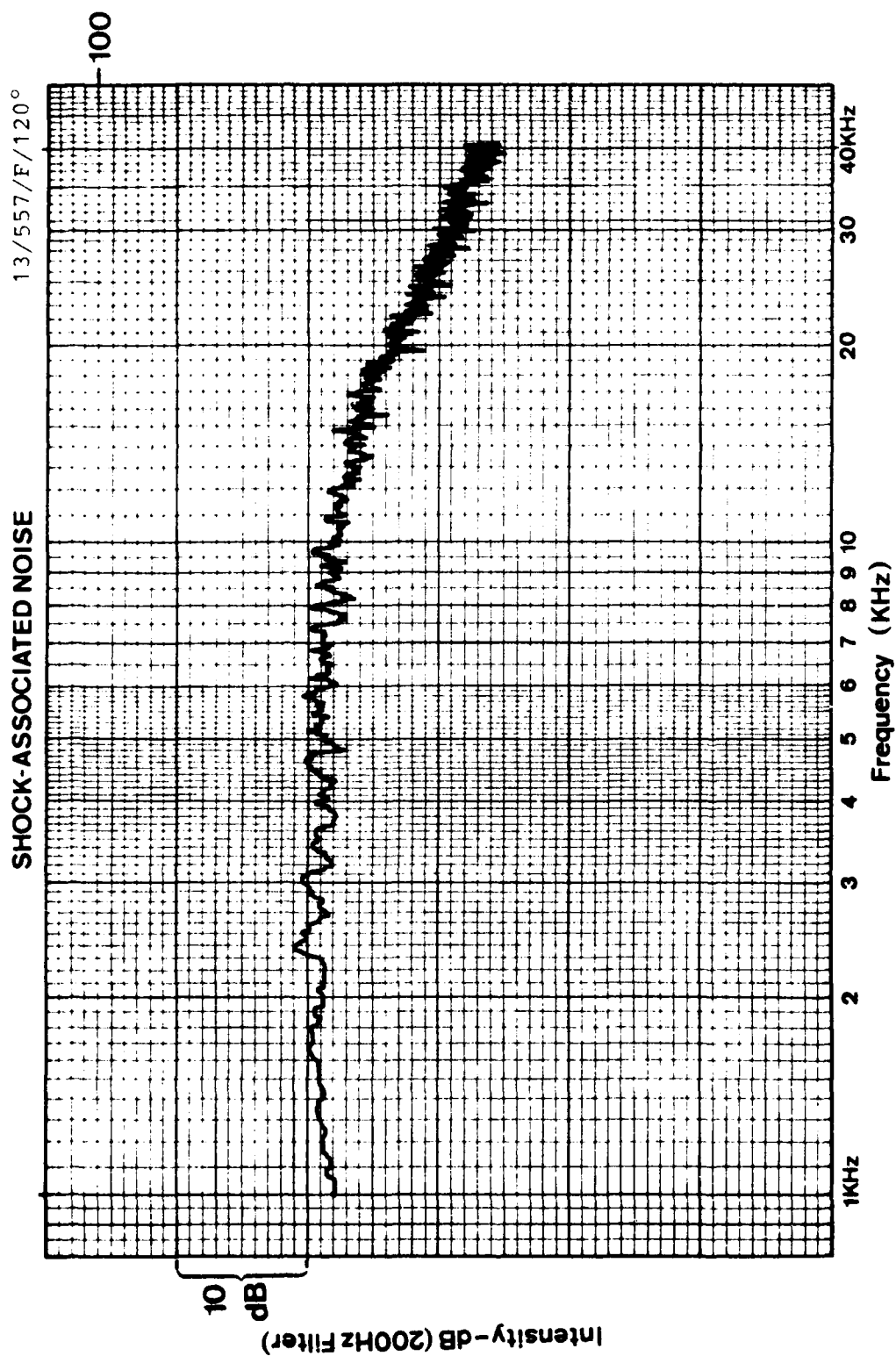


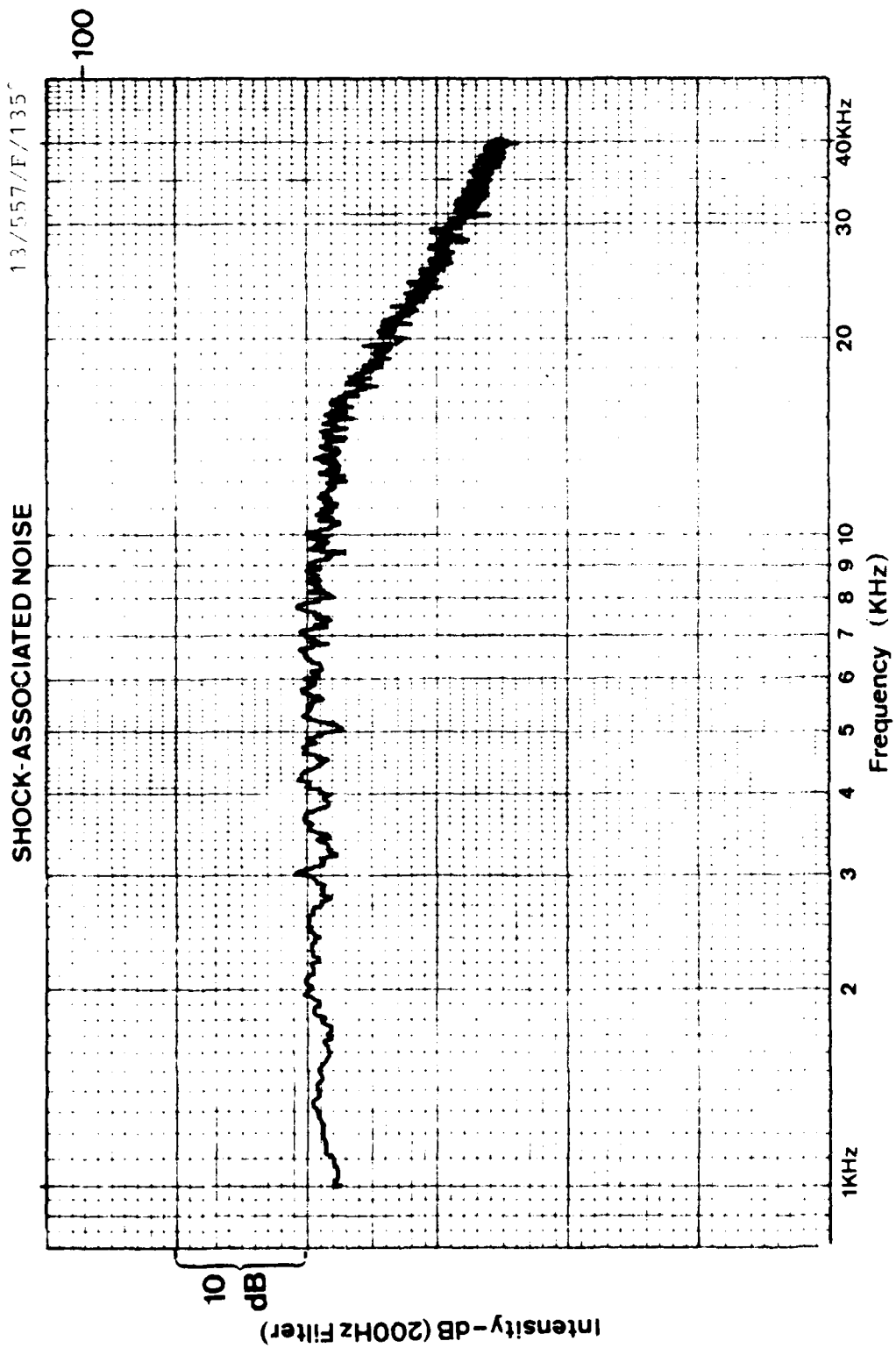


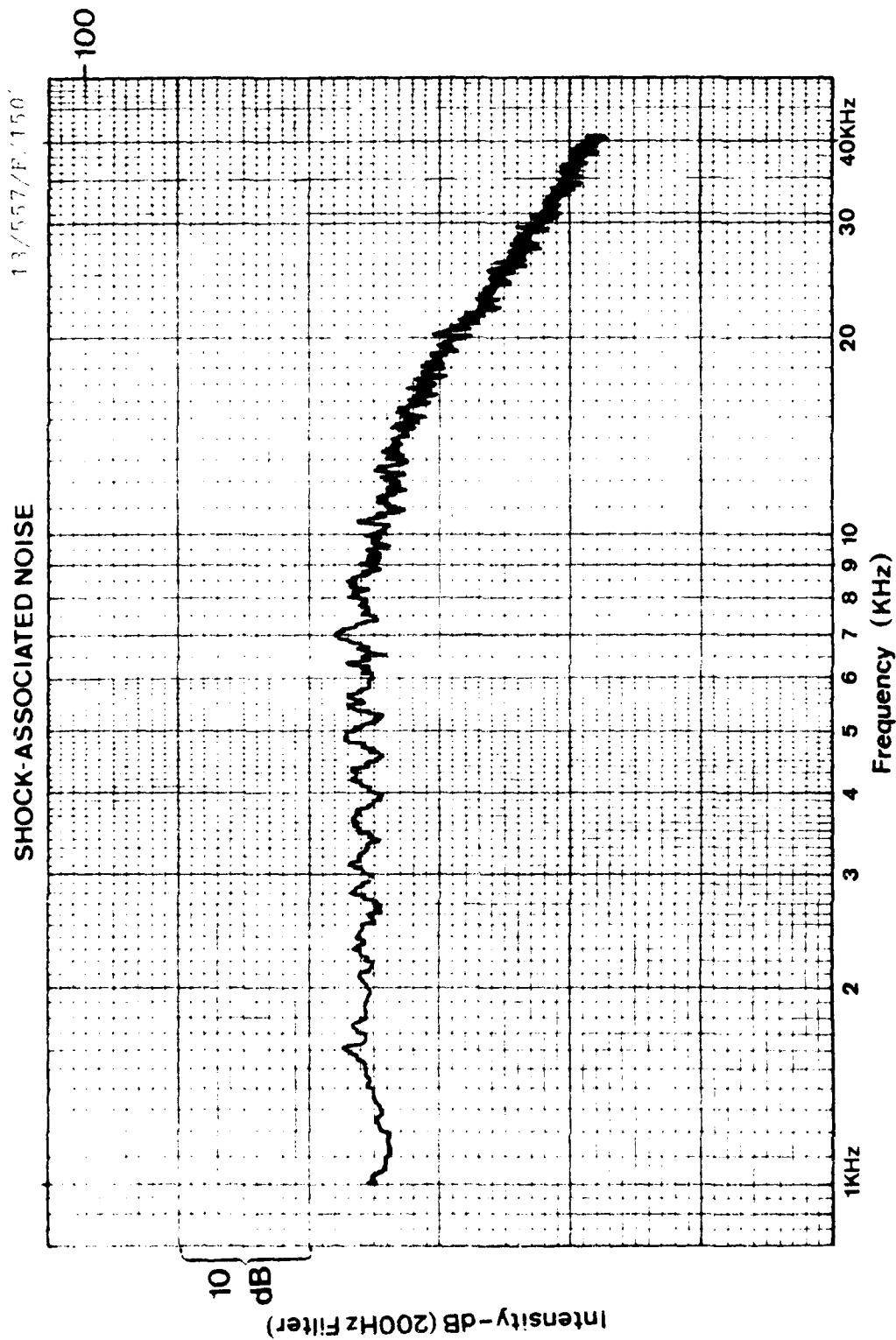


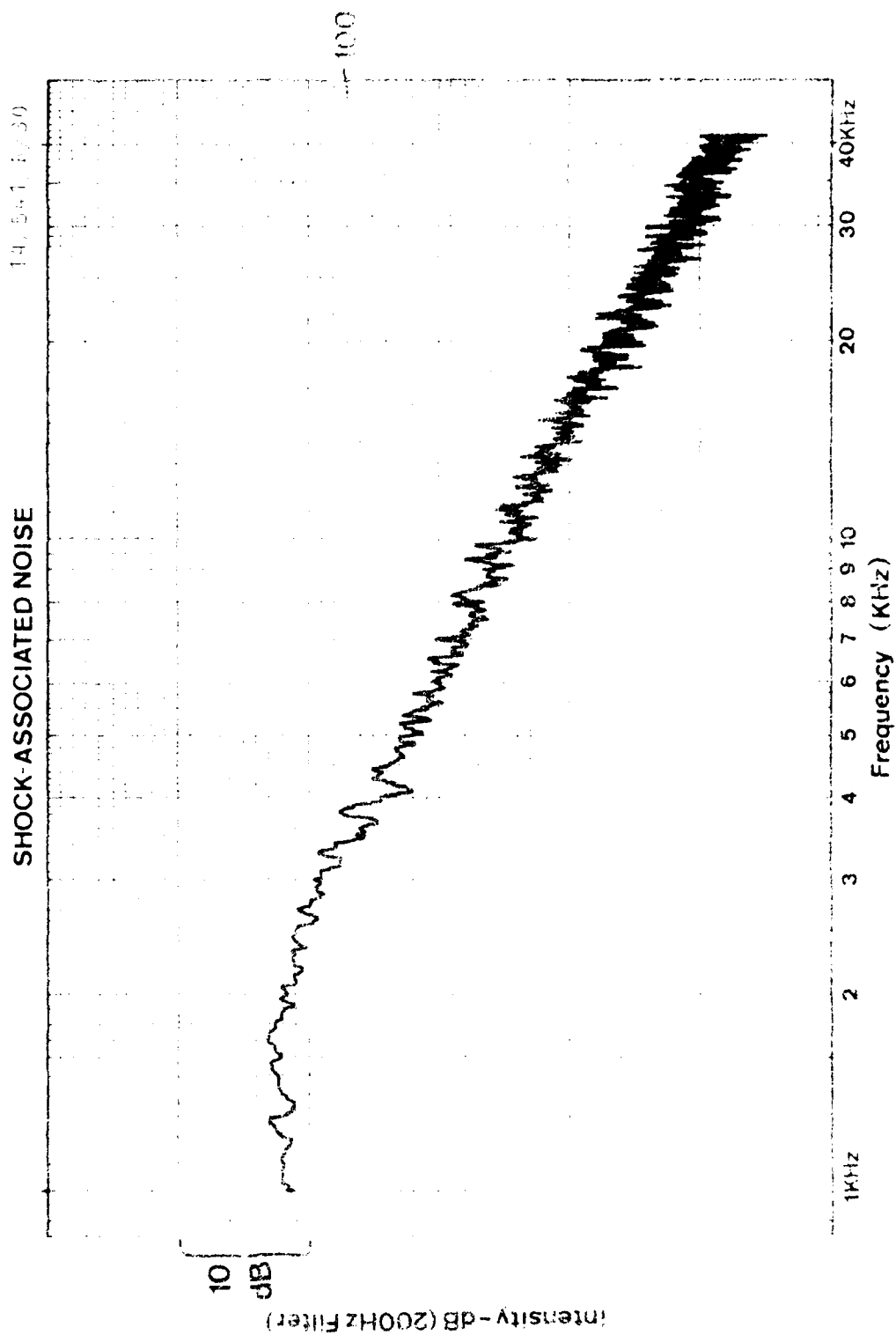


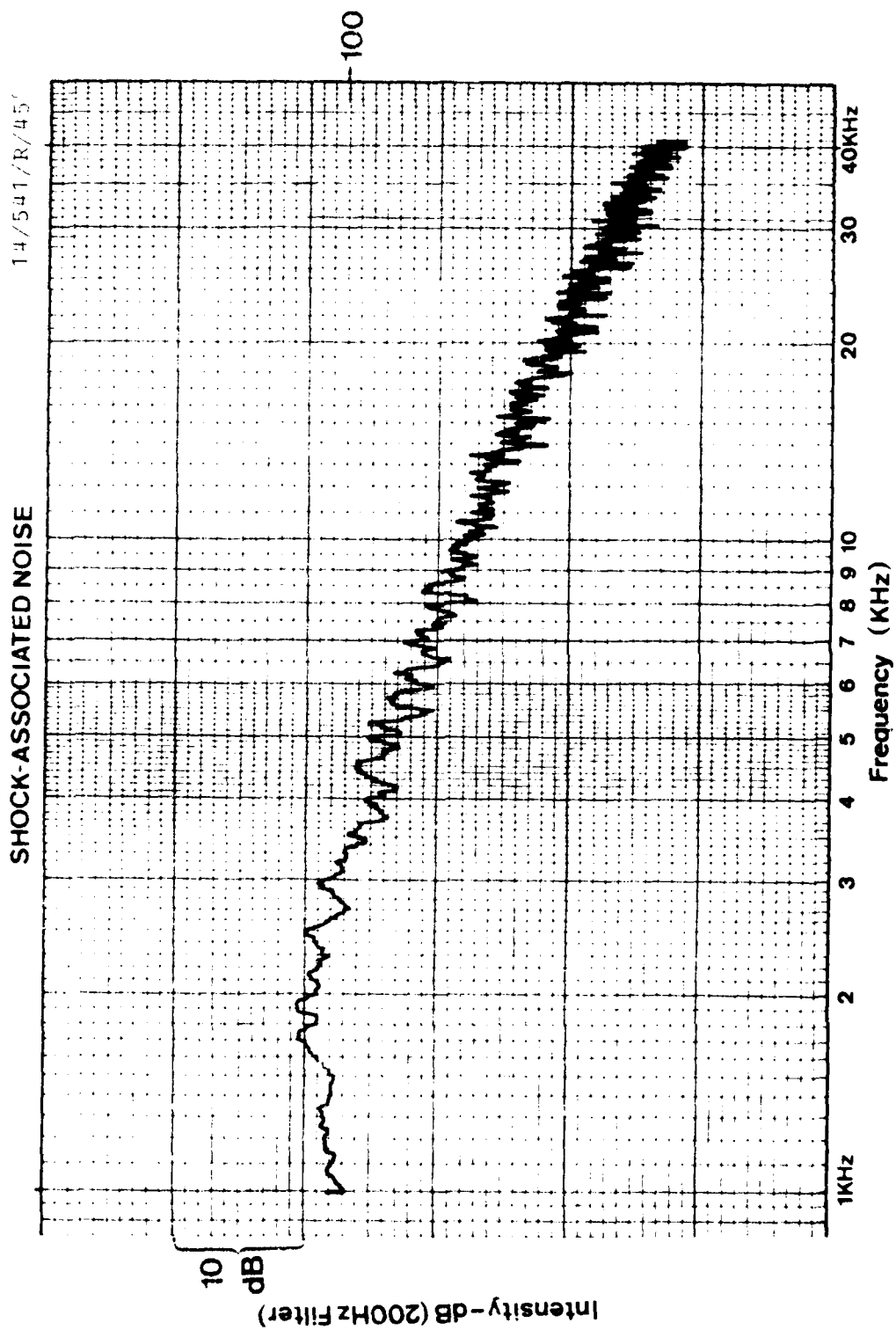






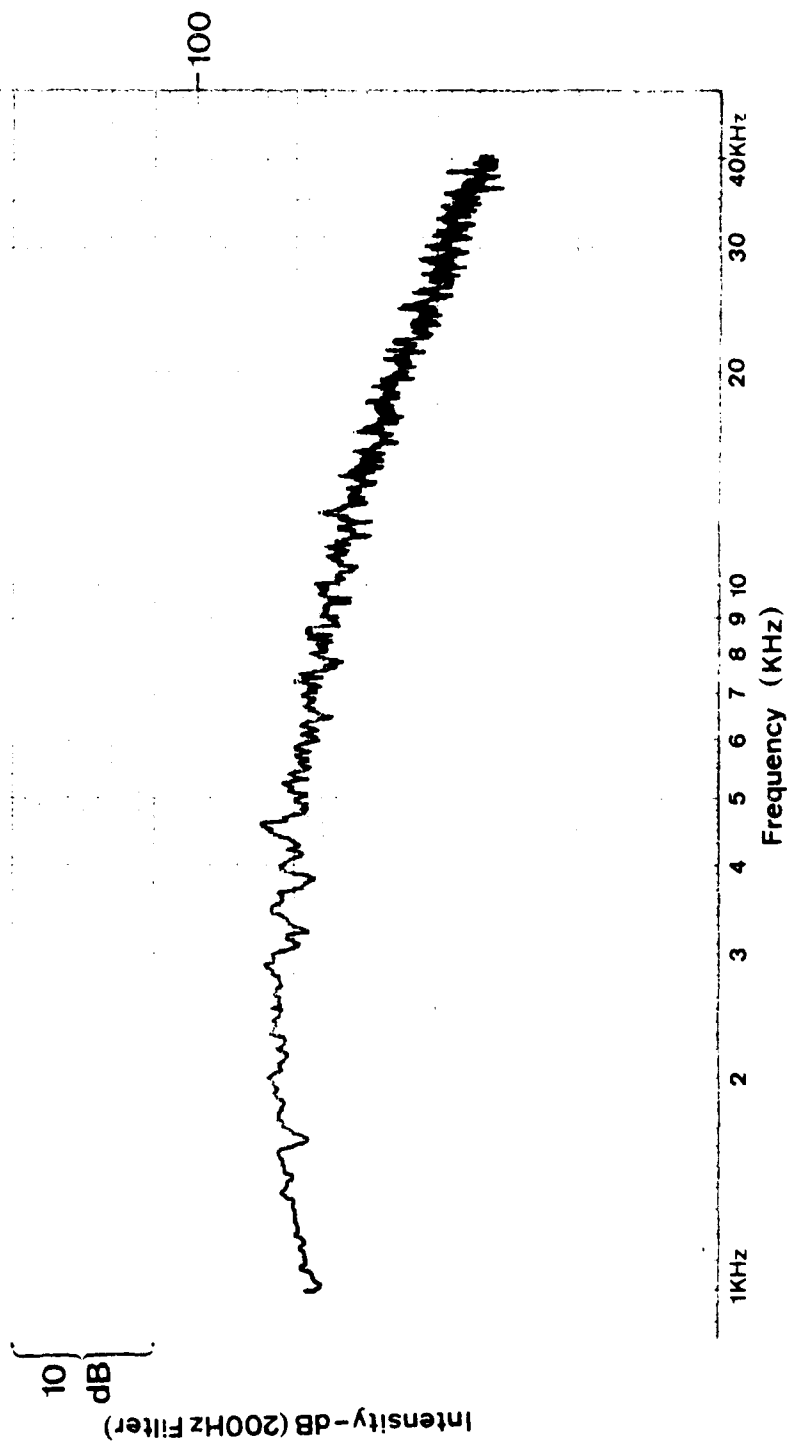


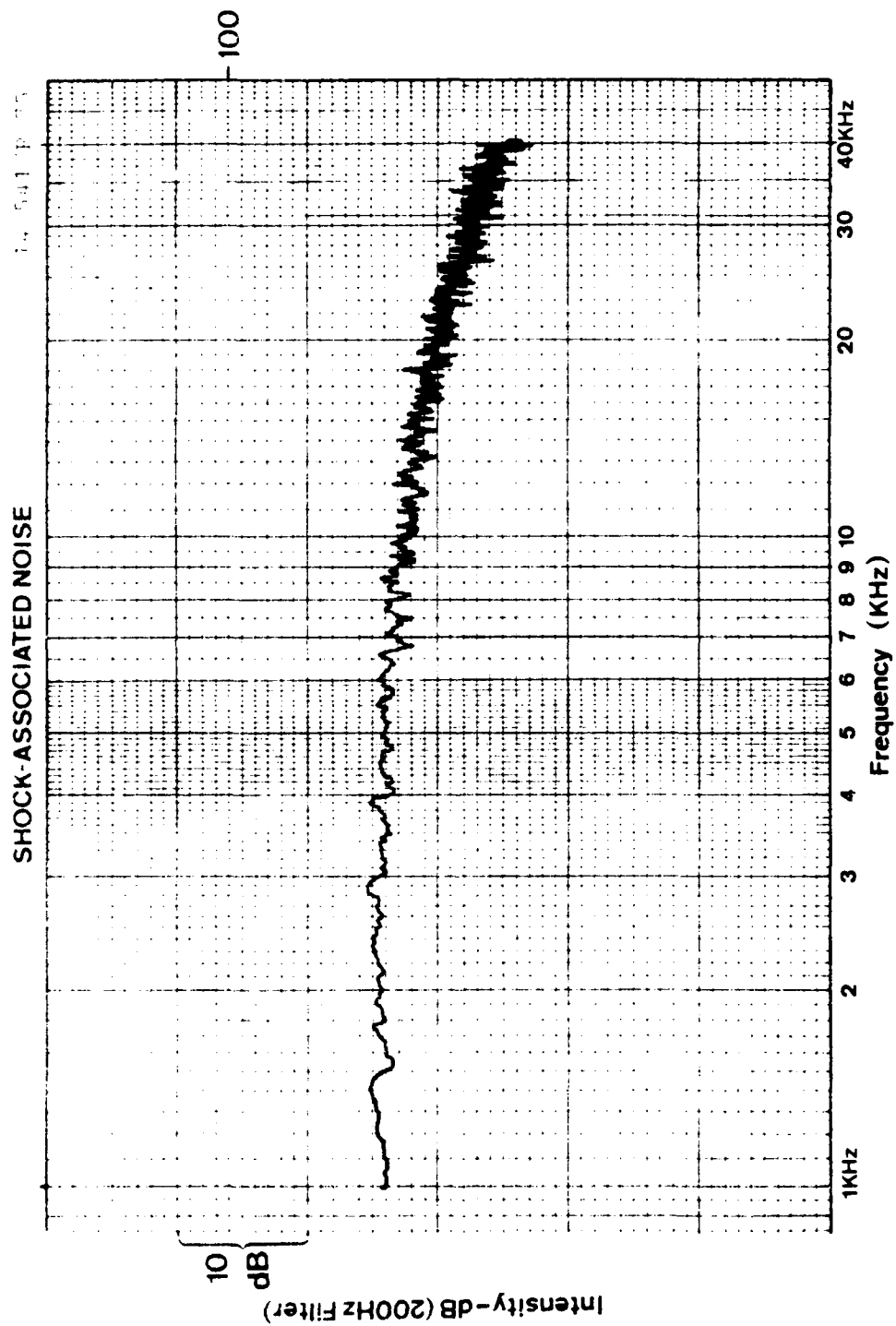


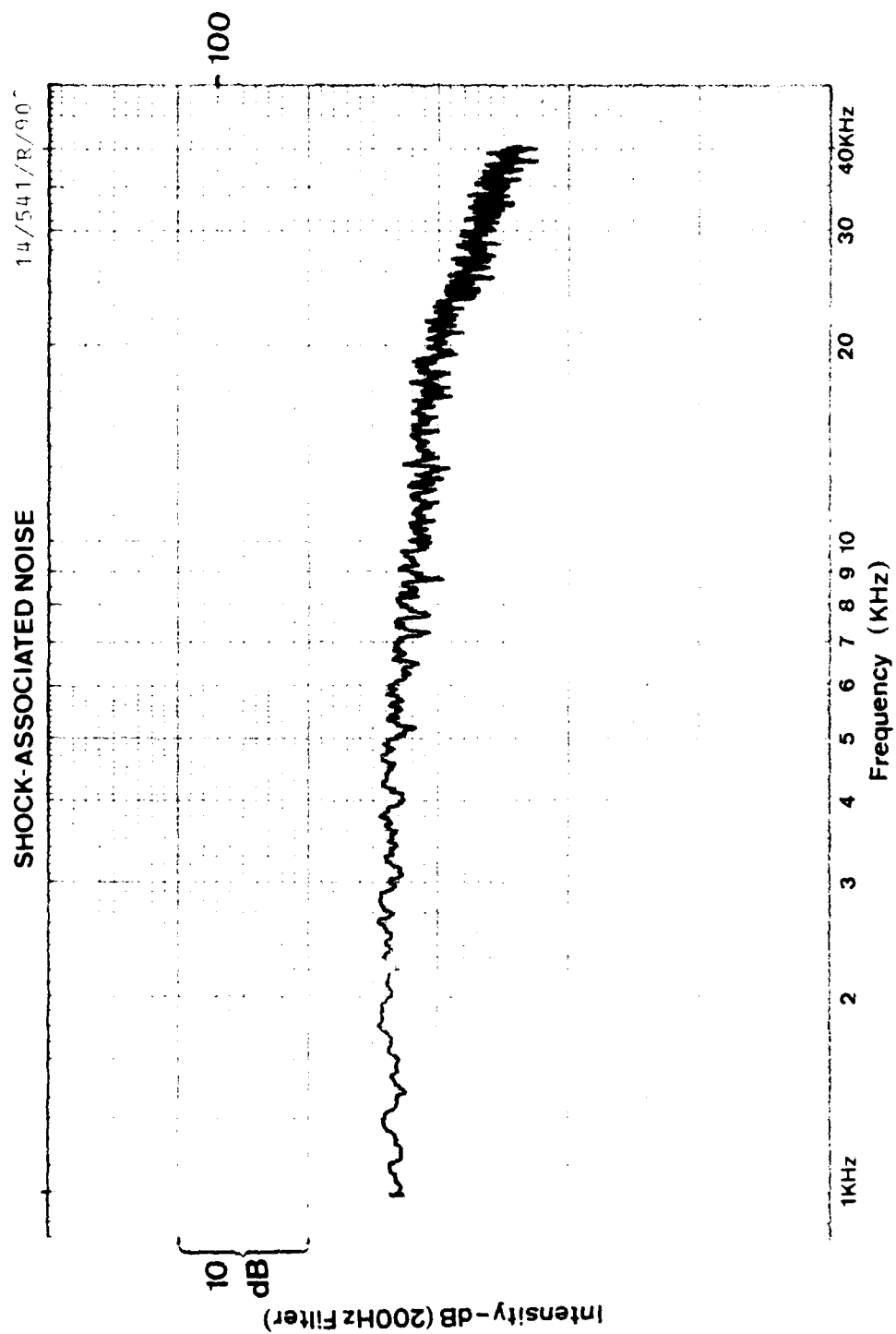


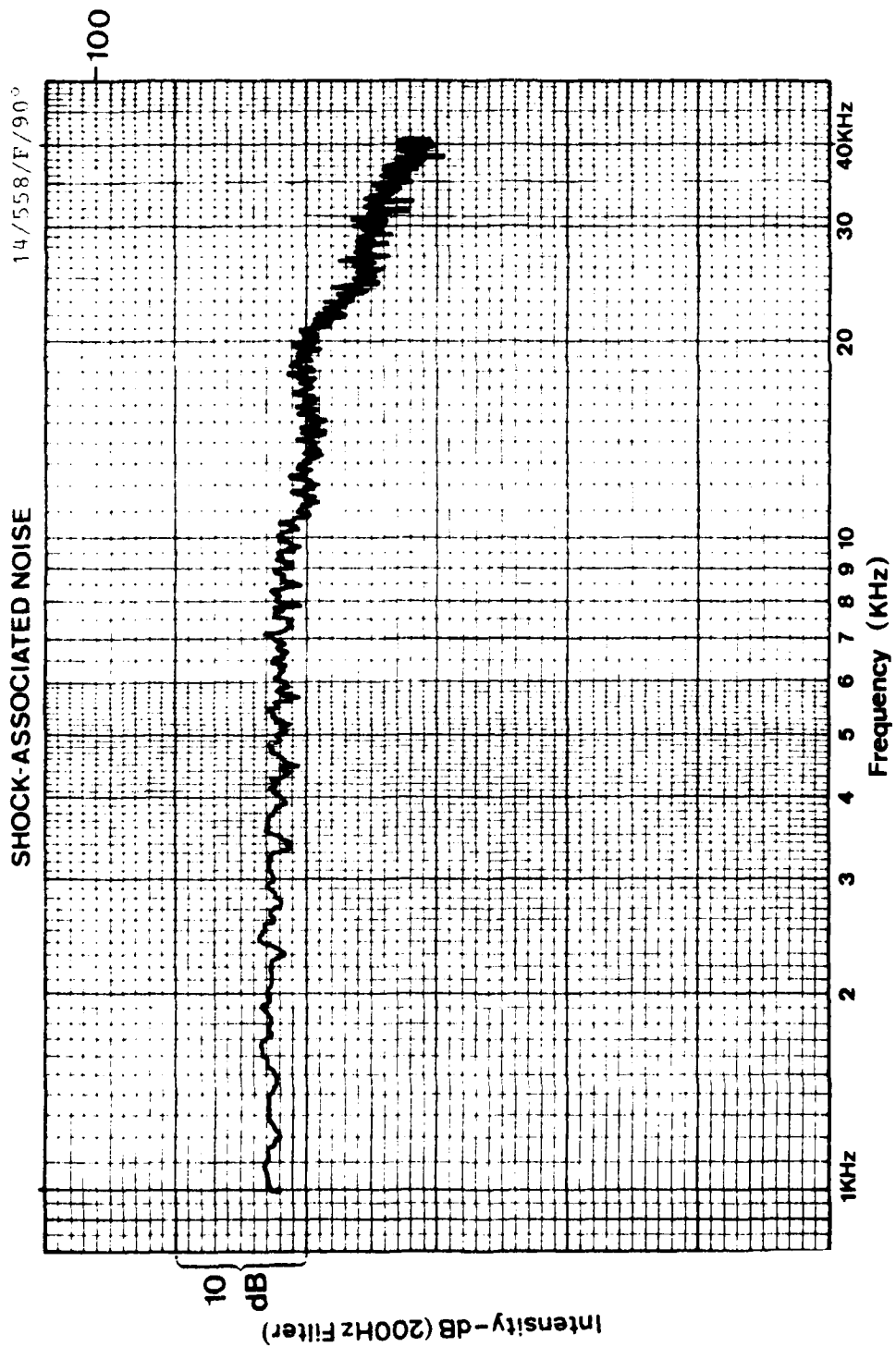
SHOCK-ASSOCIATED NOISE

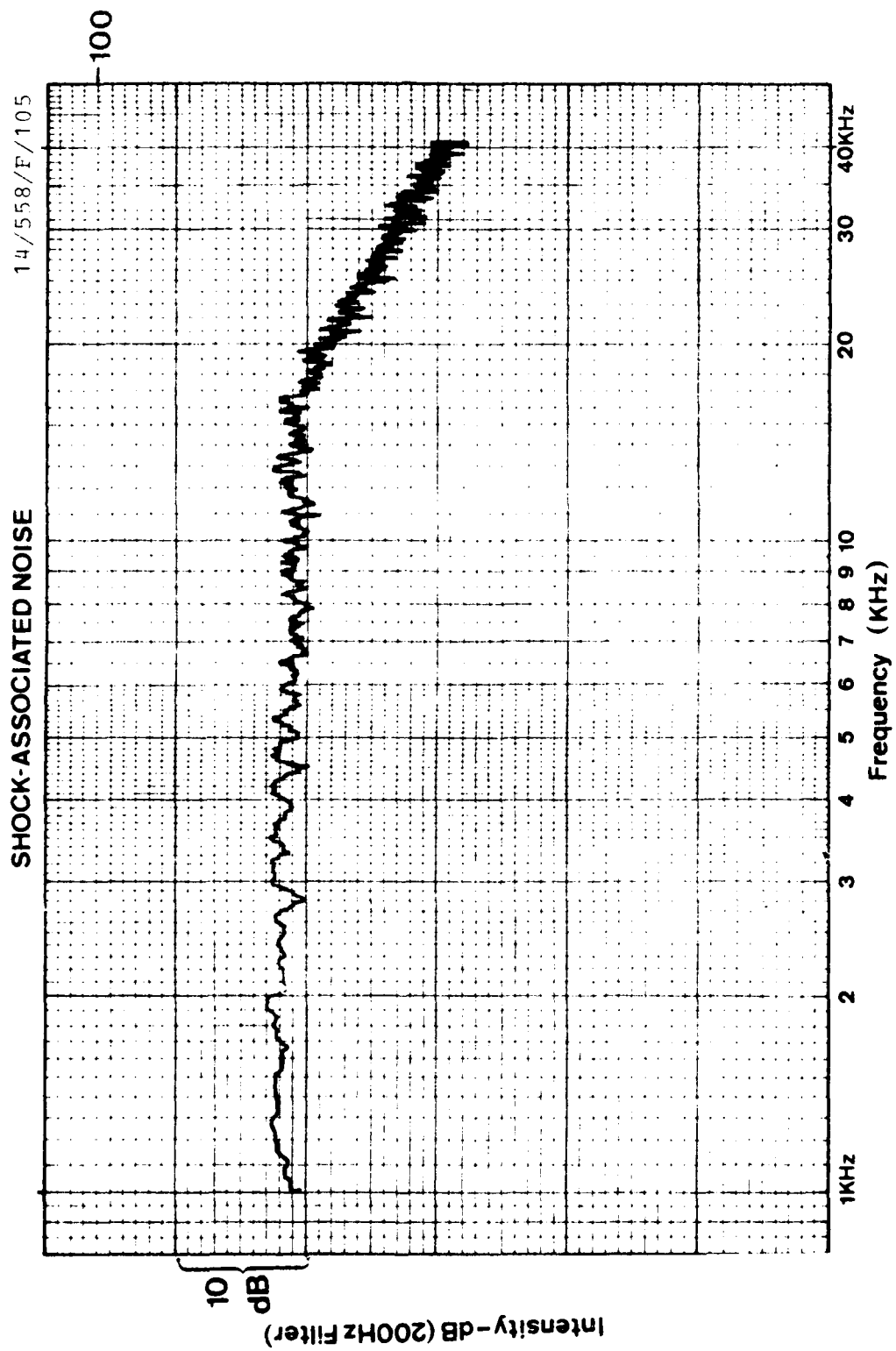
14/541/R/60

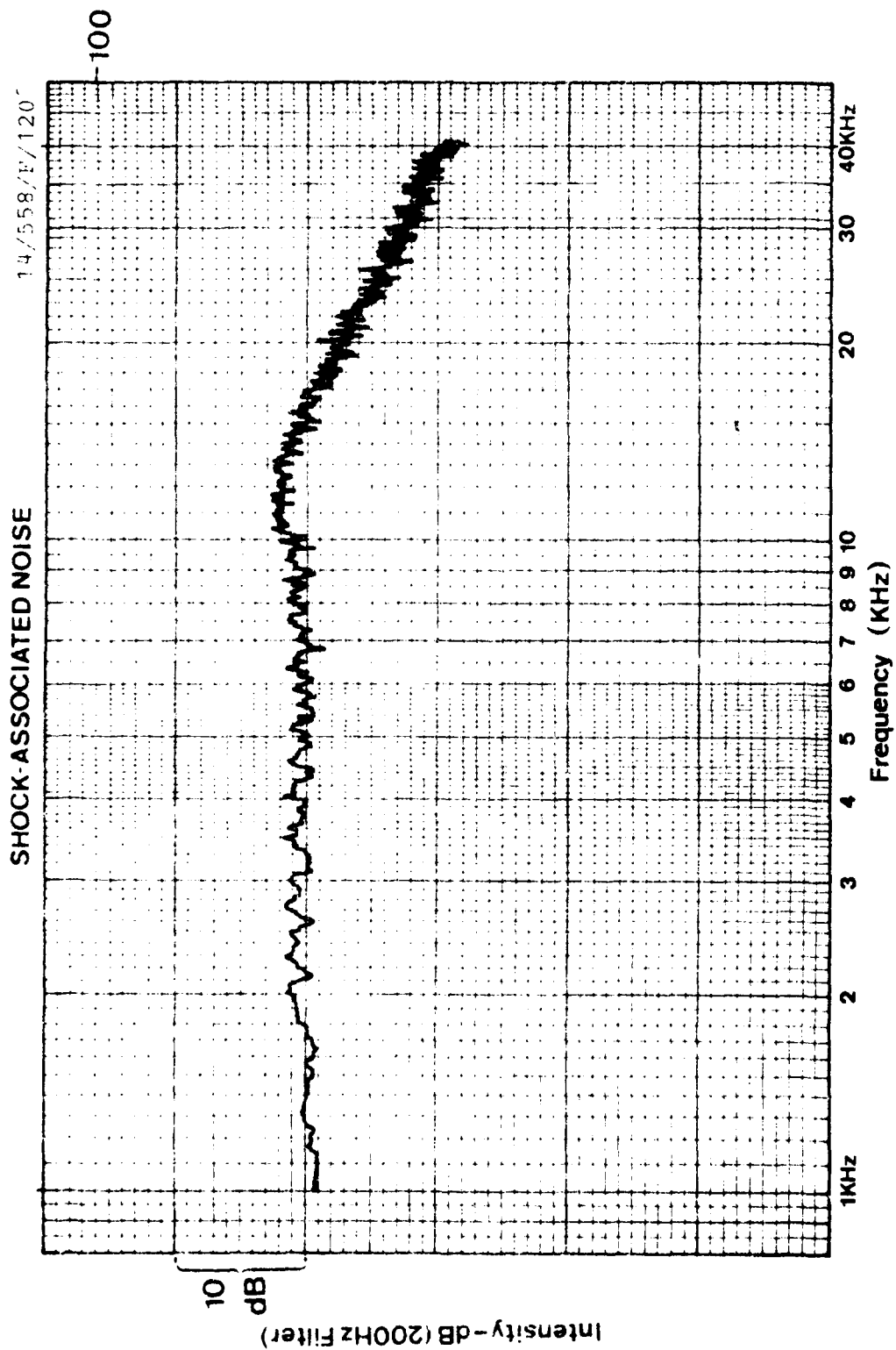


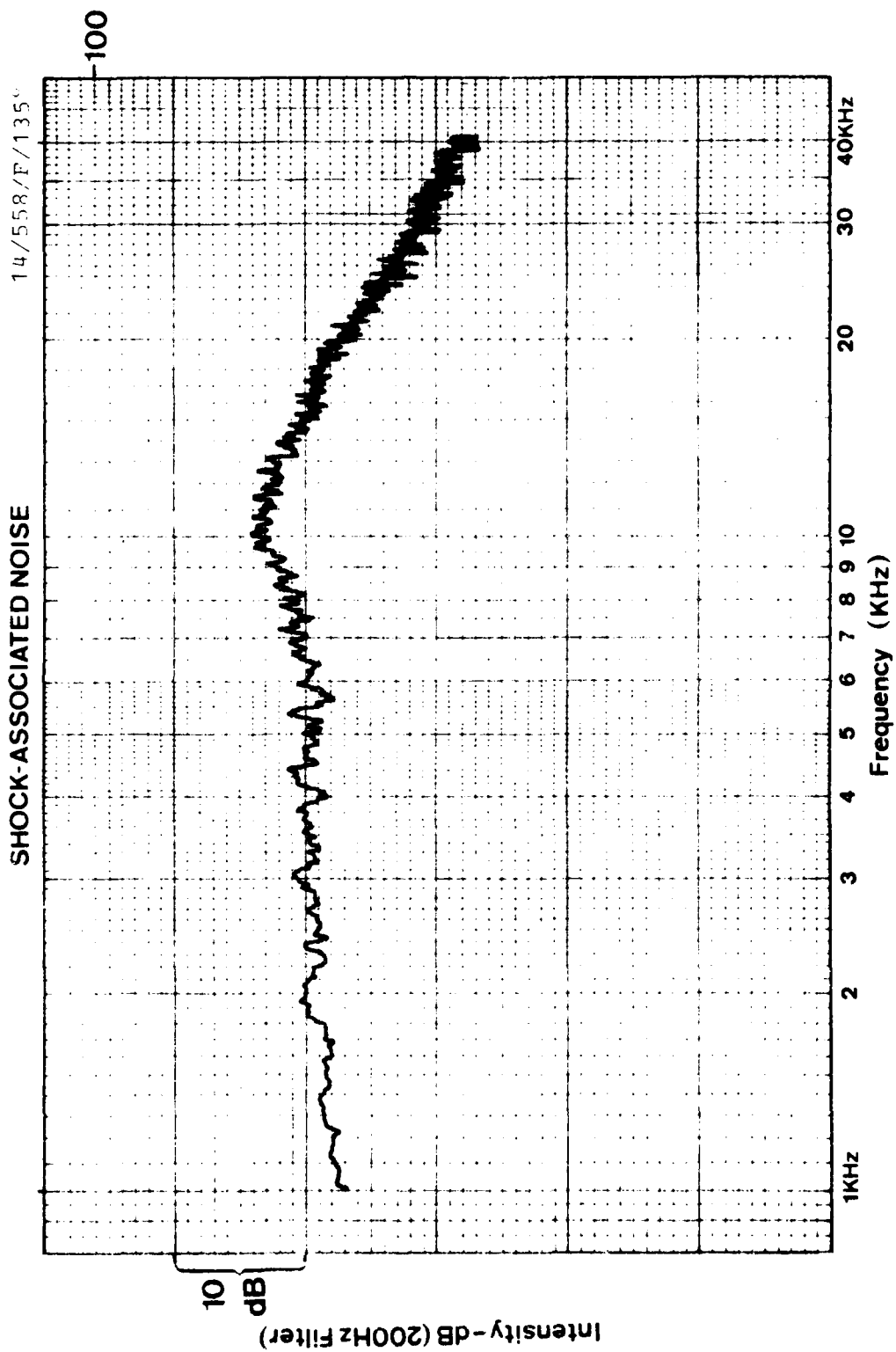


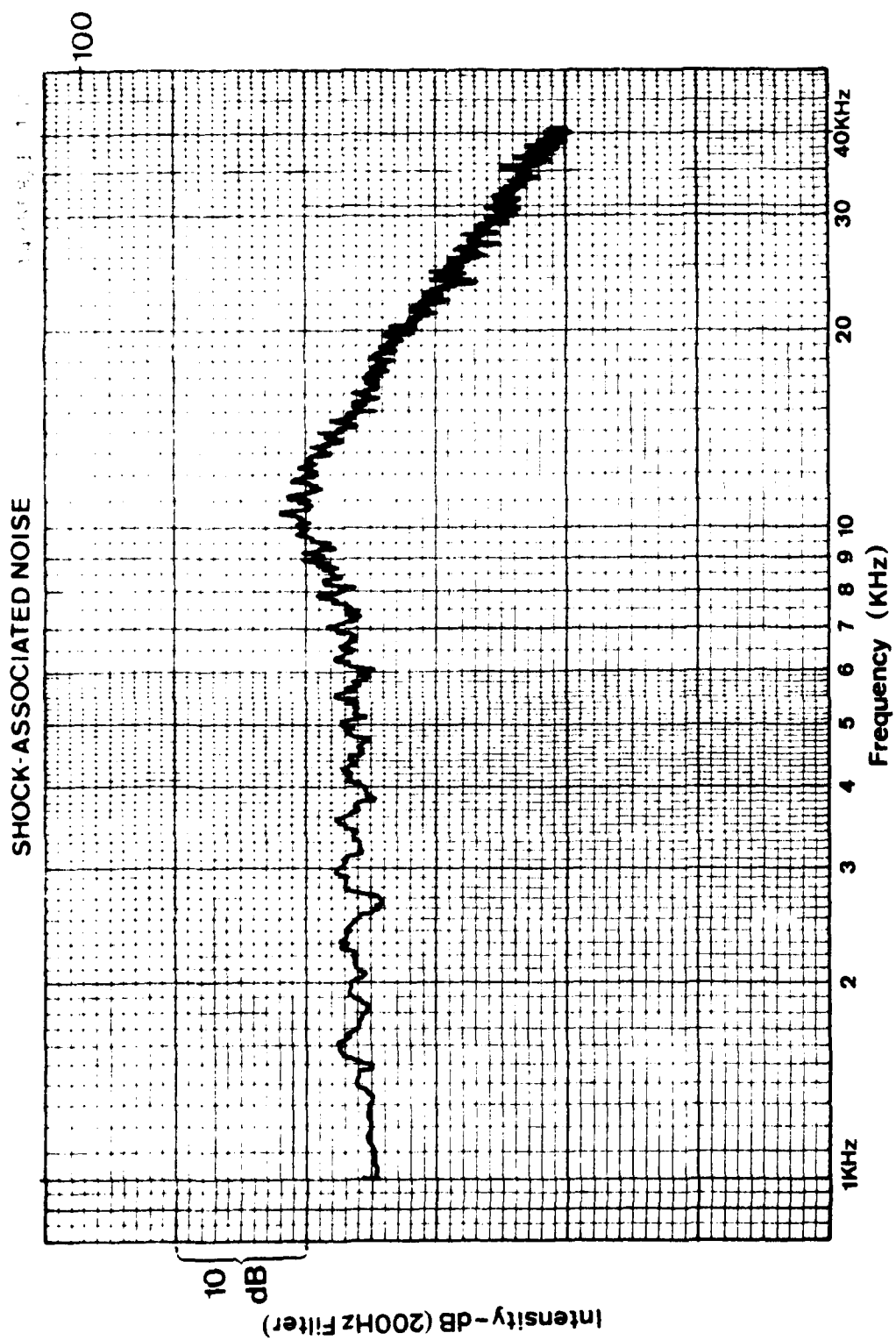


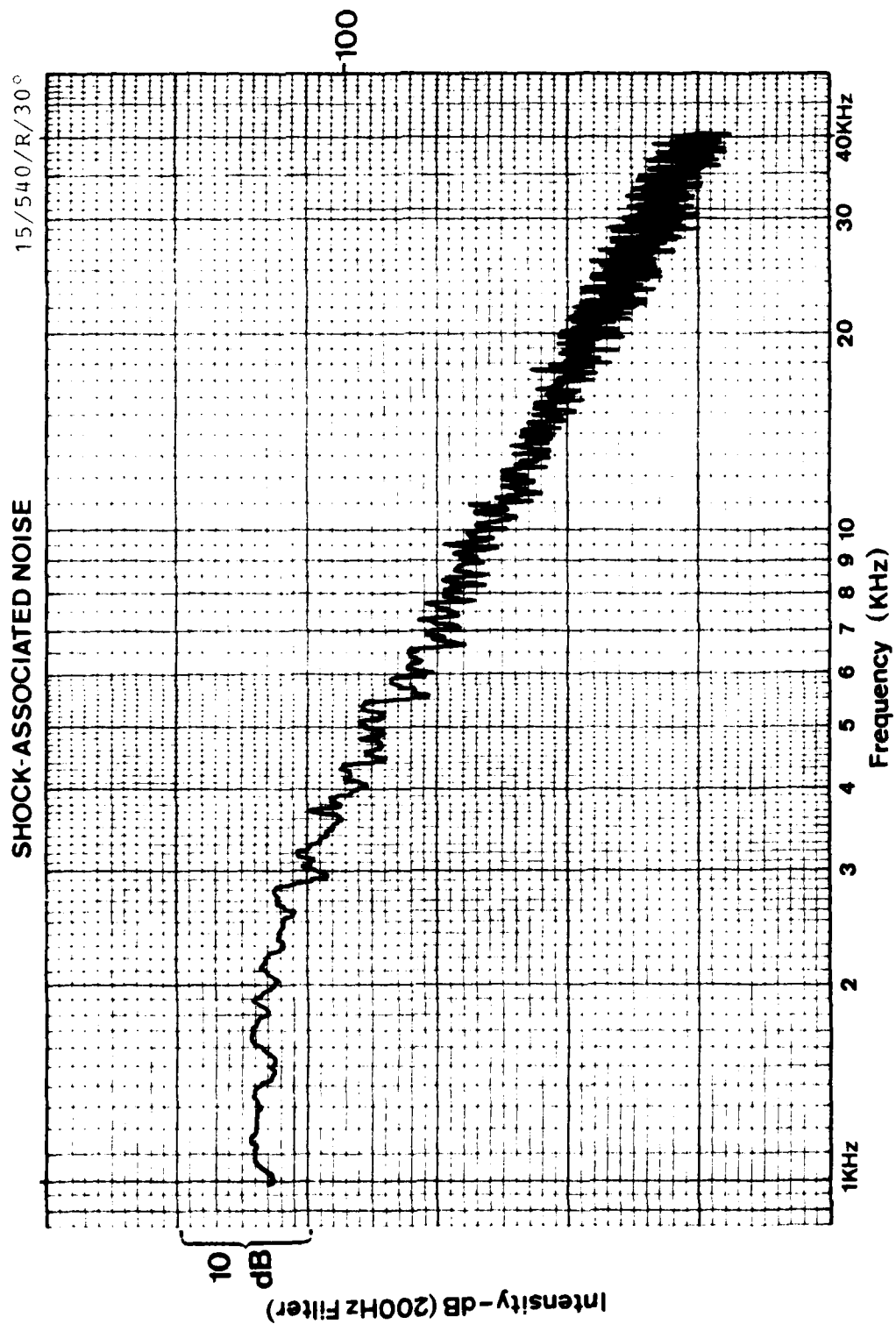


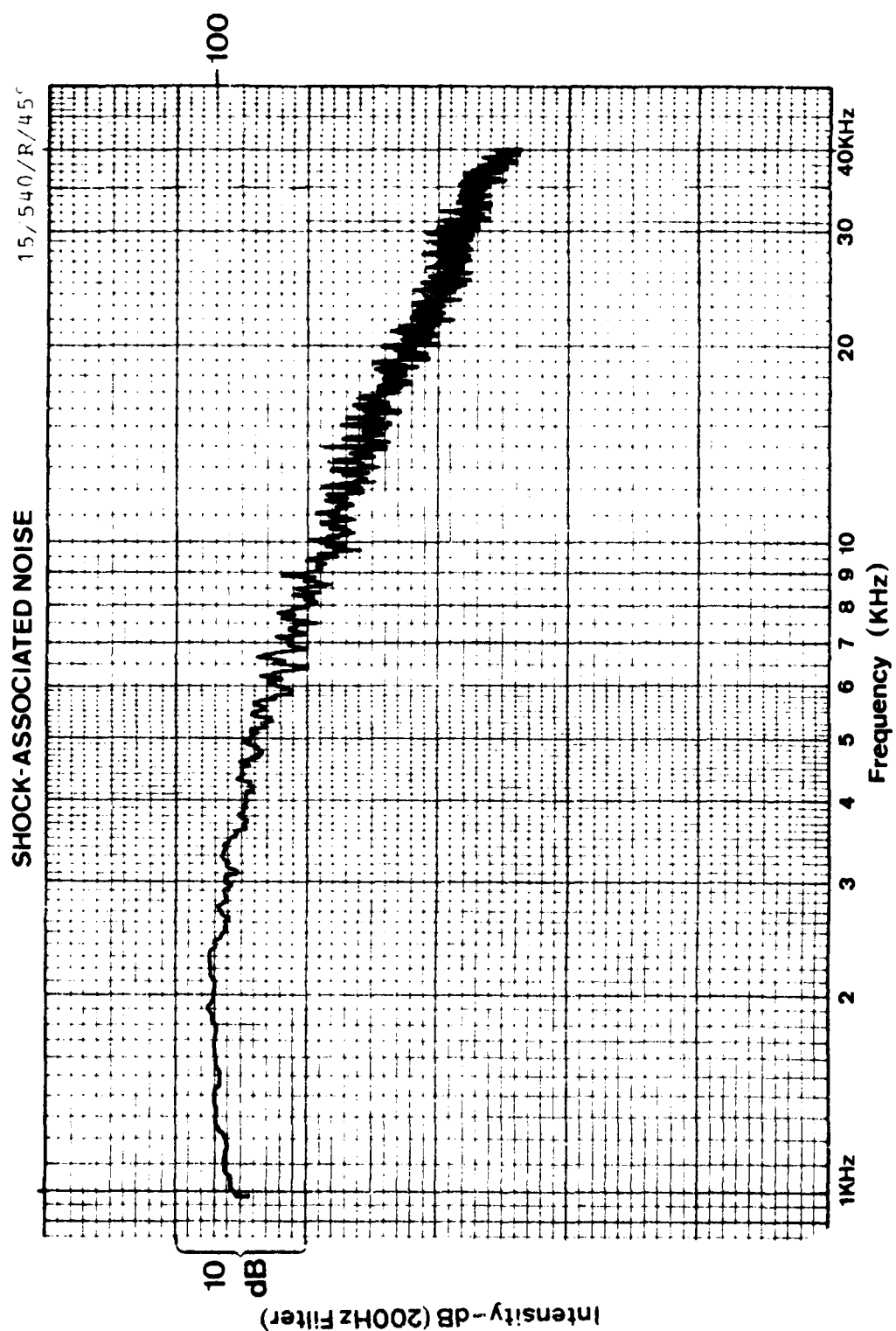


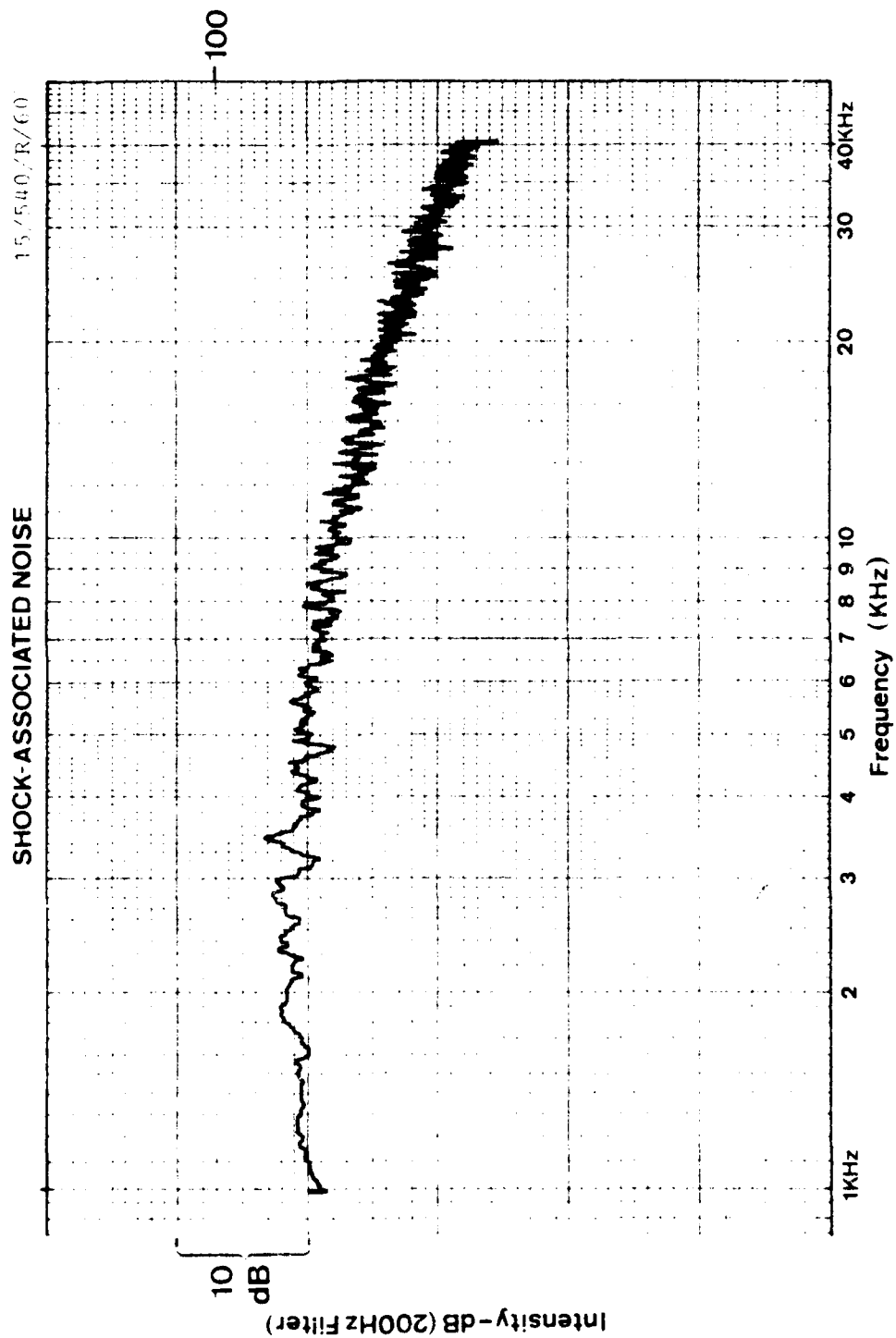


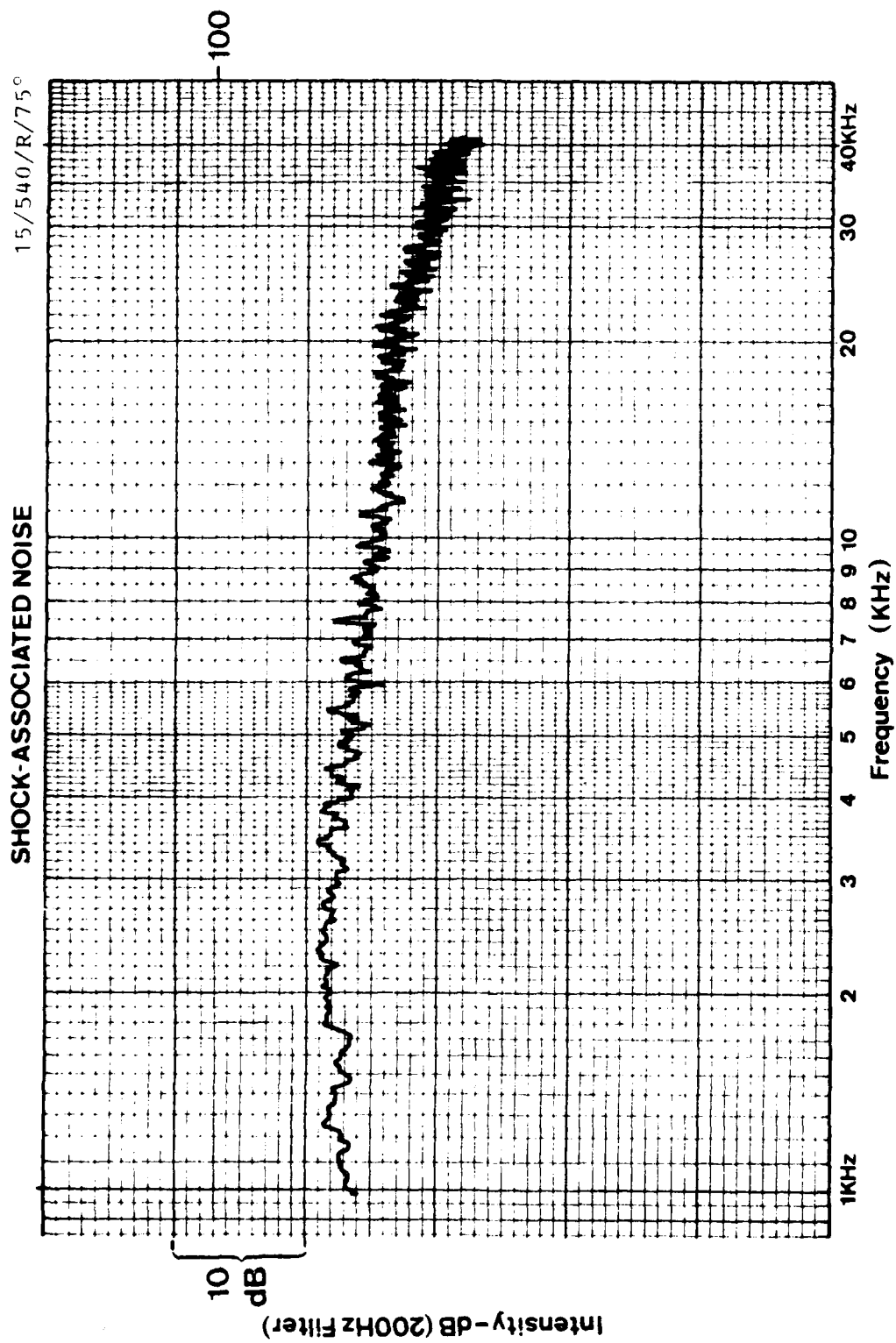


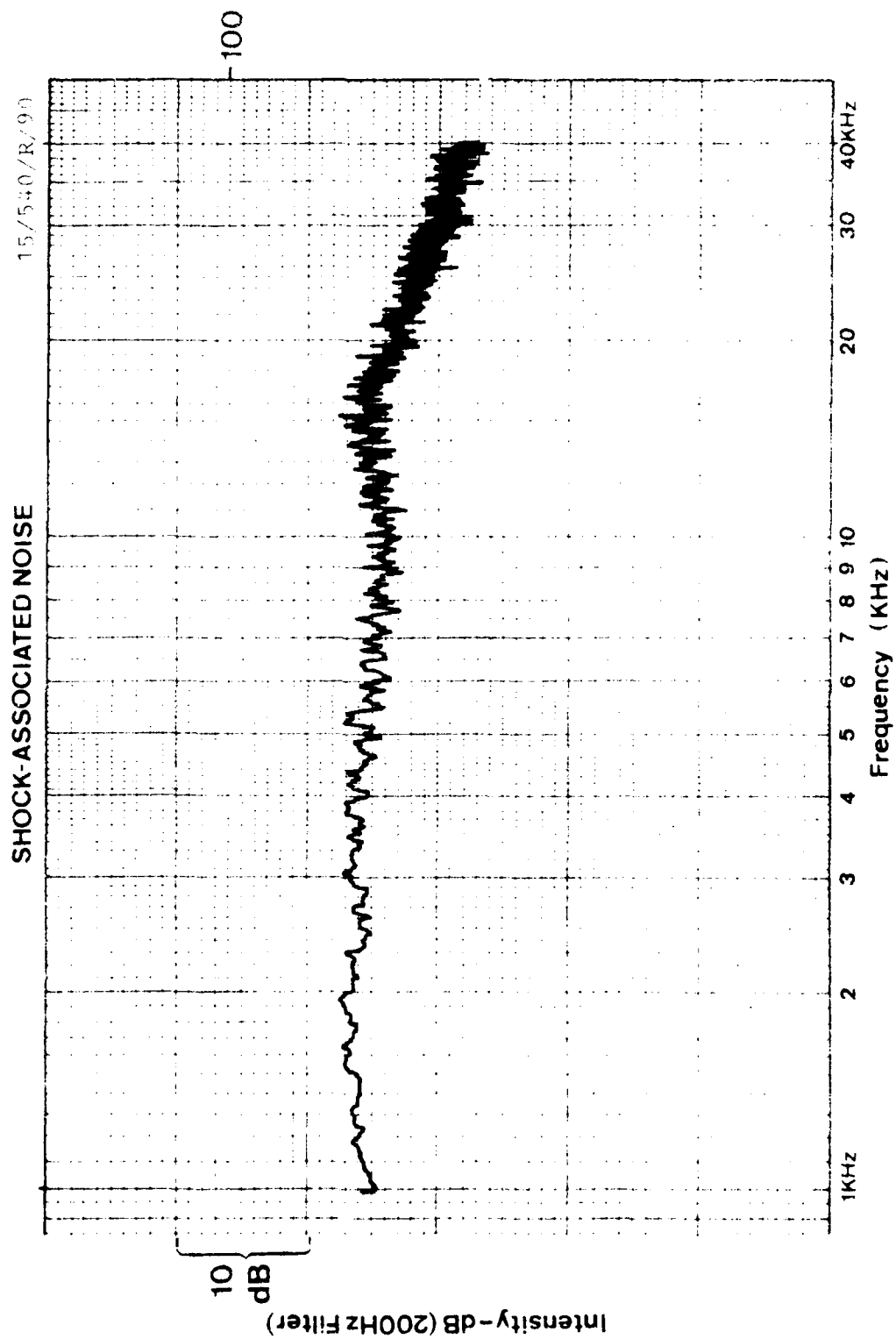


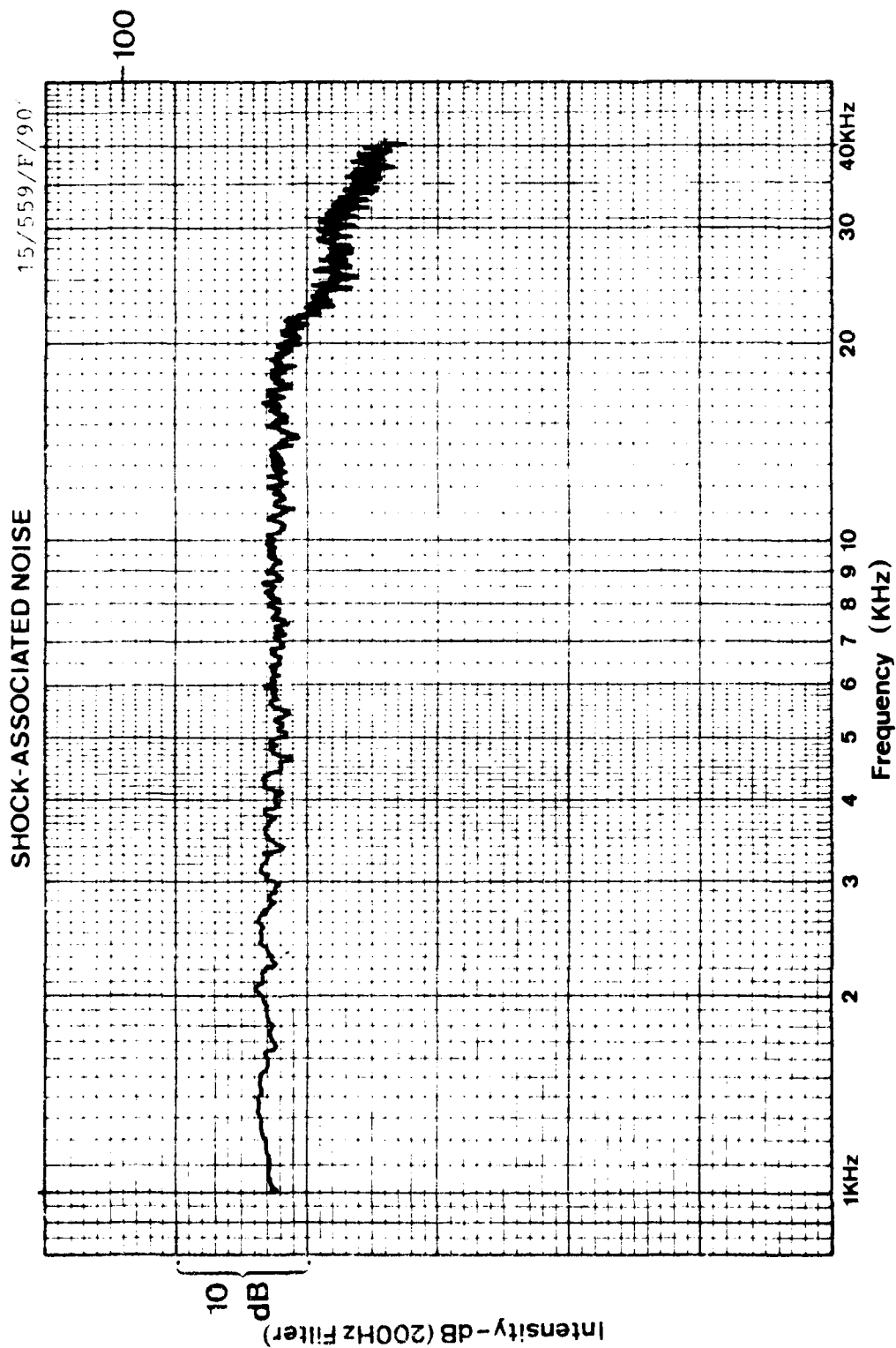


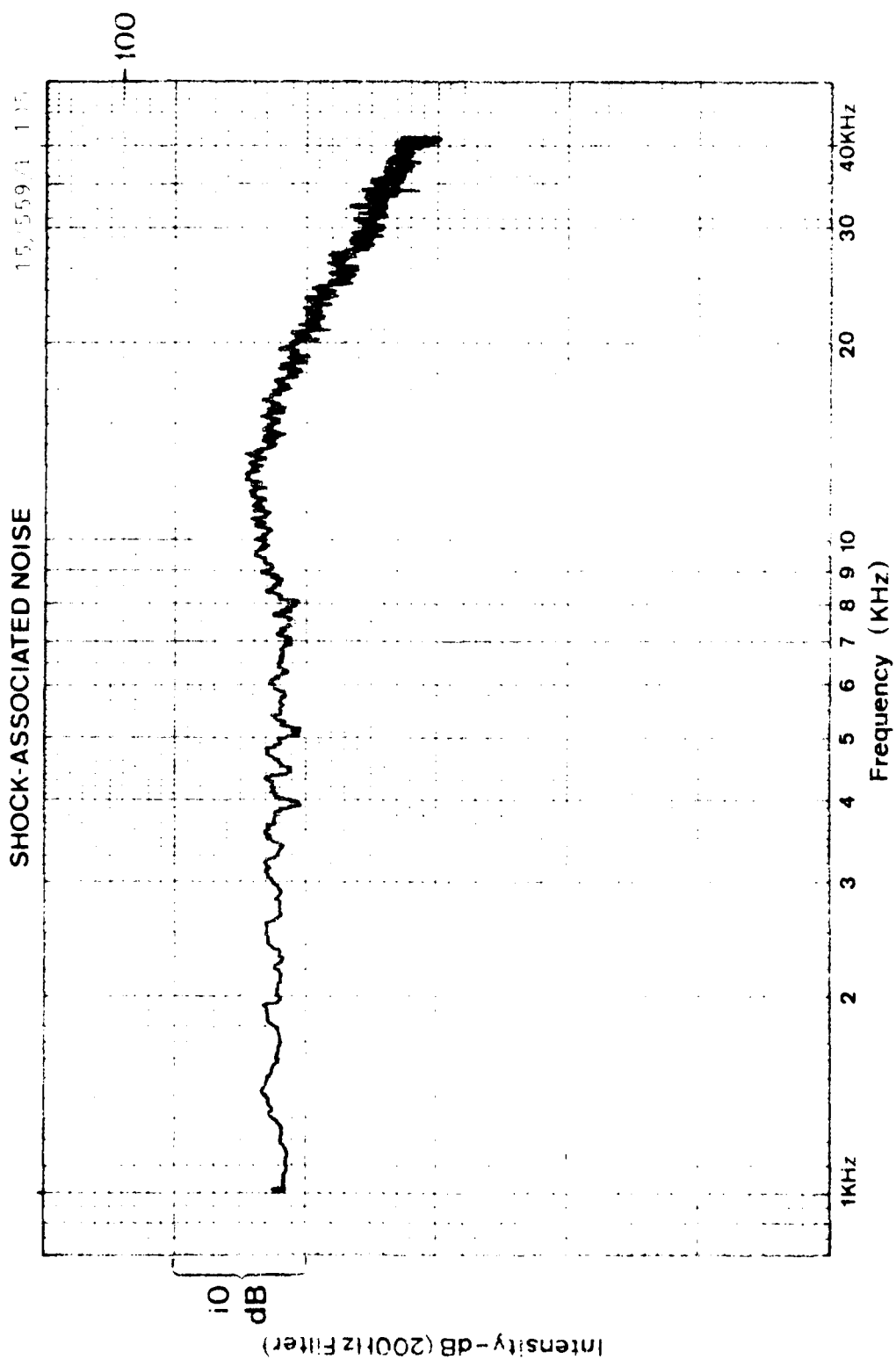


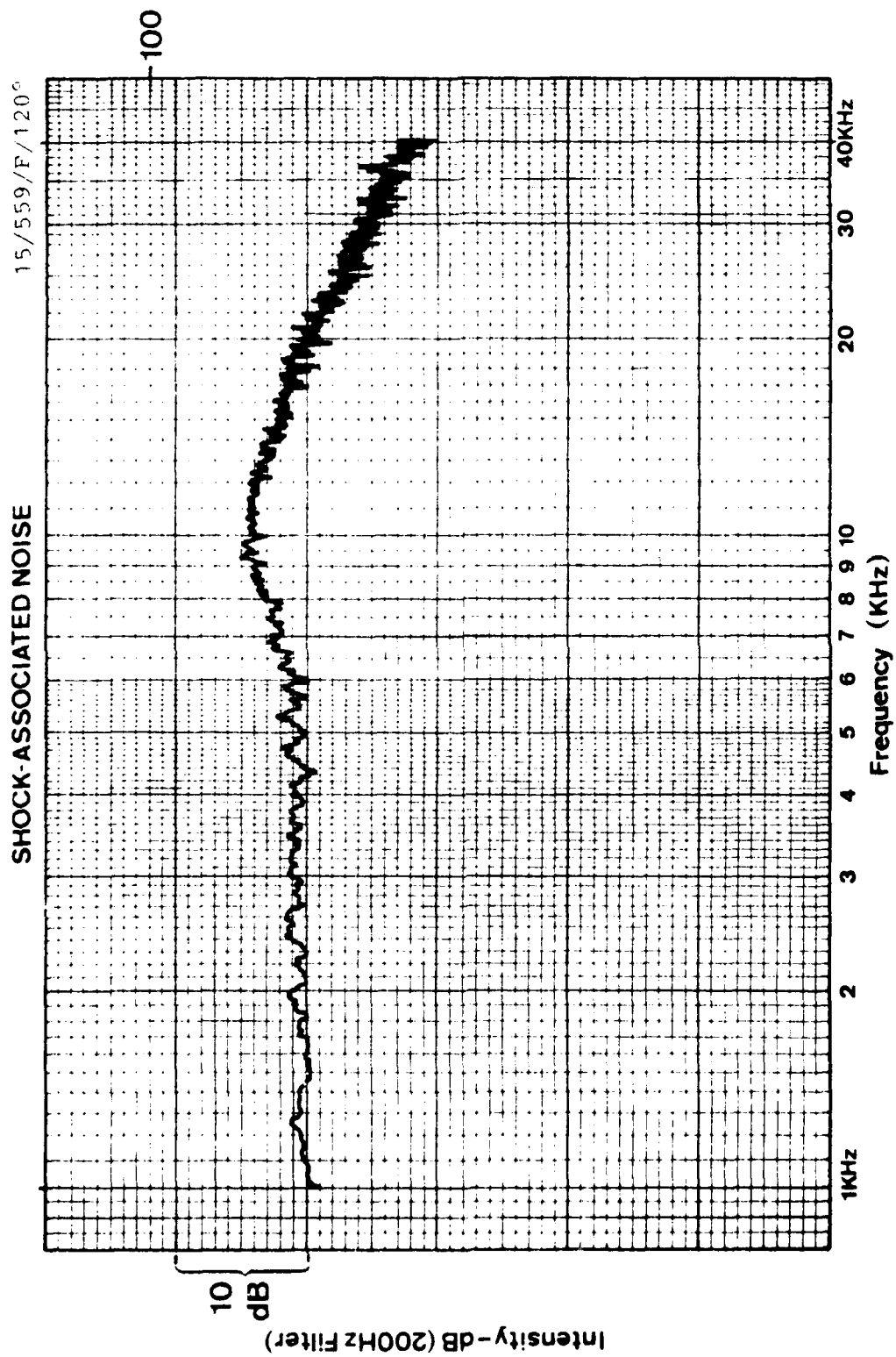


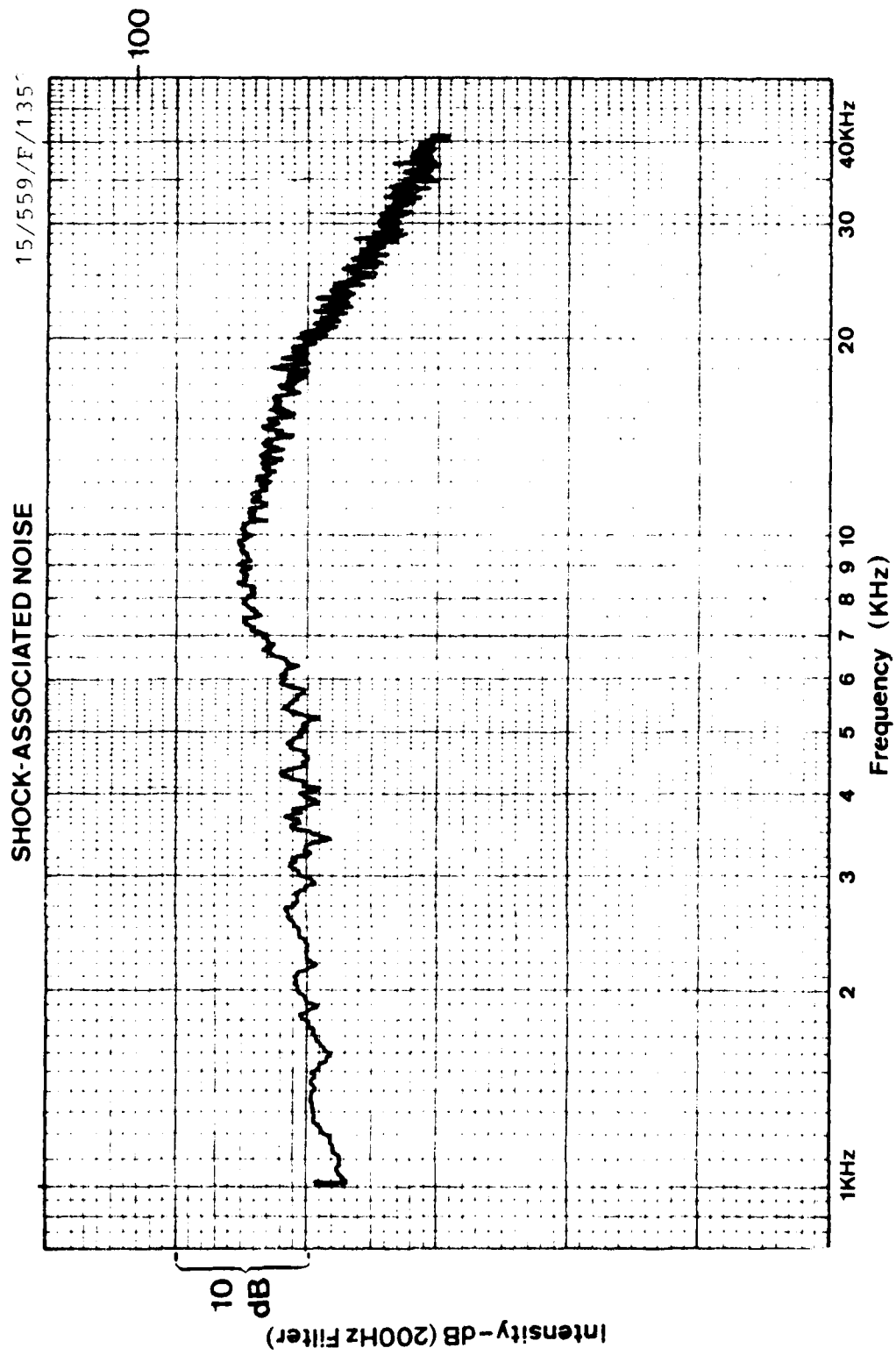


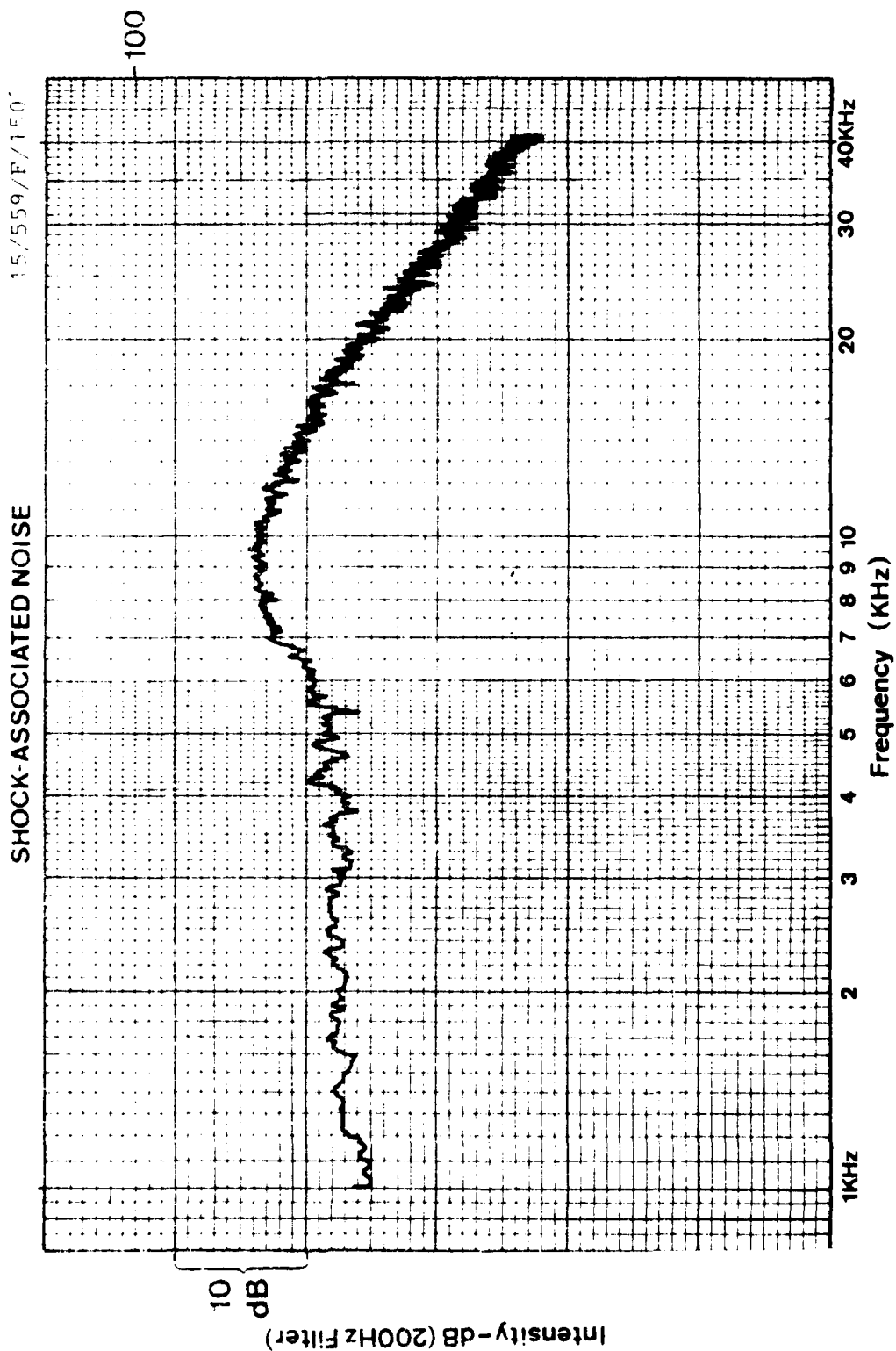


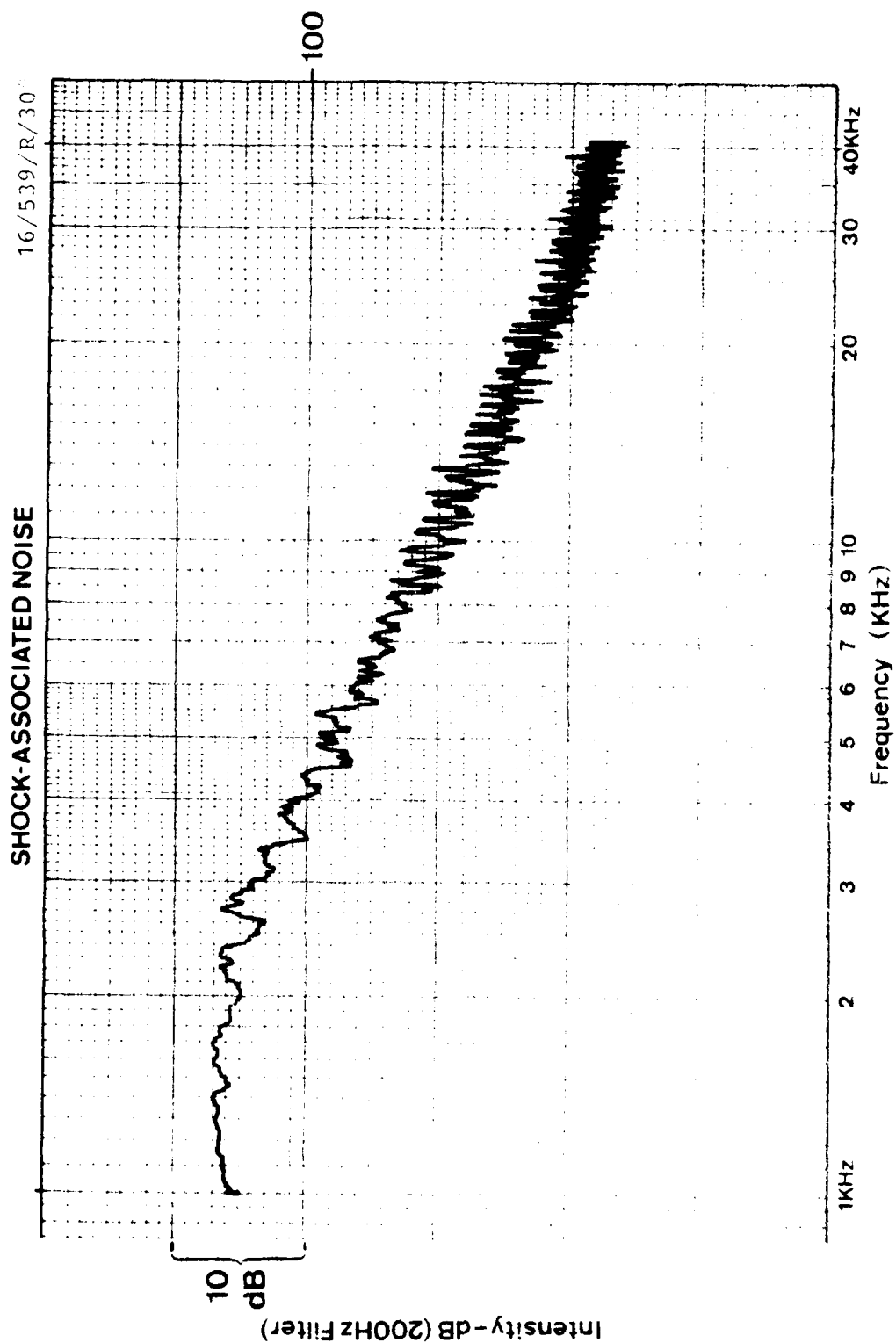


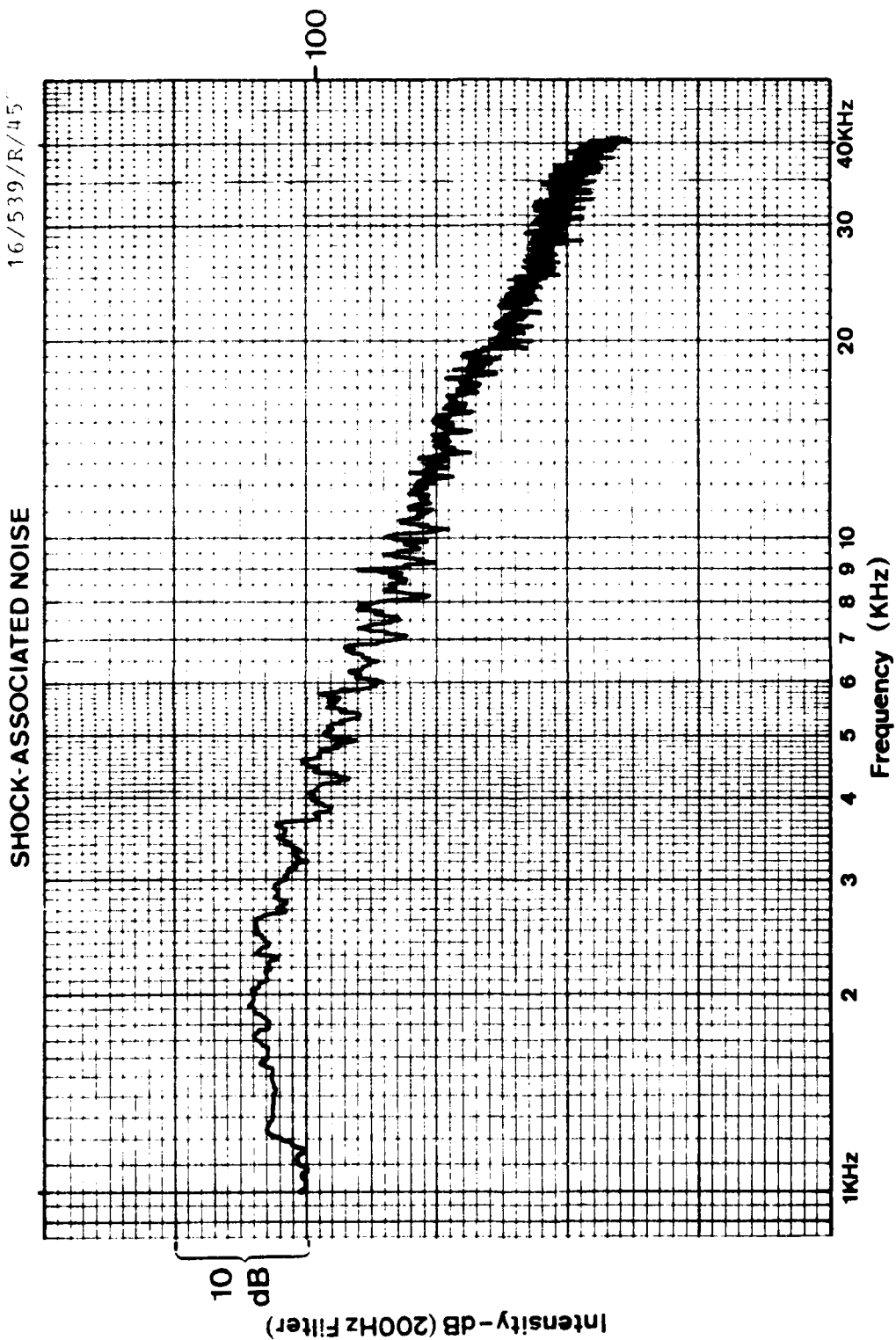


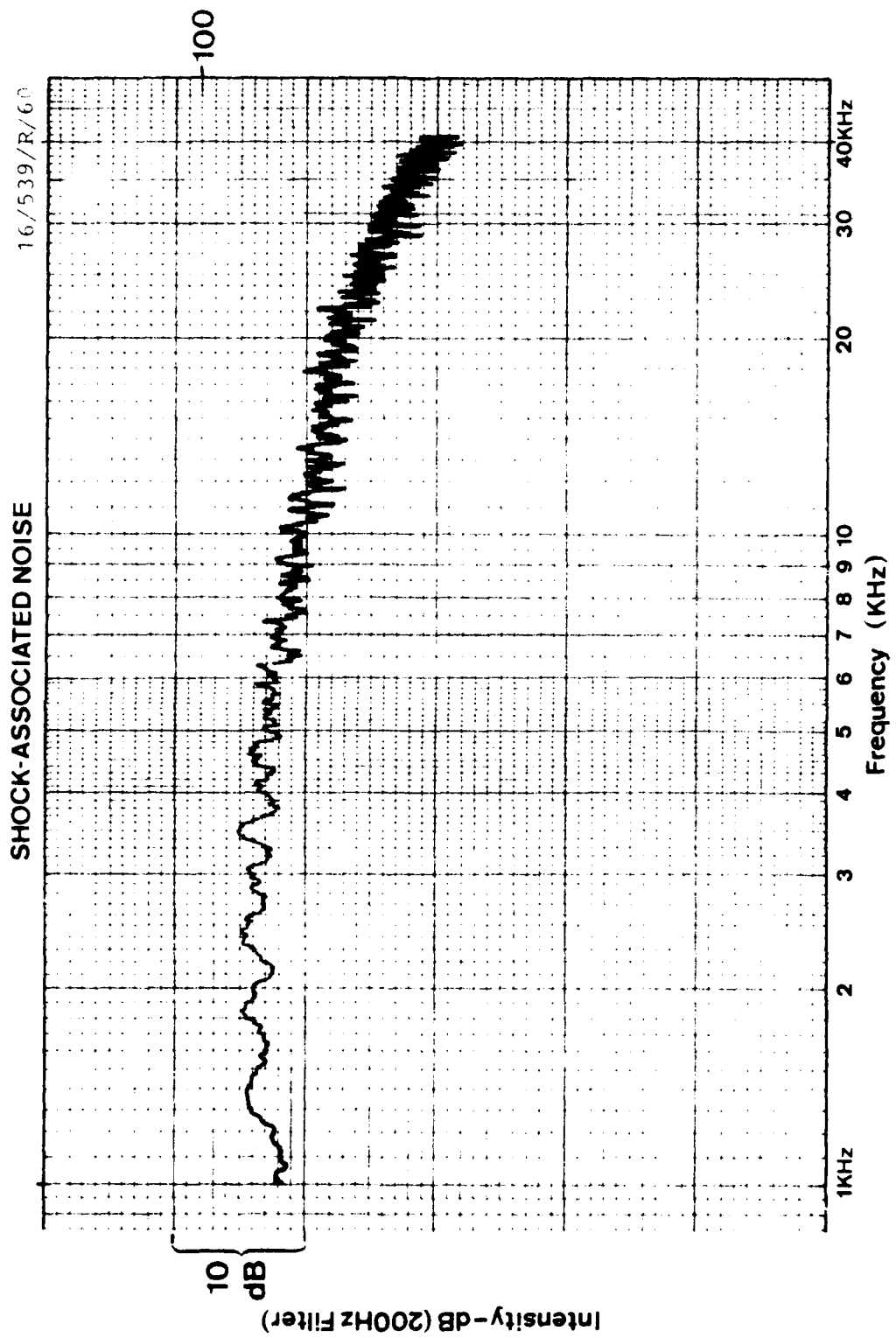






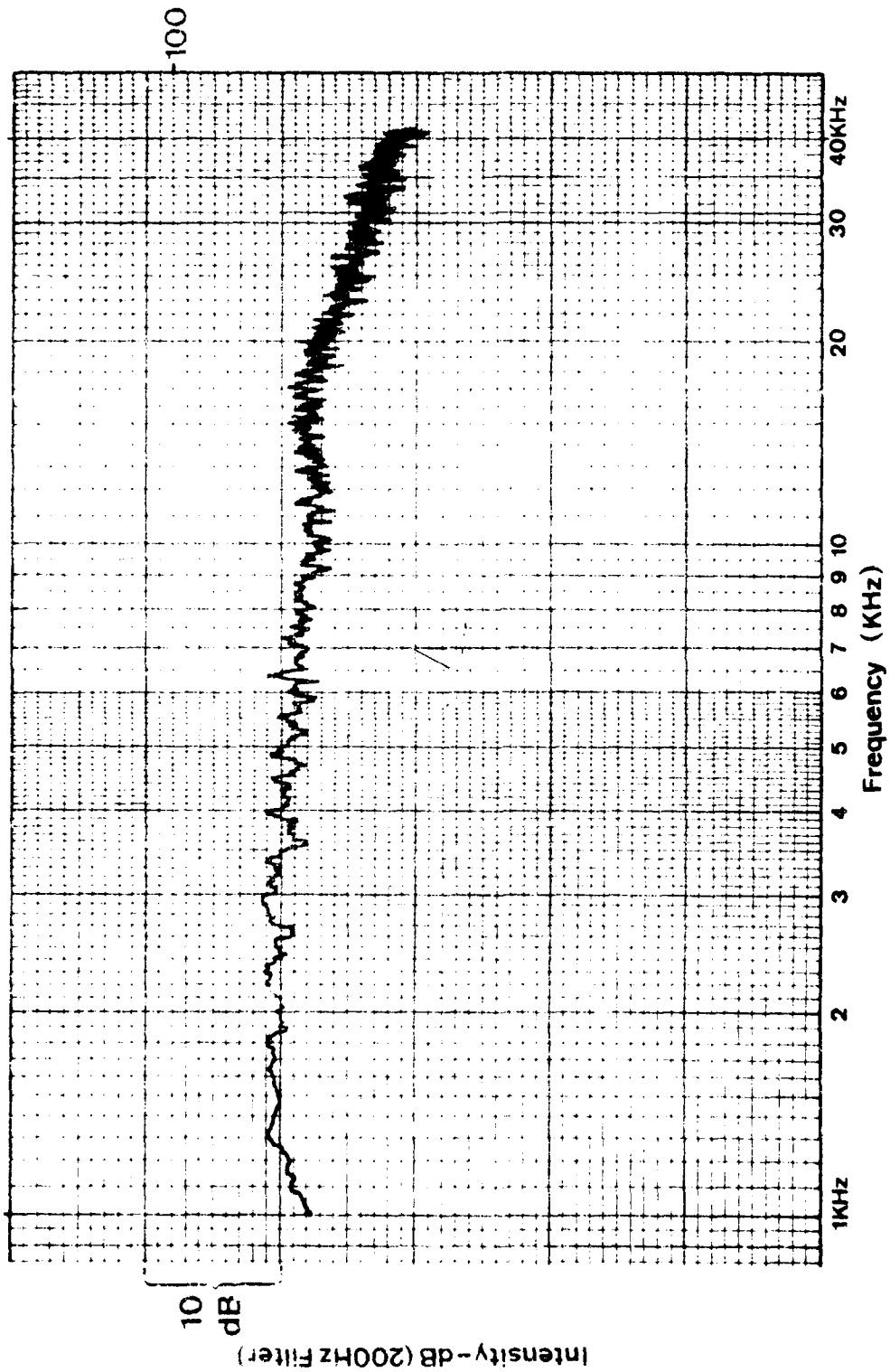


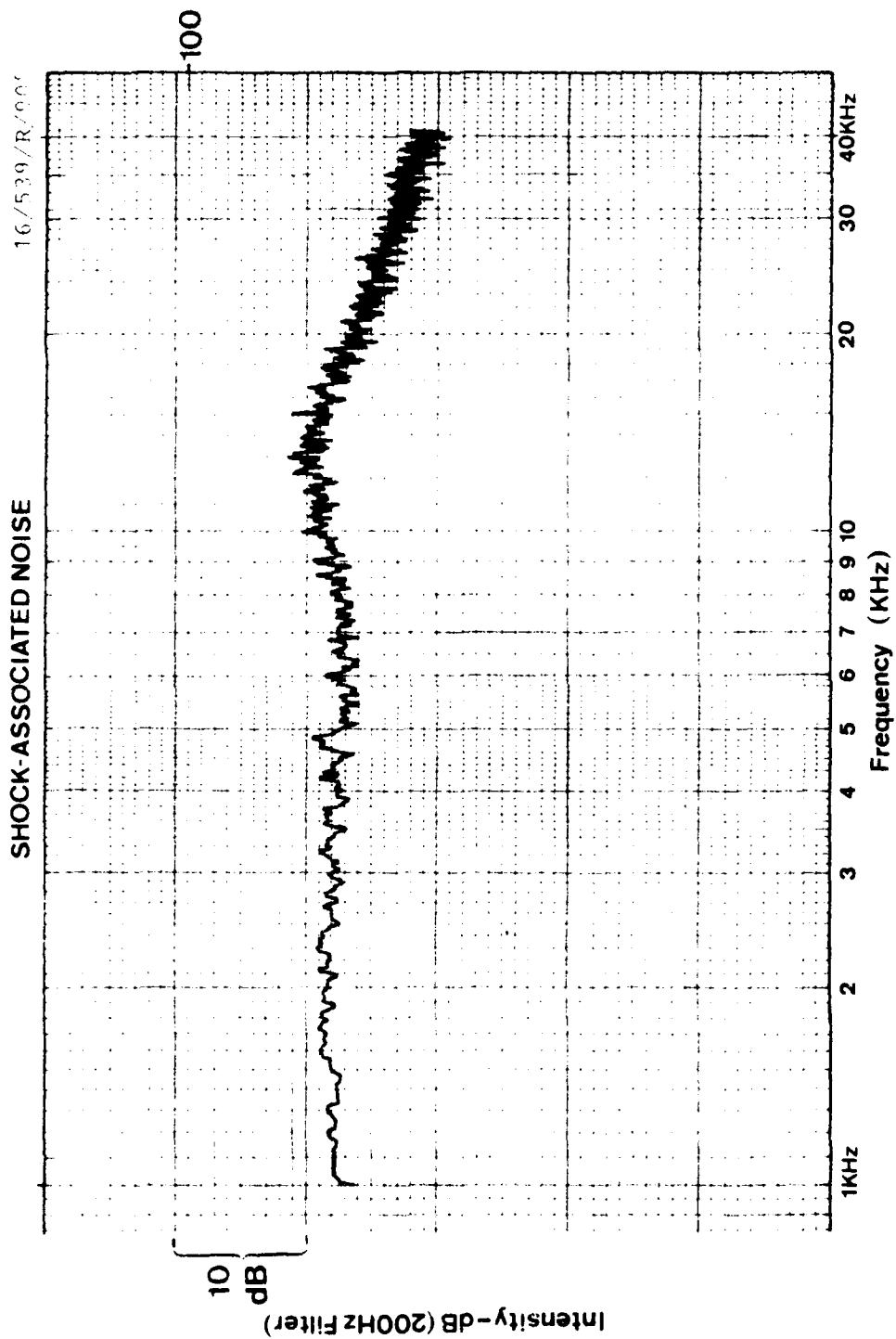


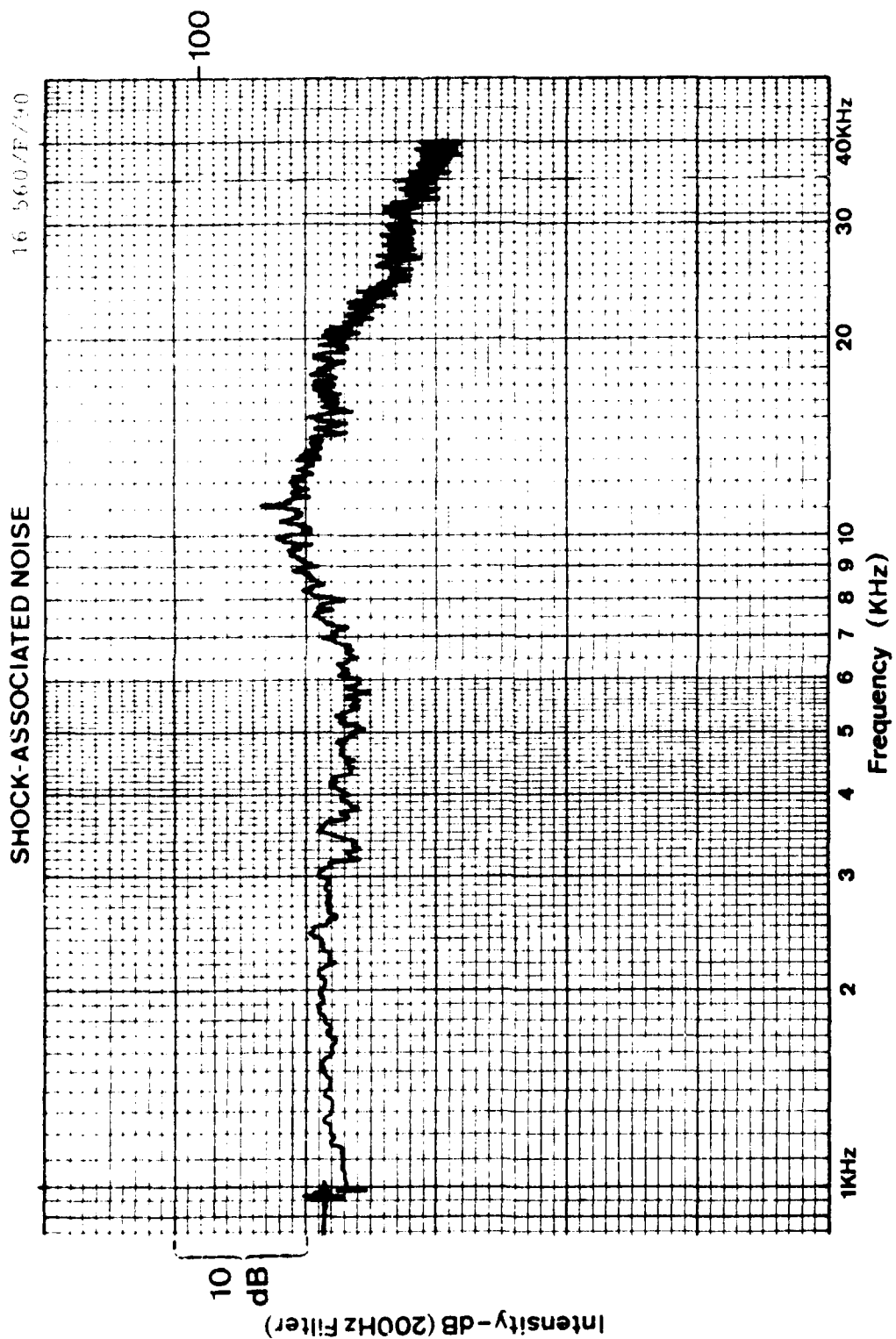


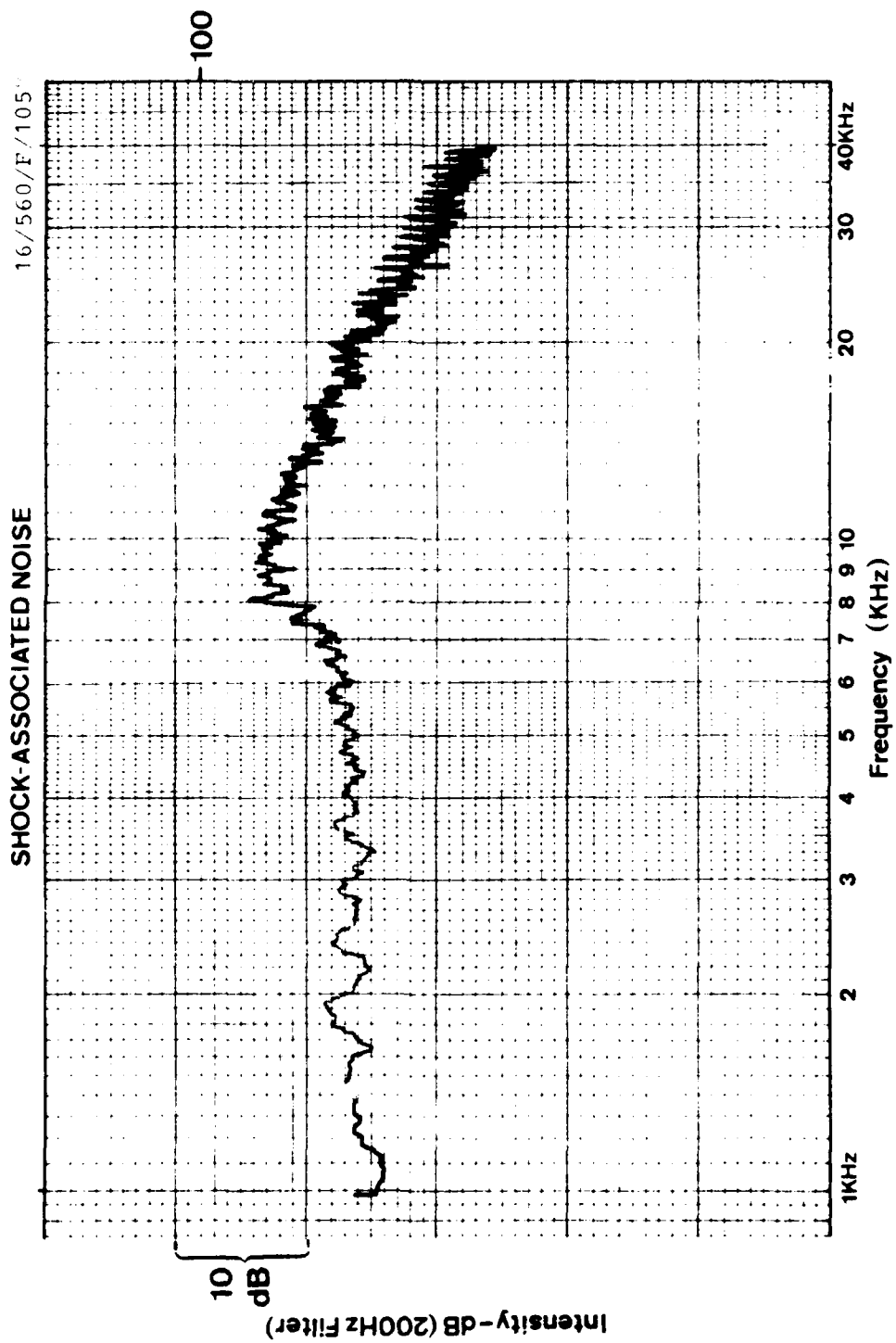
SHOCK-ASSOCIATED NOISE

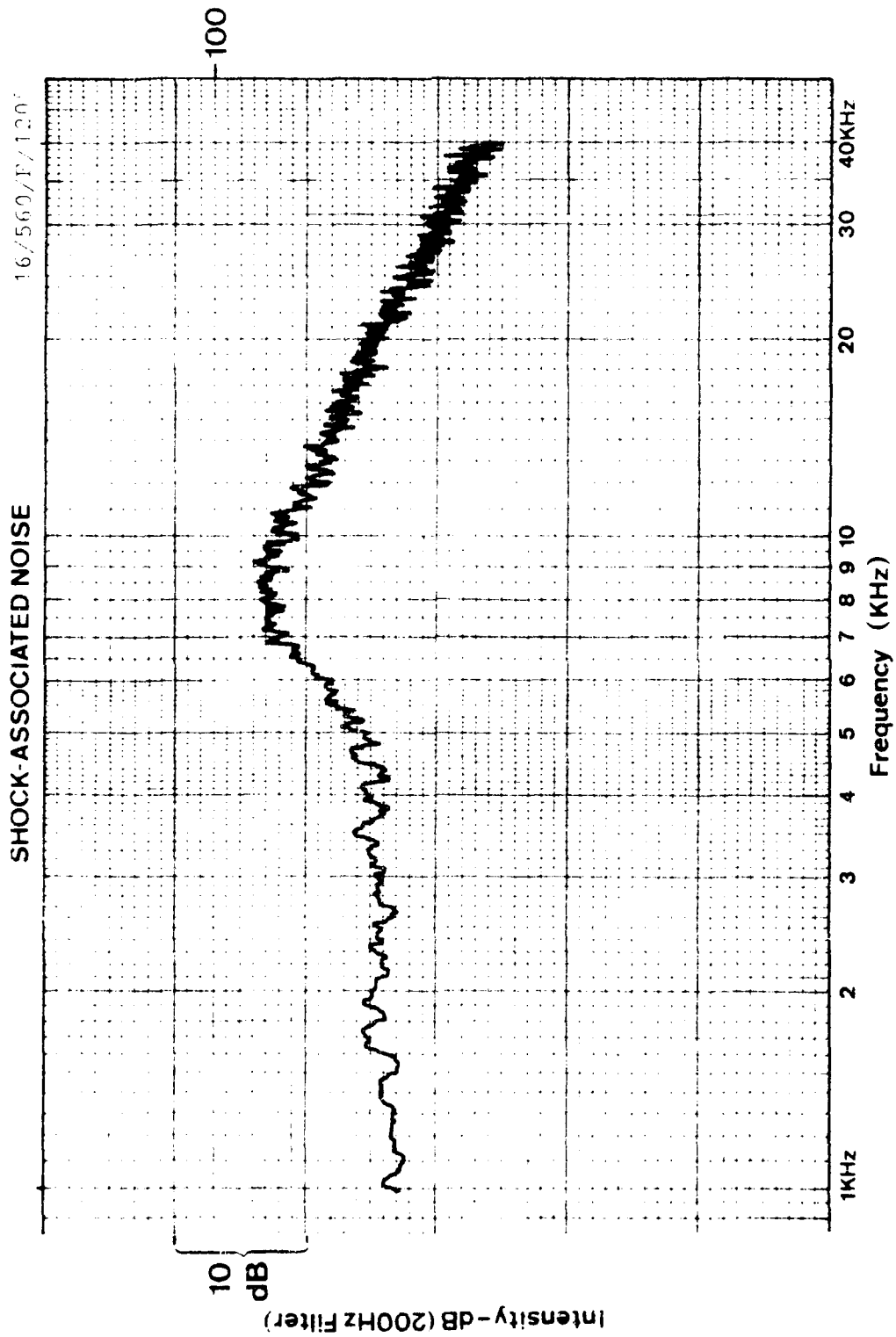
16/539/R/75"

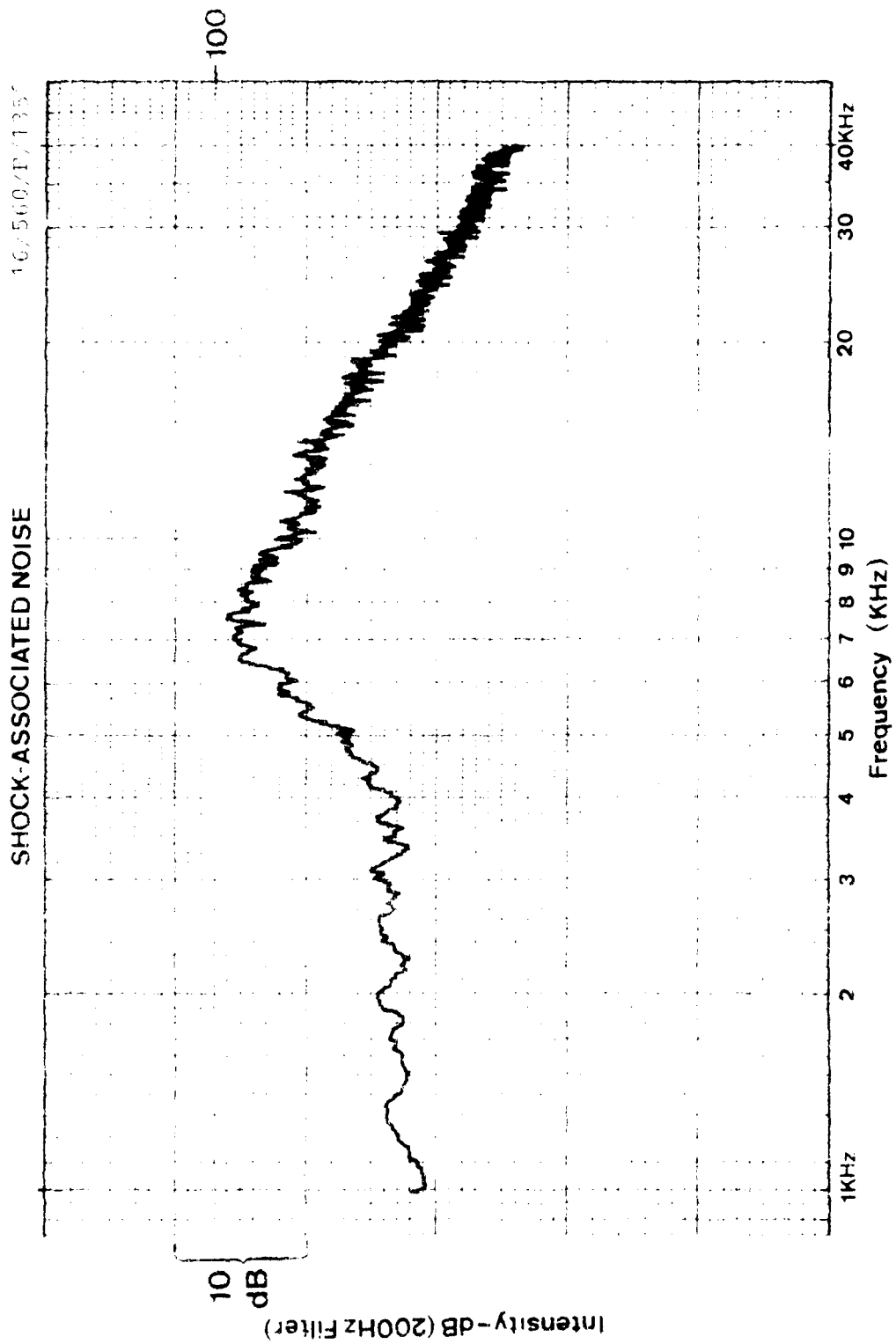


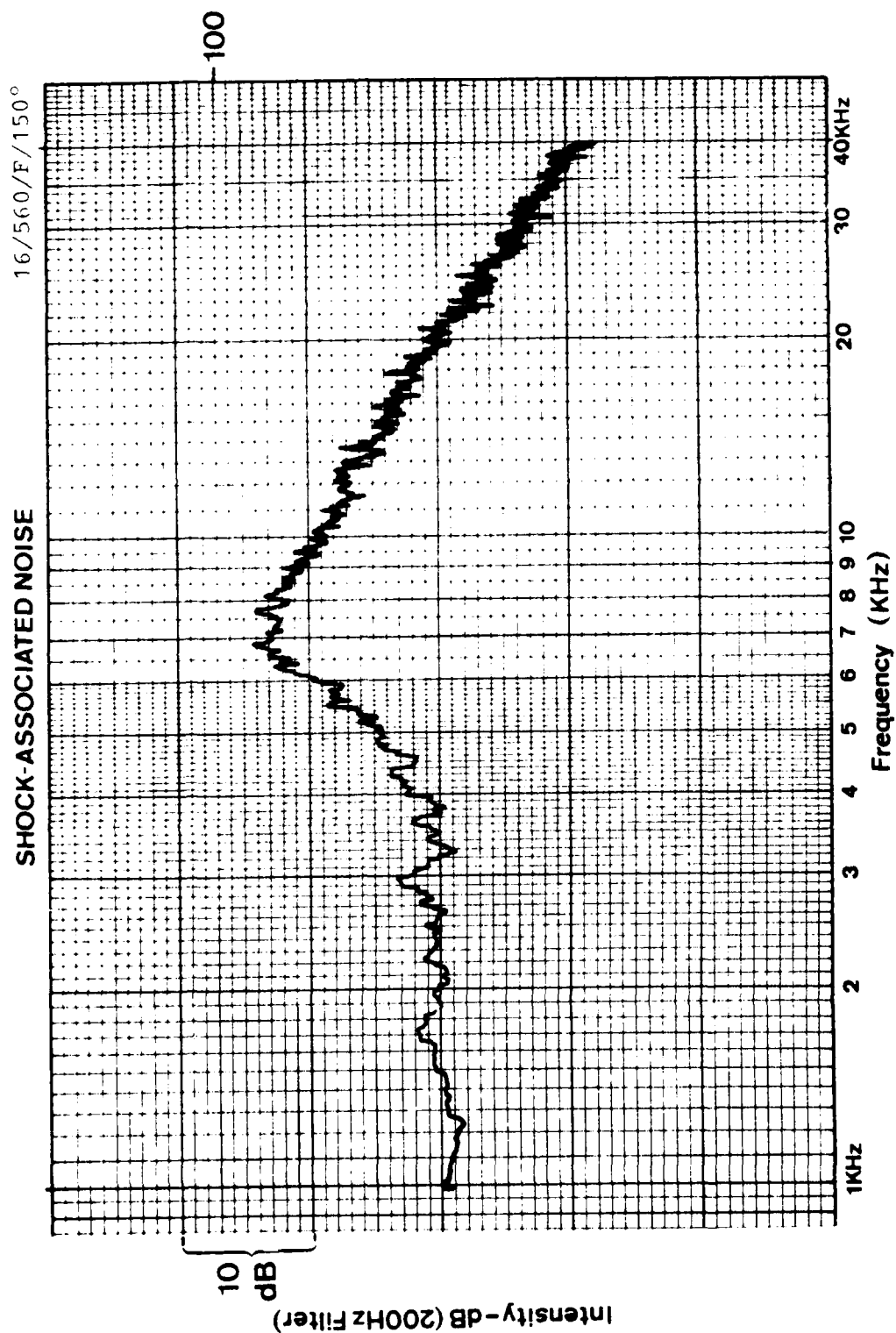


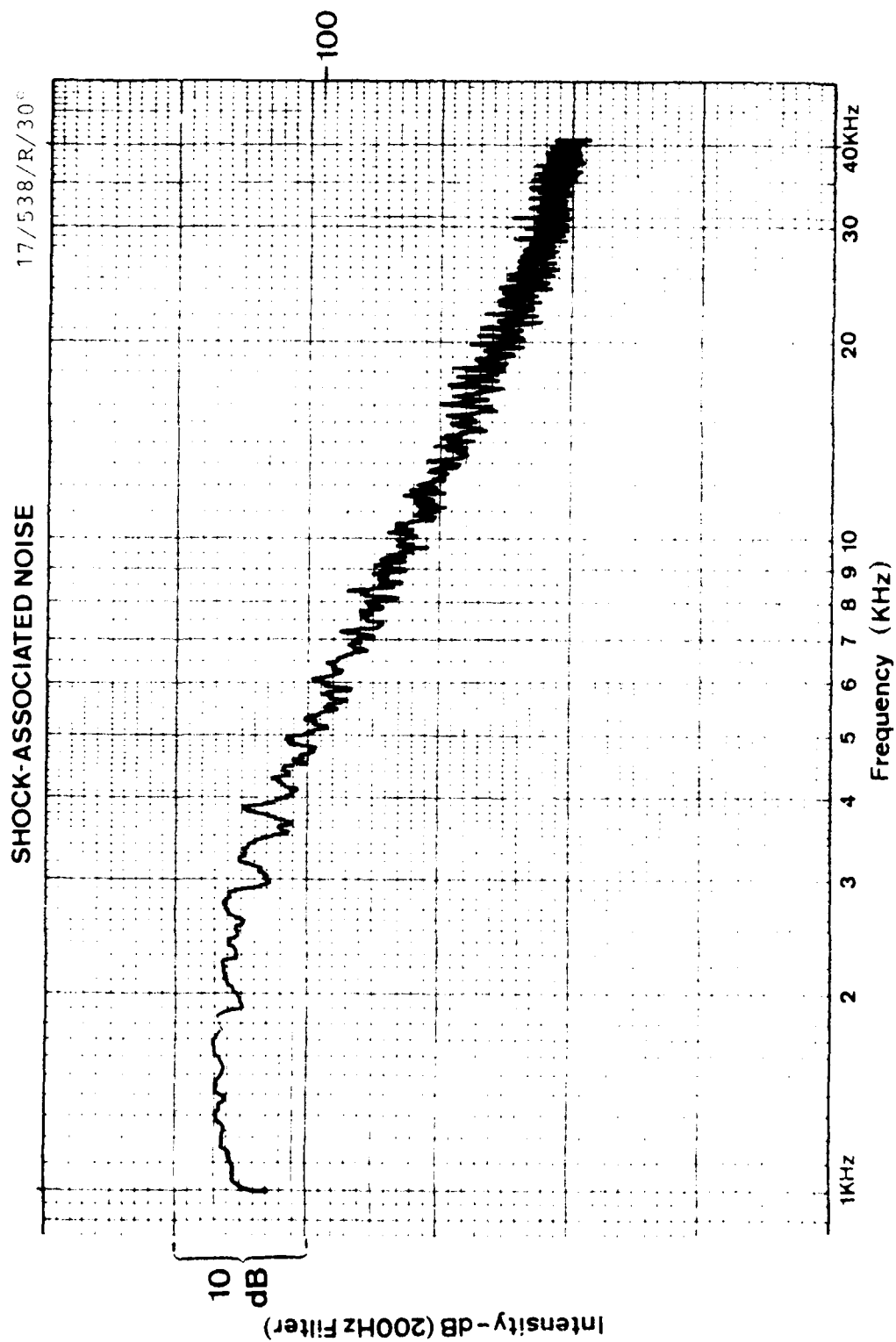


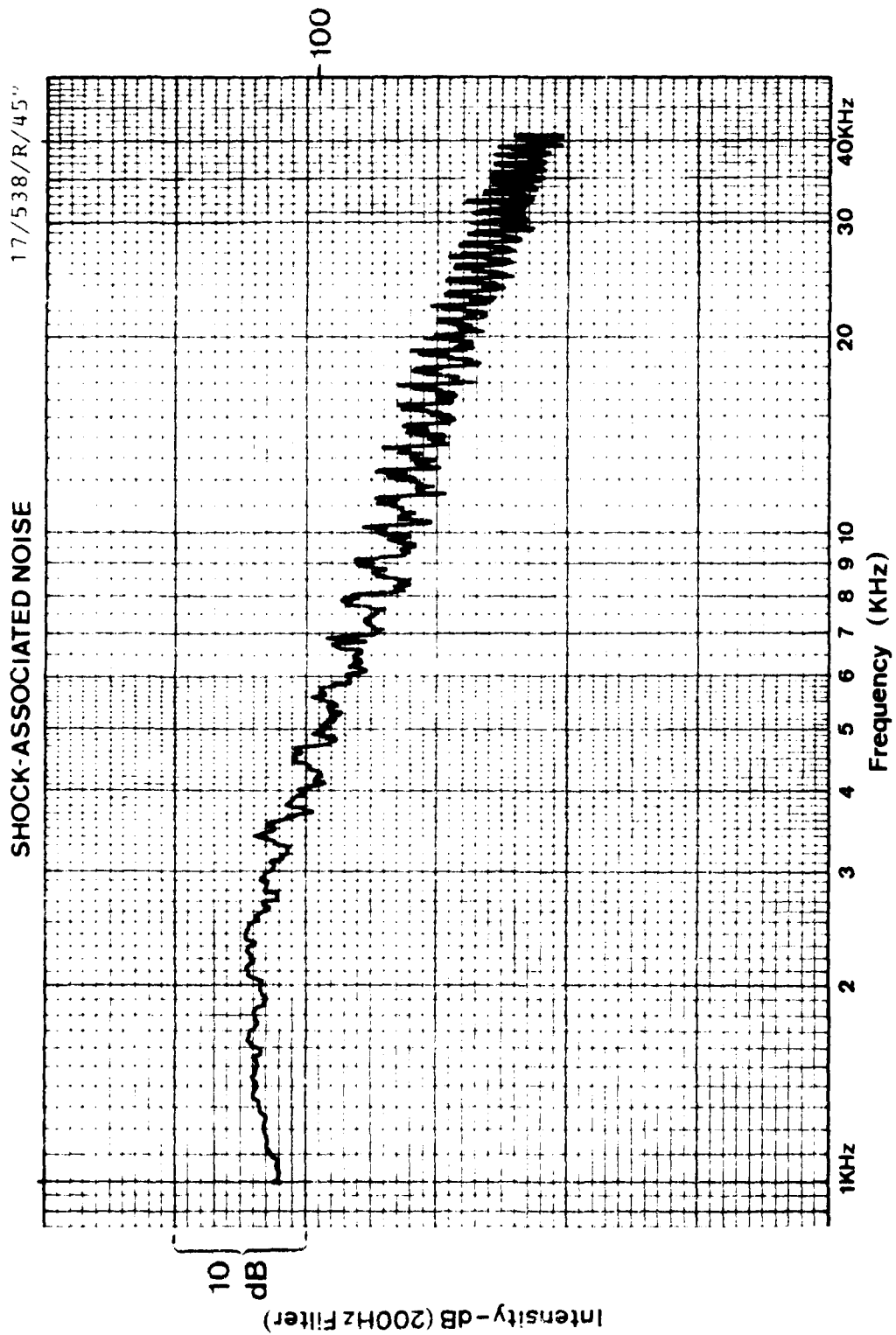


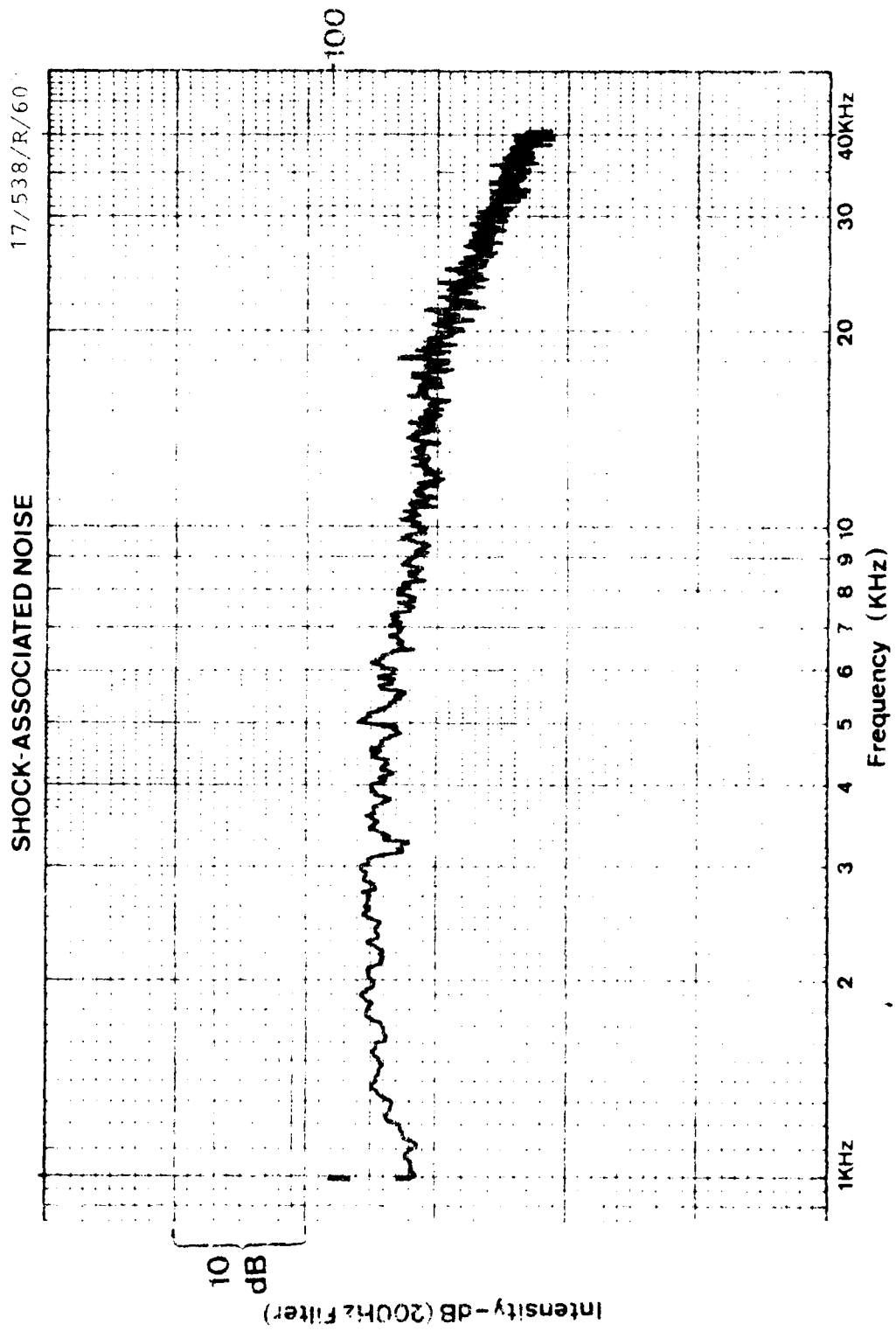


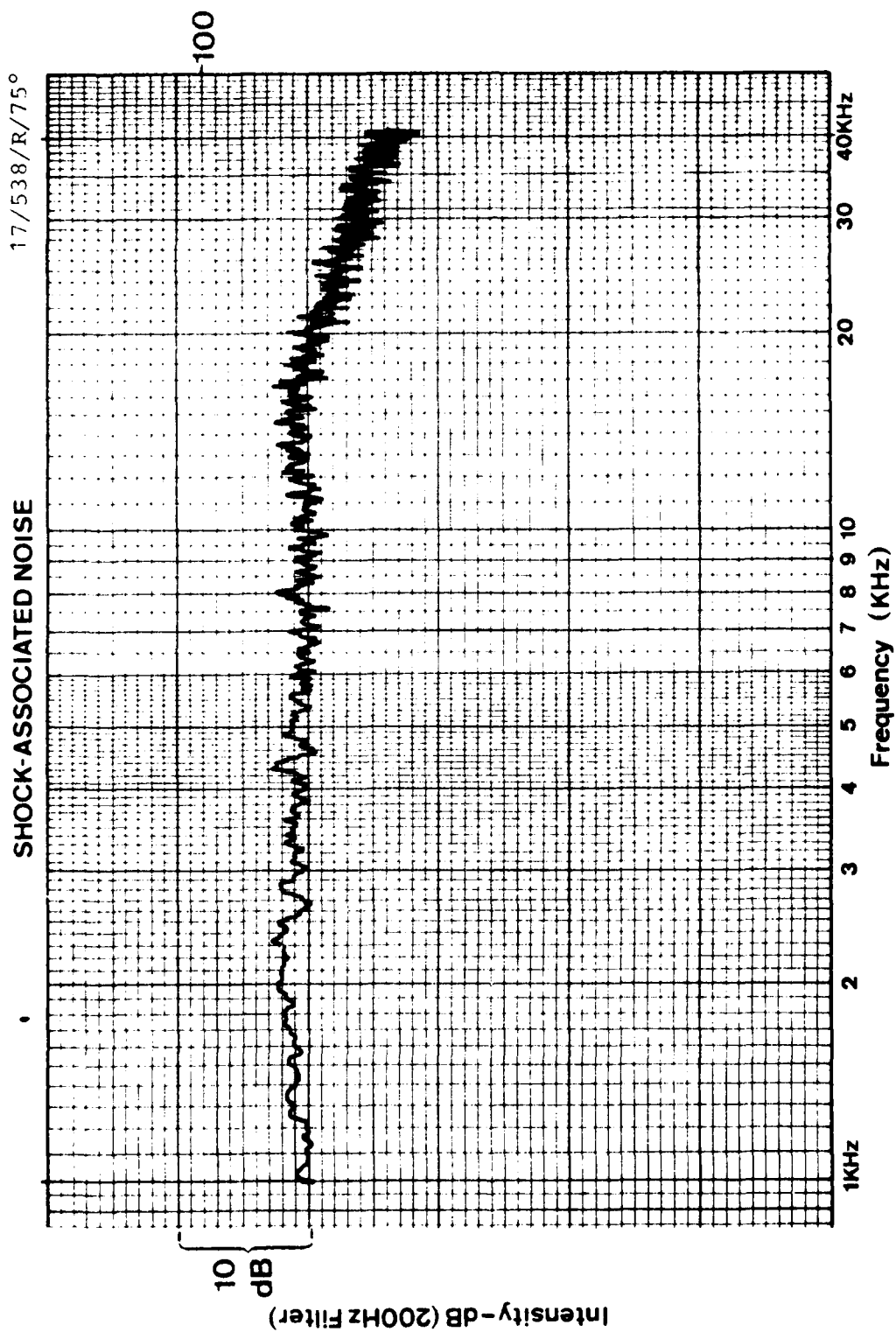


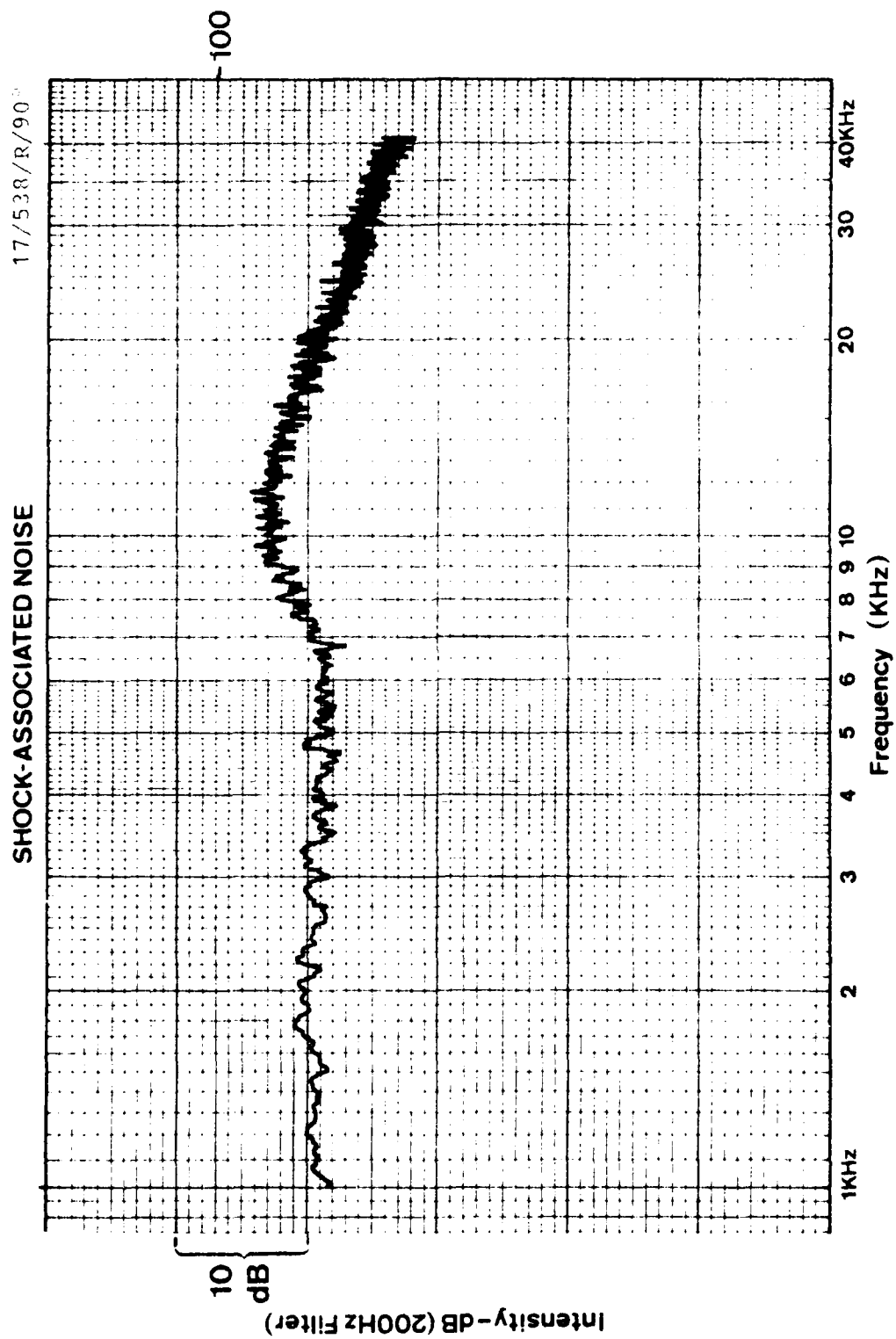






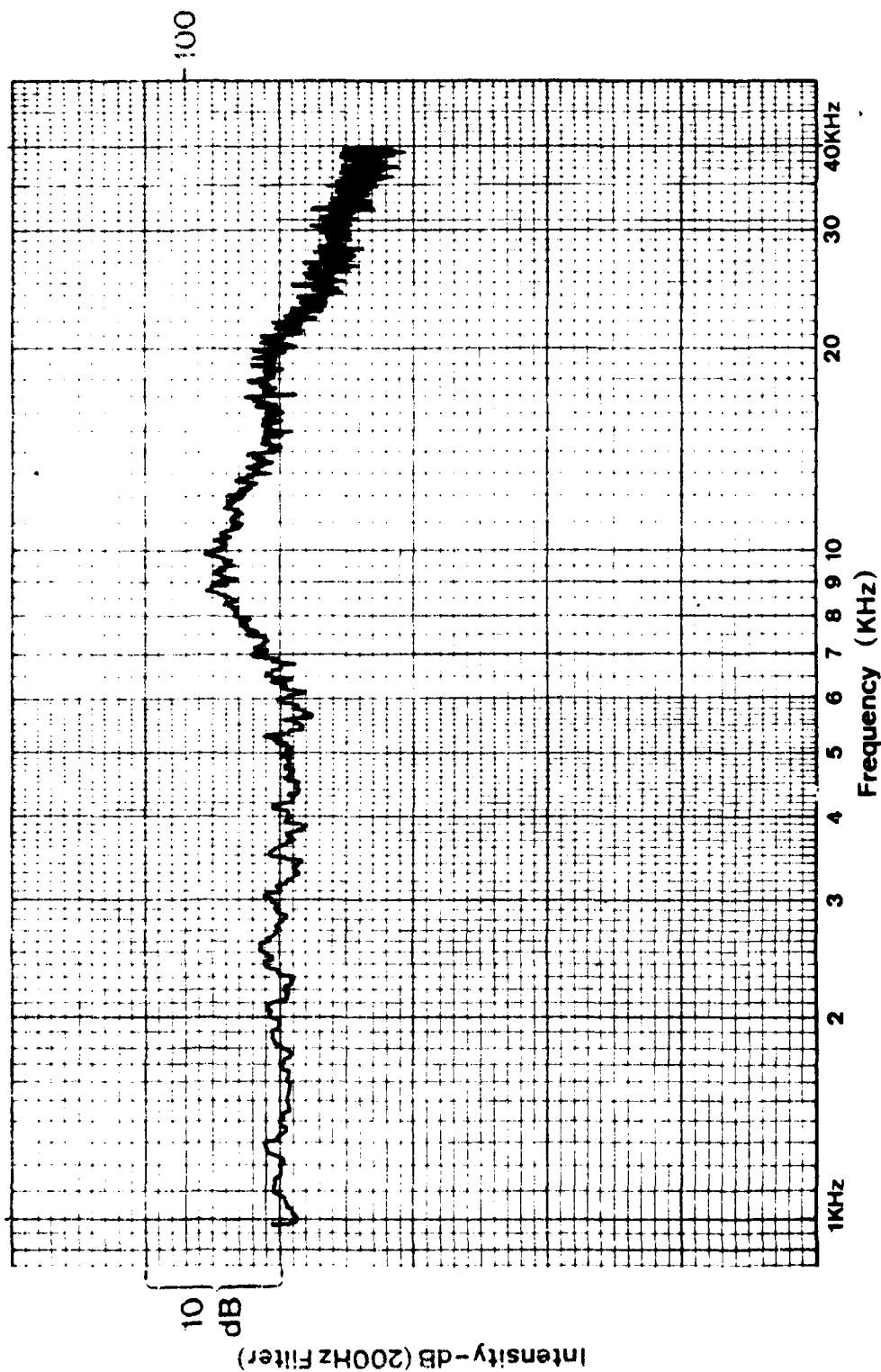


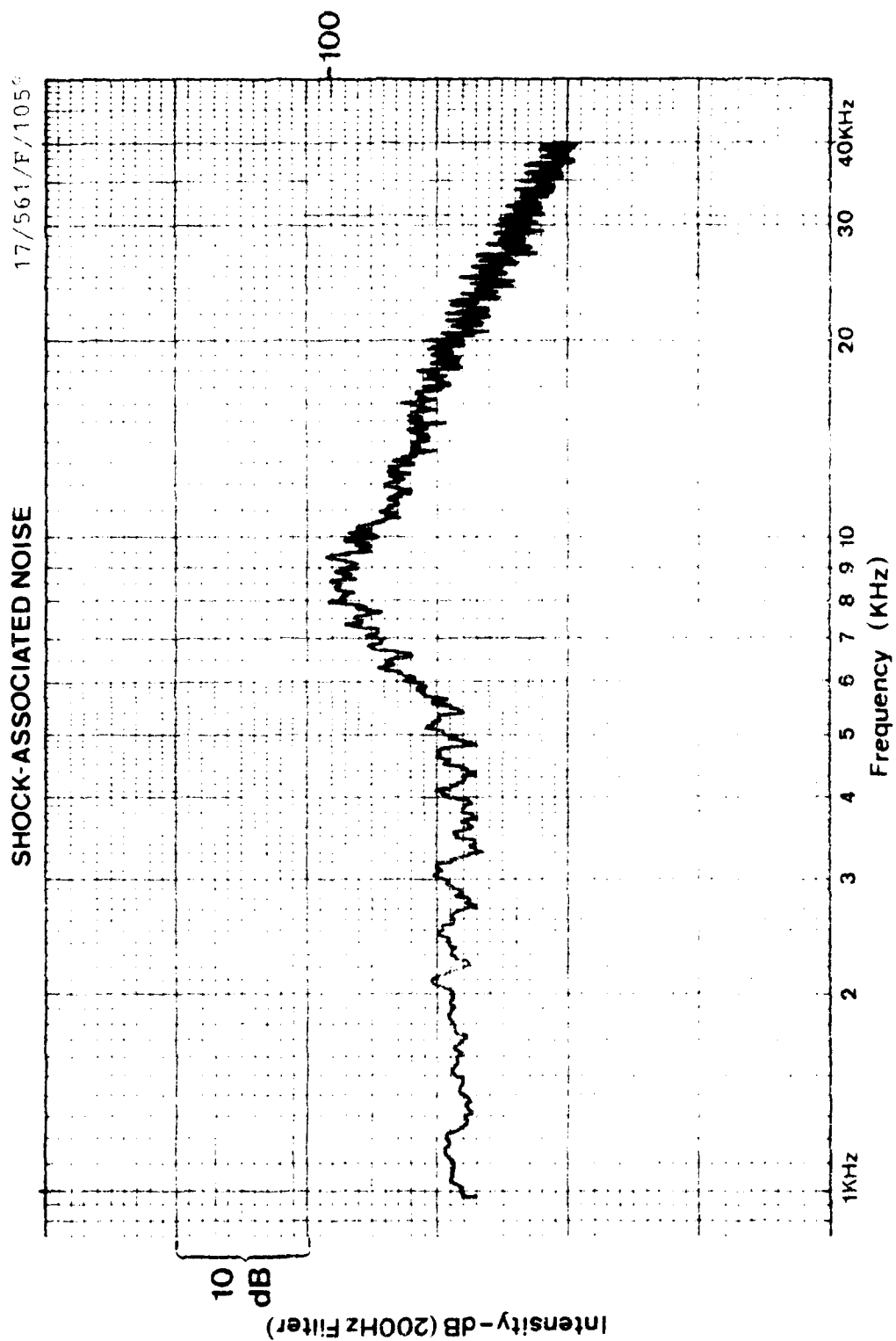


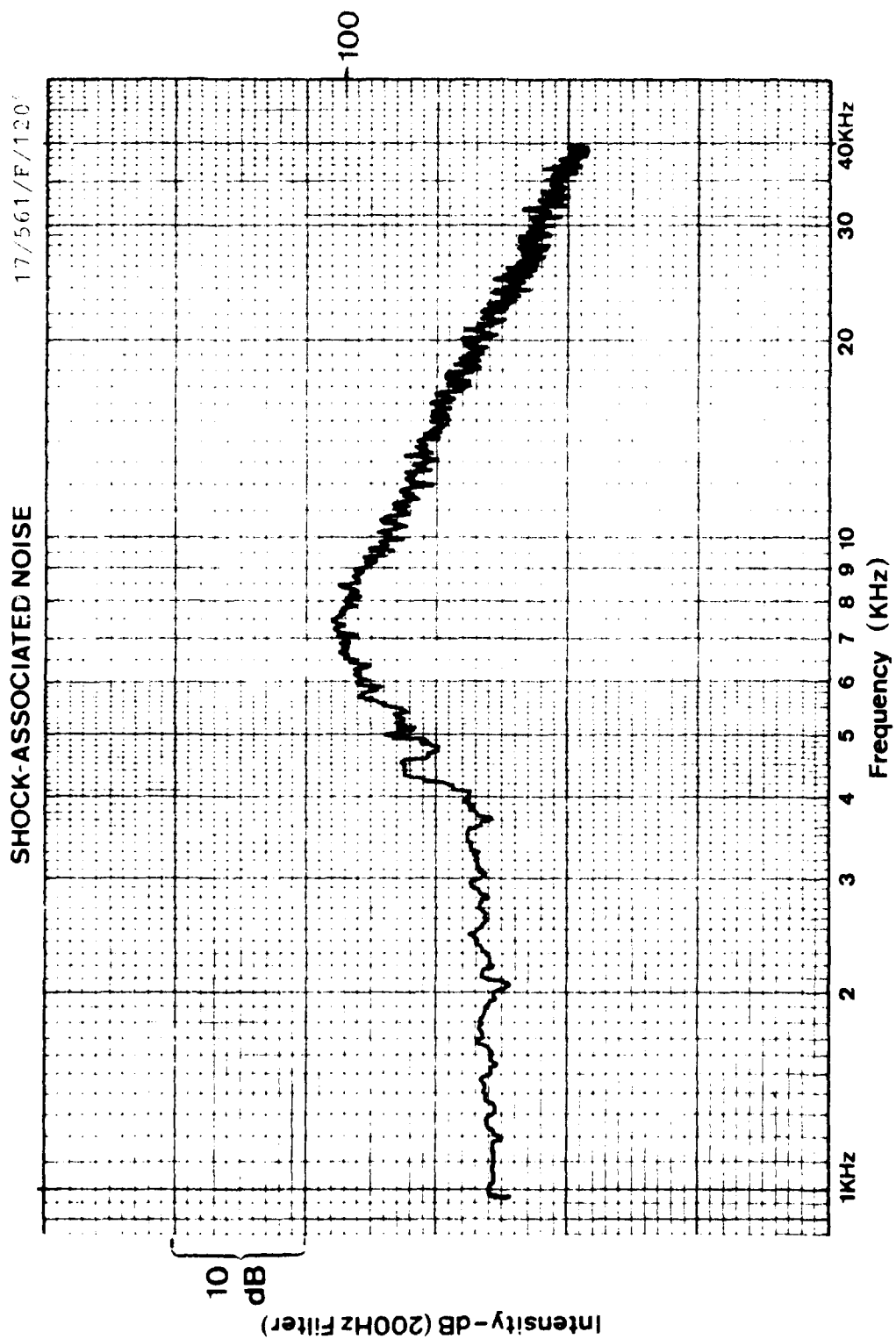


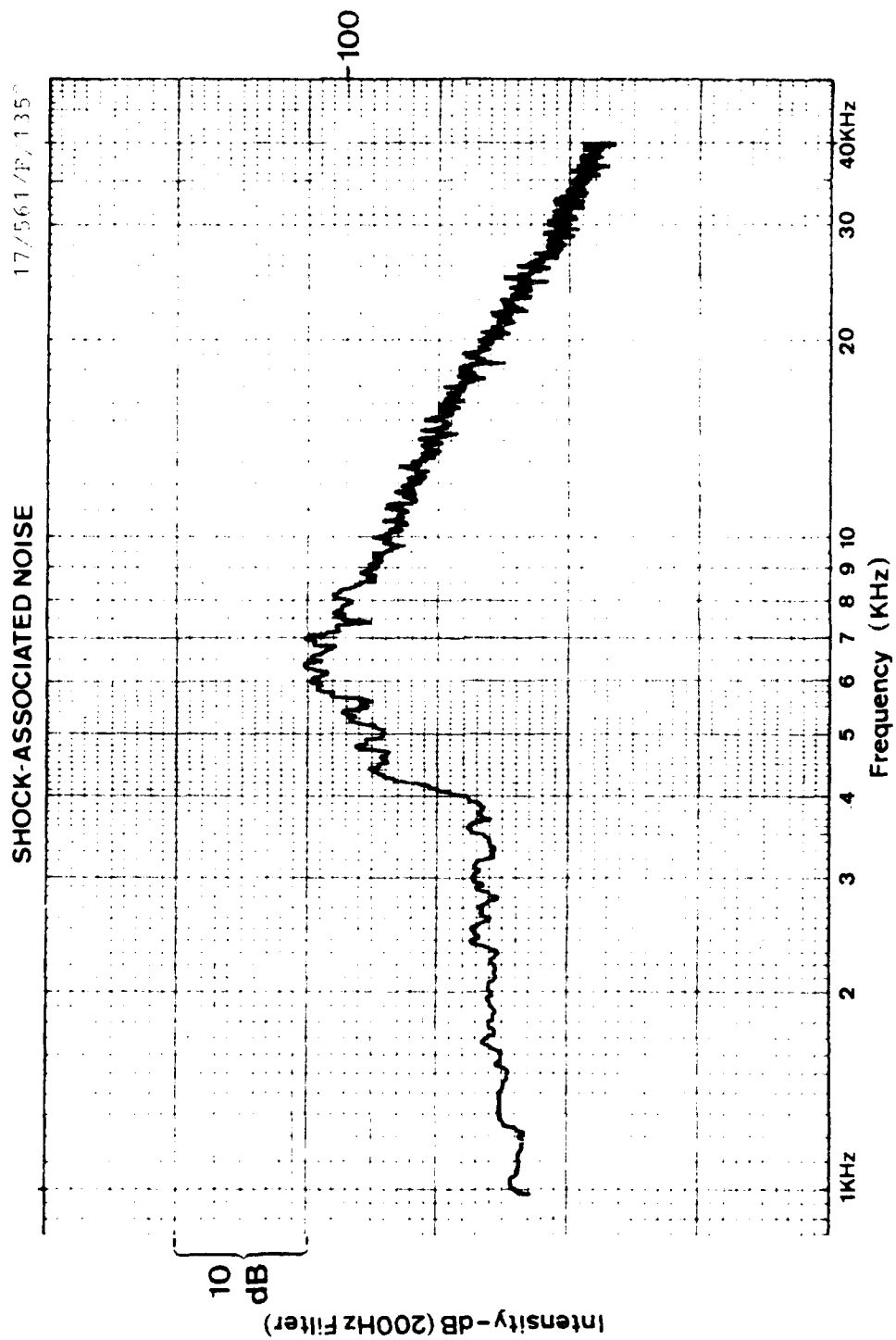
SHOCK-ASSOCIATED NOISE

12/5614/99



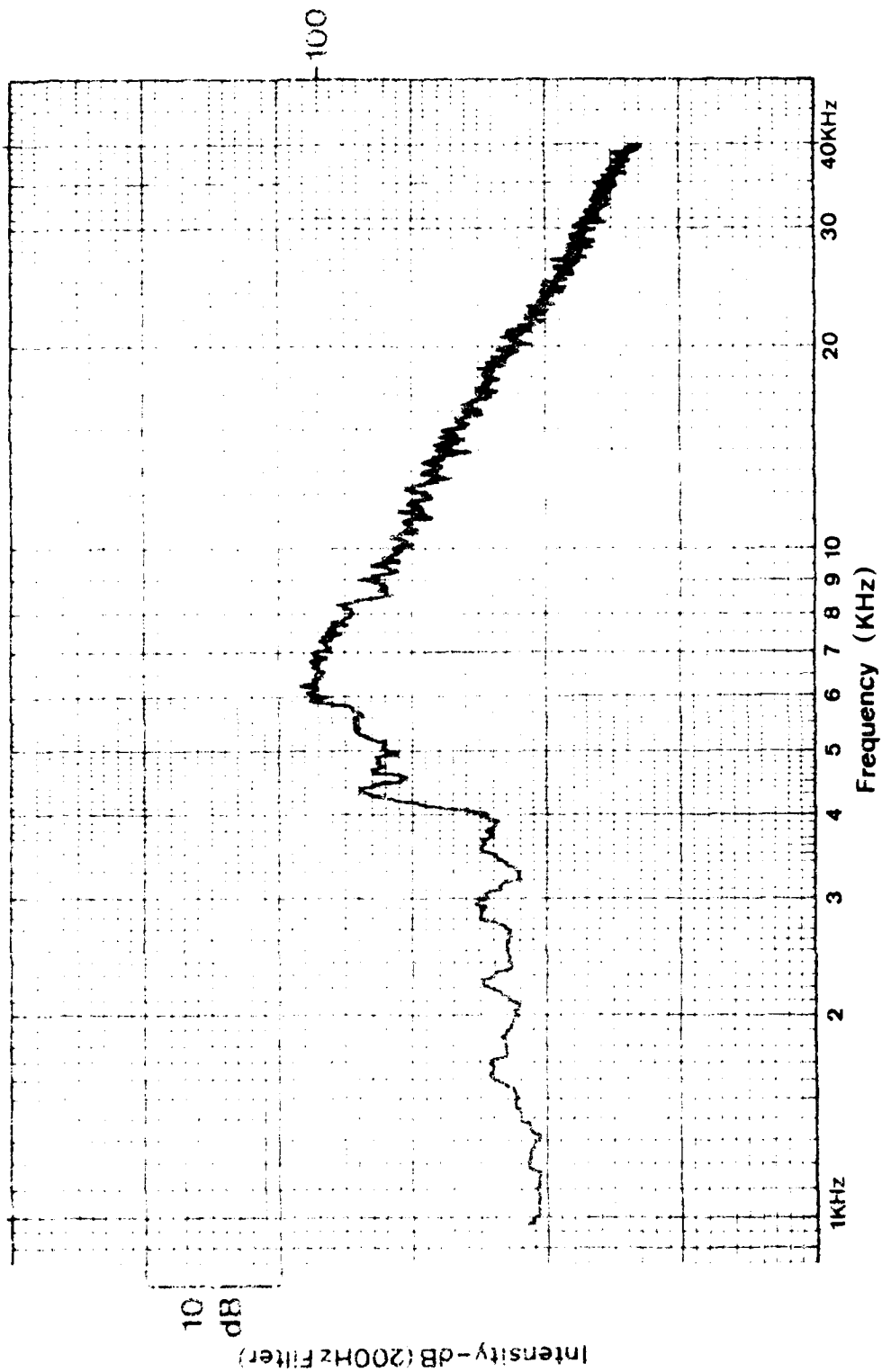






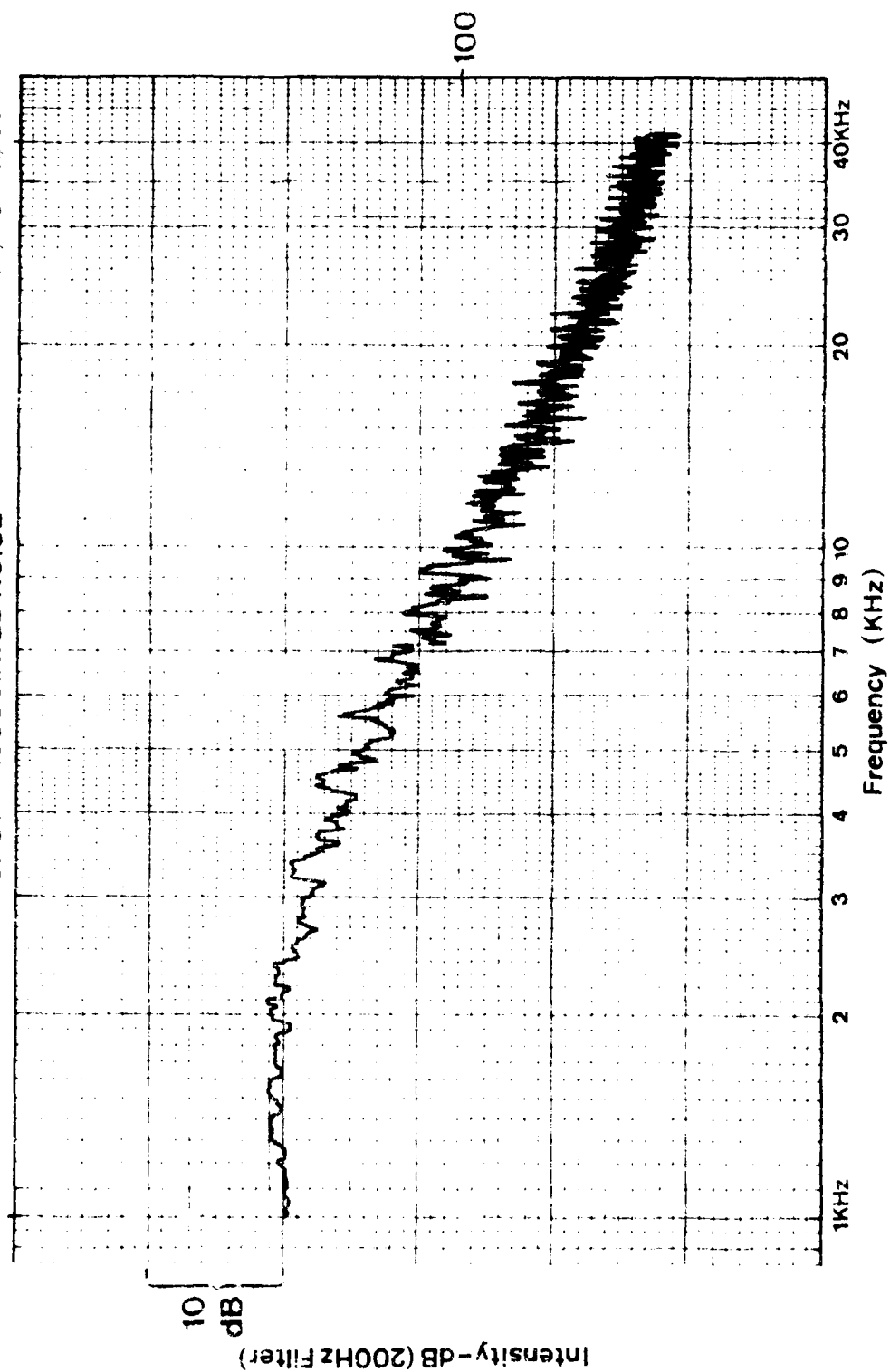
SHOCK-ASSOCIATED NOISE

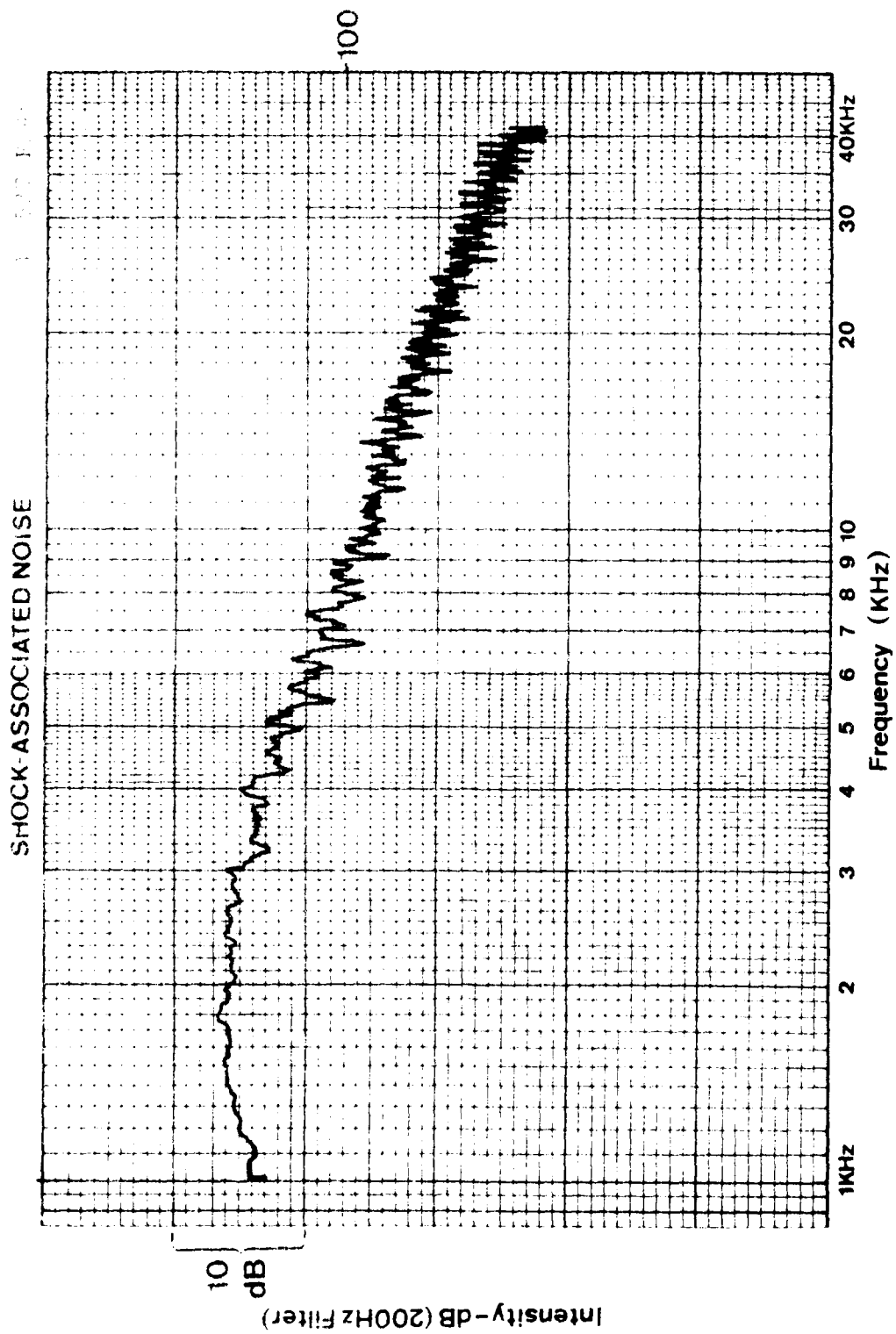
17, 161, 171, 181

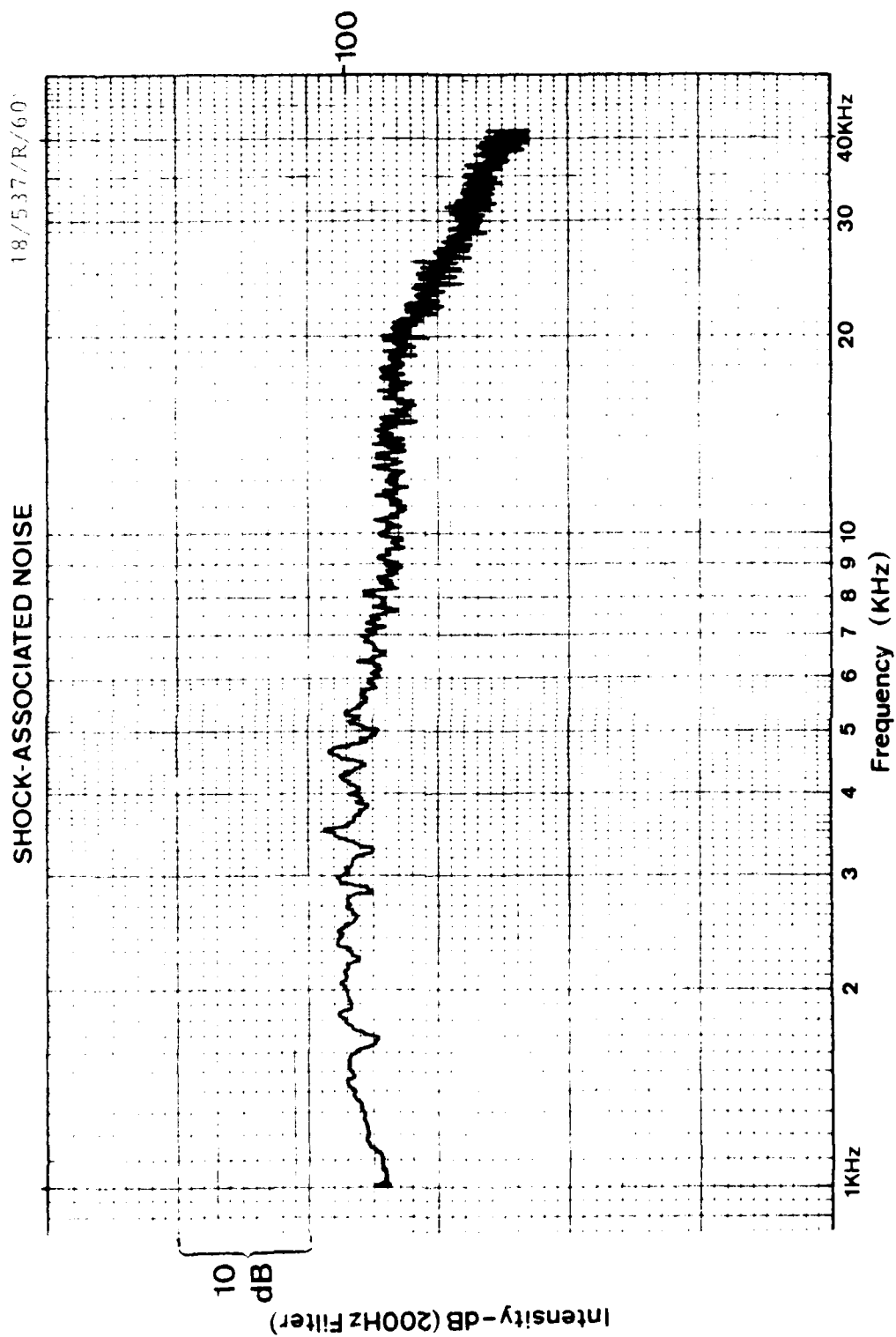


SHOCK-ASSOCIATED NOISE

18/537/R/30

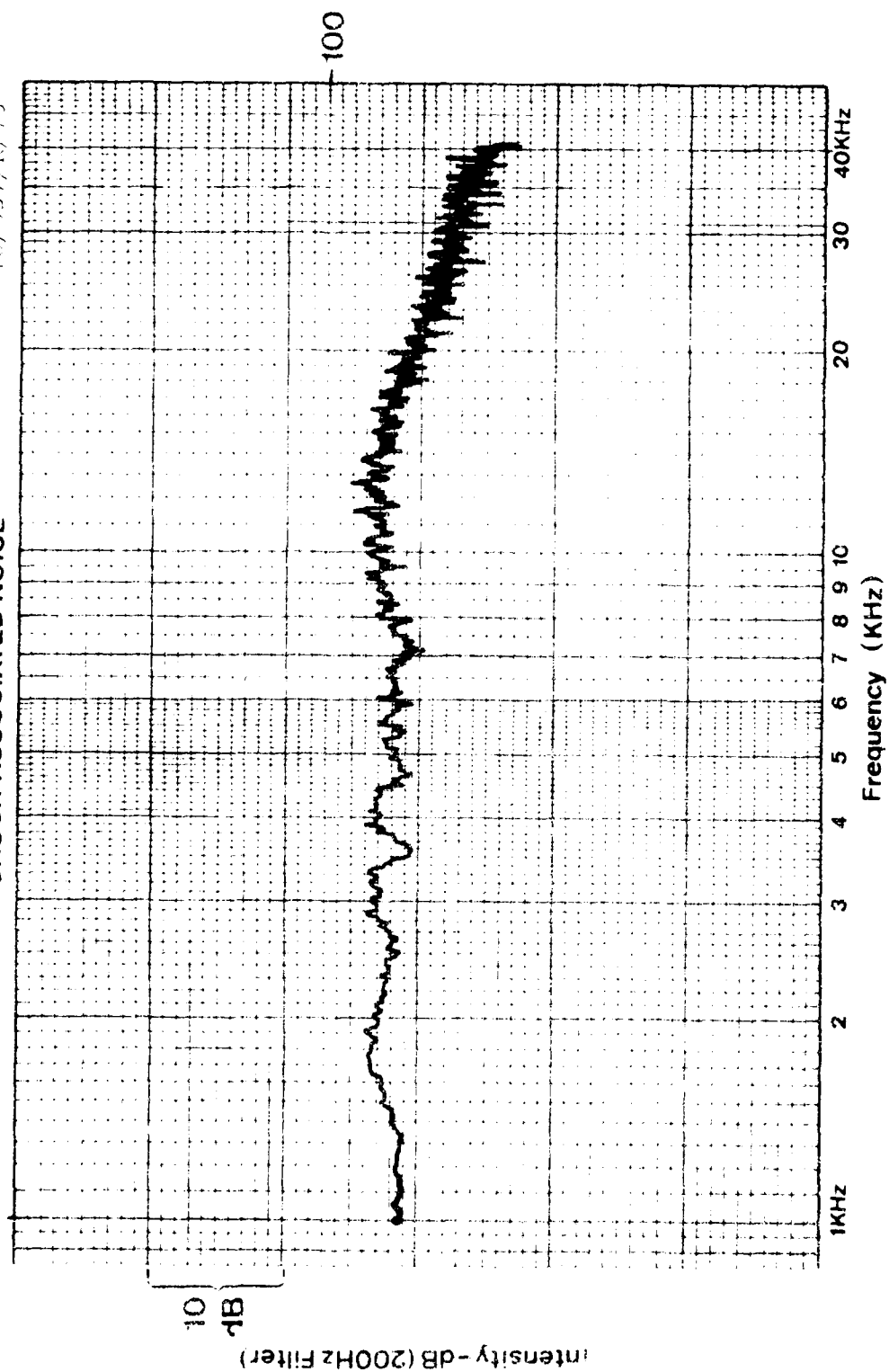






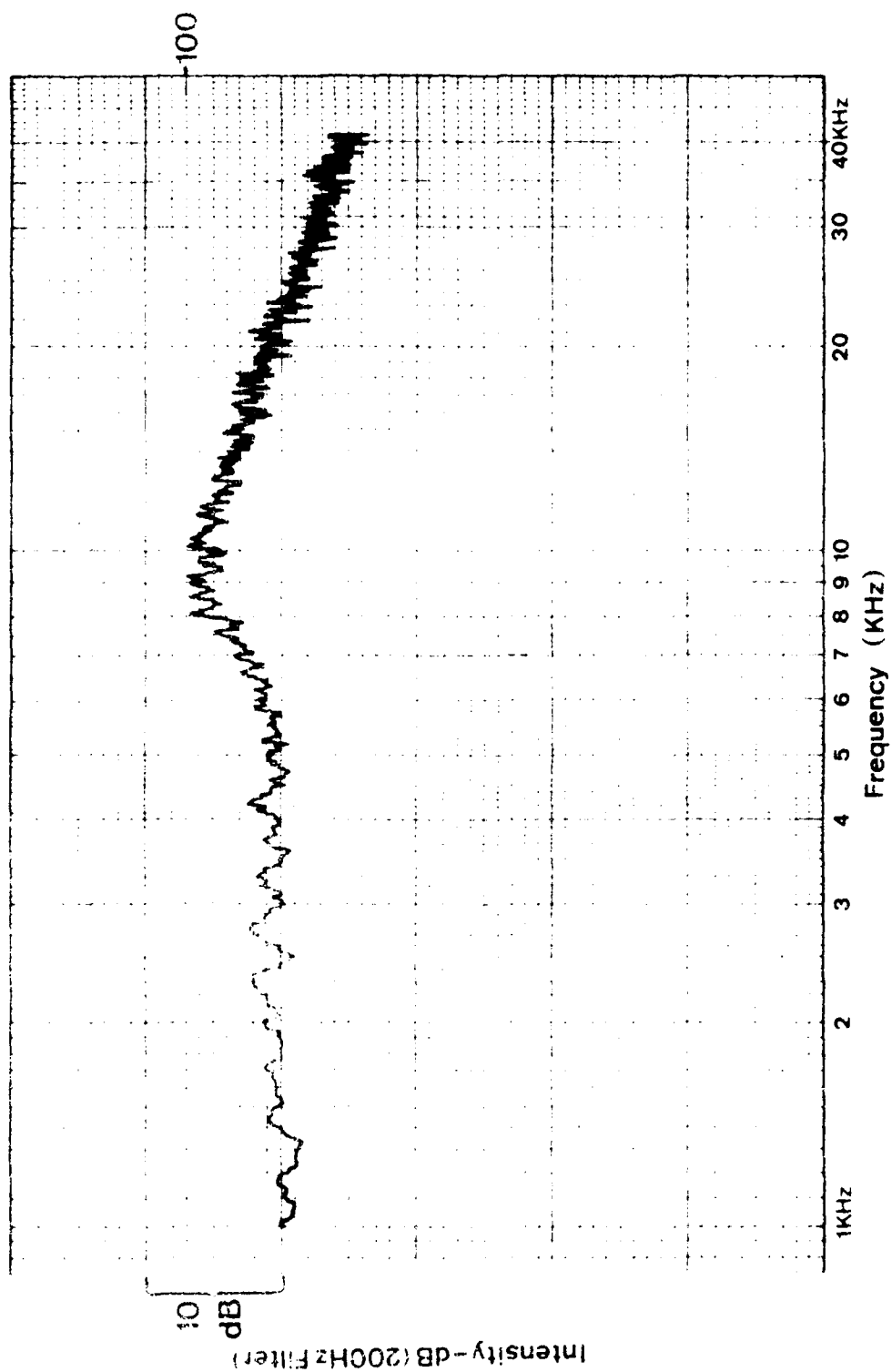
SHOCK-ASSOCIATED NOISE

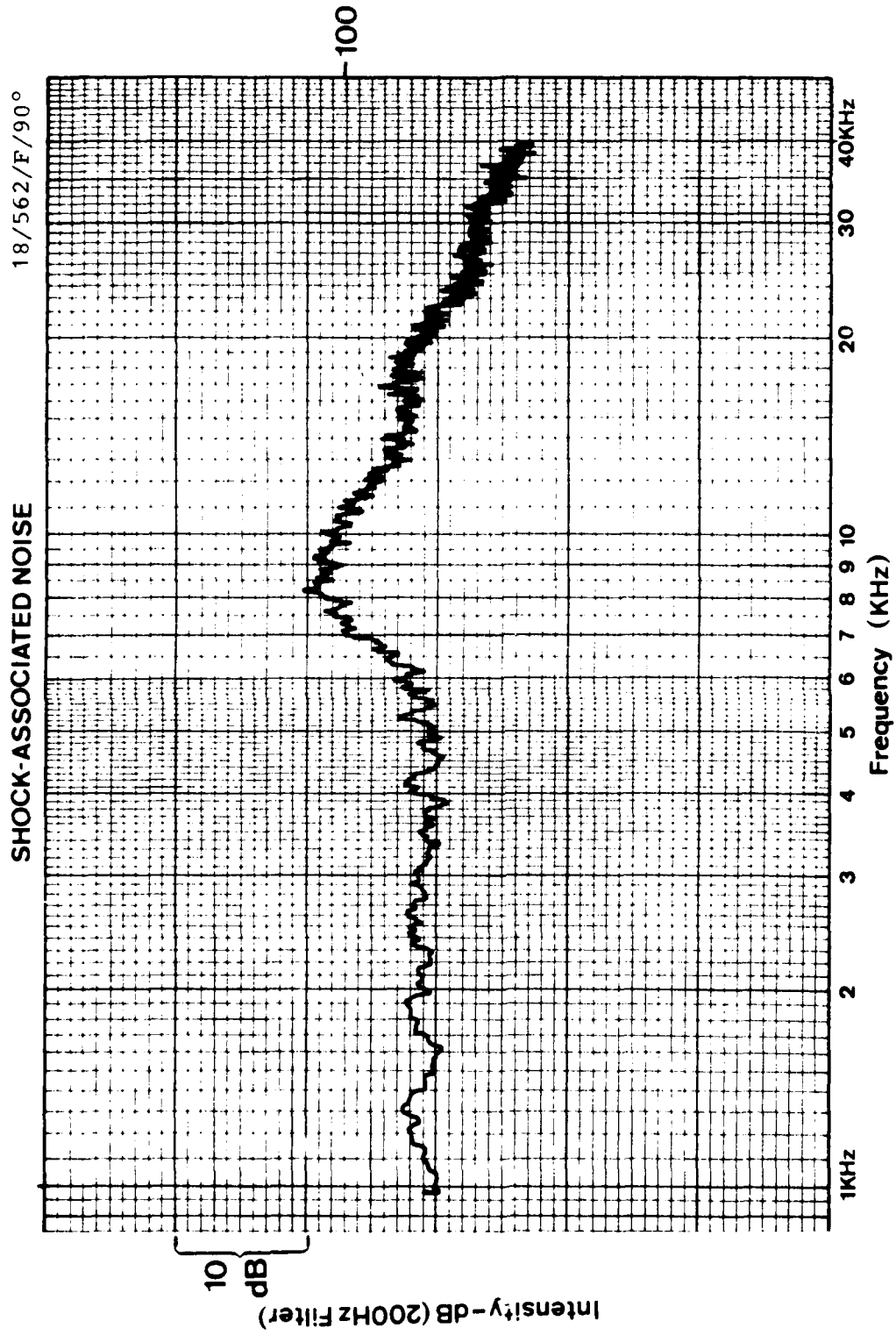
18/537/R/75



SHOCK ASSOCIATED NOISE

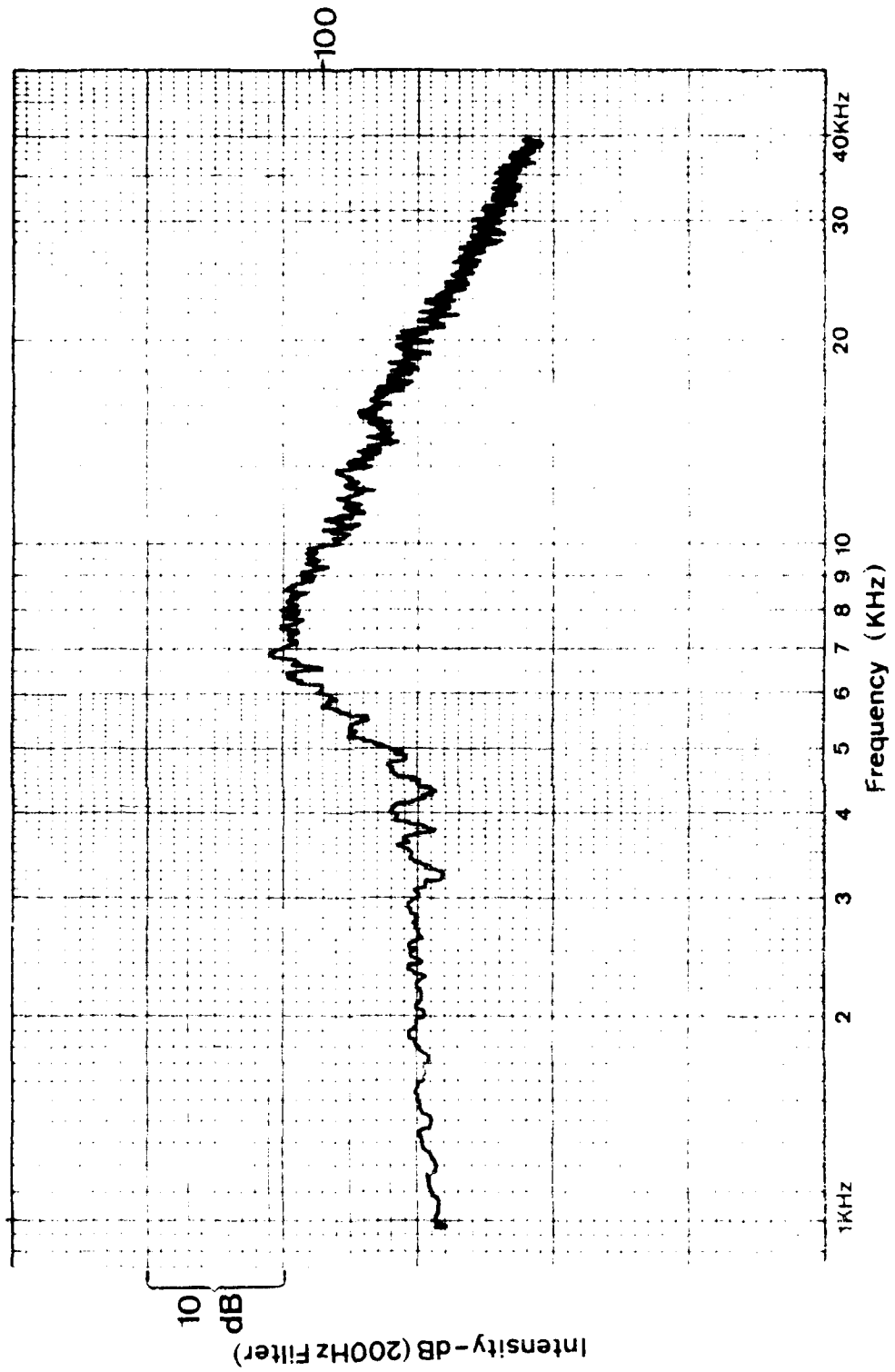
18/537 R/90°

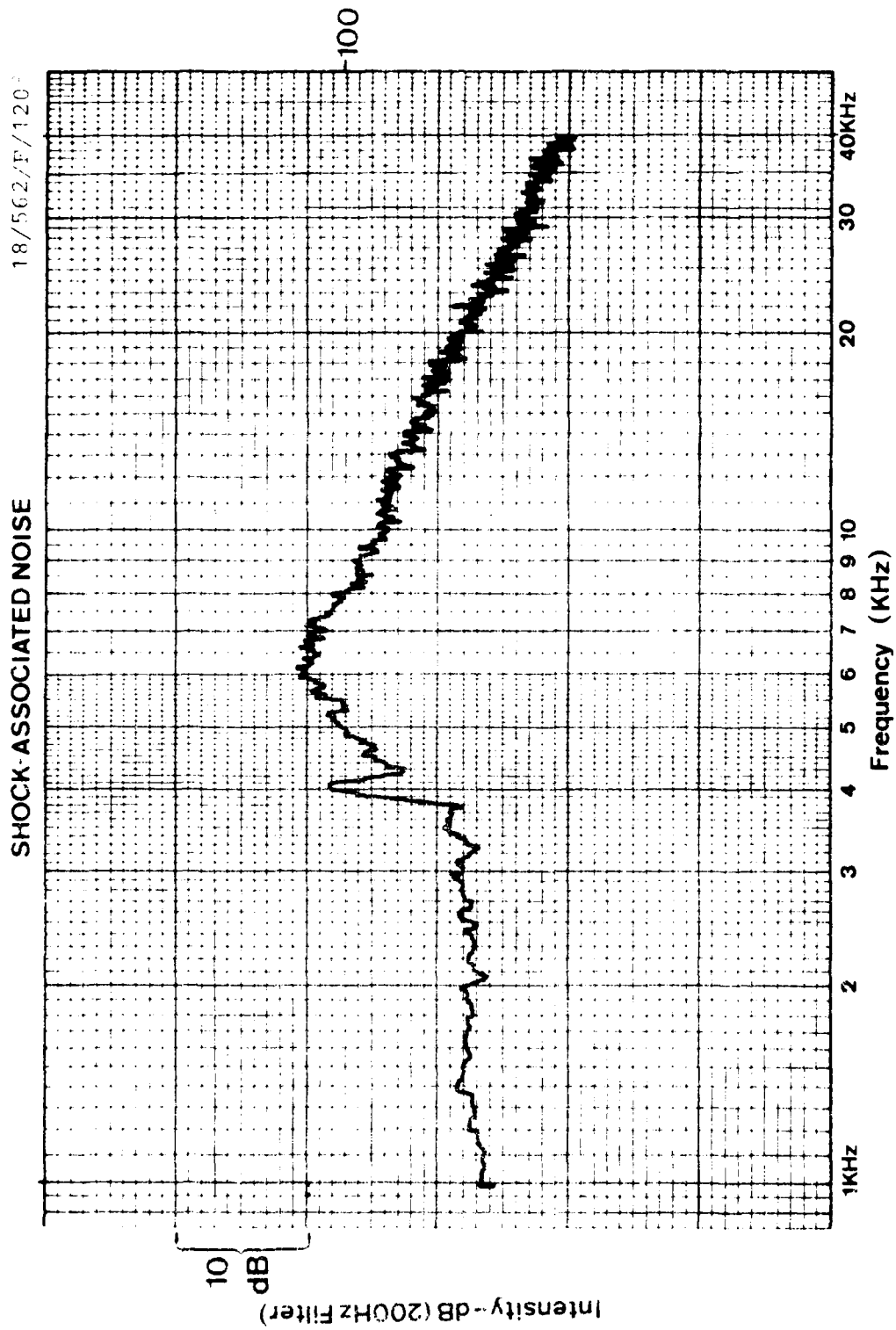




18/562/F/105

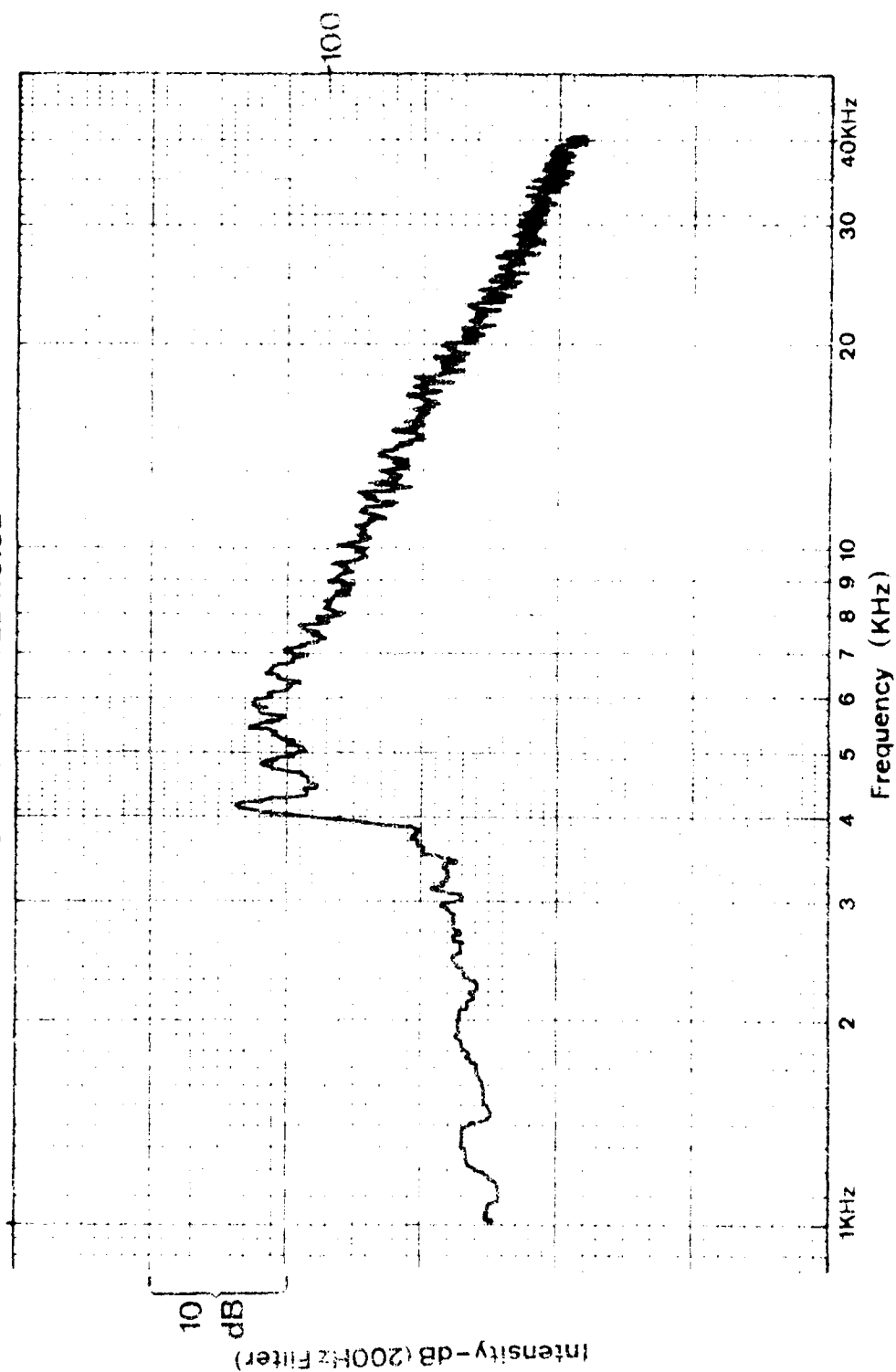
SHOCK-ASSOCIATED NOISE

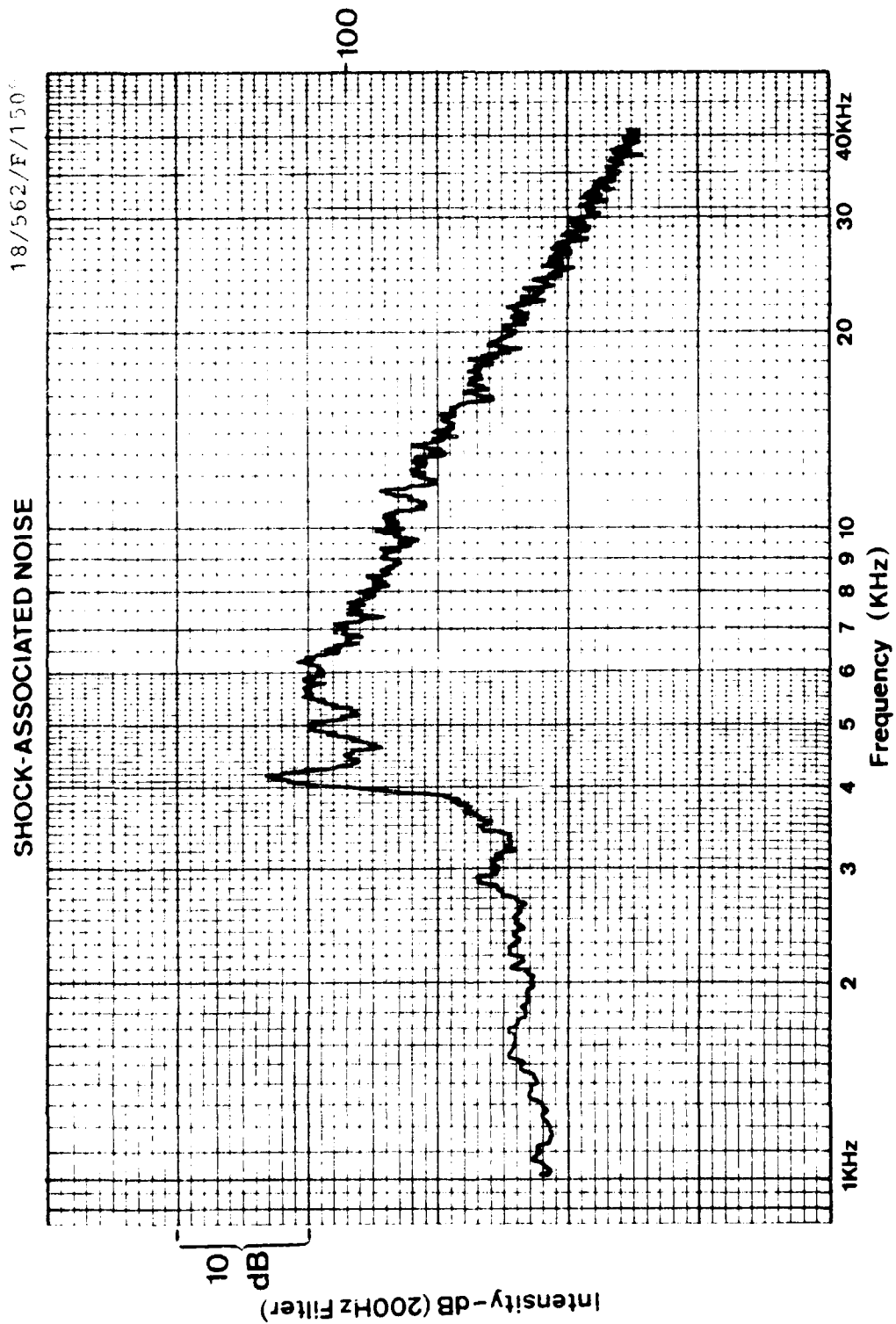


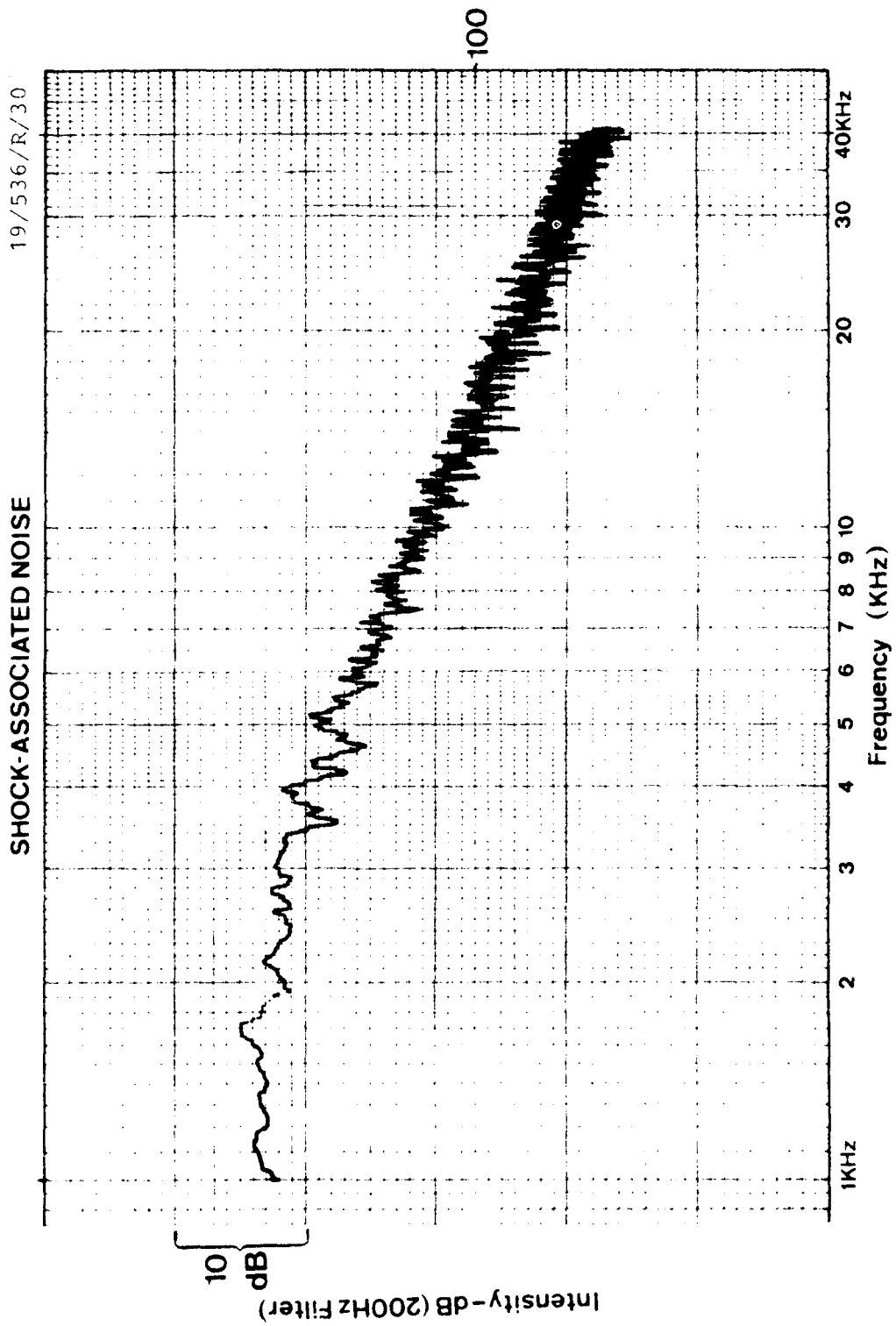


18/562/P/135

SHOCK-ASSOCIATED NOISE

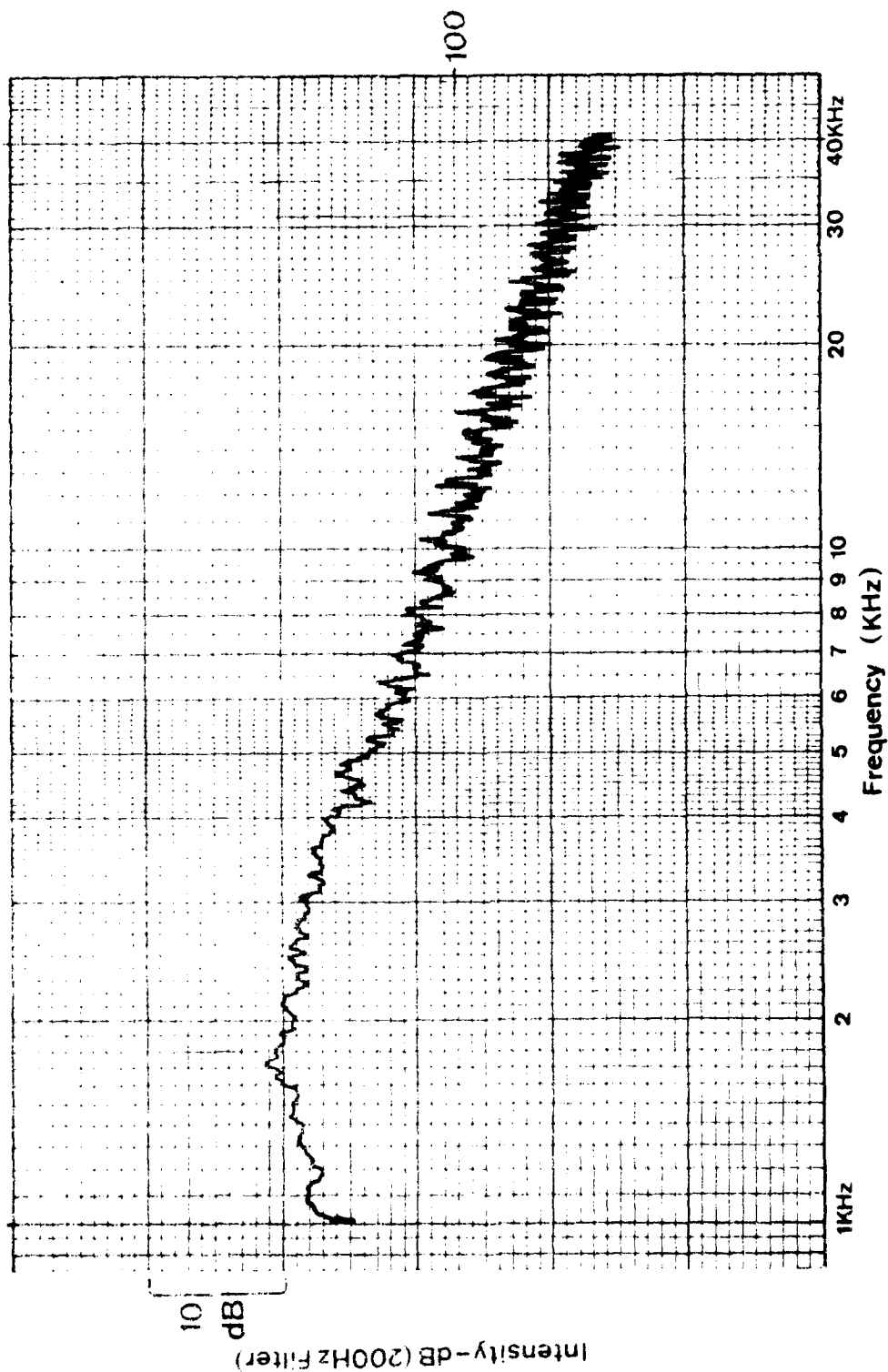


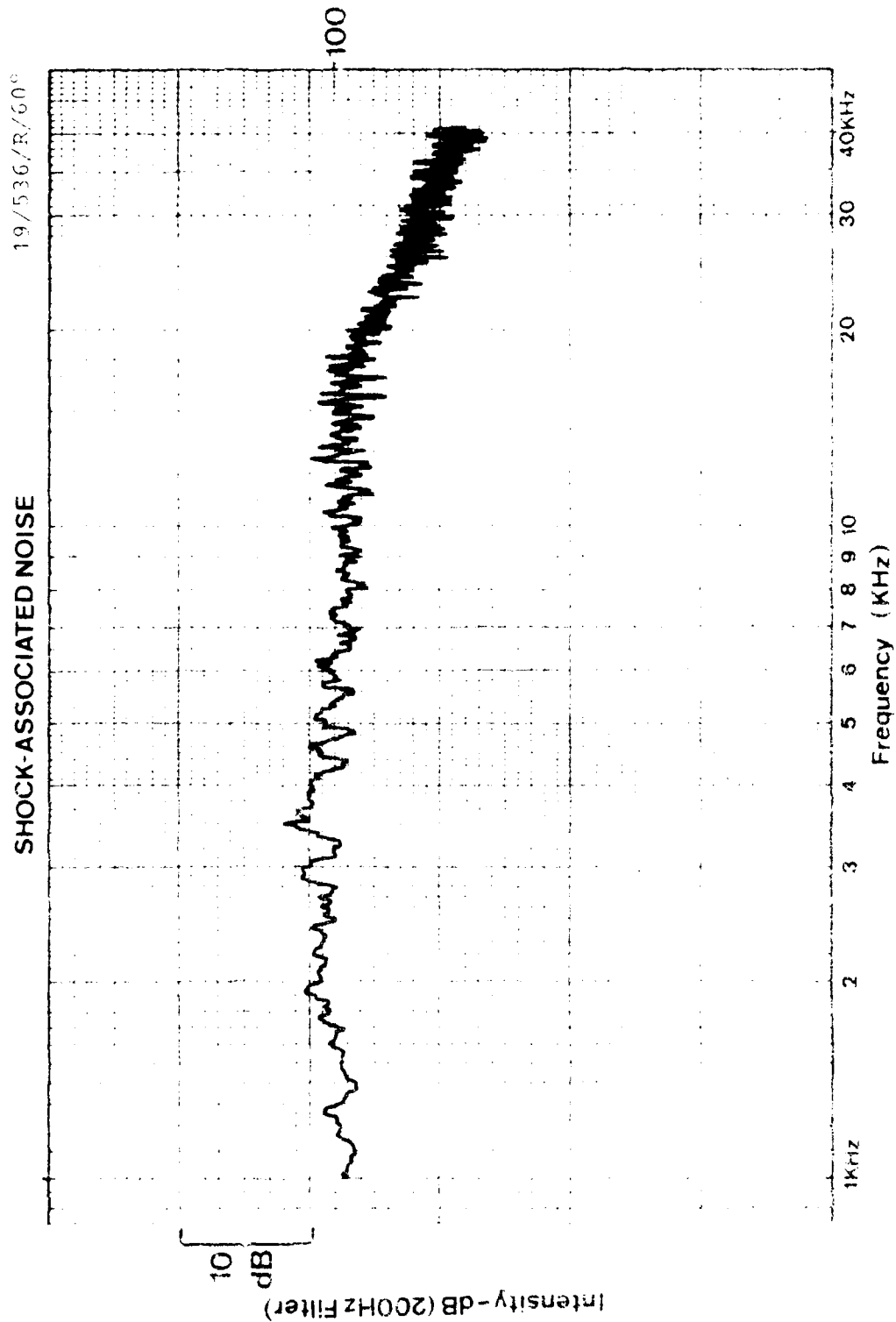


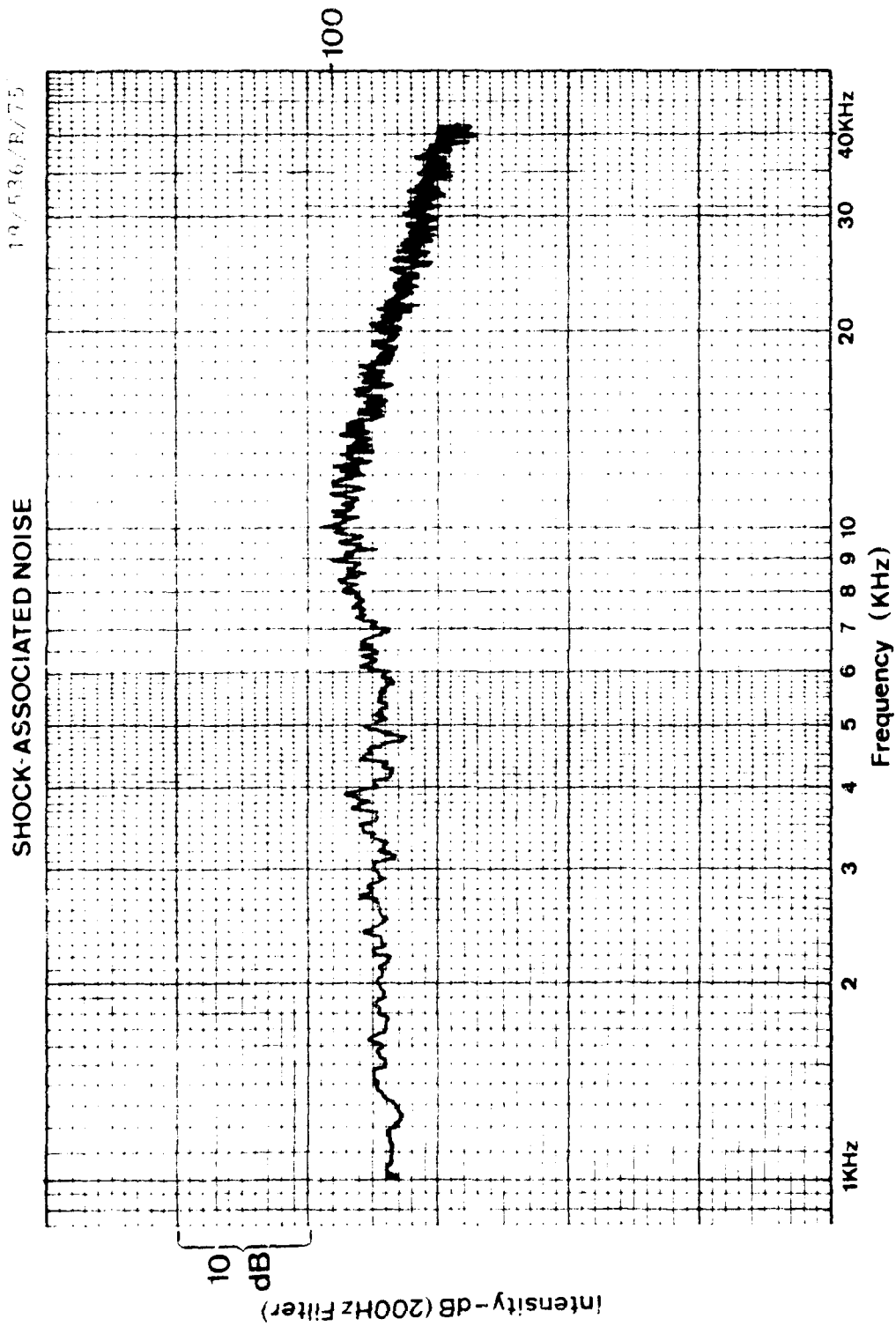


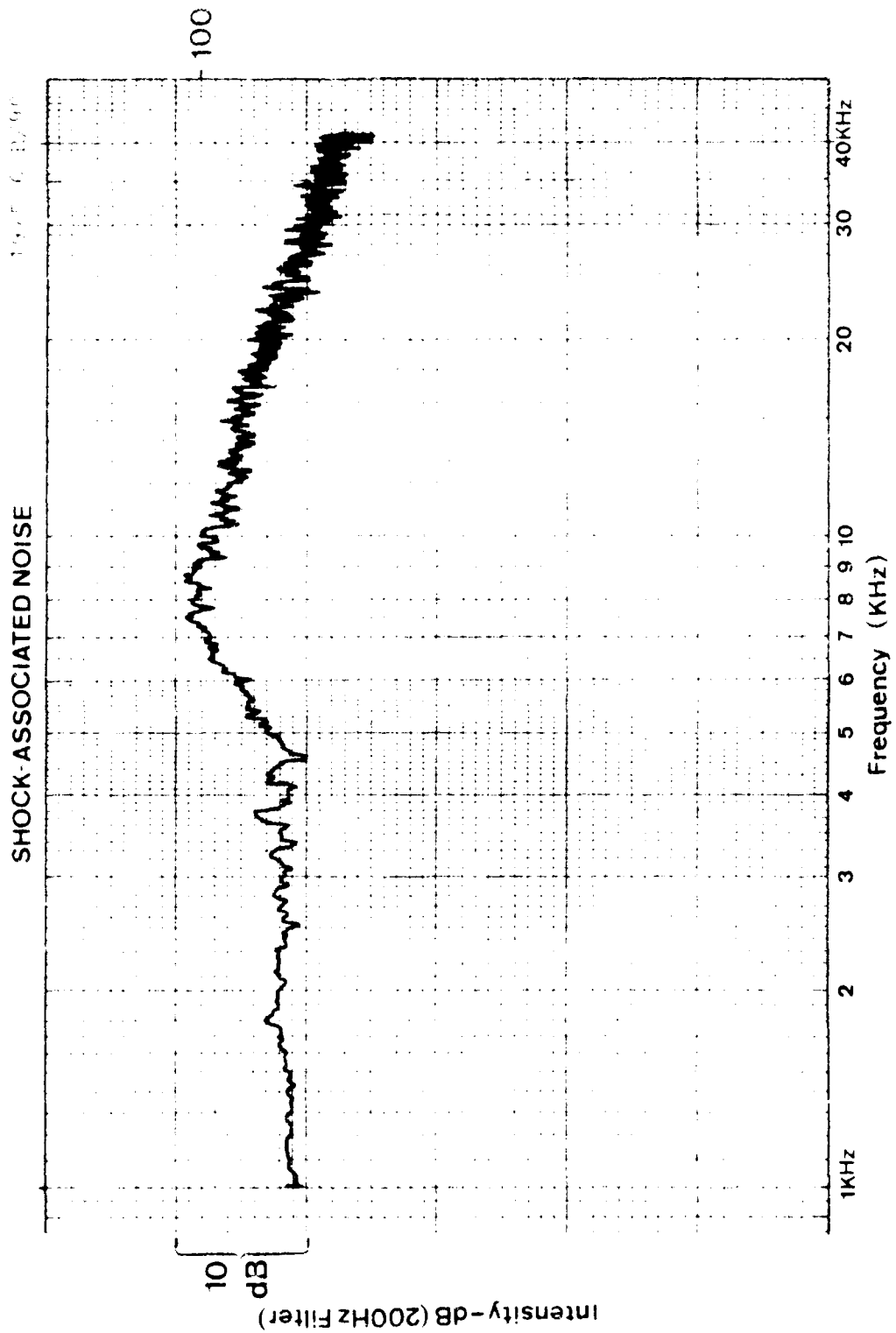
SHOCK-ASSOCIATED NOISE

19/53618-45

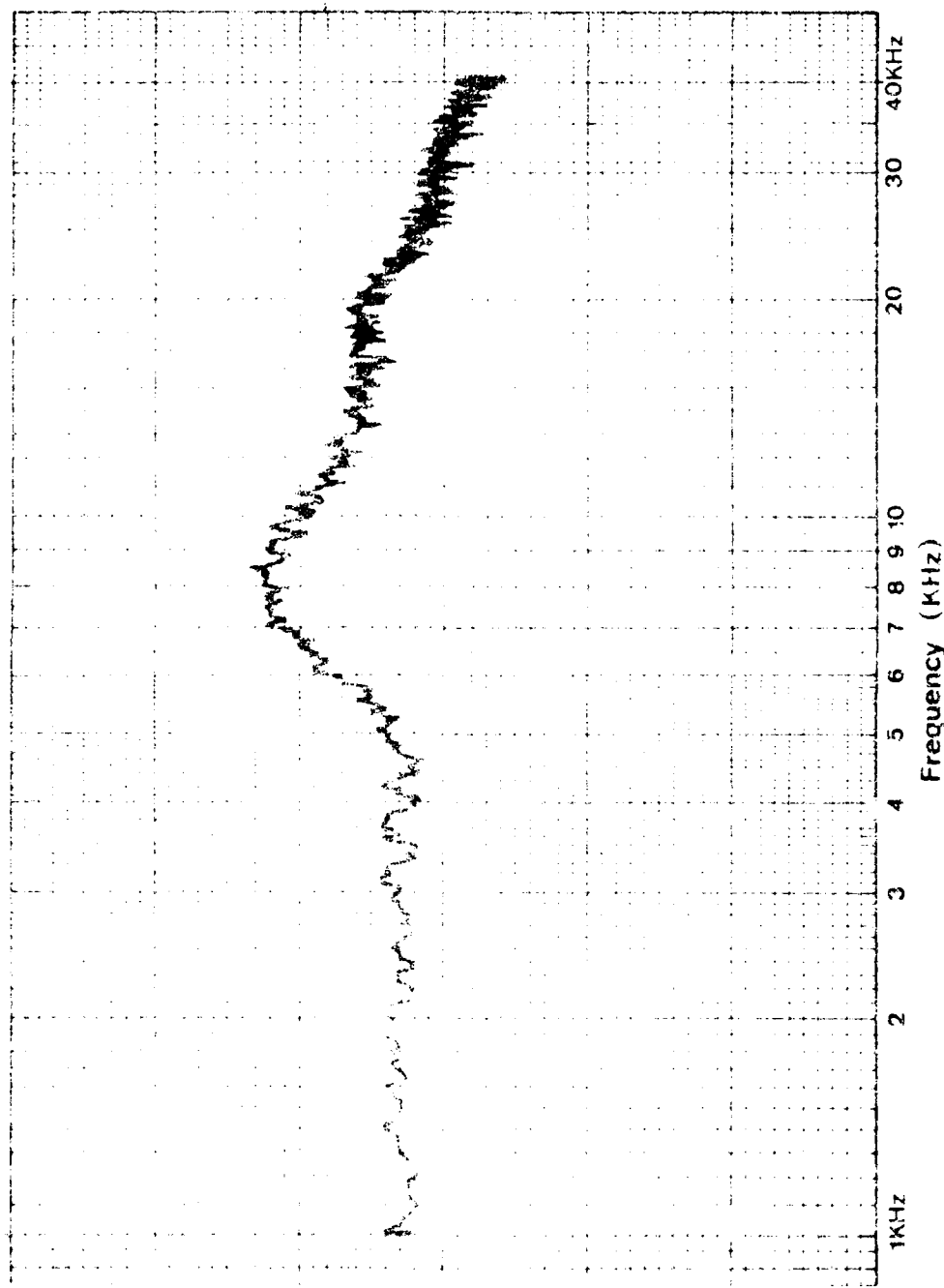








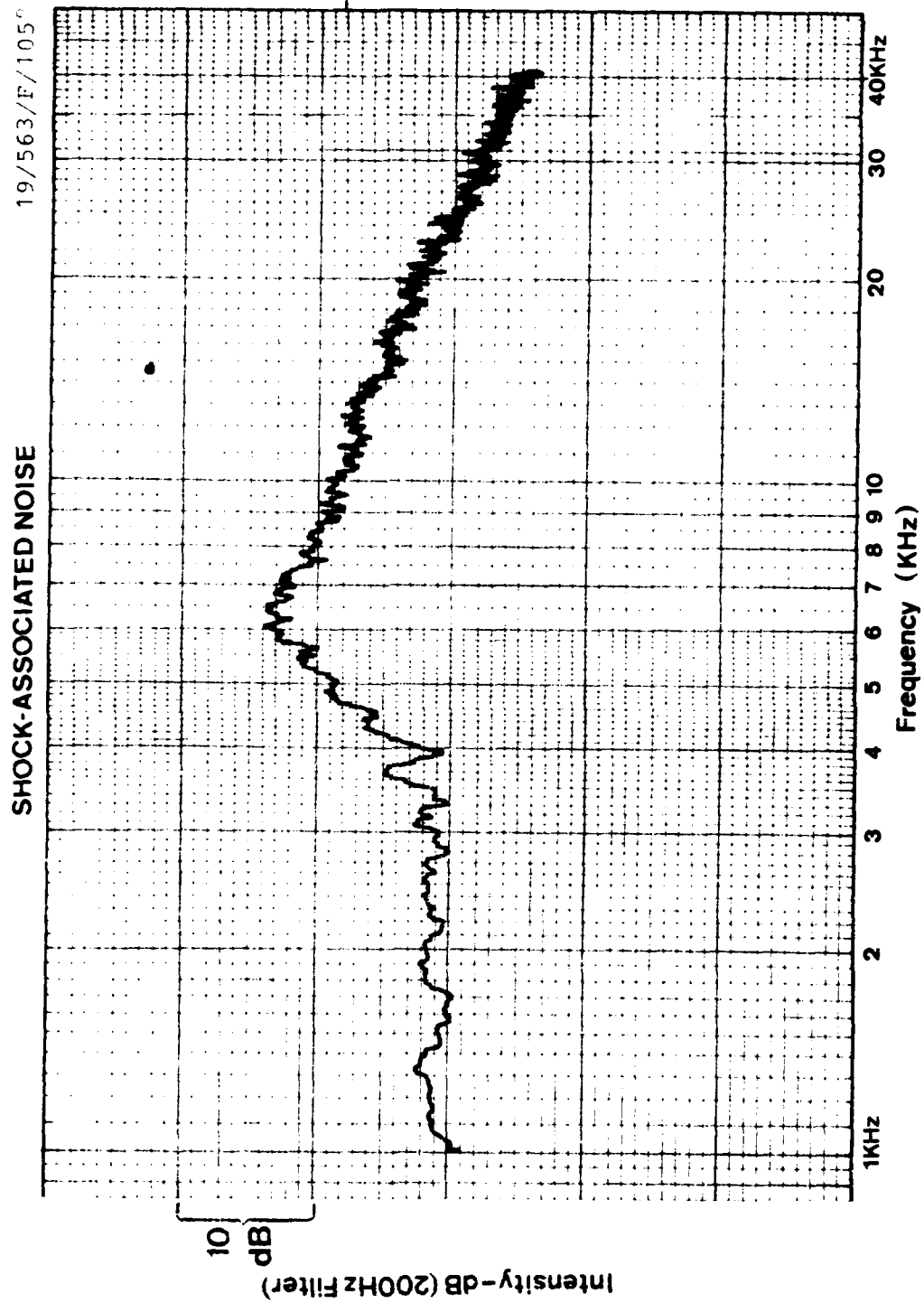
SHOCK ASSOCIATED NOISE

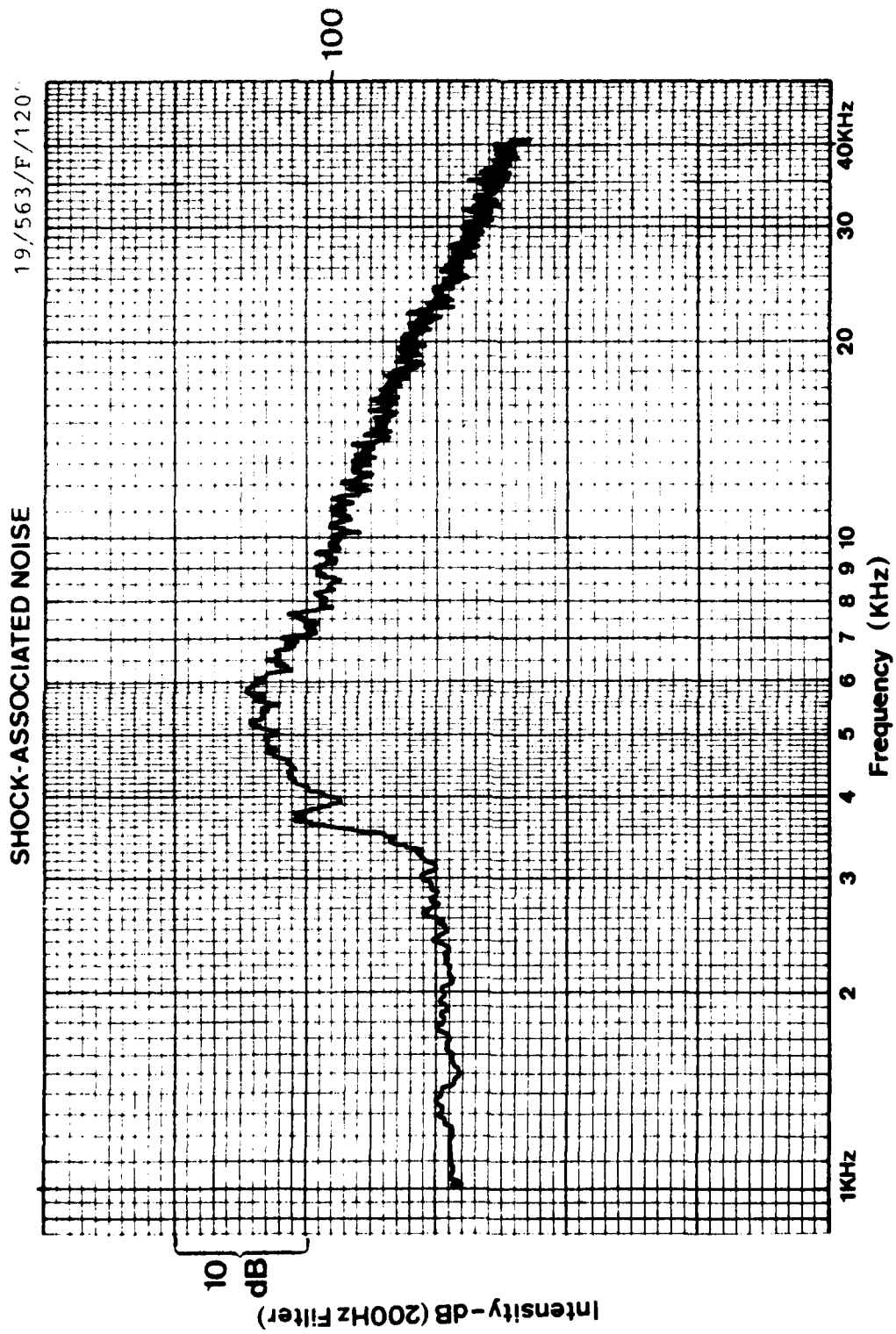


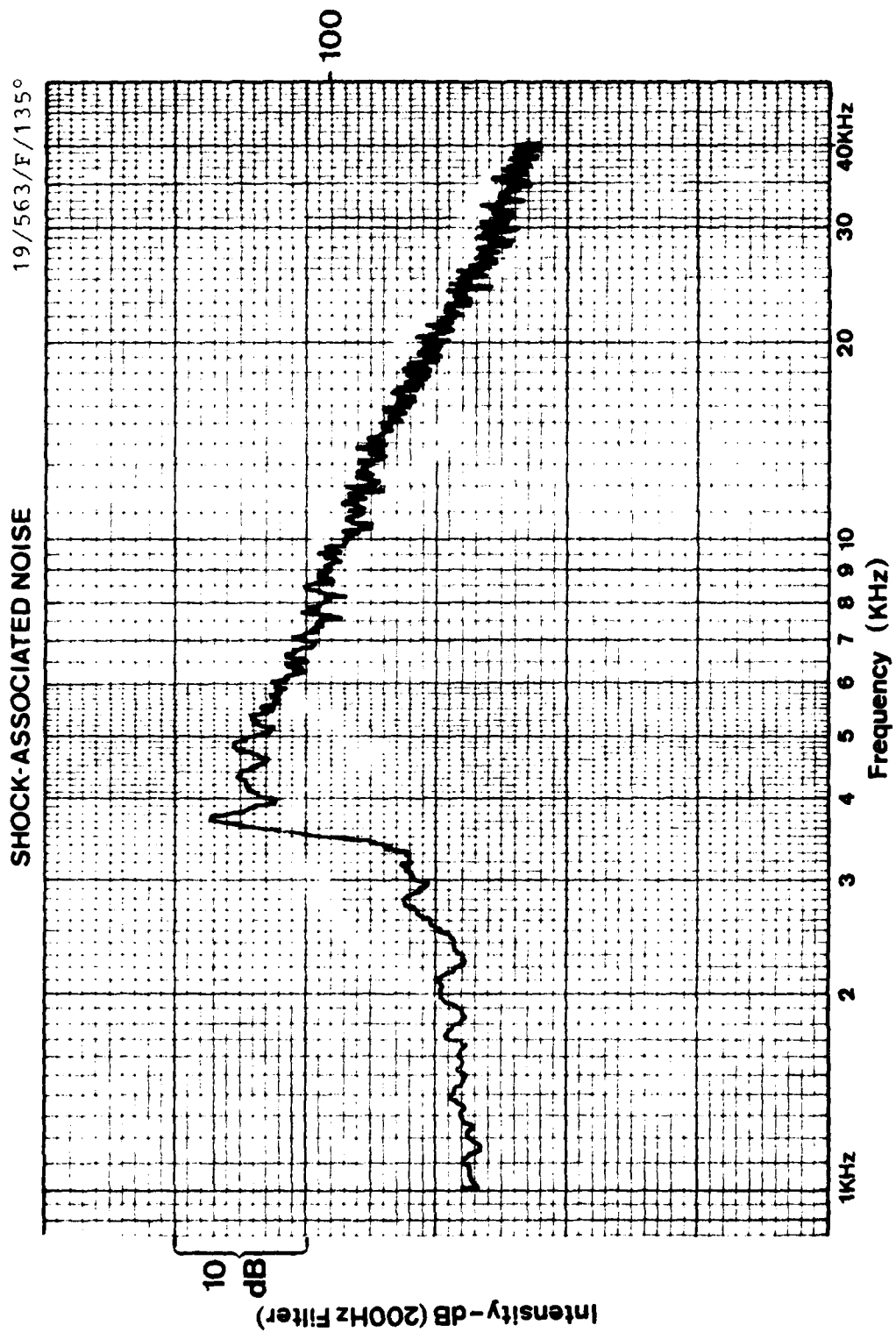
101
dB

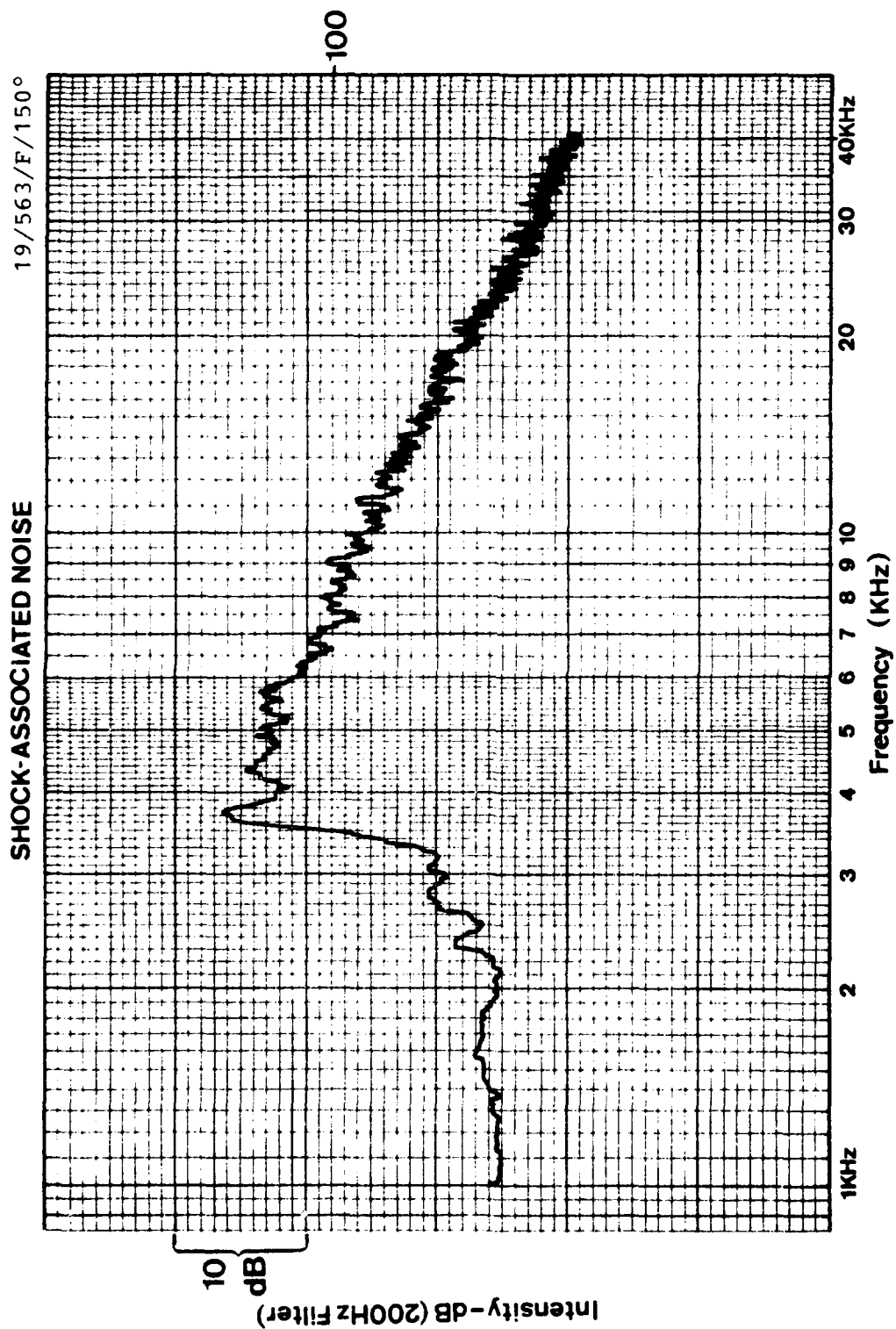
INTENSITY - 0.0001 Hz

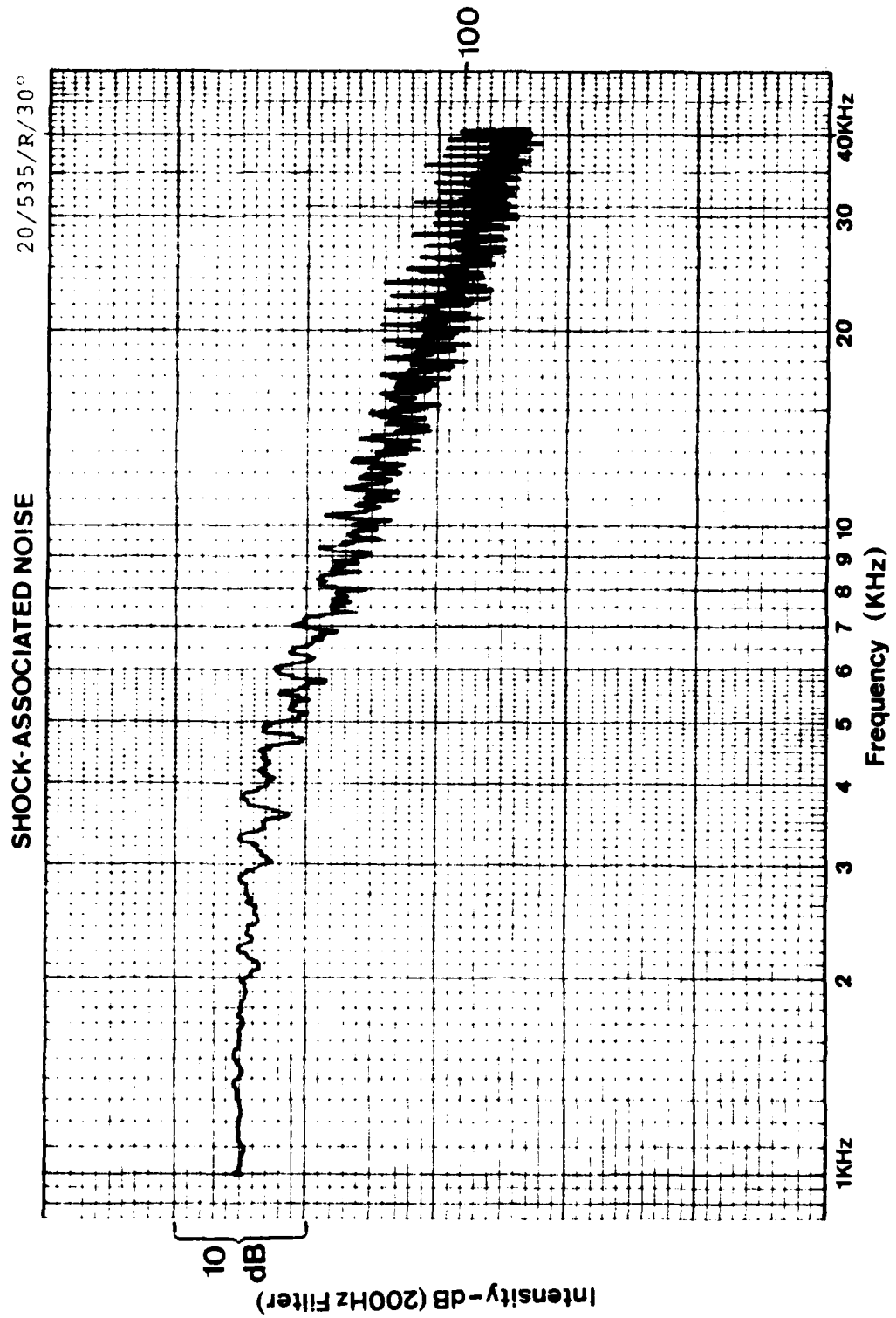
(10)

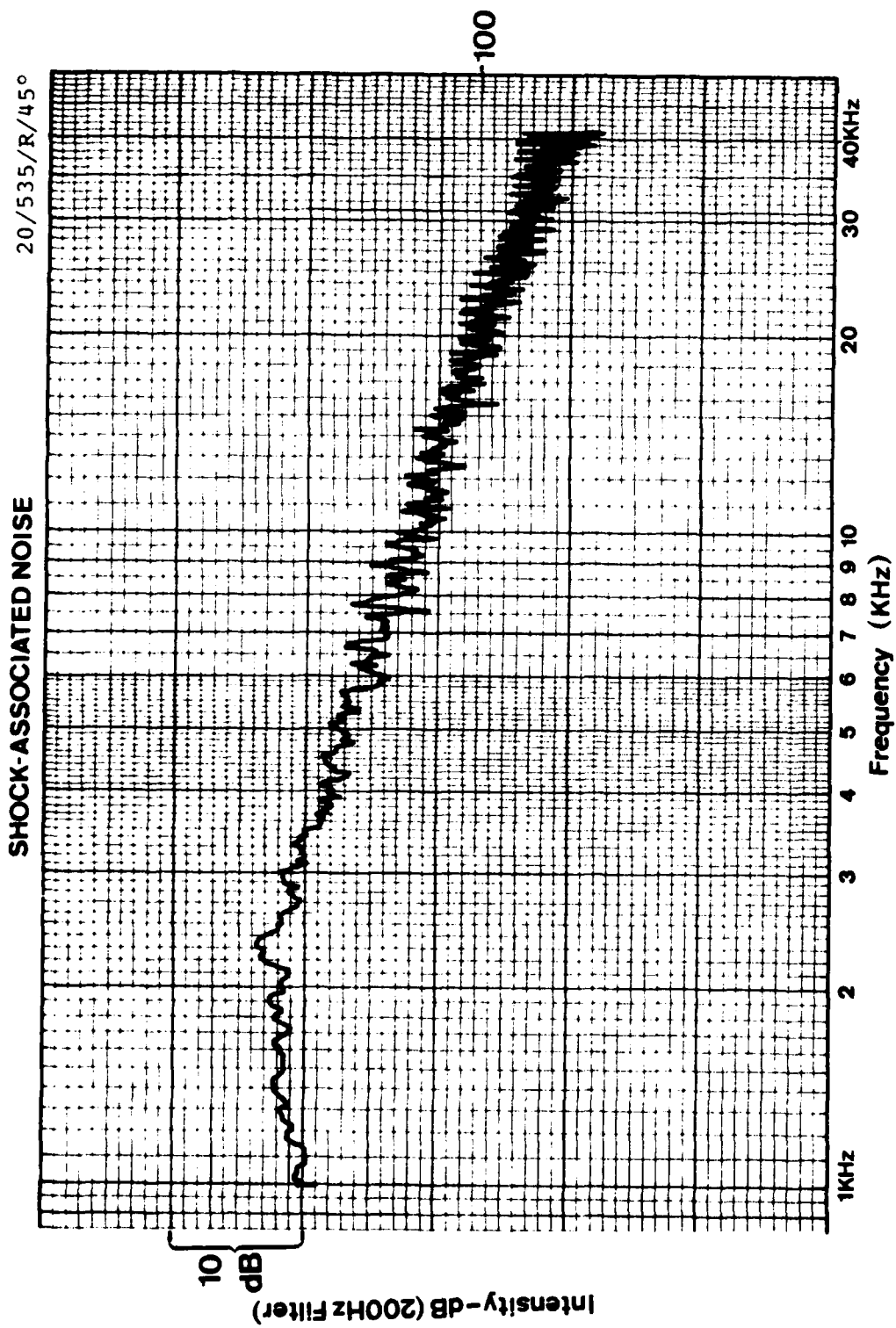


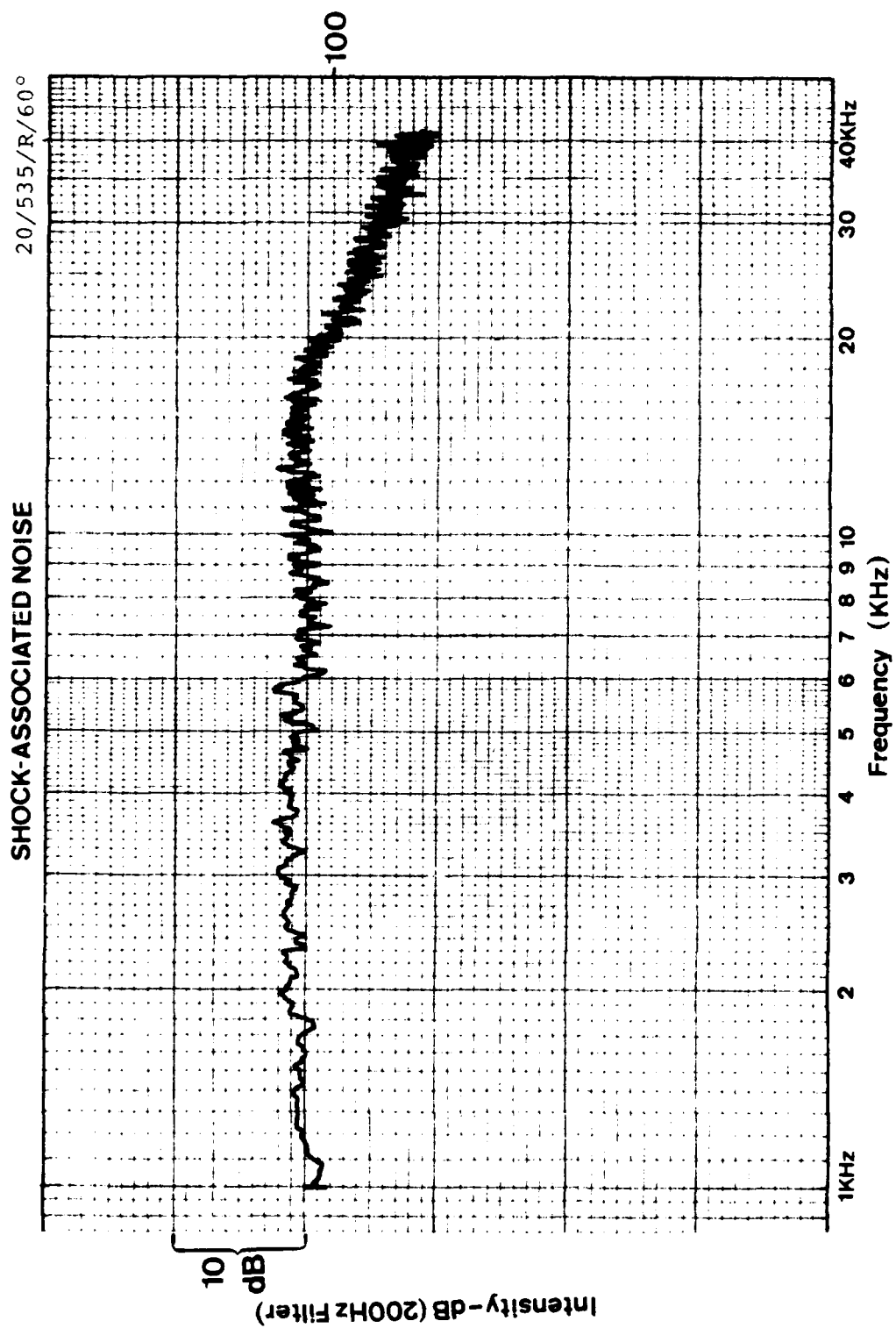


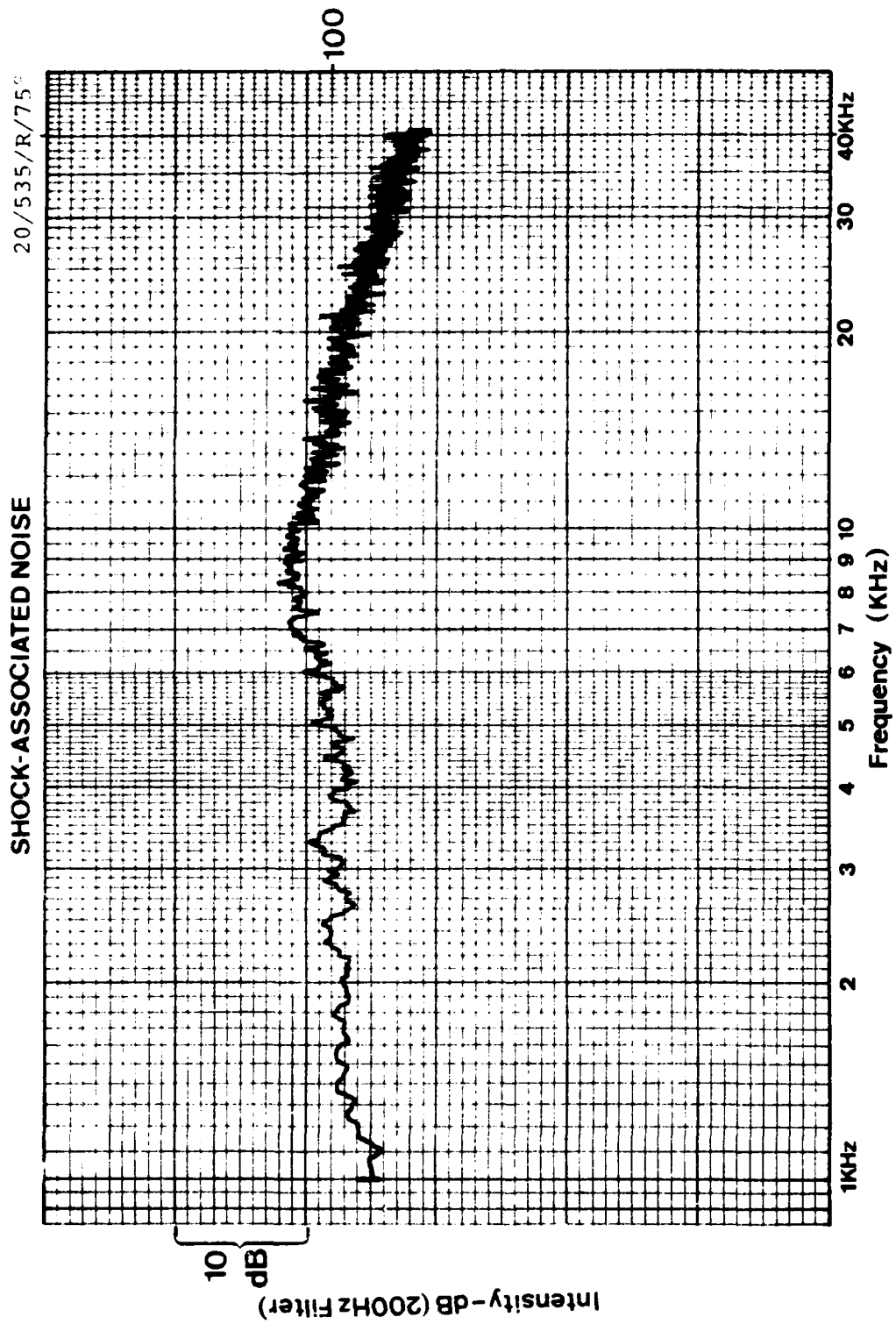


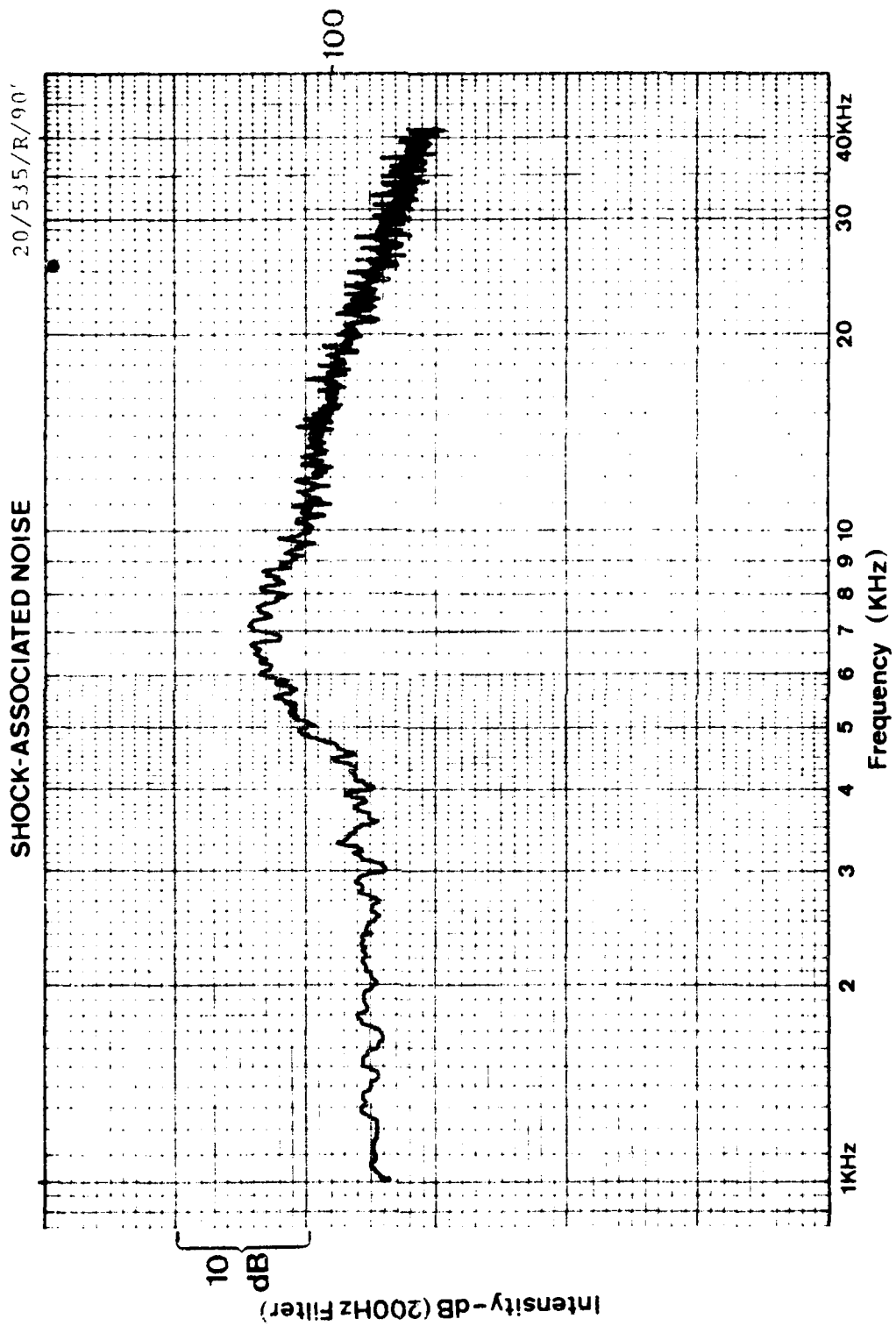


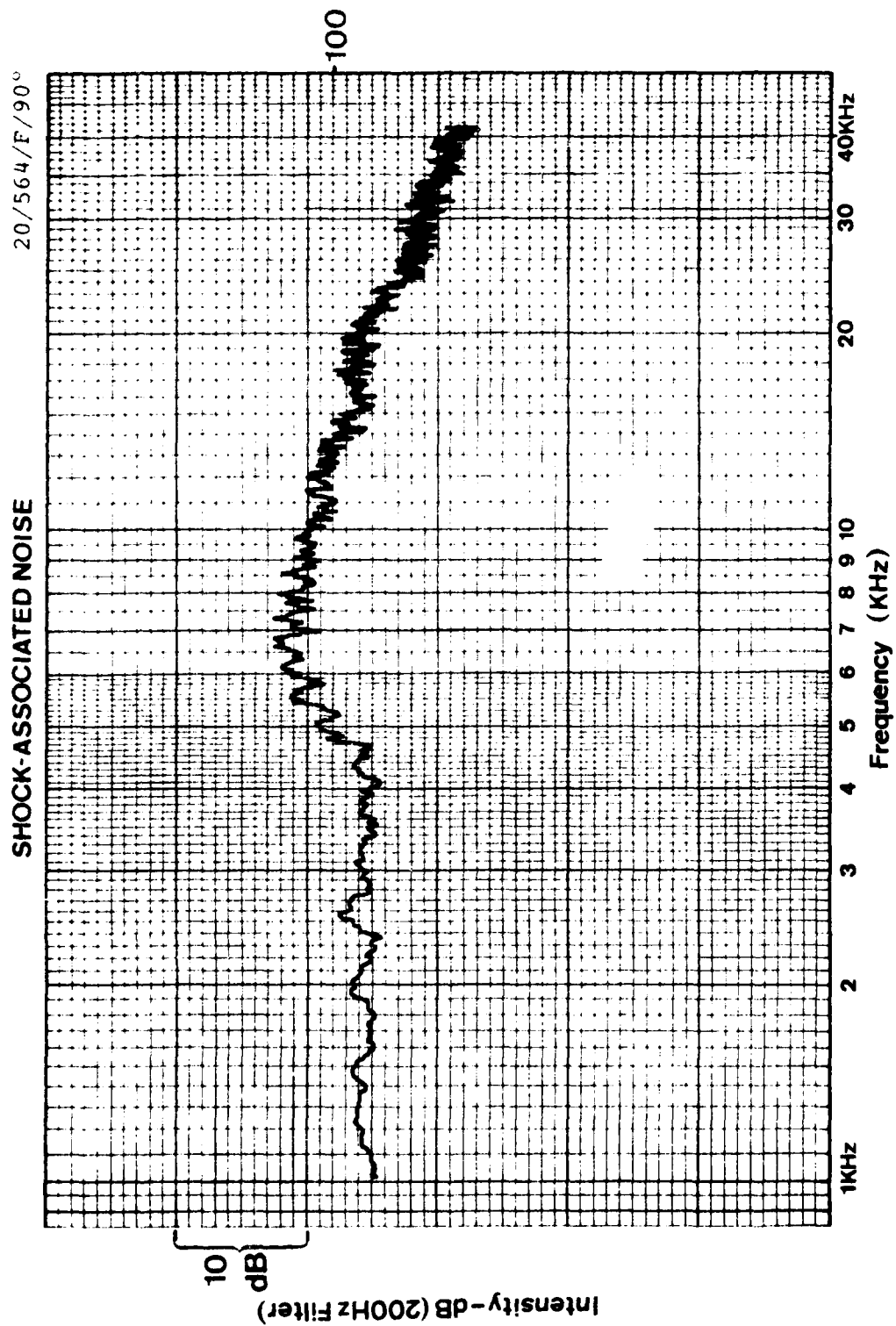


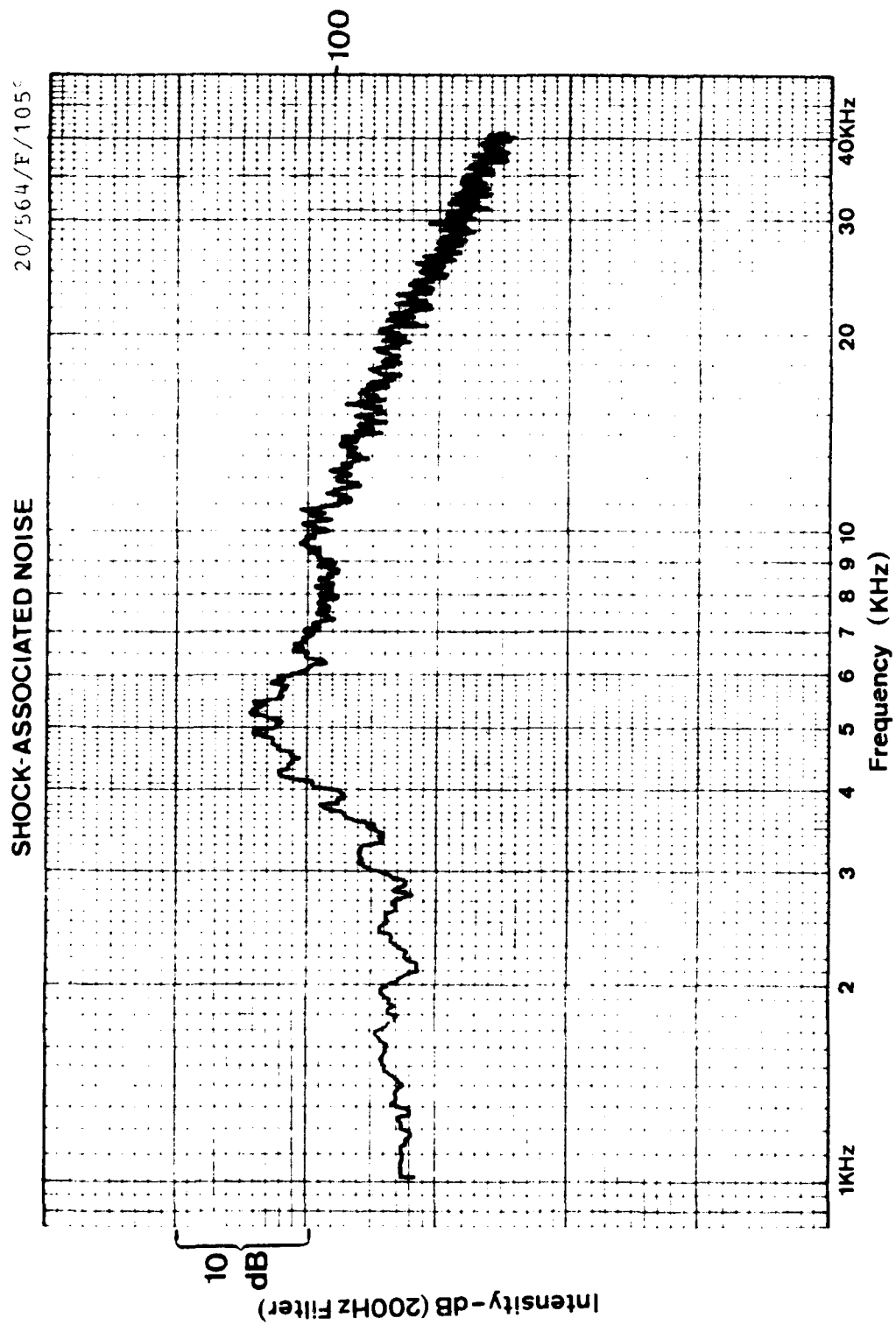


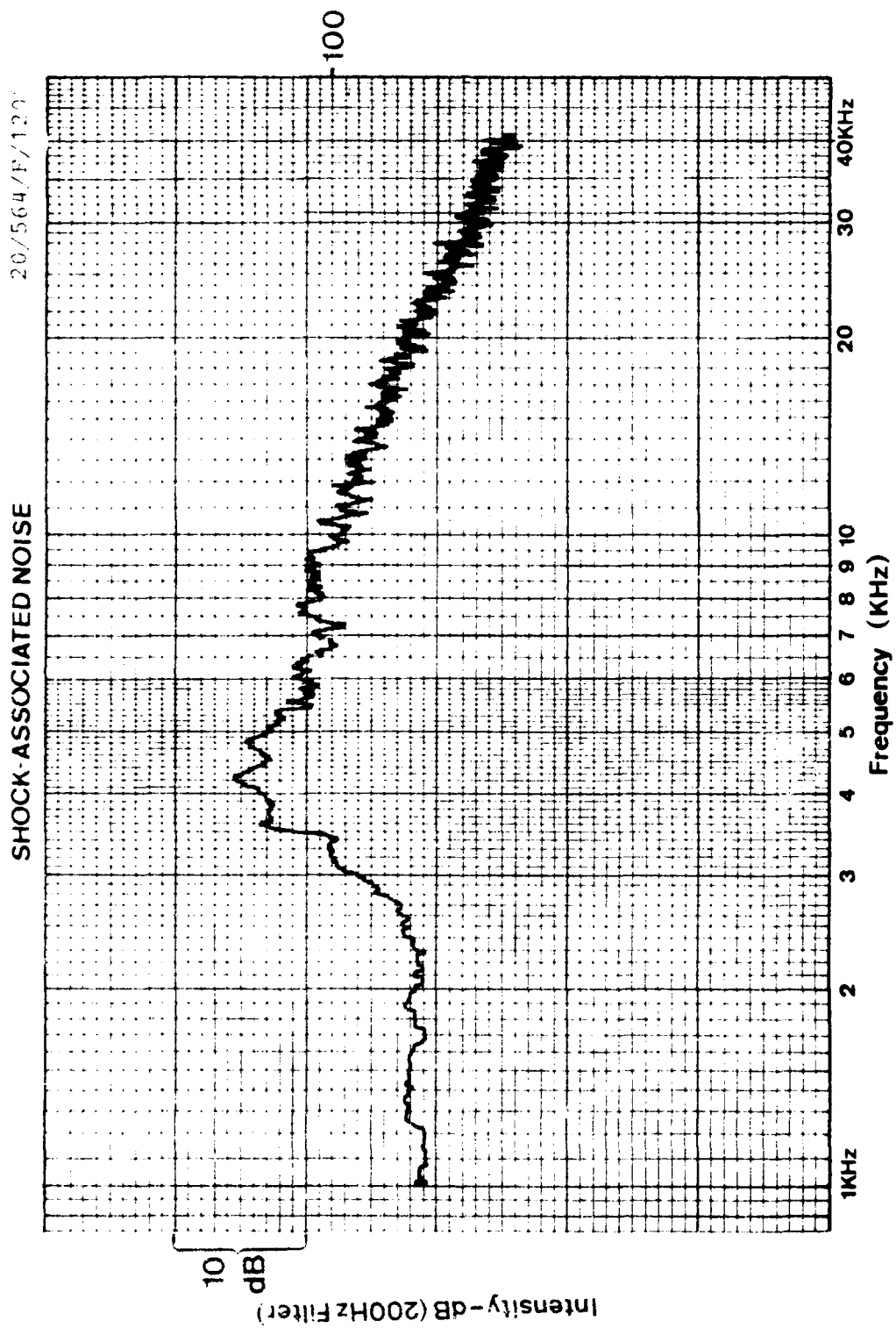


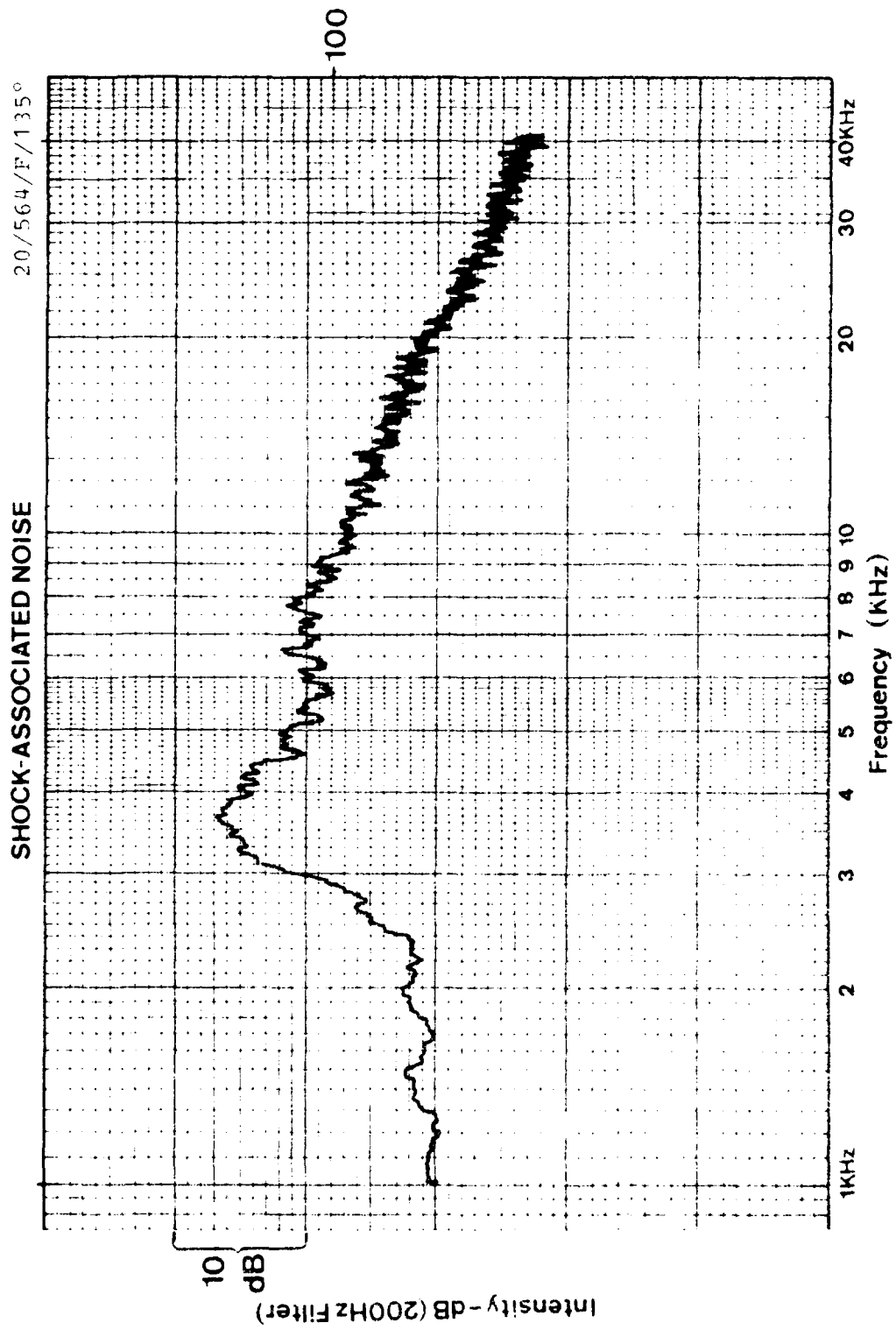


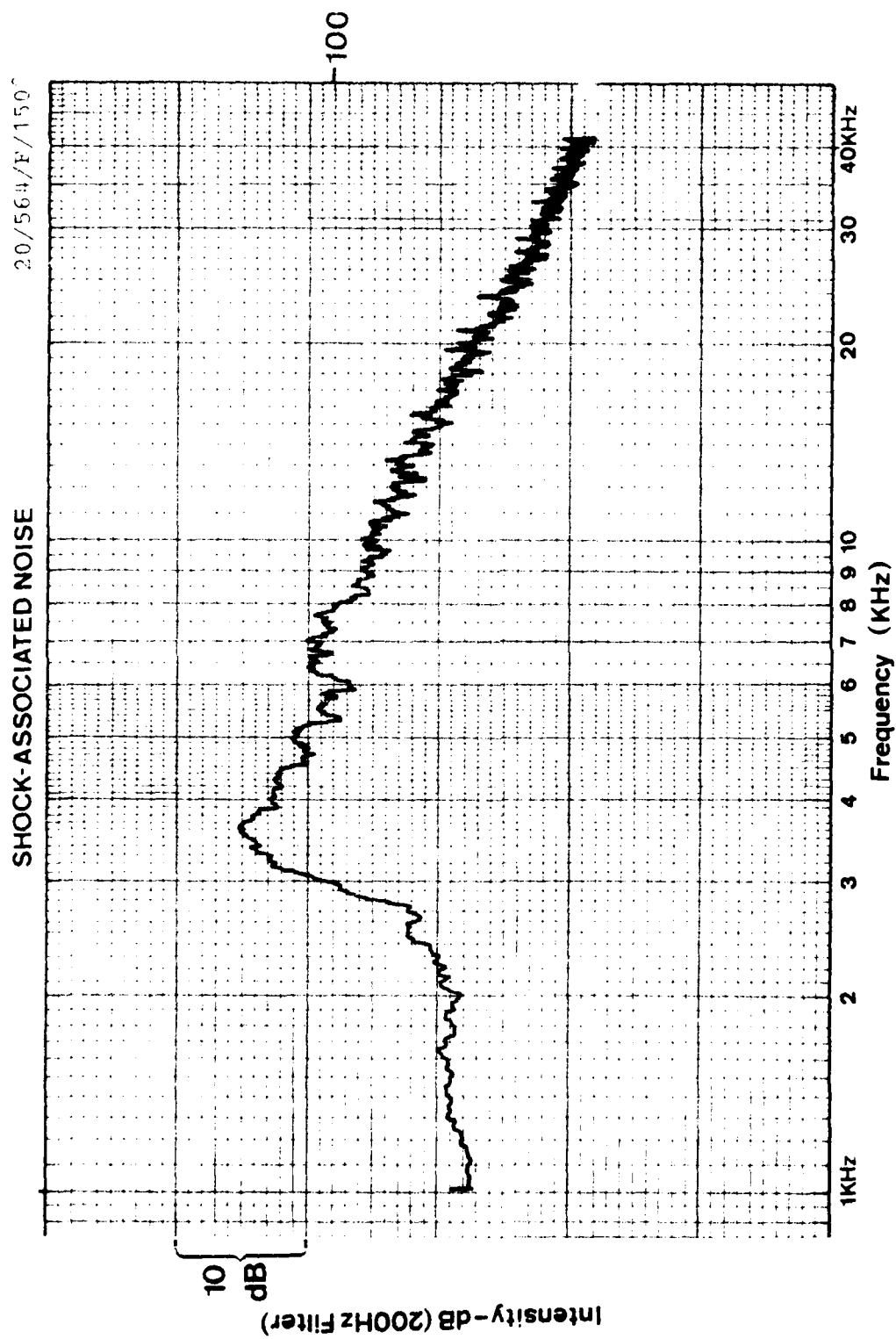






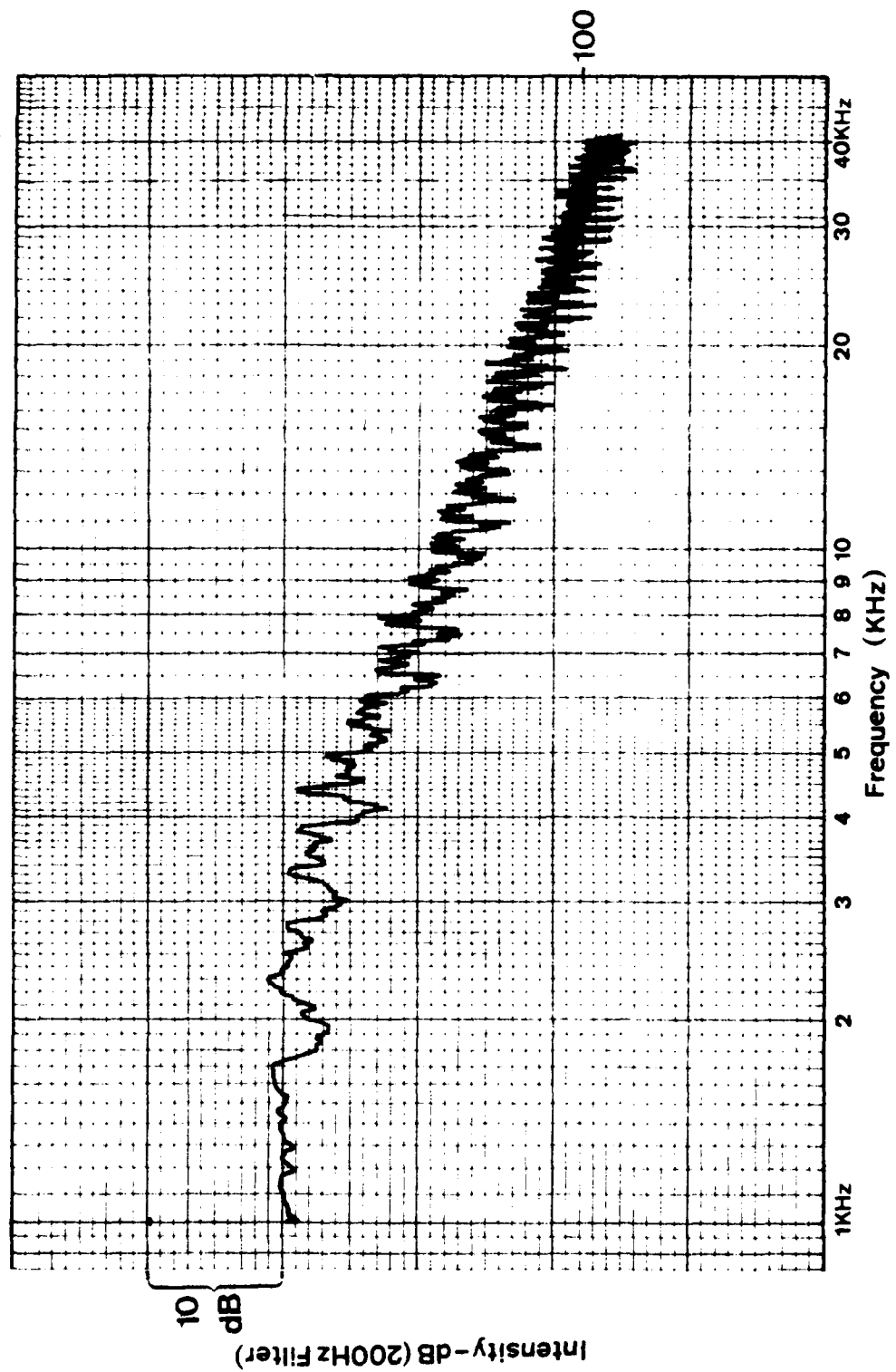


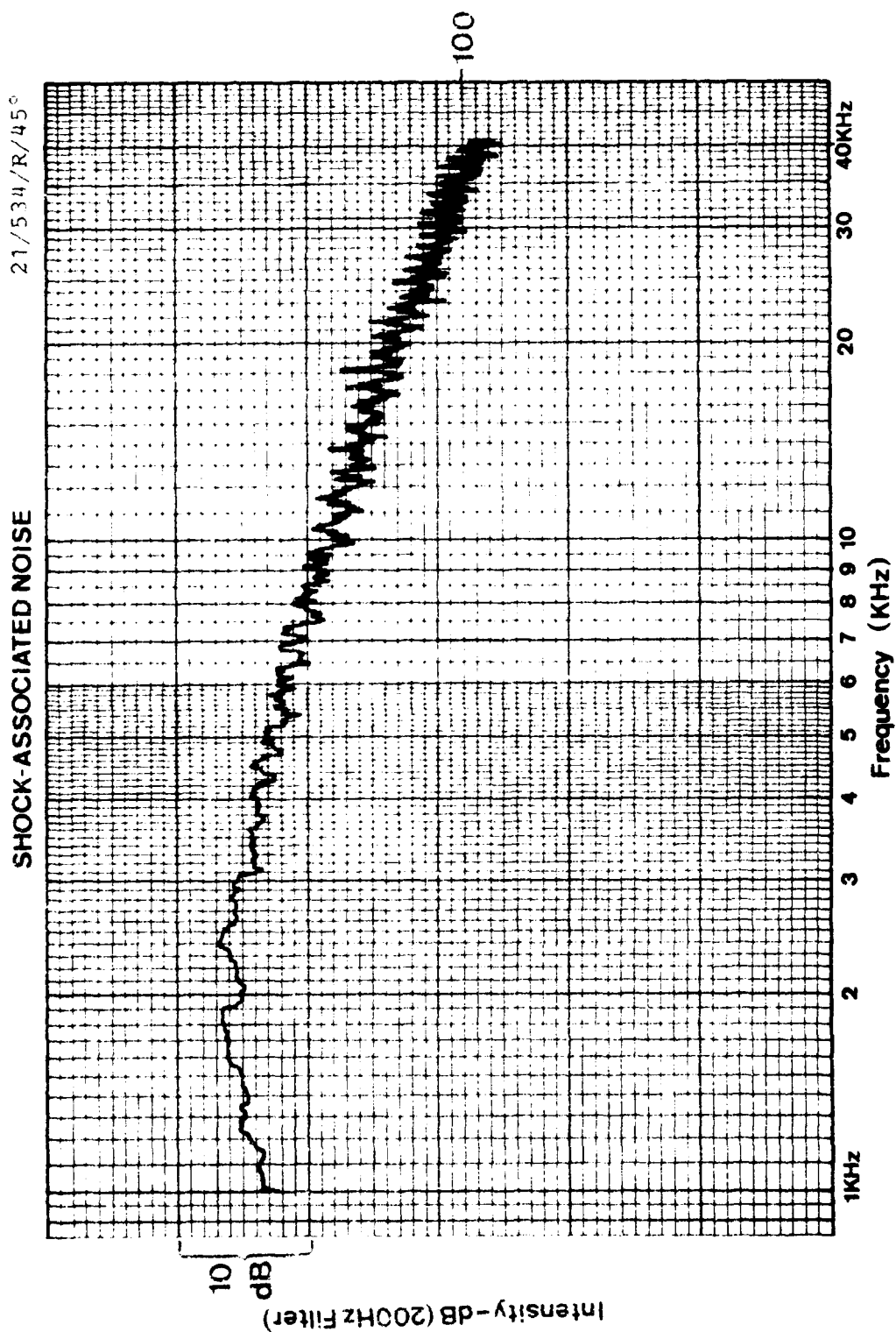


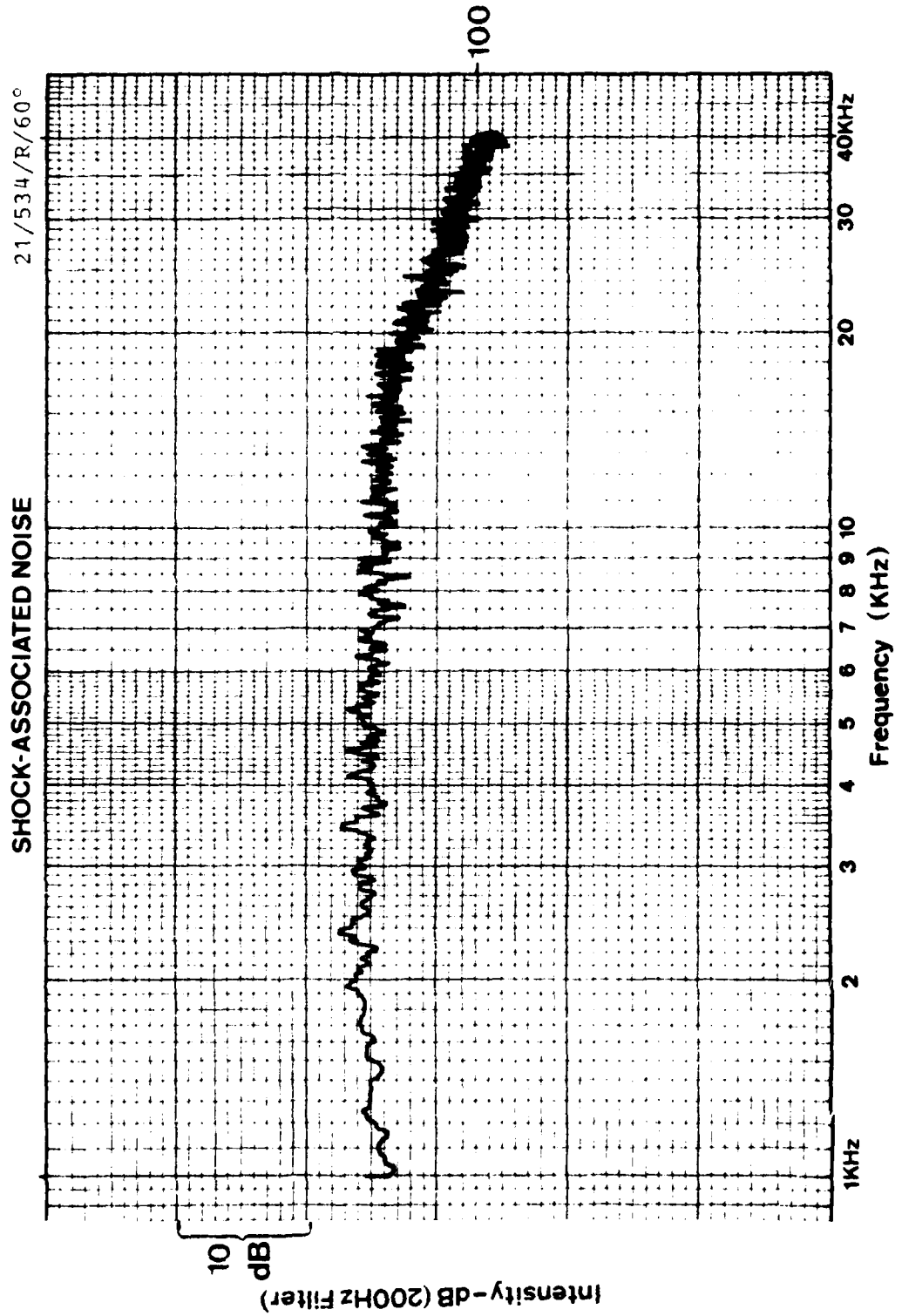


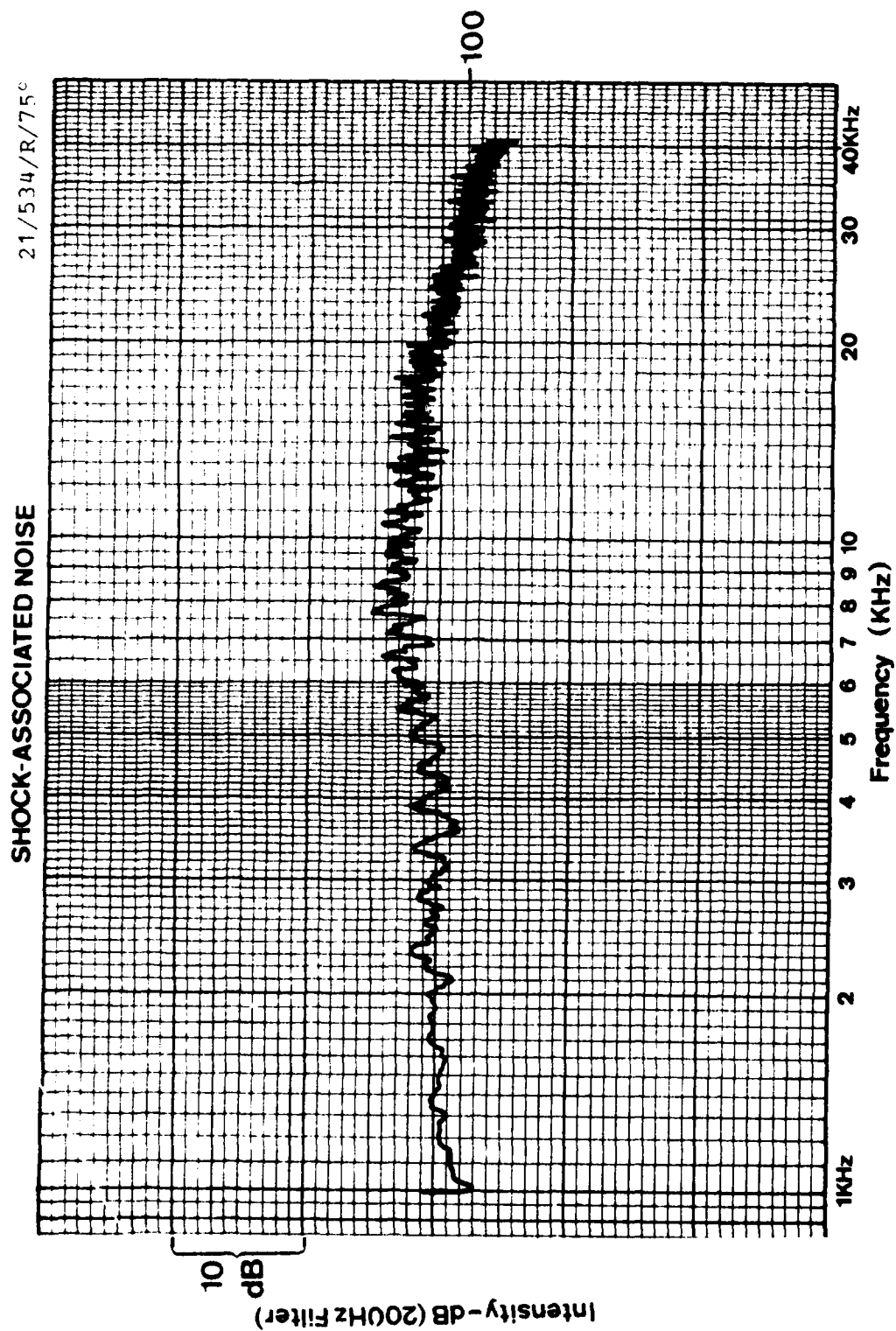
SHOCK-ASSOCIATED NOISE

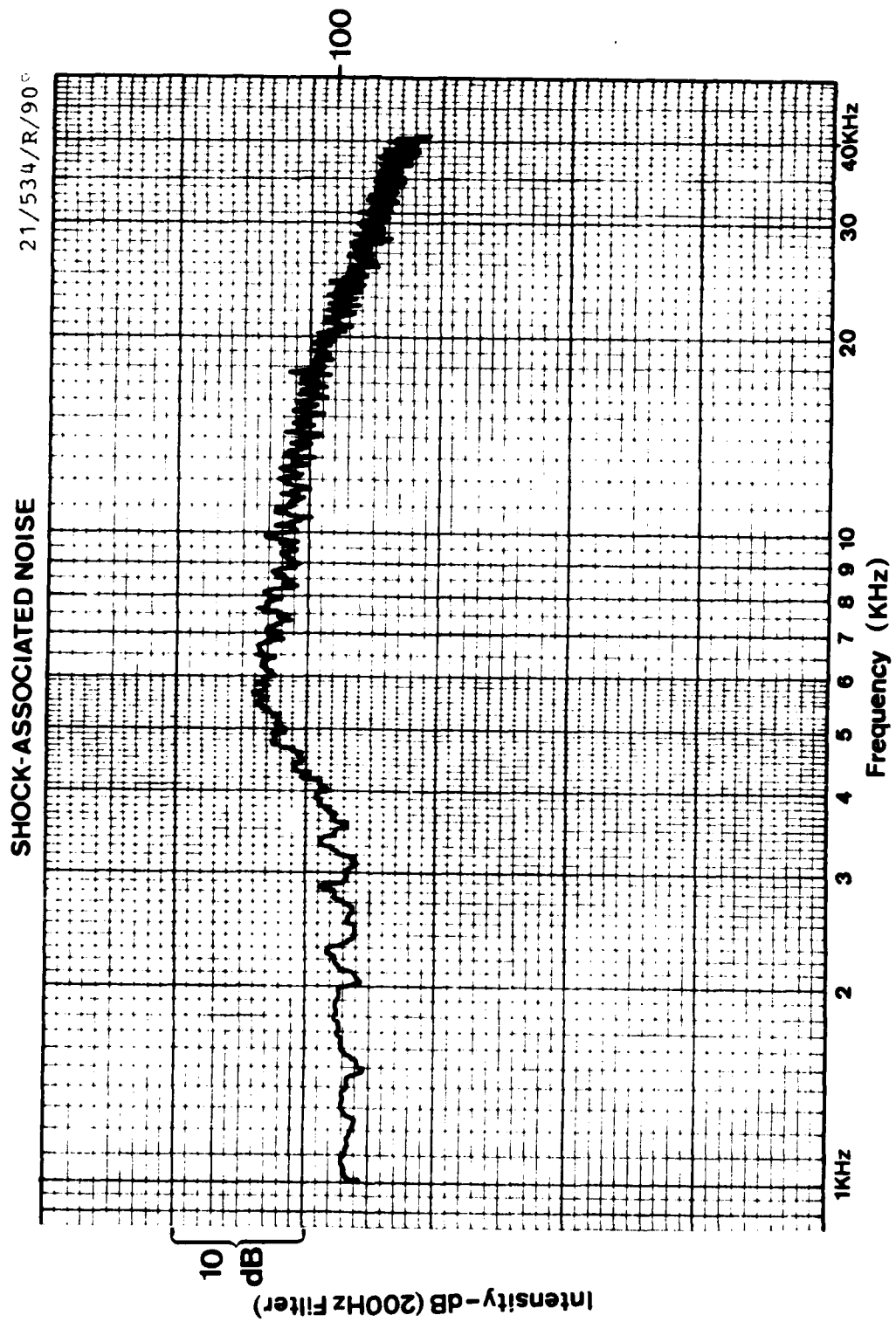
21/534/R/30

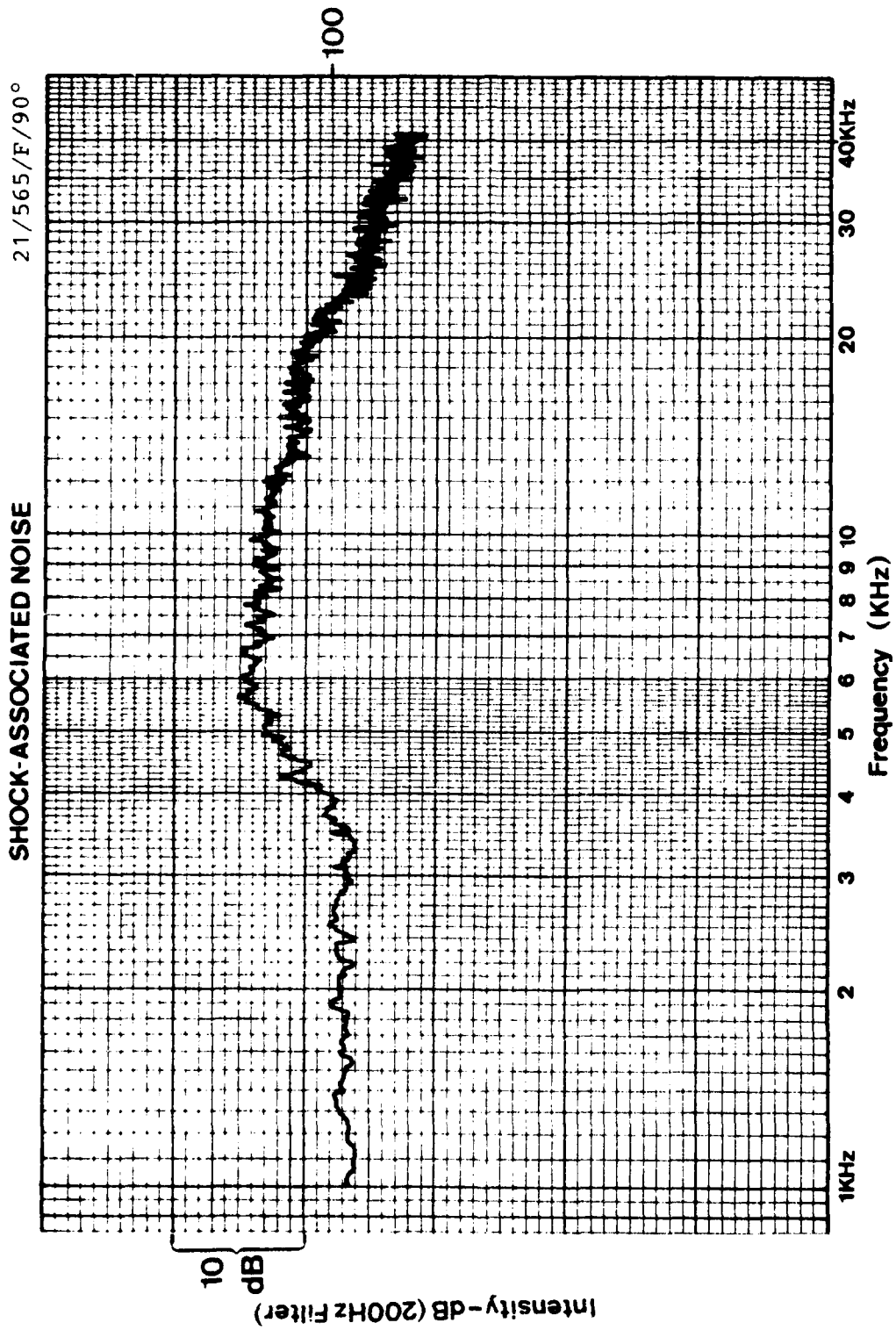


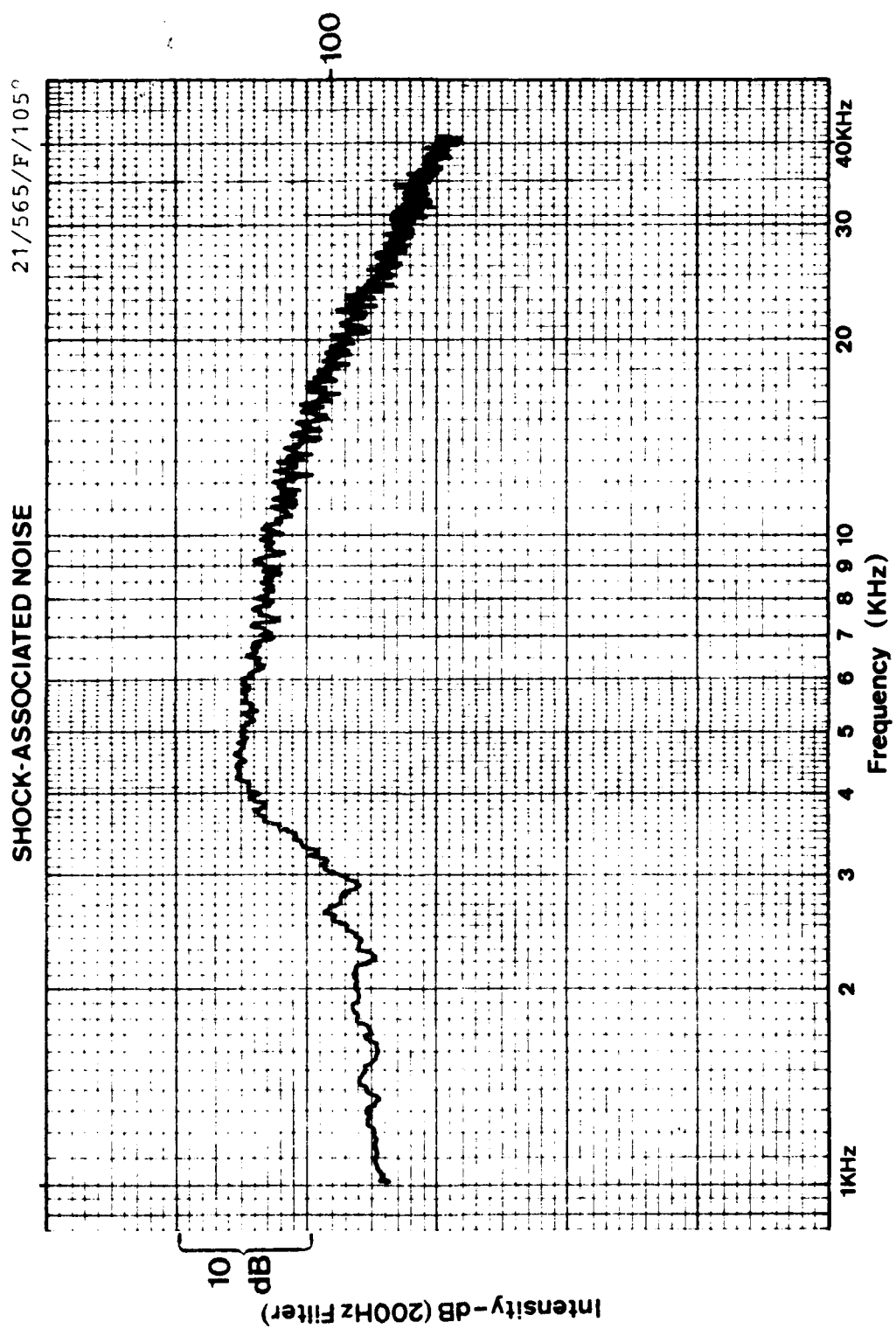


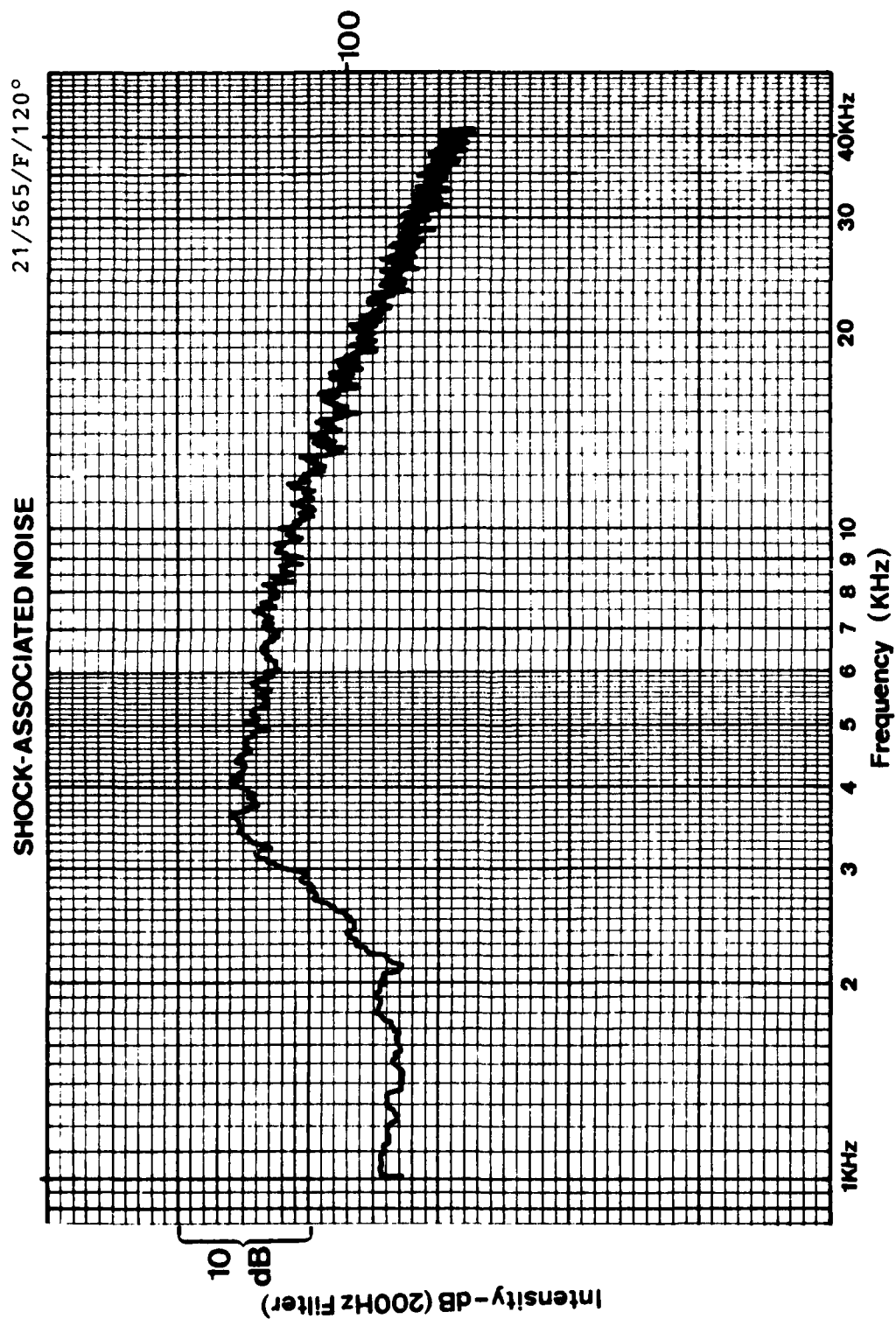


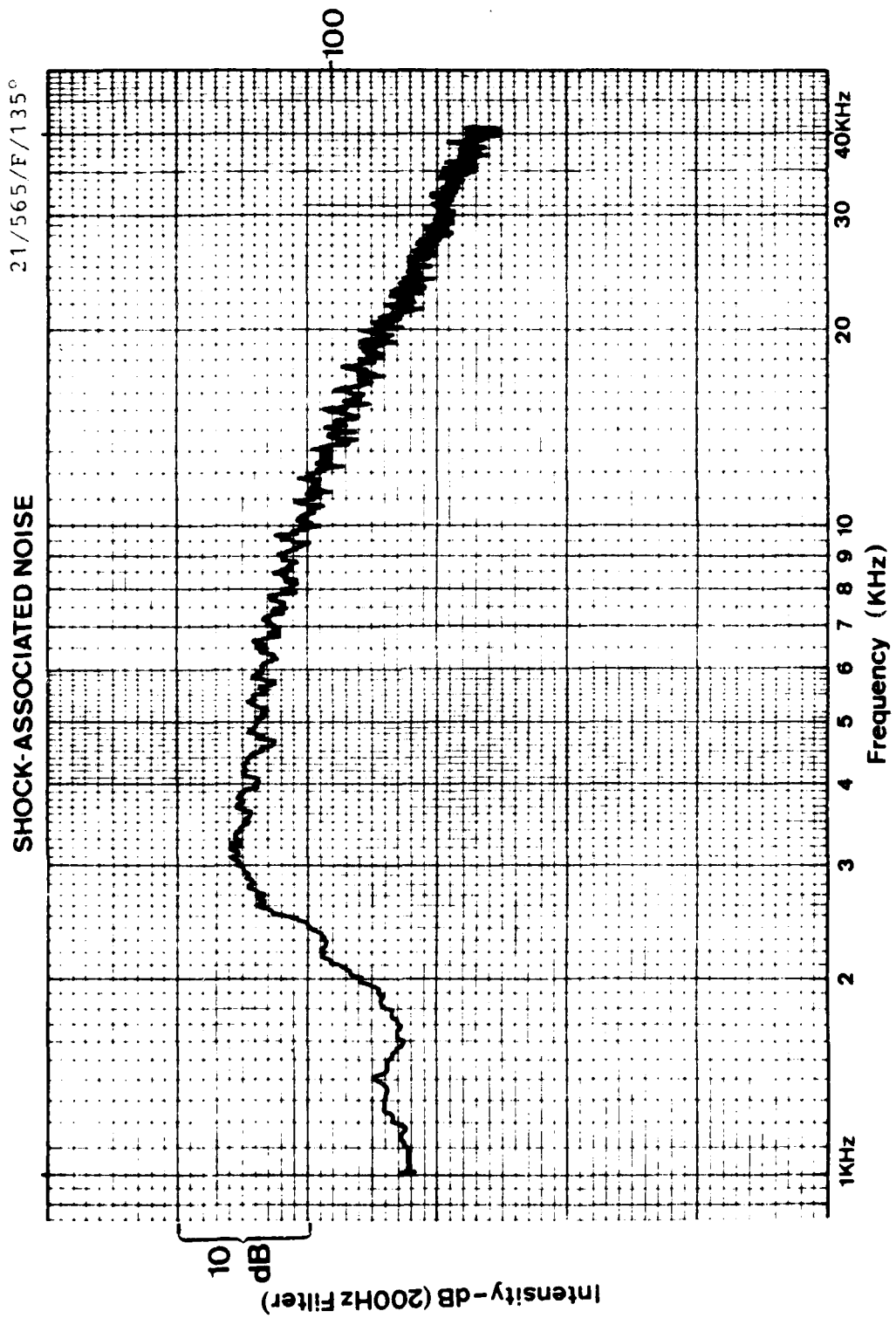


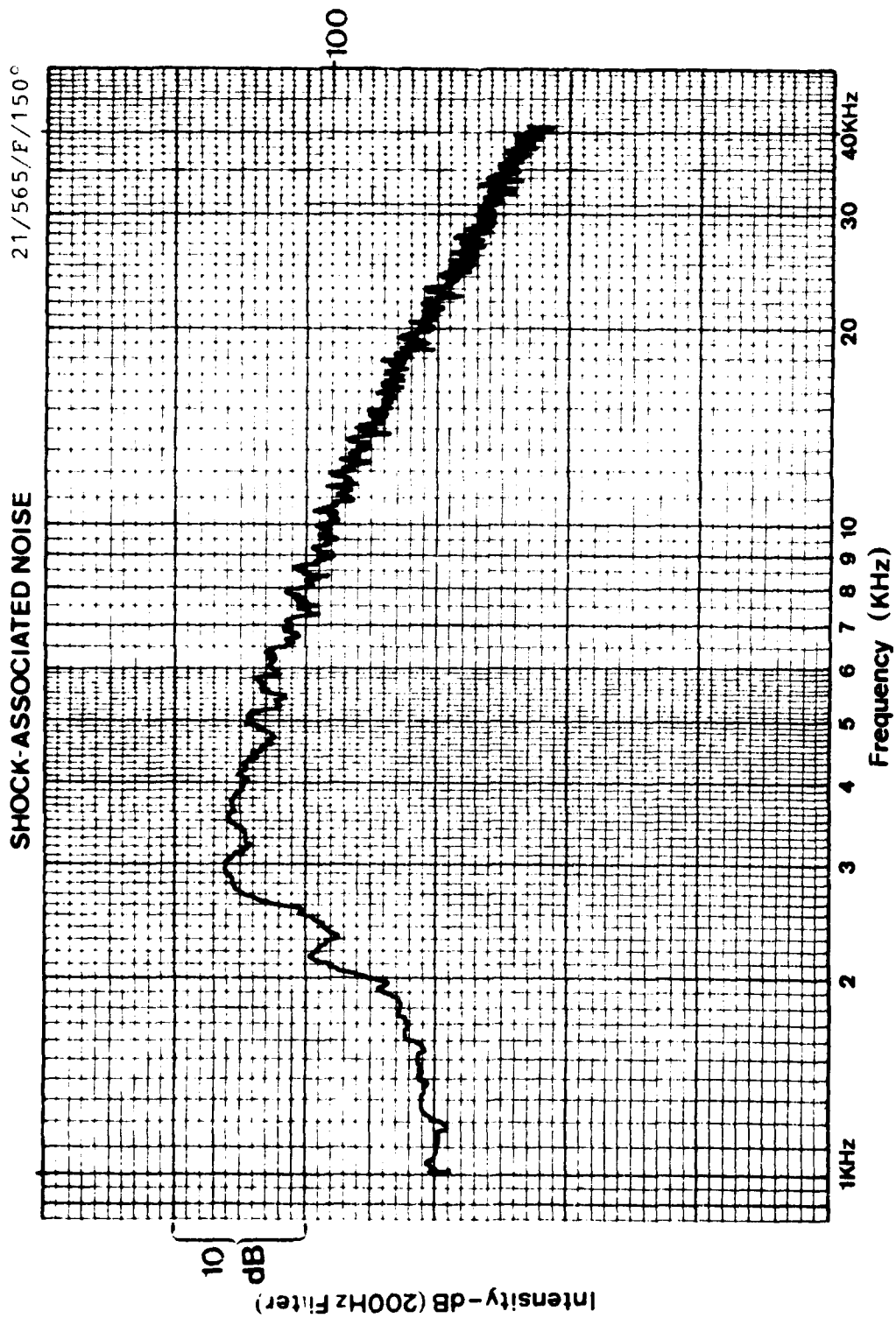


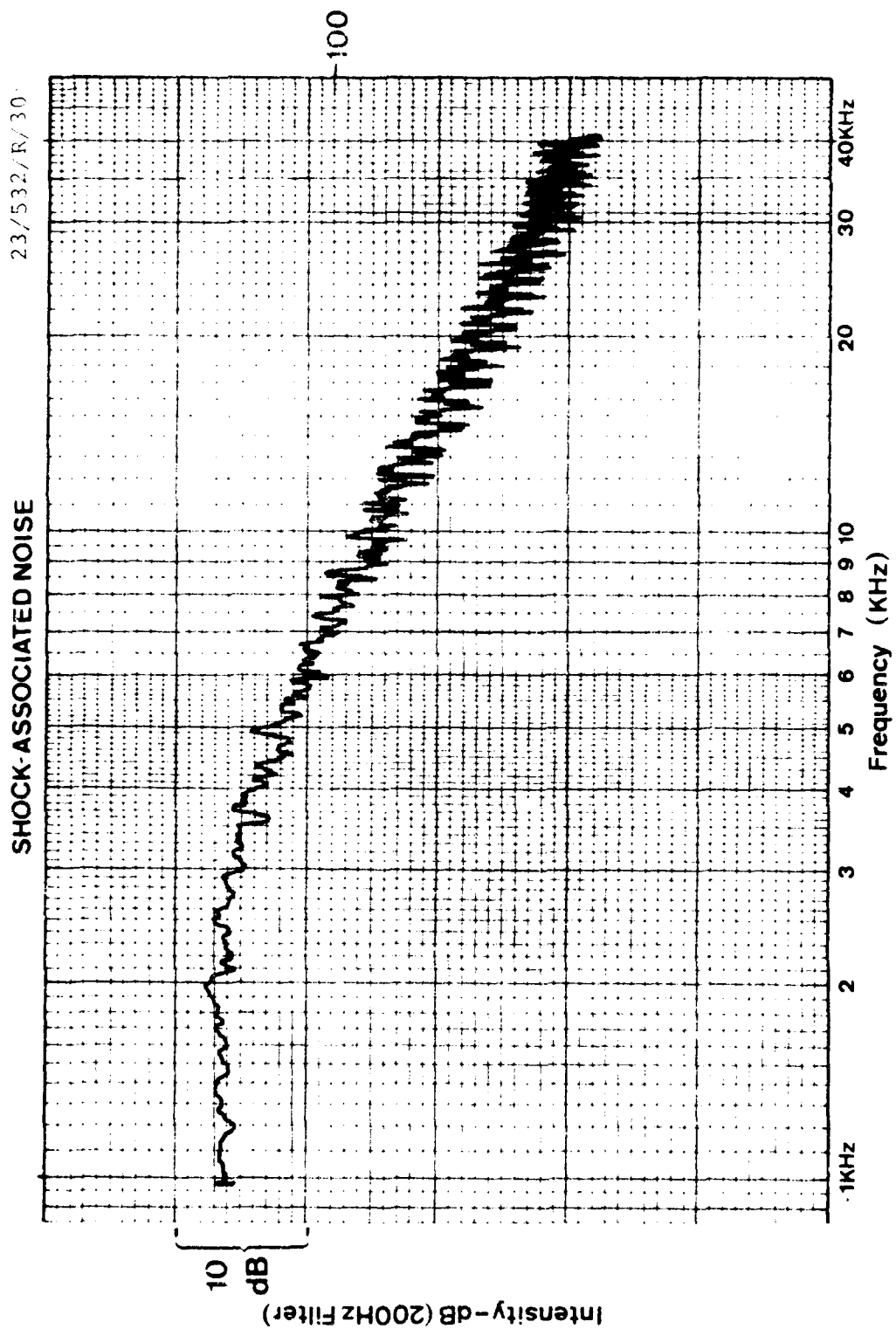


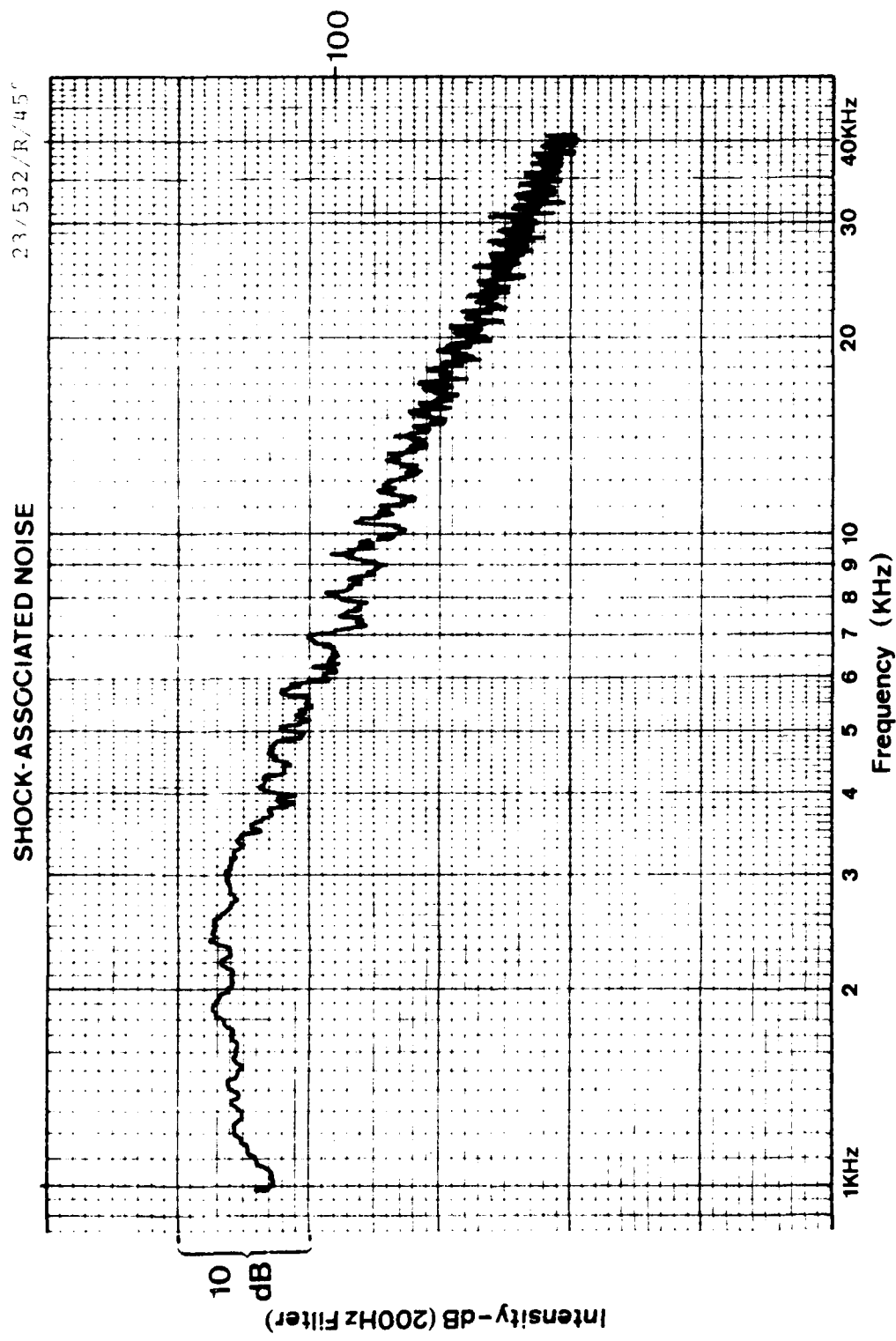


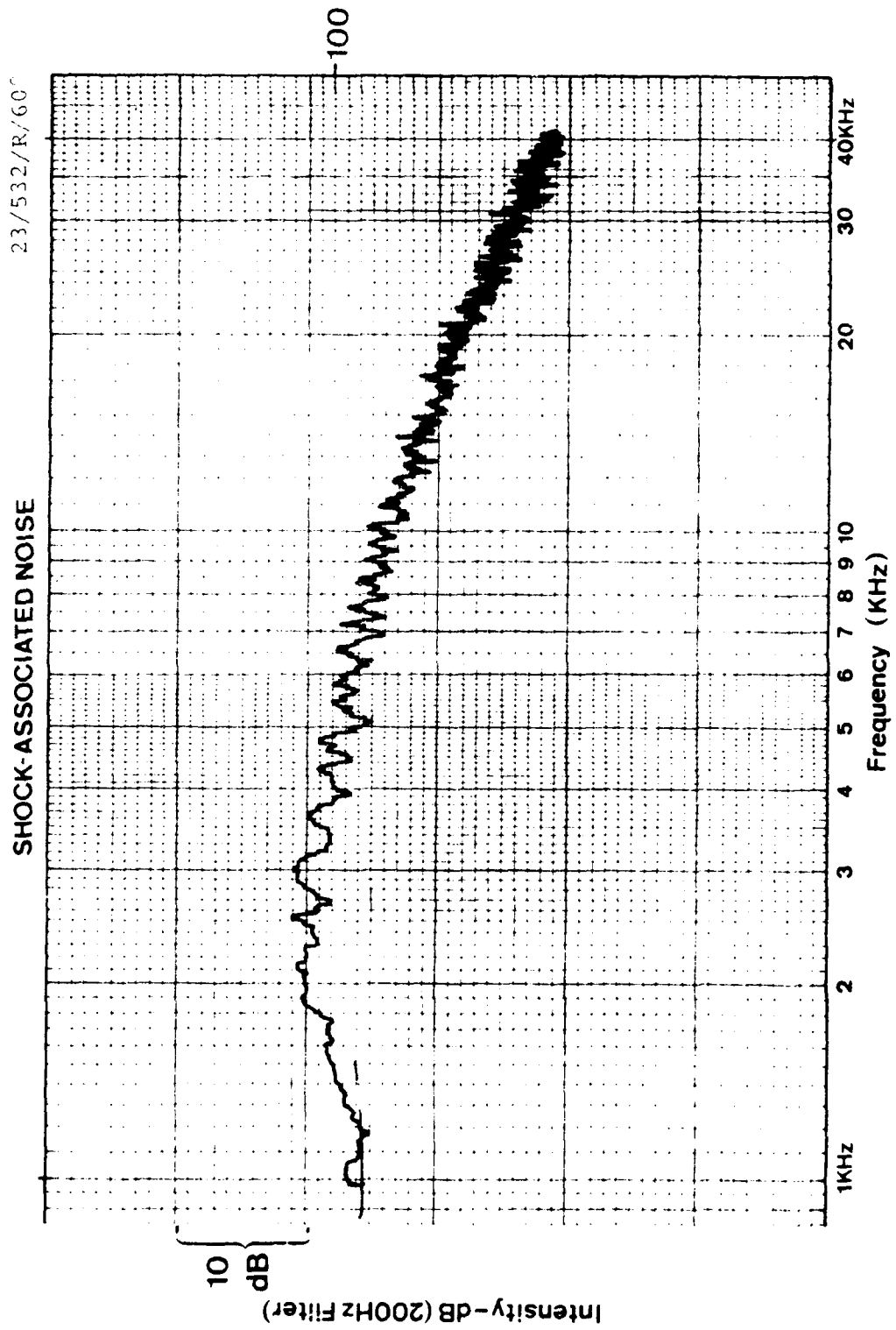






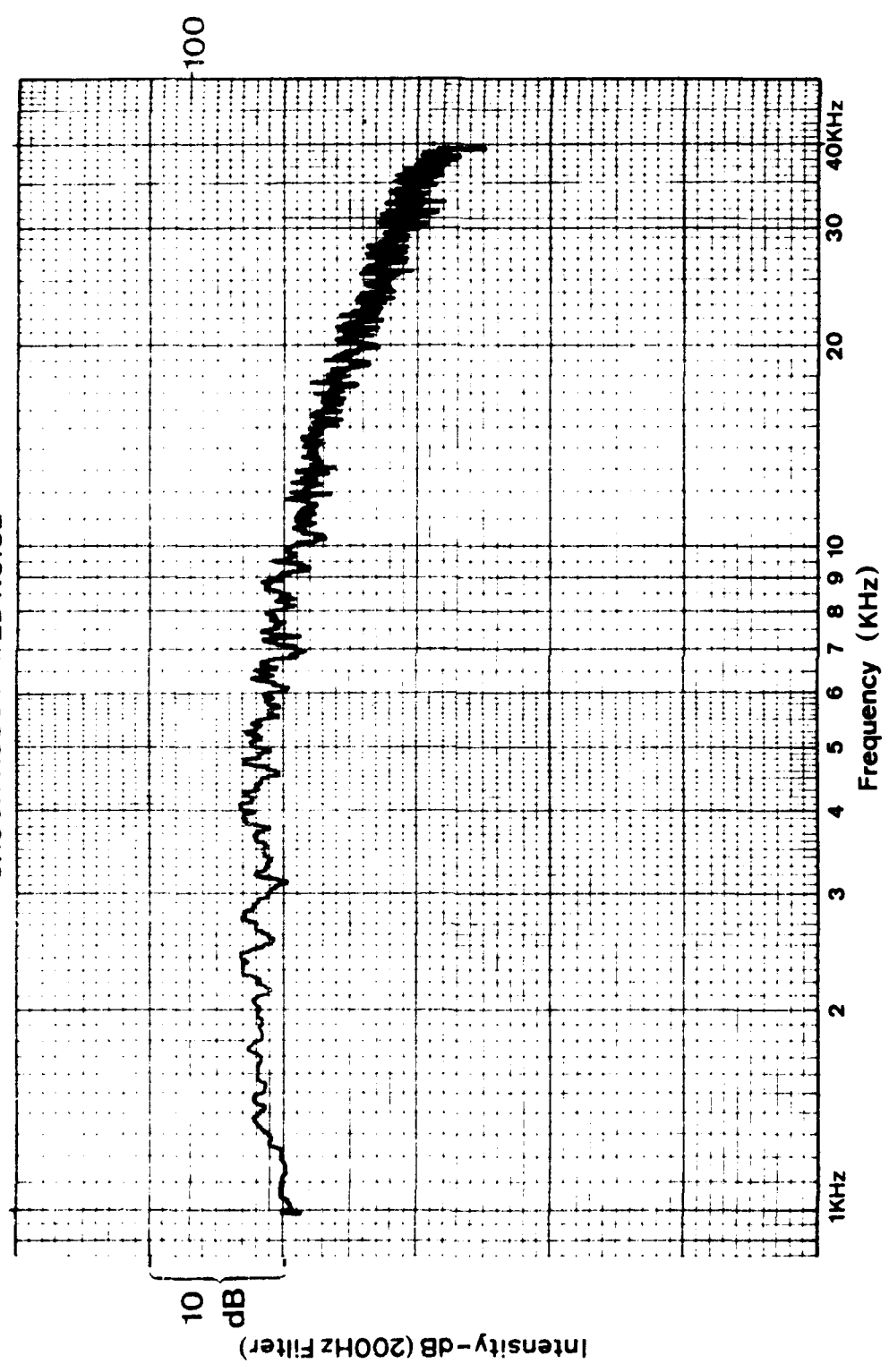






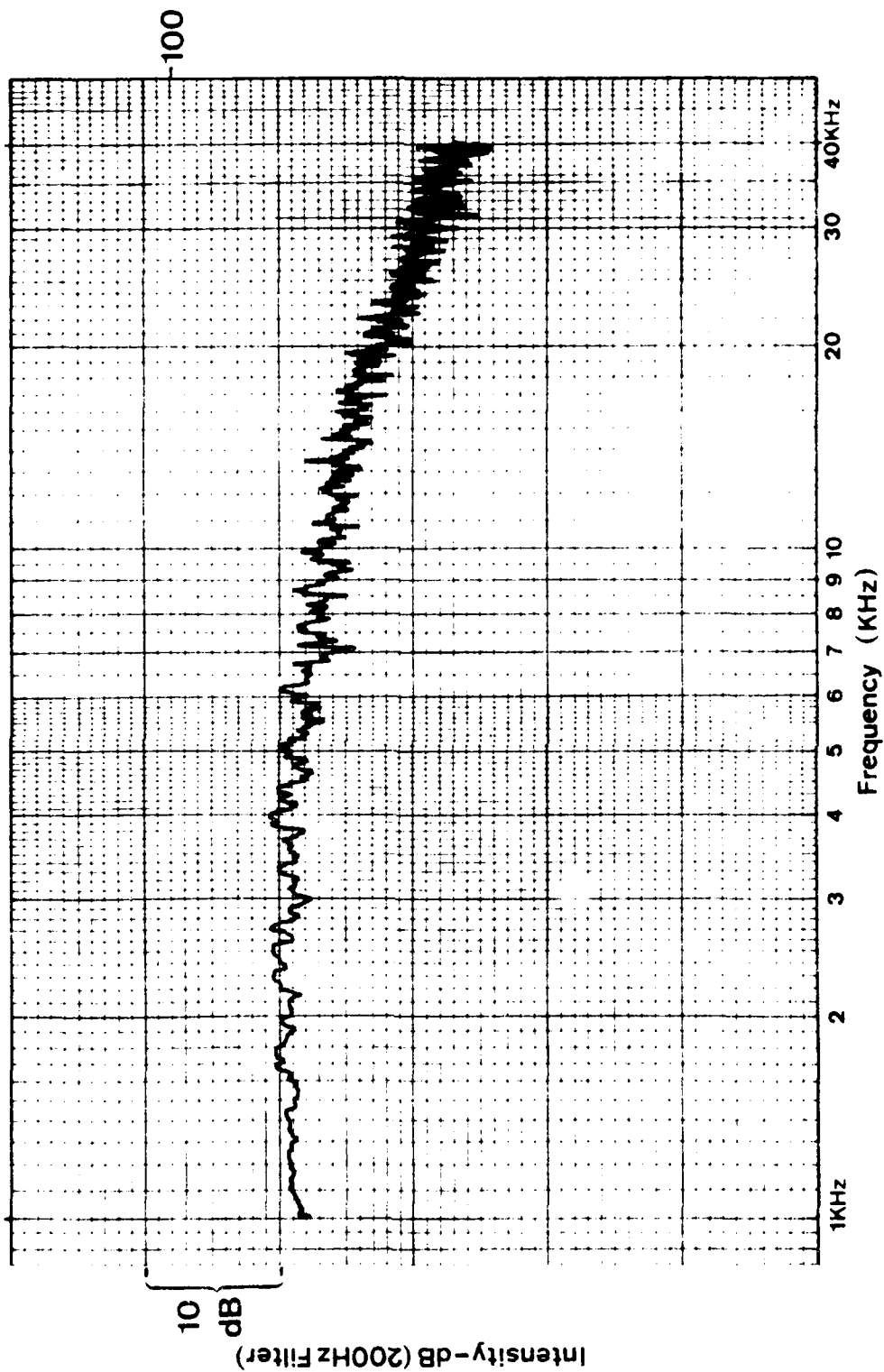
23/532/R/75

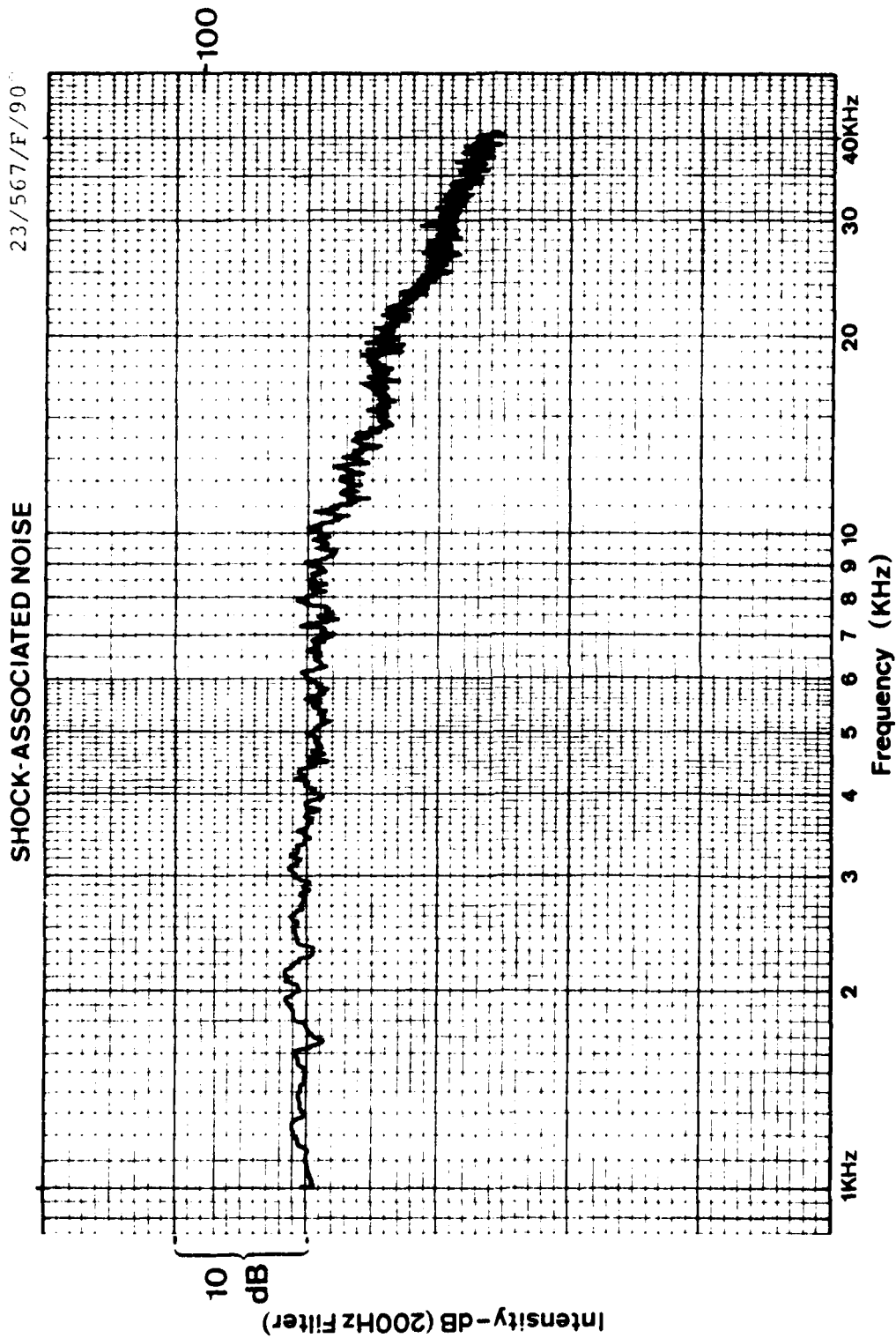
SHOCK-ASSOCIATED NOISE

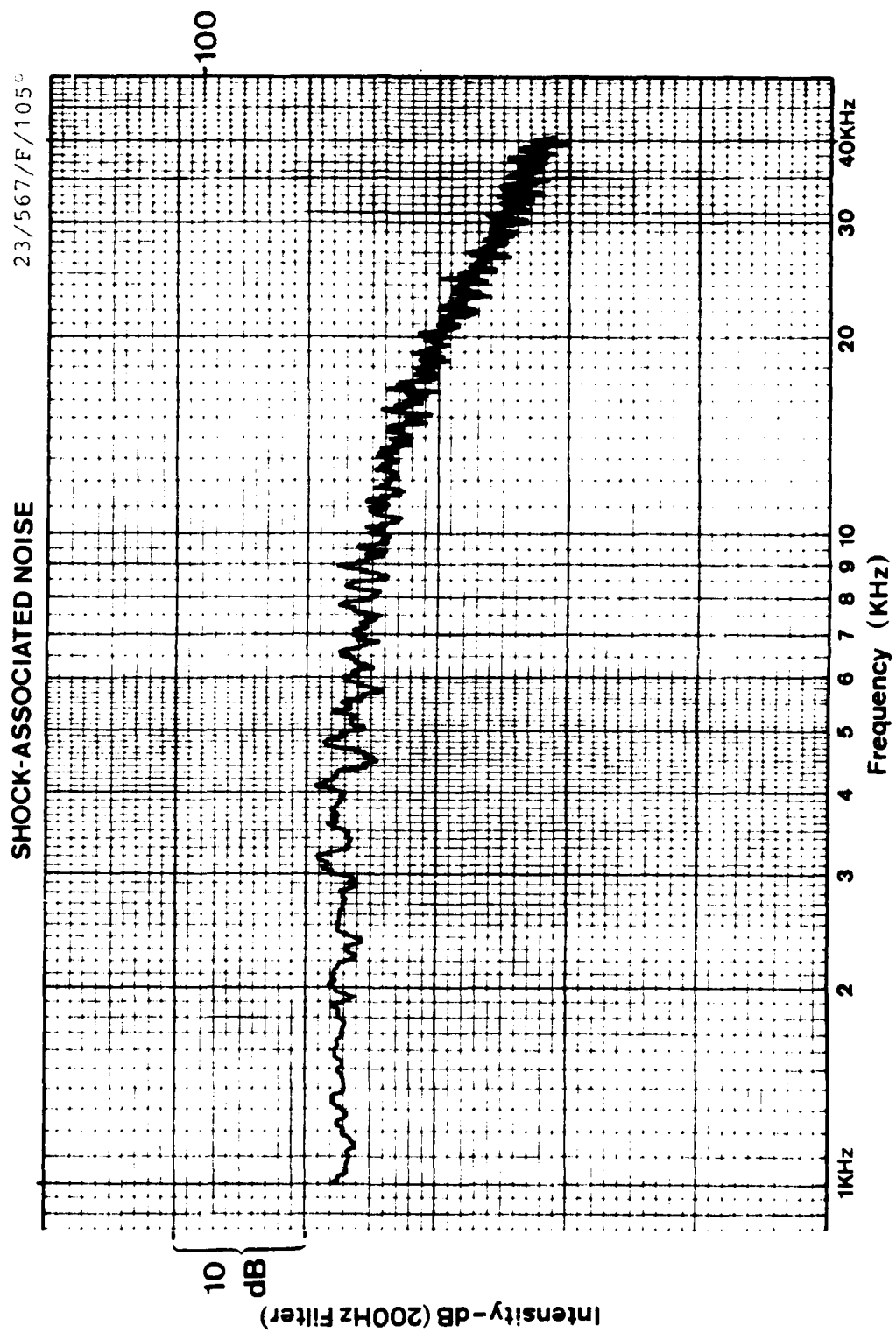


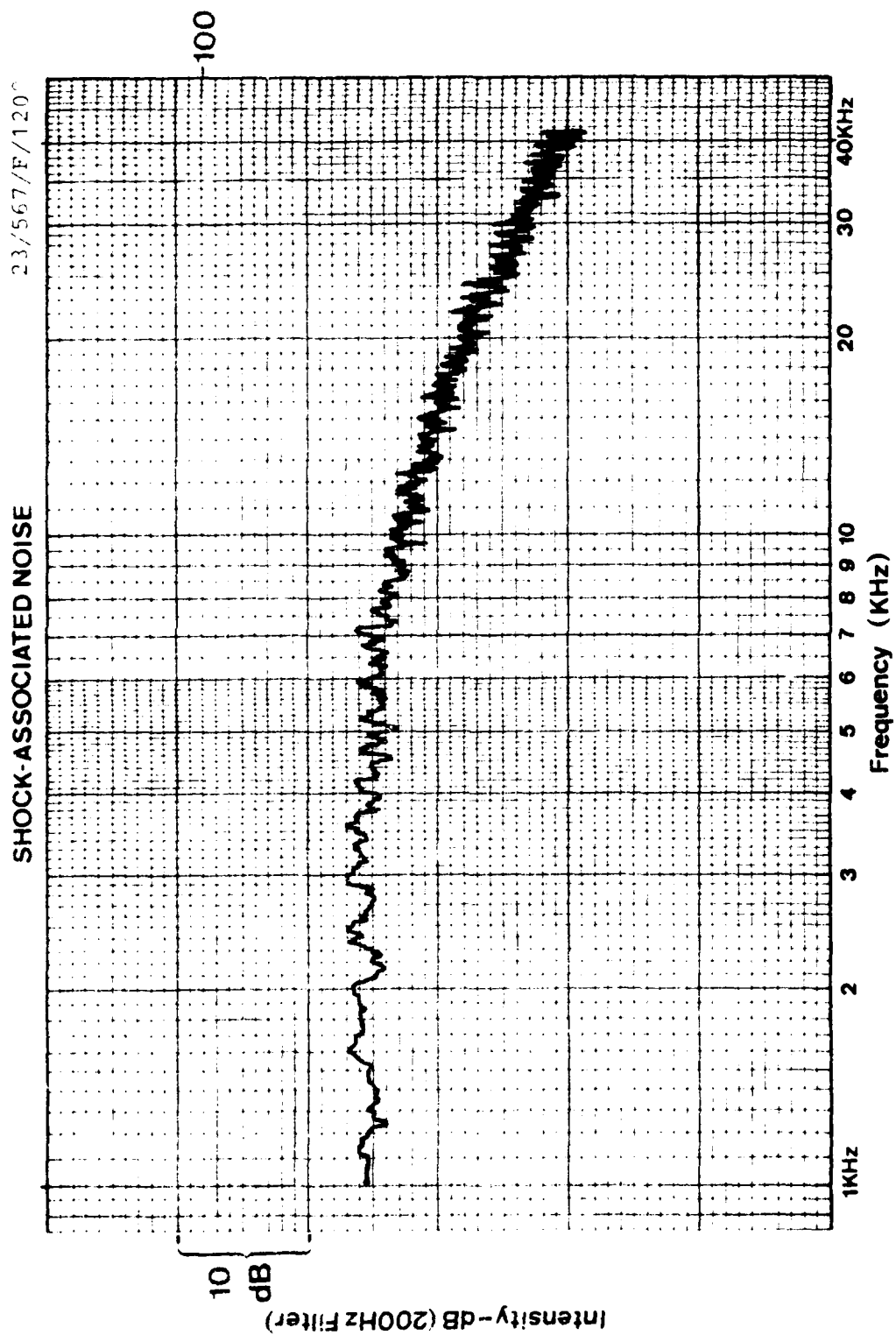
23/532/R/90

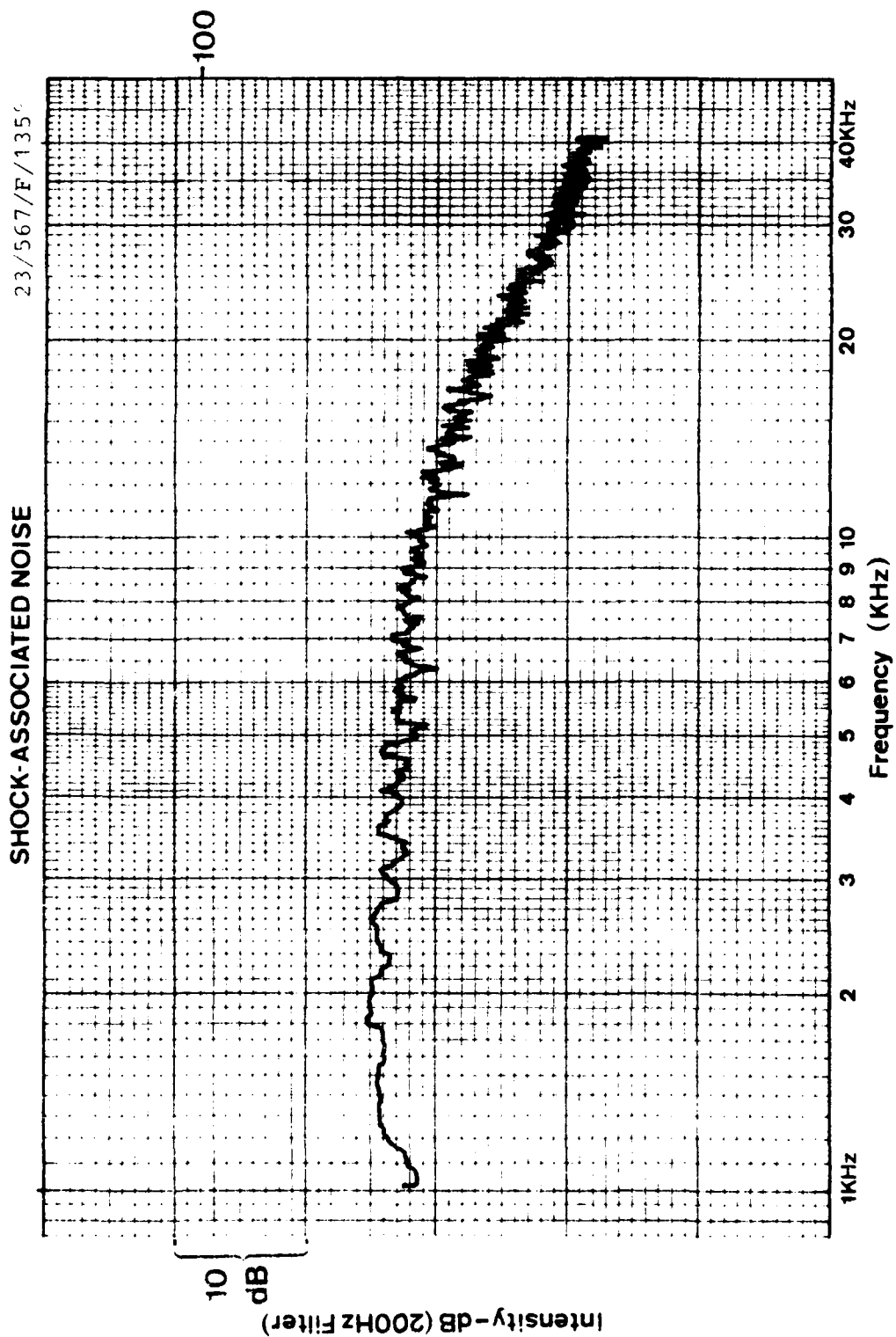
SHOCK-ASSOCIATED NOISE

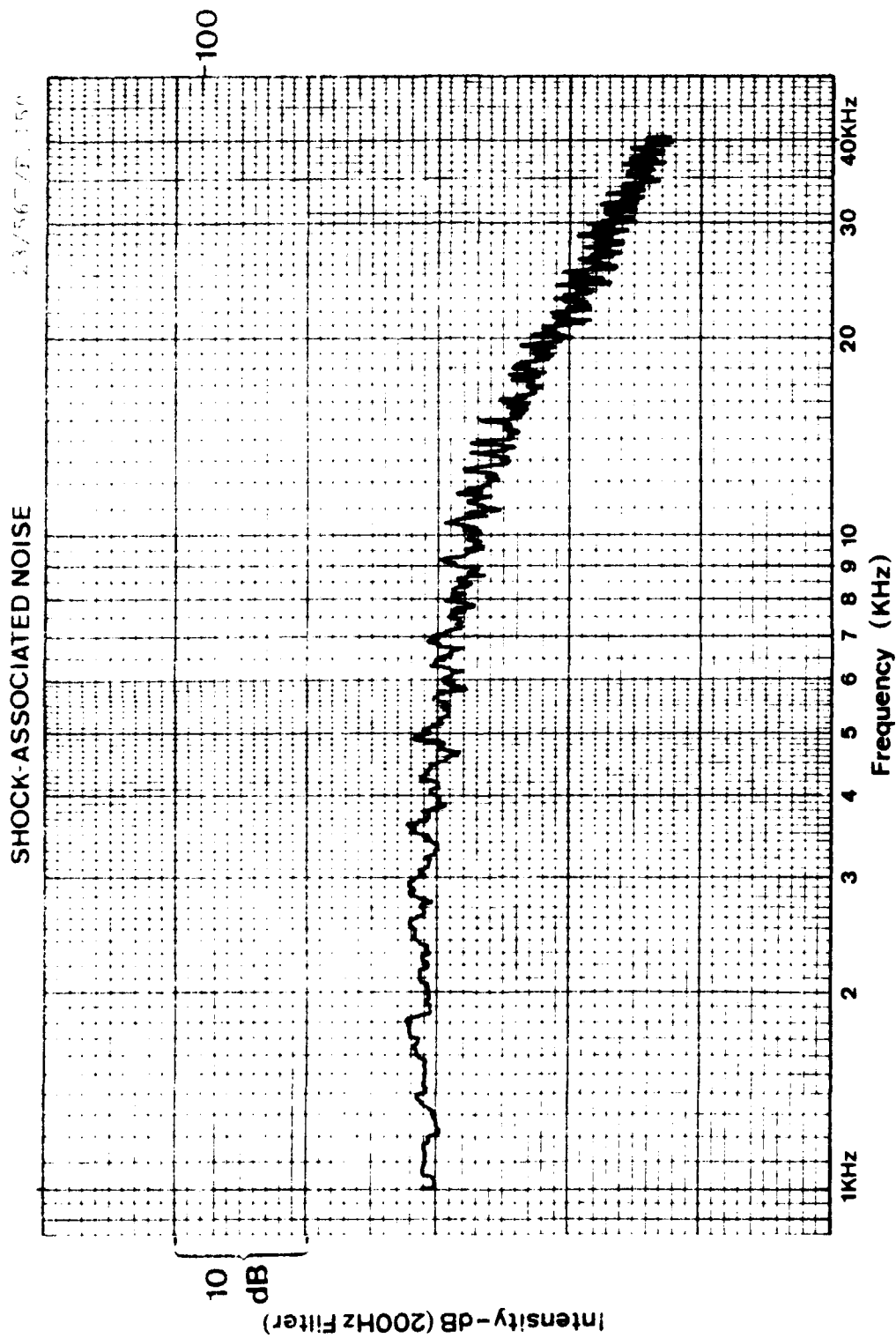


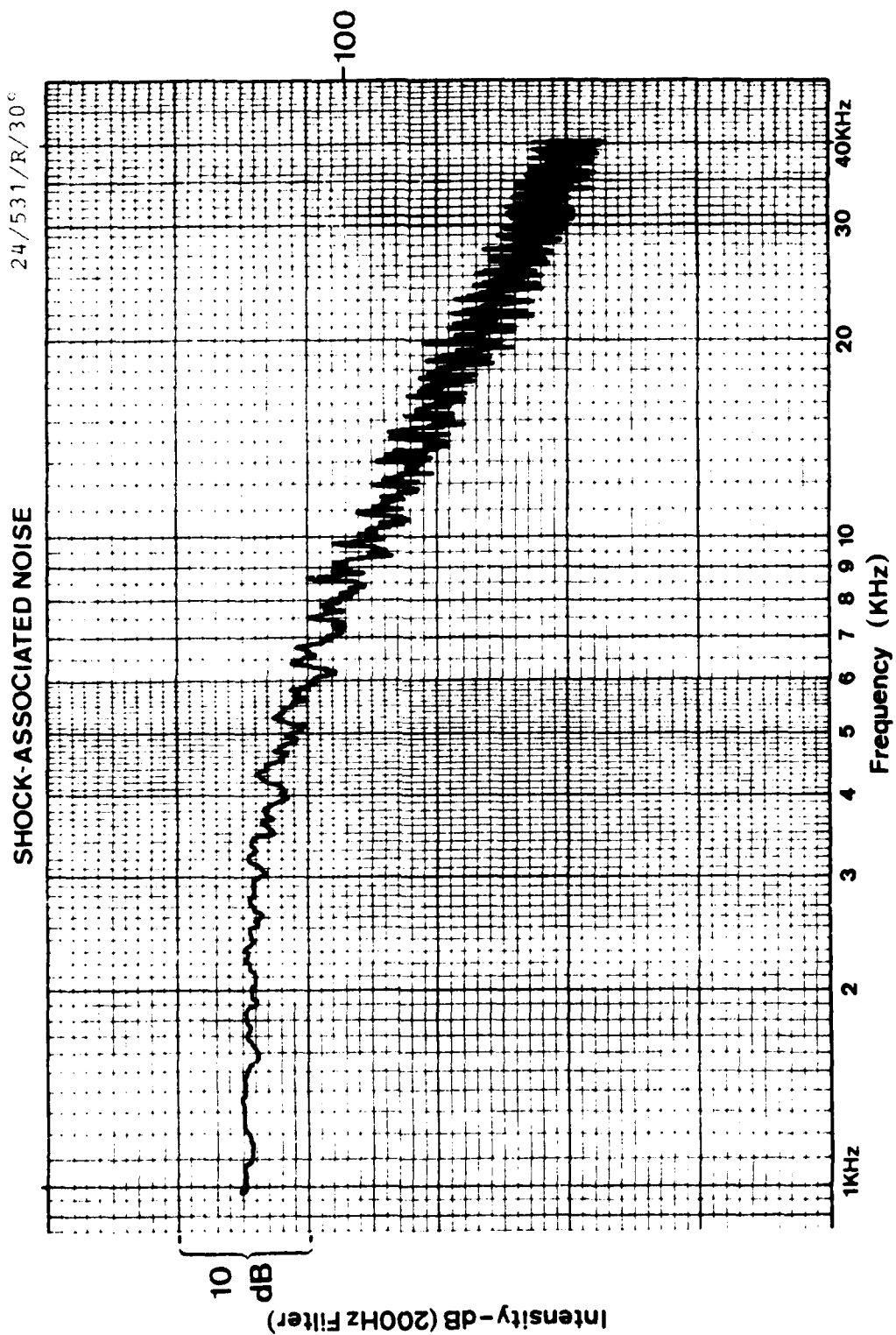


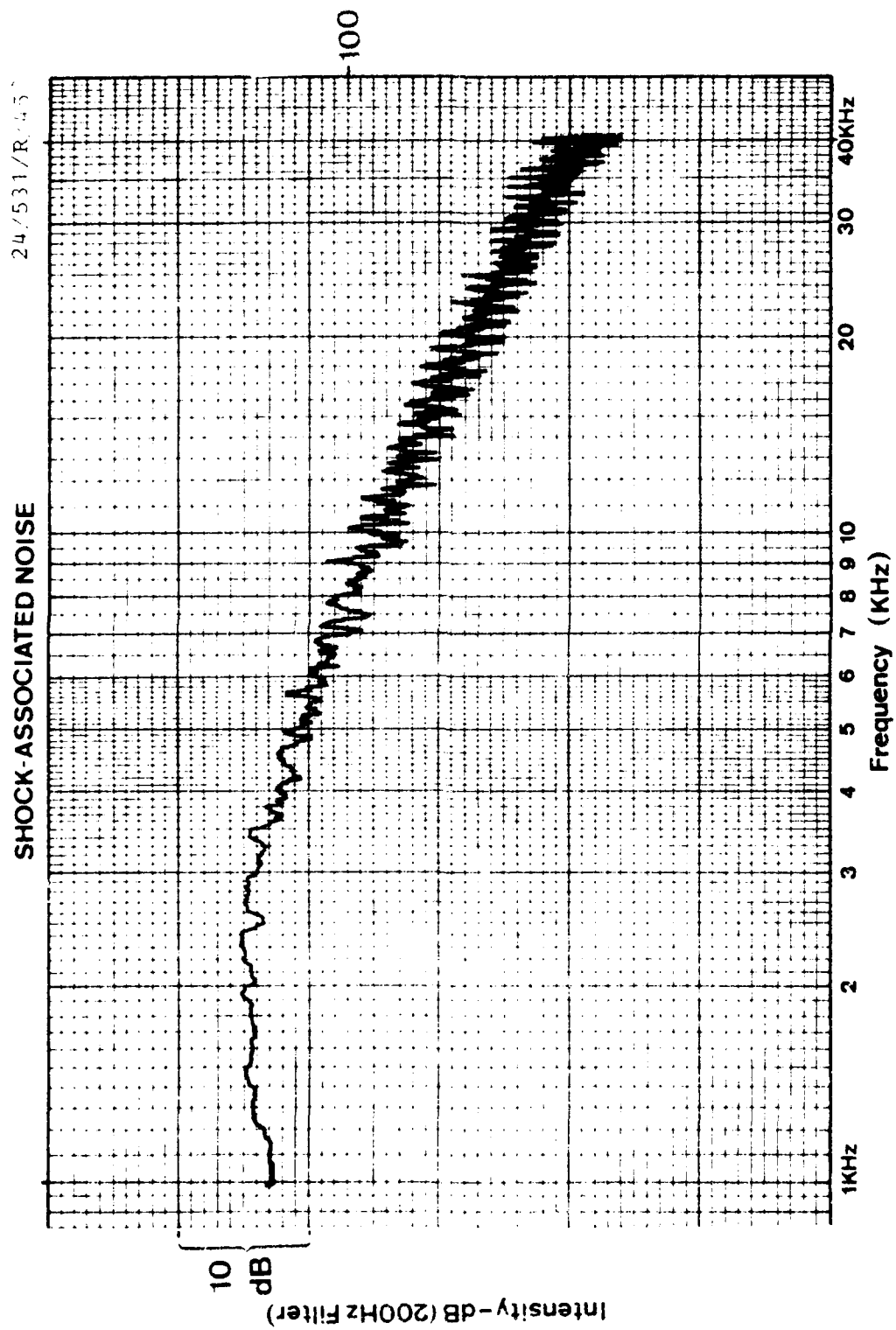


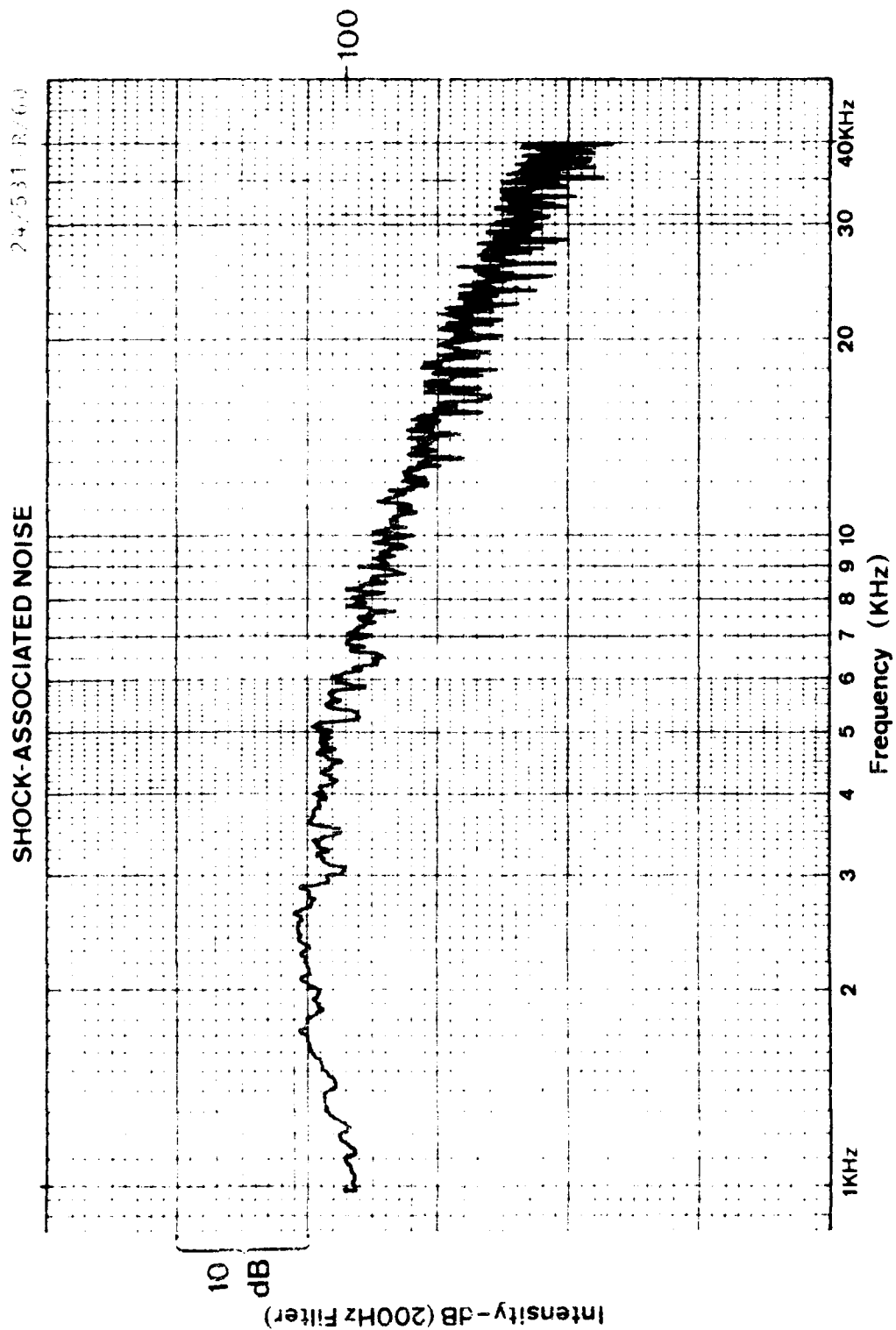


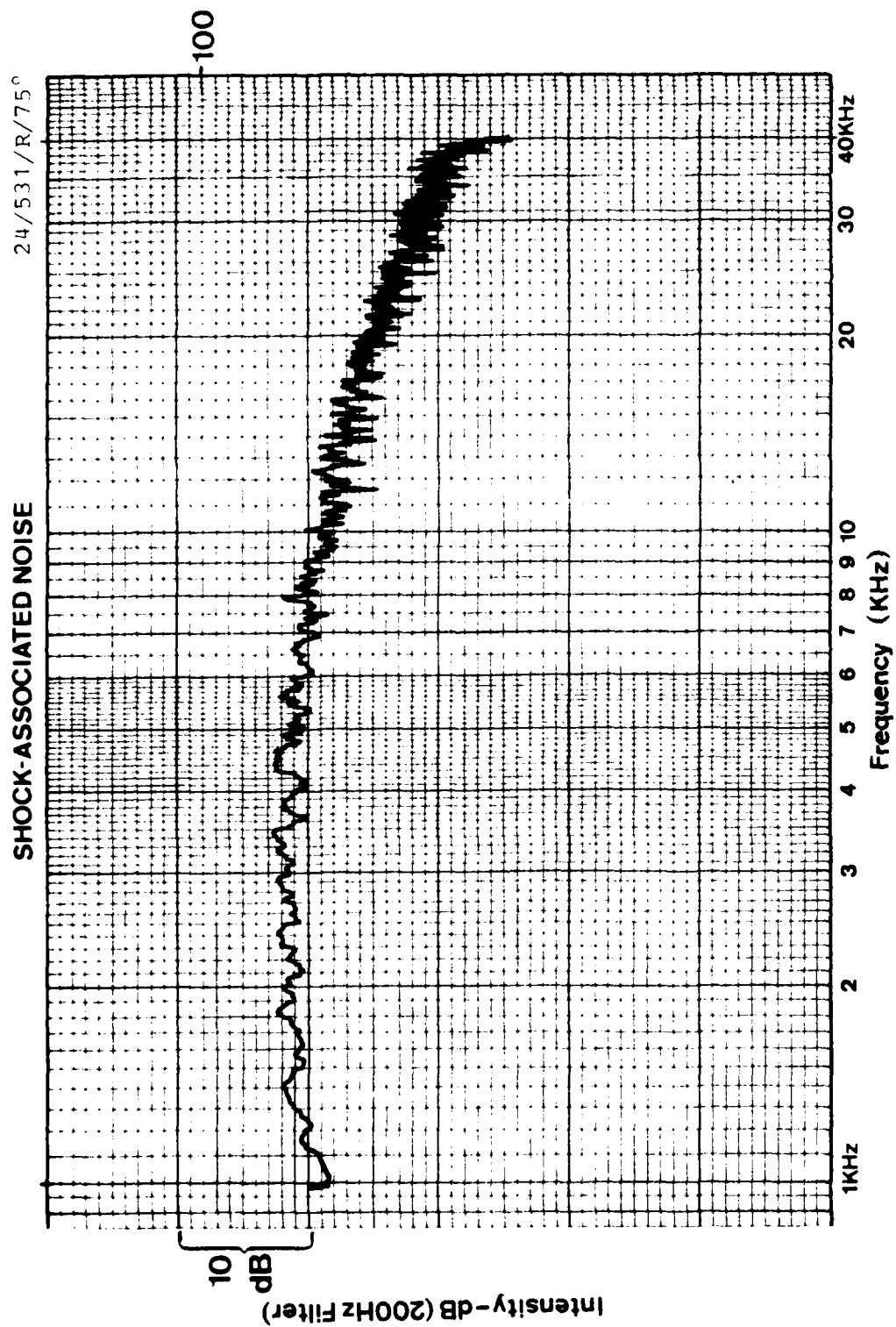


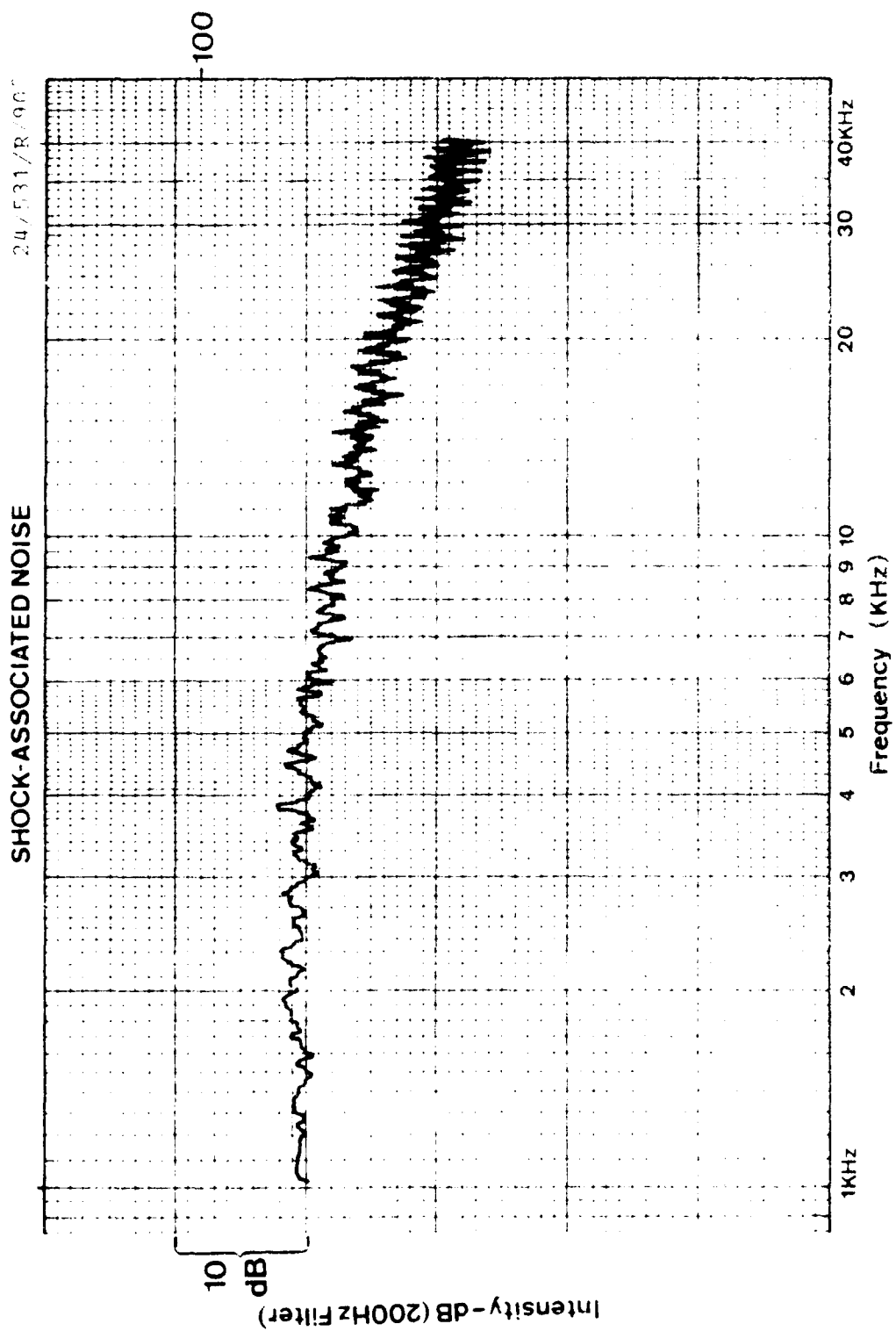






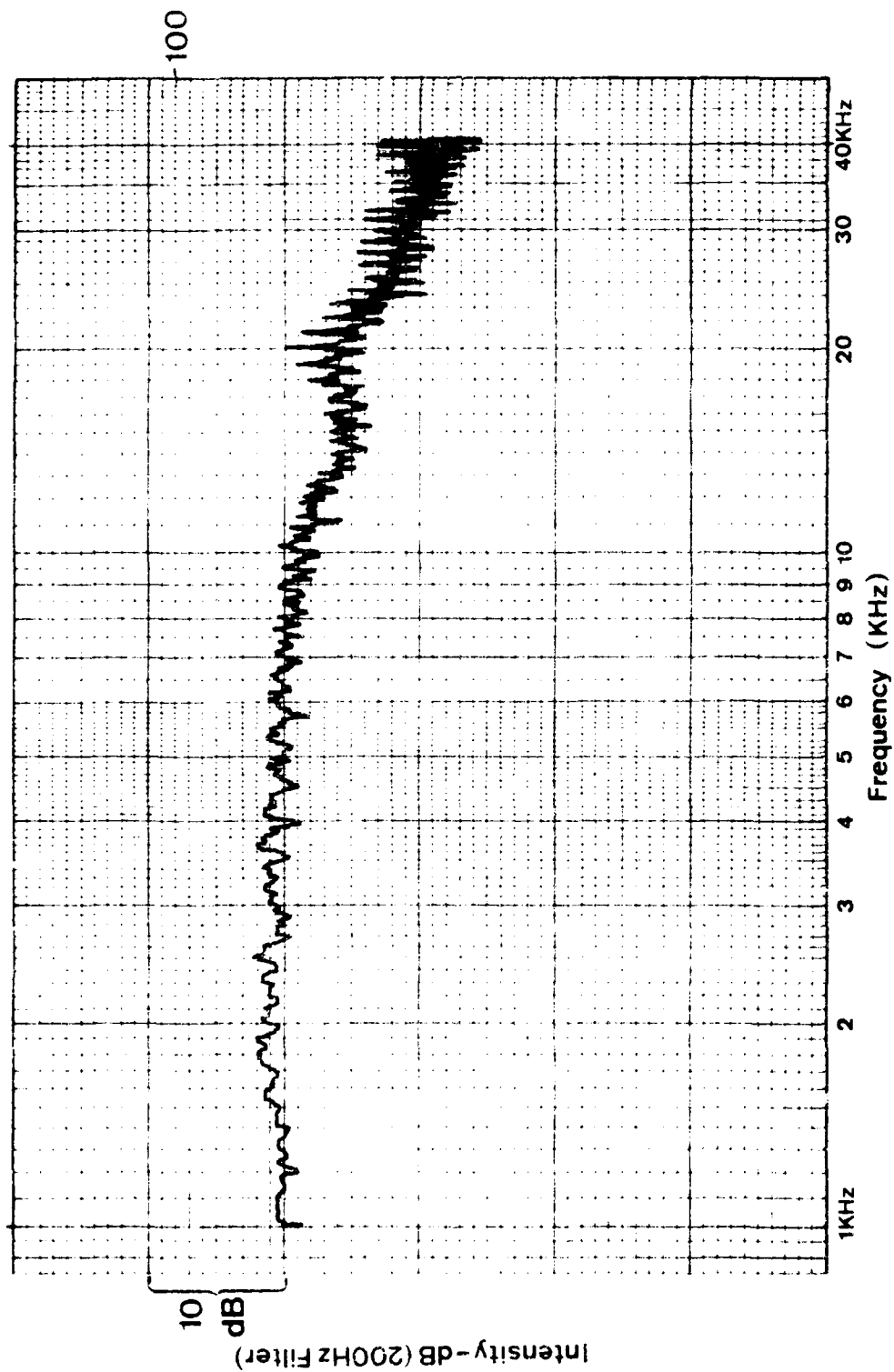


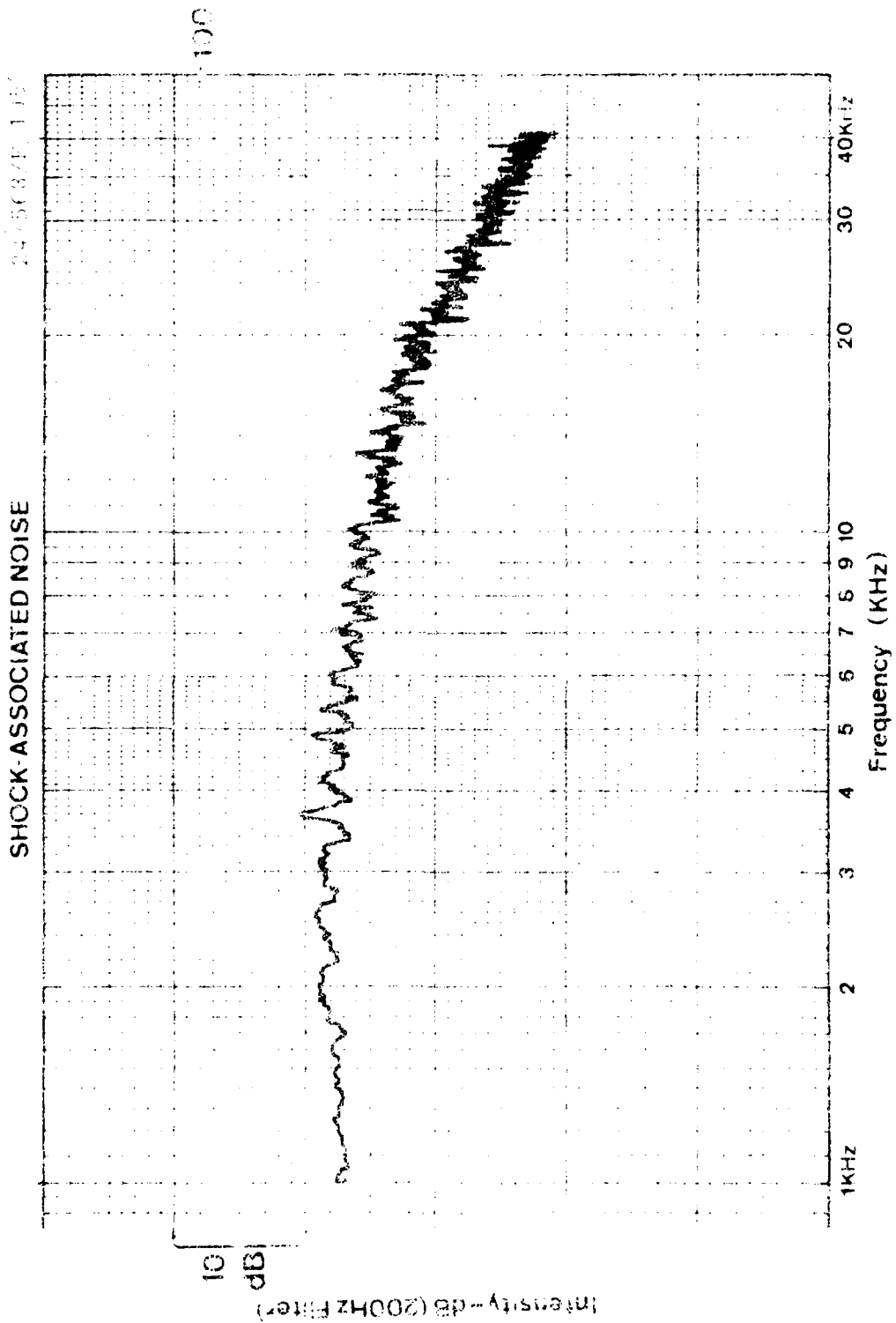




SHOCK-ASSOCIATED NOISE

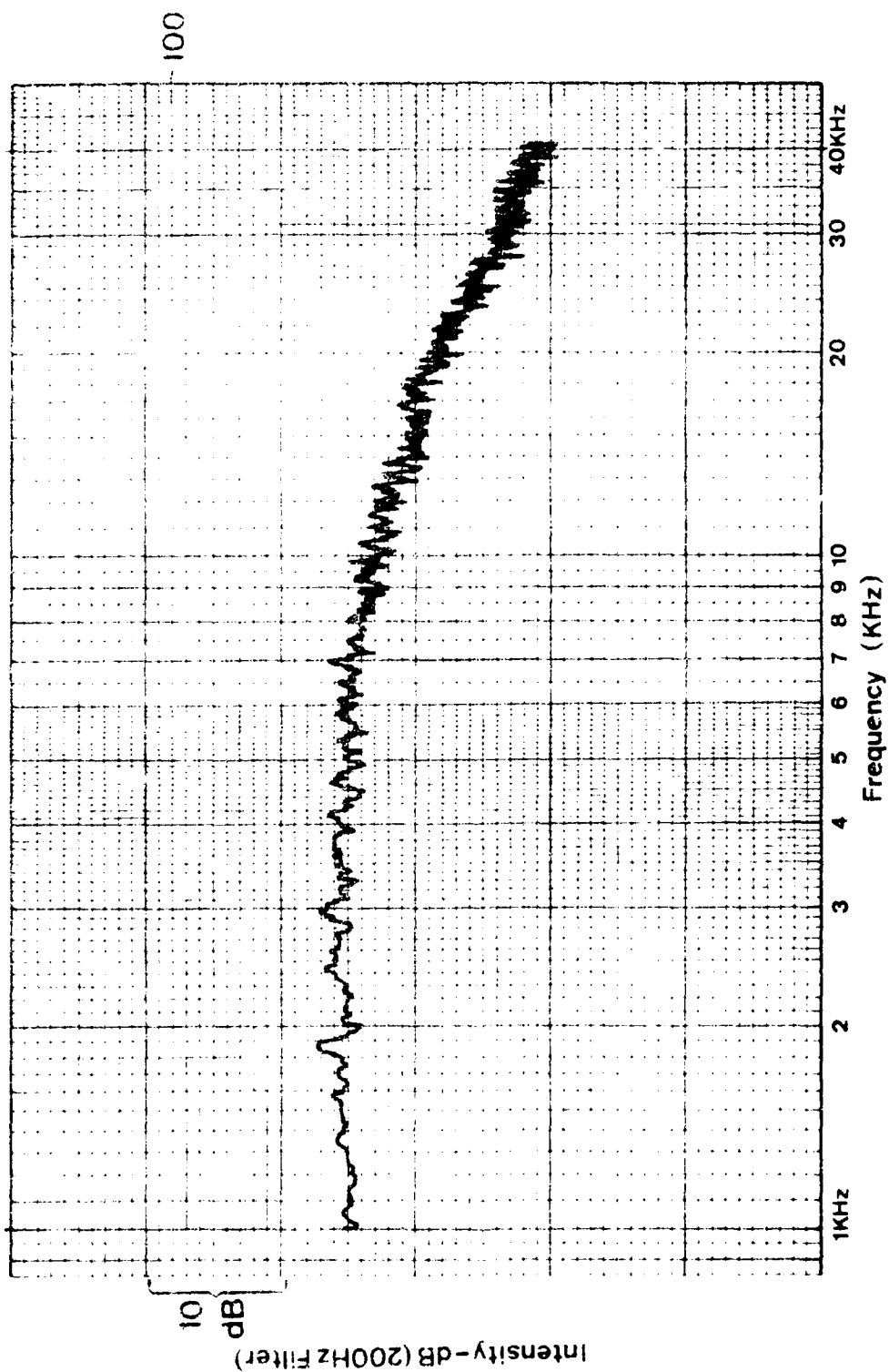
24 568/F/69

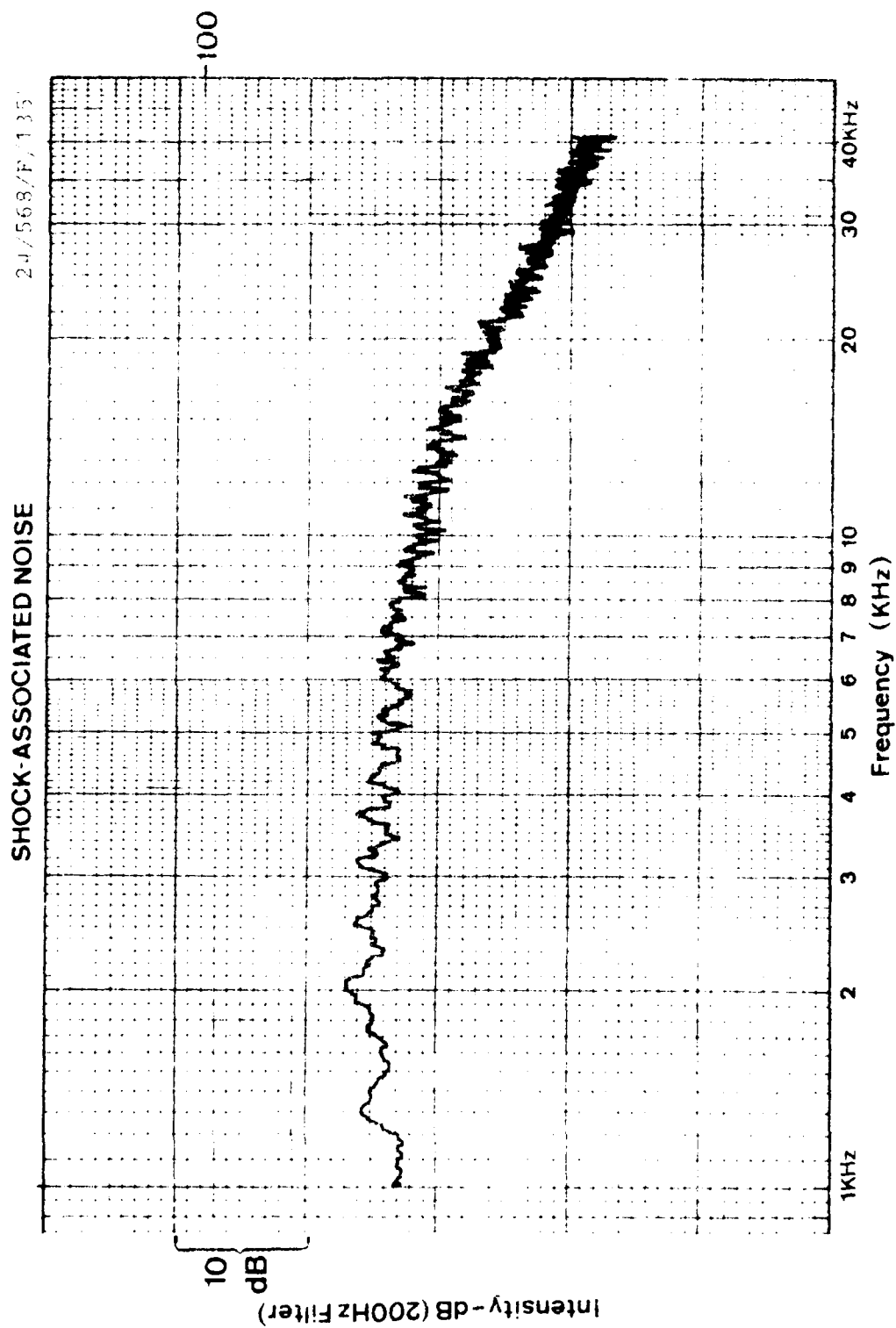




SHOCK ASSOCIATED NOISE

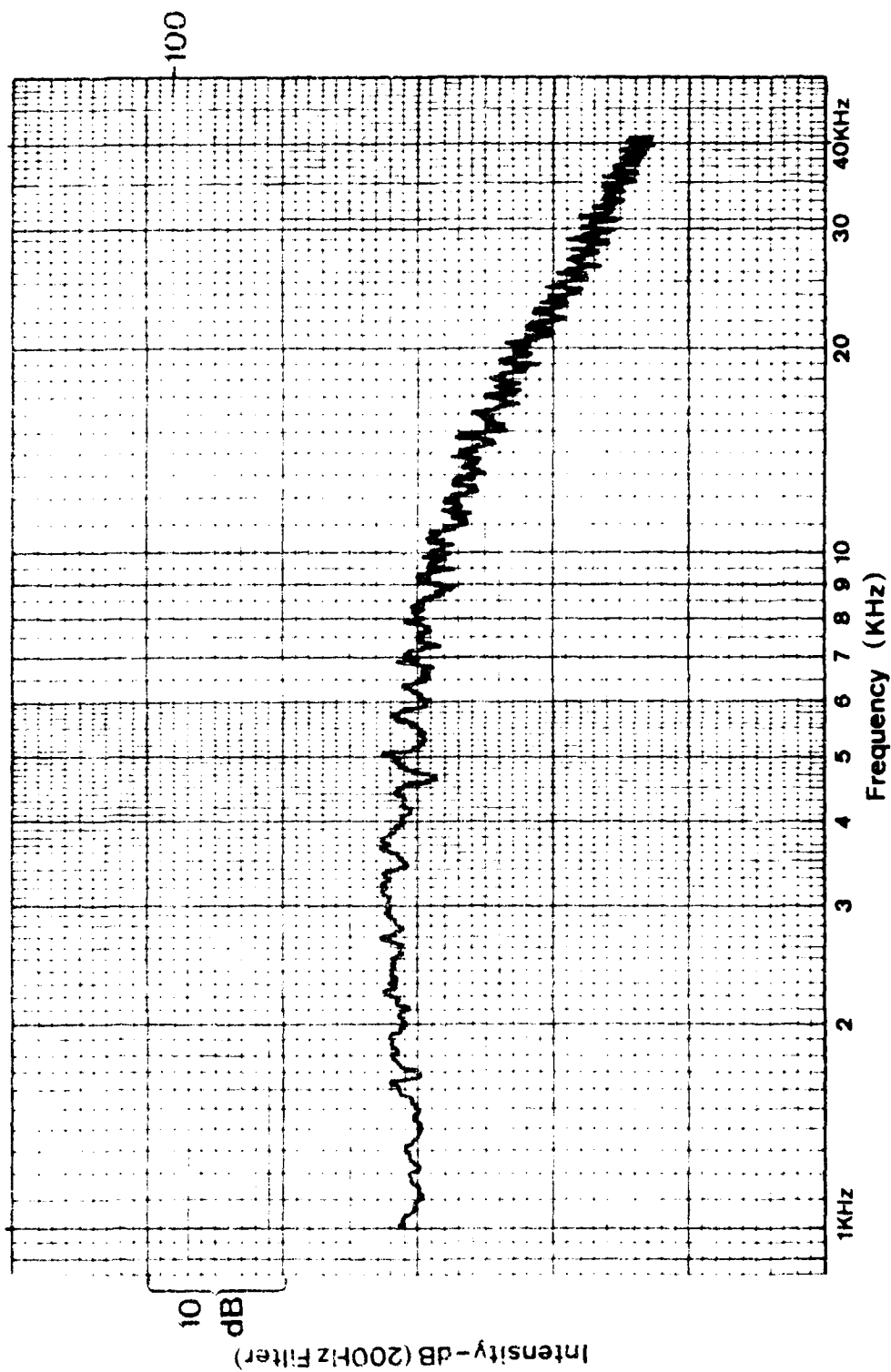
2-1563-77-004

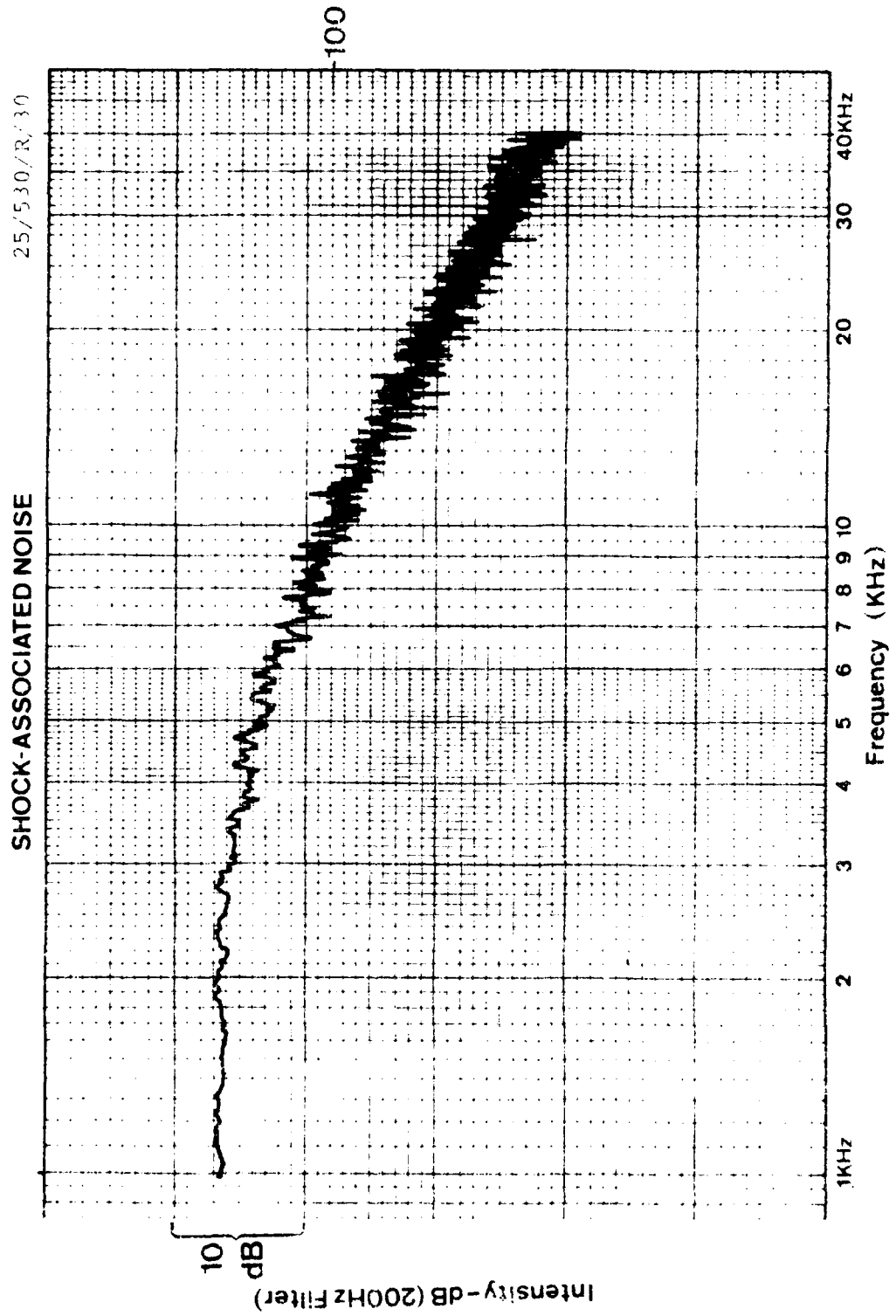


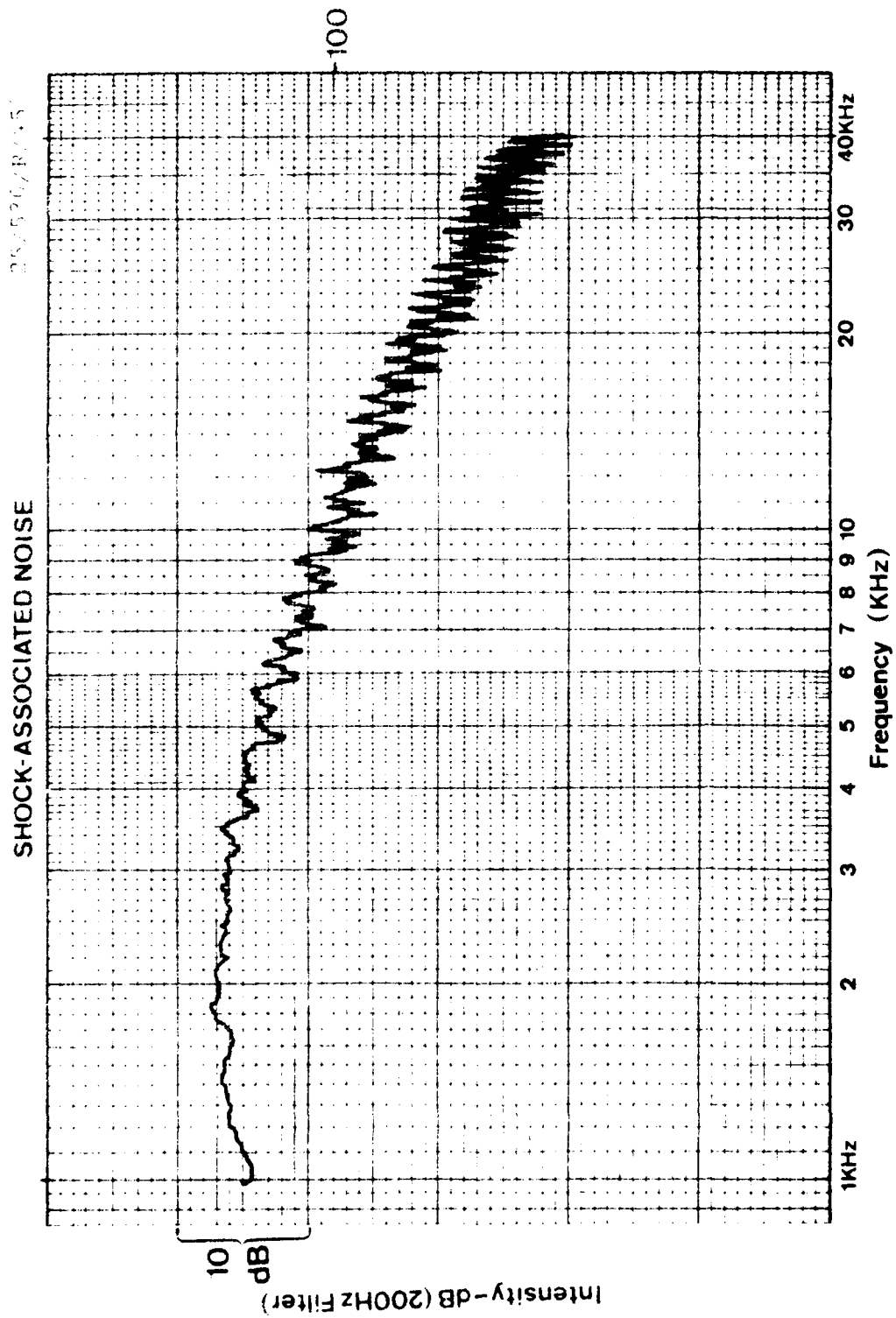


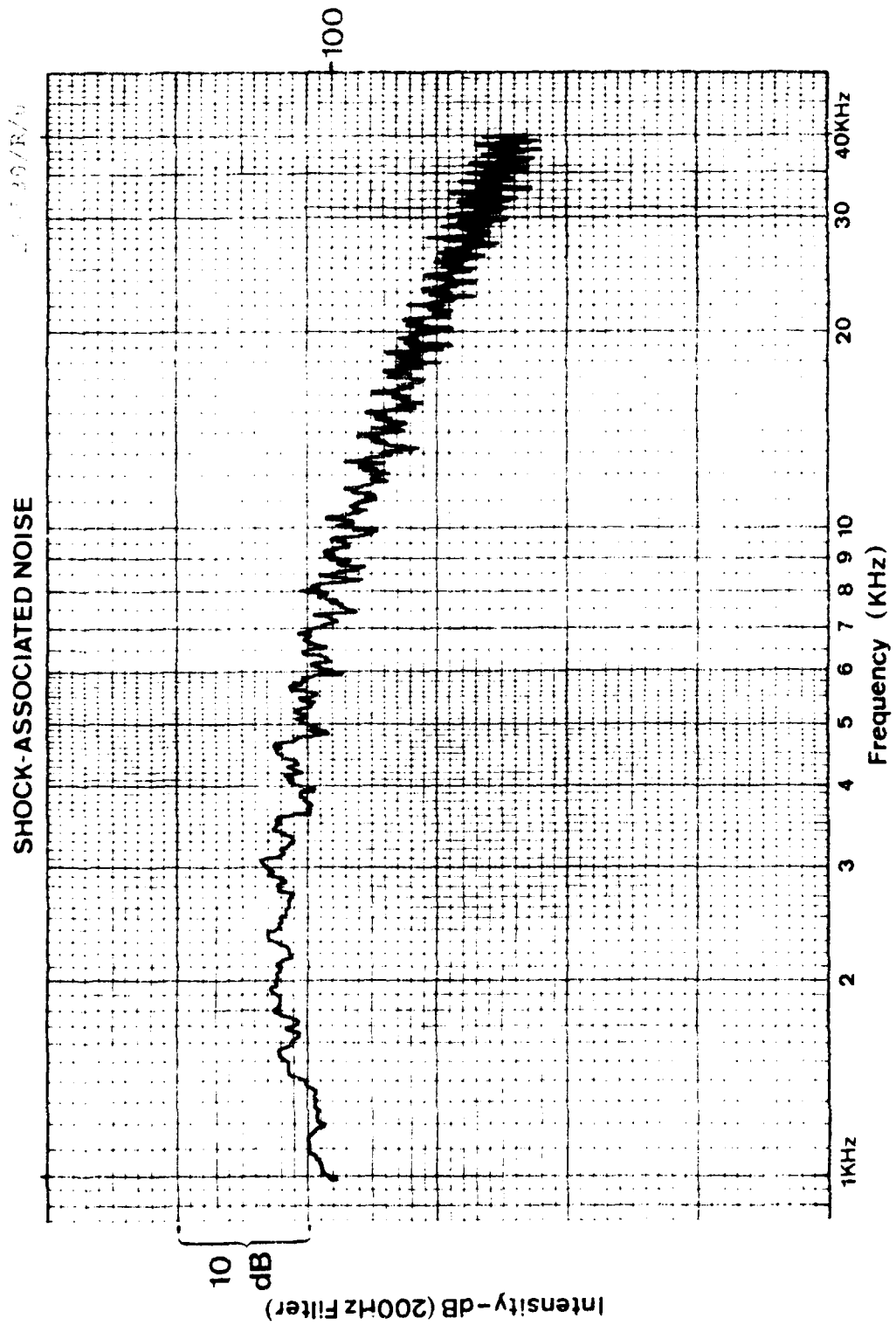
24/568/E-150

SHOCK-ASSOCIATED NOISE



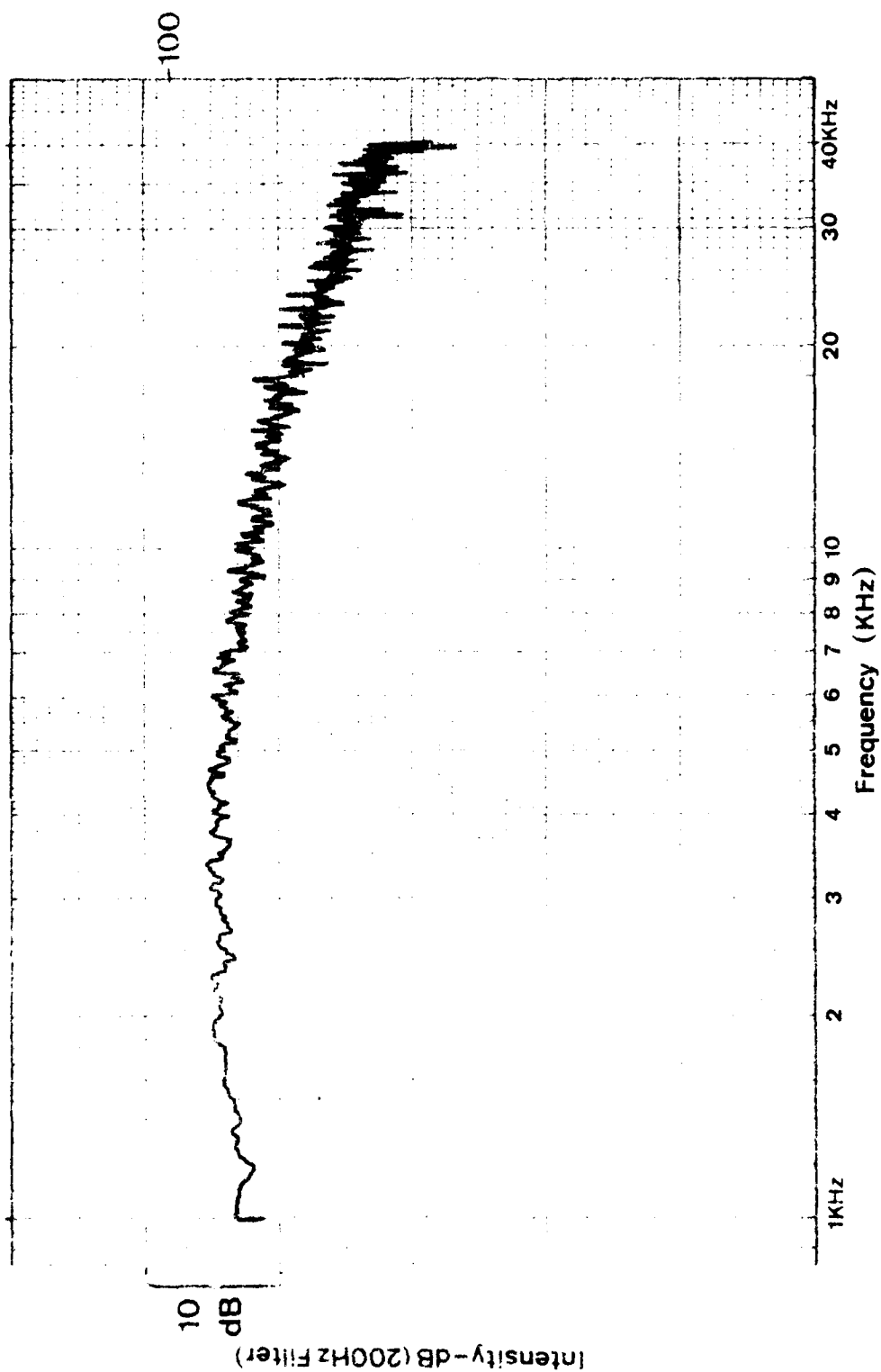


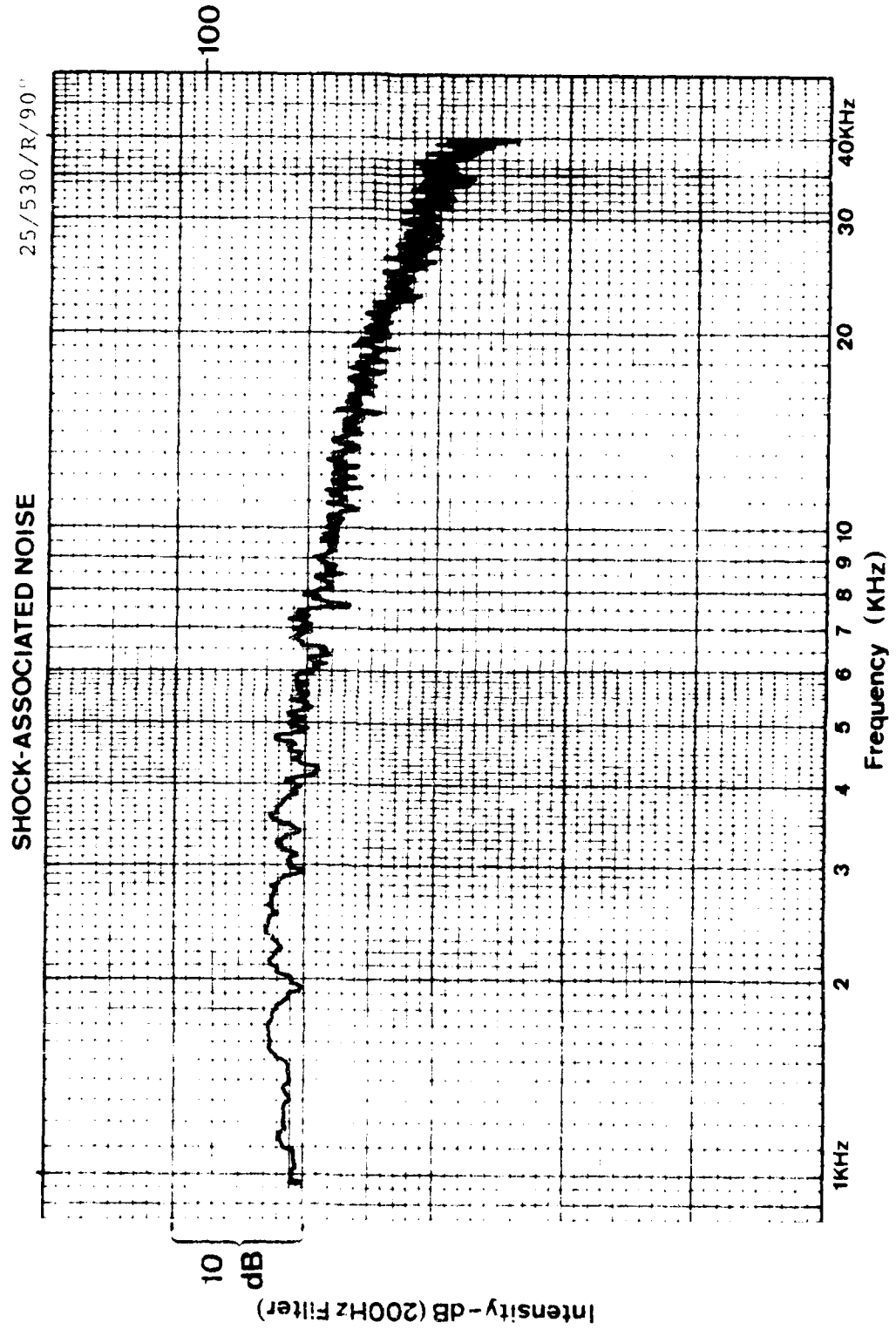


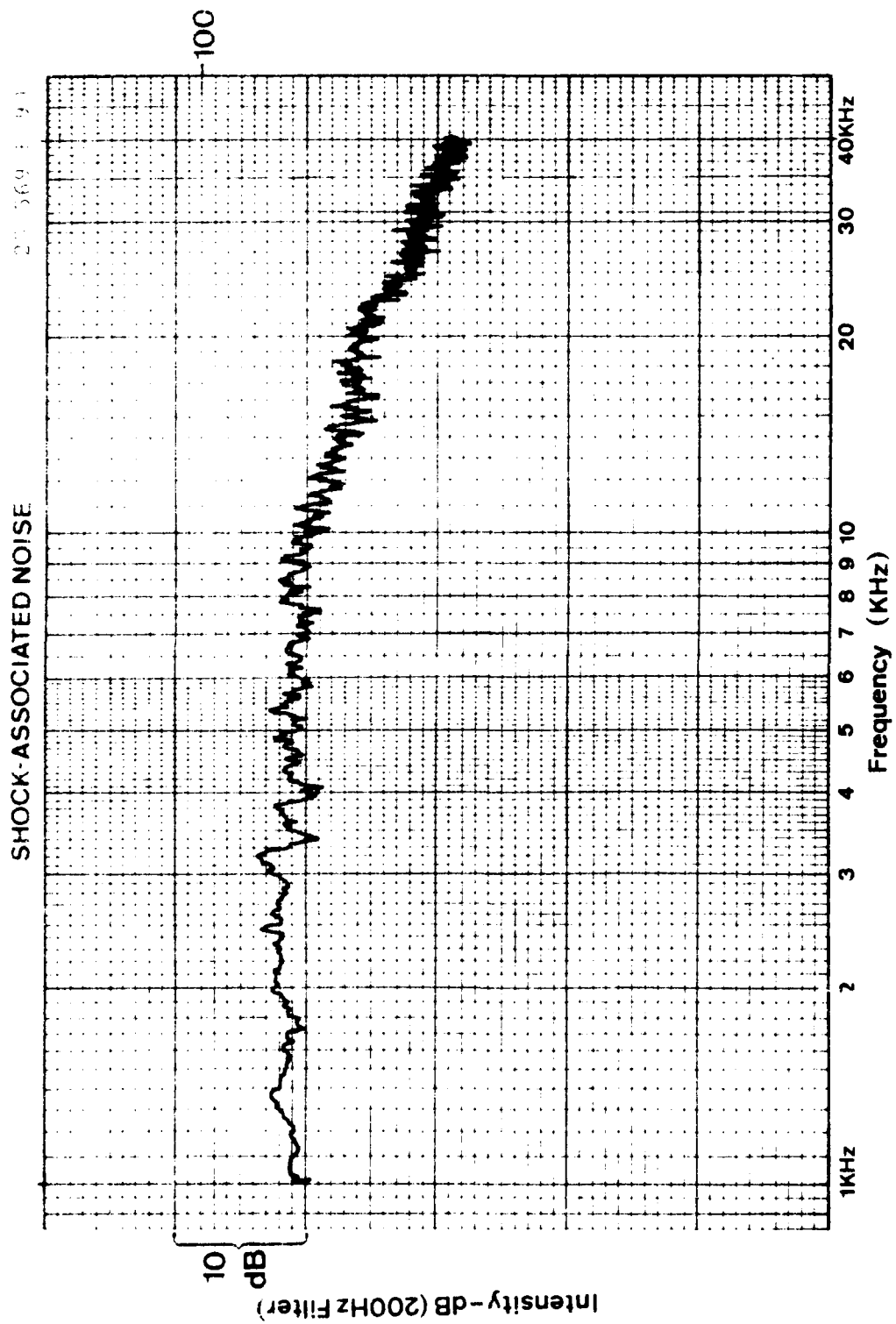


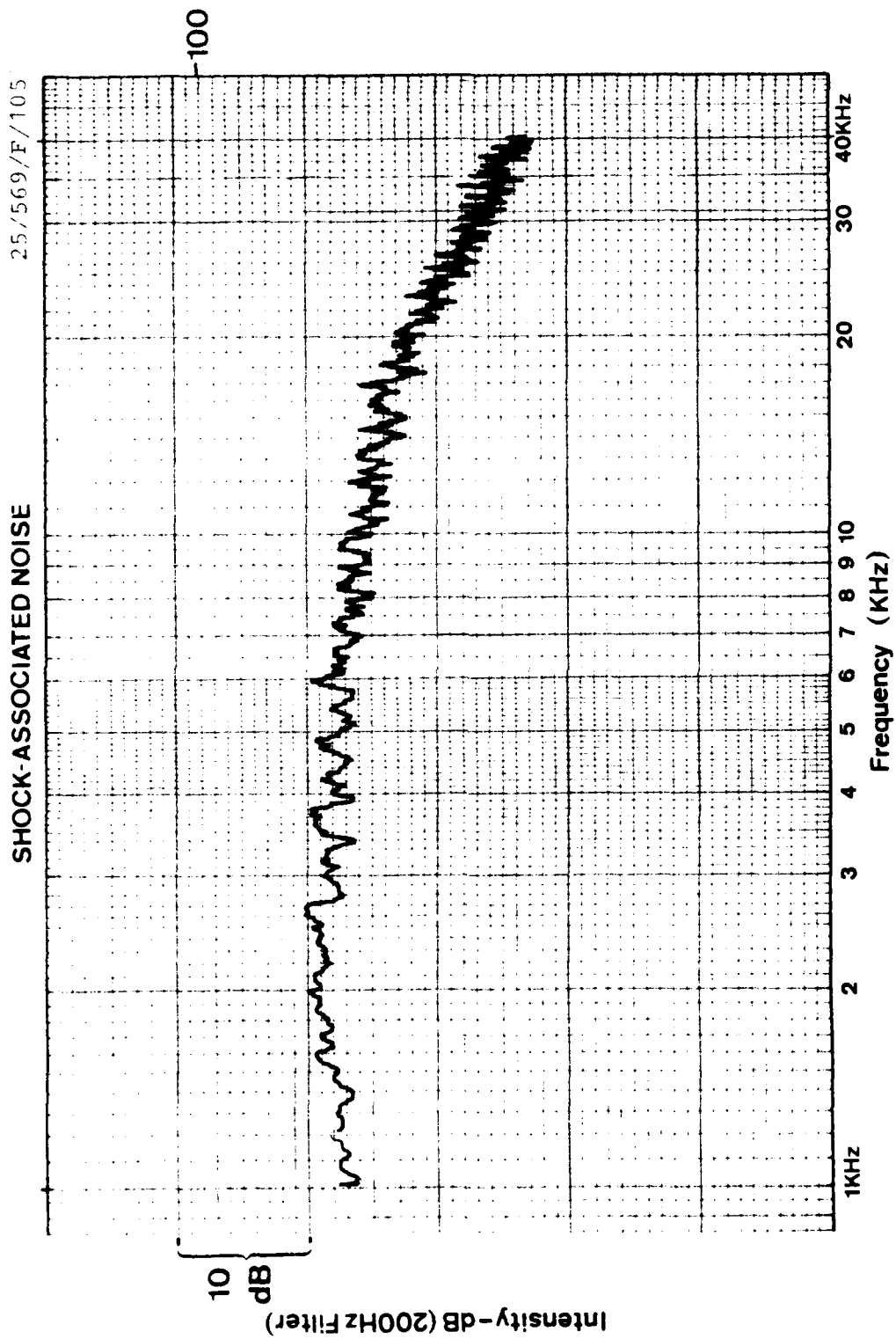
SHOCK-ASSOCIATED NOISE

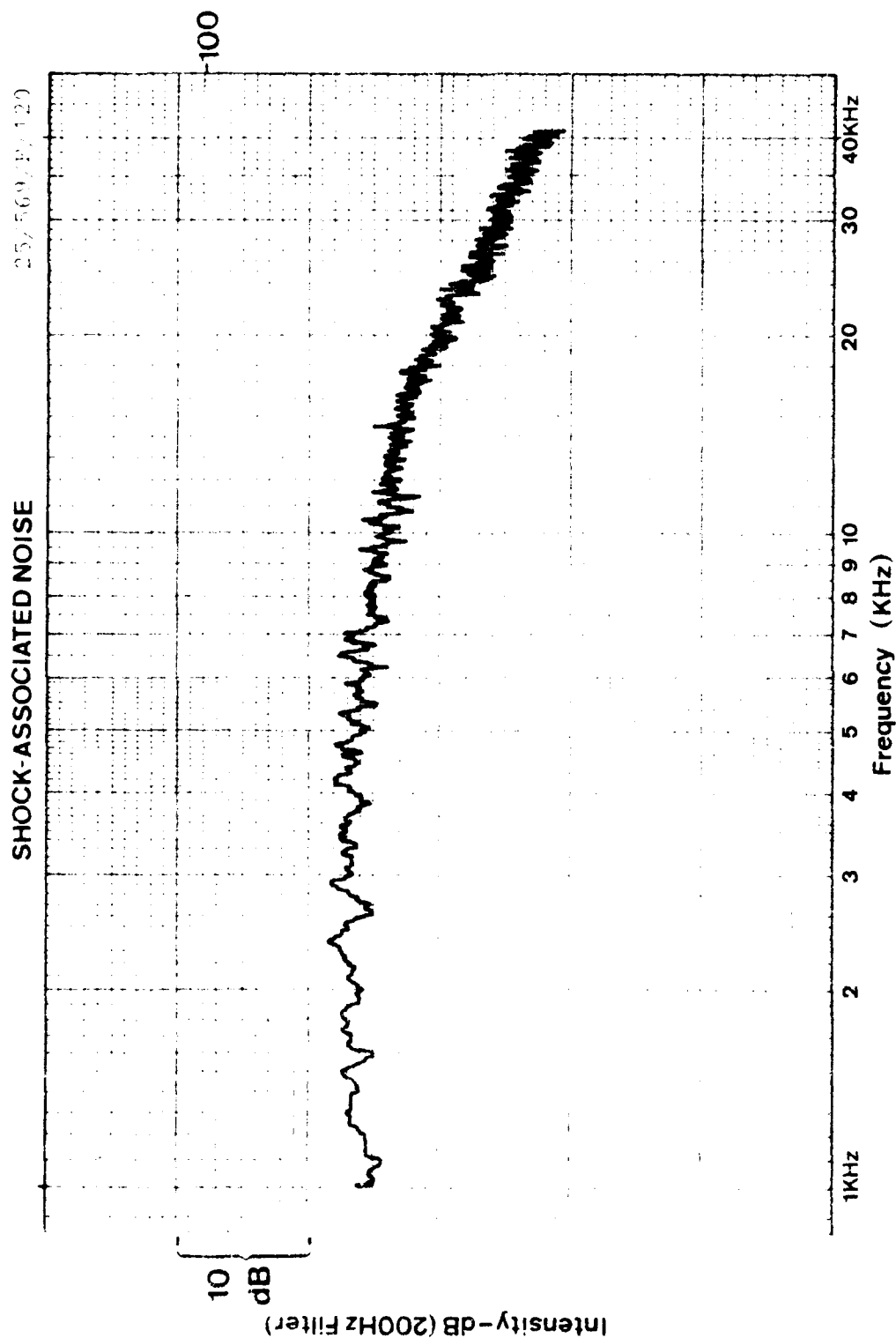
25/520/R/75





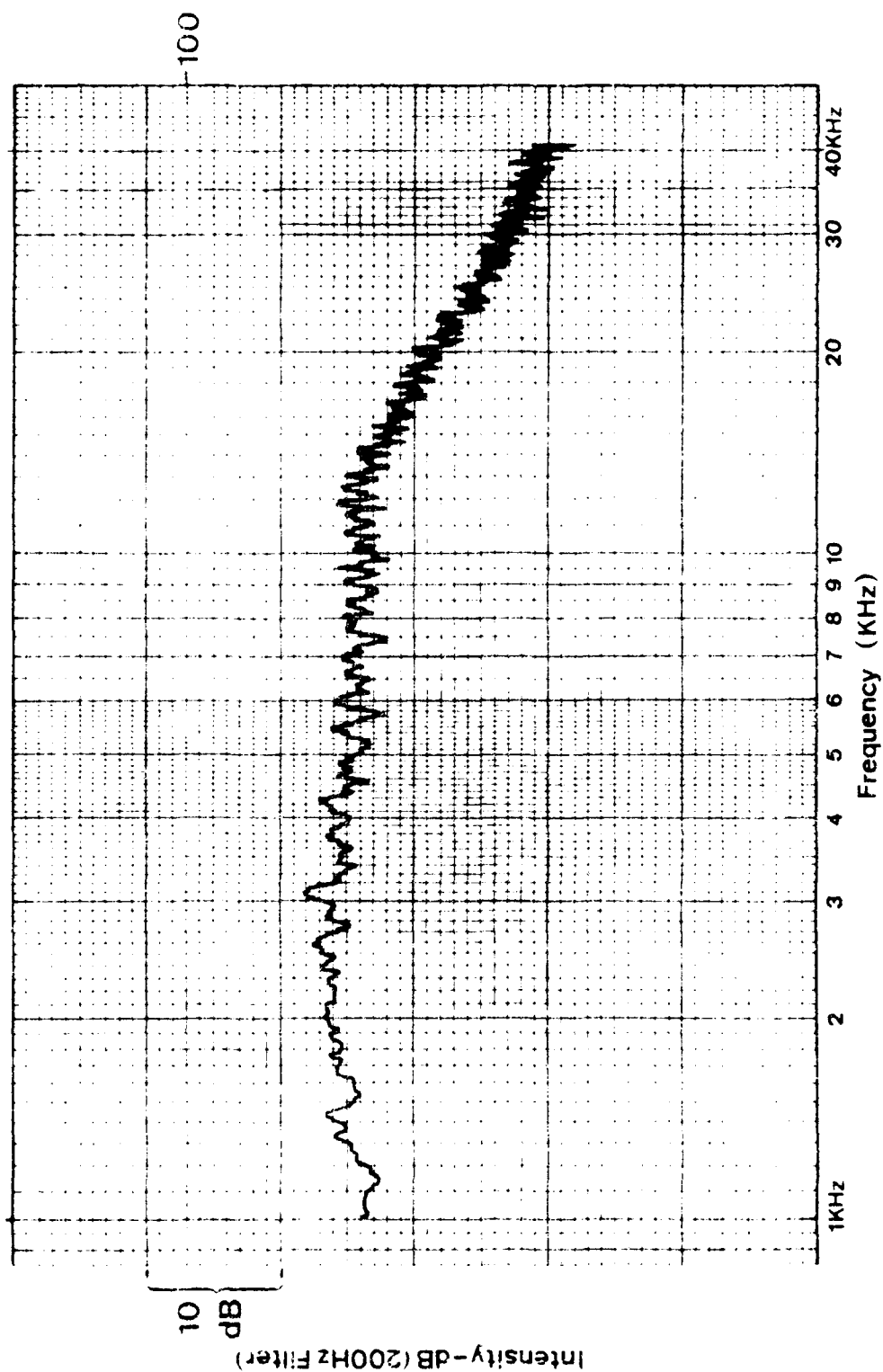


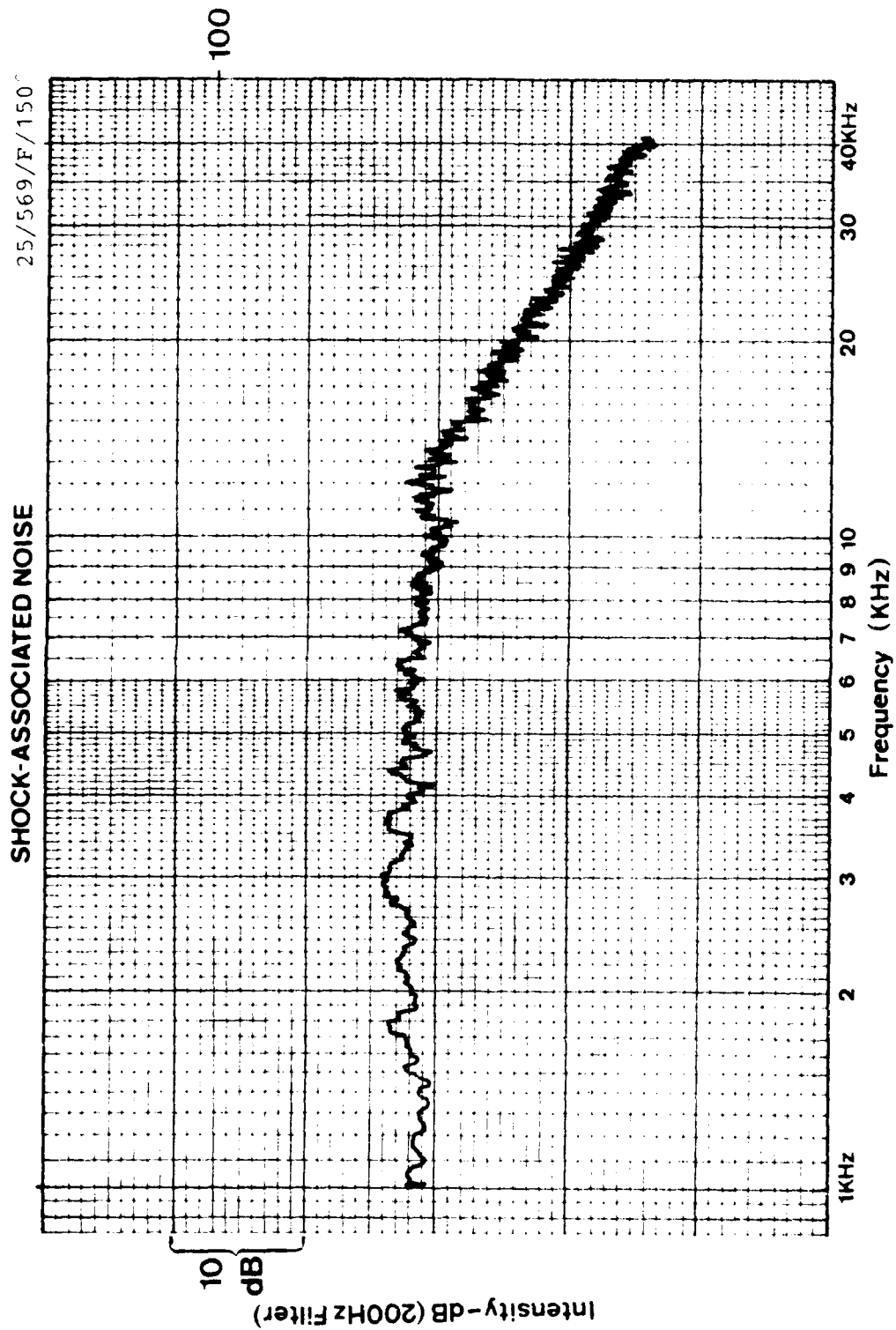




SHOCK-ASSOCIATED NOISE

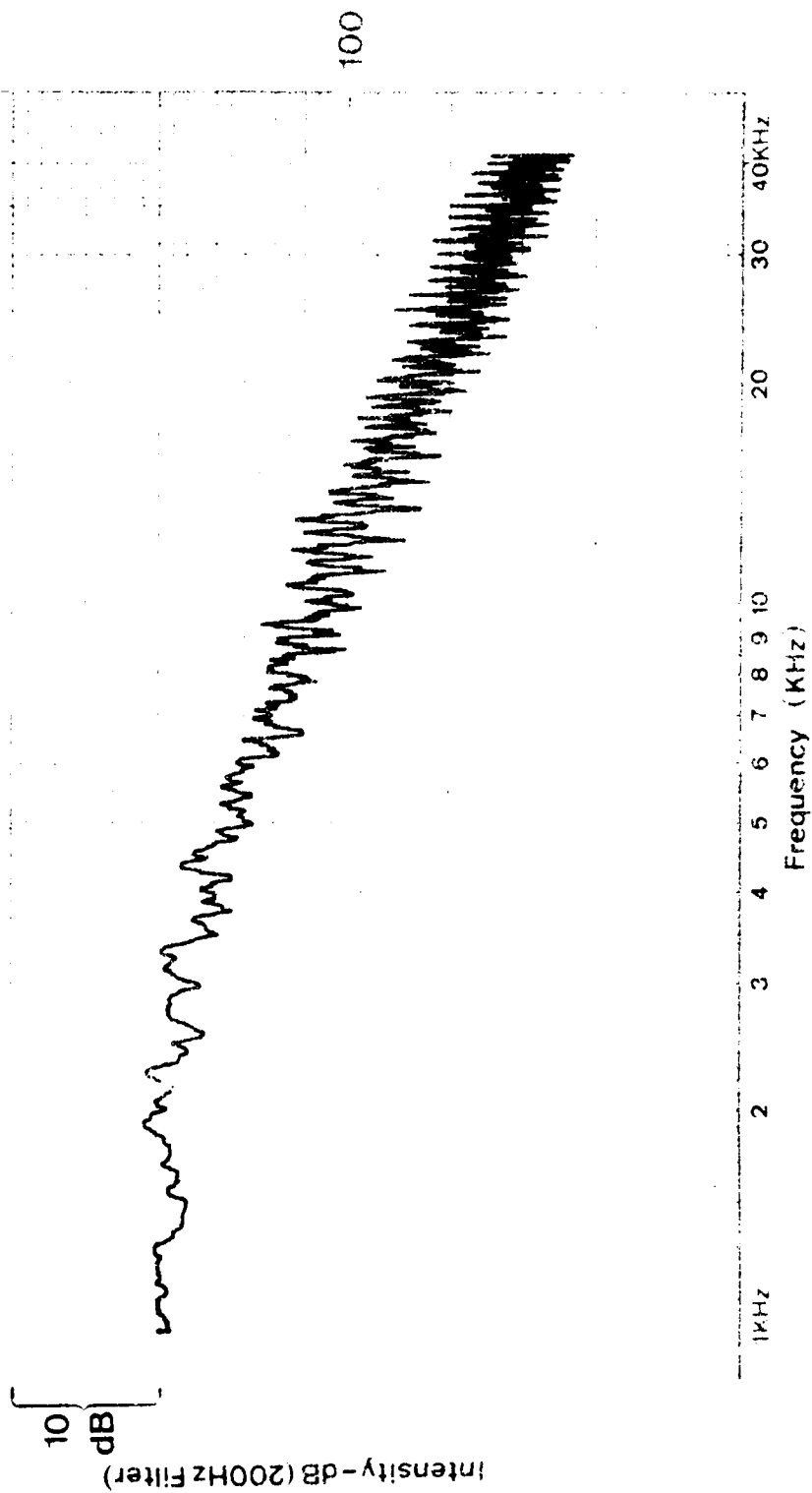
25,000/P-113





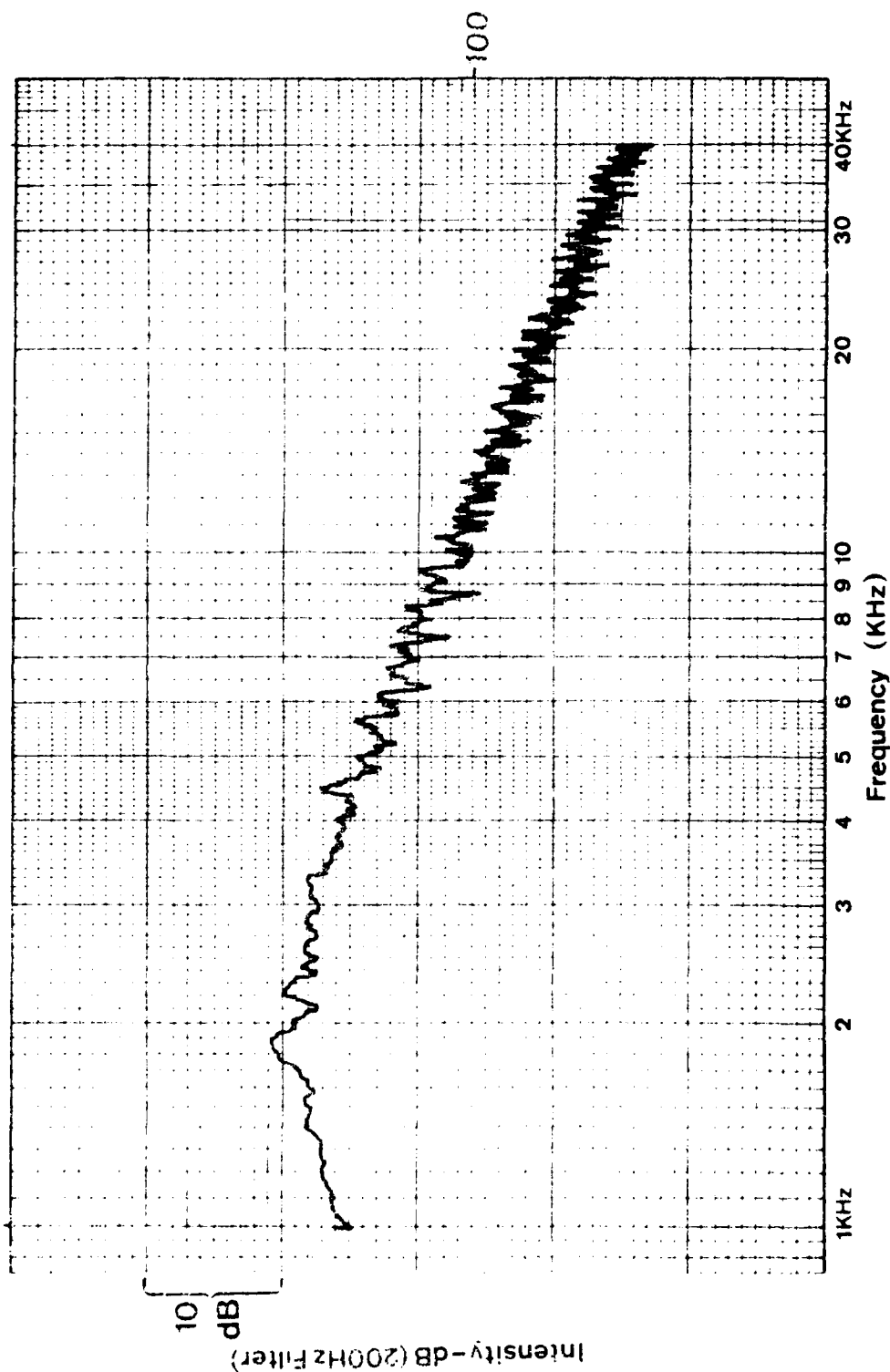
SHOCK-ASSOCIATED NOISE

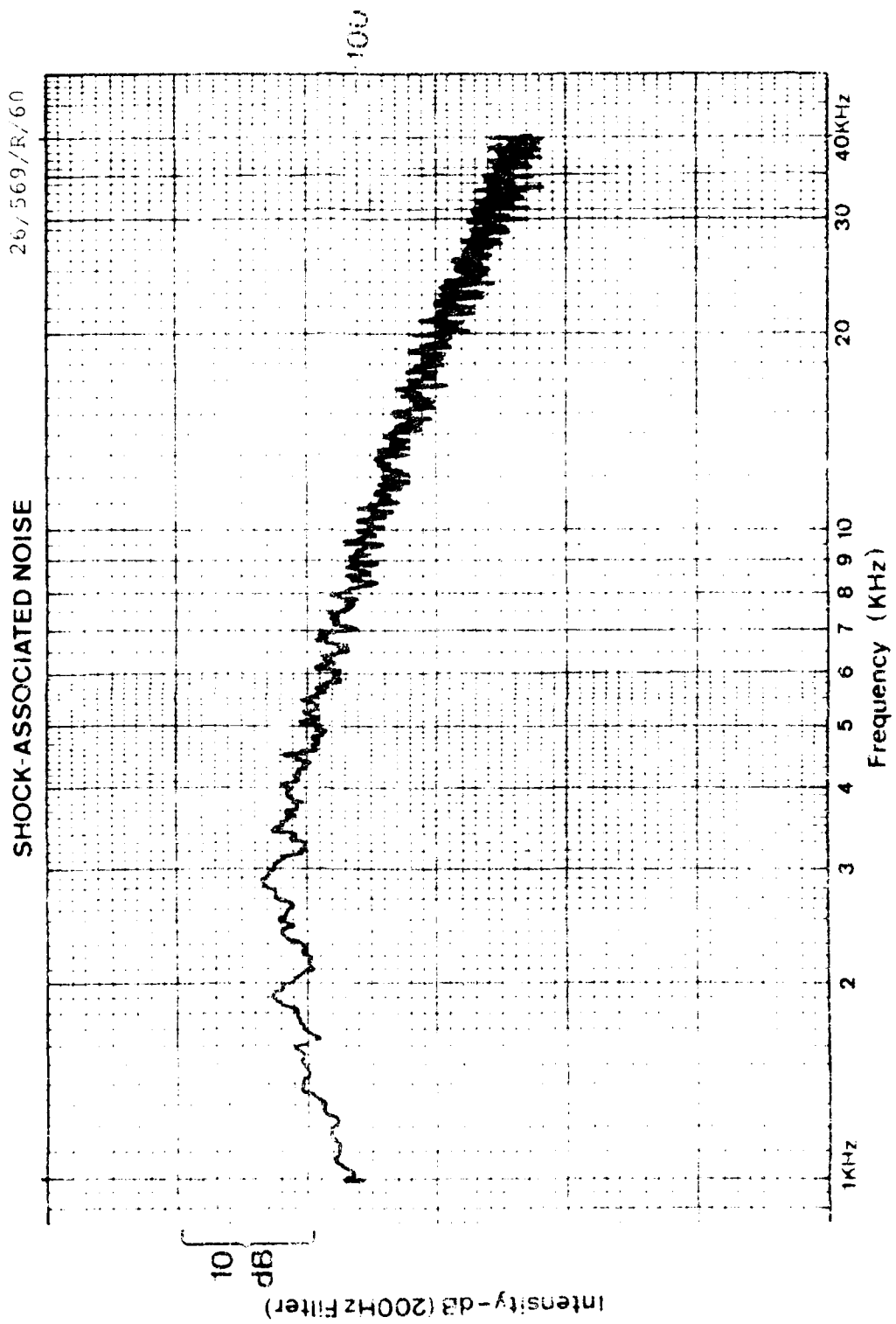
26/529/R/30

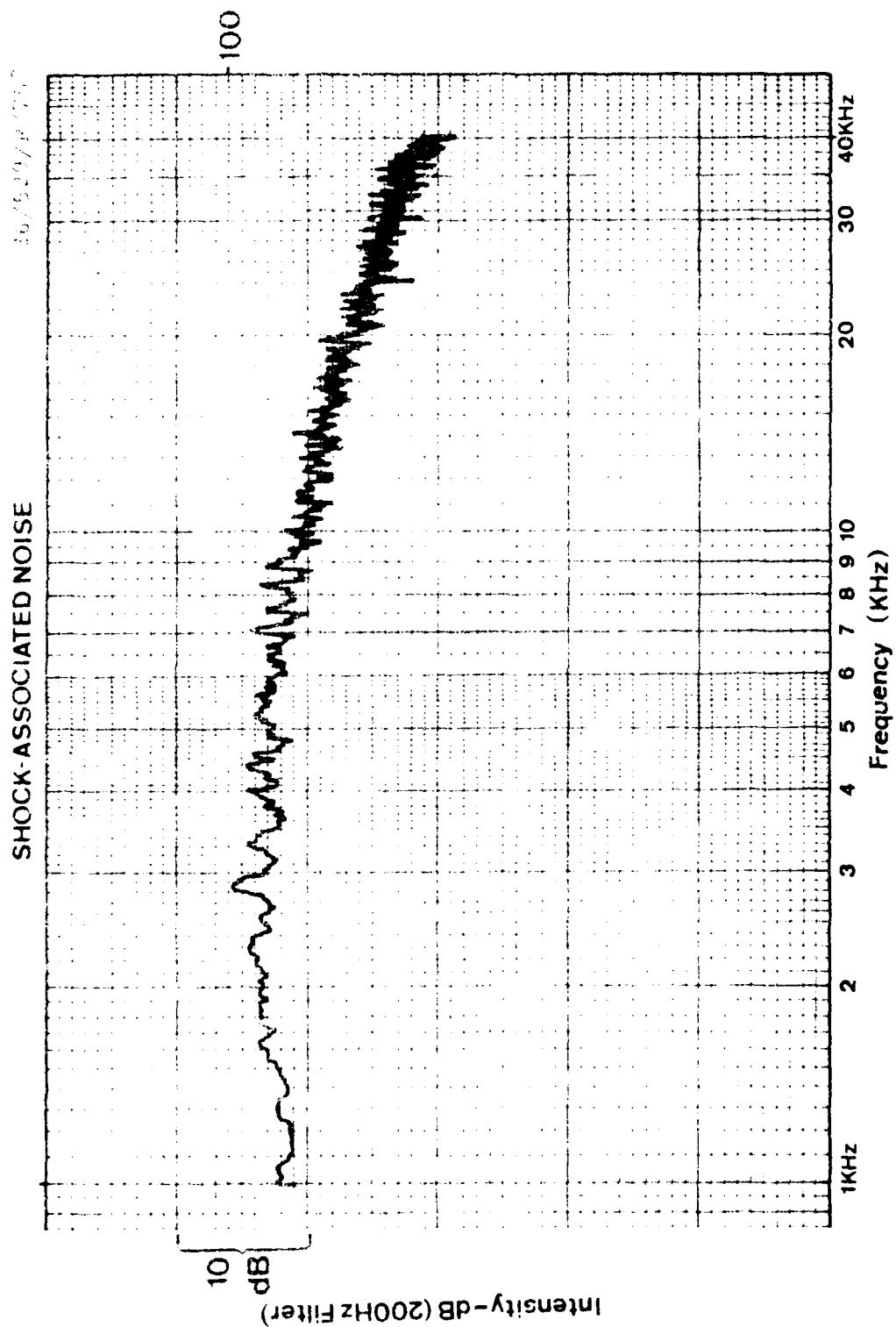


SHOCK-ASSOCIATED NOISE

26/529/R/45

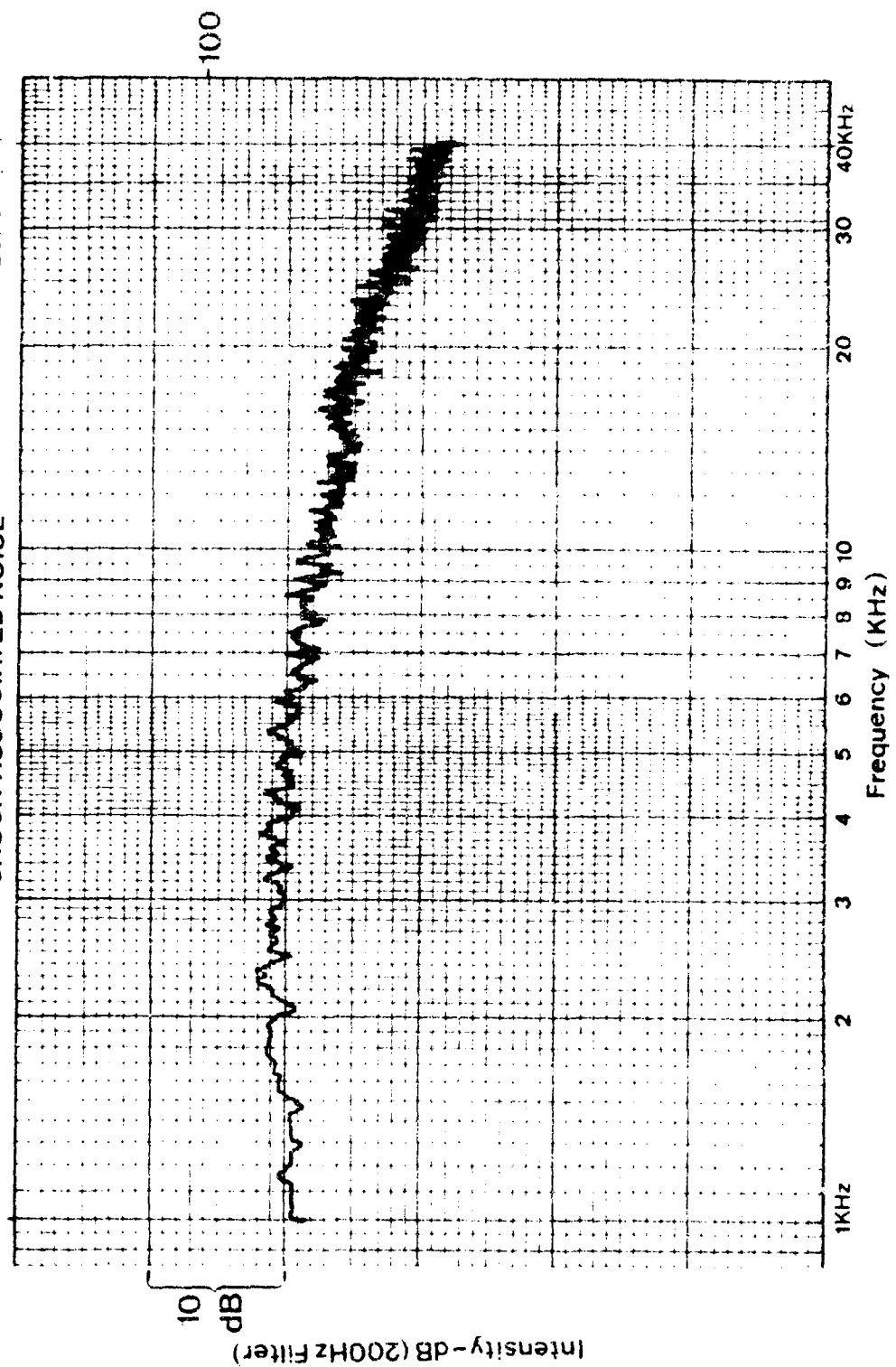






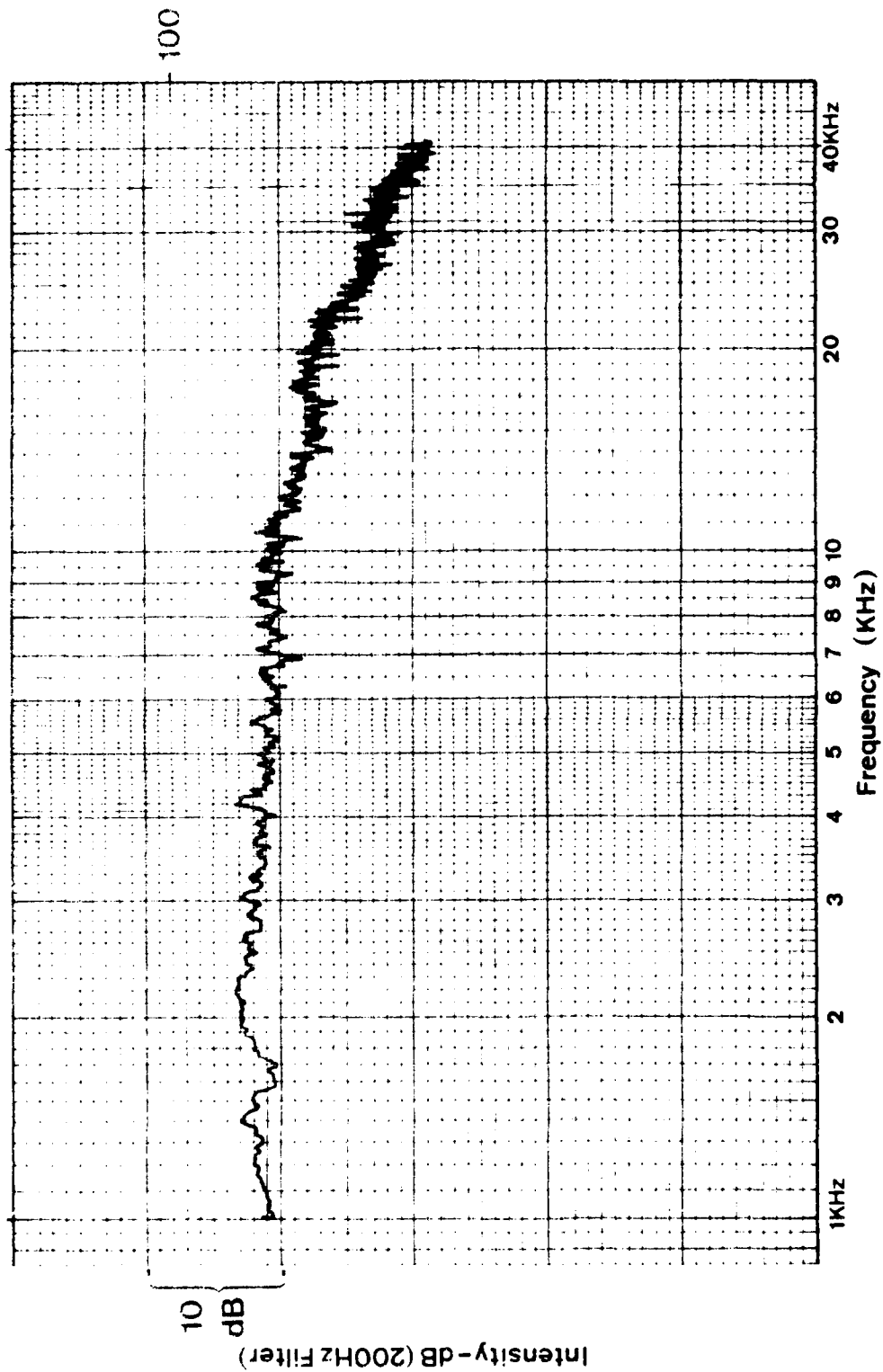
SHOCK-ASSOCIATED NOISE

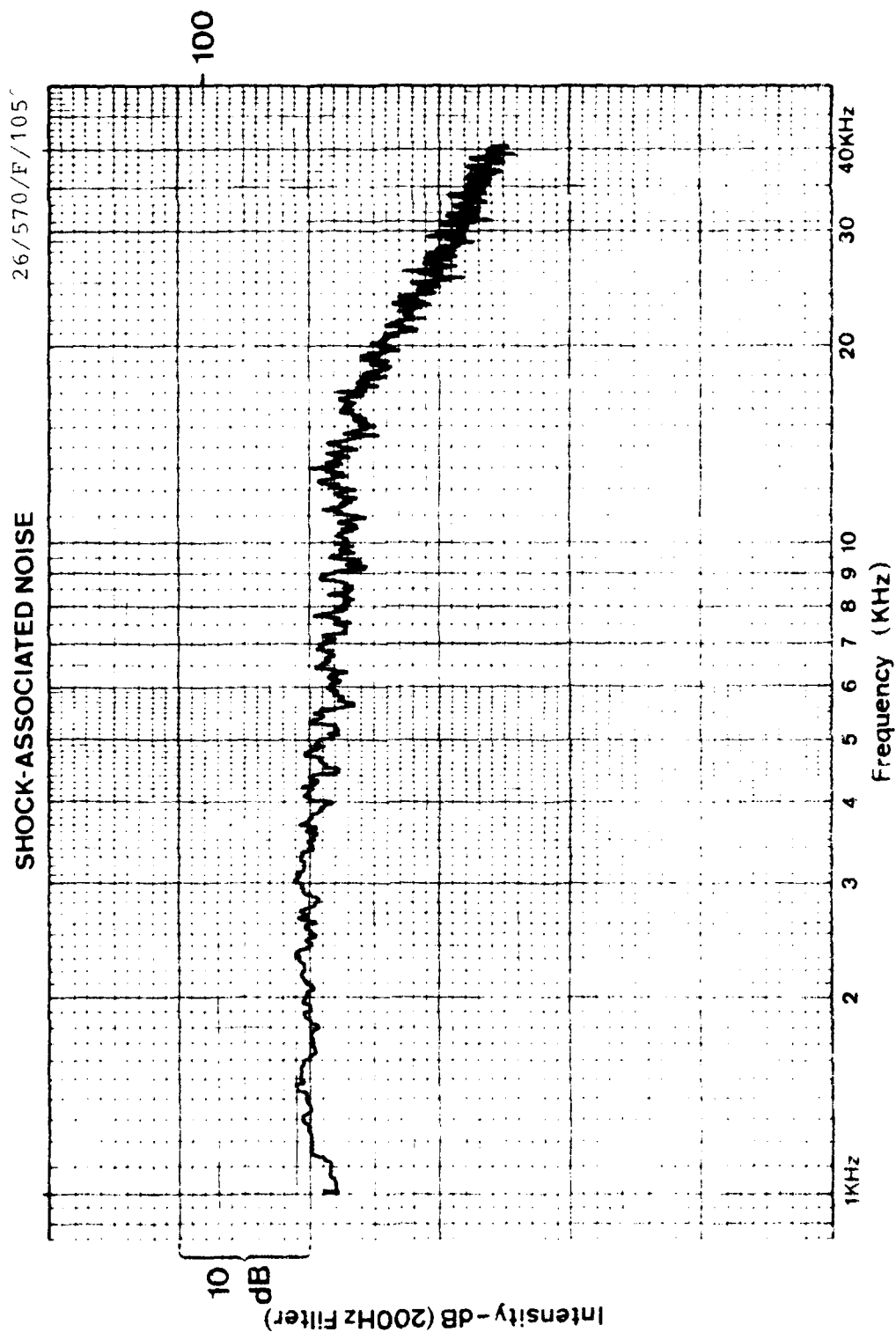
26/529/R/90



SHOCK-ASSOCIATED NOISE

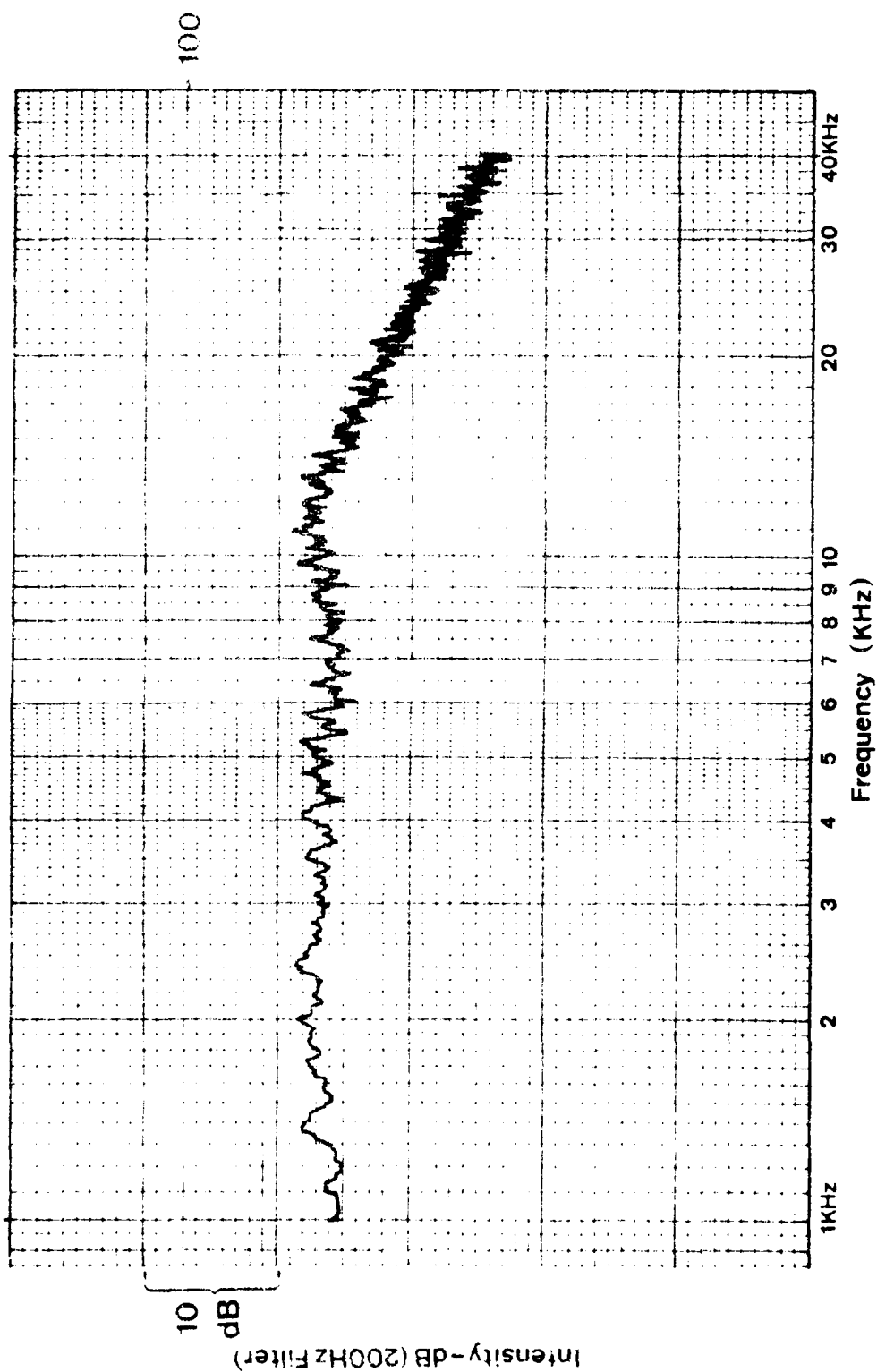
26/570/P-91





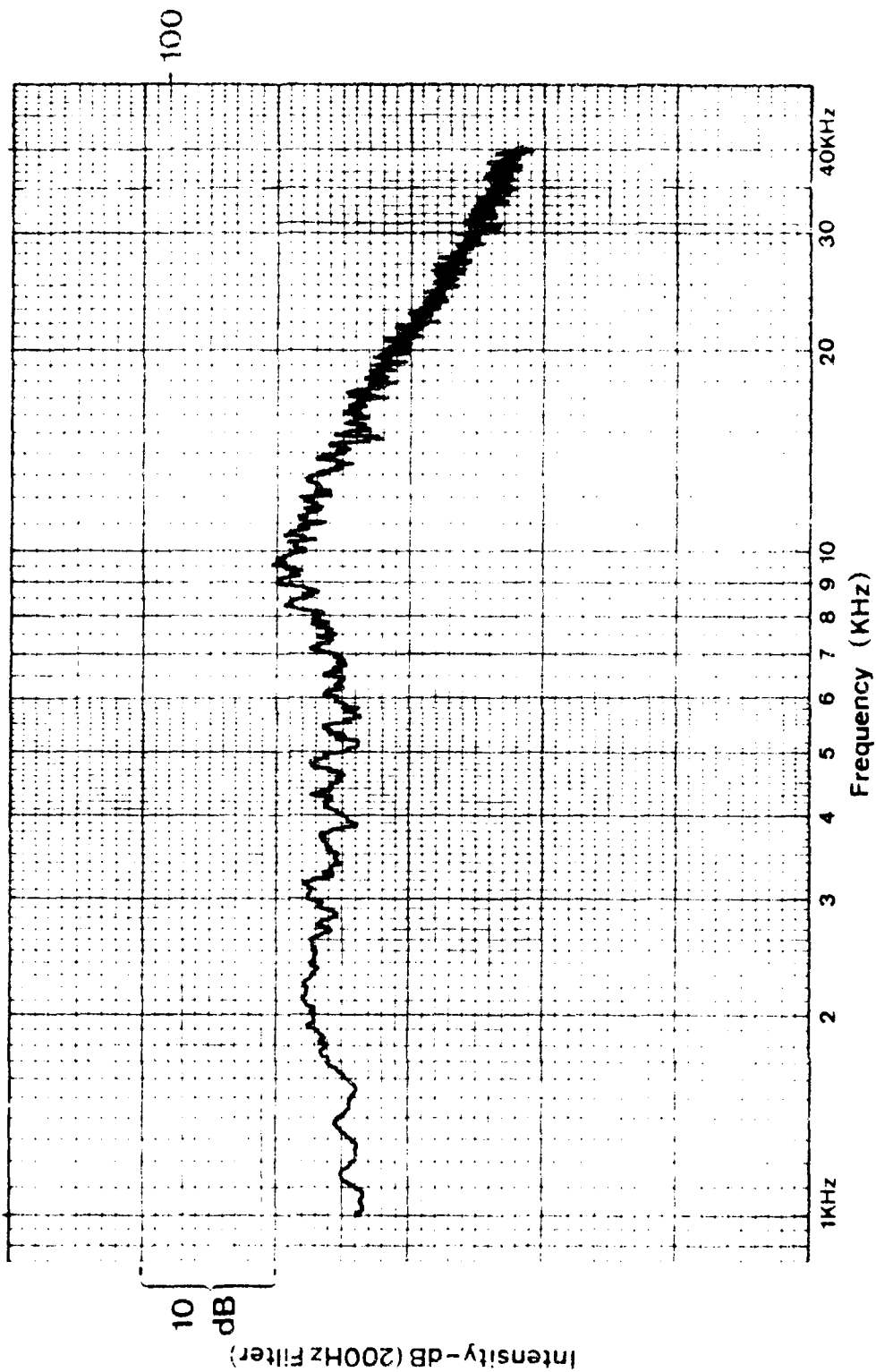
SHOCK-ASSOCIATED NOISE

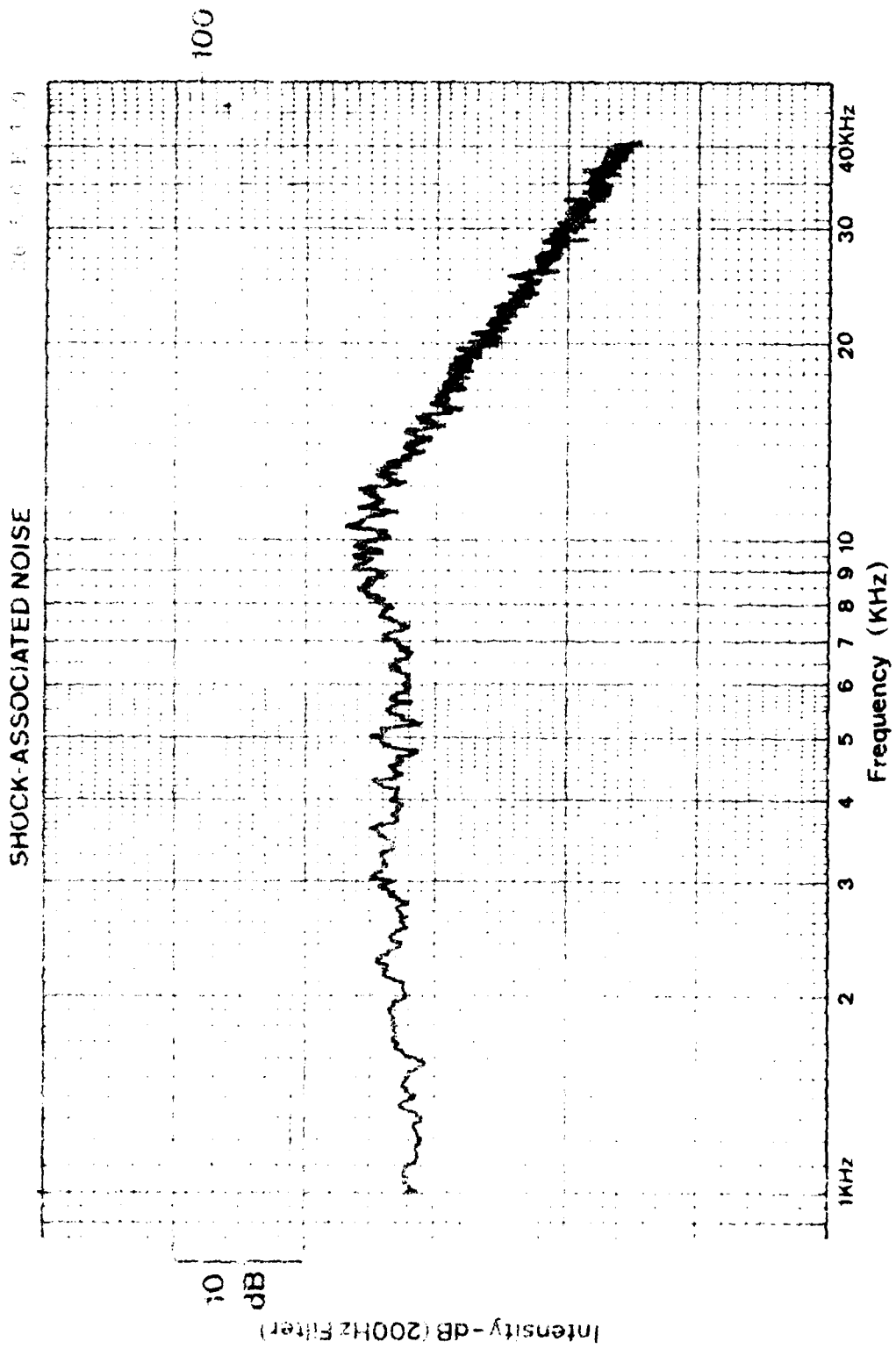
20 57 1.4 120



SHOCK-ASSOCIATED NOISE

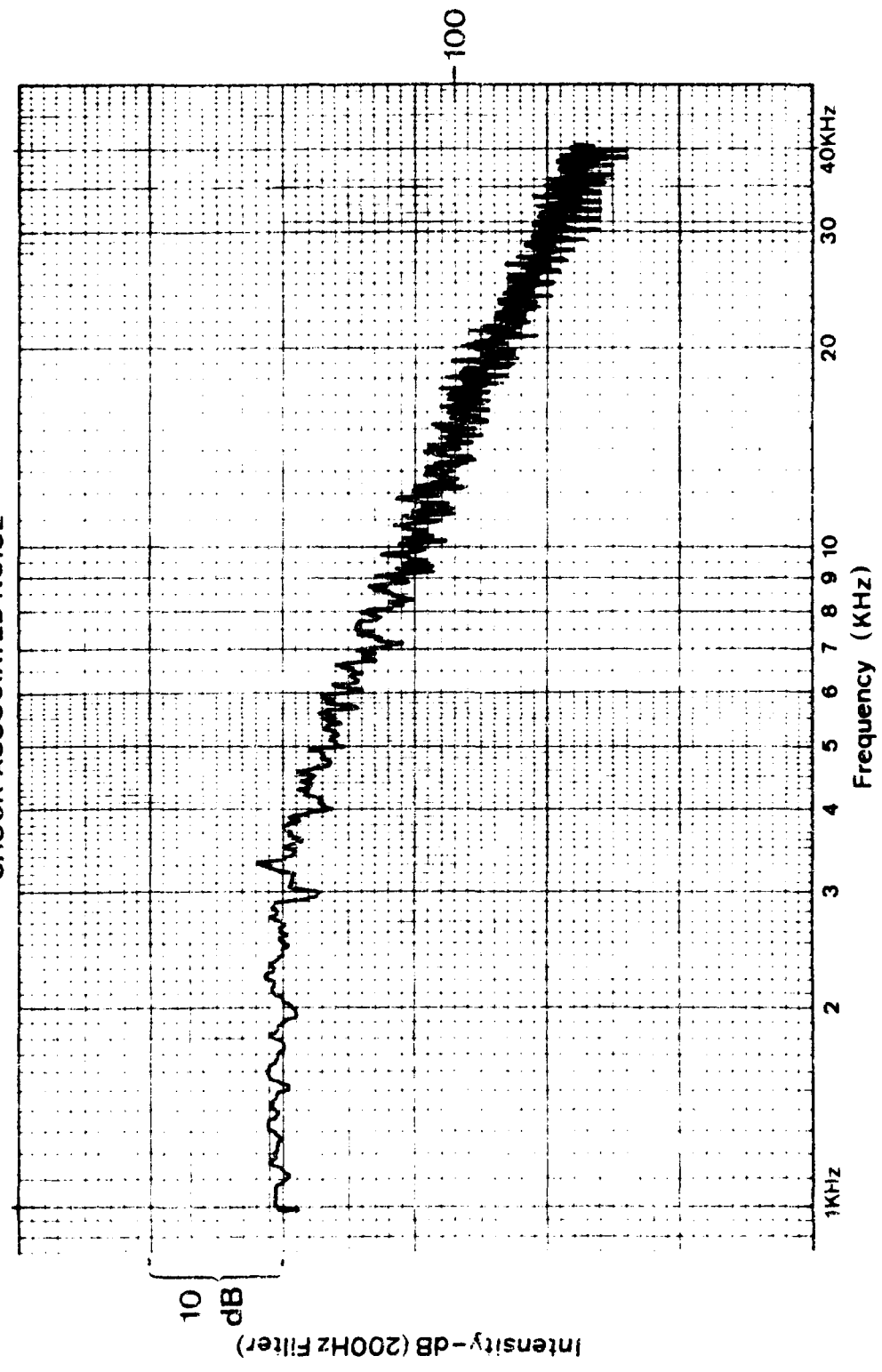
26/570/P/135



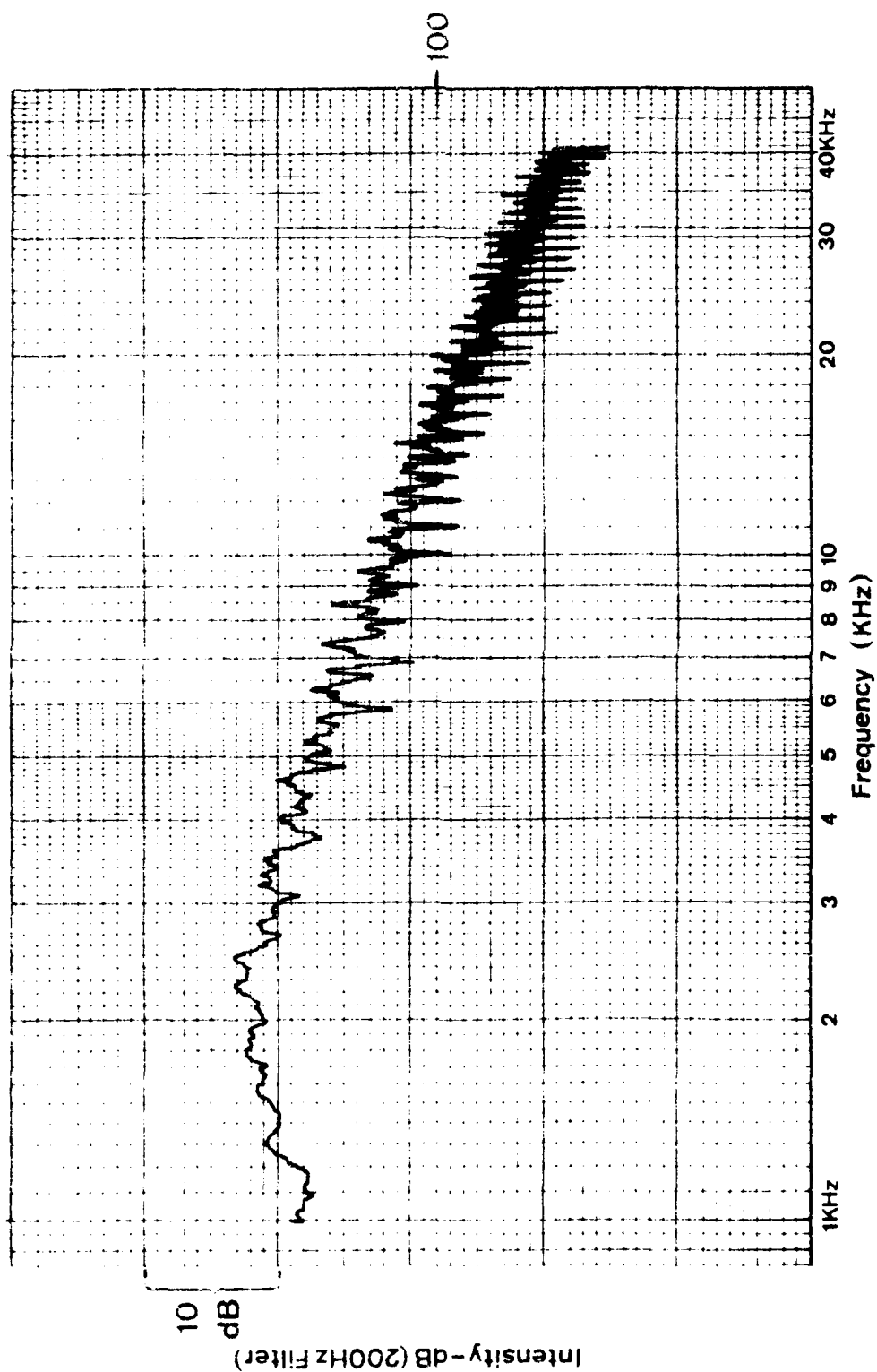


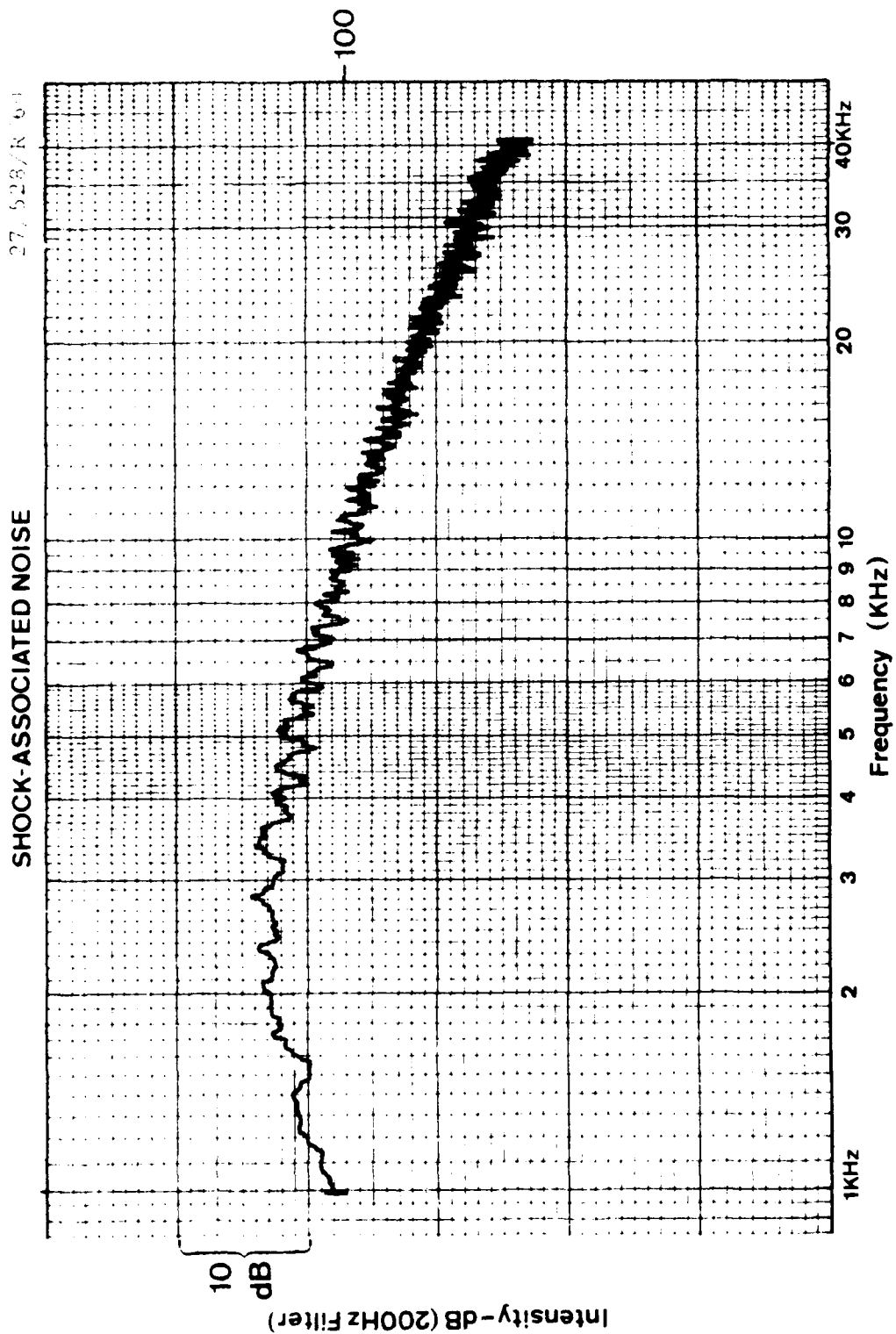
27/528/R/30

SHOCK-ASSOCIATED NOISE

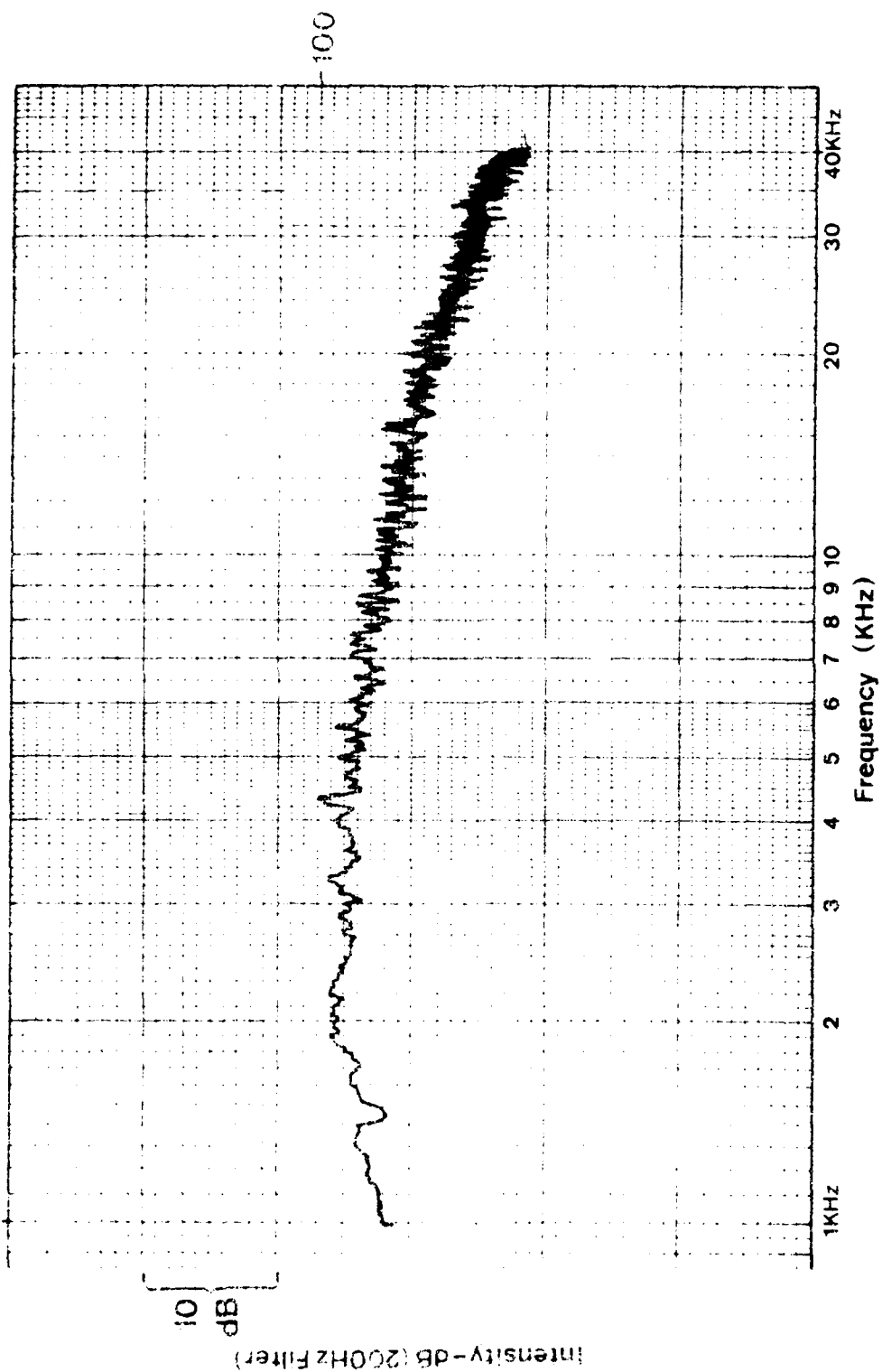


SHOCK-ASSOCIATED NOISE



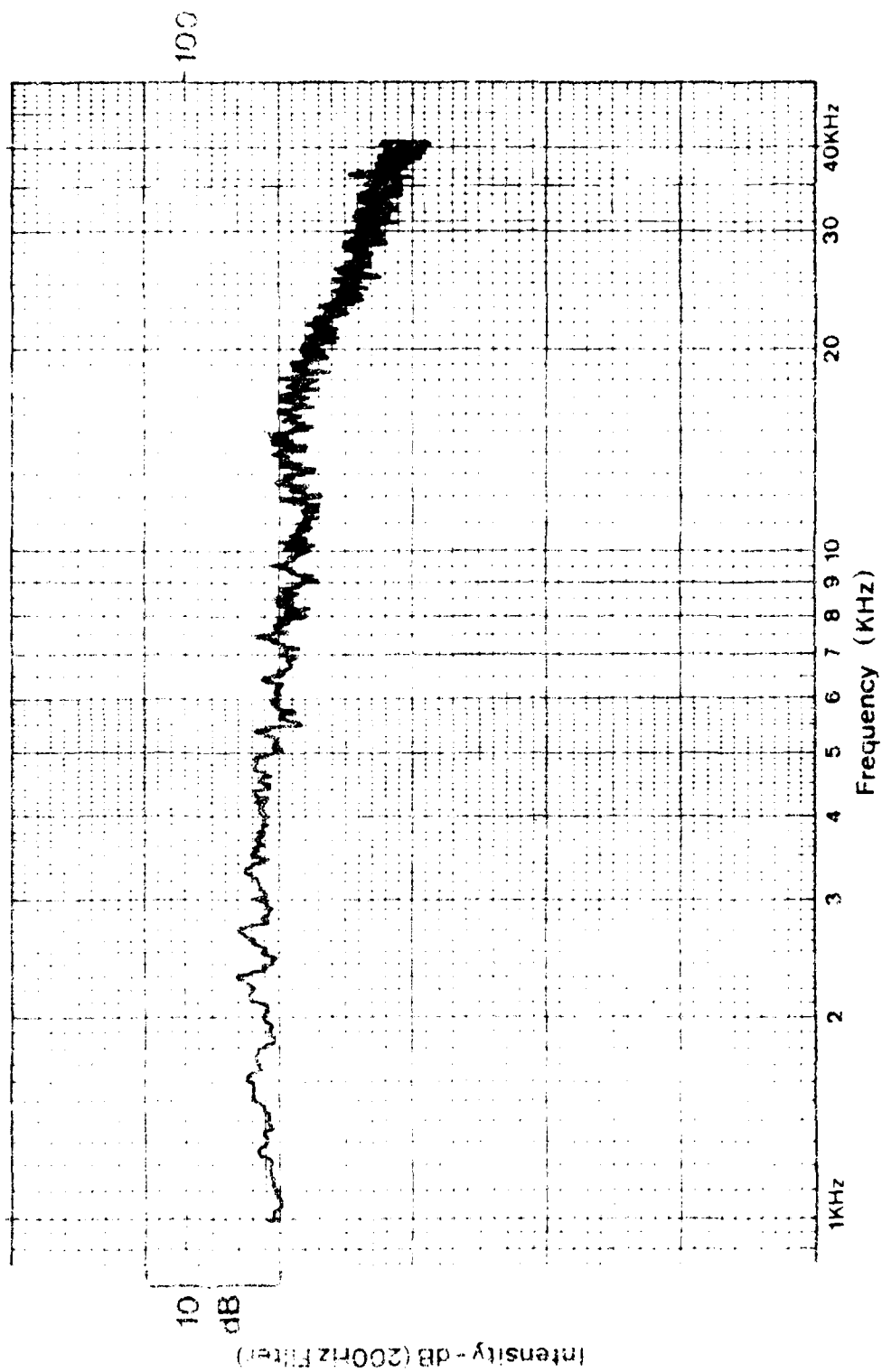


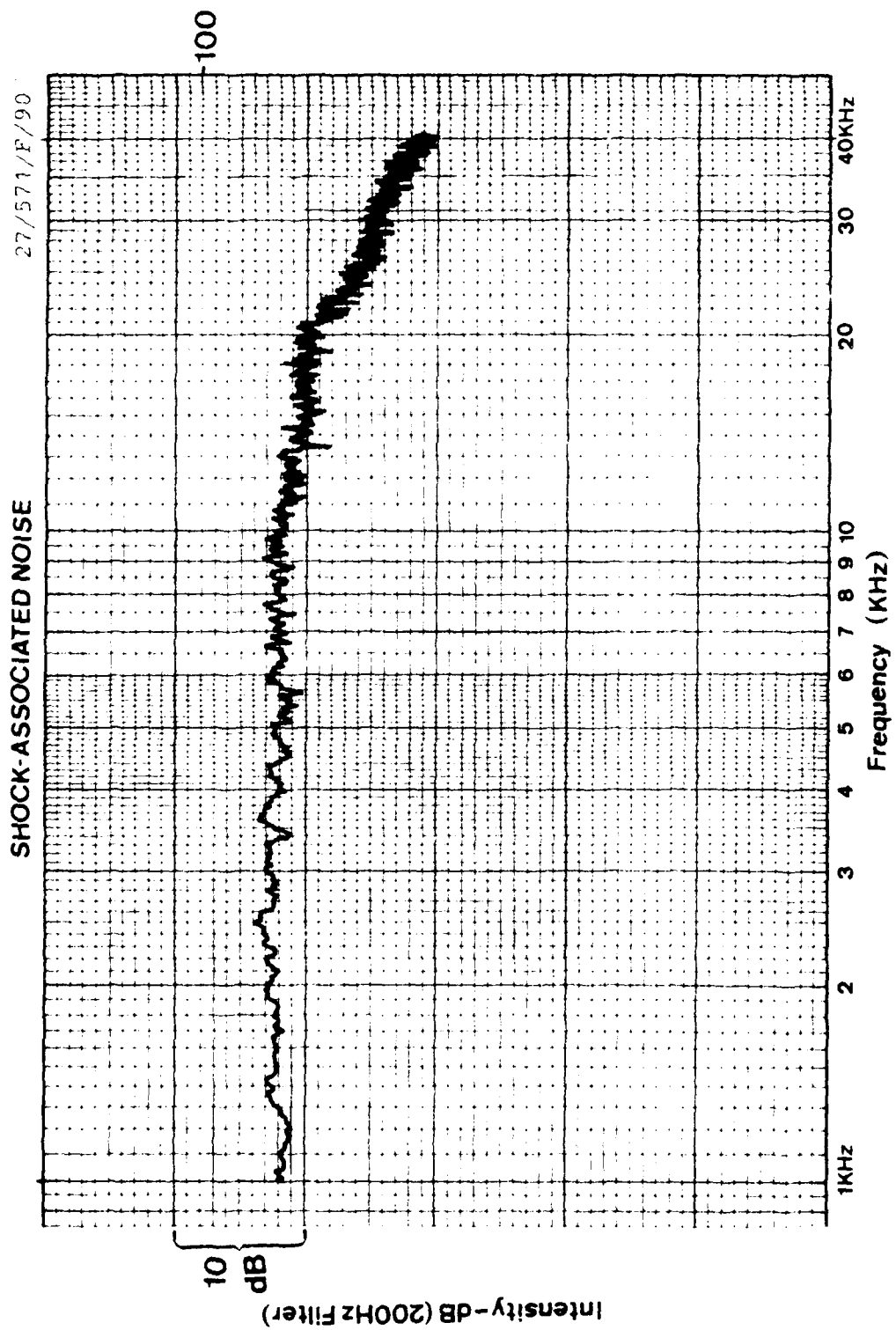
SHOCK-ASSOCIATED NOISE



SHOCK-ASSOCIATED NOISE

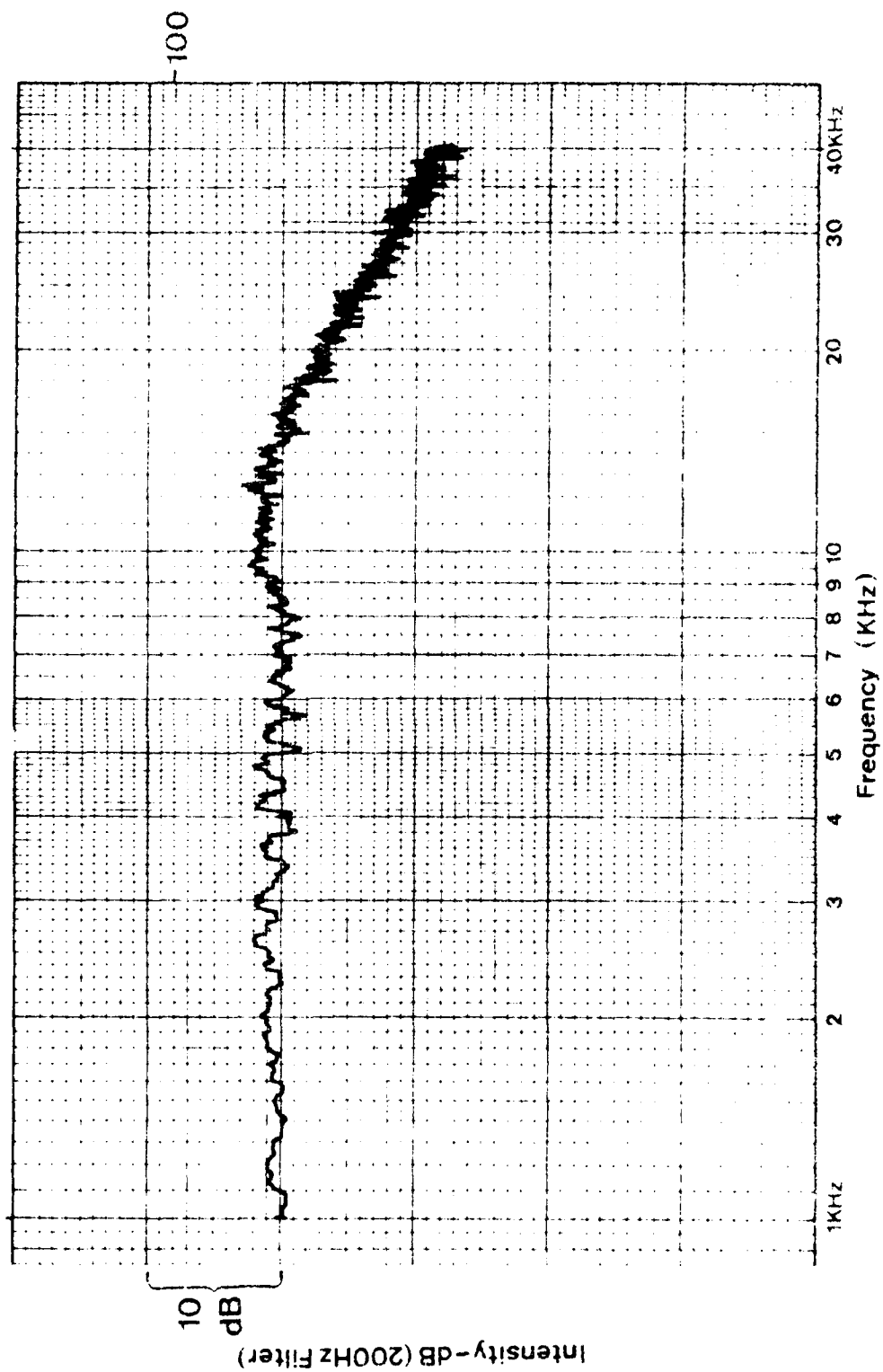
27 123 2 19

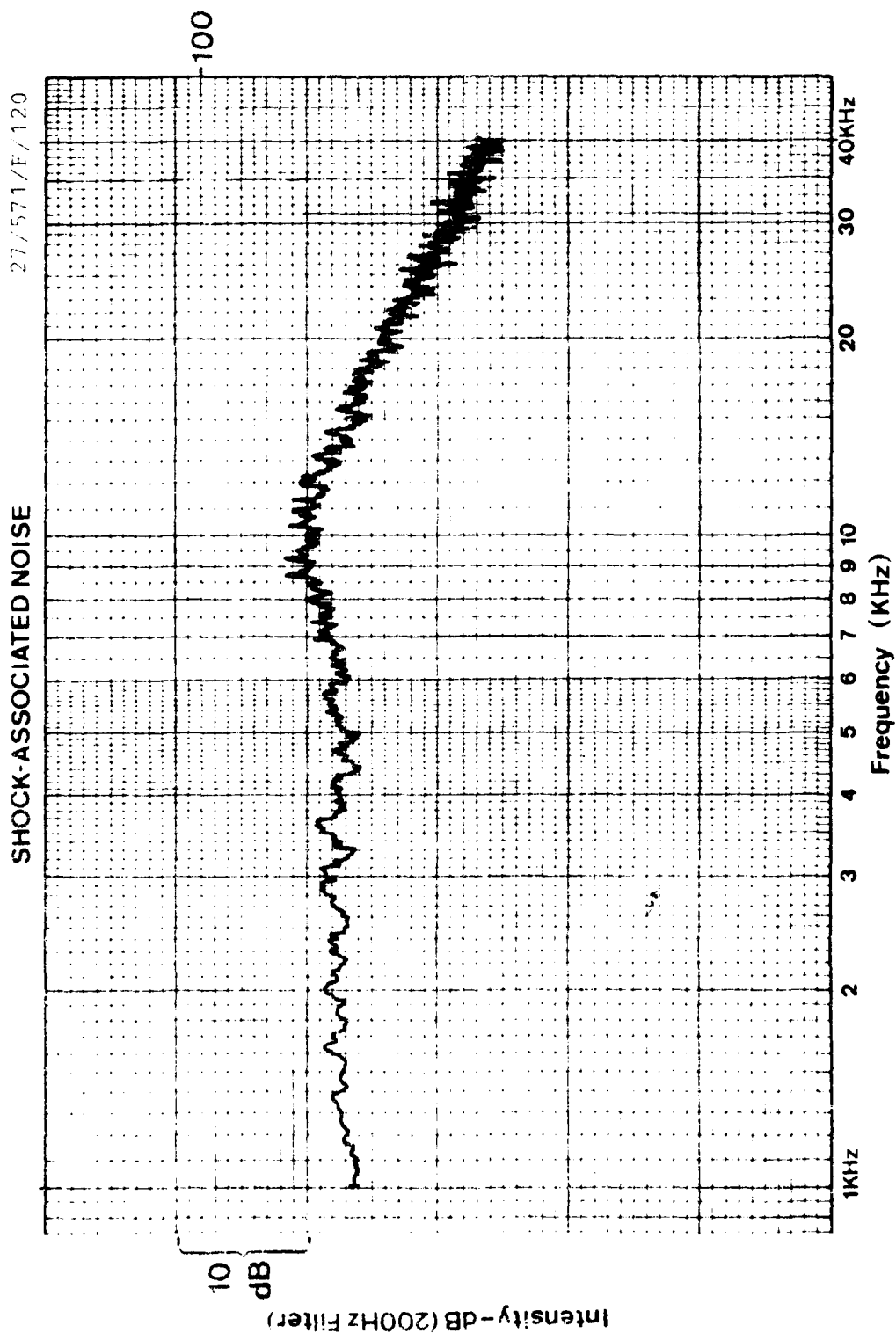




SHOCK-ASSOCIATED NOISE

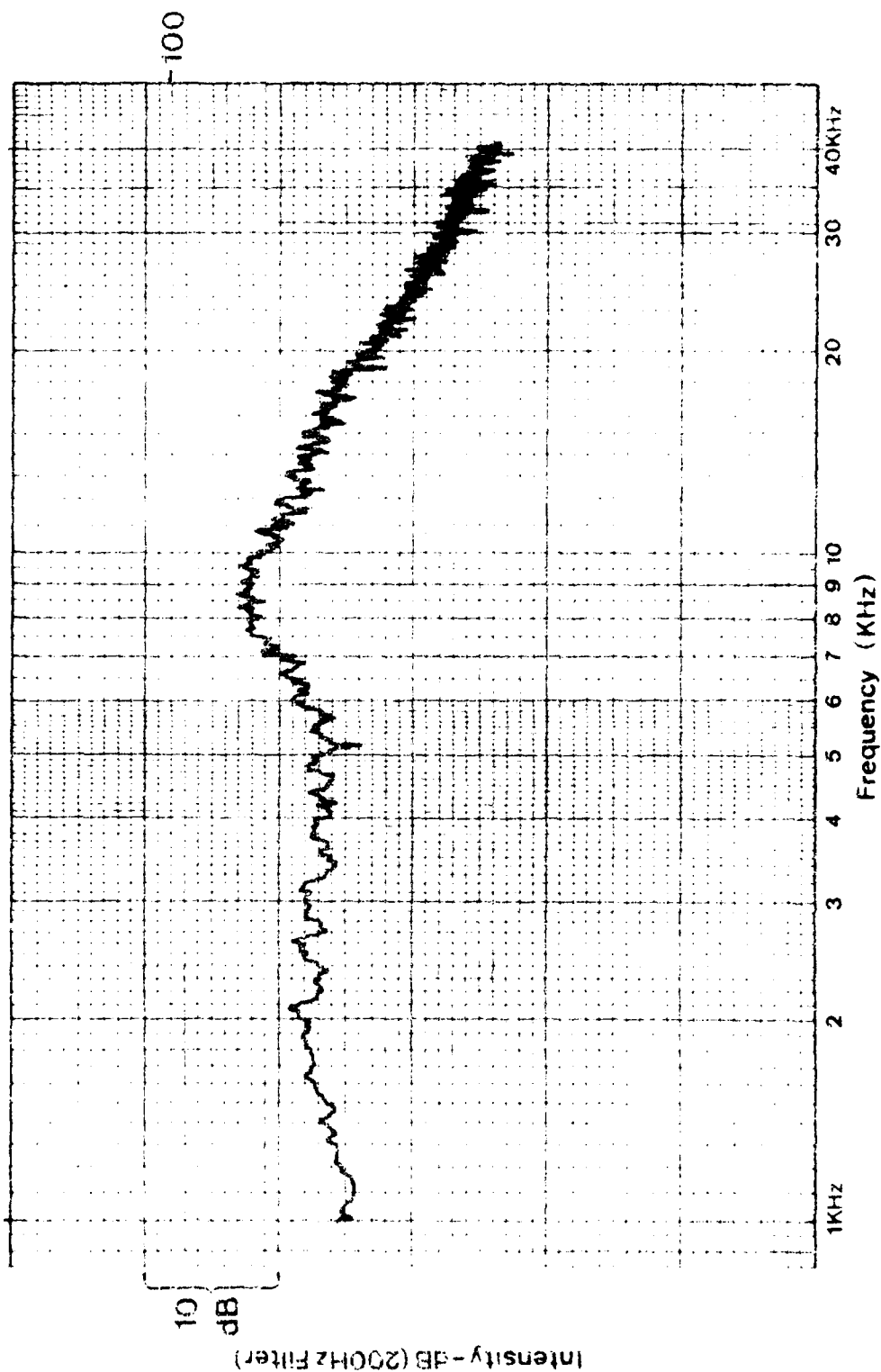
27/571, F 105

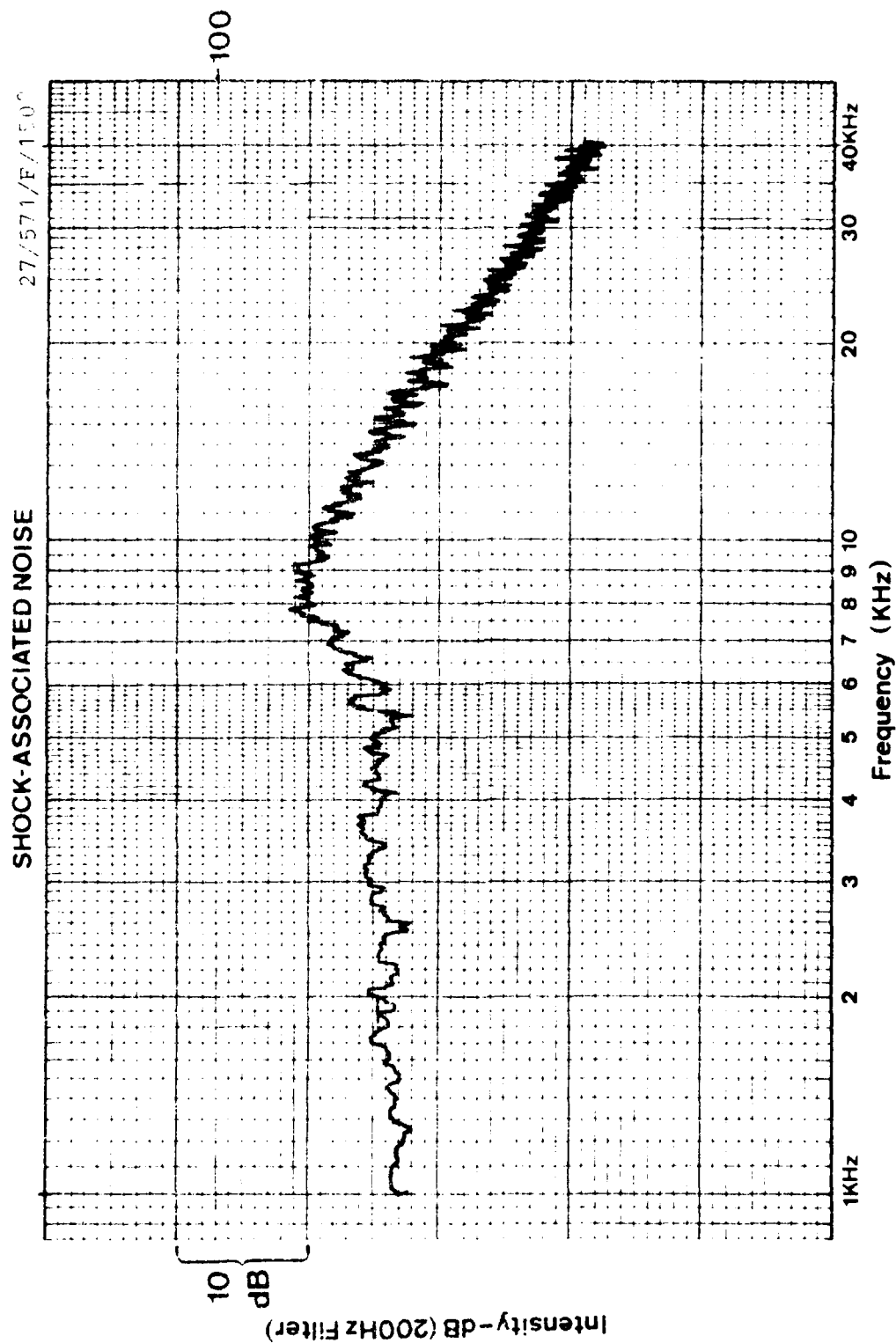




SHOCK-ASSOCIATED NOISE

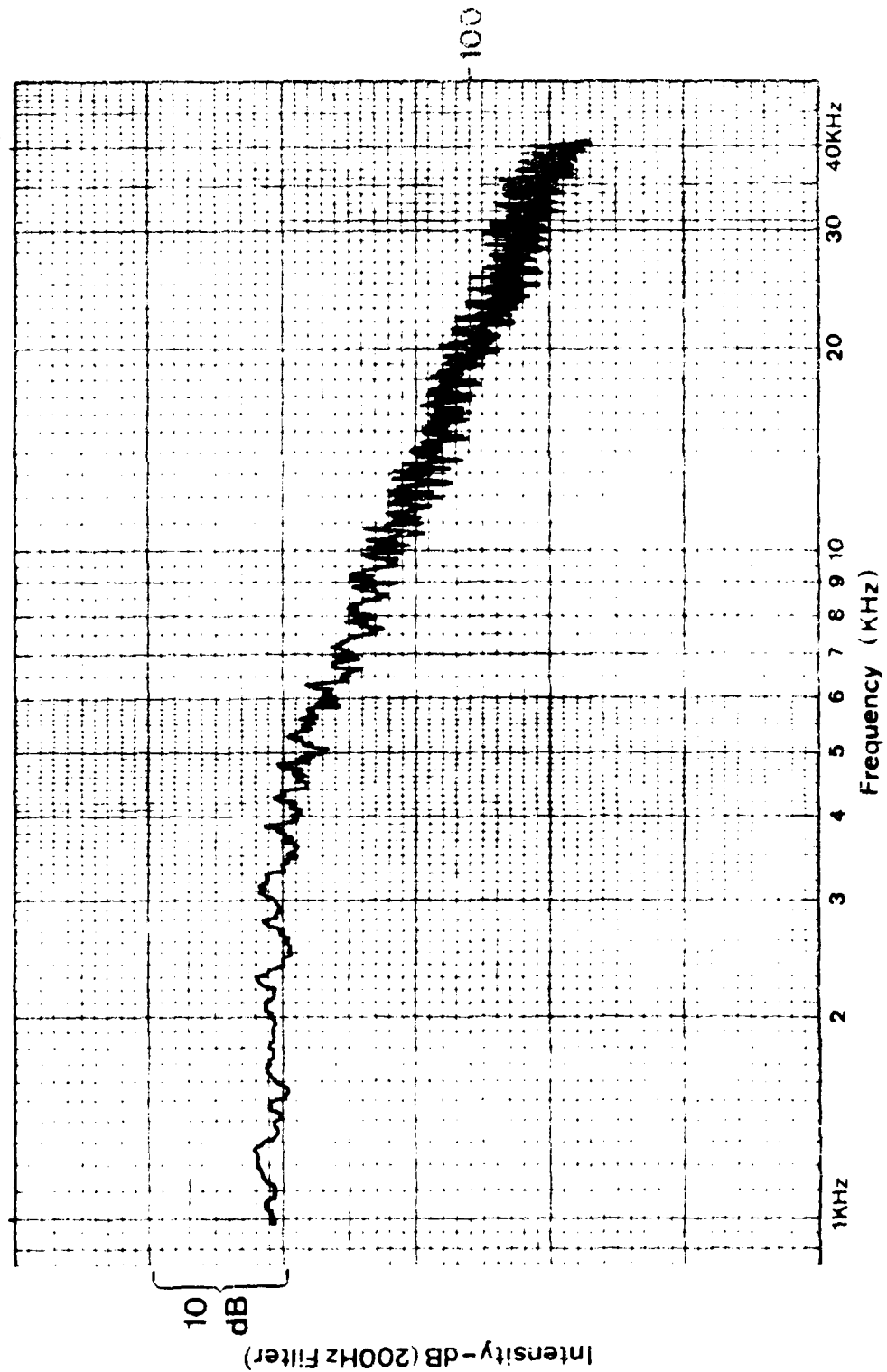
07/571/F/135





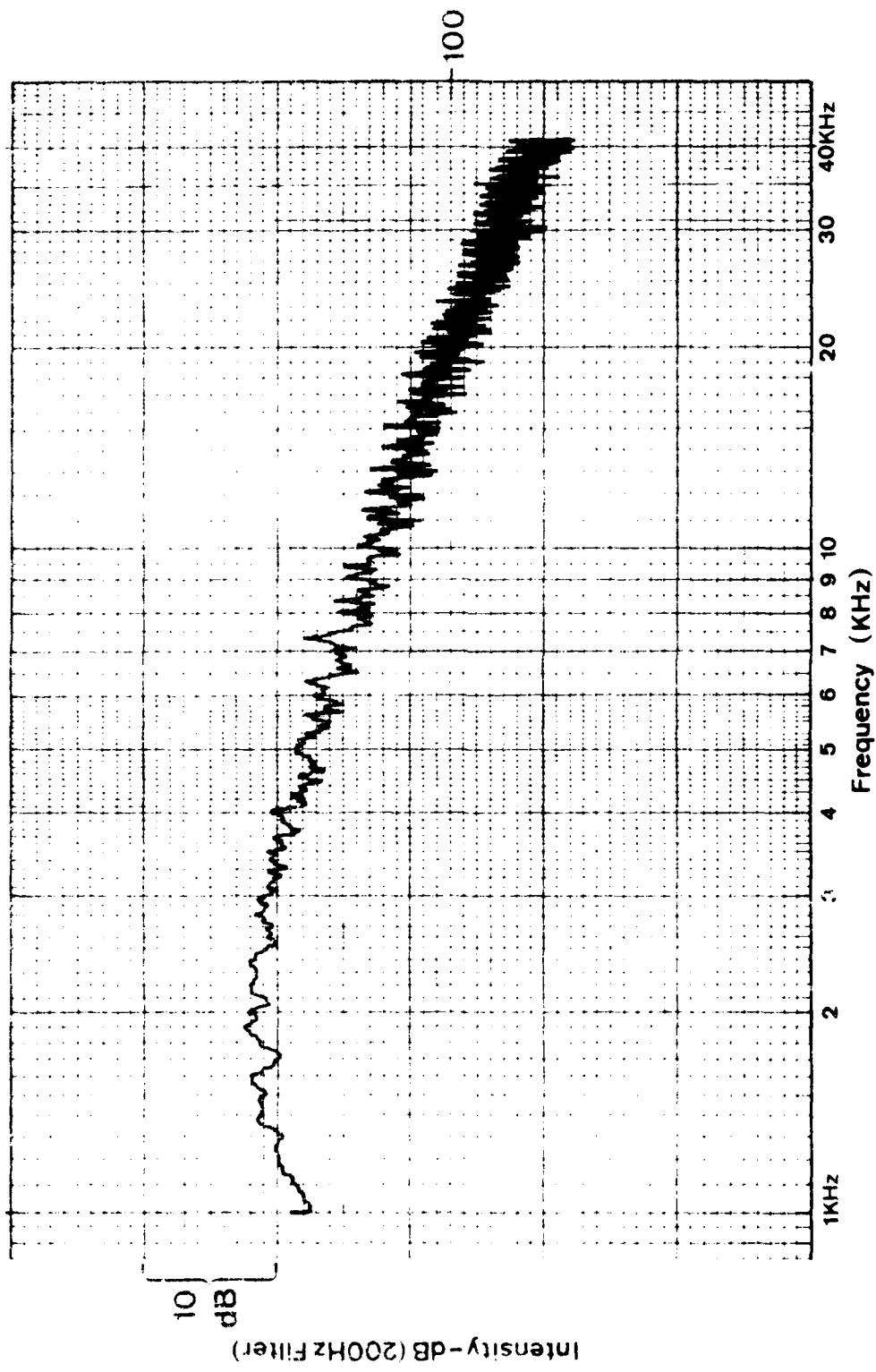
SHOCK-ASSOCIATED NOISE

28/527/R/30



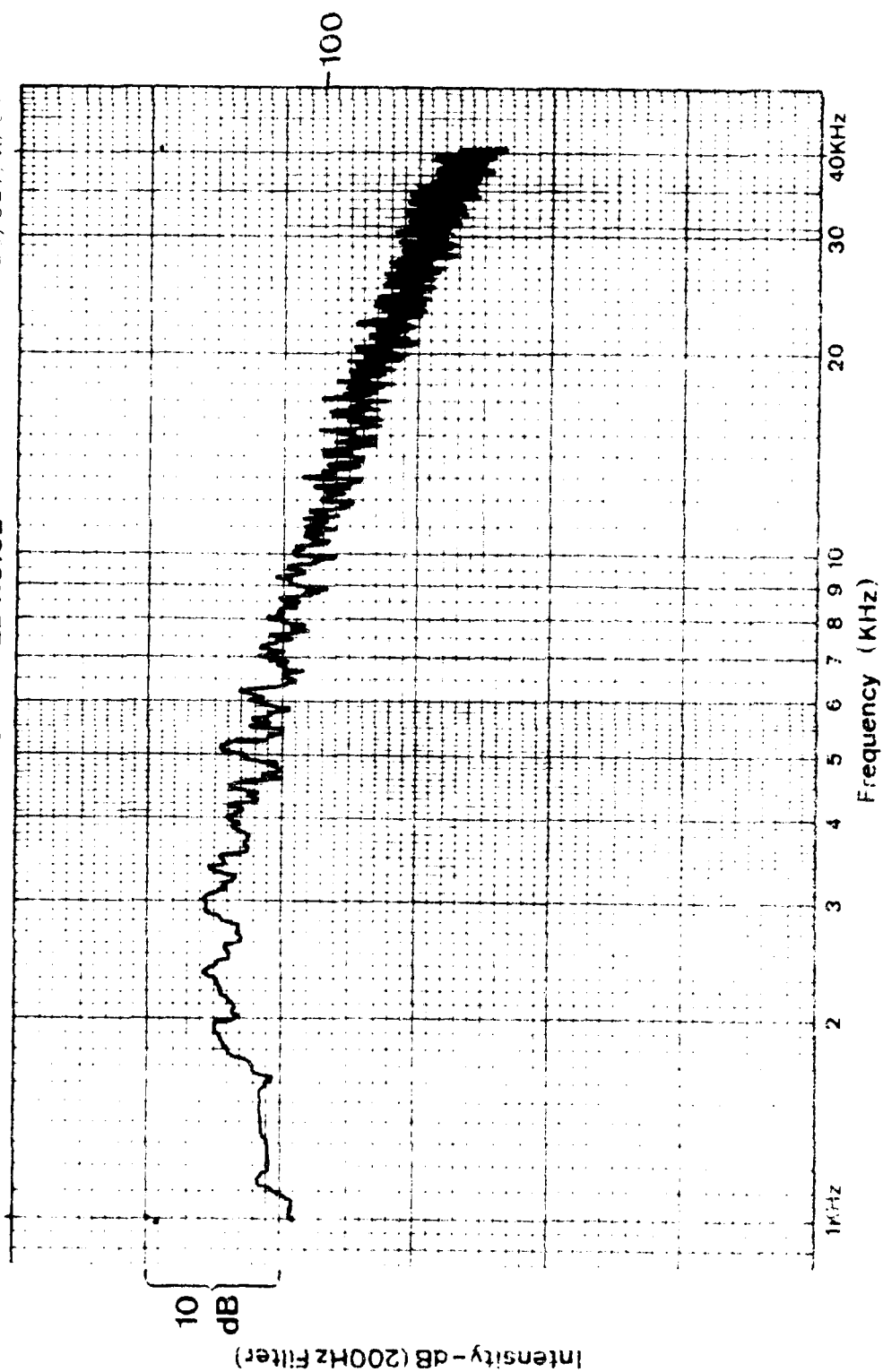
SHOCK-ASSOCIATED NOISE

1-527

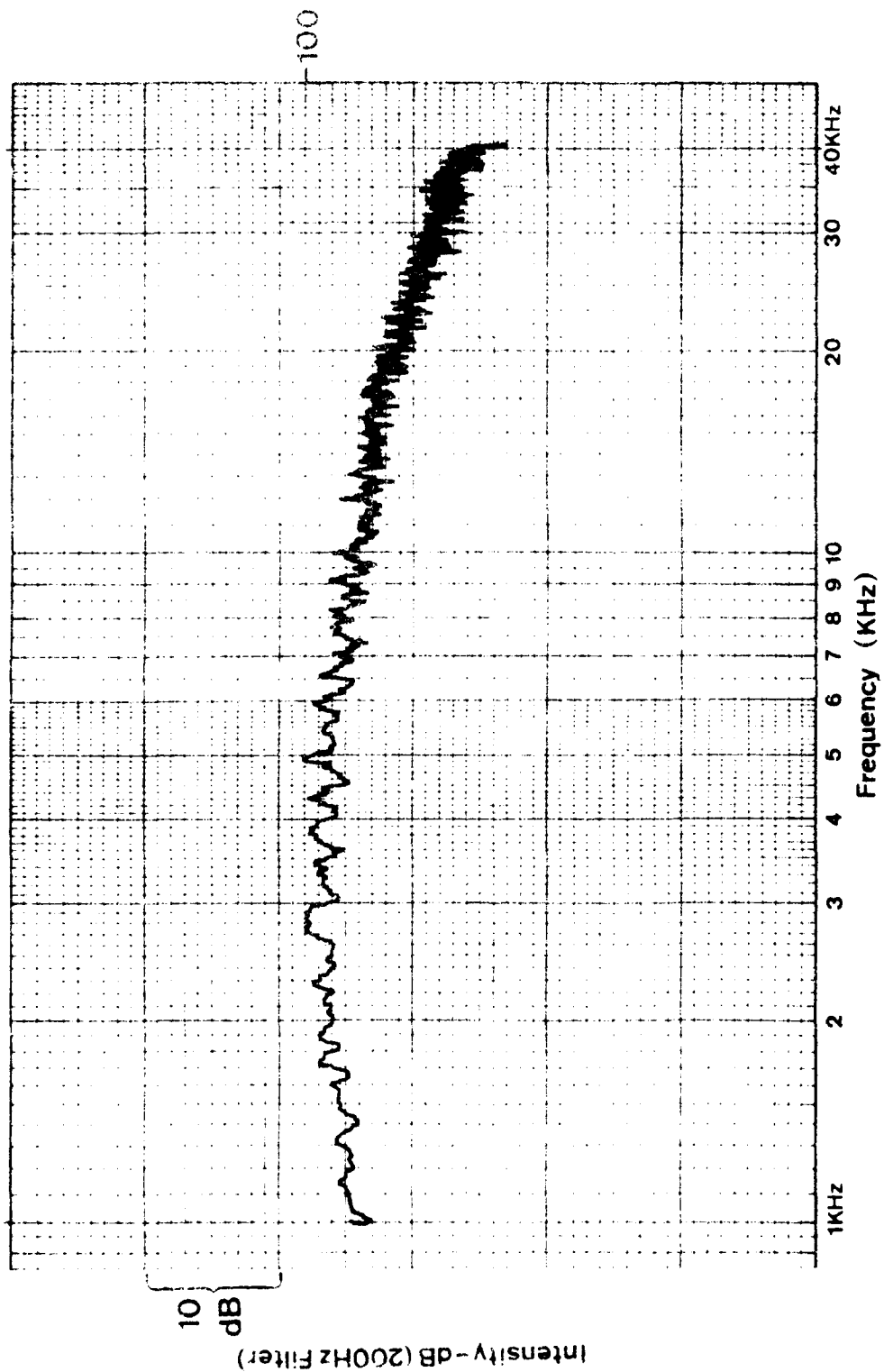


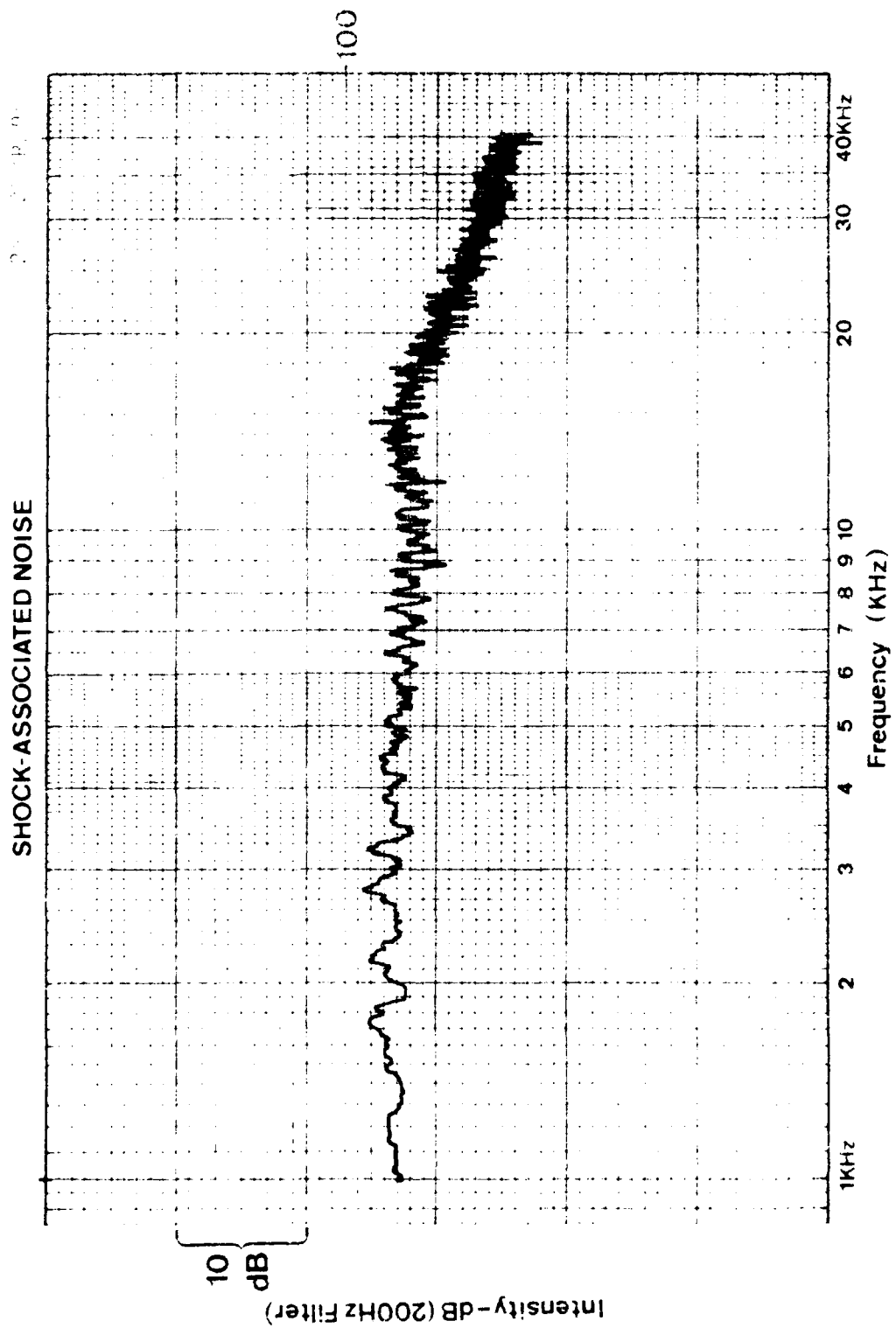
SHOCK-ASSOCIATED NOISE

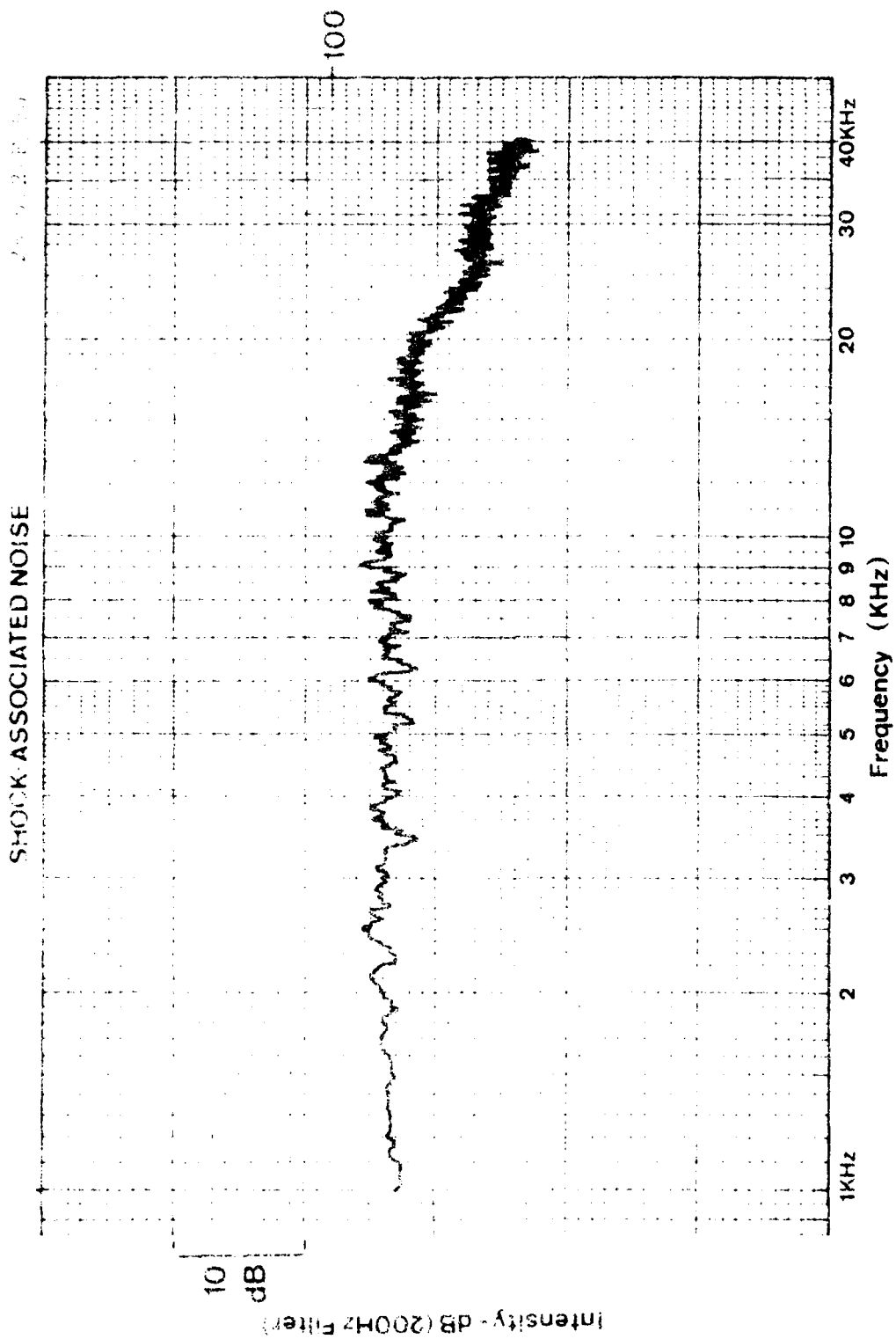
28/527/R/60

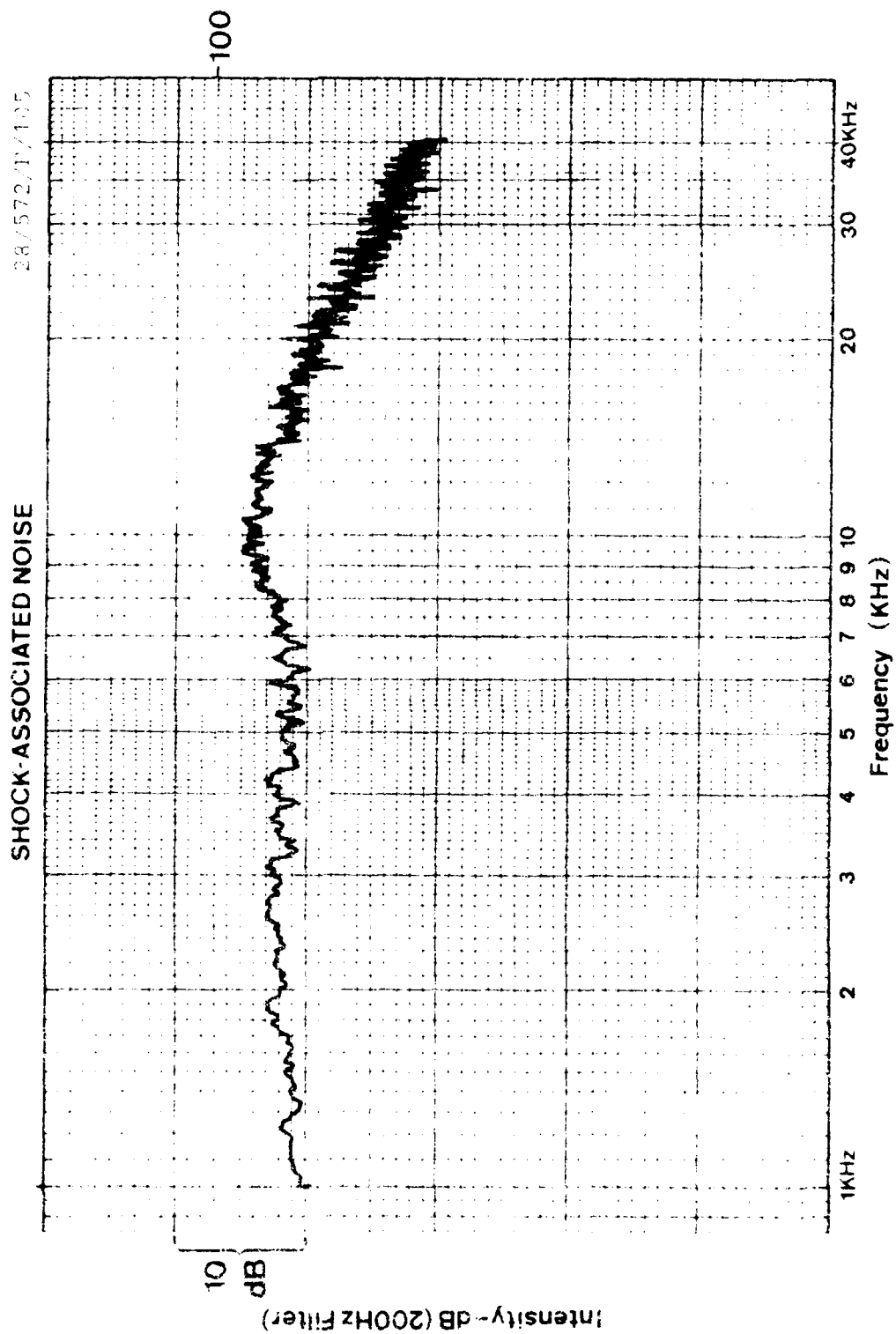


SHOCK-ASSOCIATED NOISE

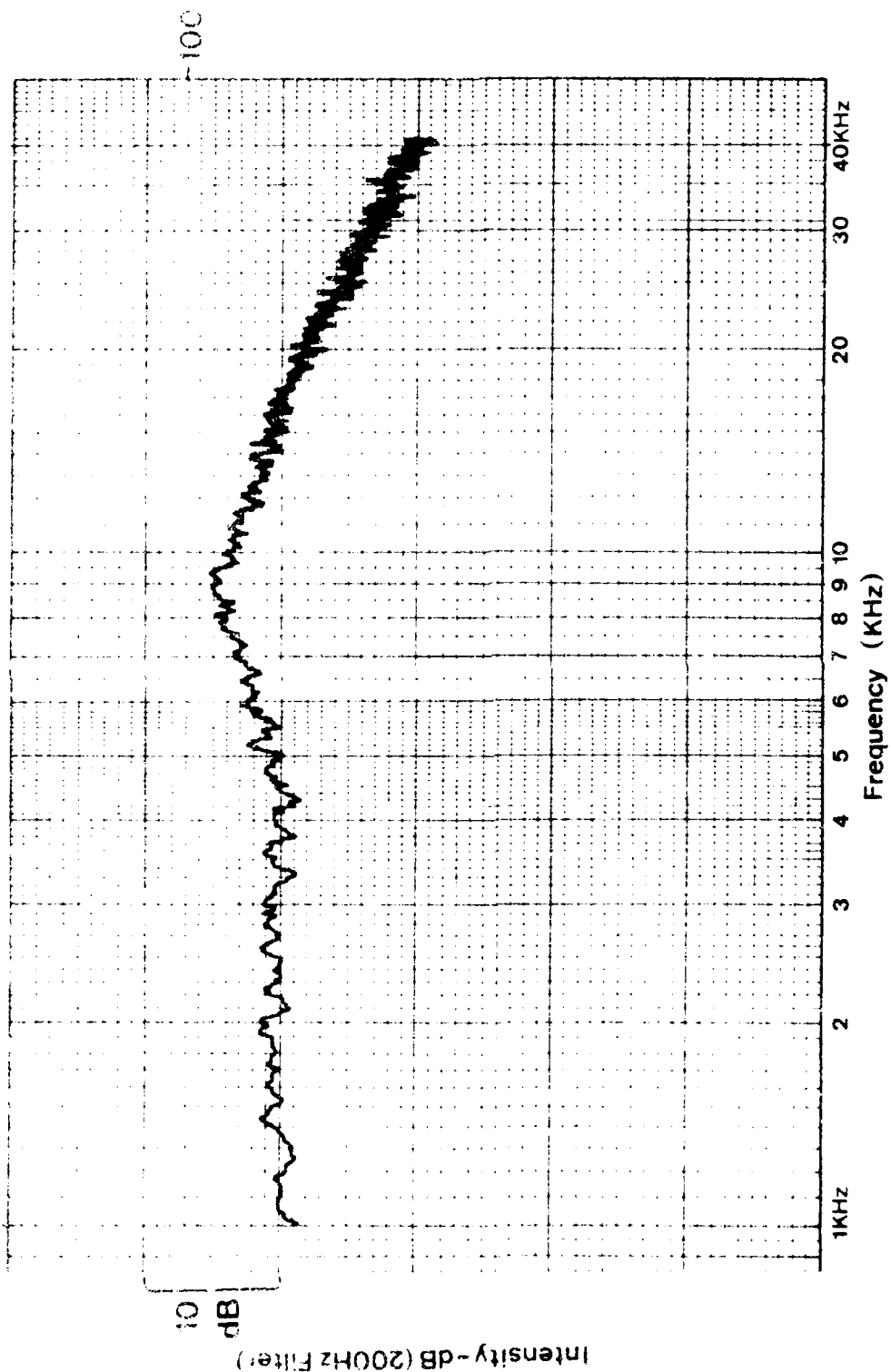


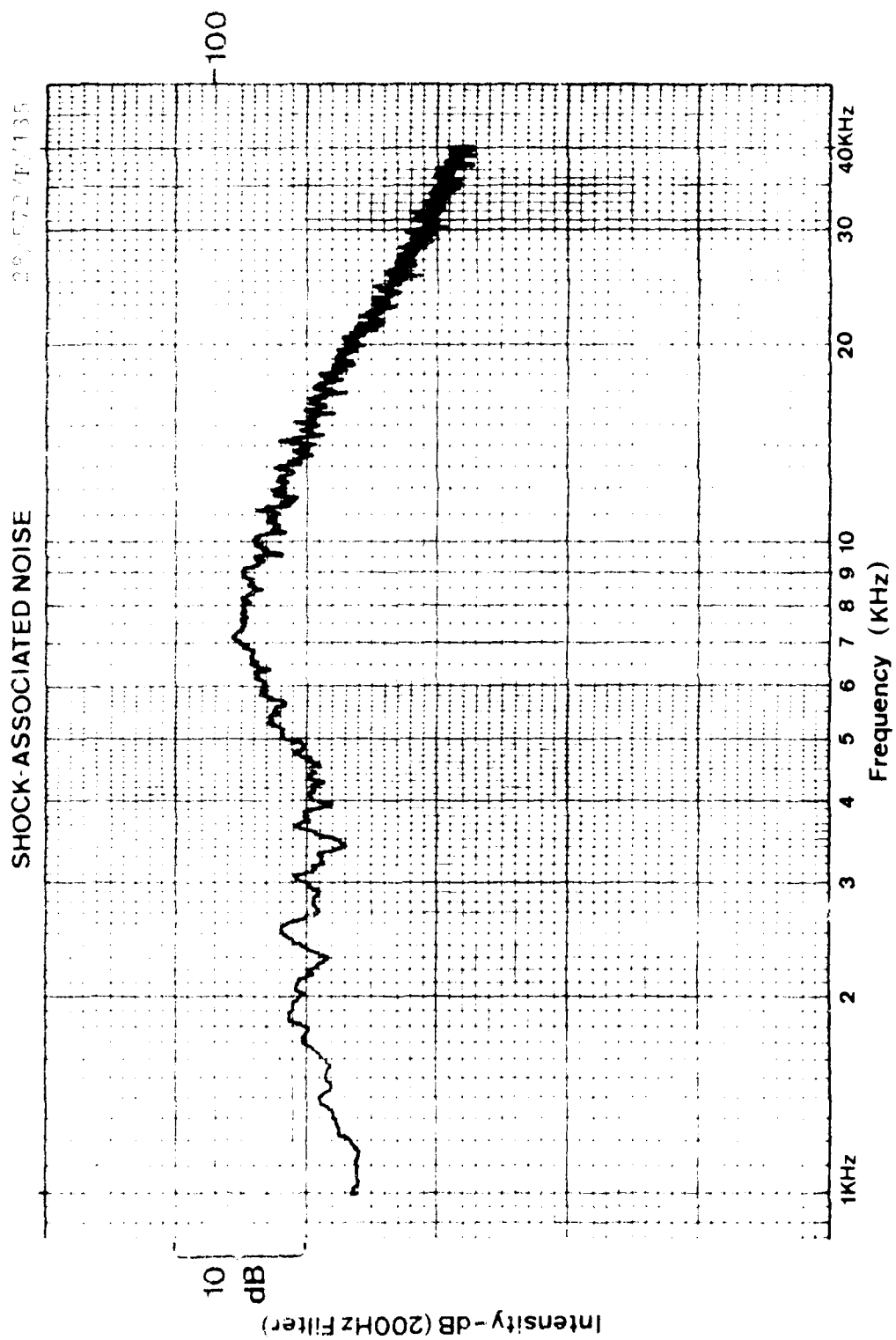


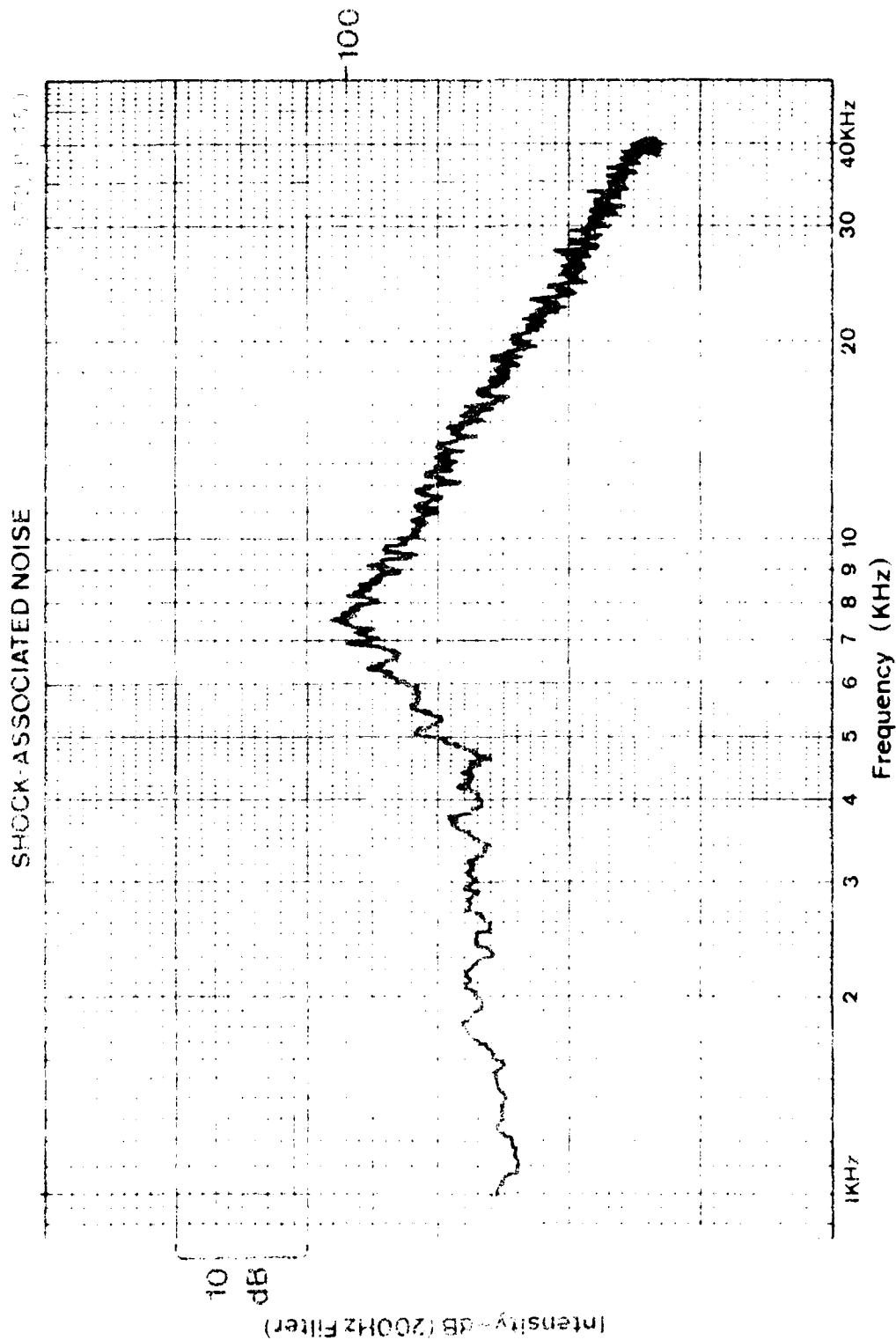




SHOCK-ASSOCIATED NOISE

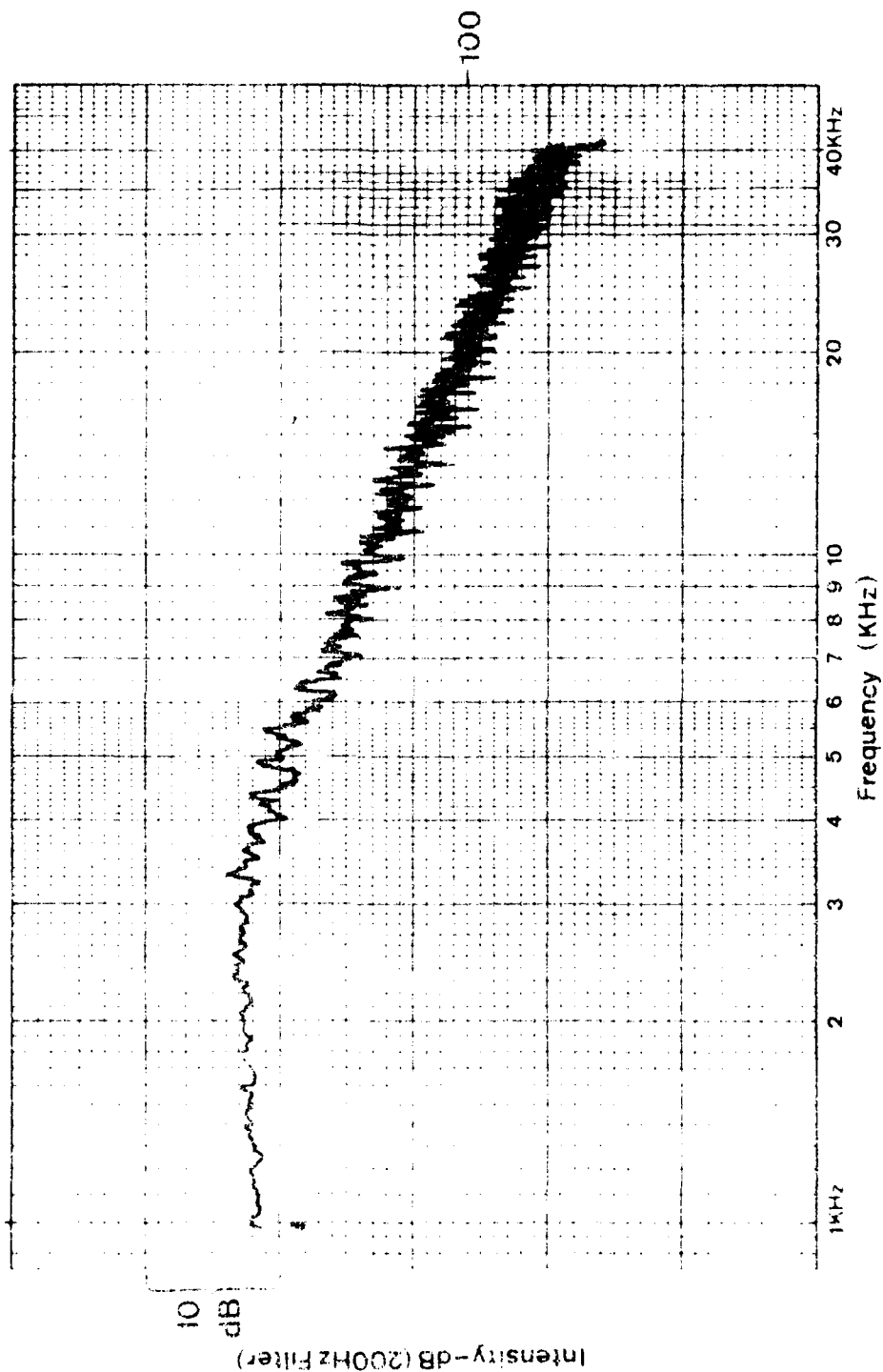


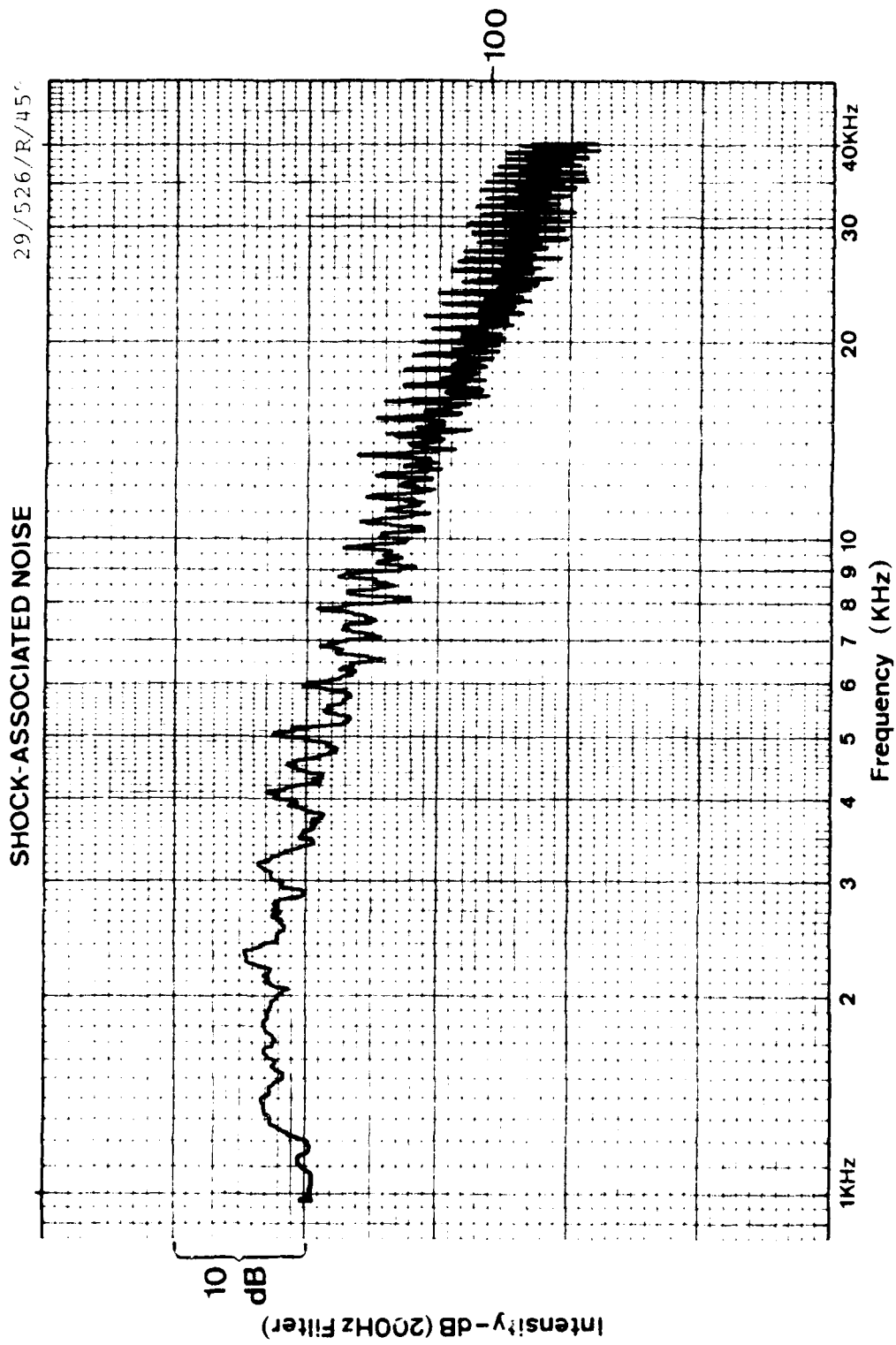


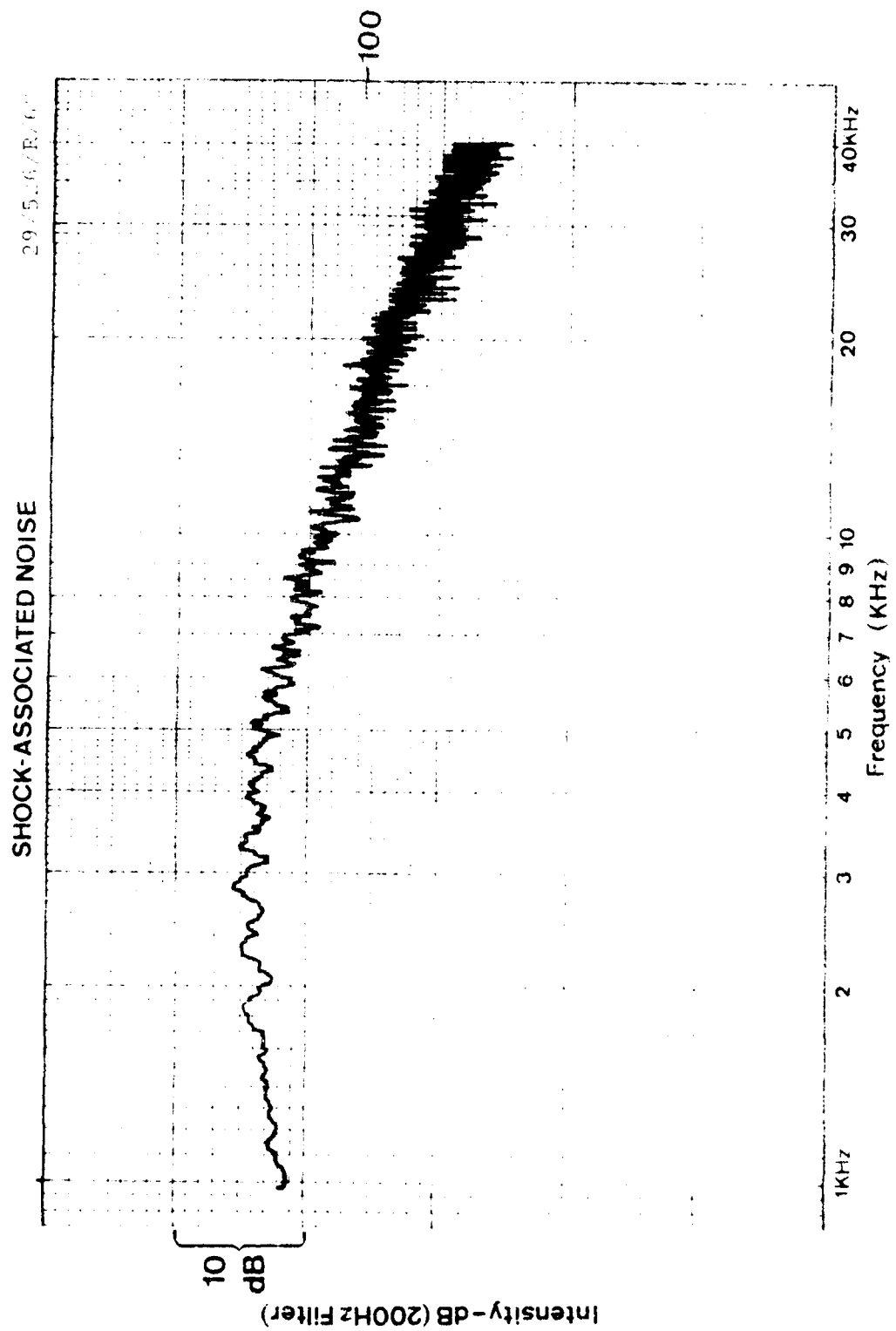


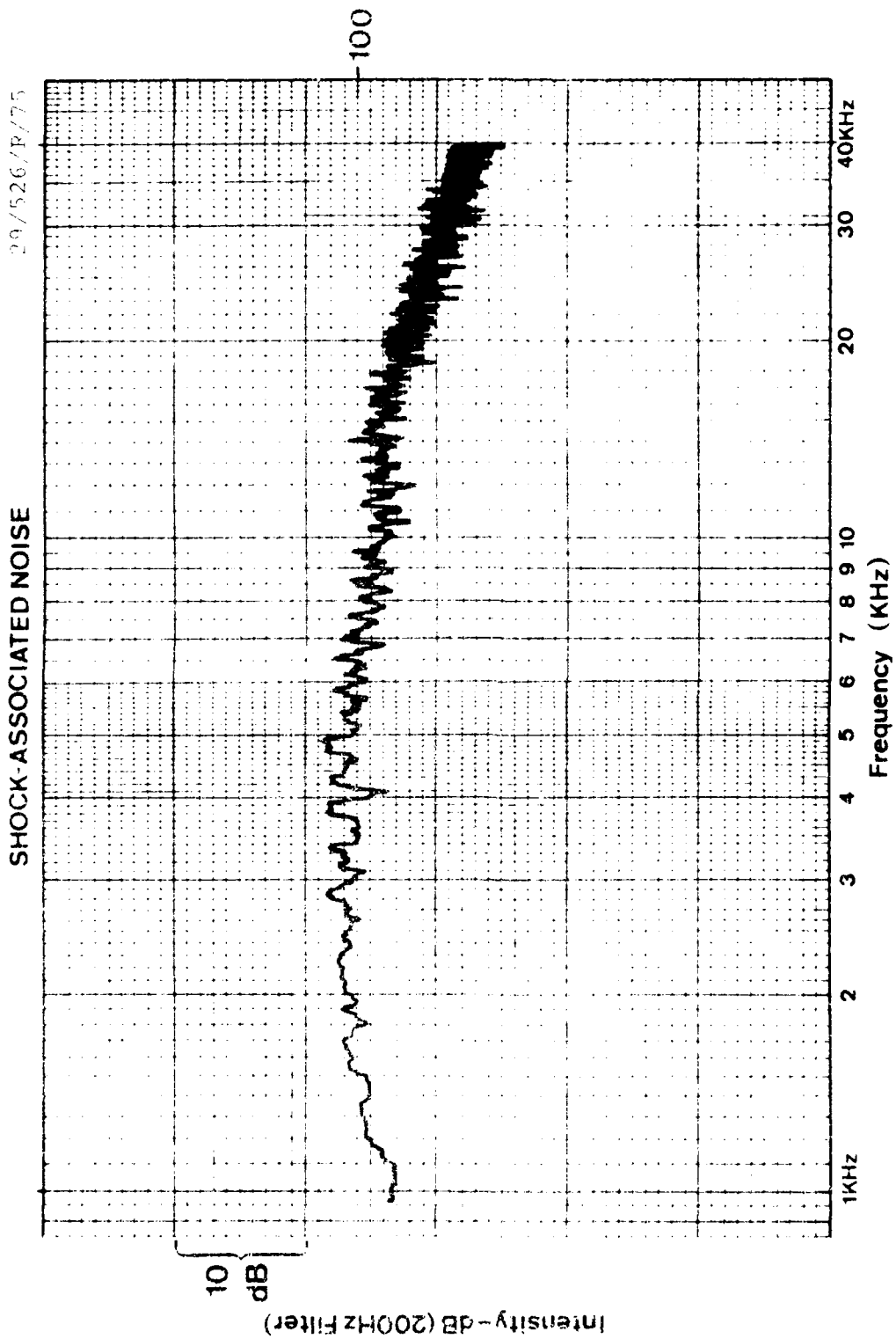
SHOCK-ASSOCIATED NOISE

29 FEB 64 R 120



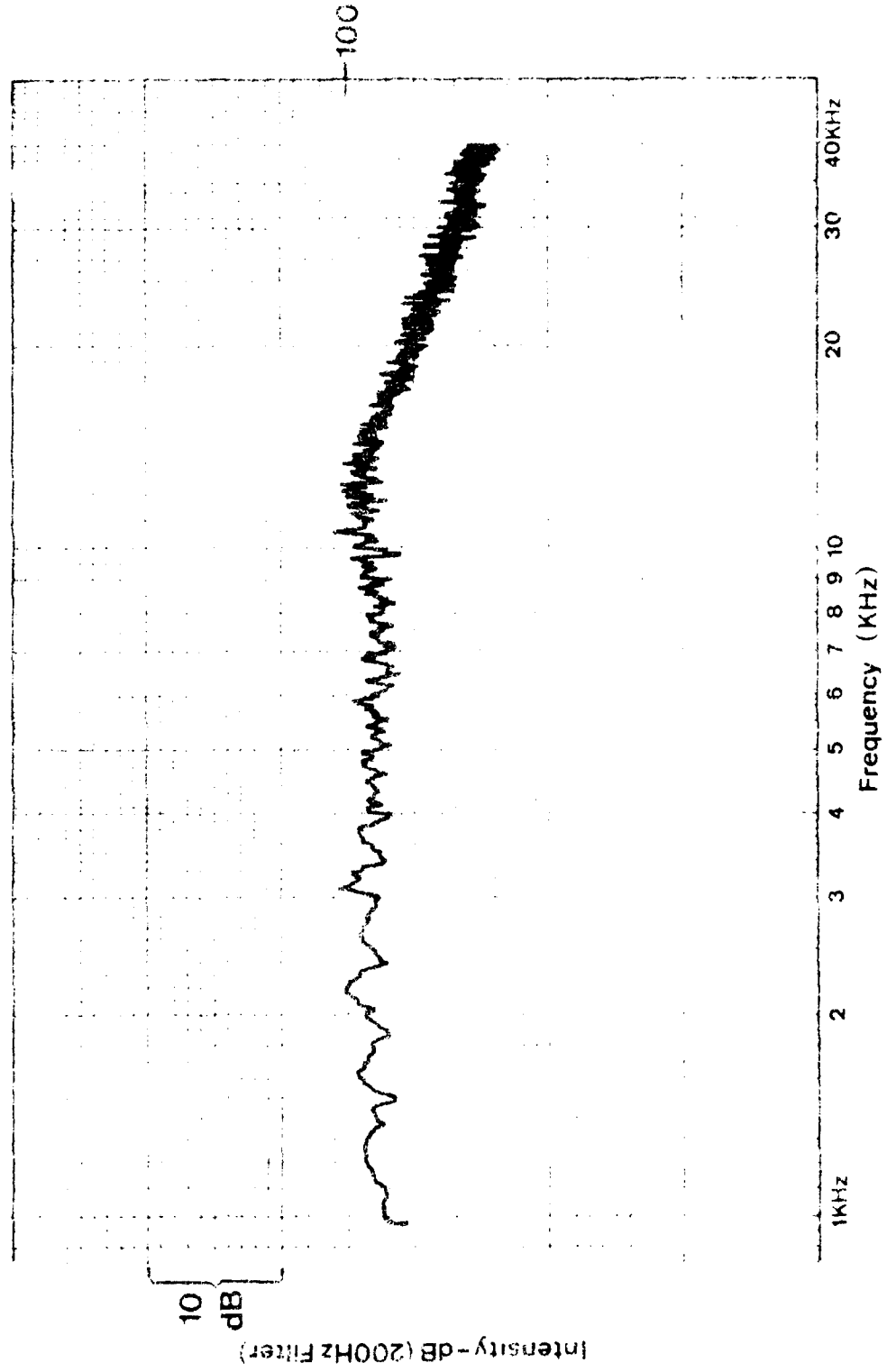


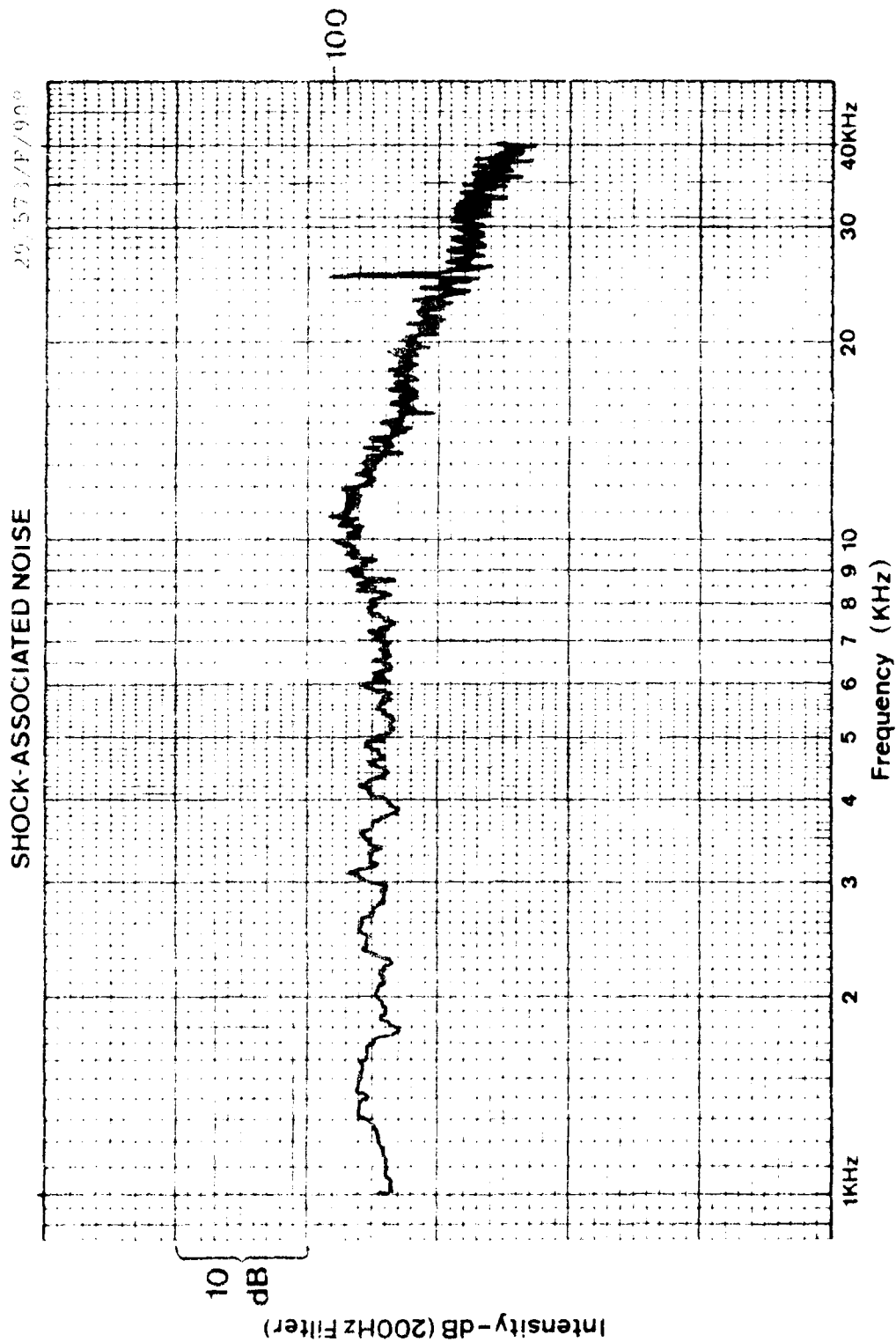


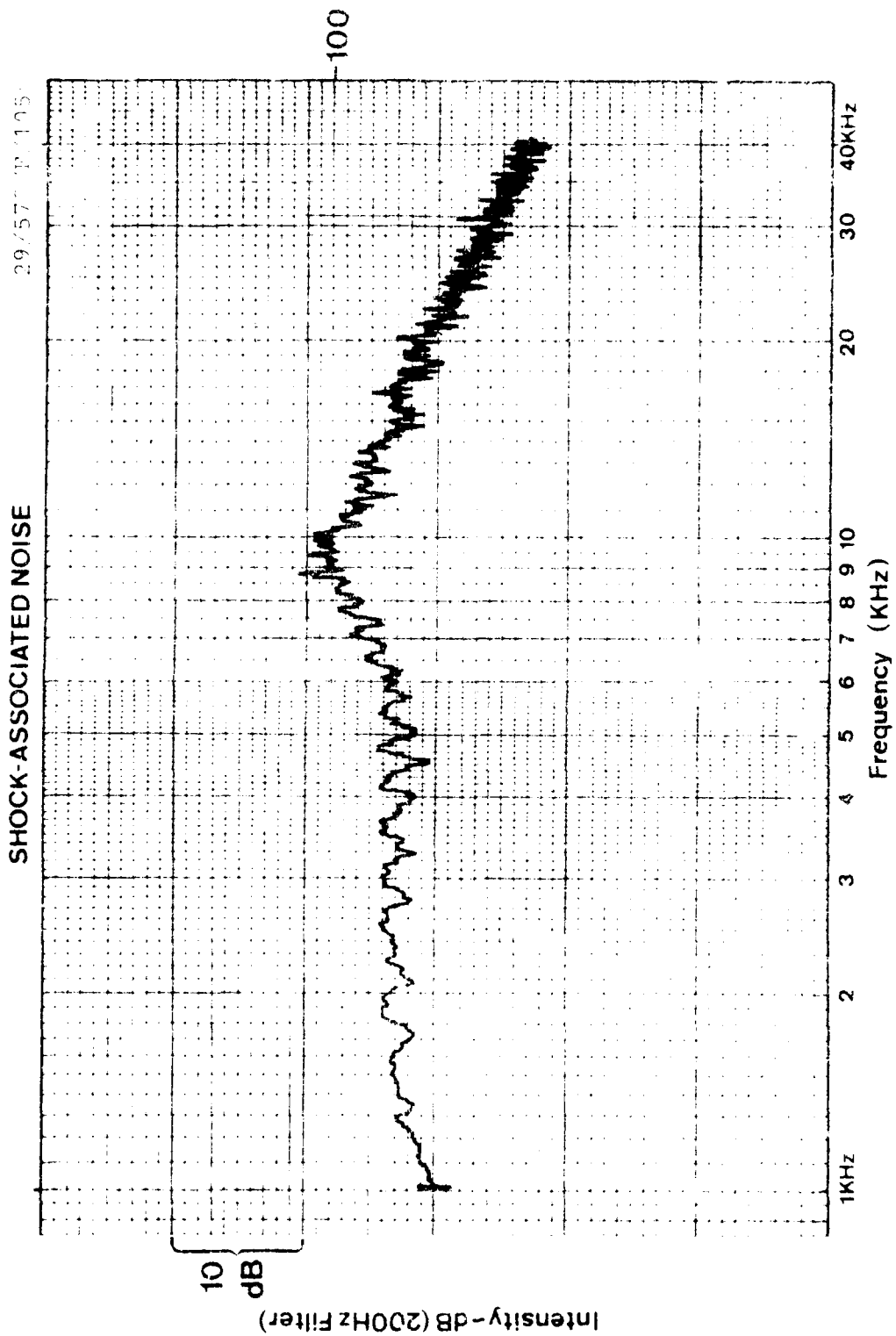


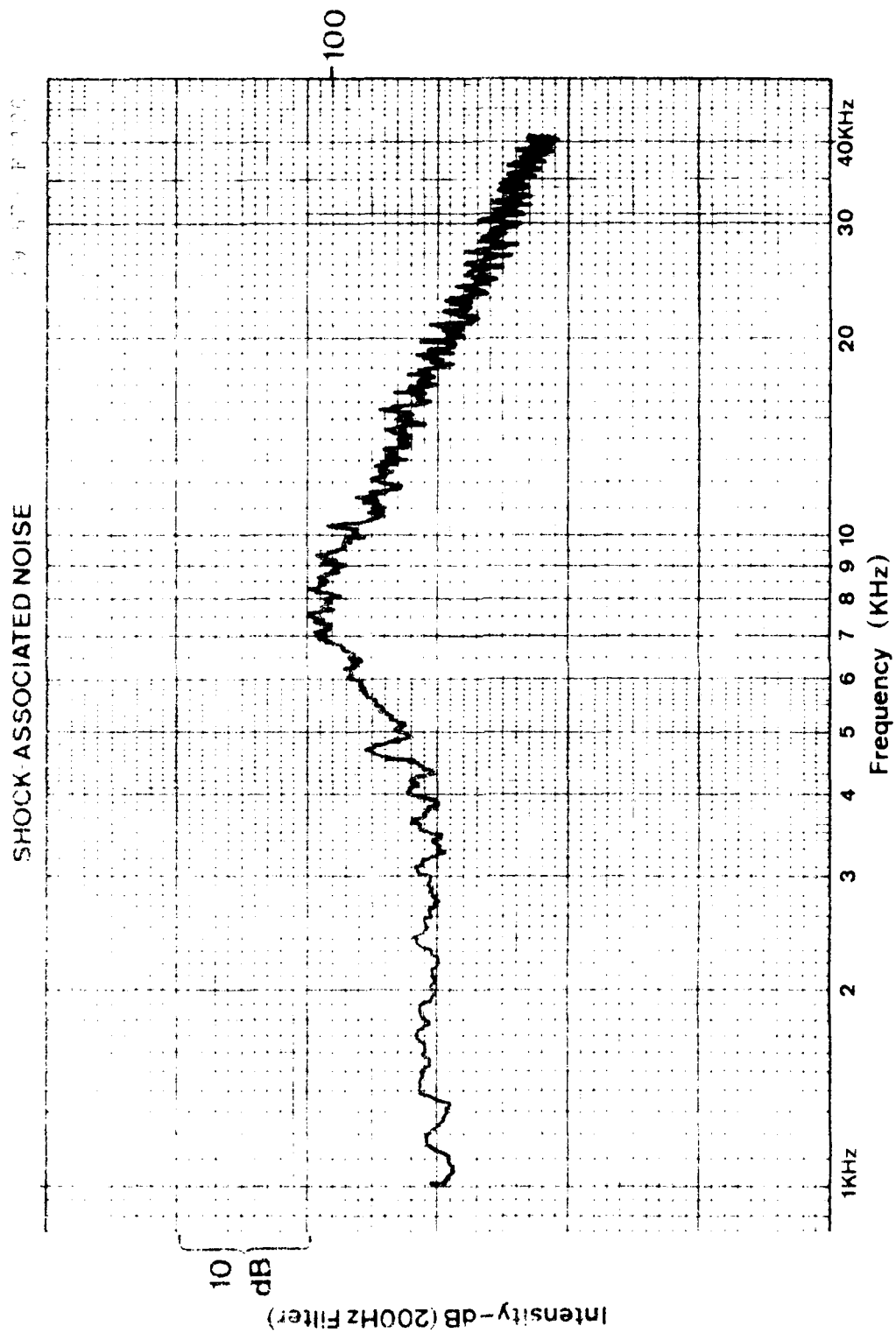
29/521/R 194

SHOCK-ASSOCIATED NOISE



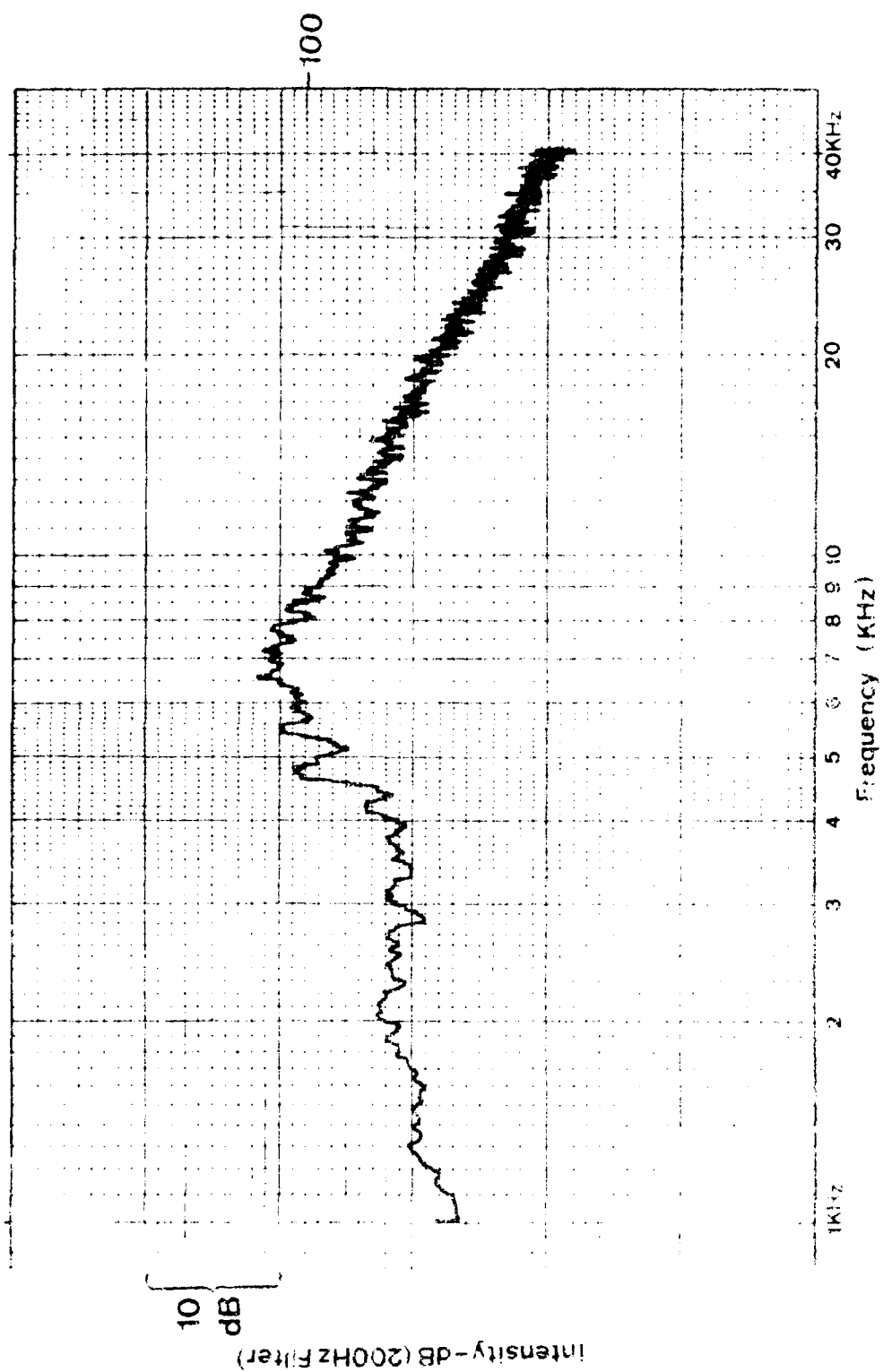




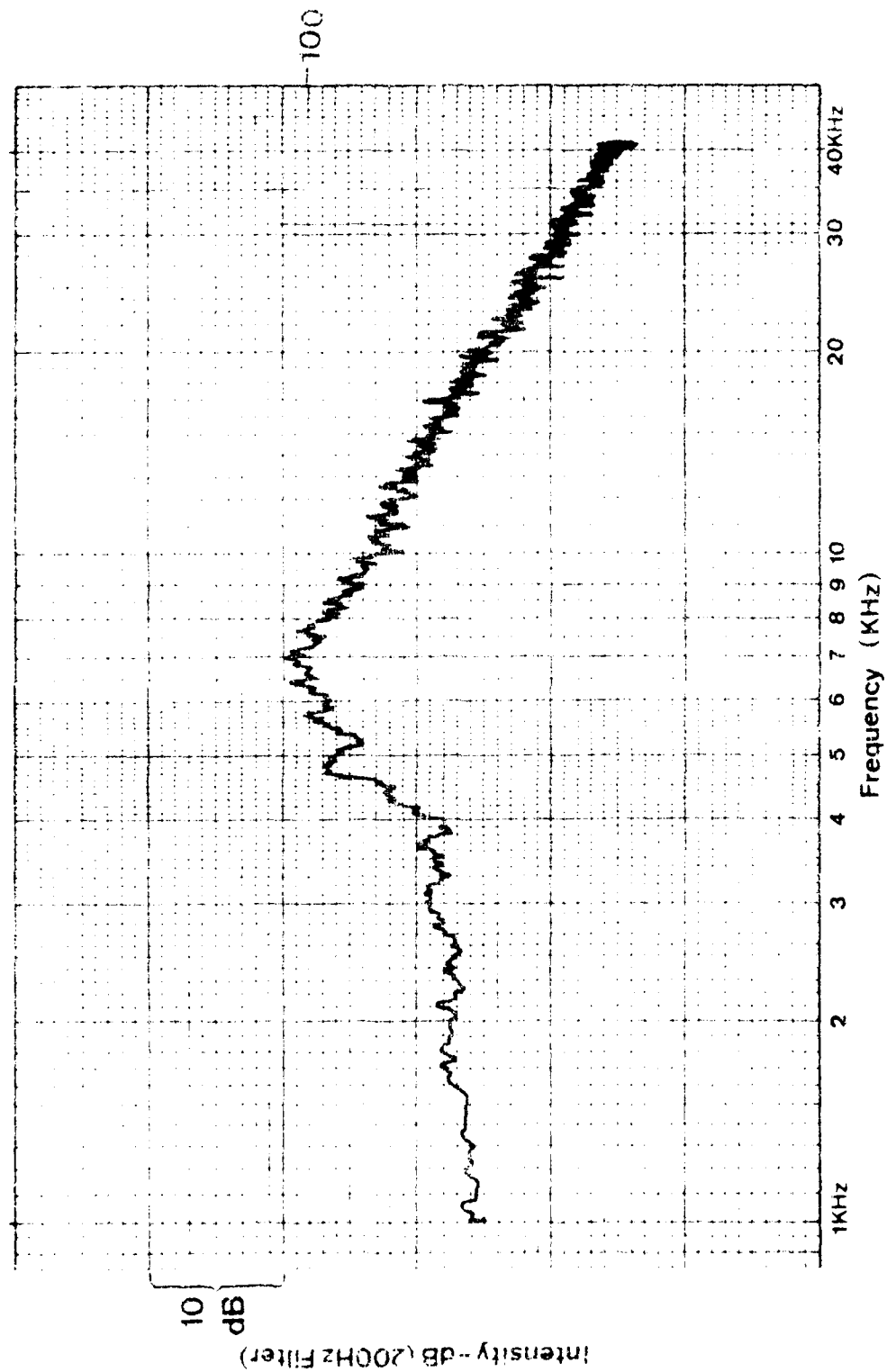


SHOCK-ASSOCIATED NOISE

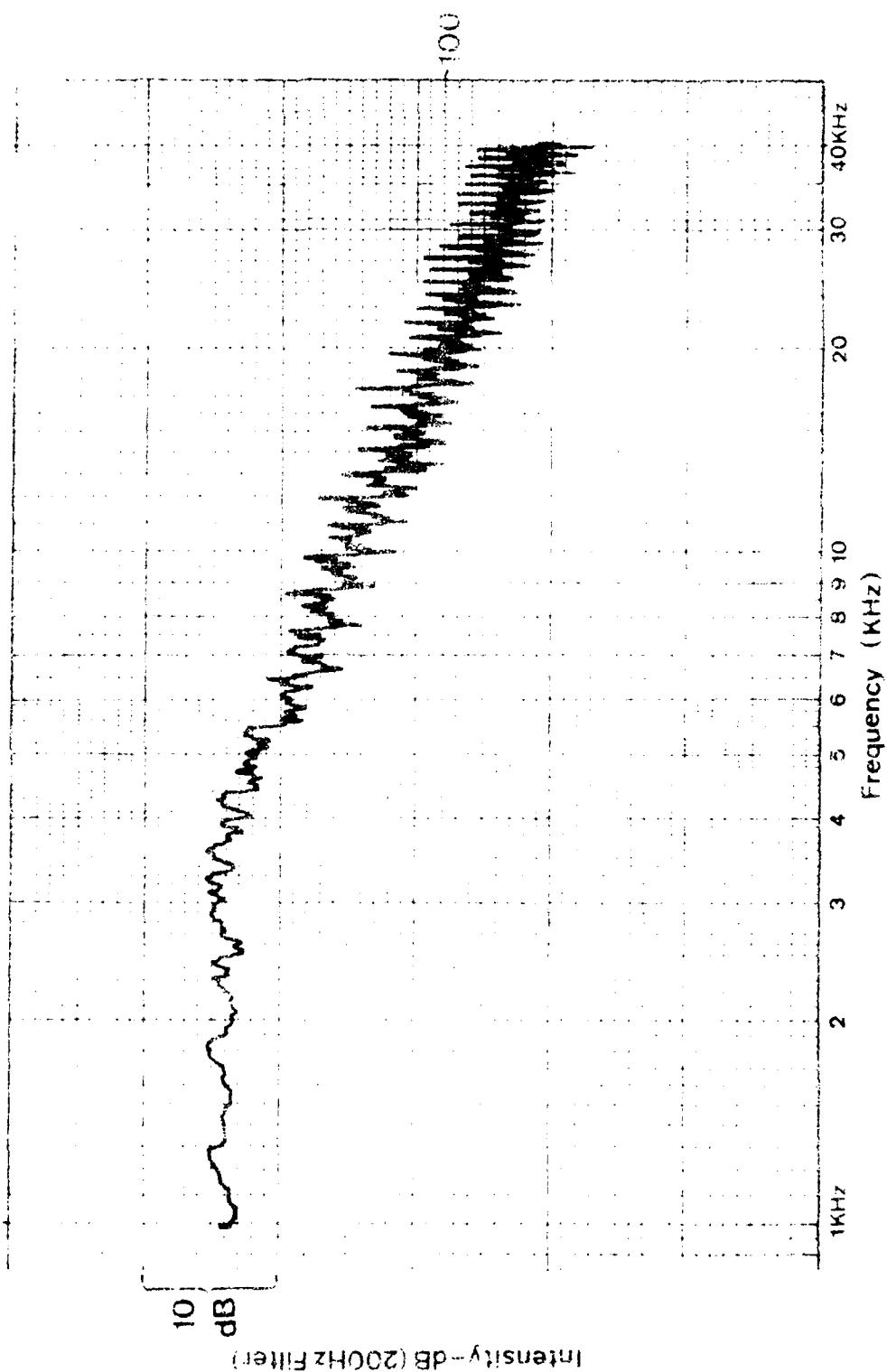
29 SEP 67 P/135



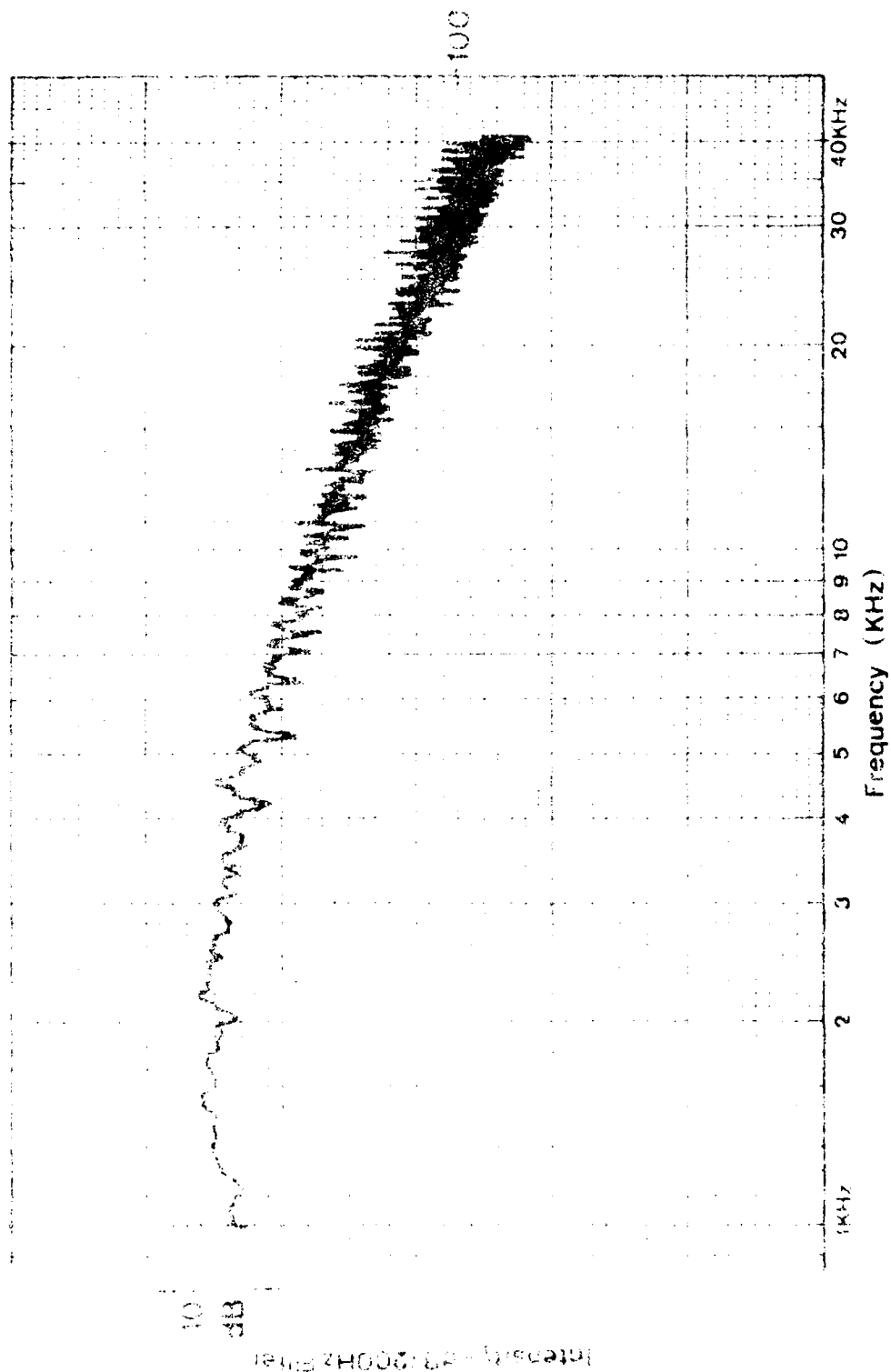
SHOCK-ASSOCIATED NOISE

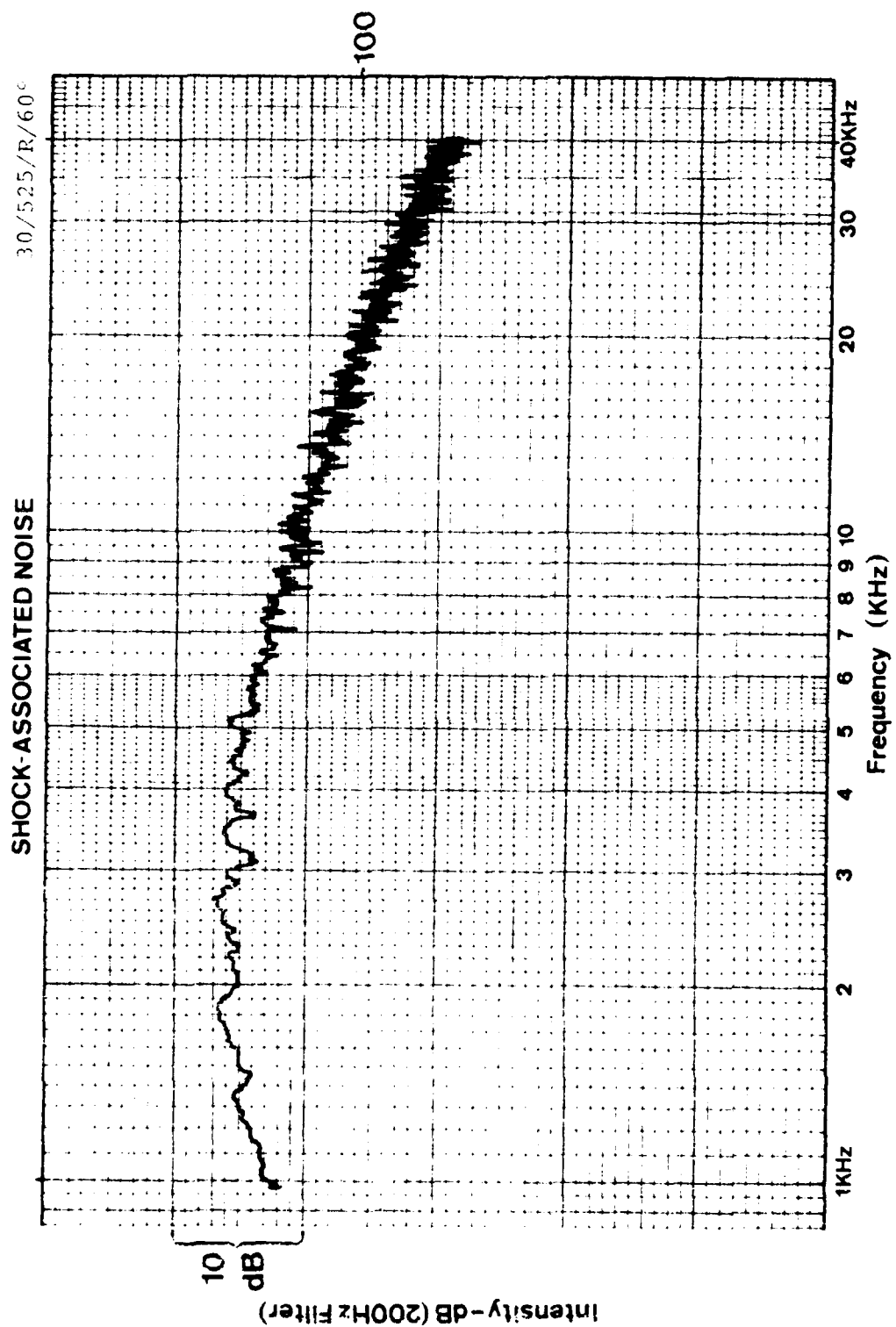


SHOCK ASSOCIATED NOISE

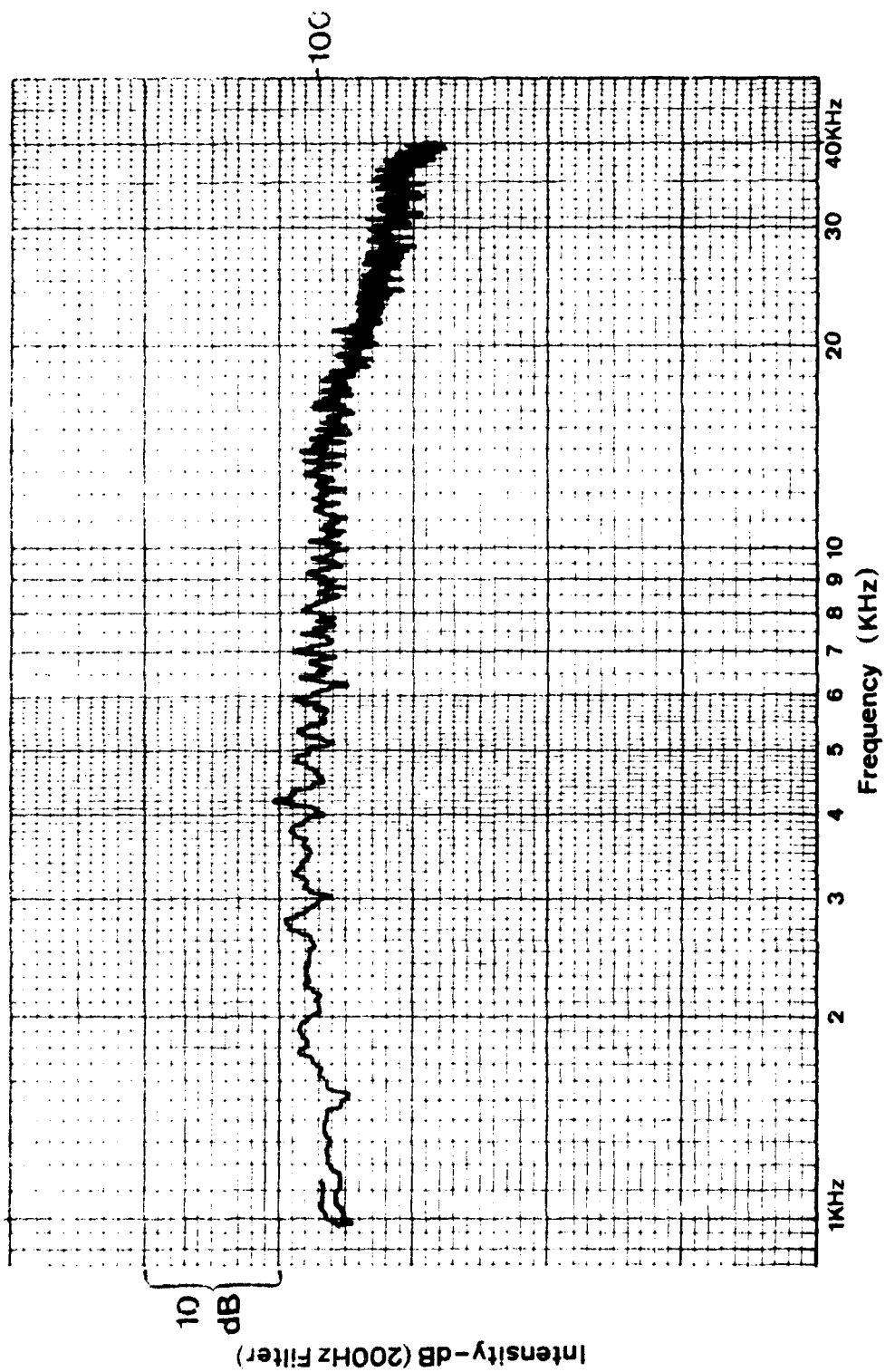


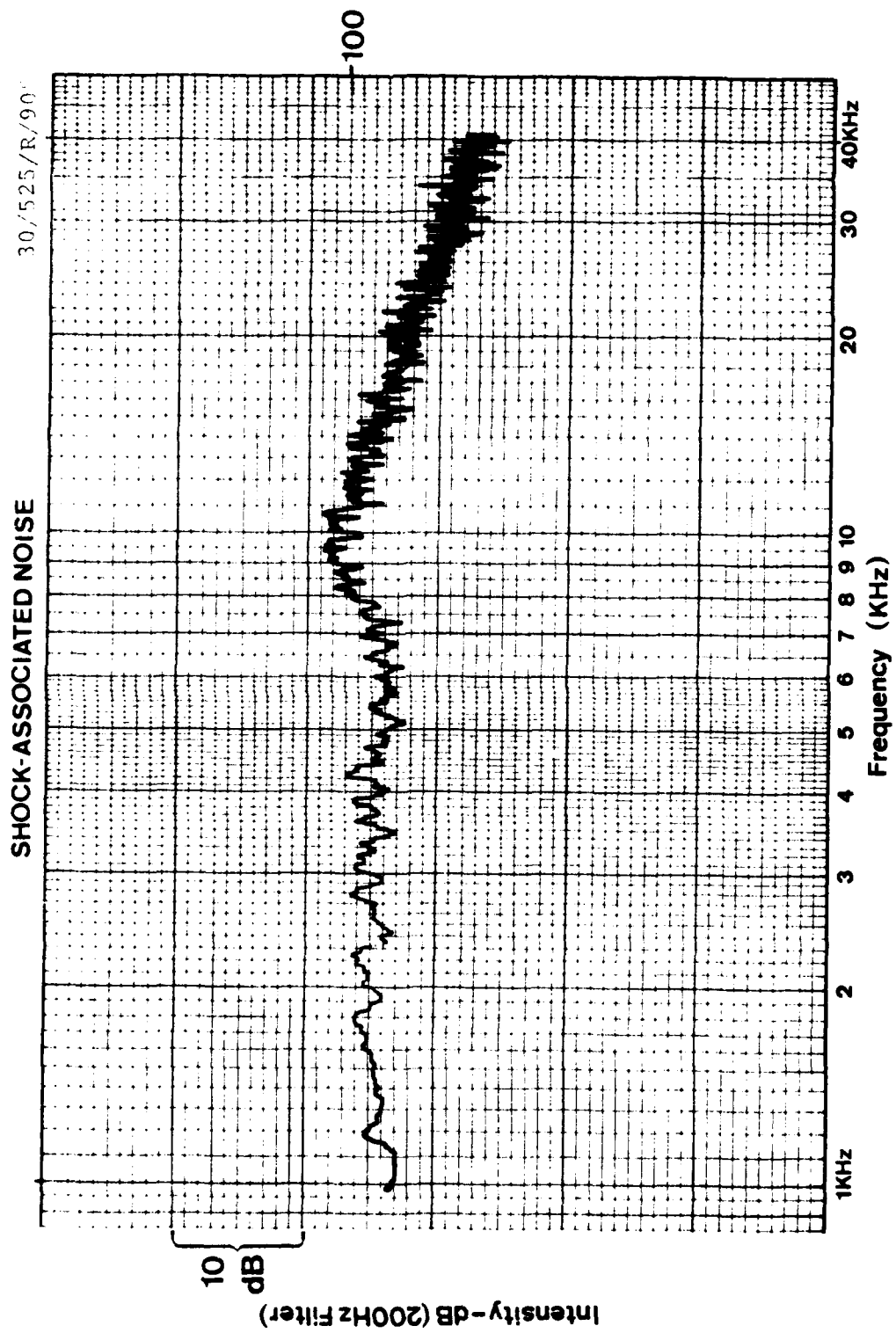
SHOCK-ASSOCIATED NOISE

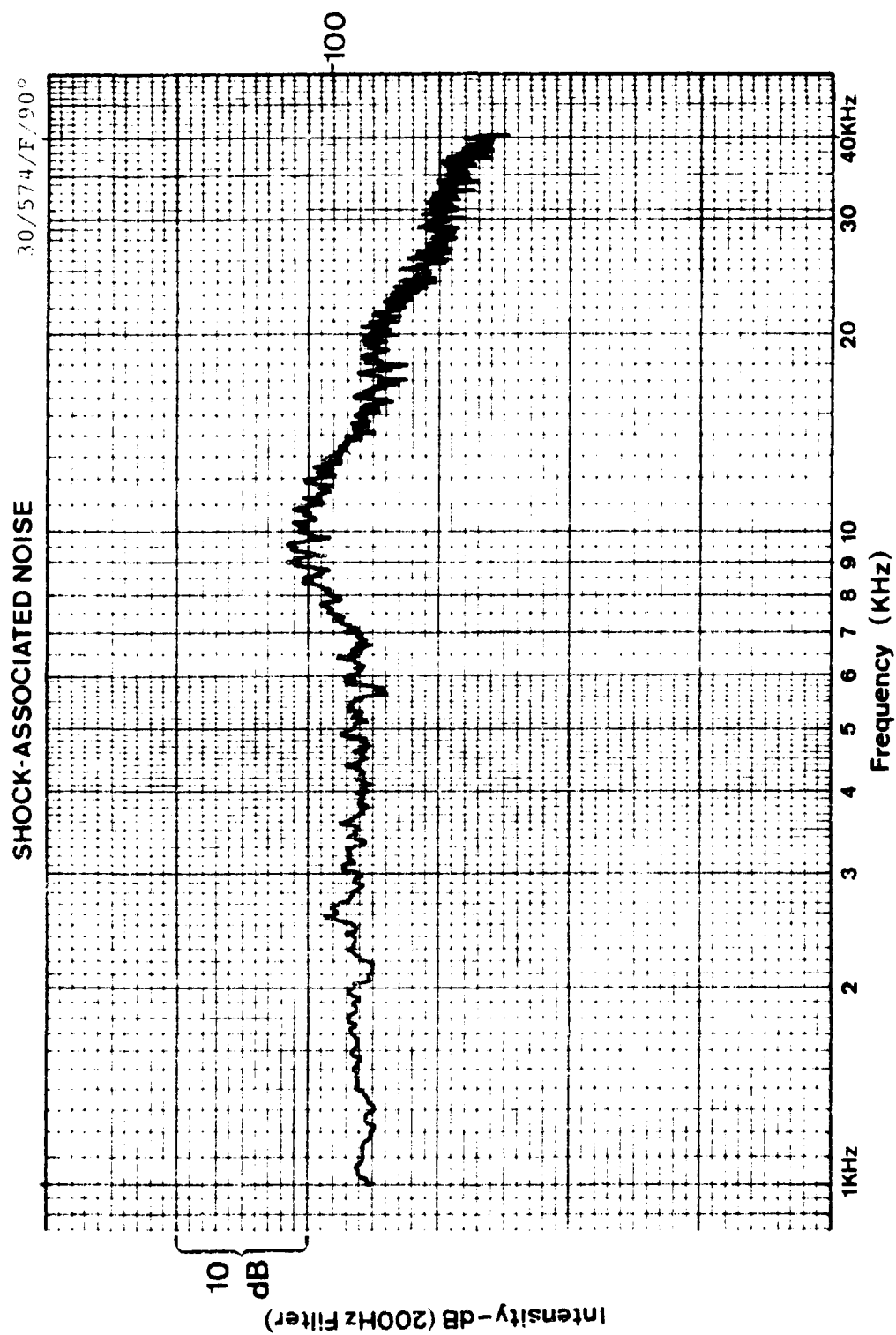


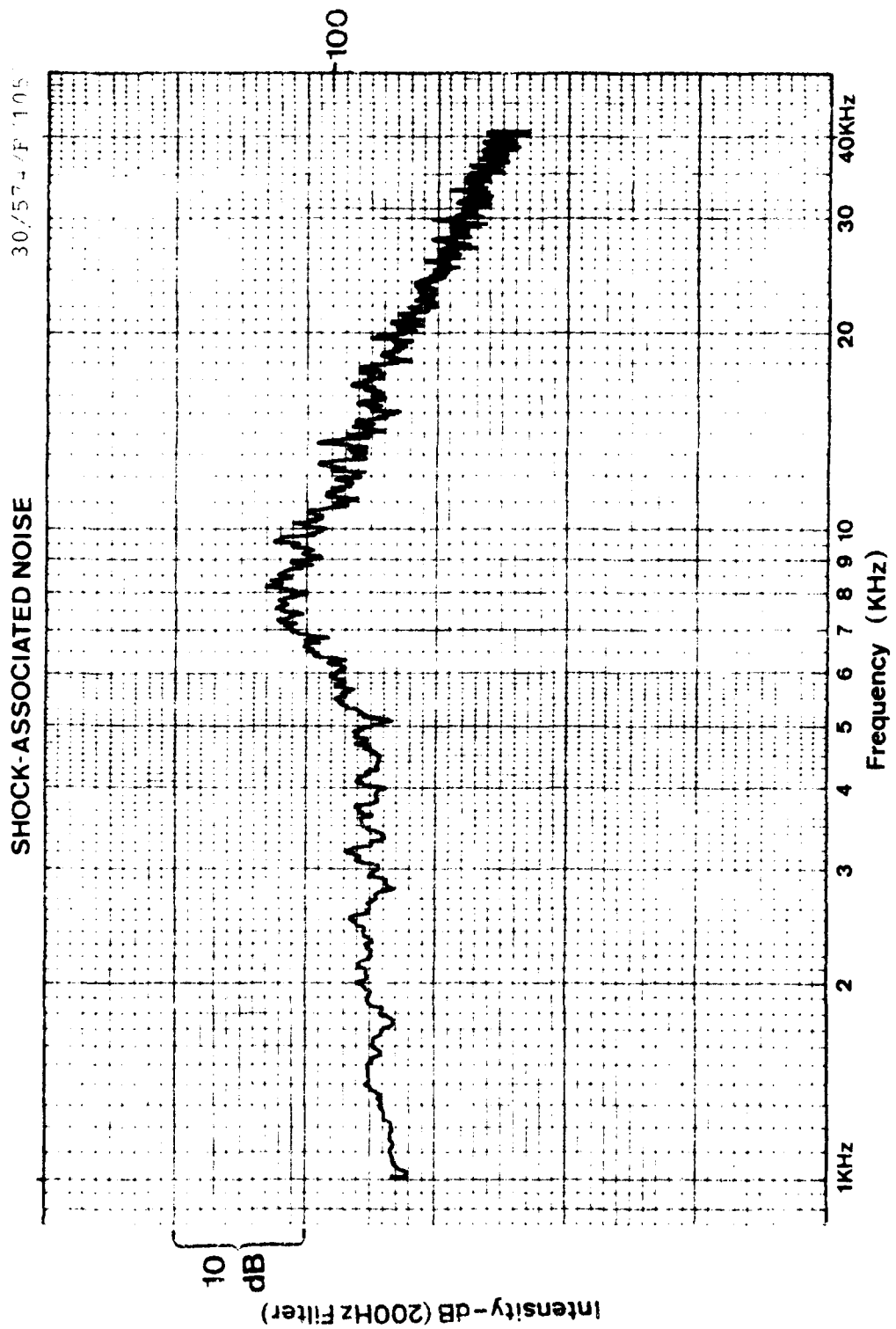


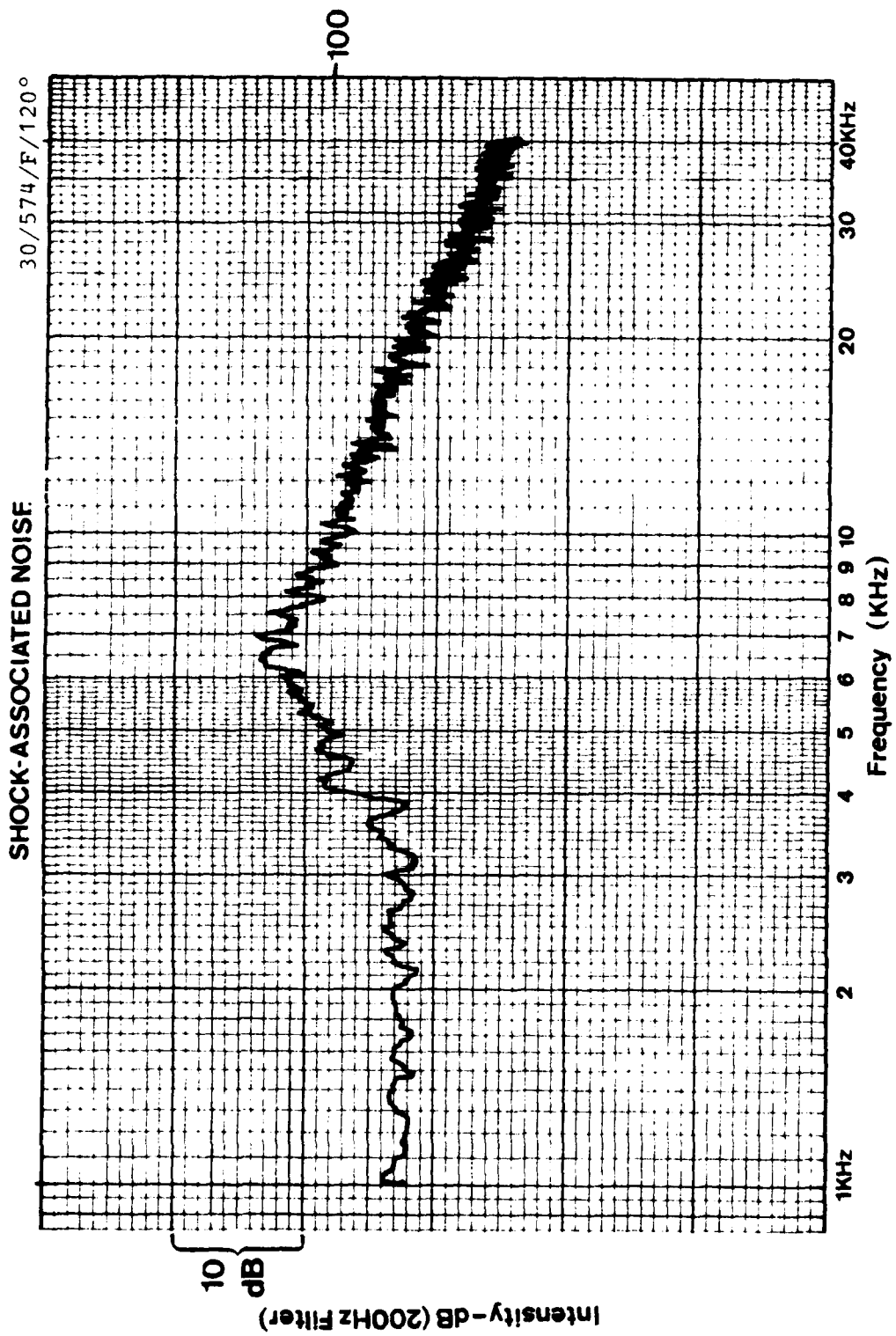
SHOCK-ASSOCIATED NOISE

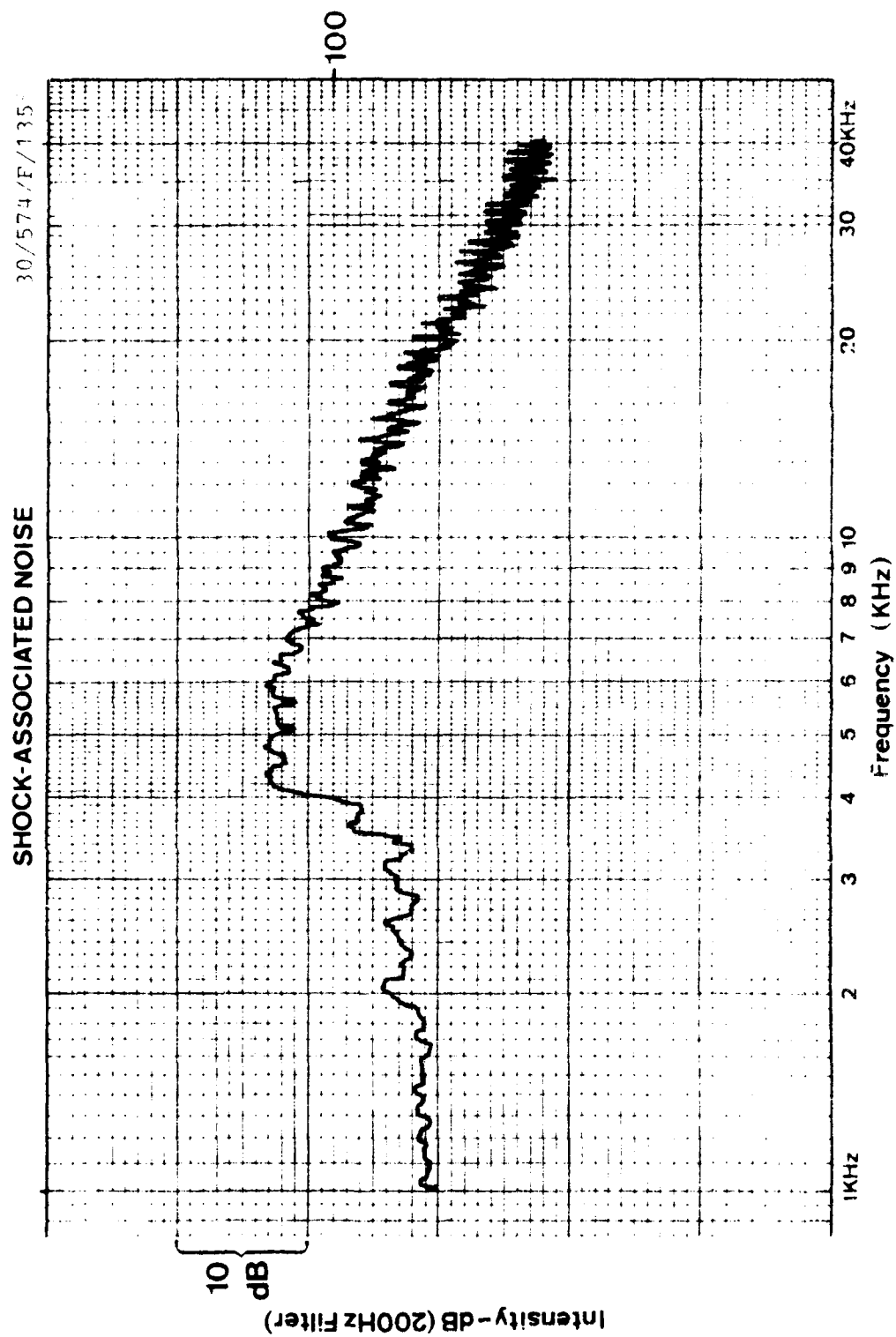


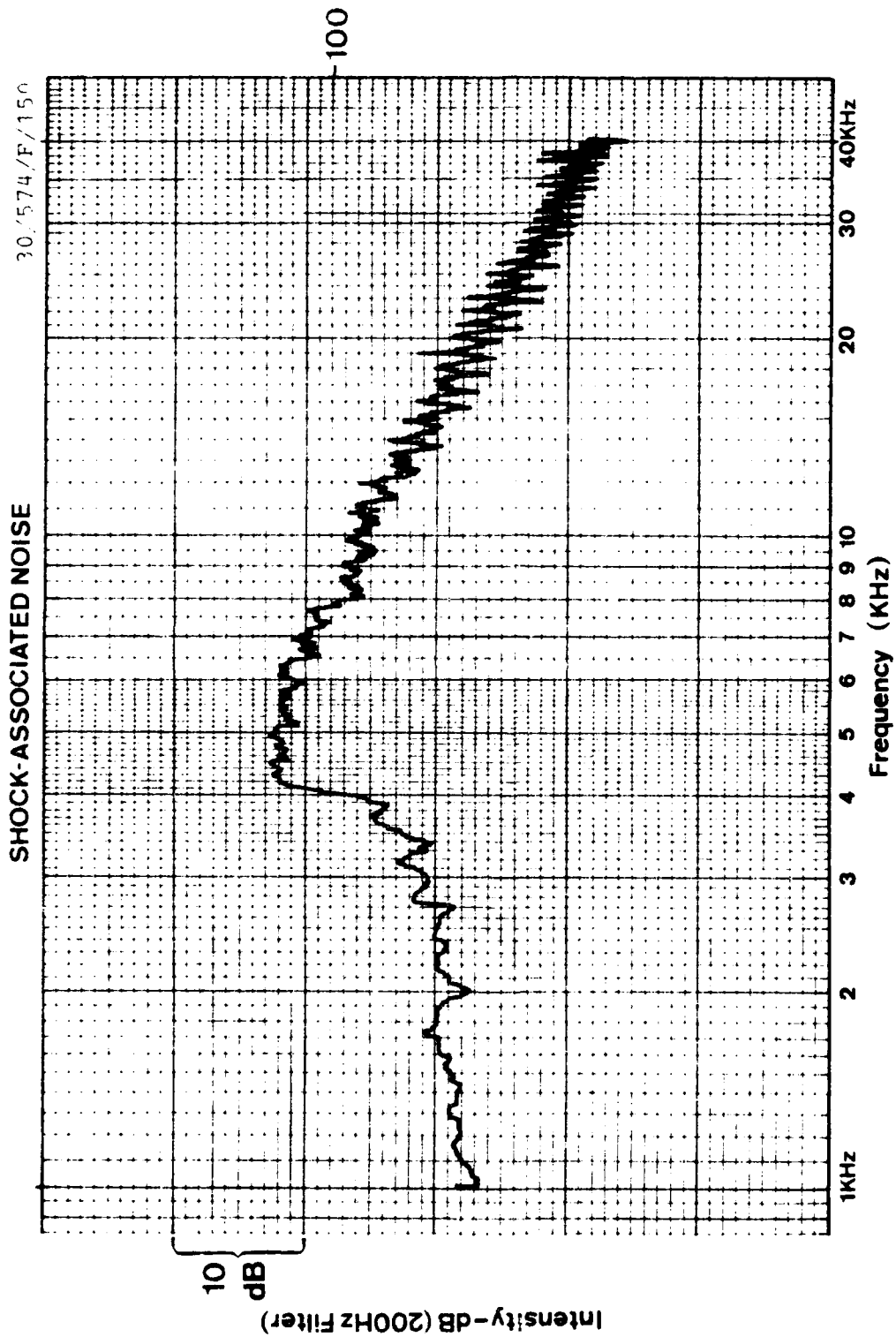


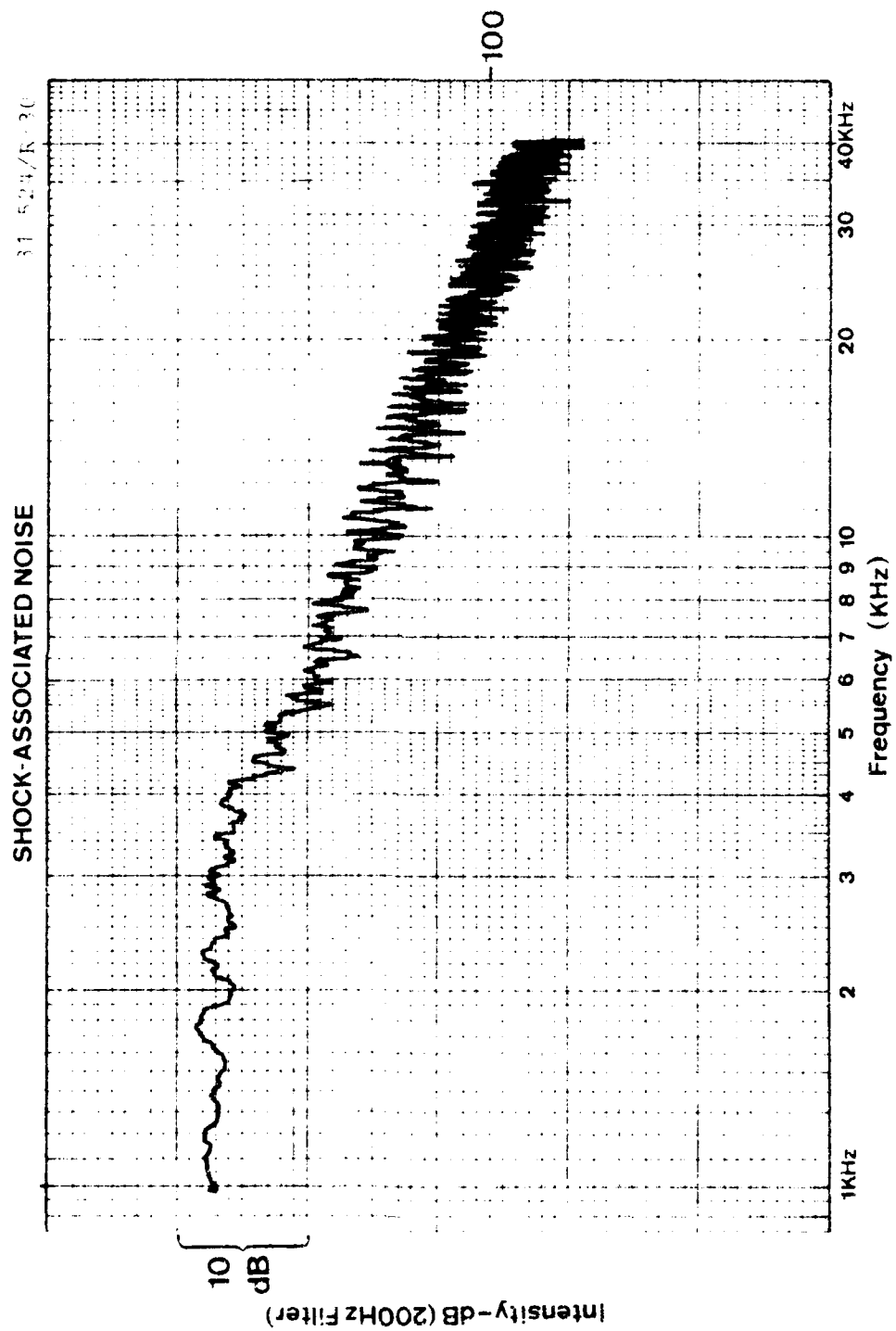


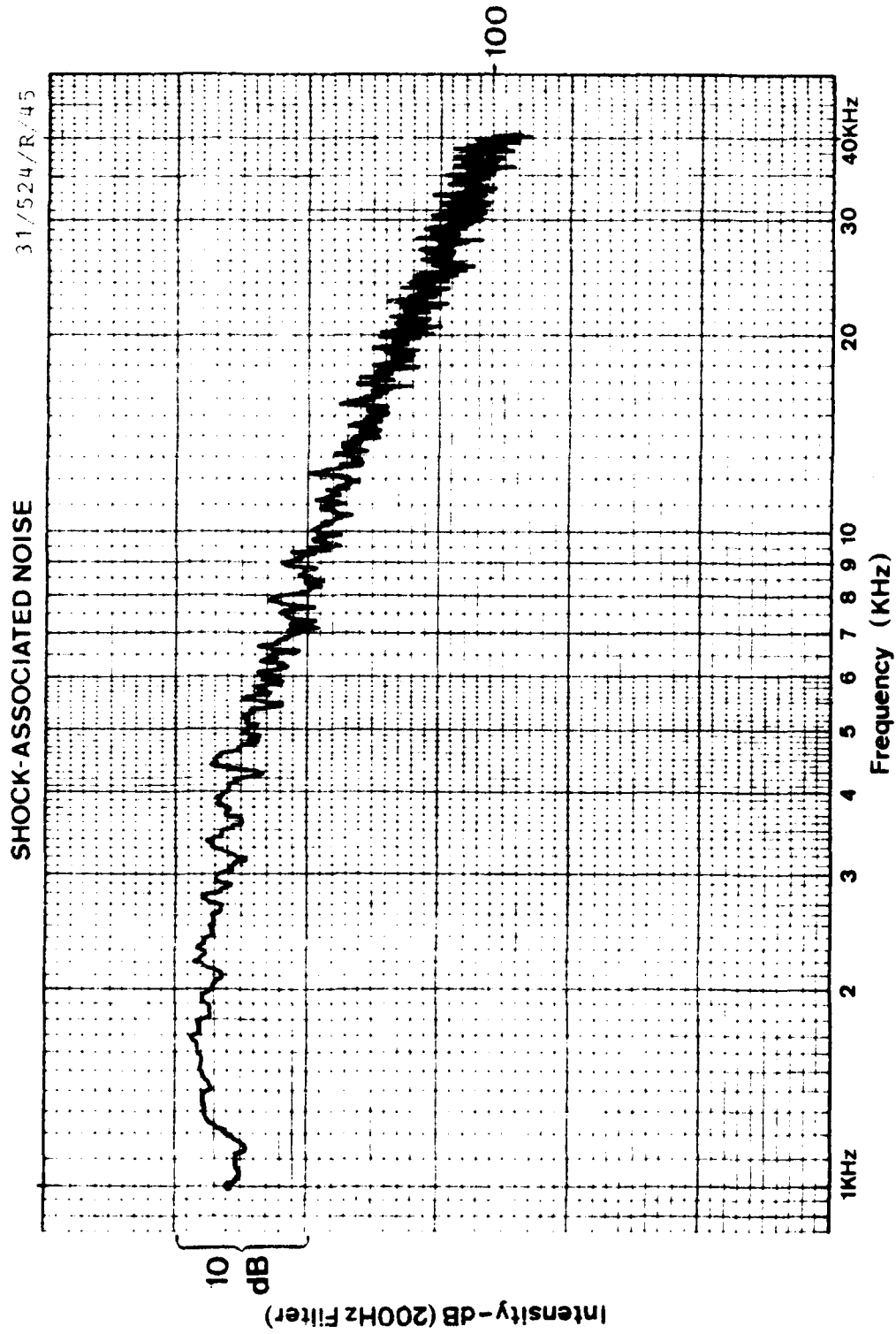


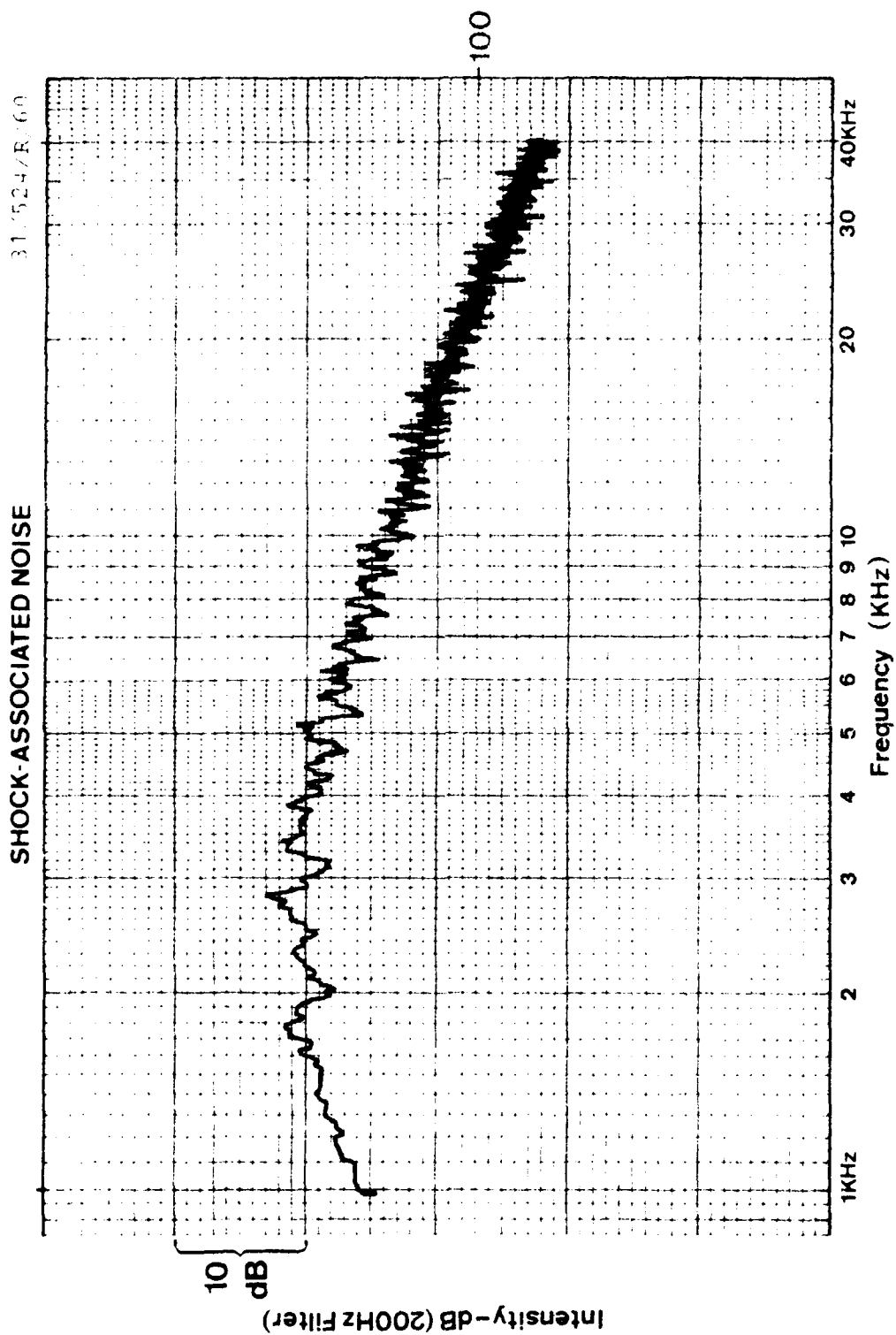




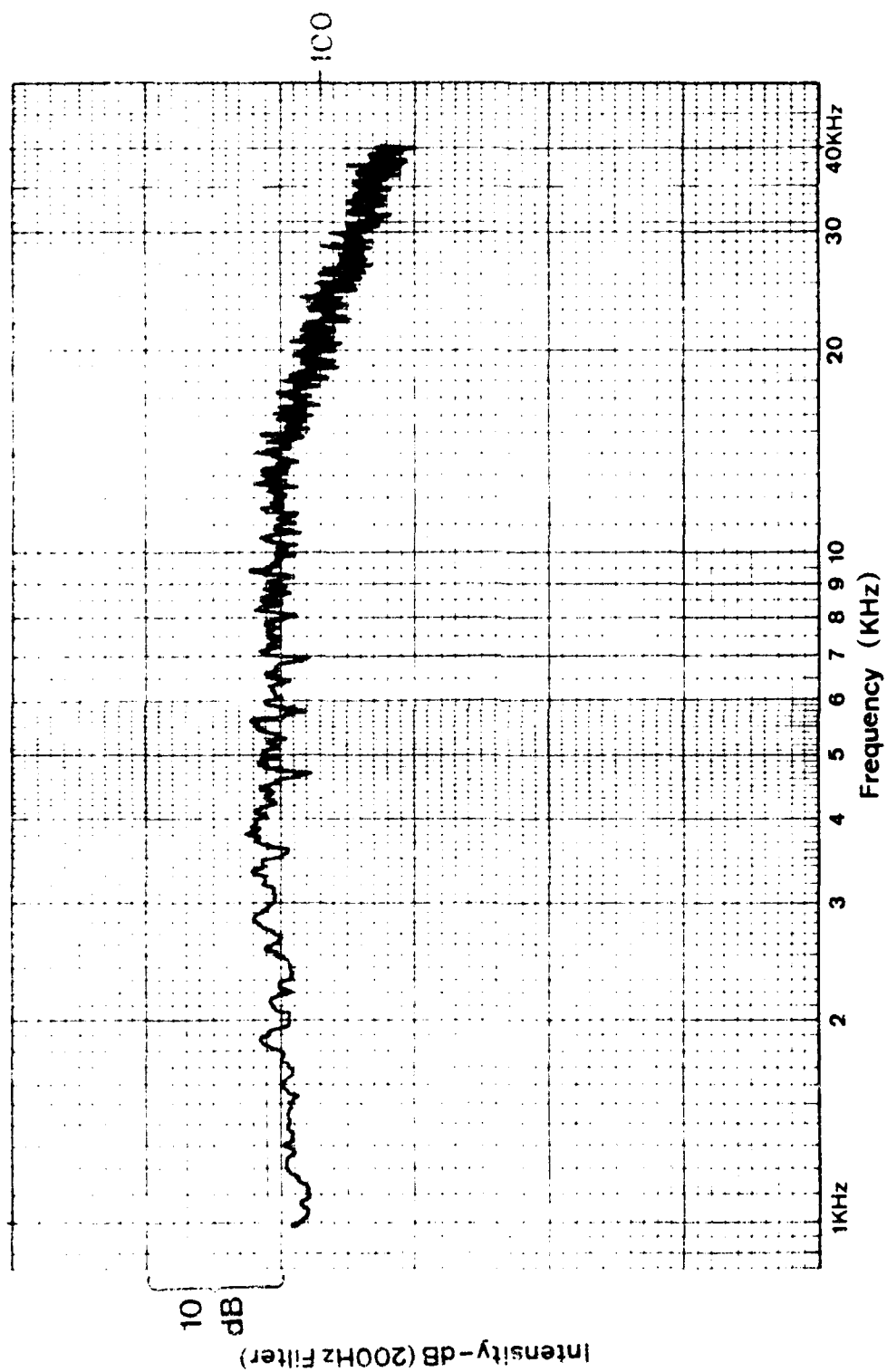


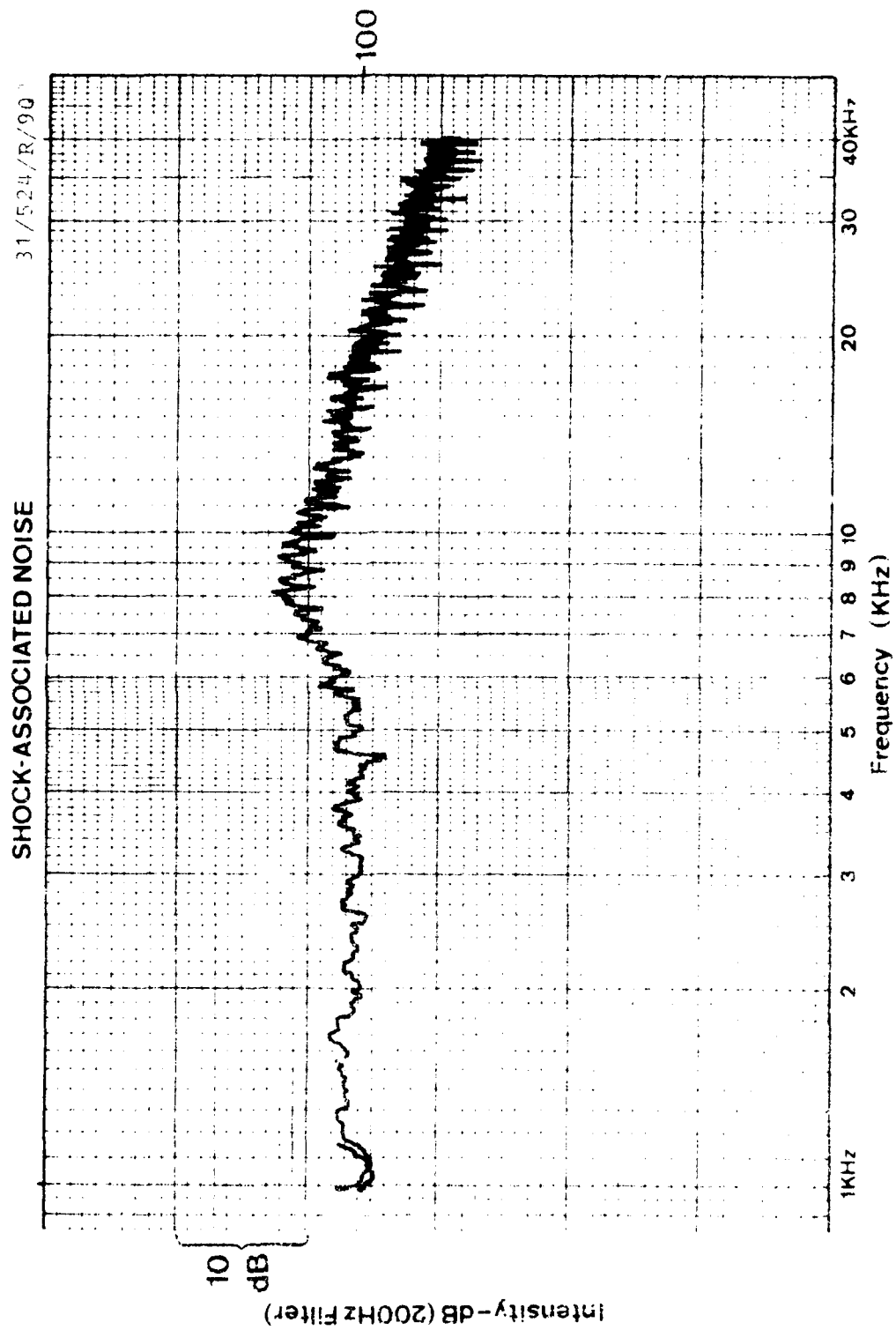






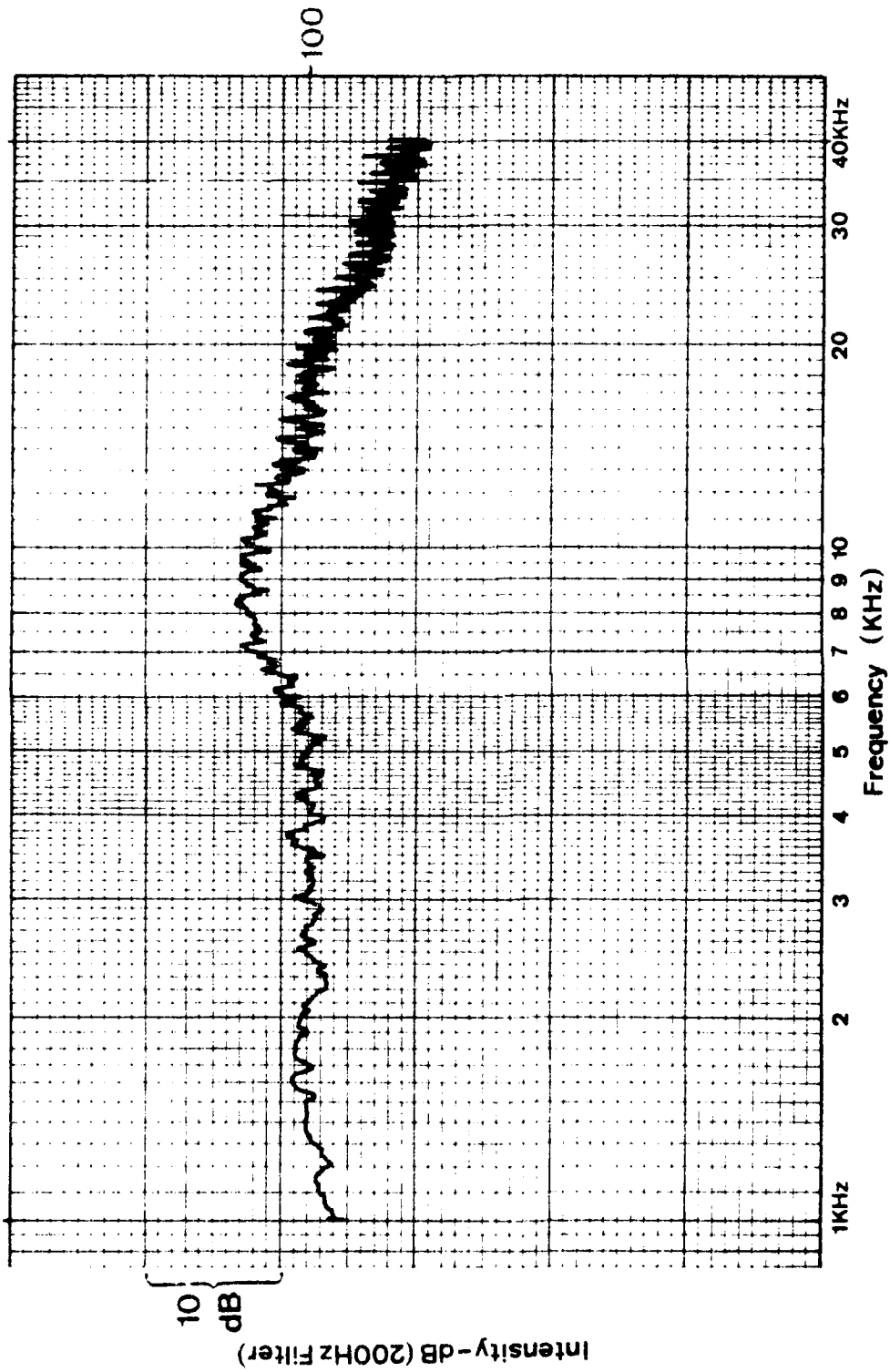
SHOCK-ASSOCIATED NOISE

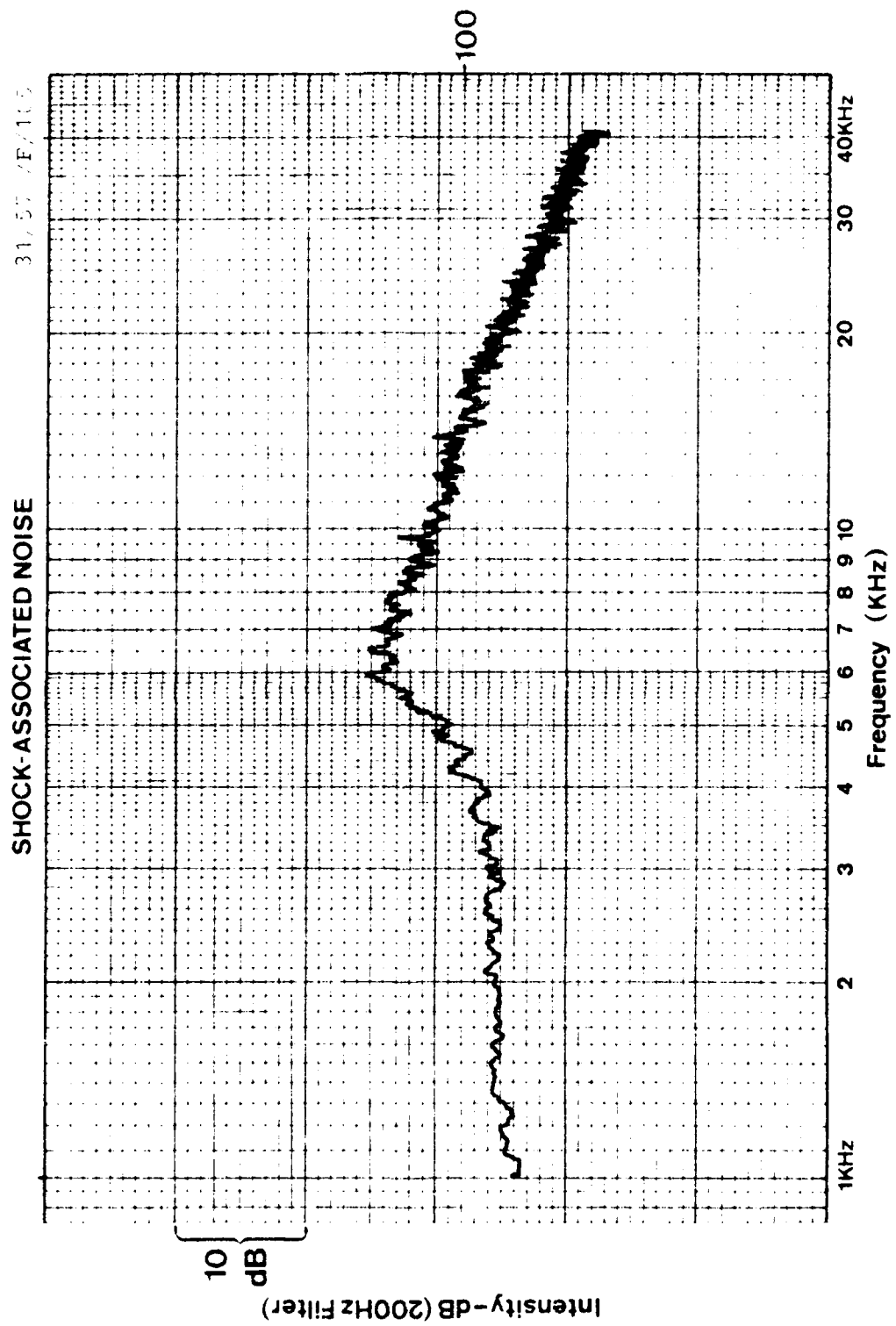


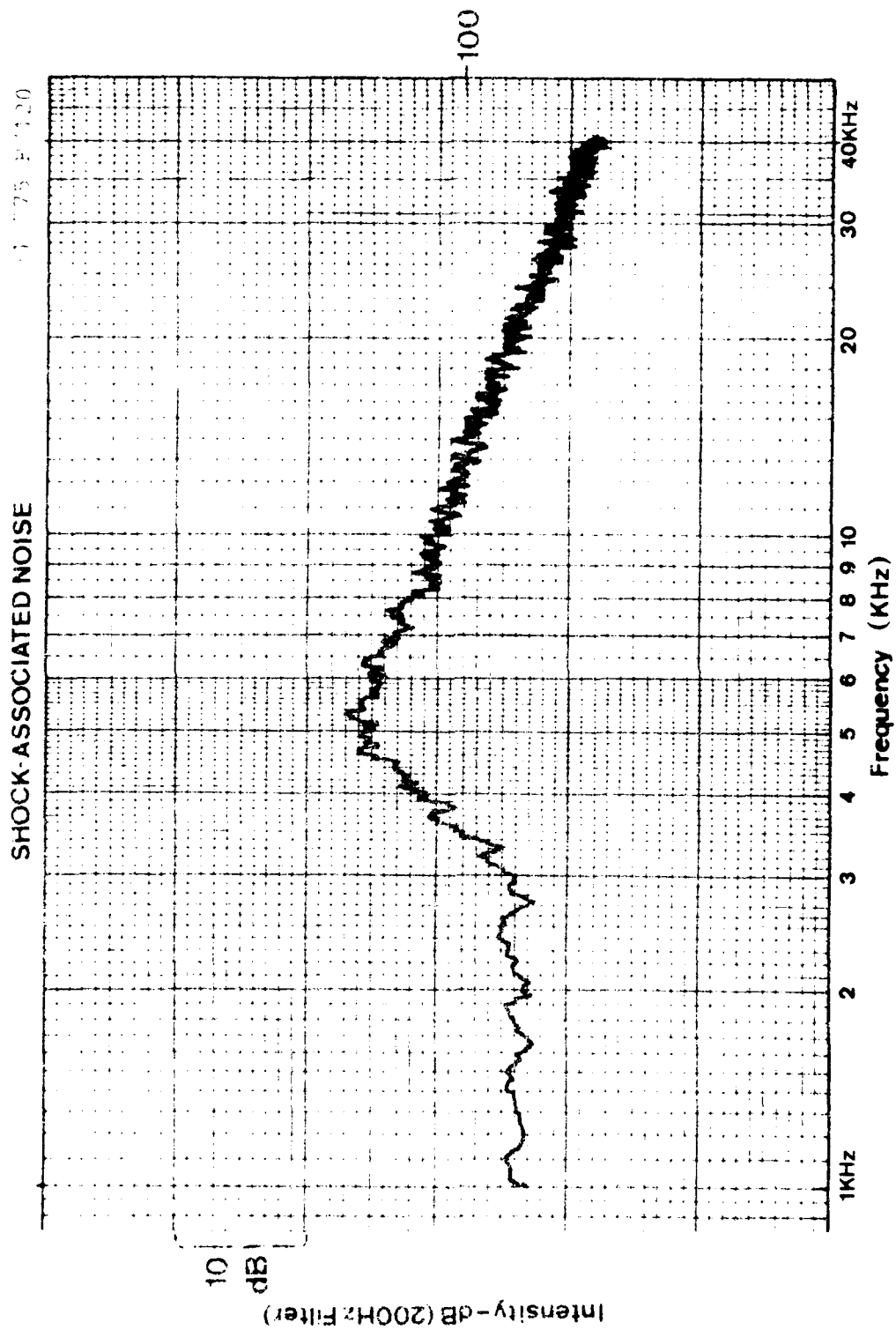


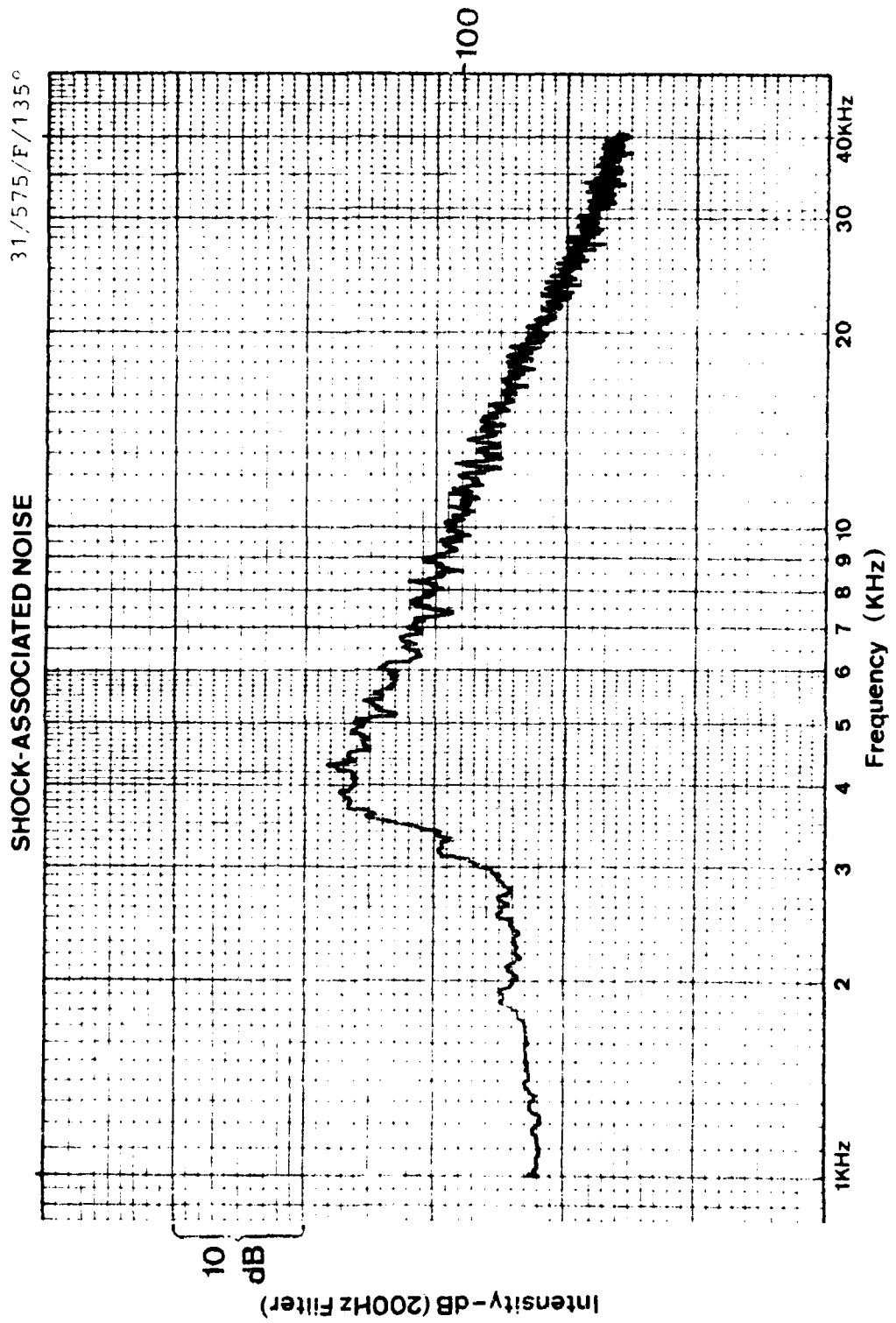
SHOCK-ASSOCIATED NOISE

31/575, F/90

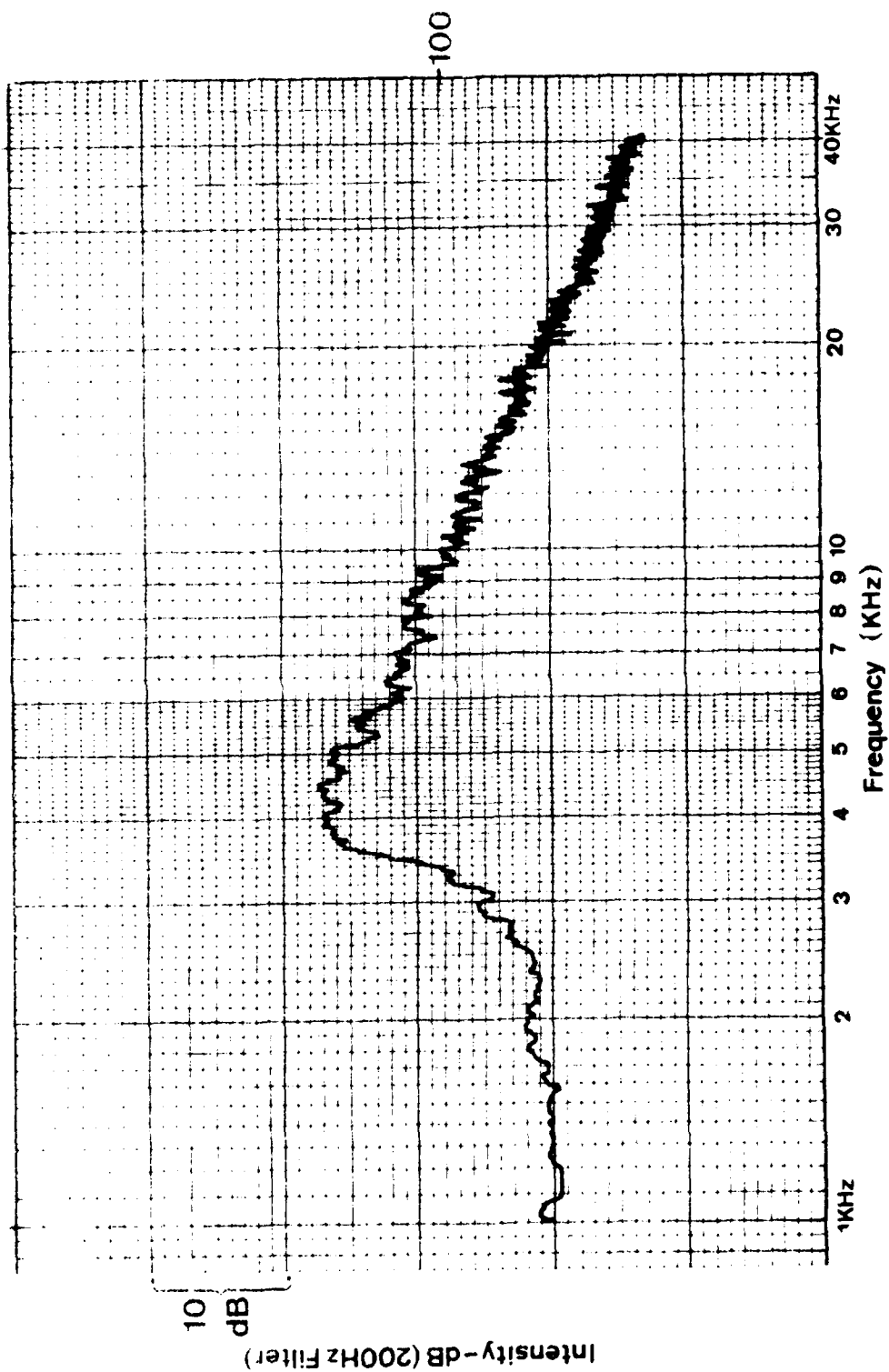


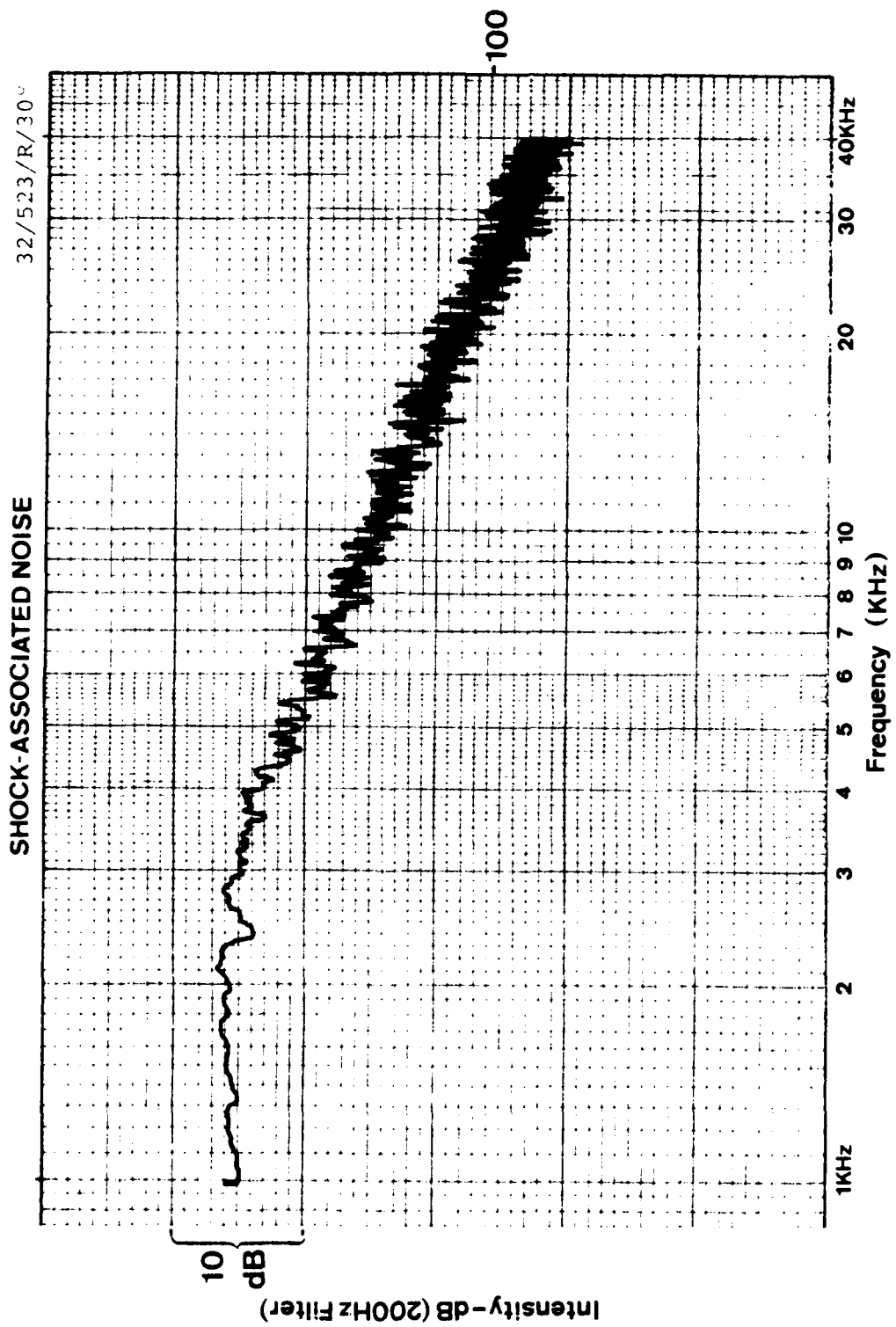






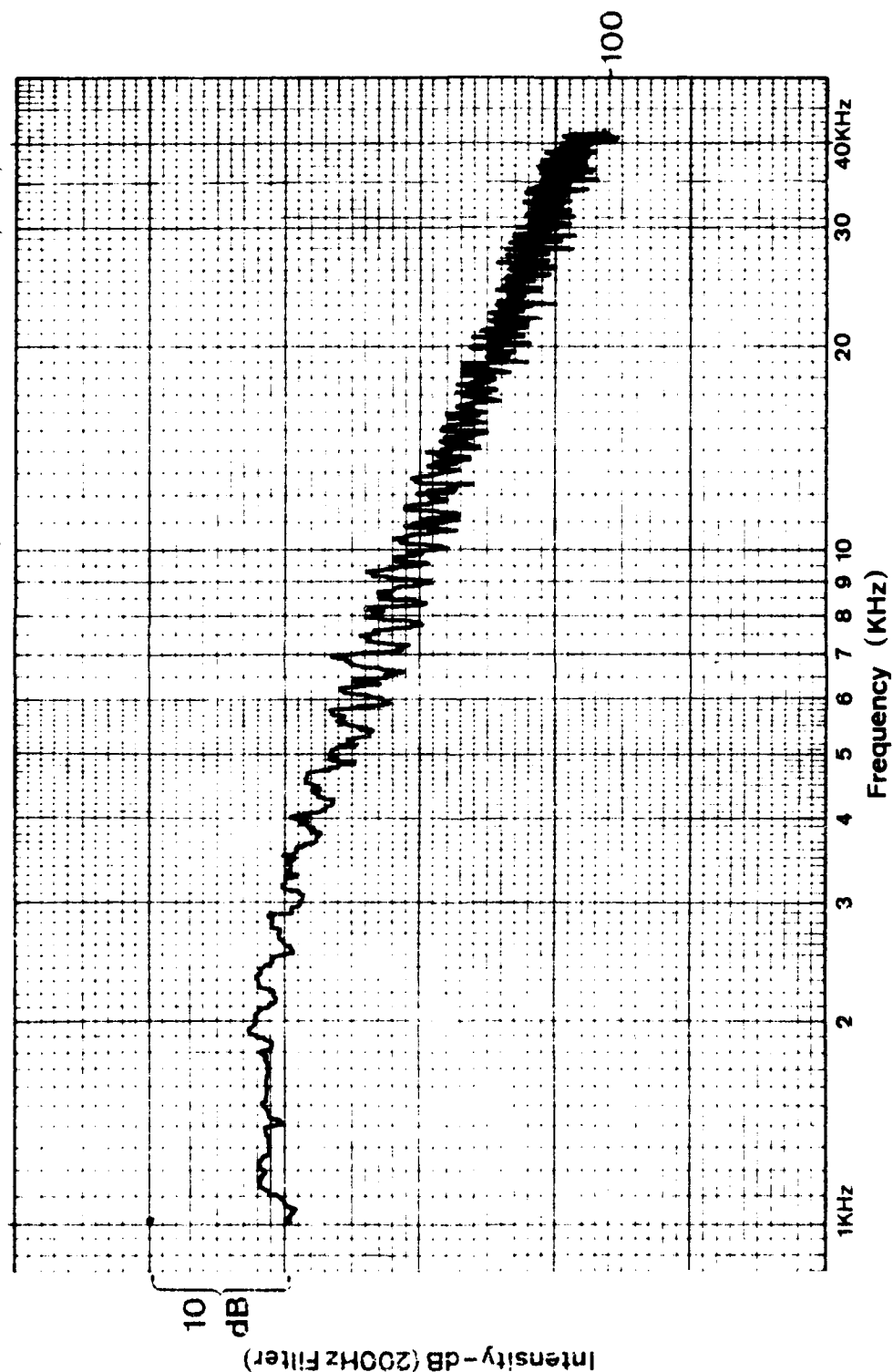
SHOCK-ASSOCIATED NOISE





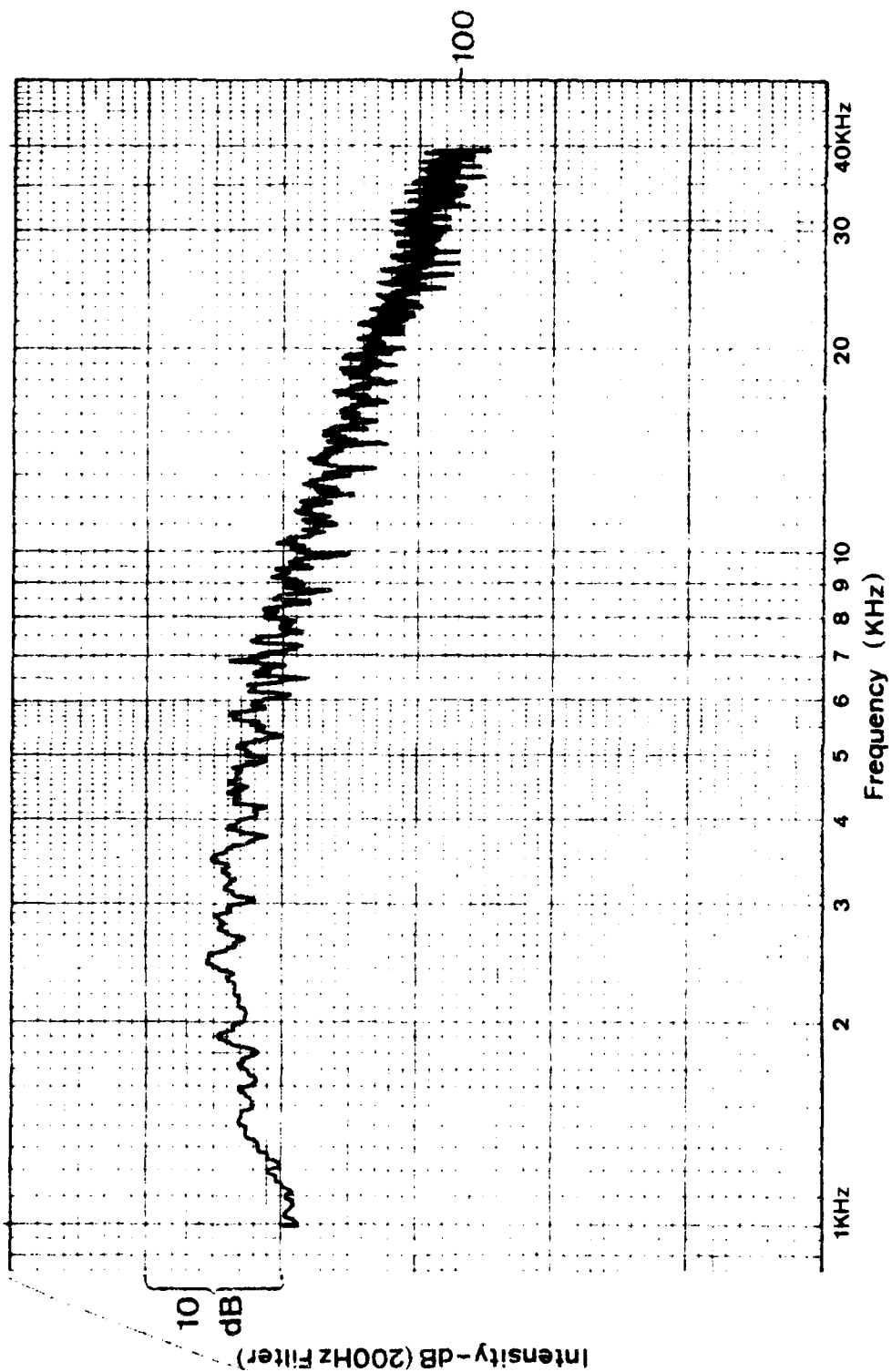
SHOCK-ASSOCIATED NOISE

32/523/P/45



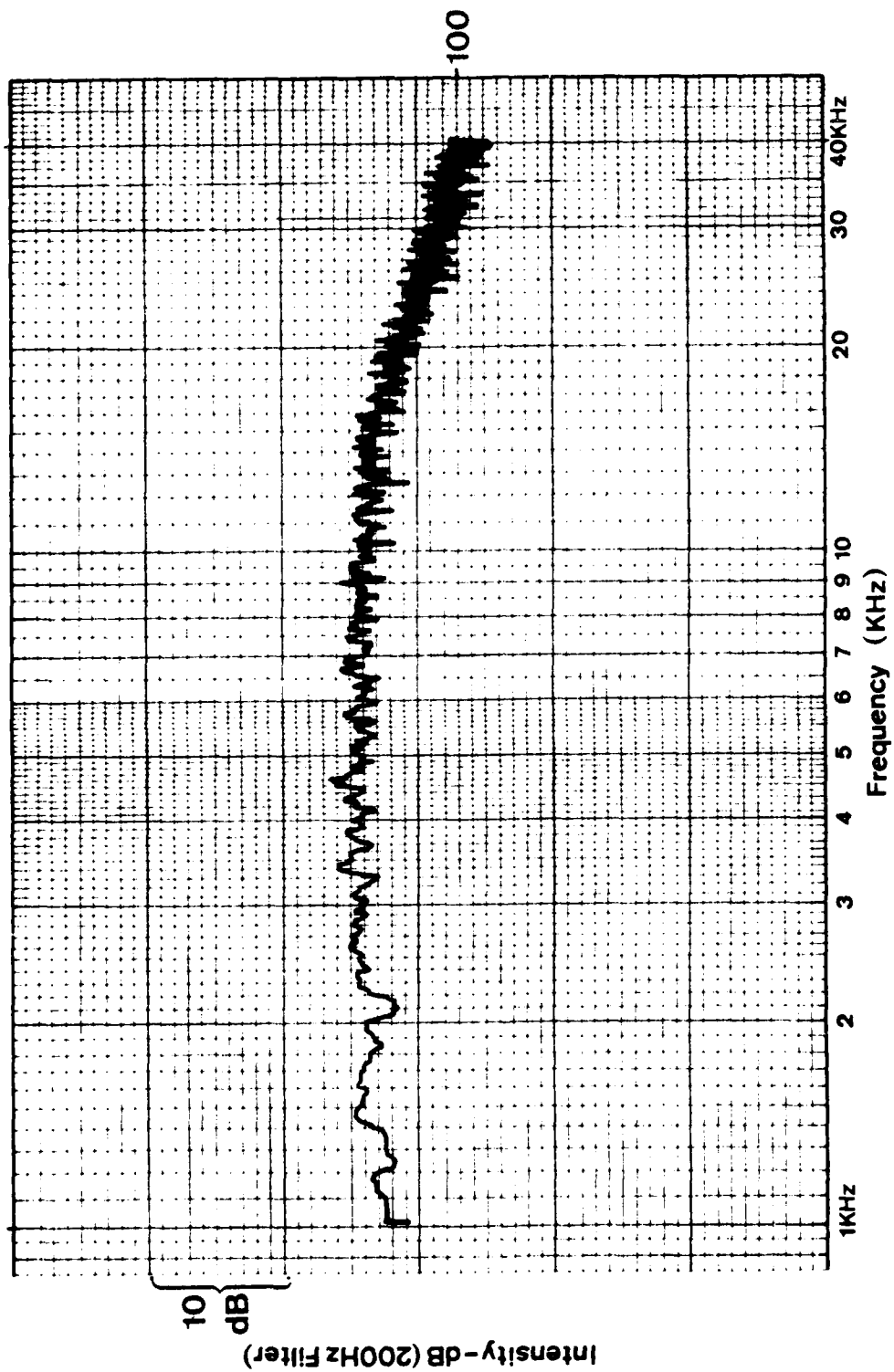
SHOCK-ASSOCIATED NOISE

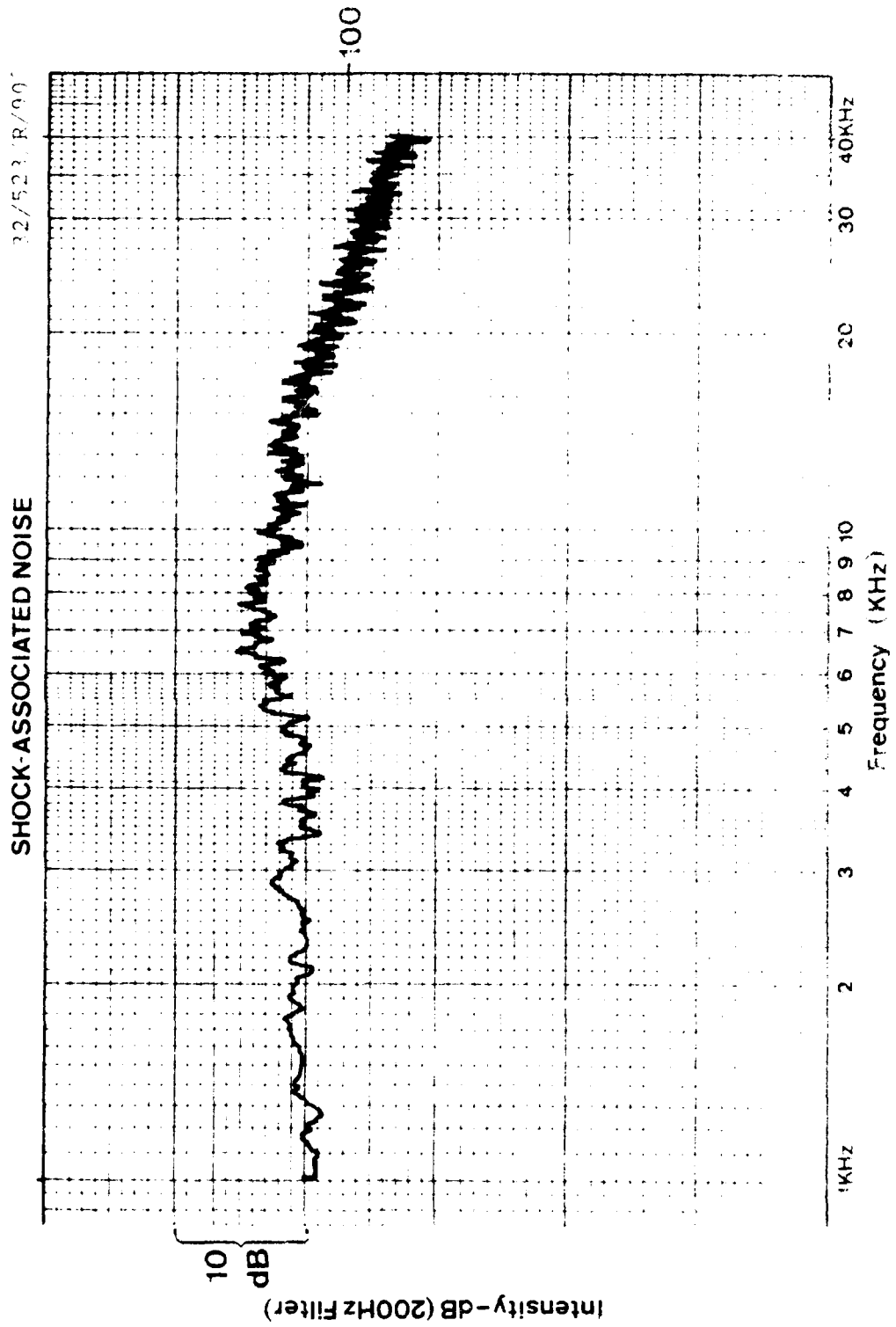
32/523/R/60



32/523/R/75°

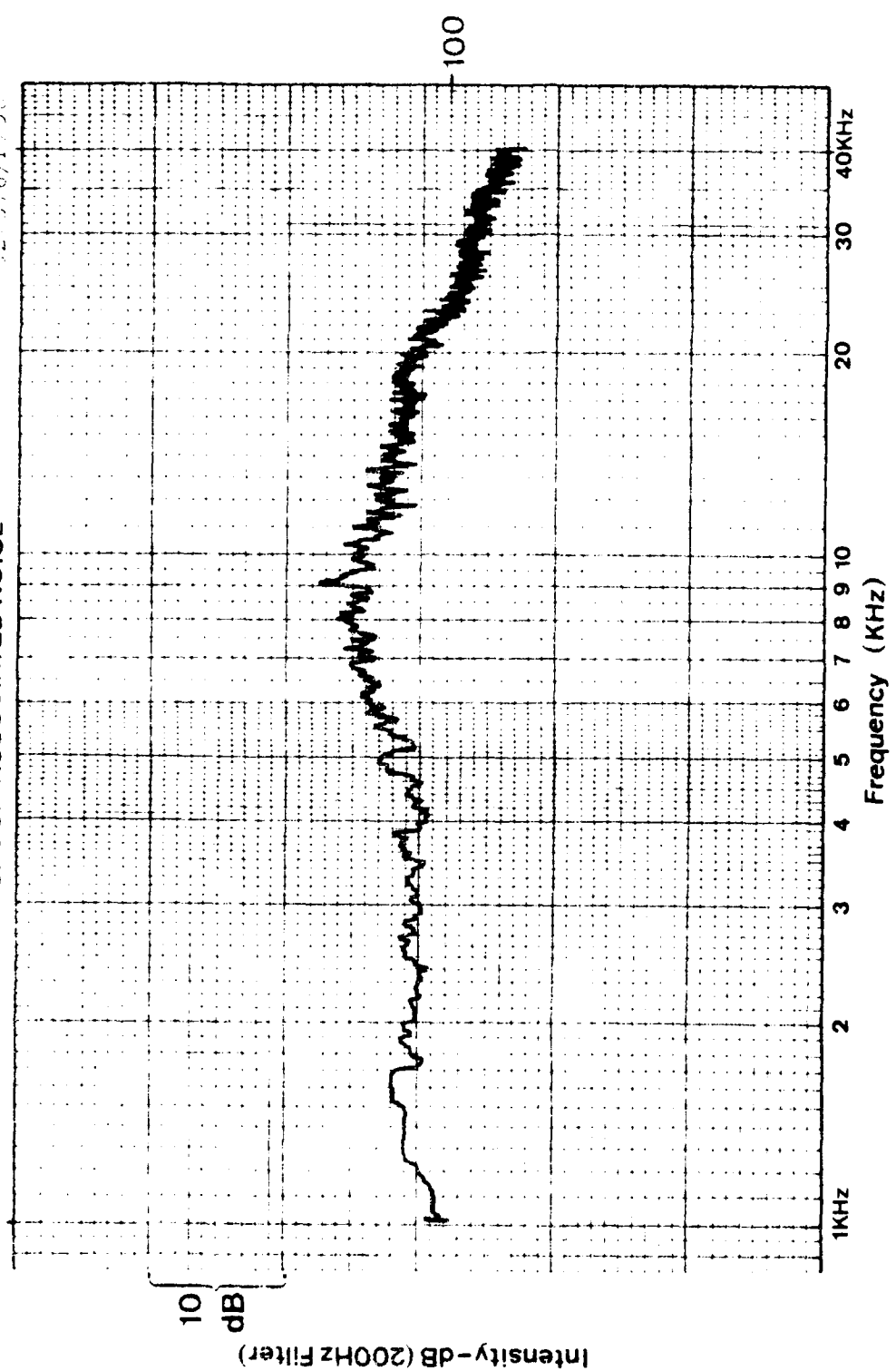
SHOCK-ASSOCIATED NOISE





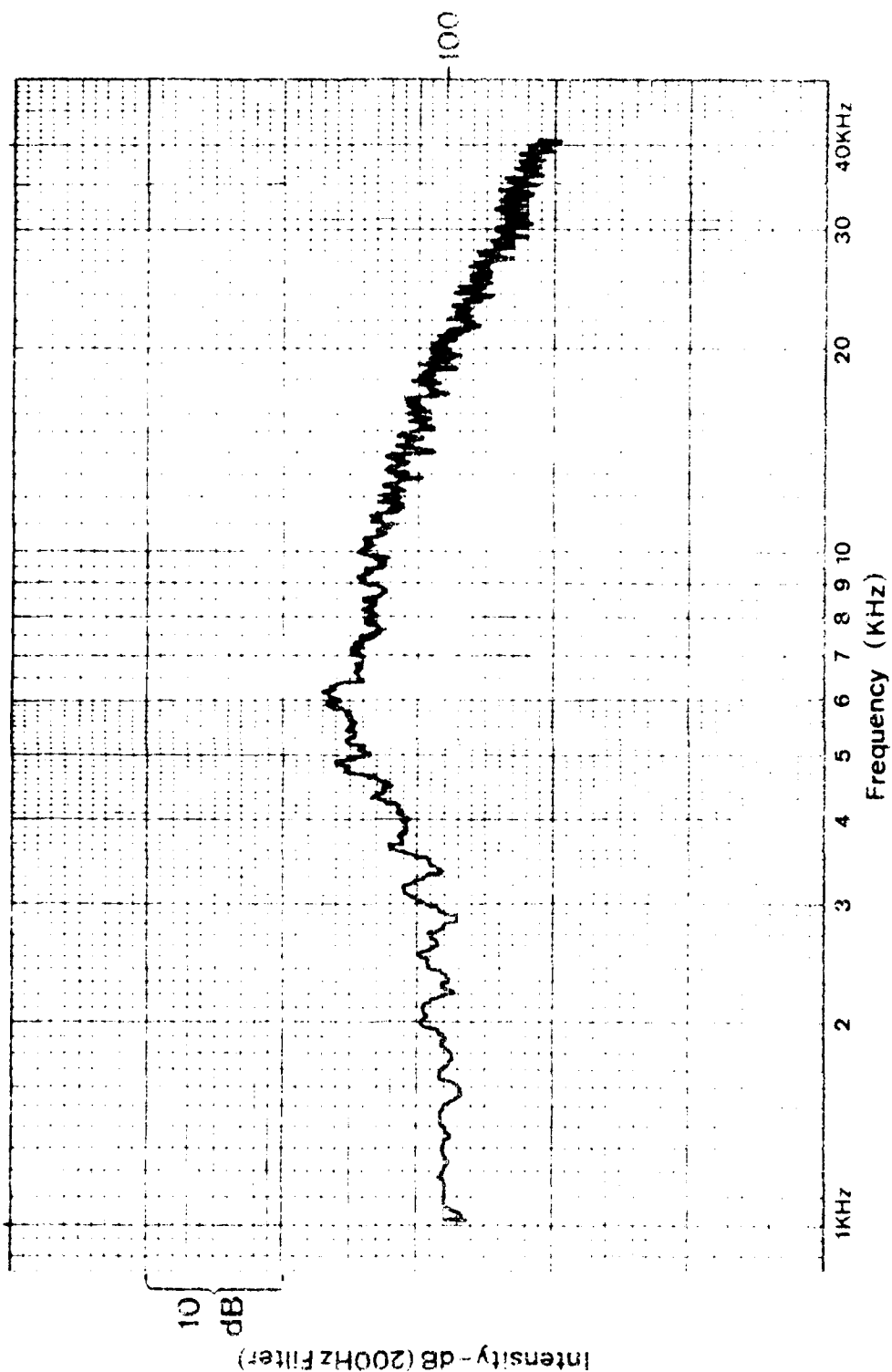
SHOCK-ASSOCIATED NOISE

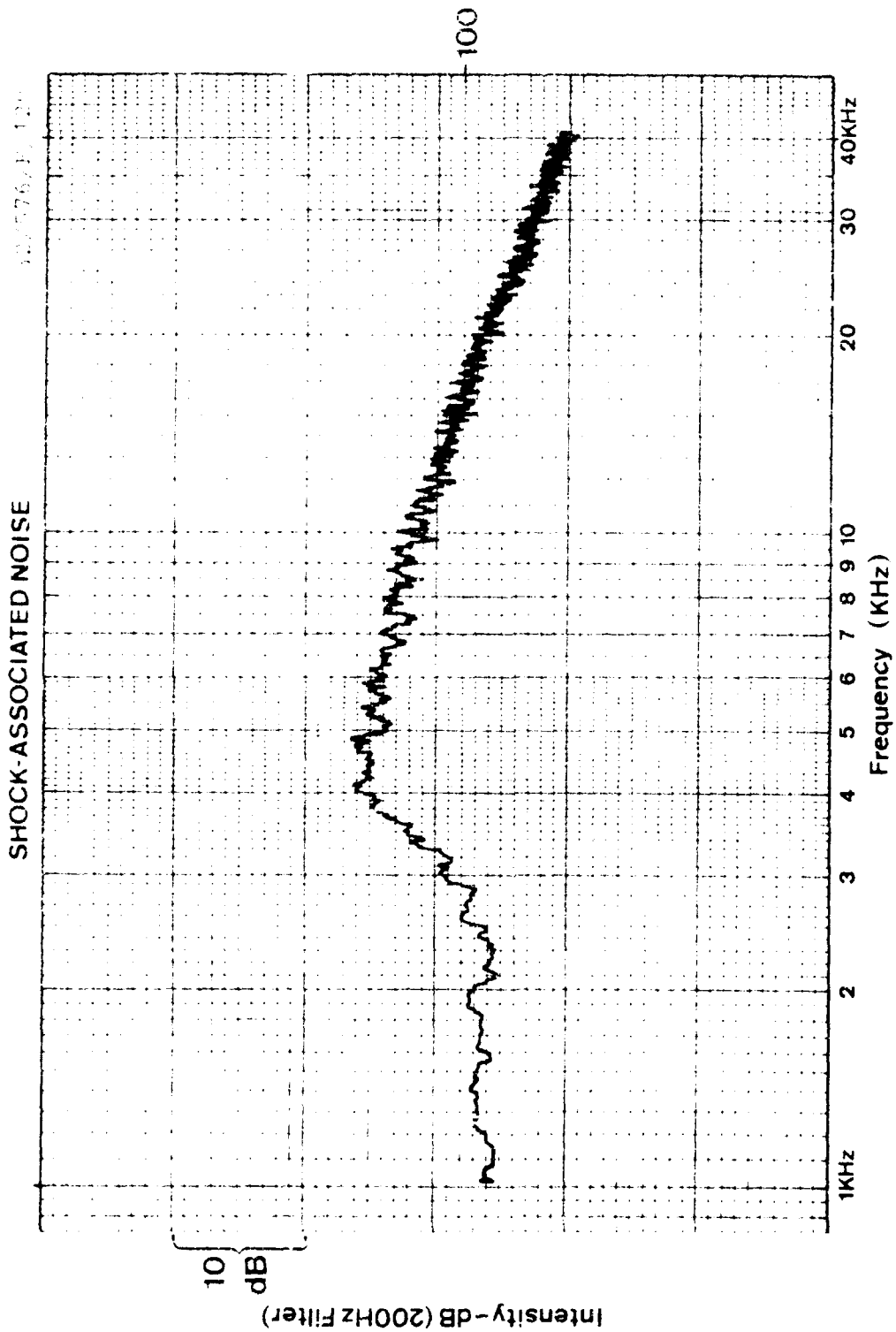
324576/P750



SHOCK-ASSOCIATED NOISE

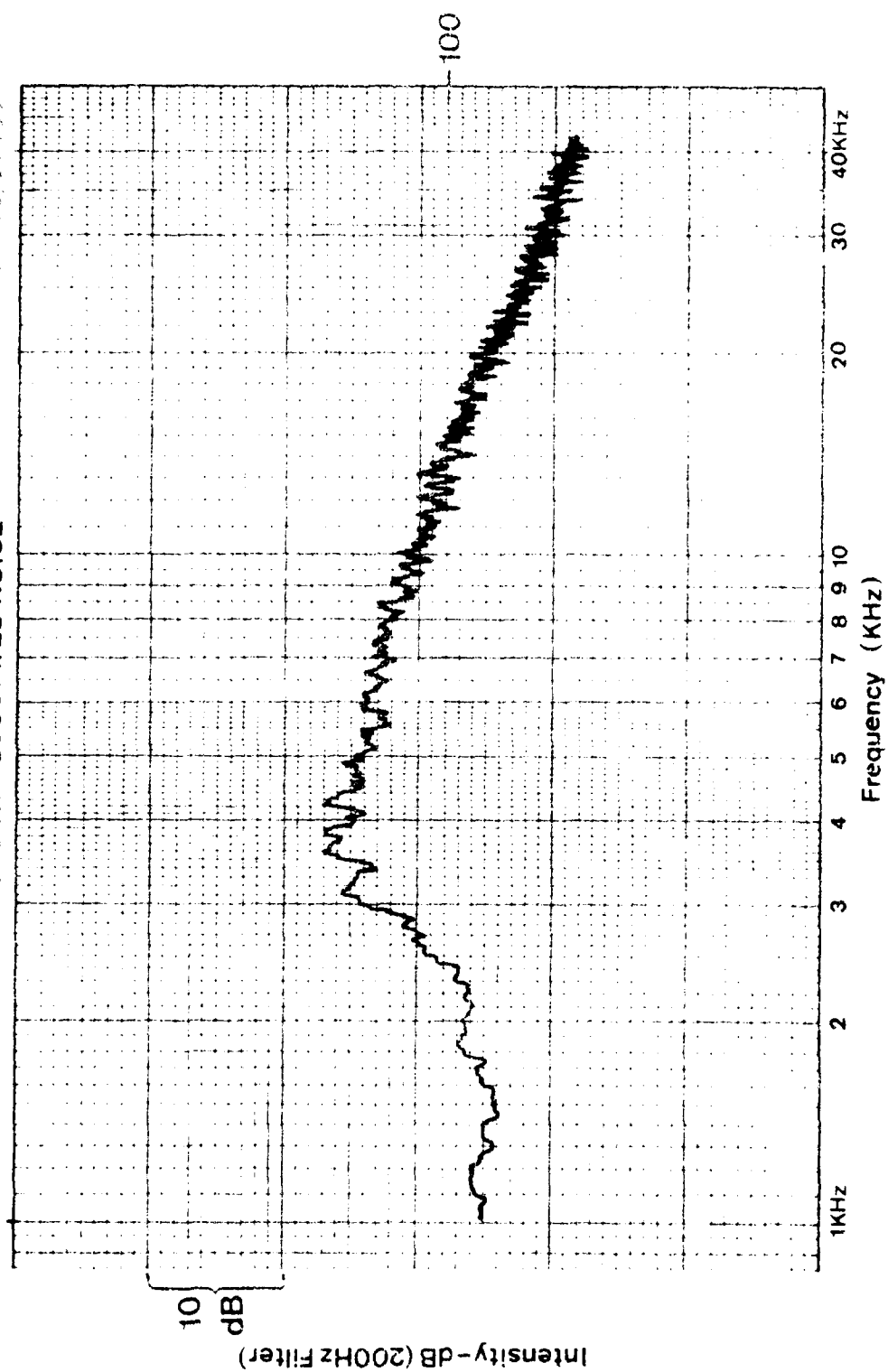
12-5767-1-105

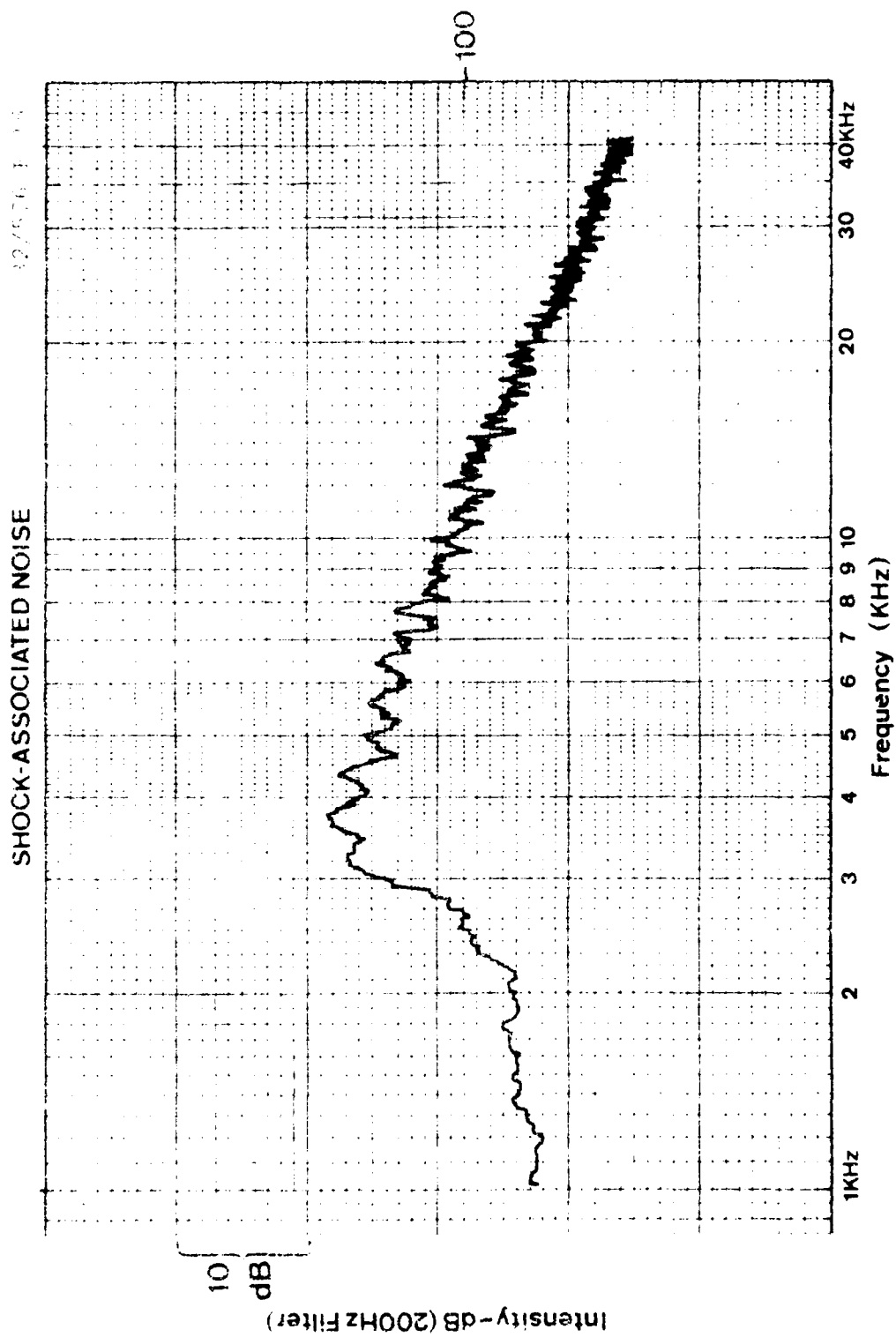




SHOCK-ASSOCIATED NOISE

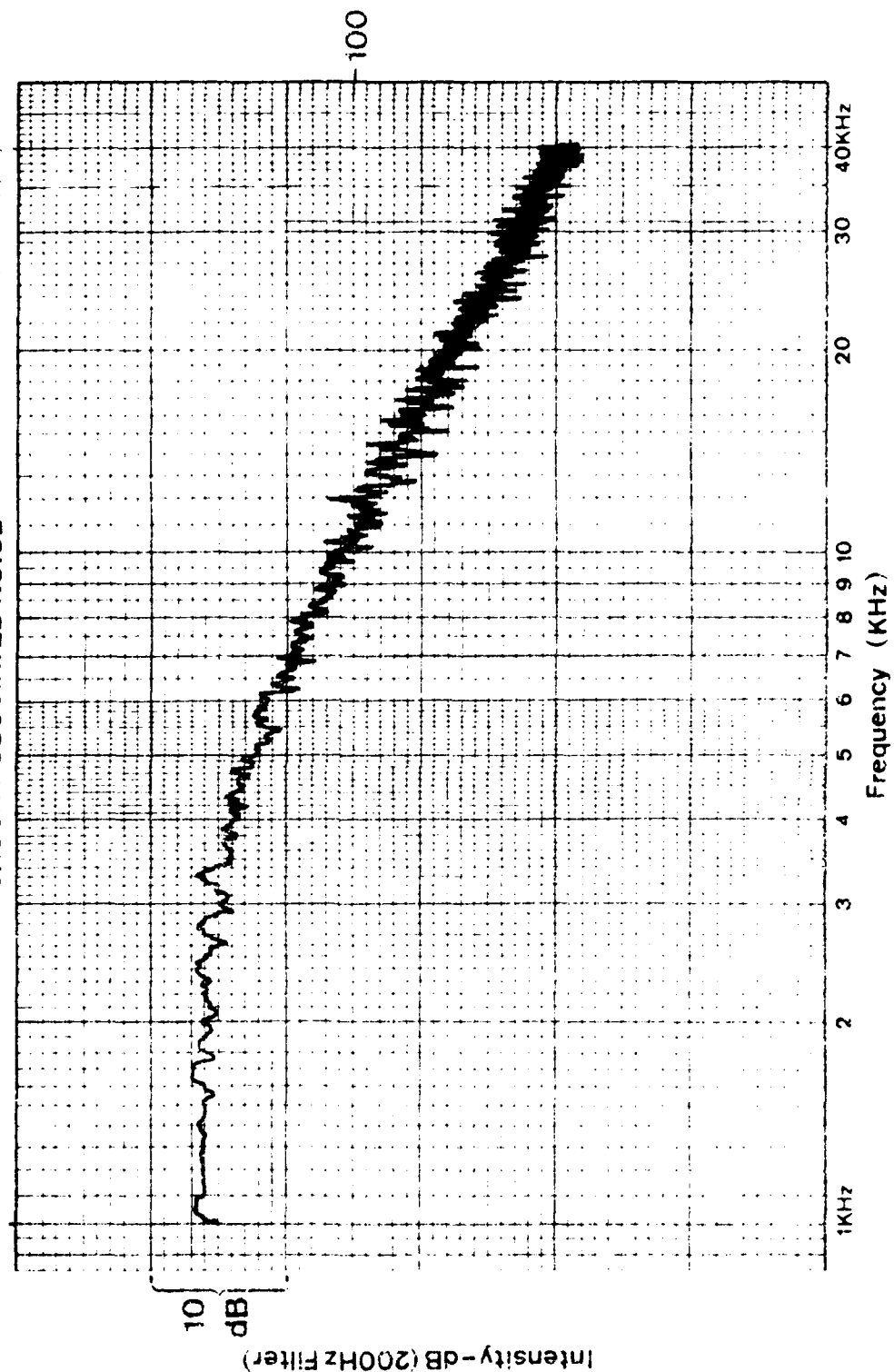
92-576, P. 135

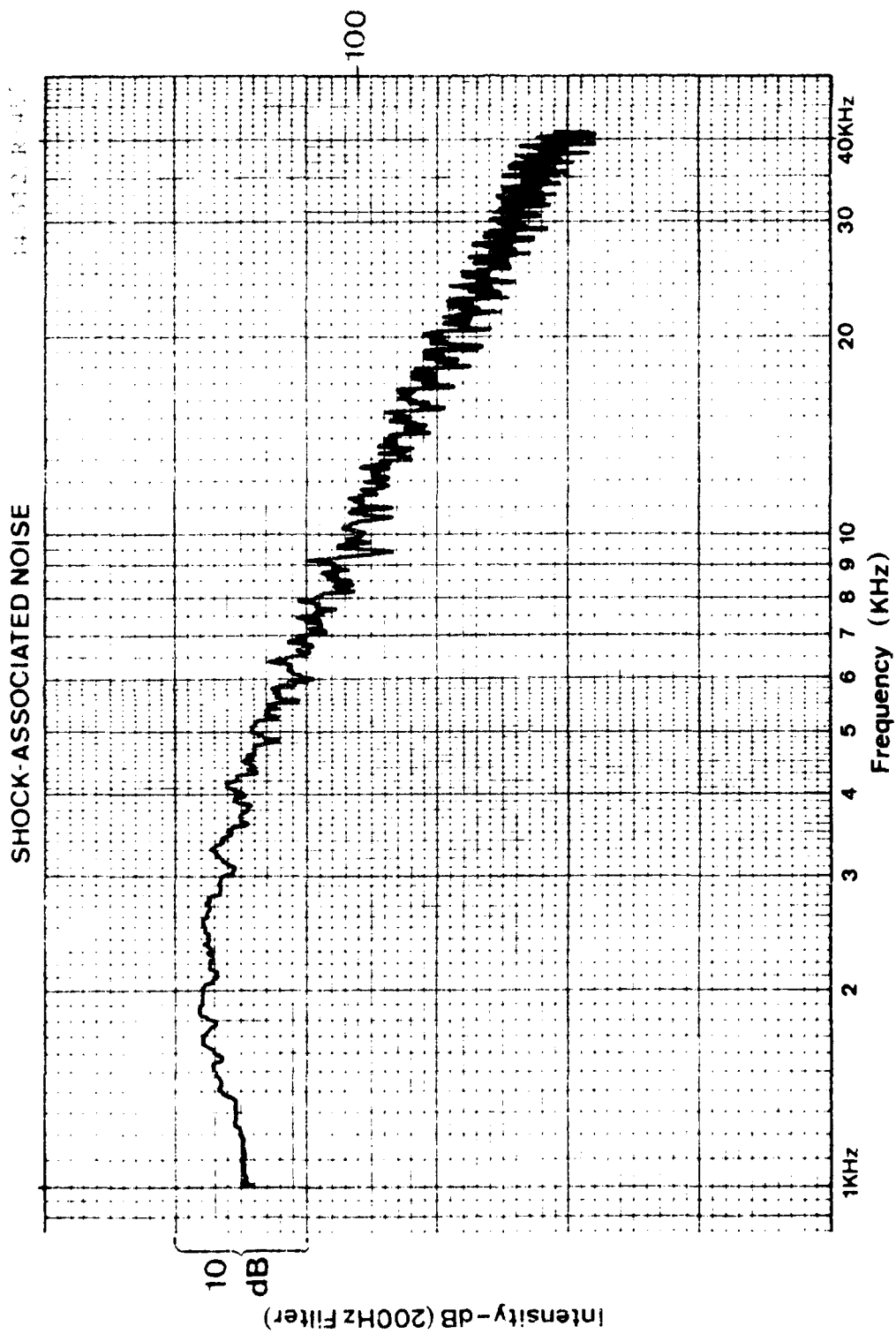


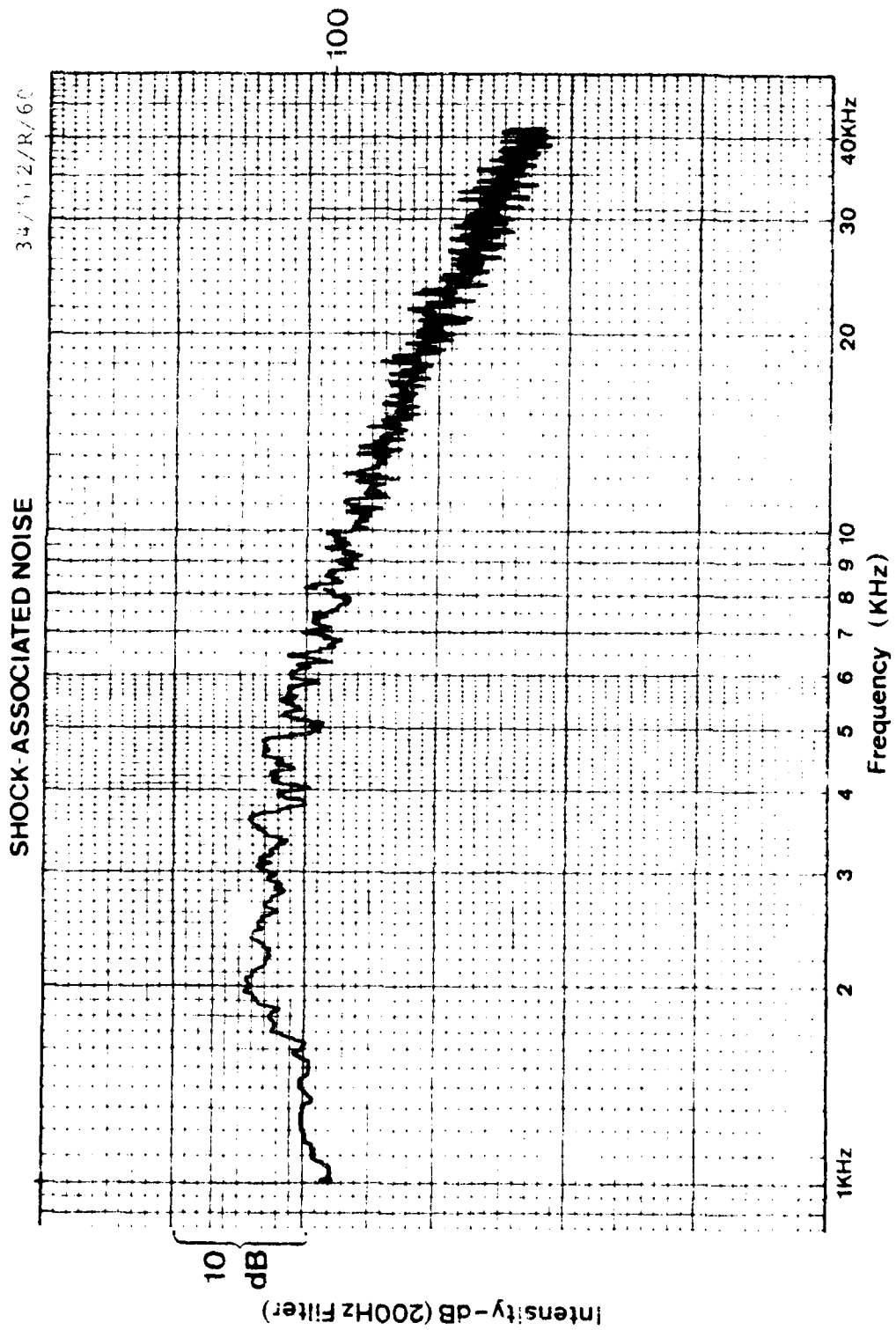


SHOCK-ASSOCIATED NOISE

34/512/R/30

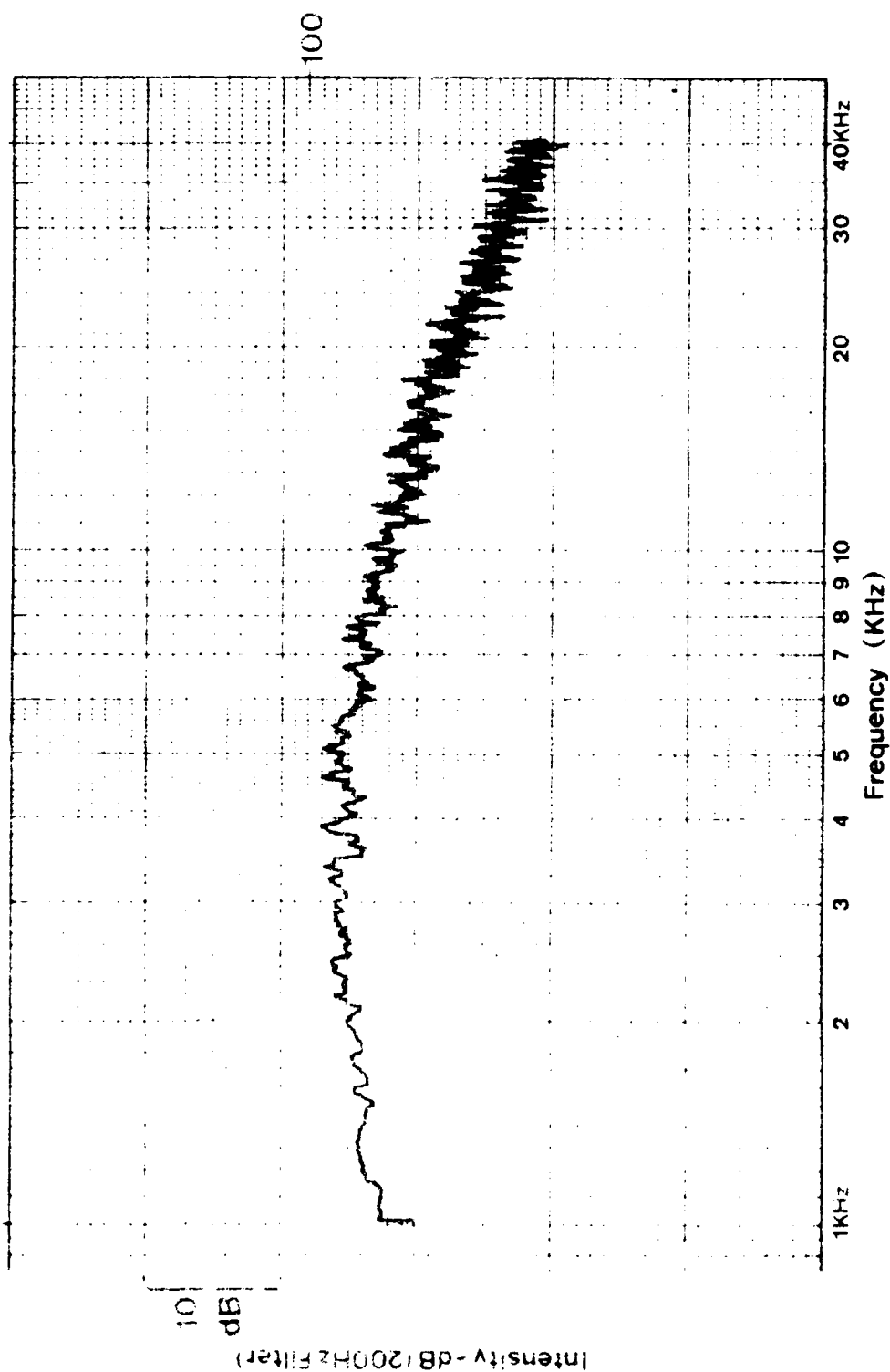






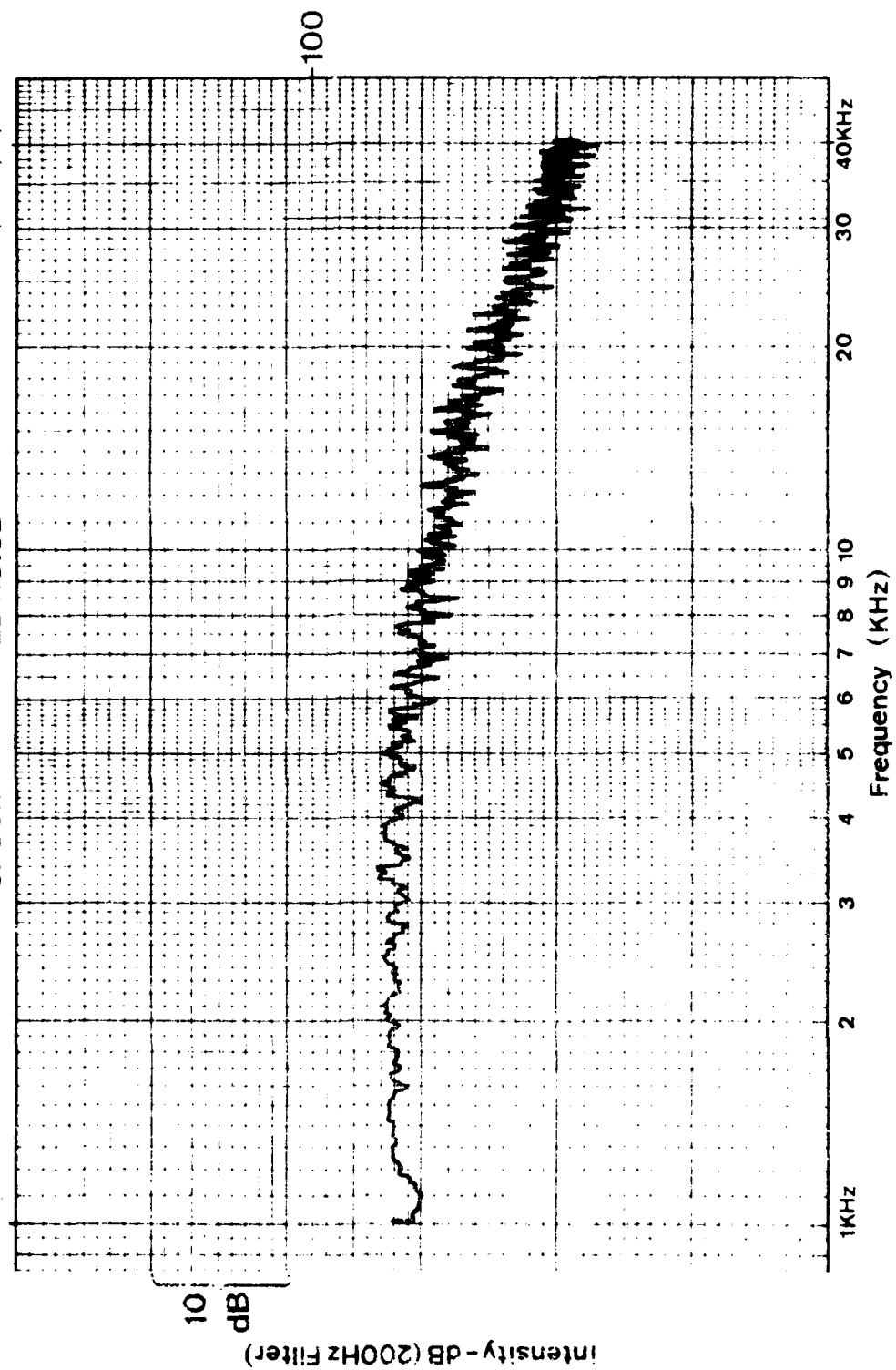
SHOCK-ASSOCIATED NOISE

34/512-5/73

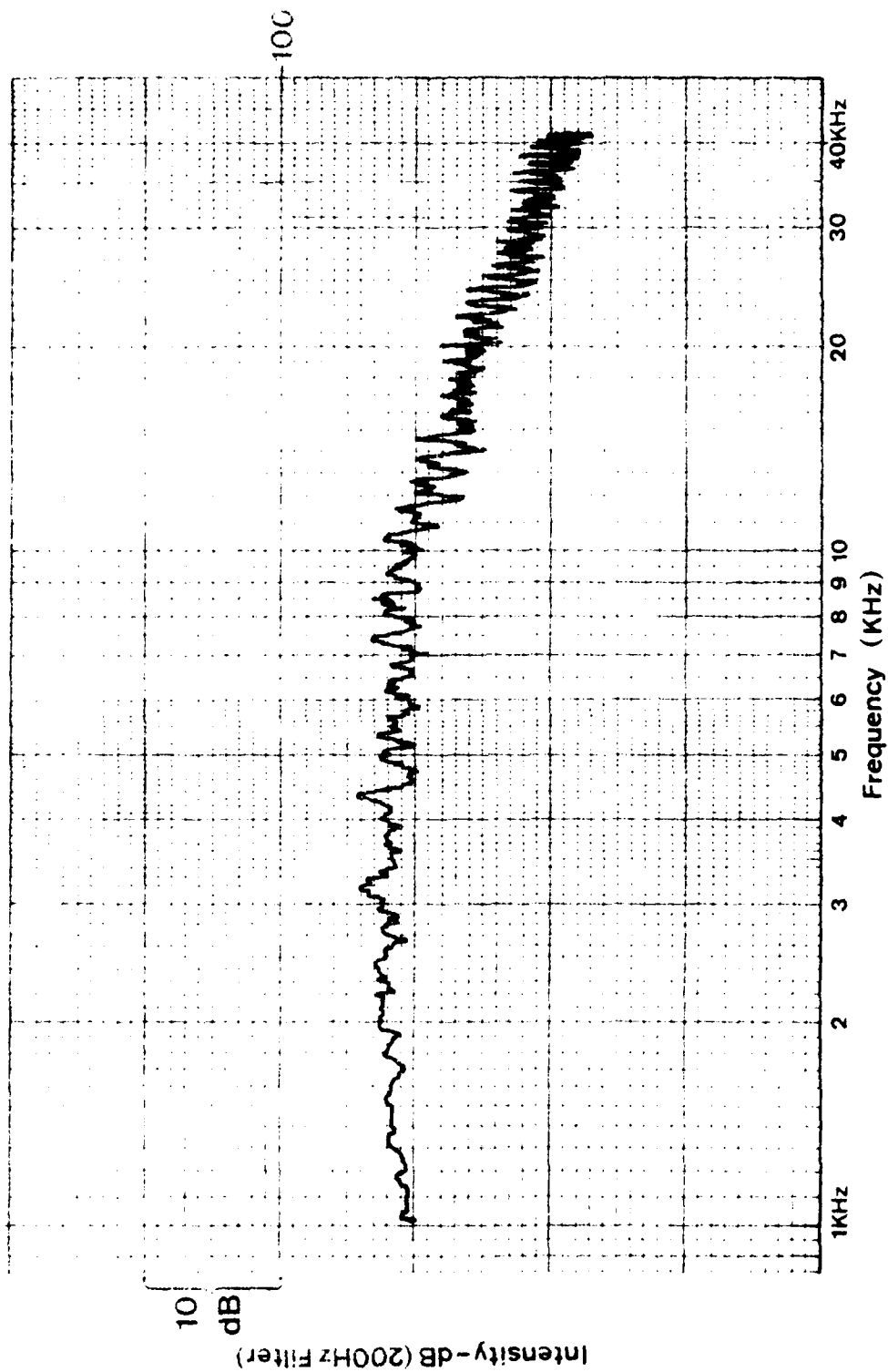


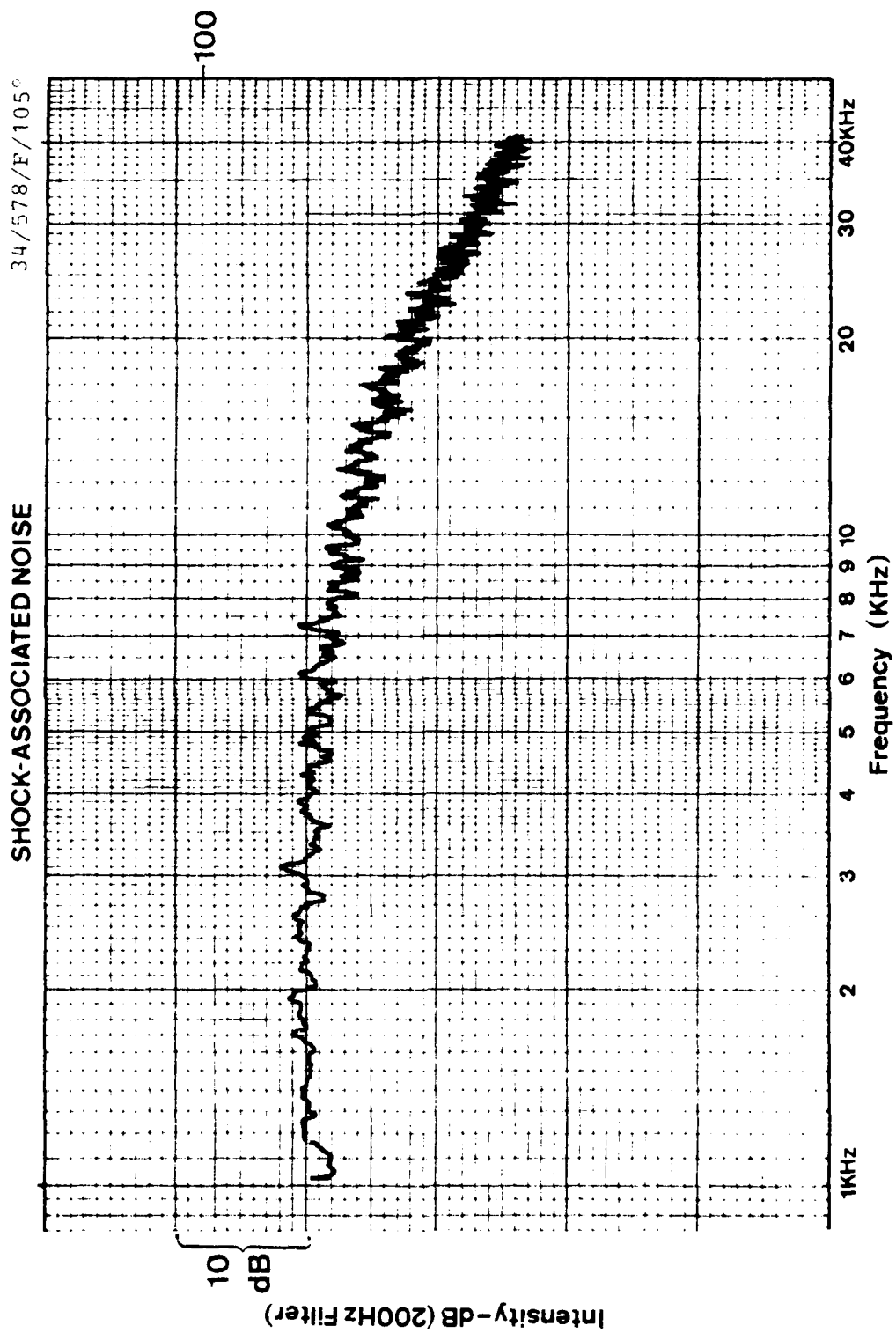
SHOCK-ASSOCIATED NOISE

34/512/R/90



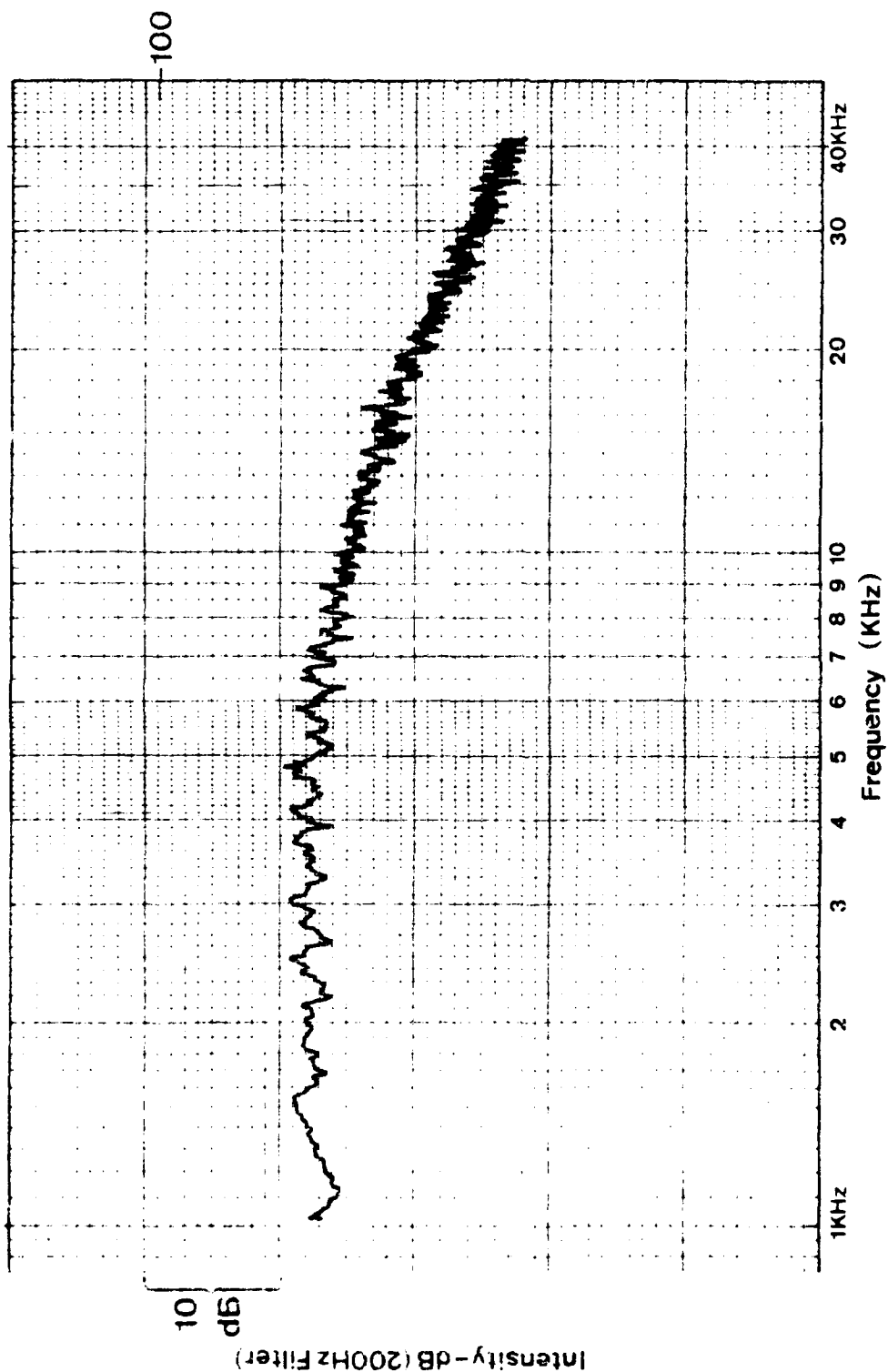
SHOCK-ASSOCIATED NOISE





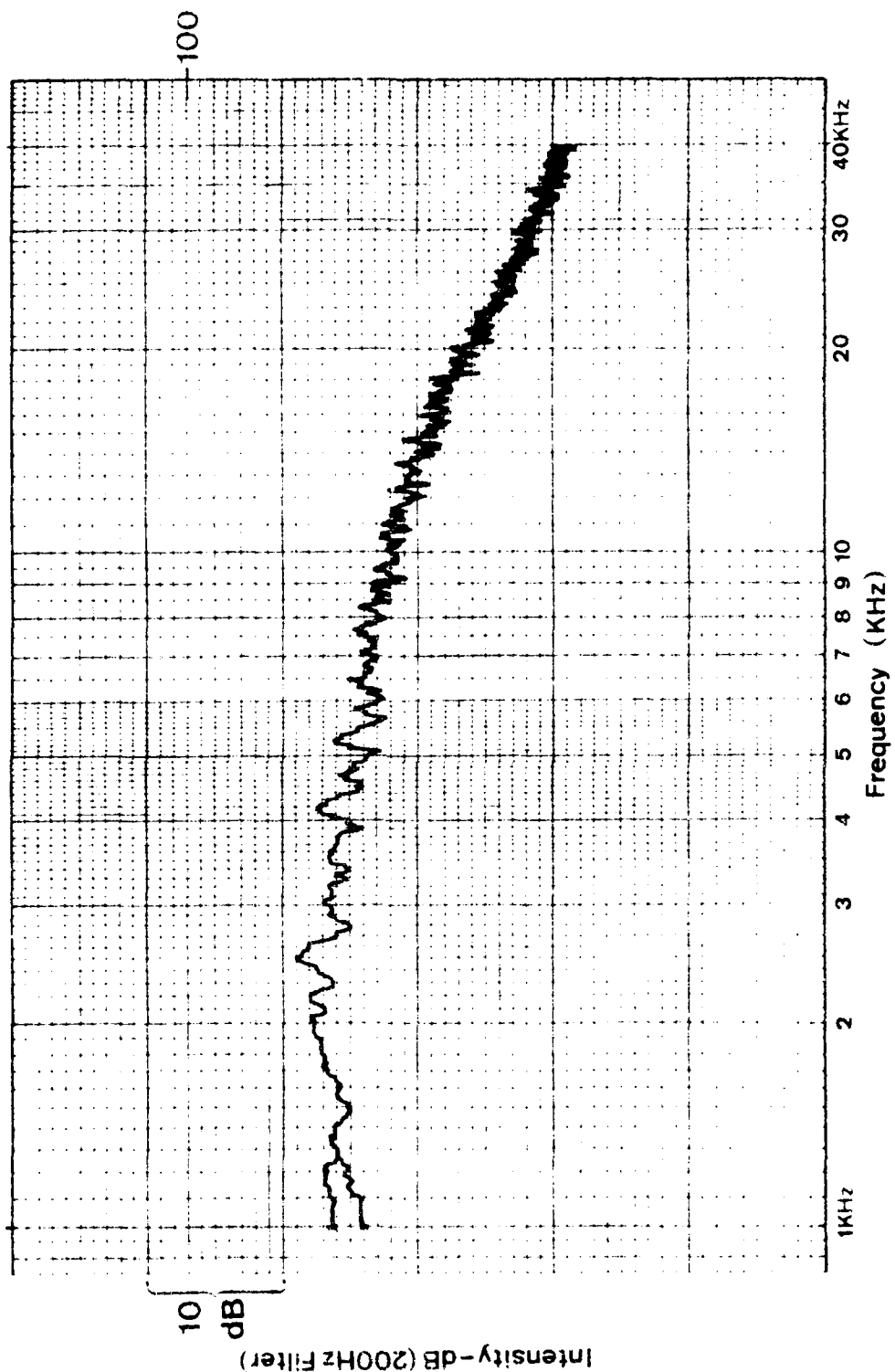
SHOCK-ASSOCIATED NOISE

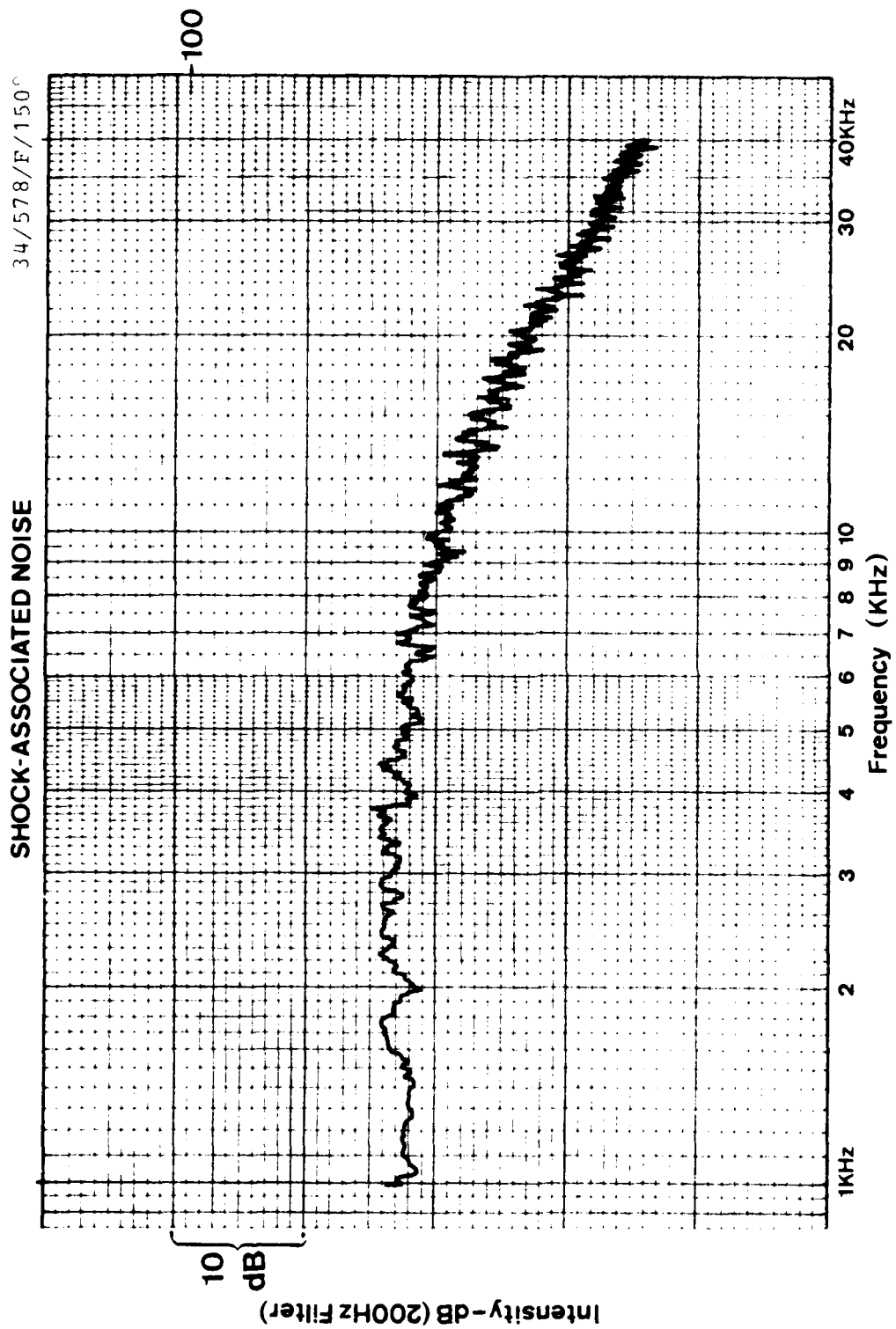
34, 578-P-129

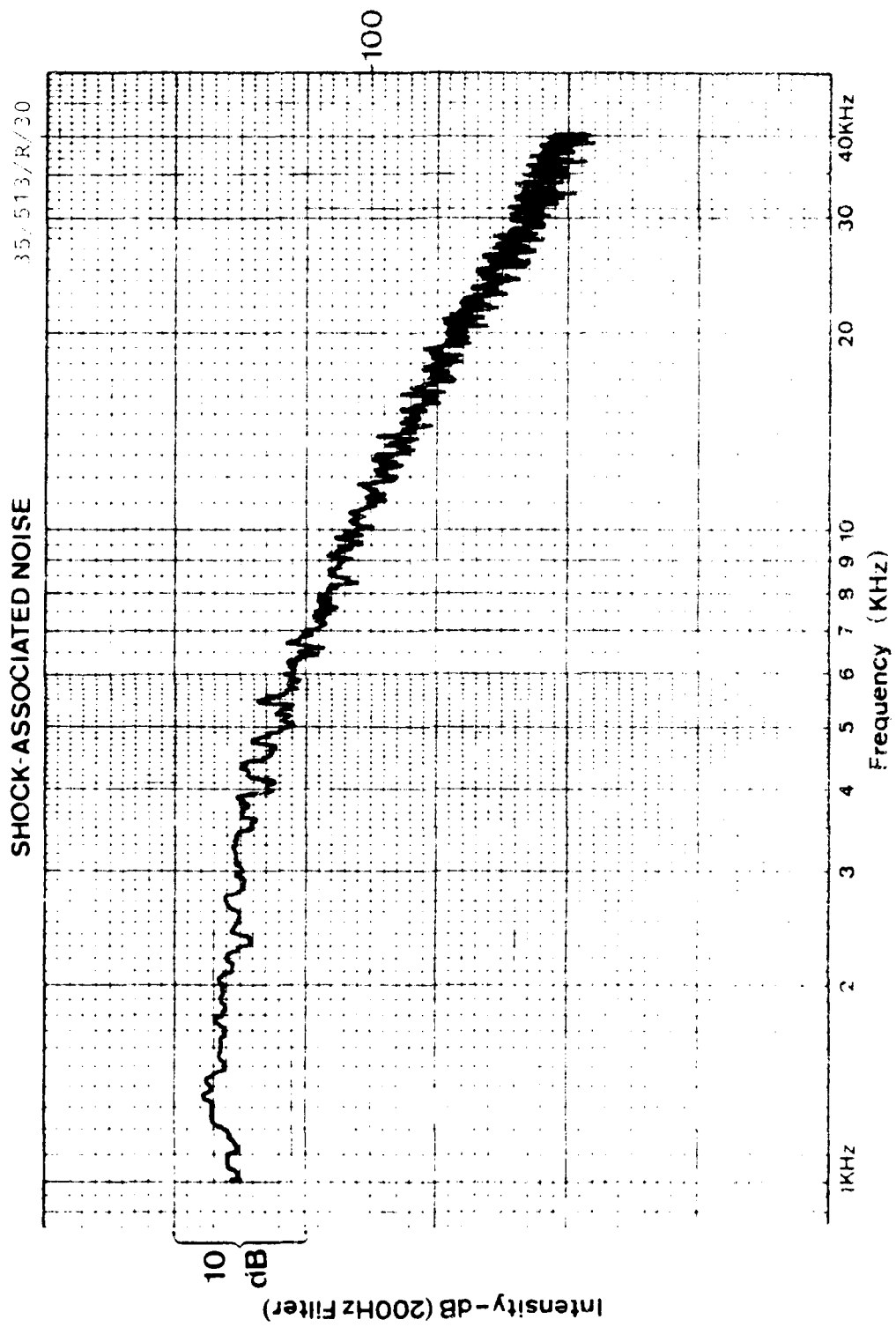


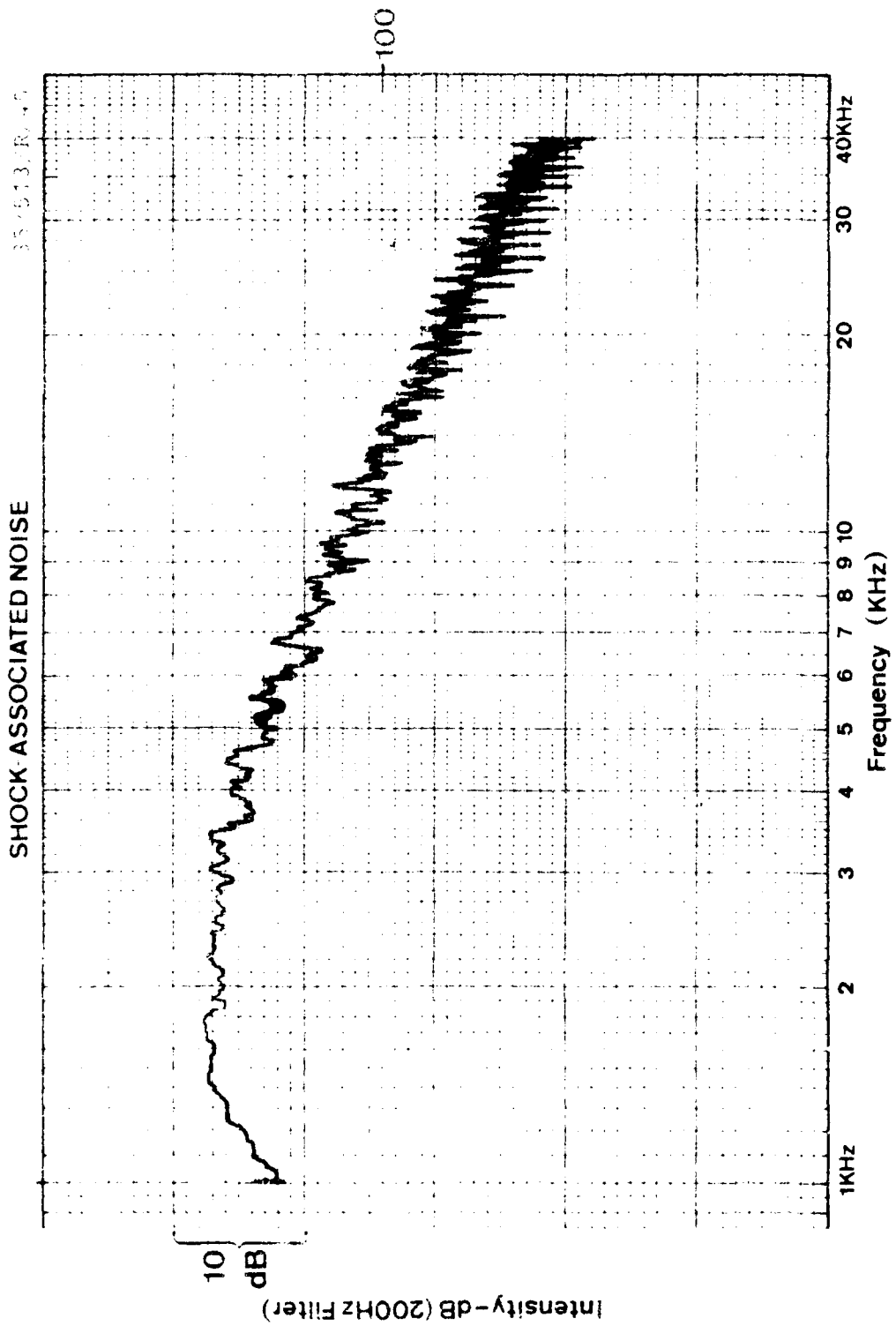
SHOCK-ASSOCIATED NOISE

34/578/F/135



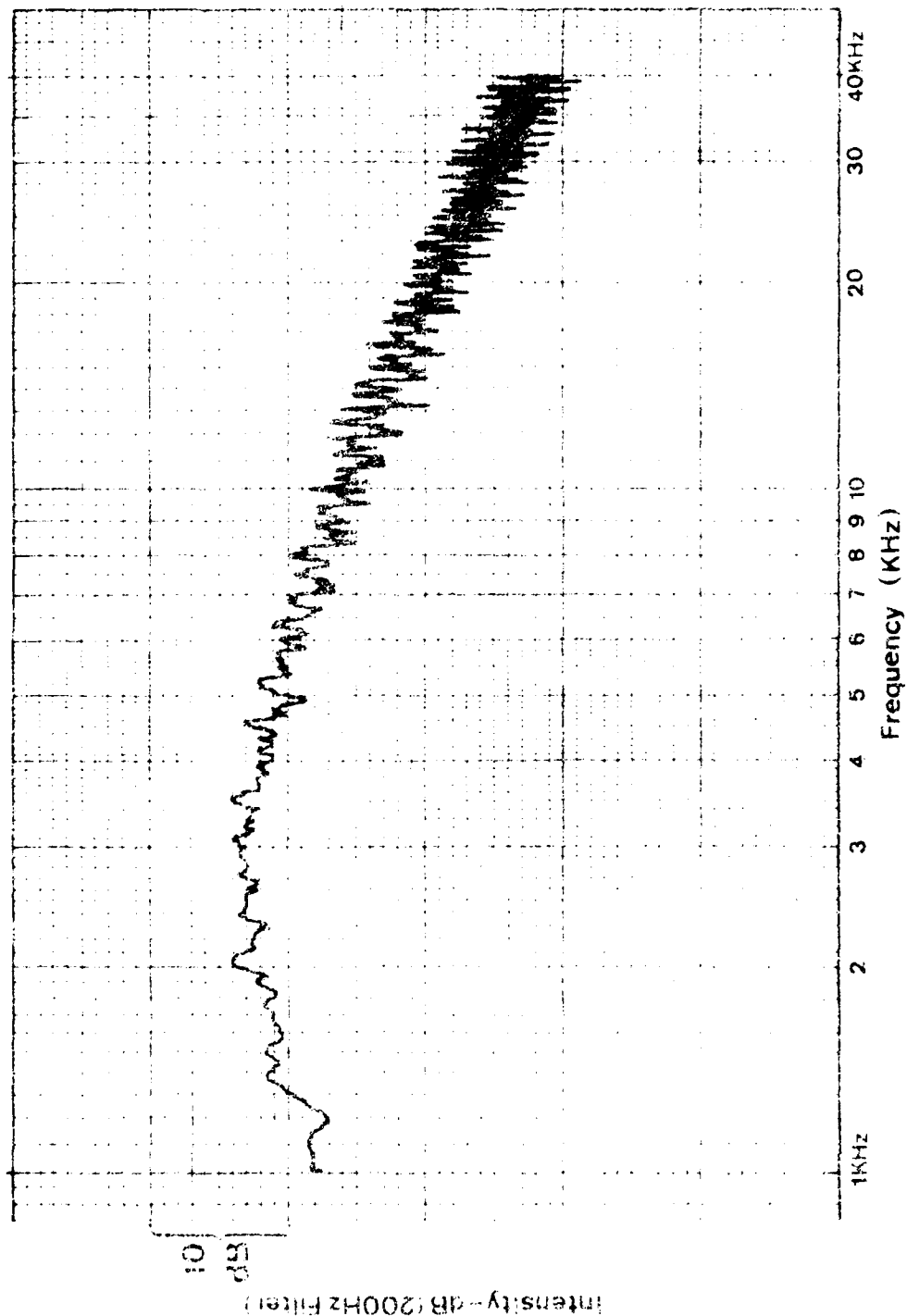


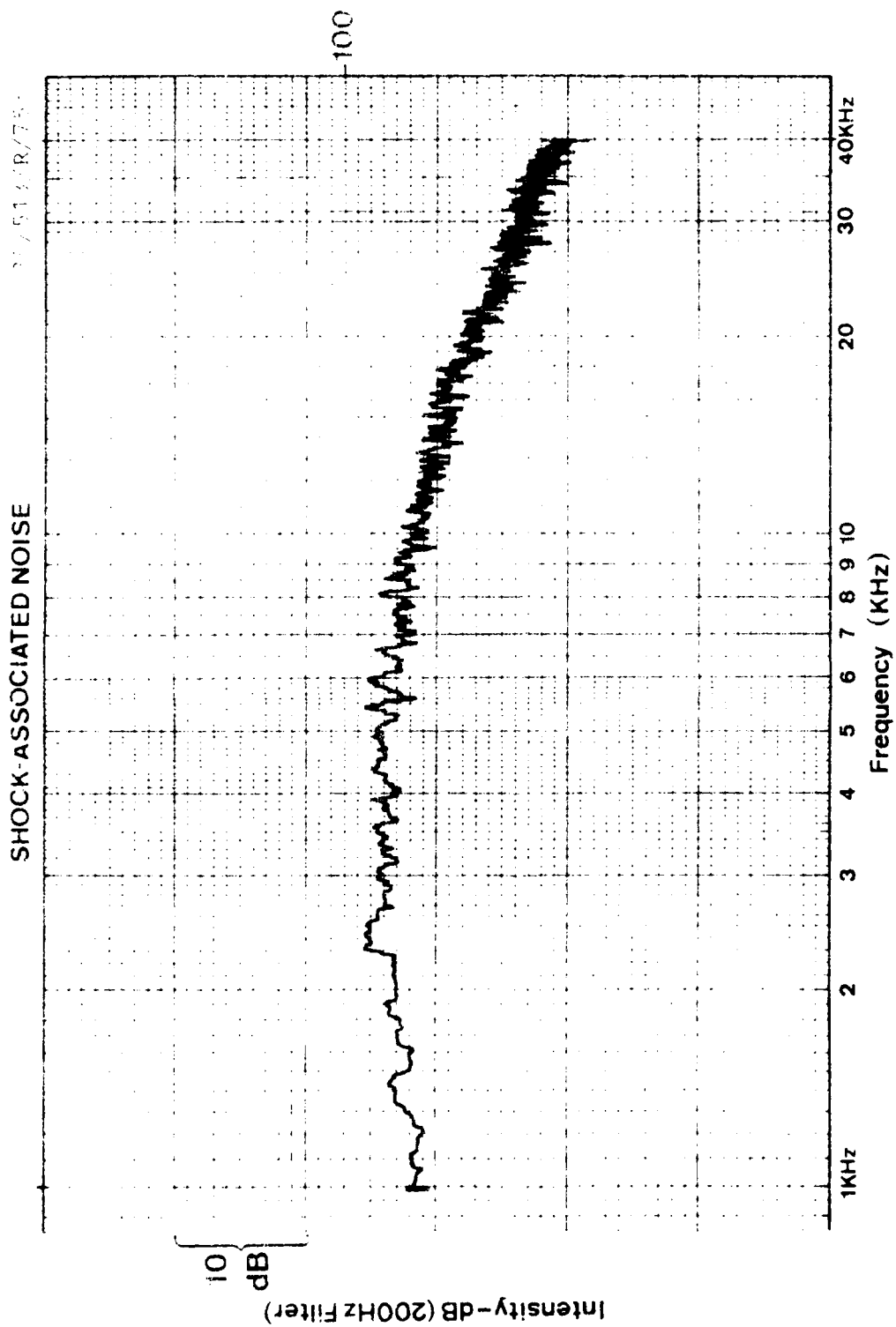


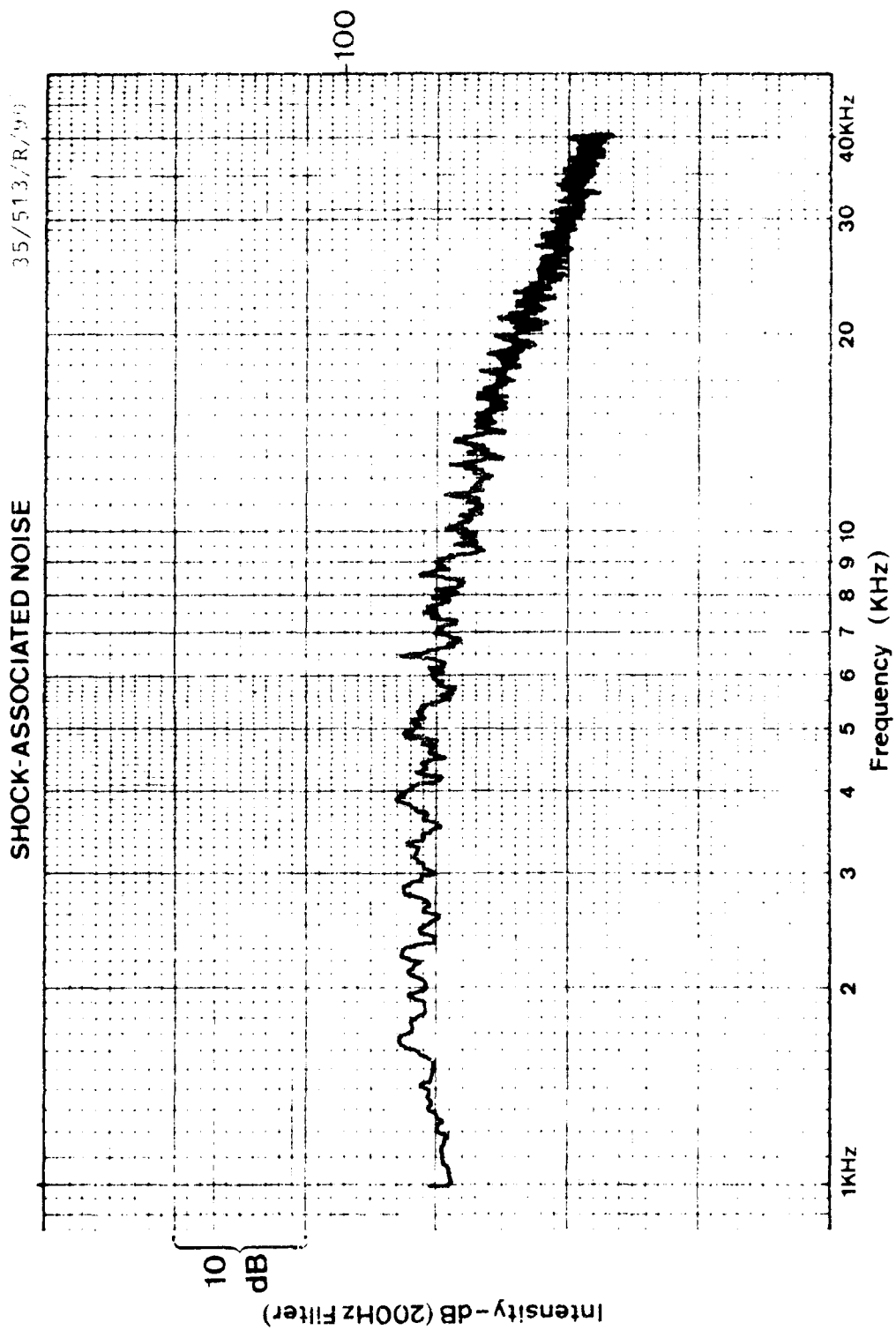


SHOCK-ASSOCIATED NOISE

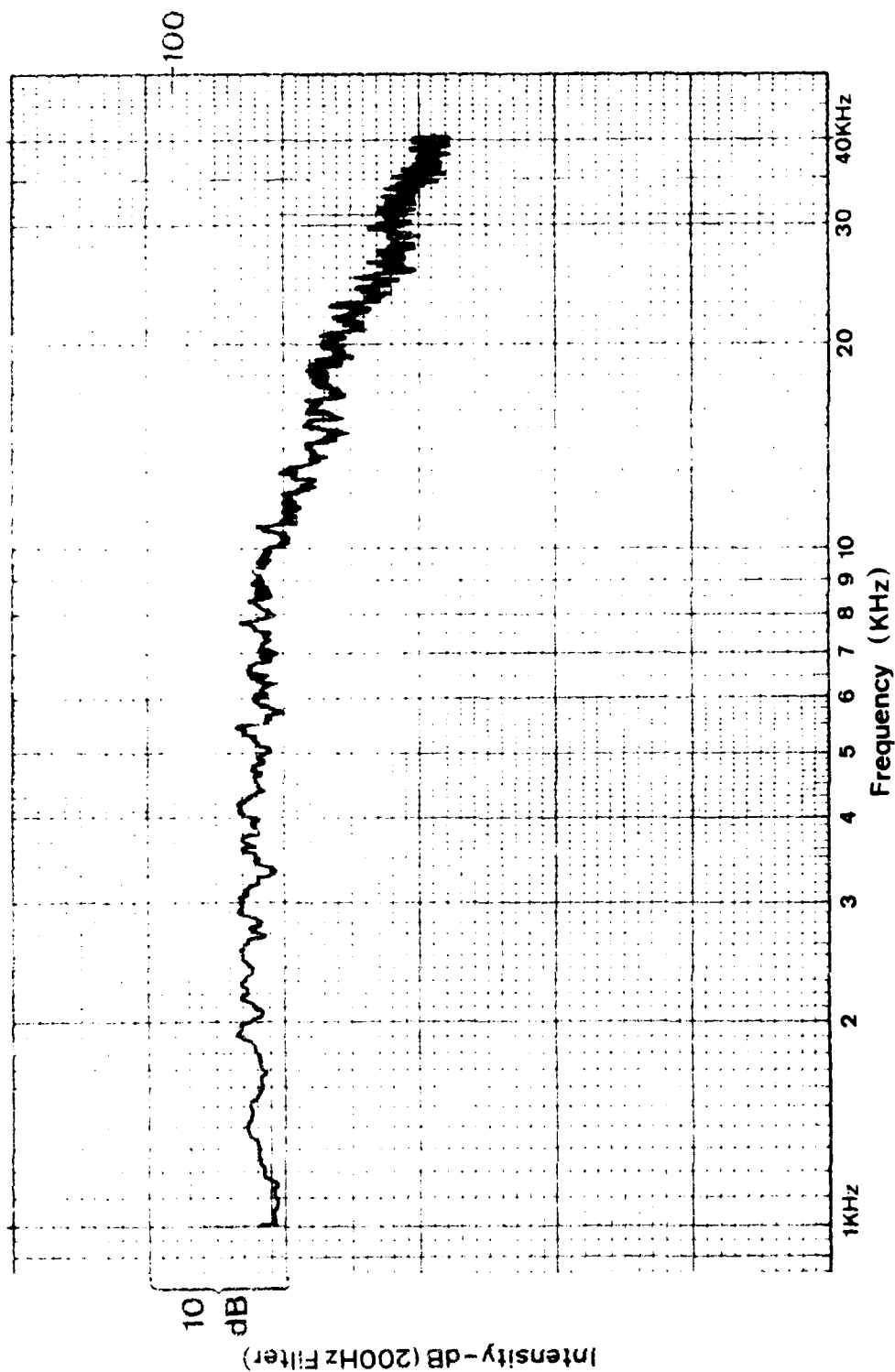
55/513/P 46

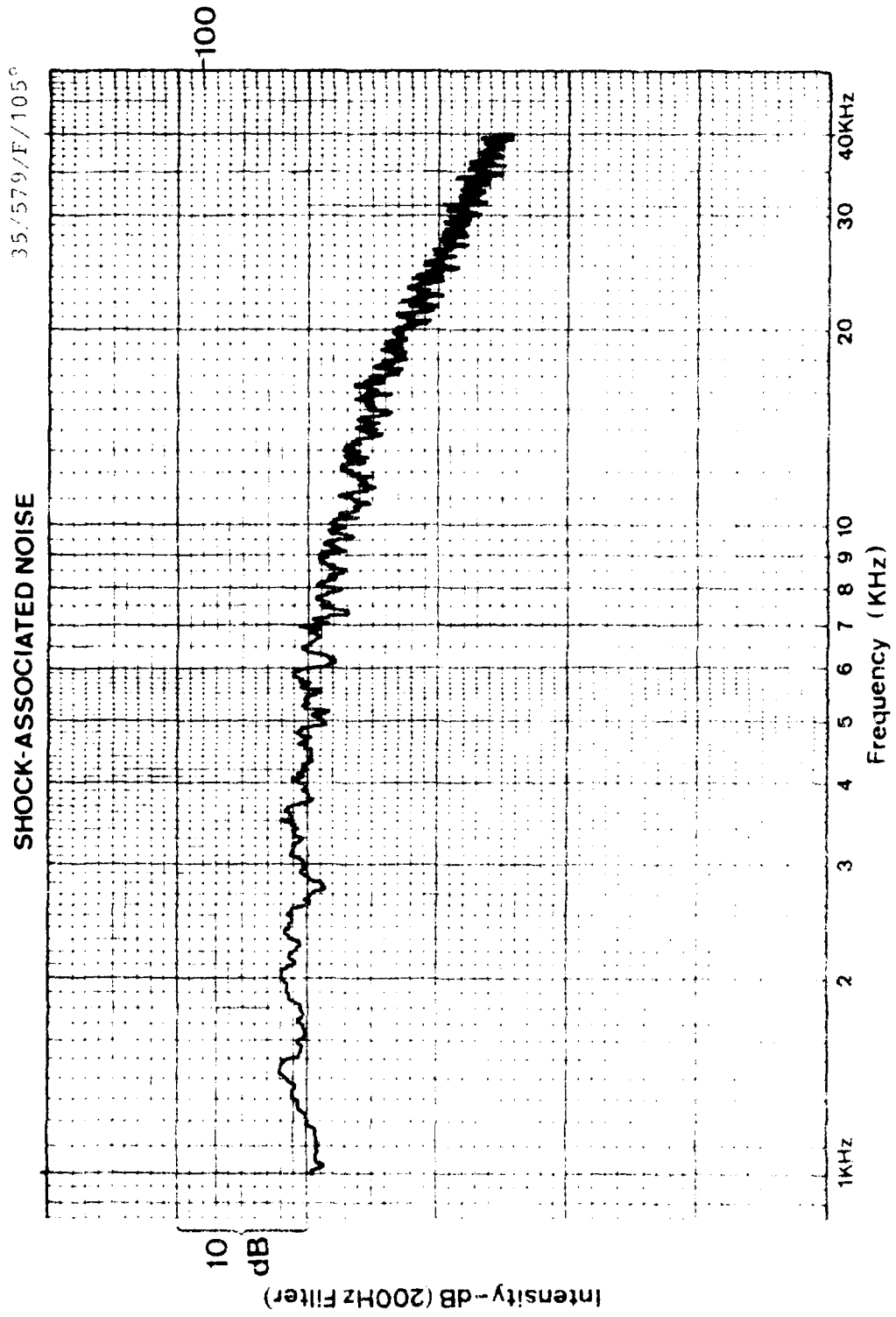


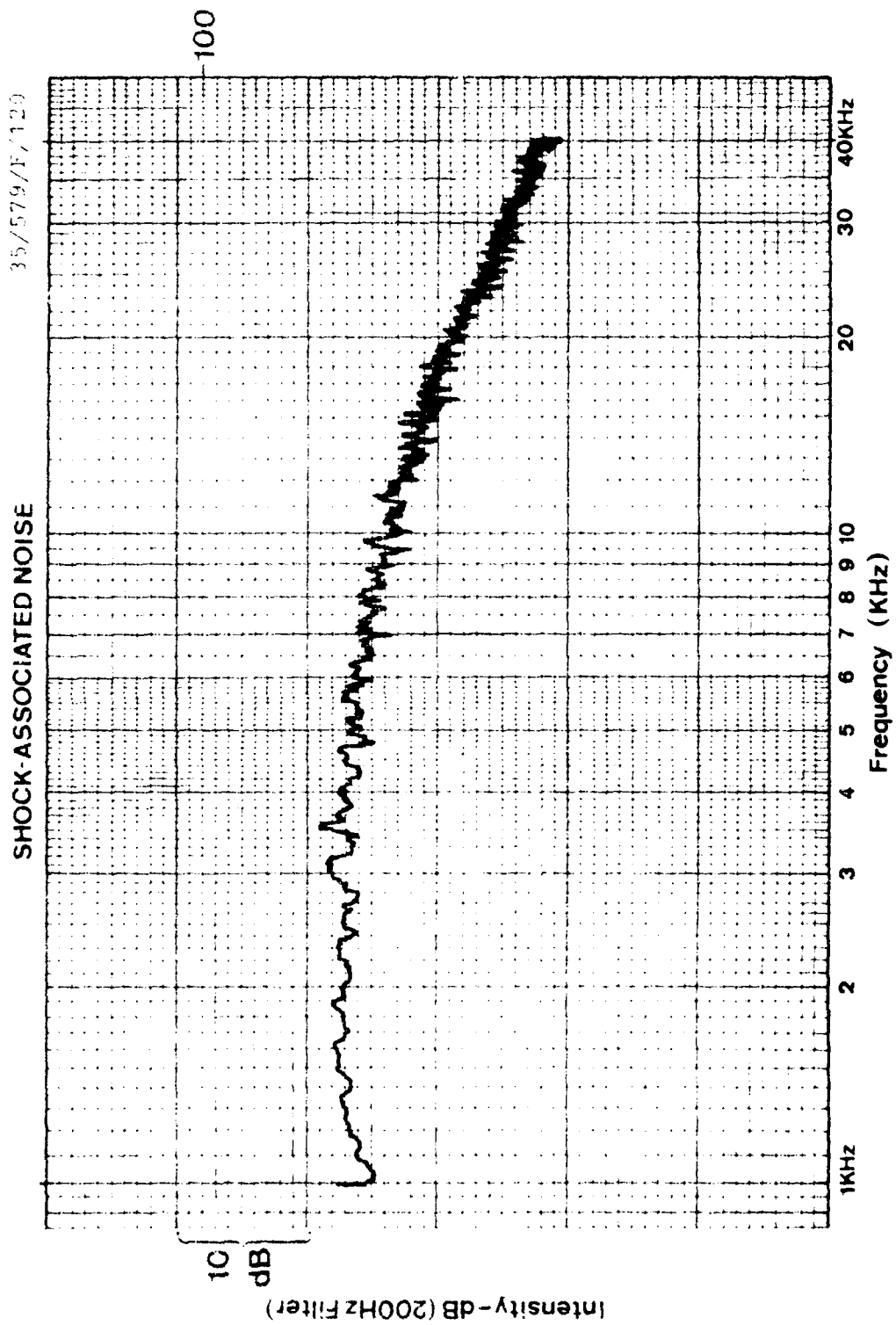


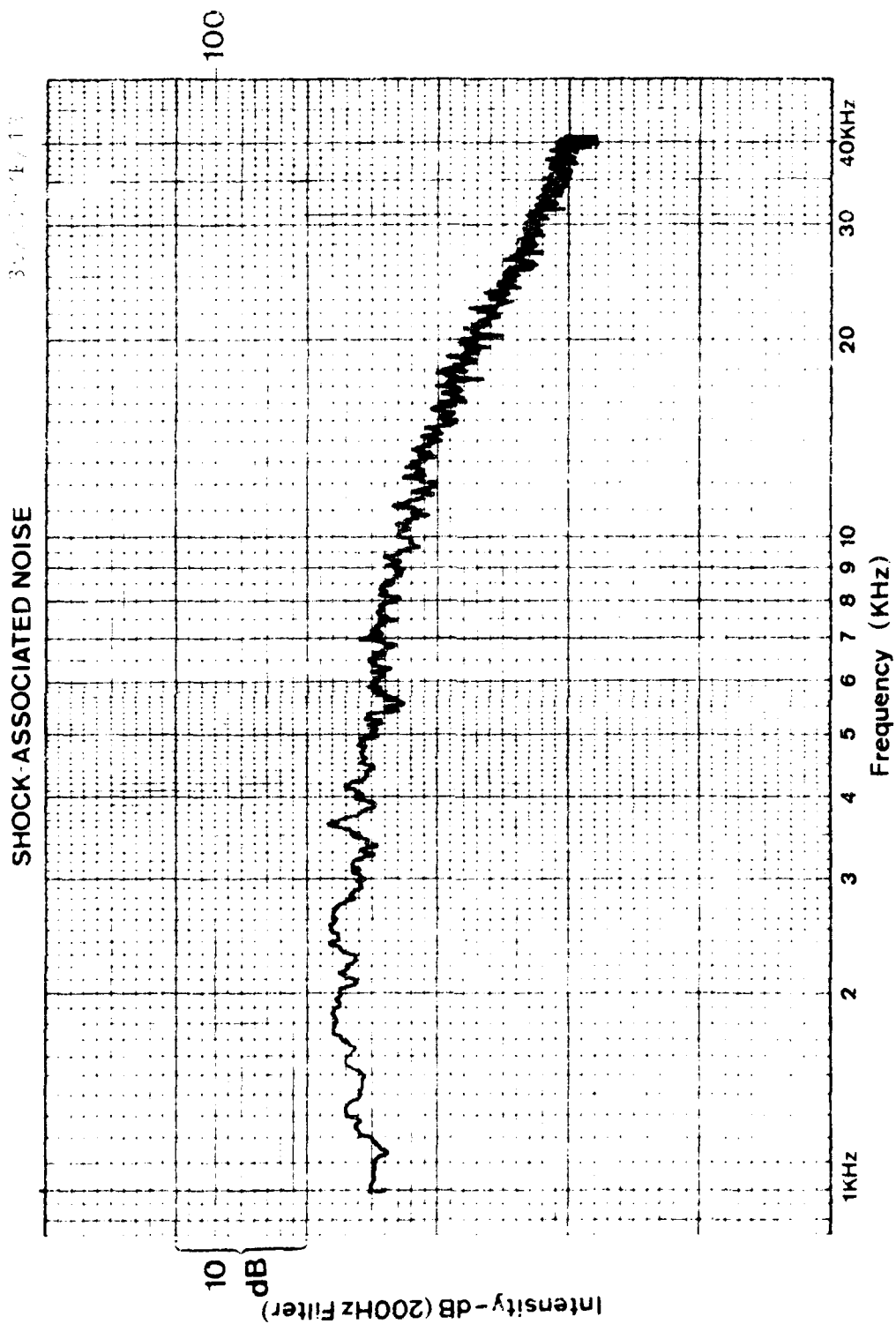


SHOCK-ASSOCIATED NOISE



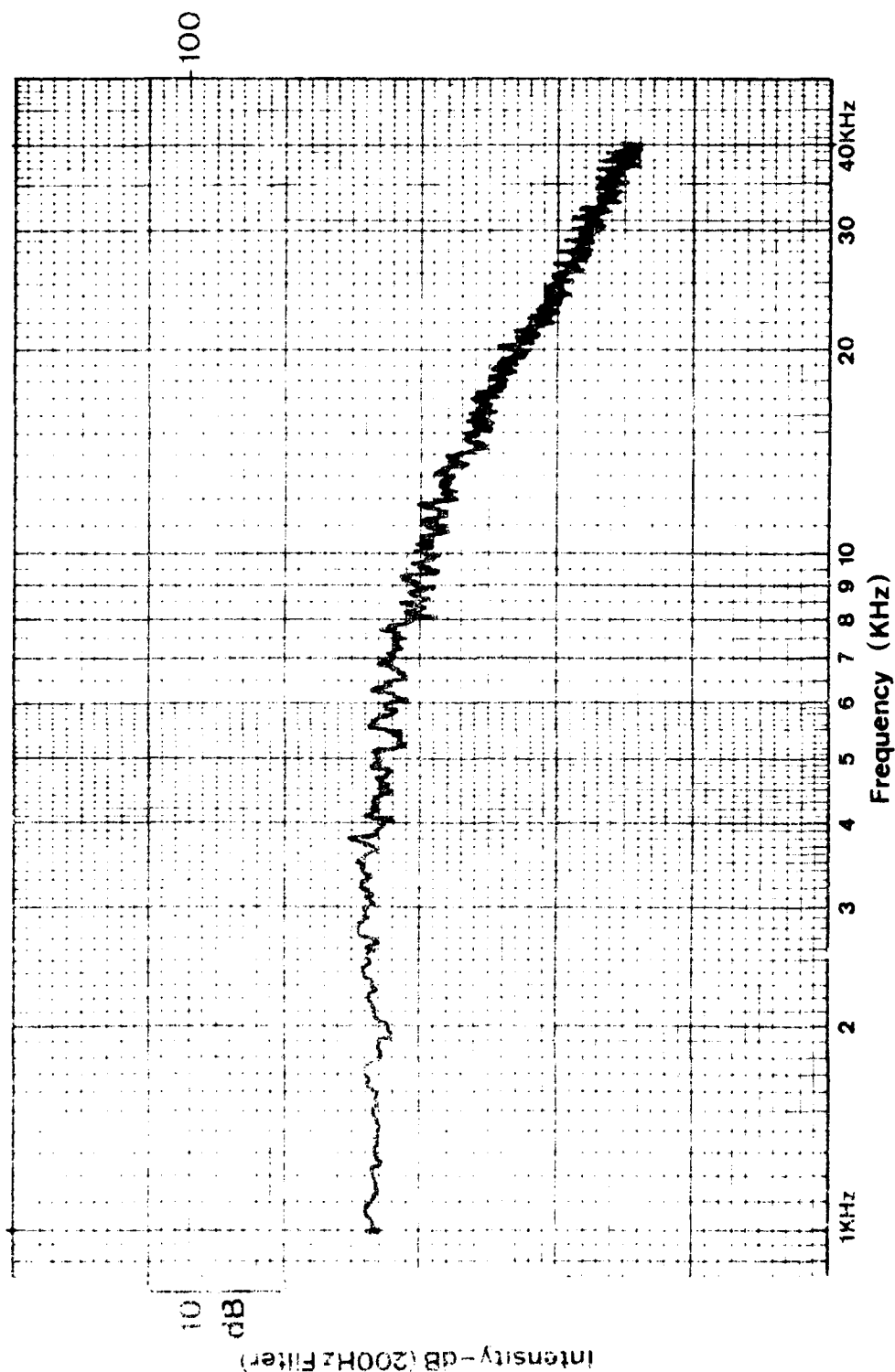






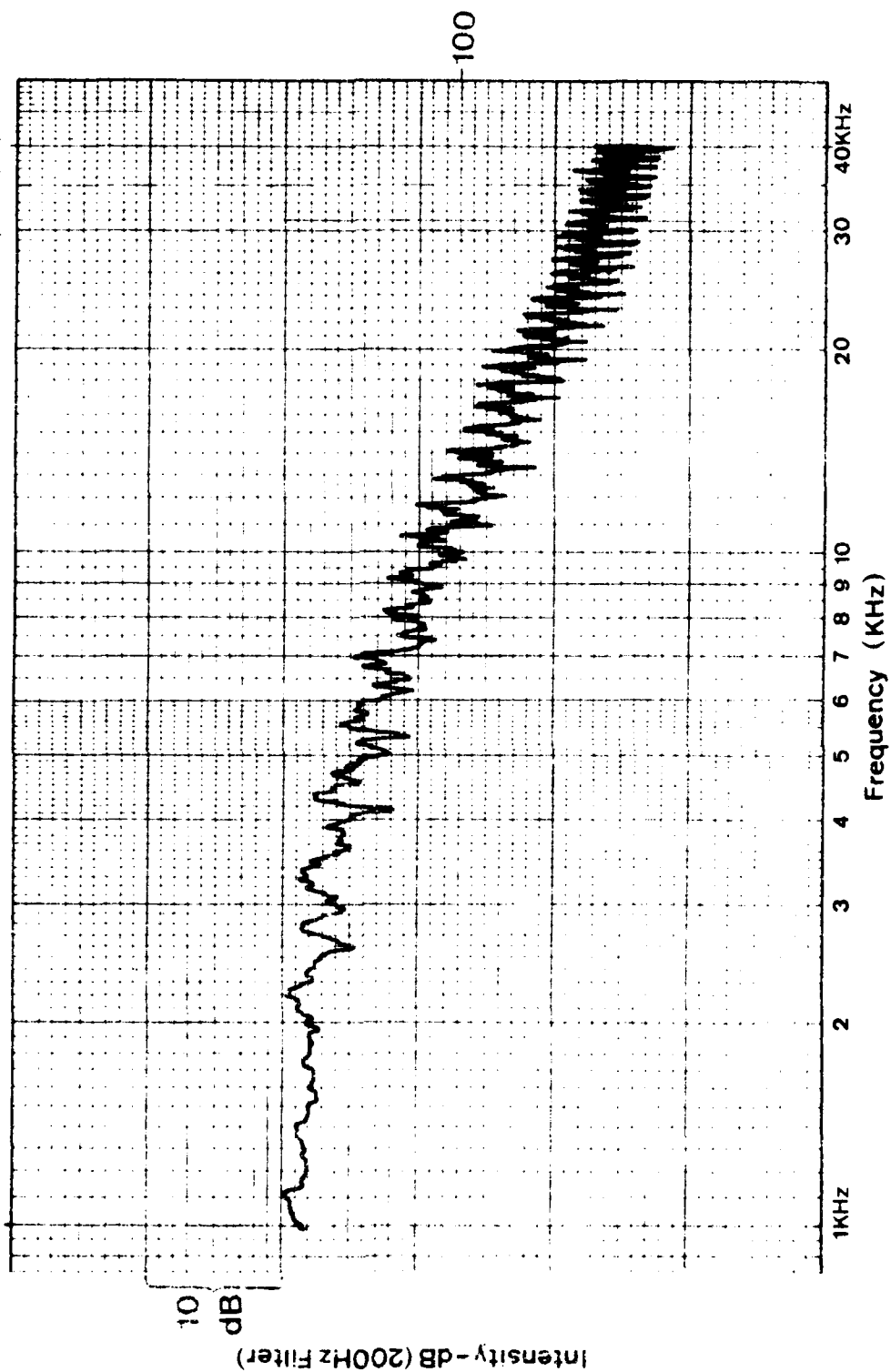
35-579/F 150

SHOCK-ASSOCIATED NOISE

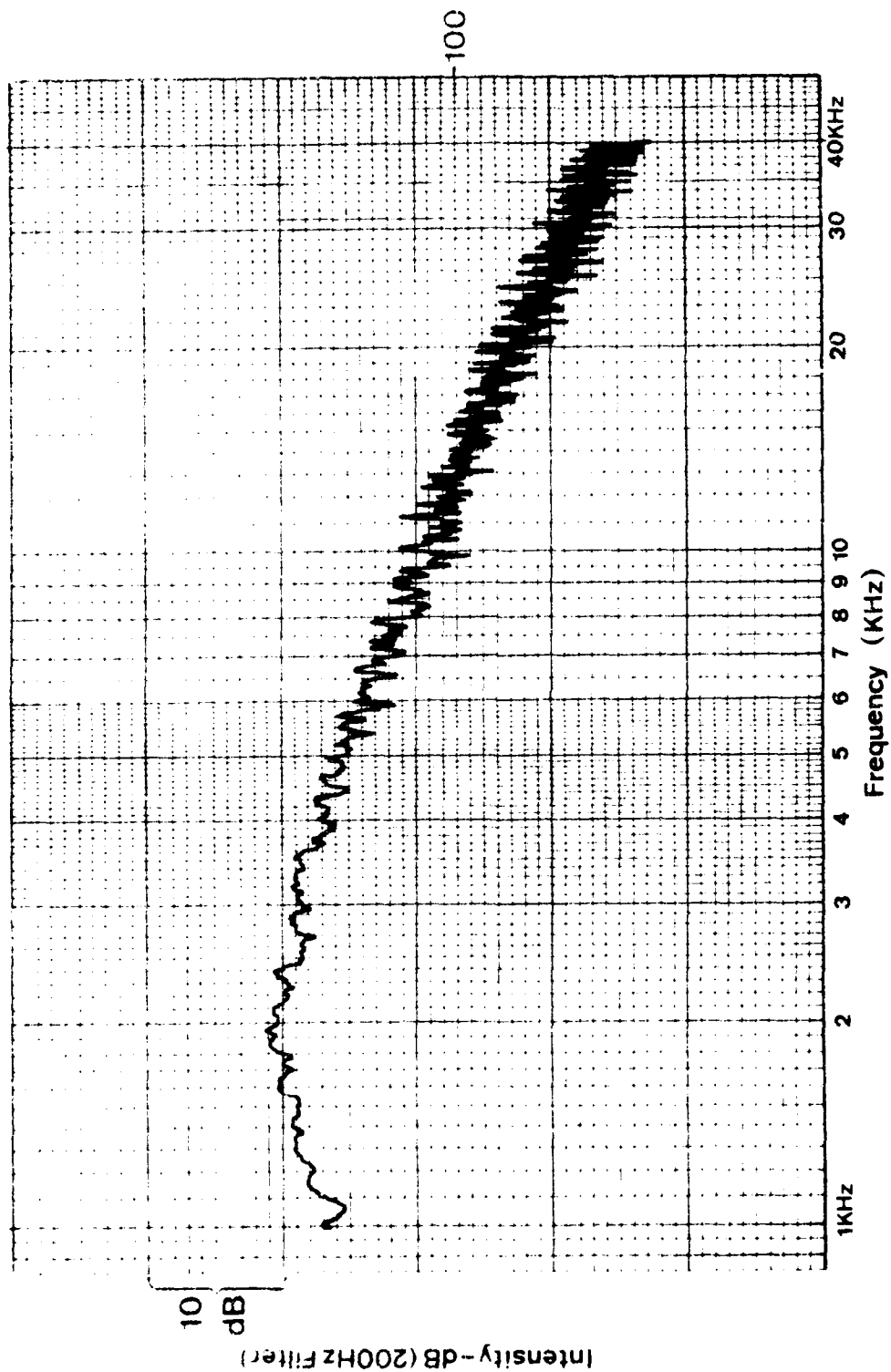


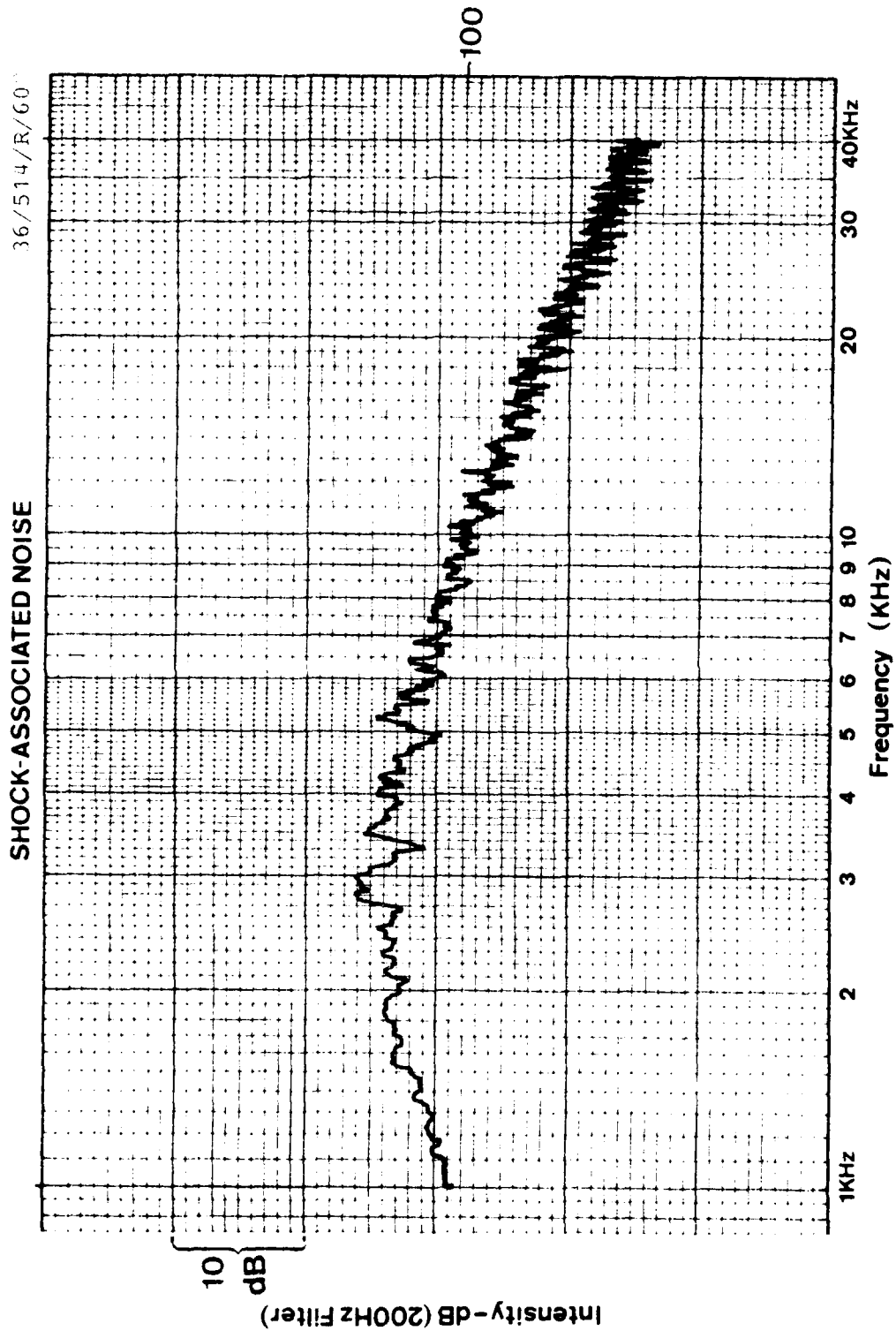
SHOCK-ASSOCIATED NOISE

36/514/R/30



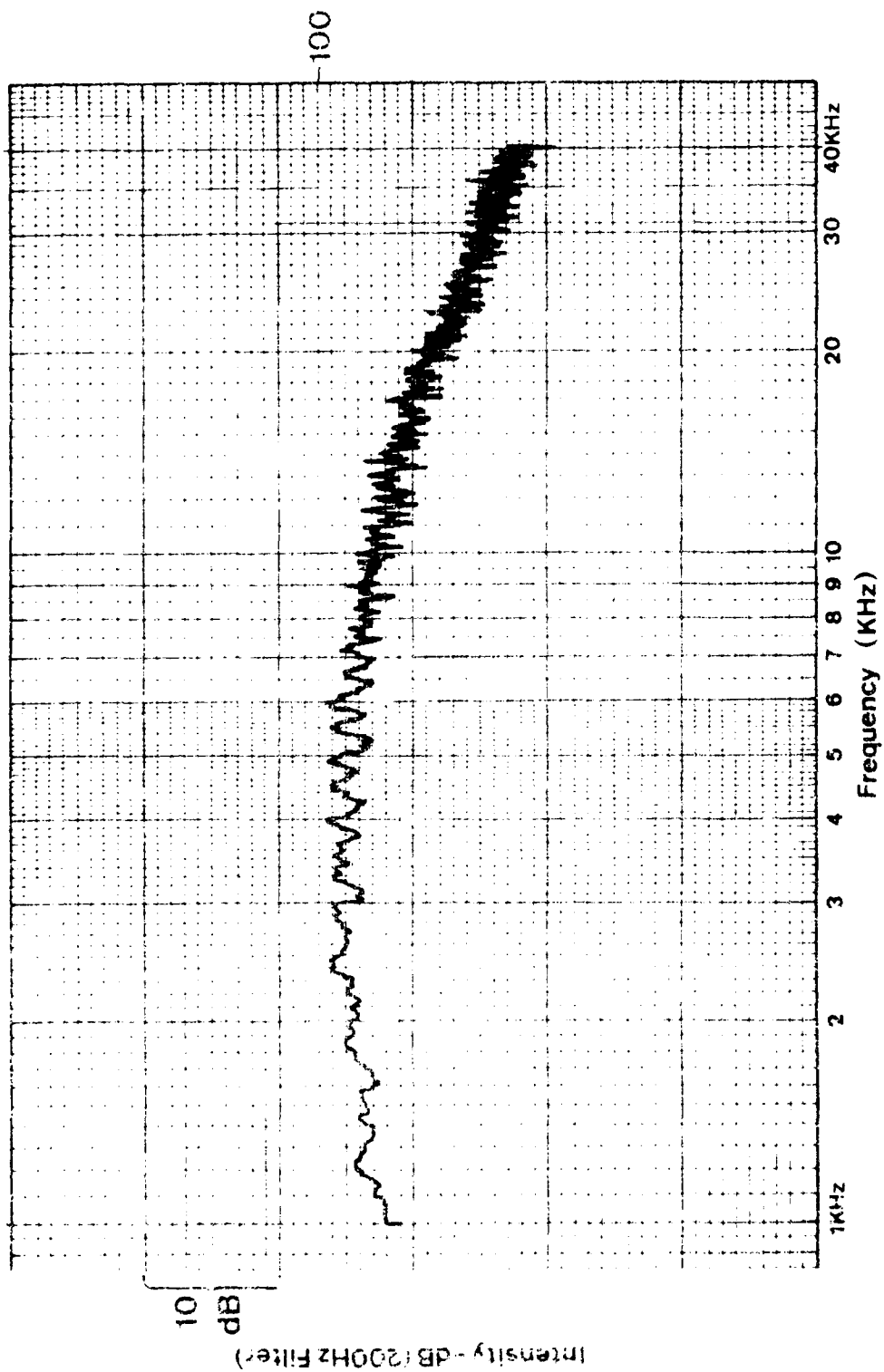
SHOCK-ASSOCIATED NOISE





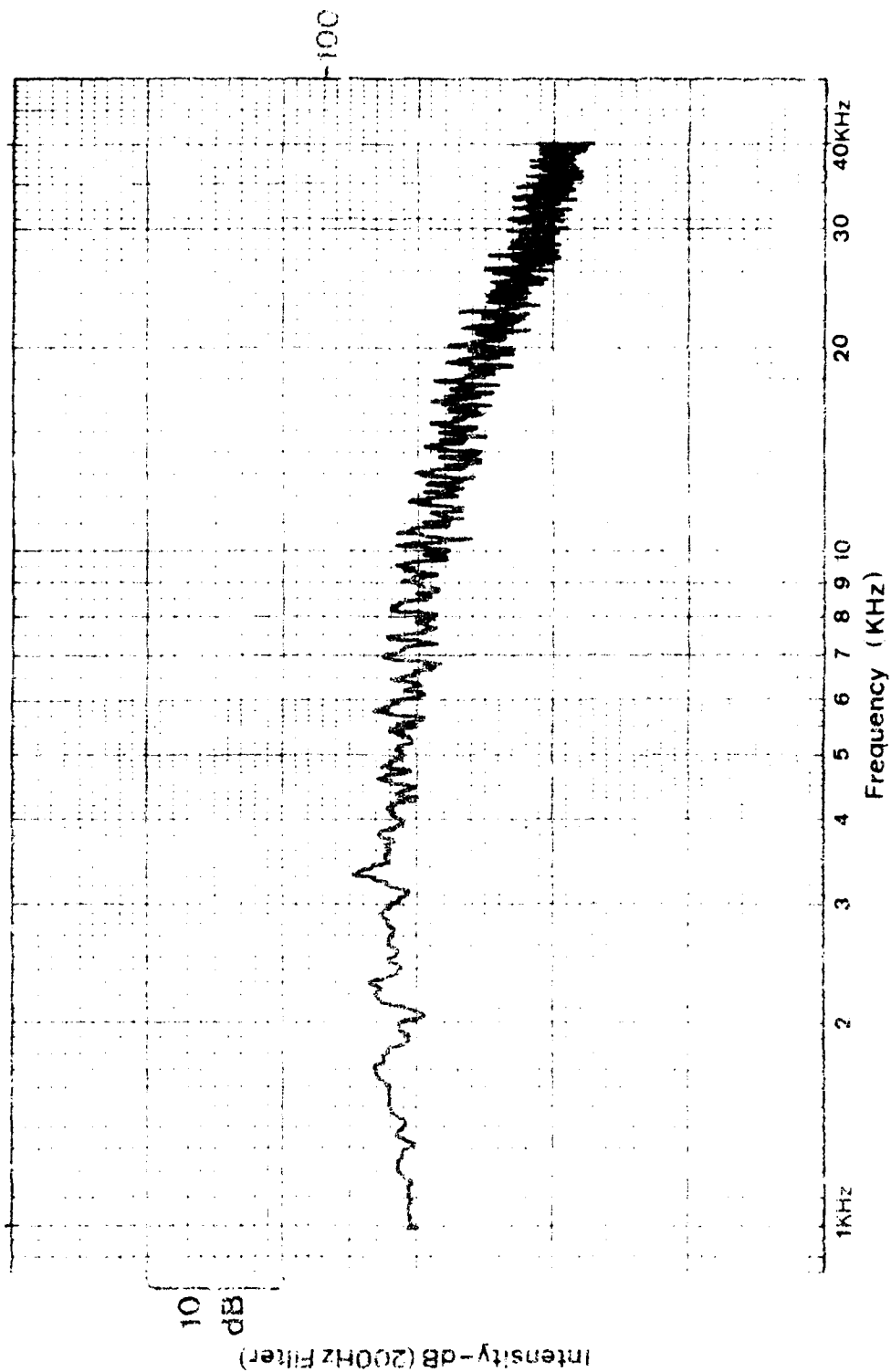
SHOCK-ASSOCIATED NOISE

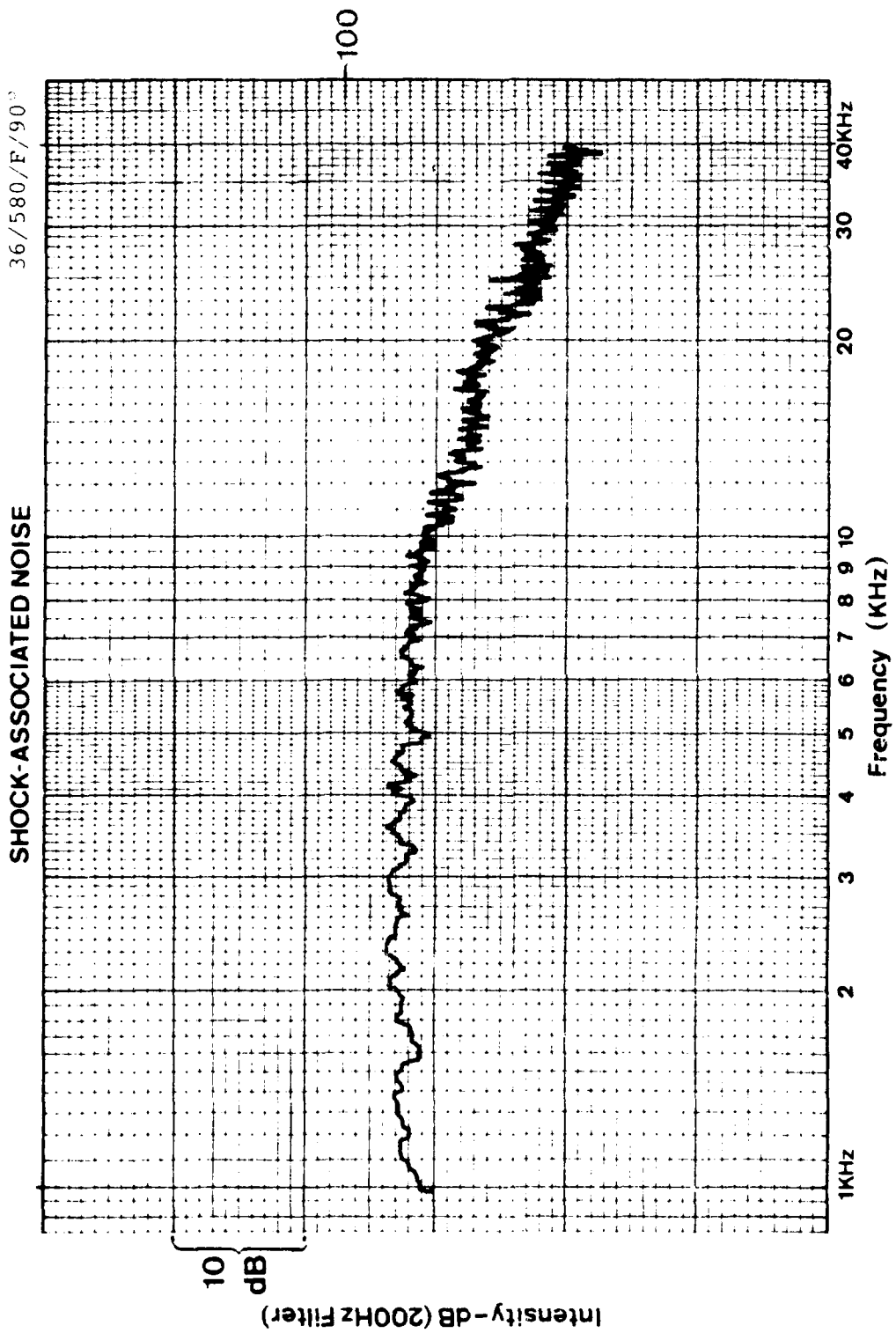
36 514-R-75

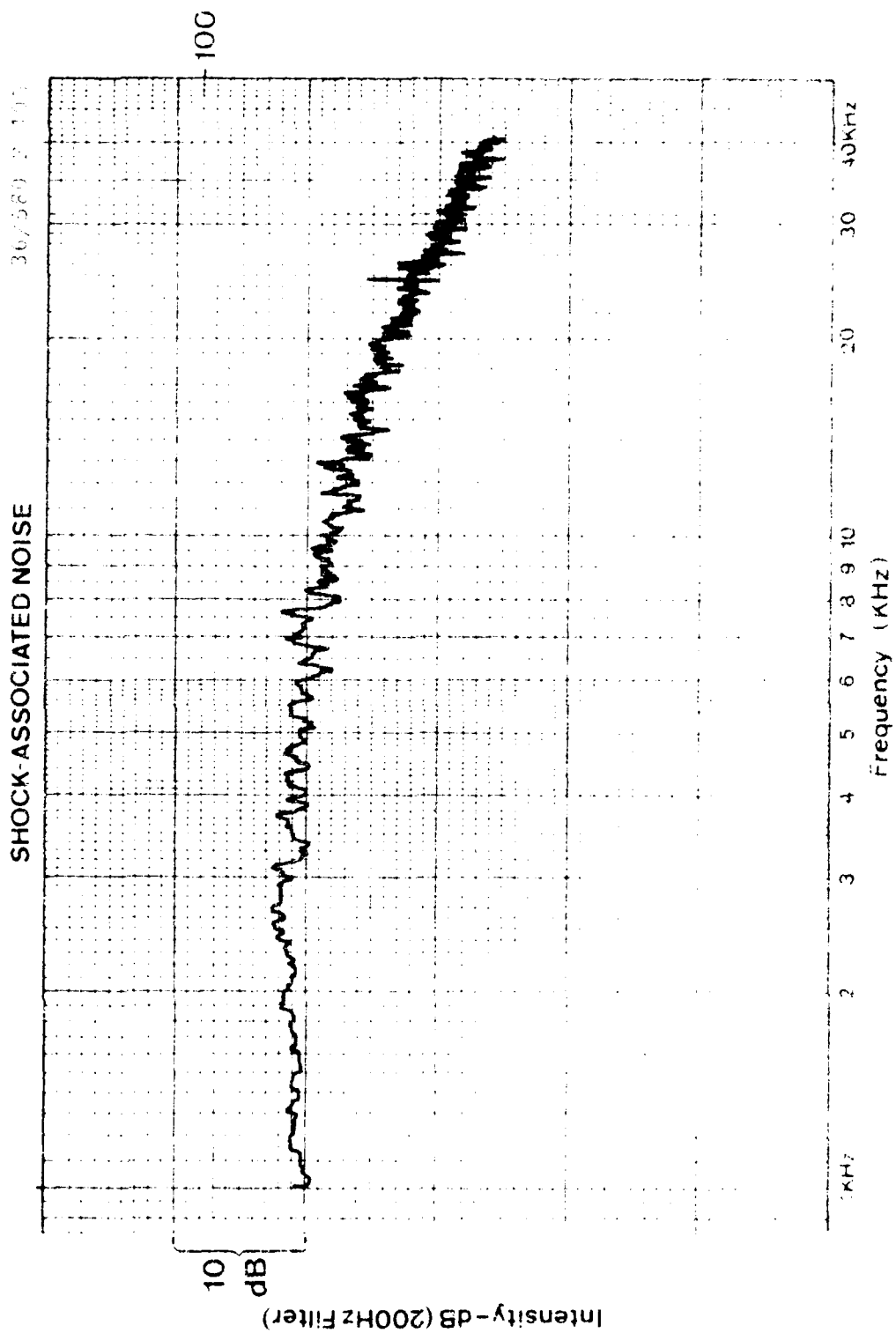


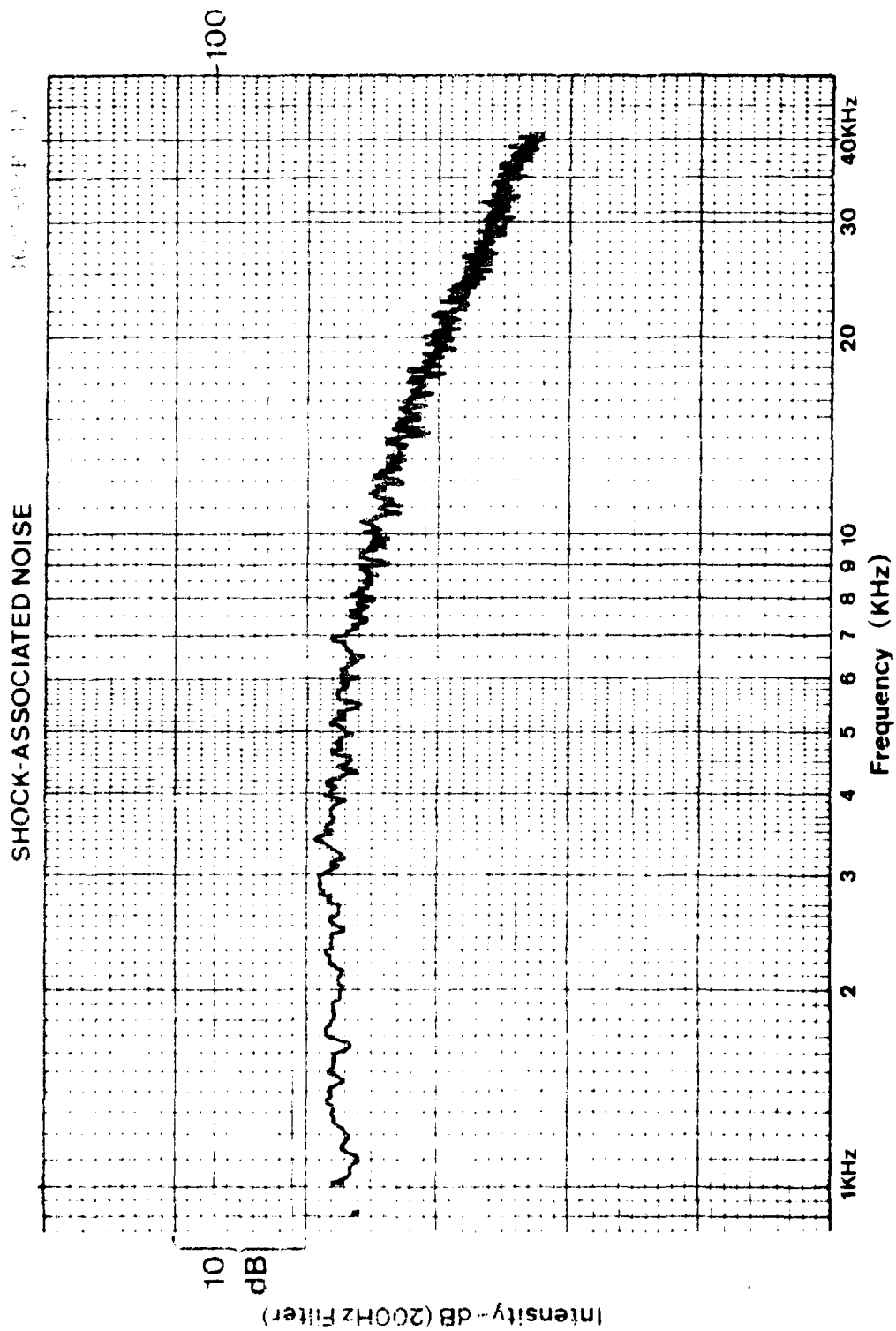
SHOCK-ASSOCIATED NOISE

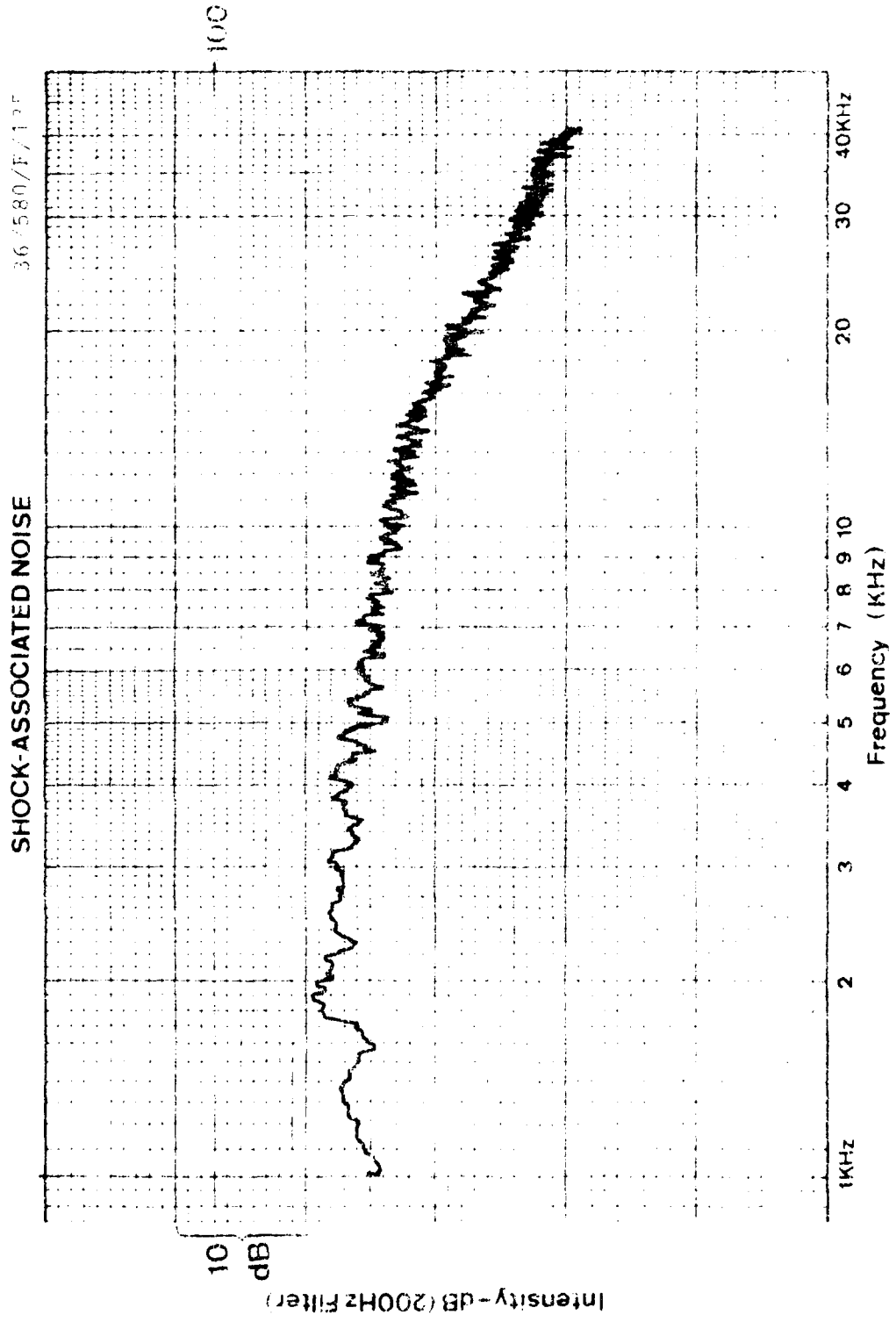
36/514/R 99

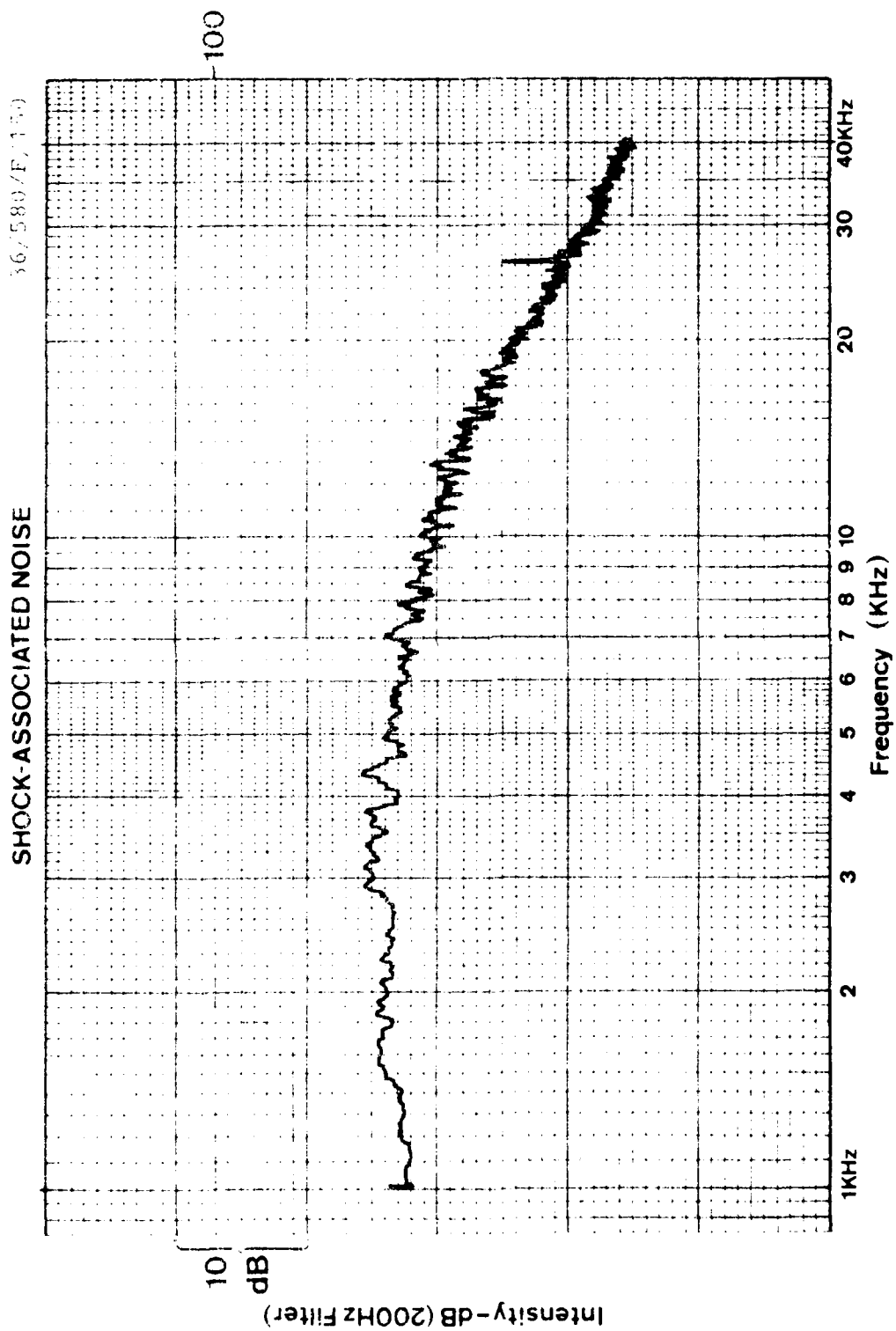


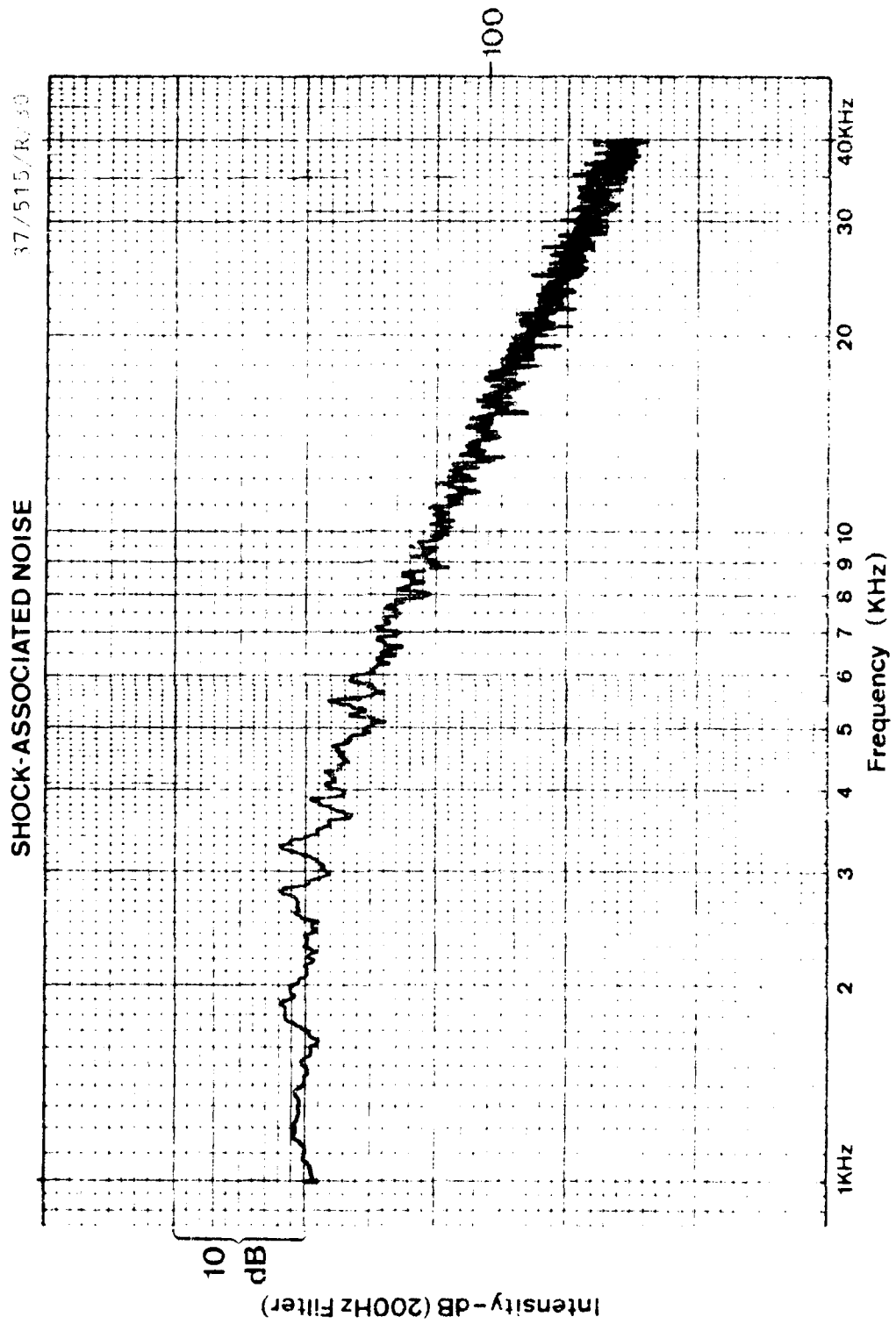


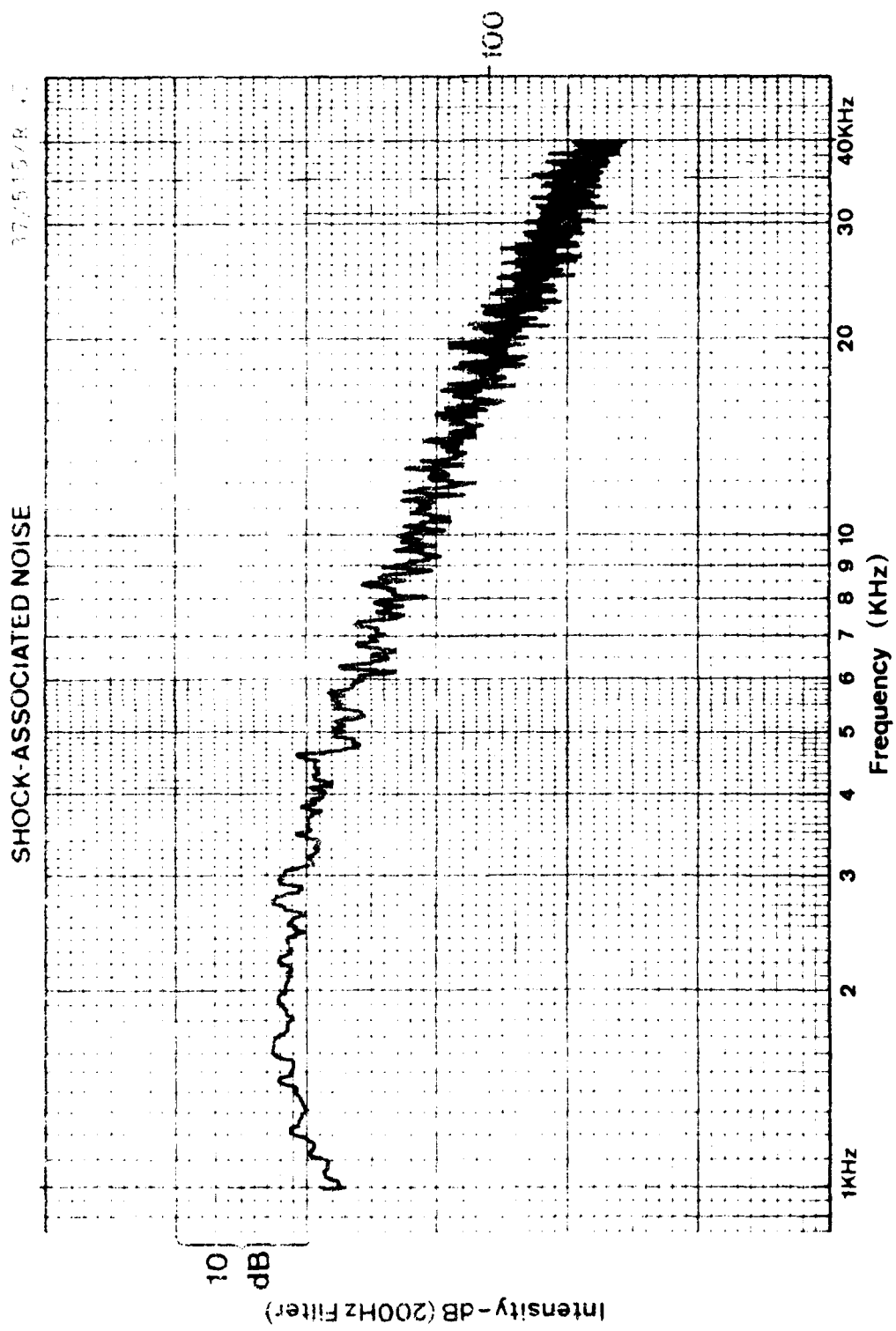






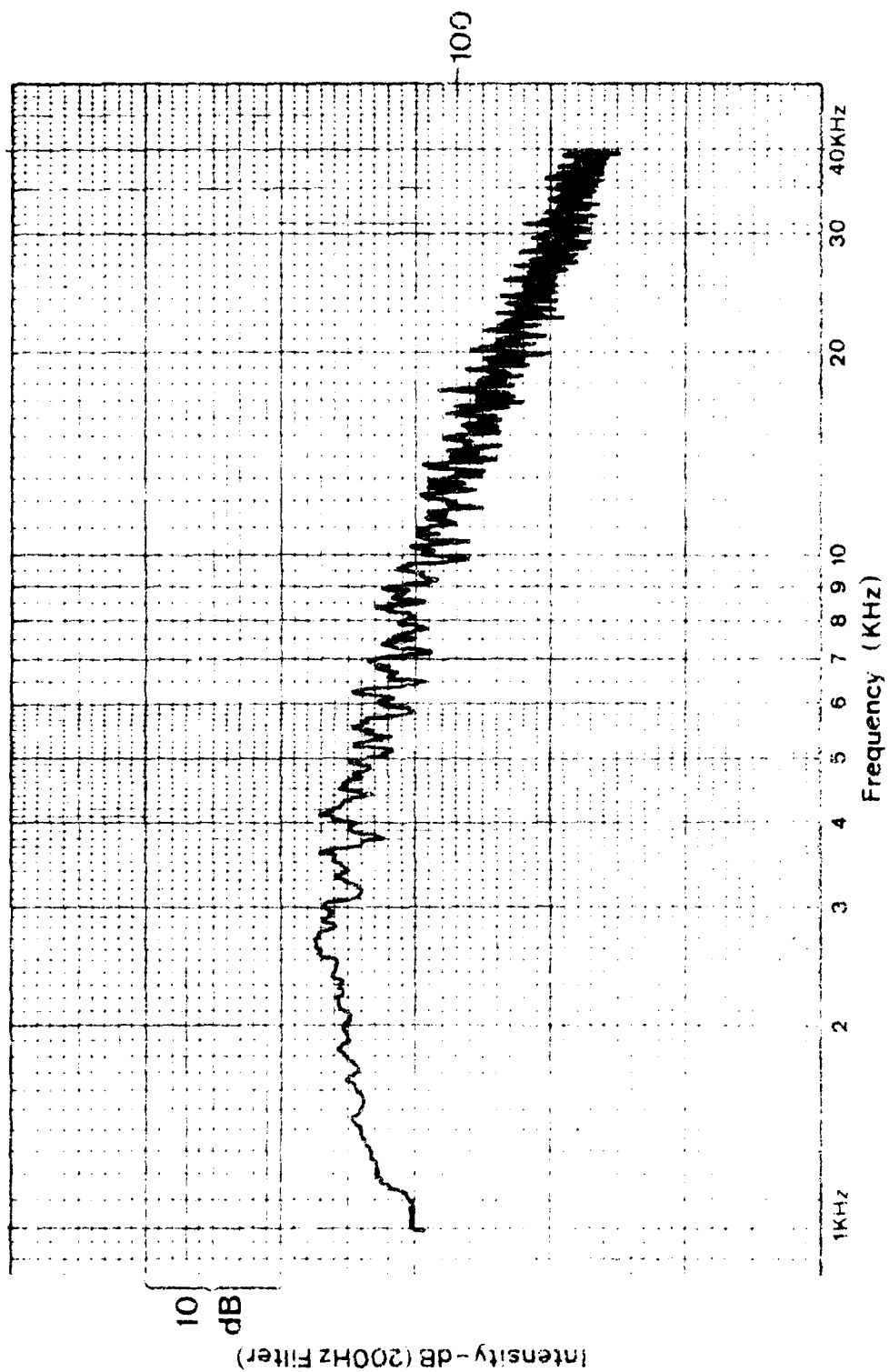






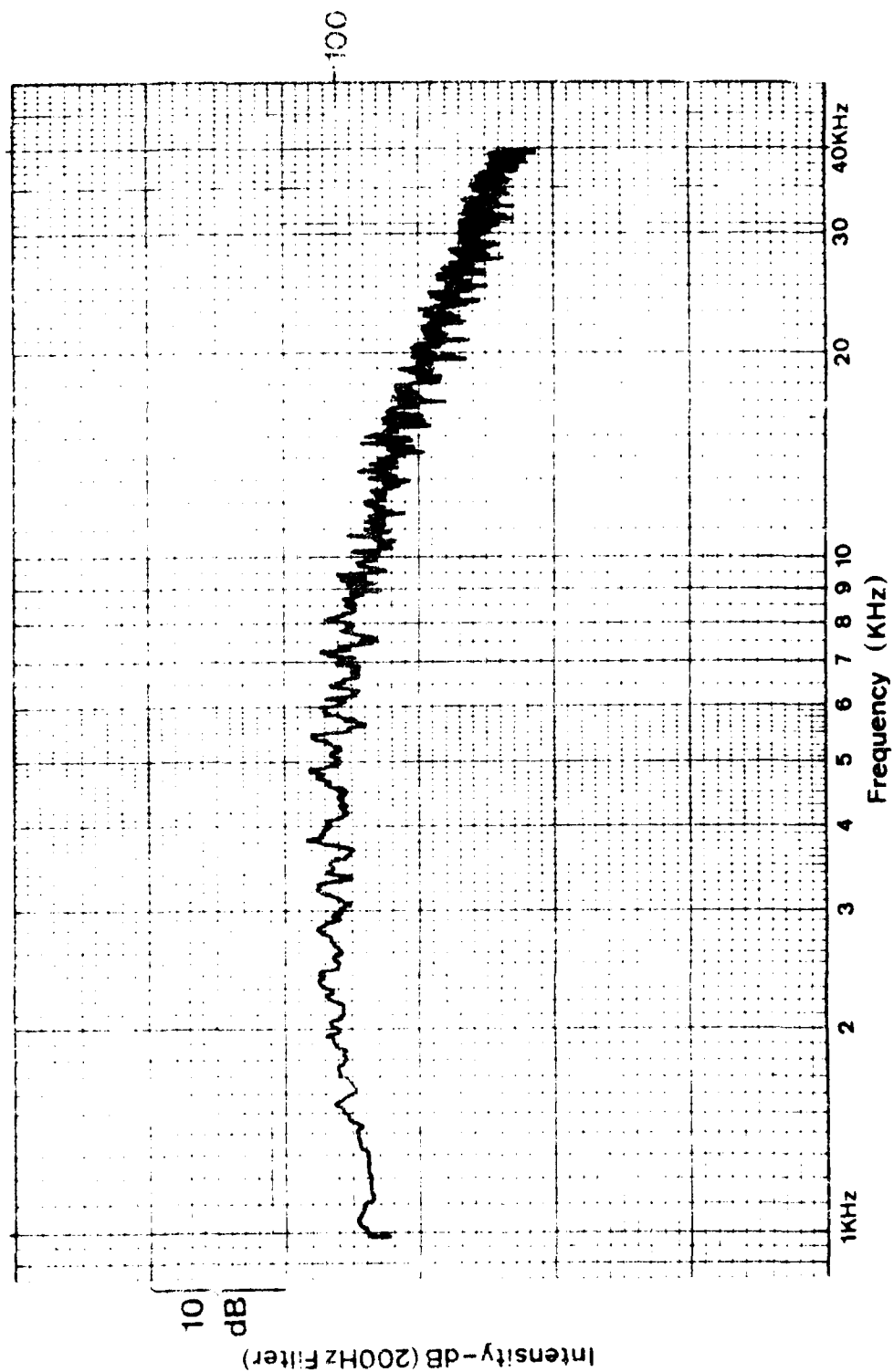
SHOCK-ASSOCIATED NOISE

37/515/R/60



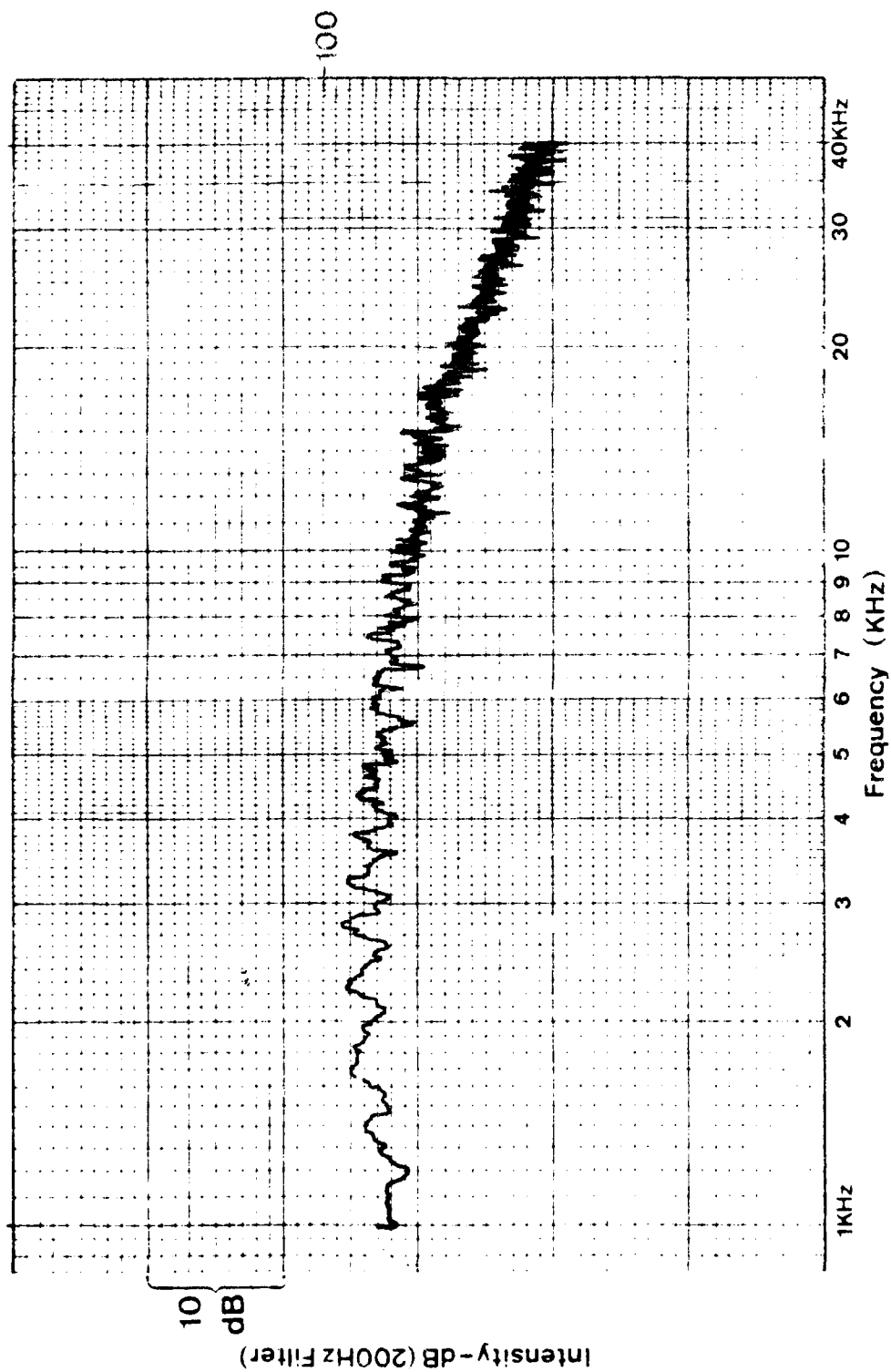
SHOCK ASSOCIATED NOISE

10-15-67



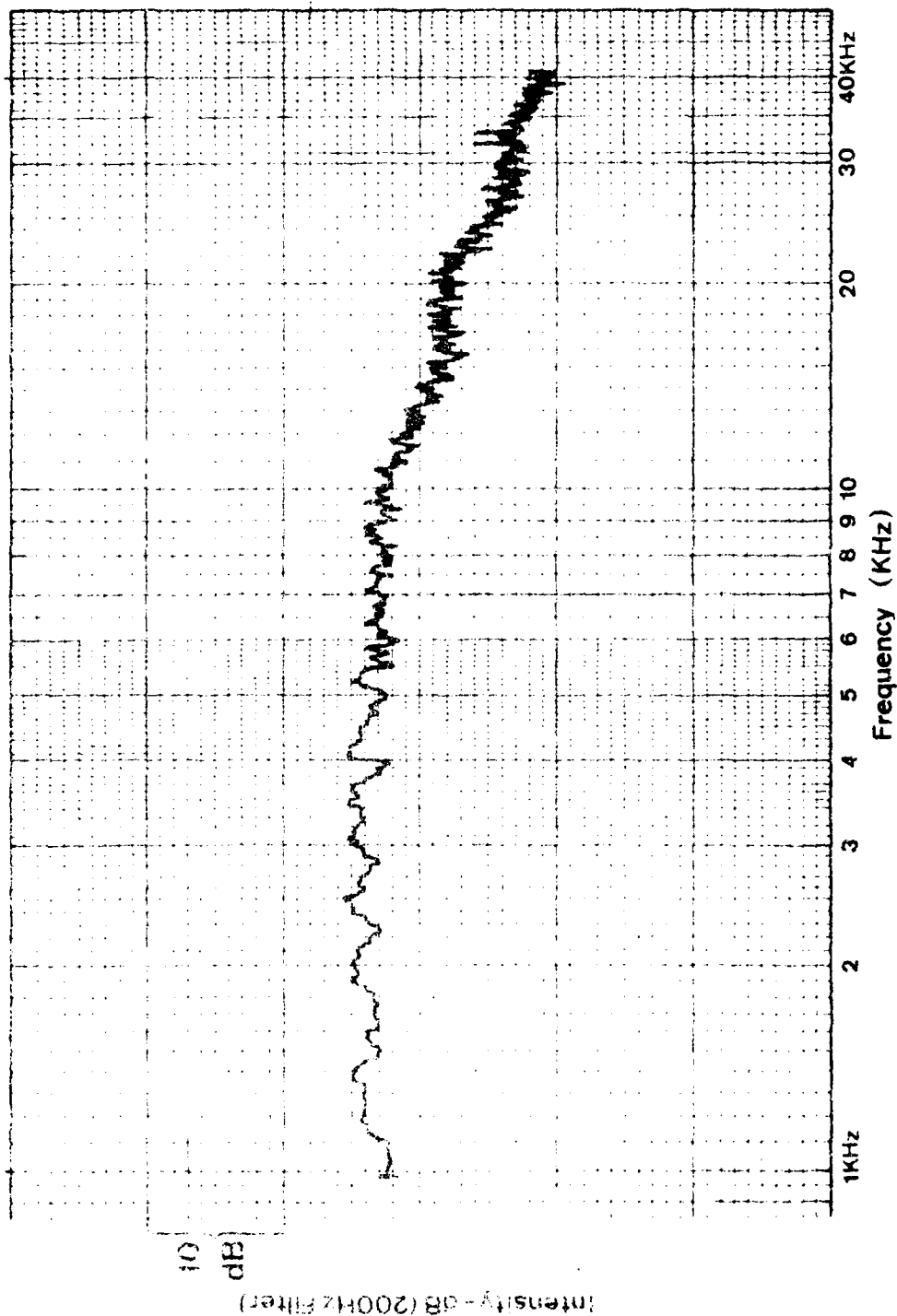
SHOCK-ASSOCIATED NOISE

37, 53, 69, 85



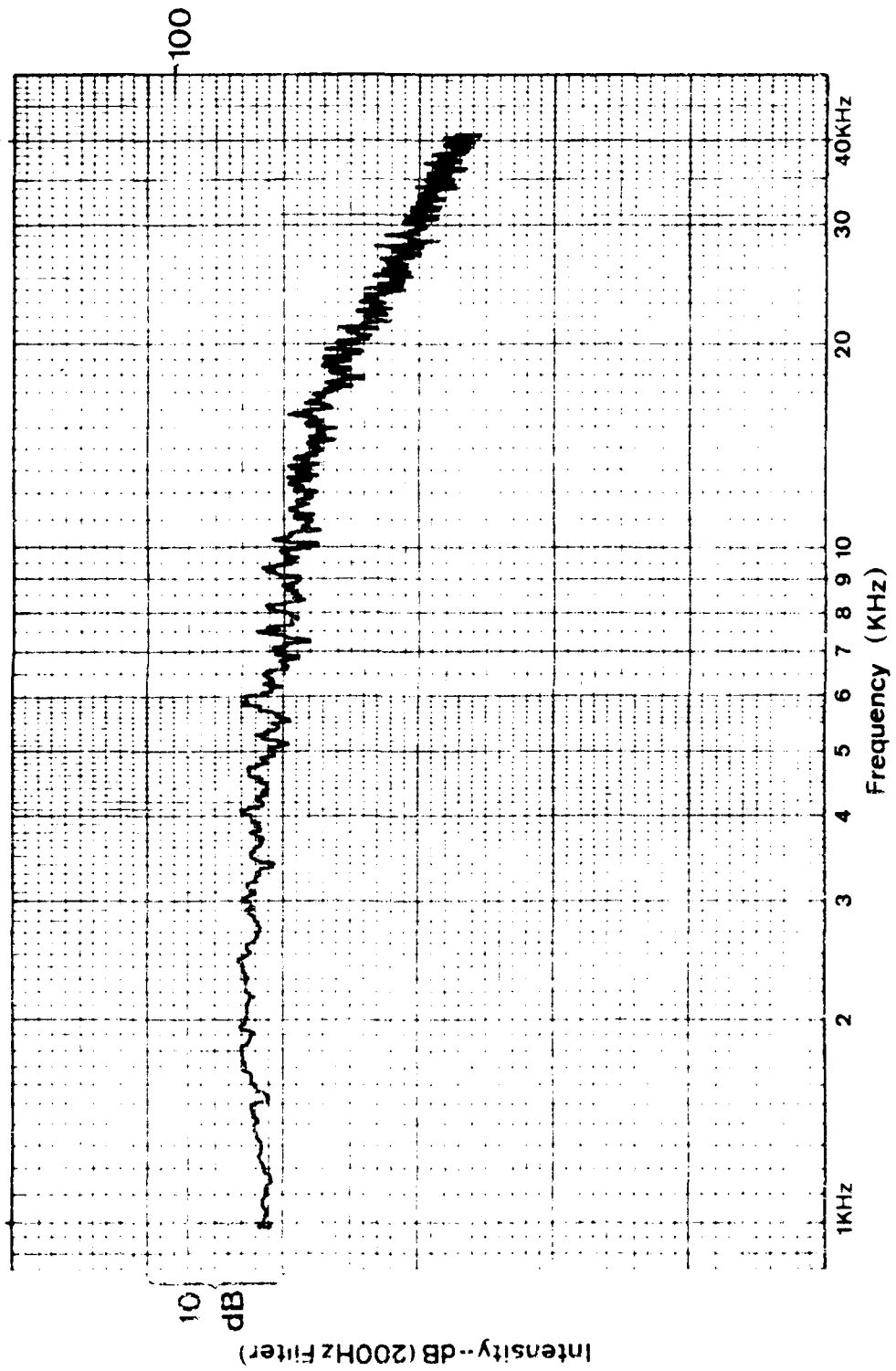
SHOCK-ASSOCIATED NOISE

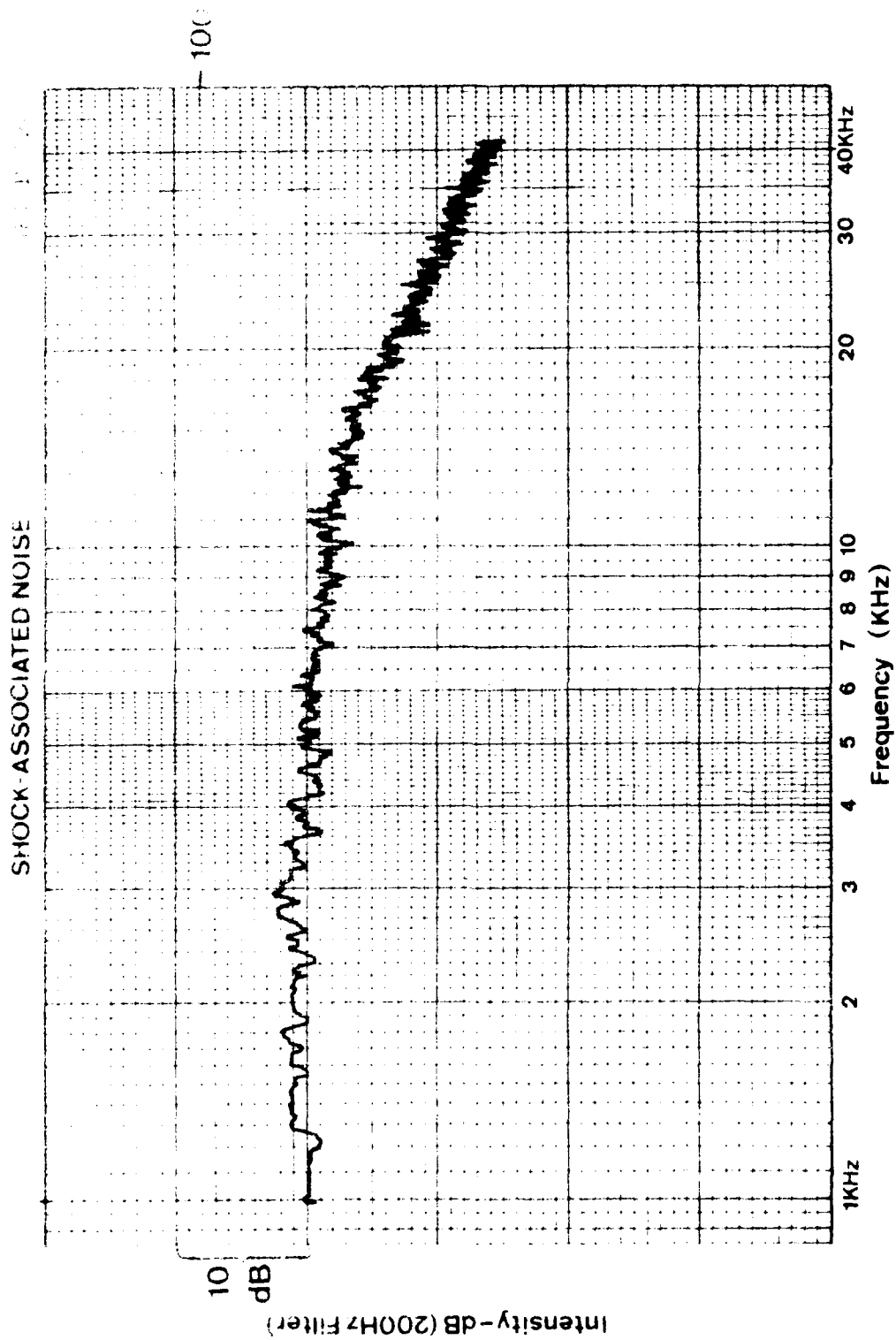
17. 10. 1 4. 90

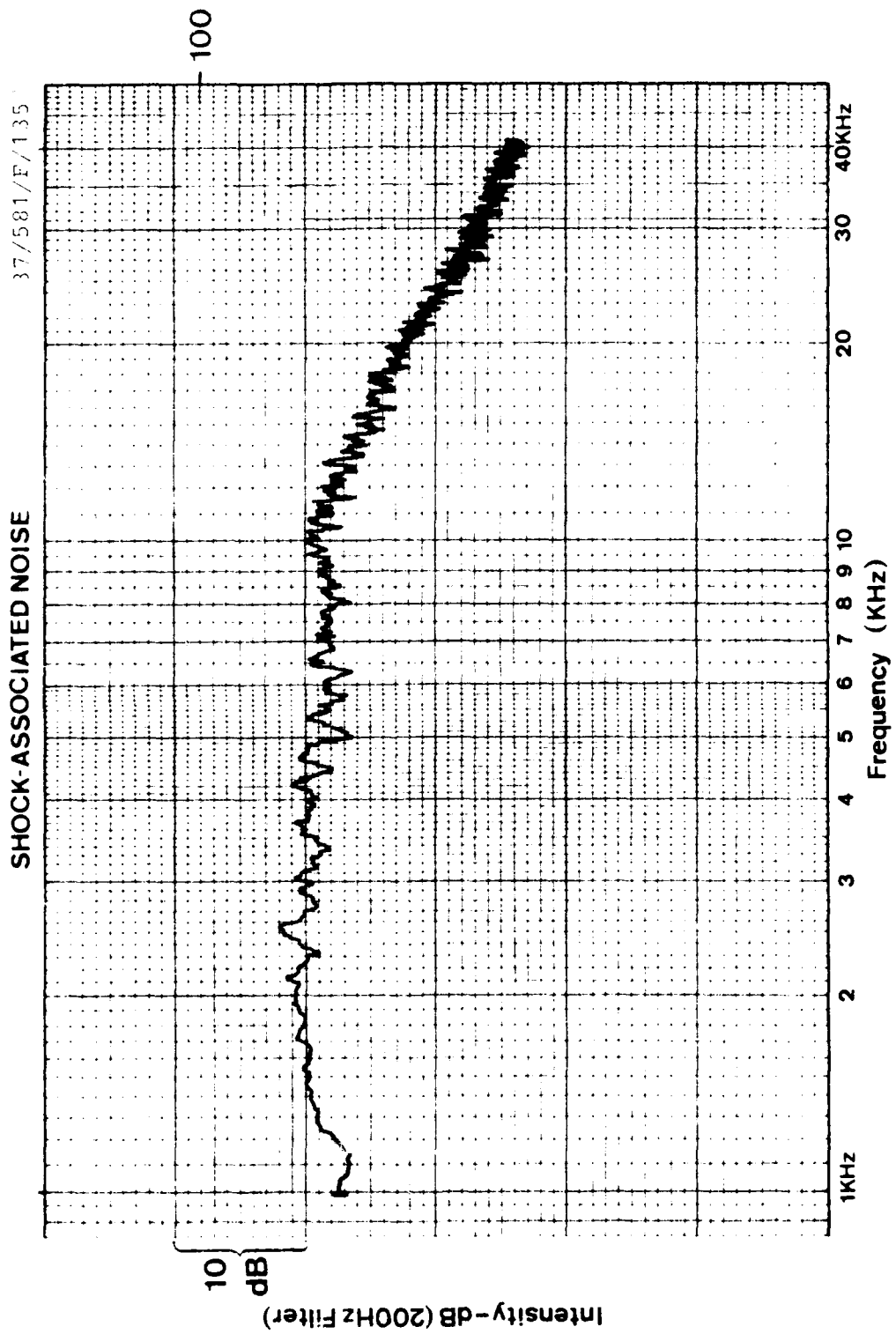


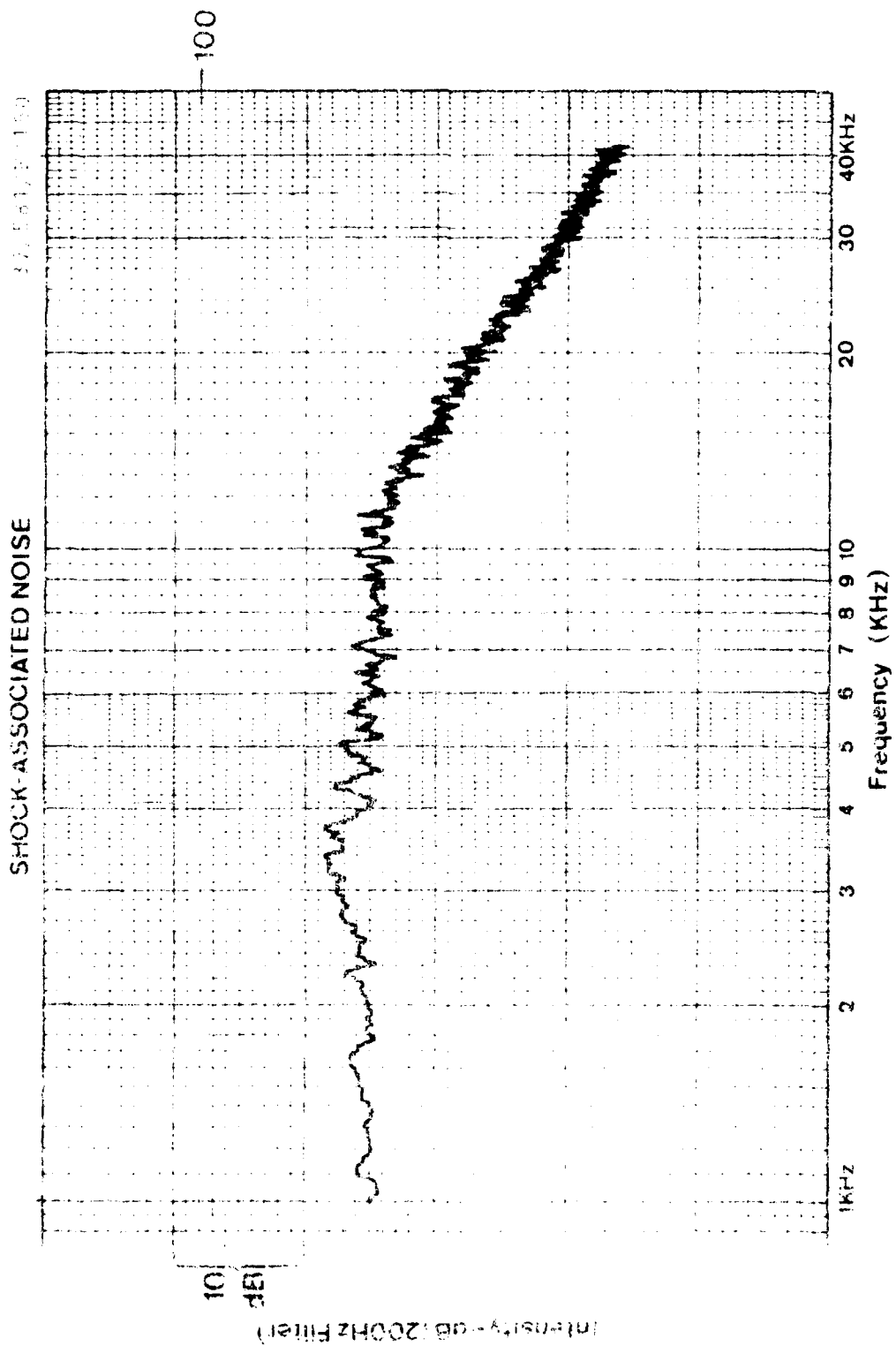
SHOCK-ASSOCIATED NOISE

37/581/F/105



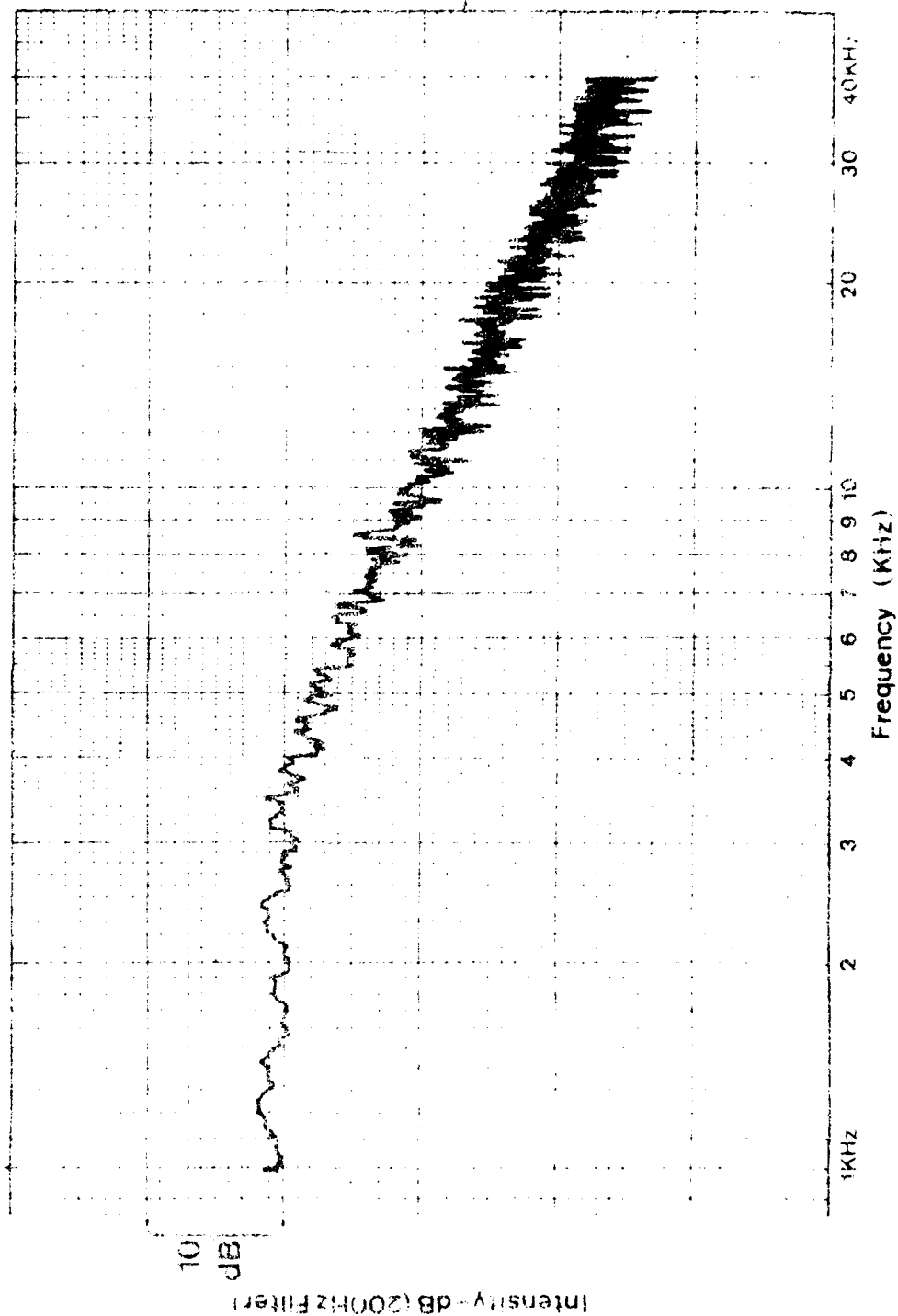


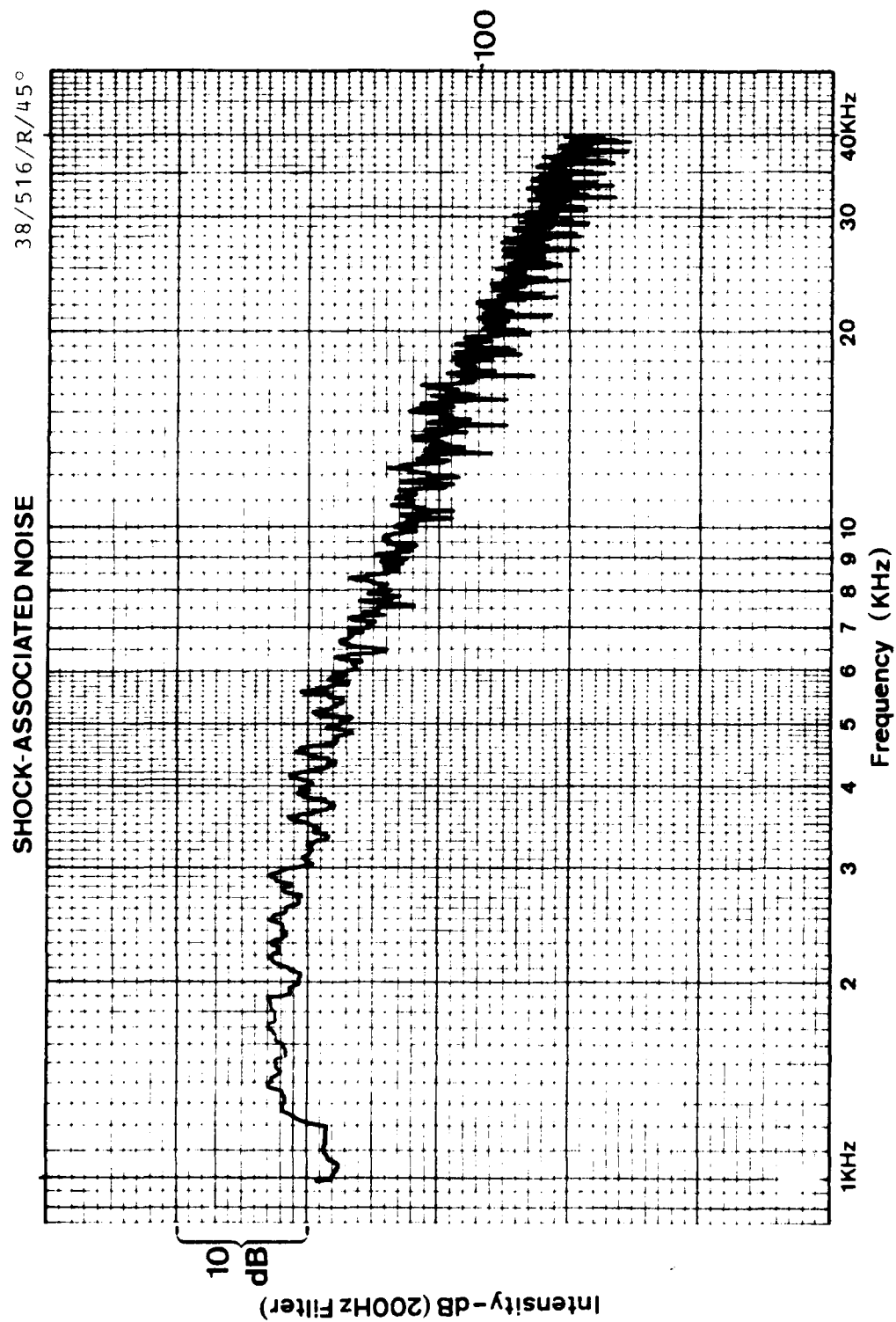




SHOCK-ASSOCIATED NOISE

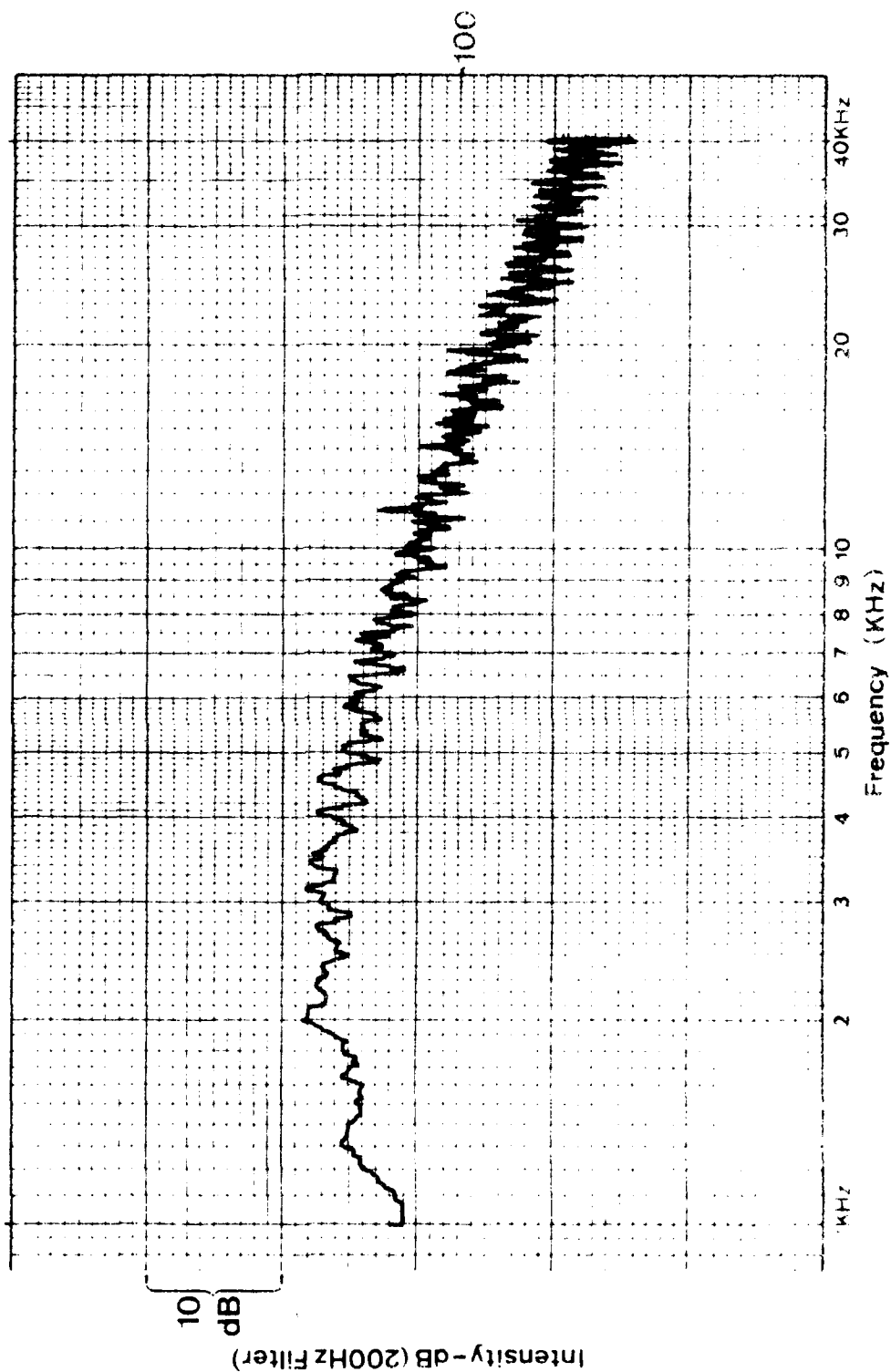
00516-103





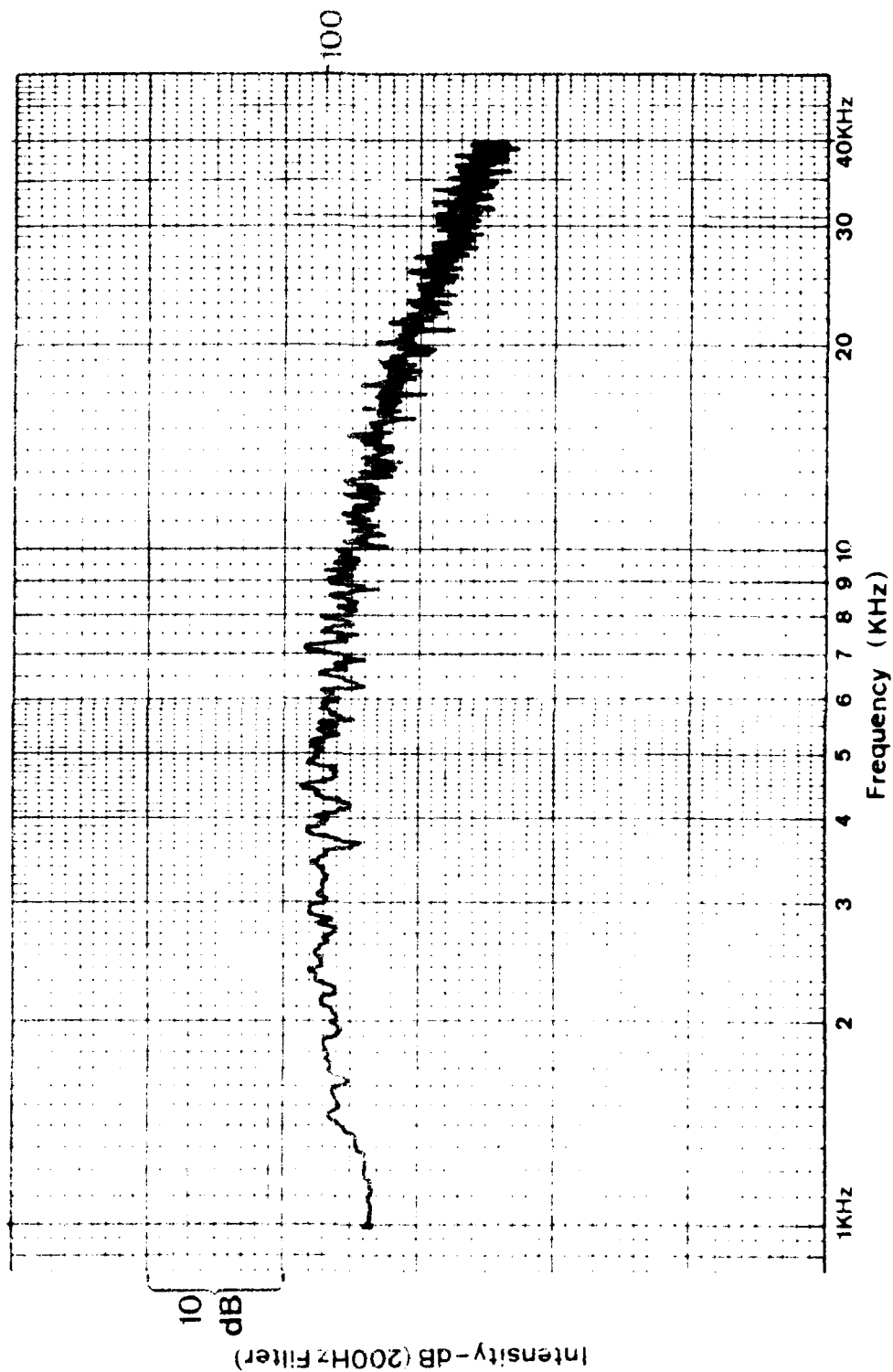
SHOCK-ASSOCIATED NOISE

38/516/R/60



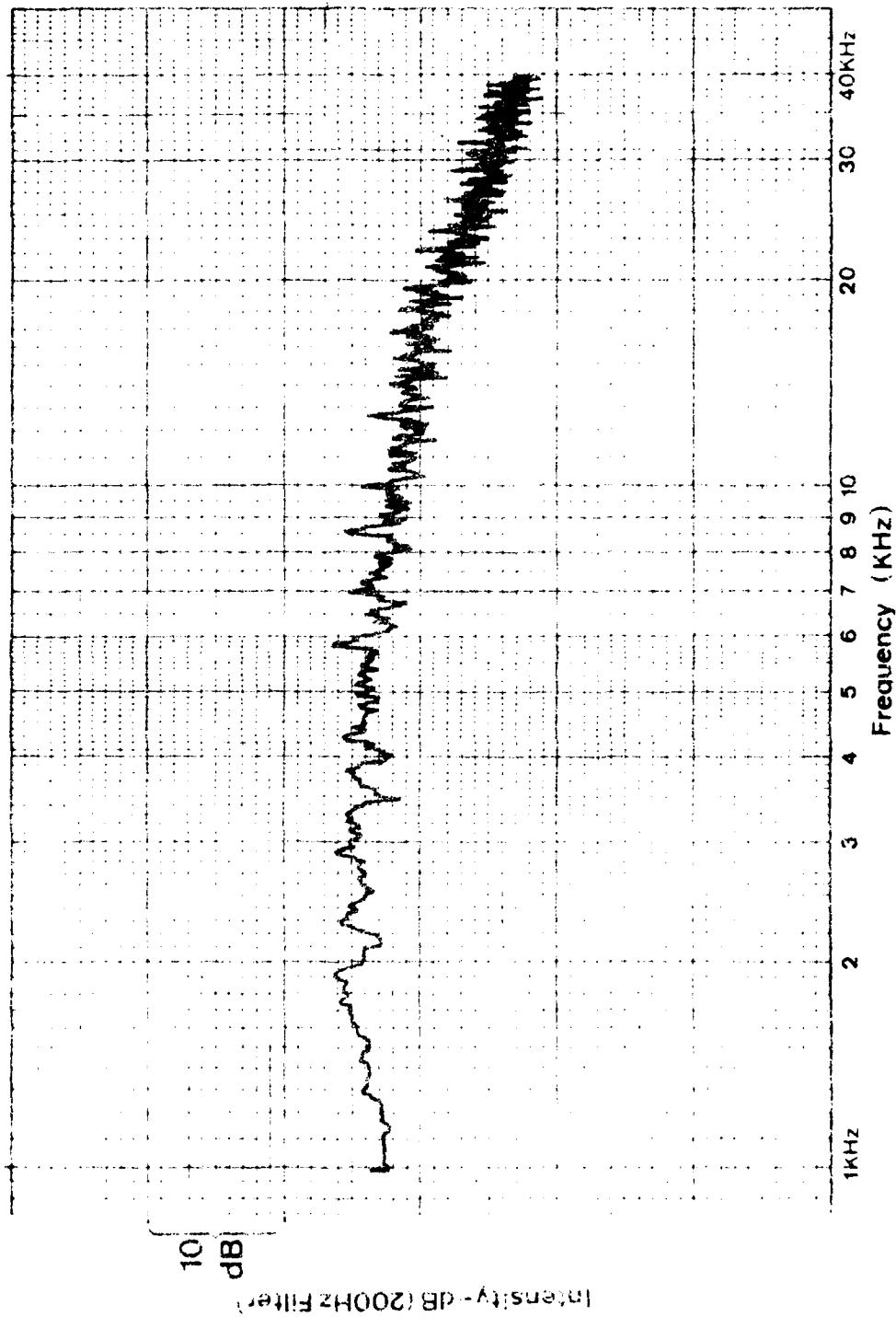
SHOCK-ASSOCIATED NOISE

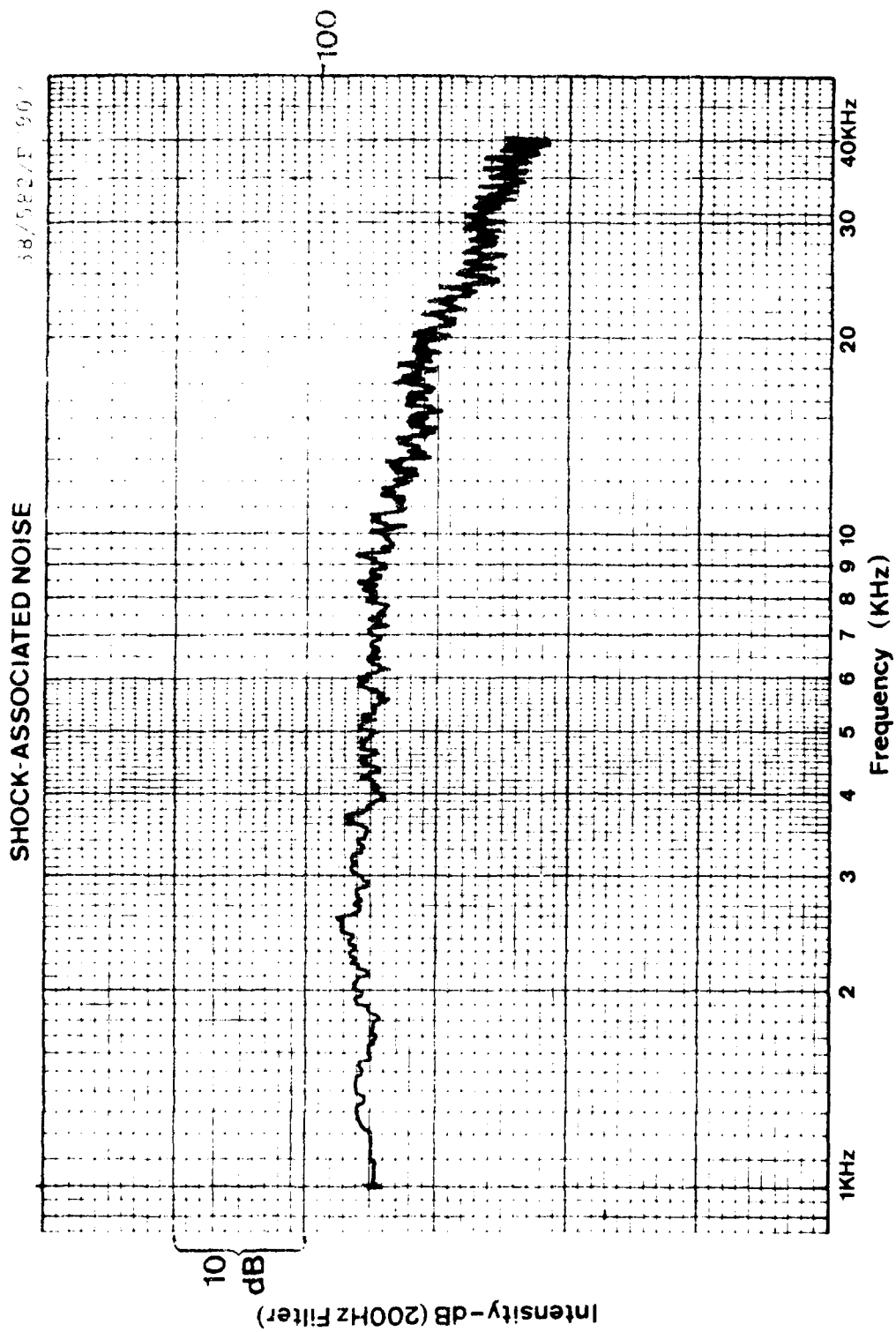
35-516/R-757

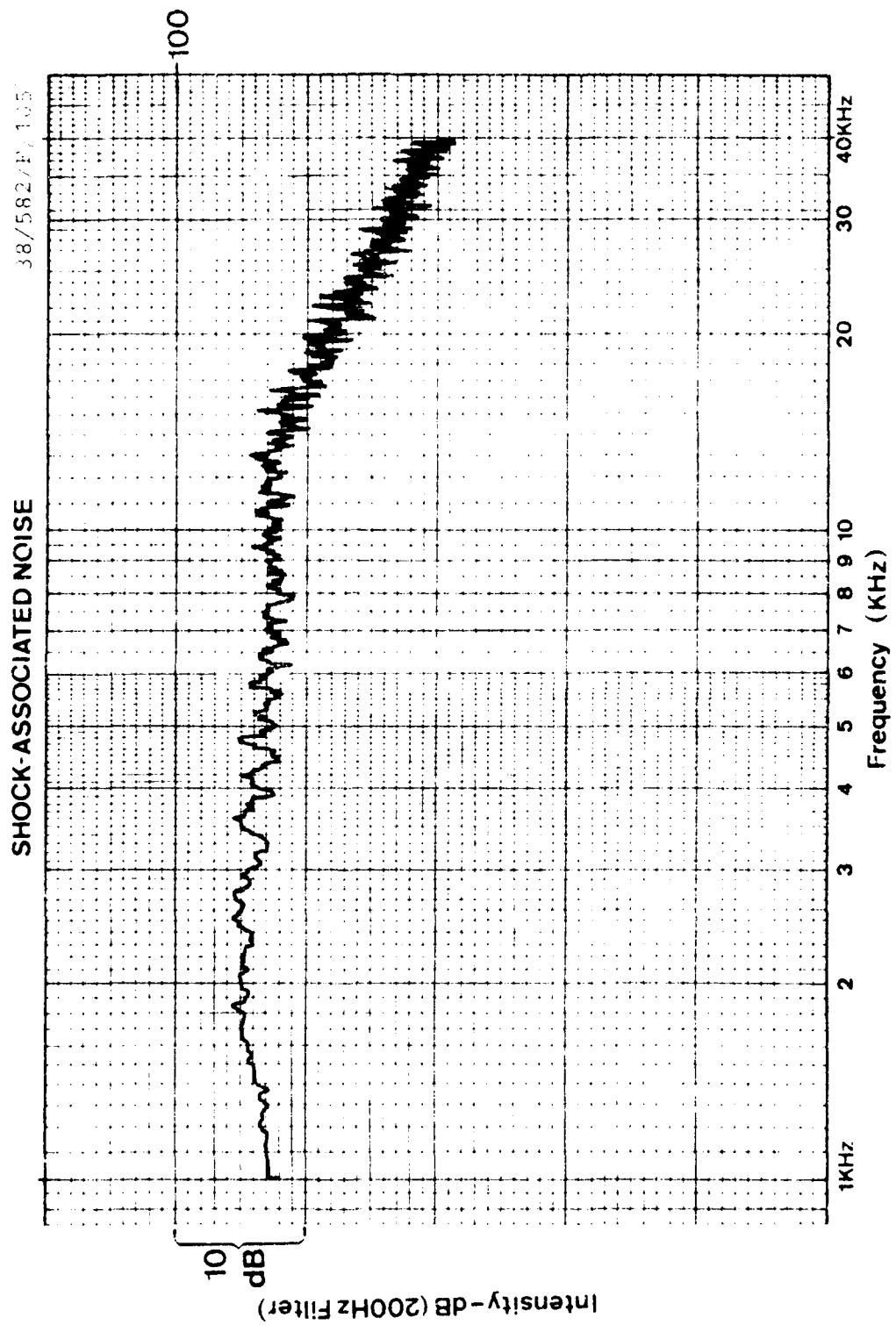


SHOCK-ASSOCIATED NOISE

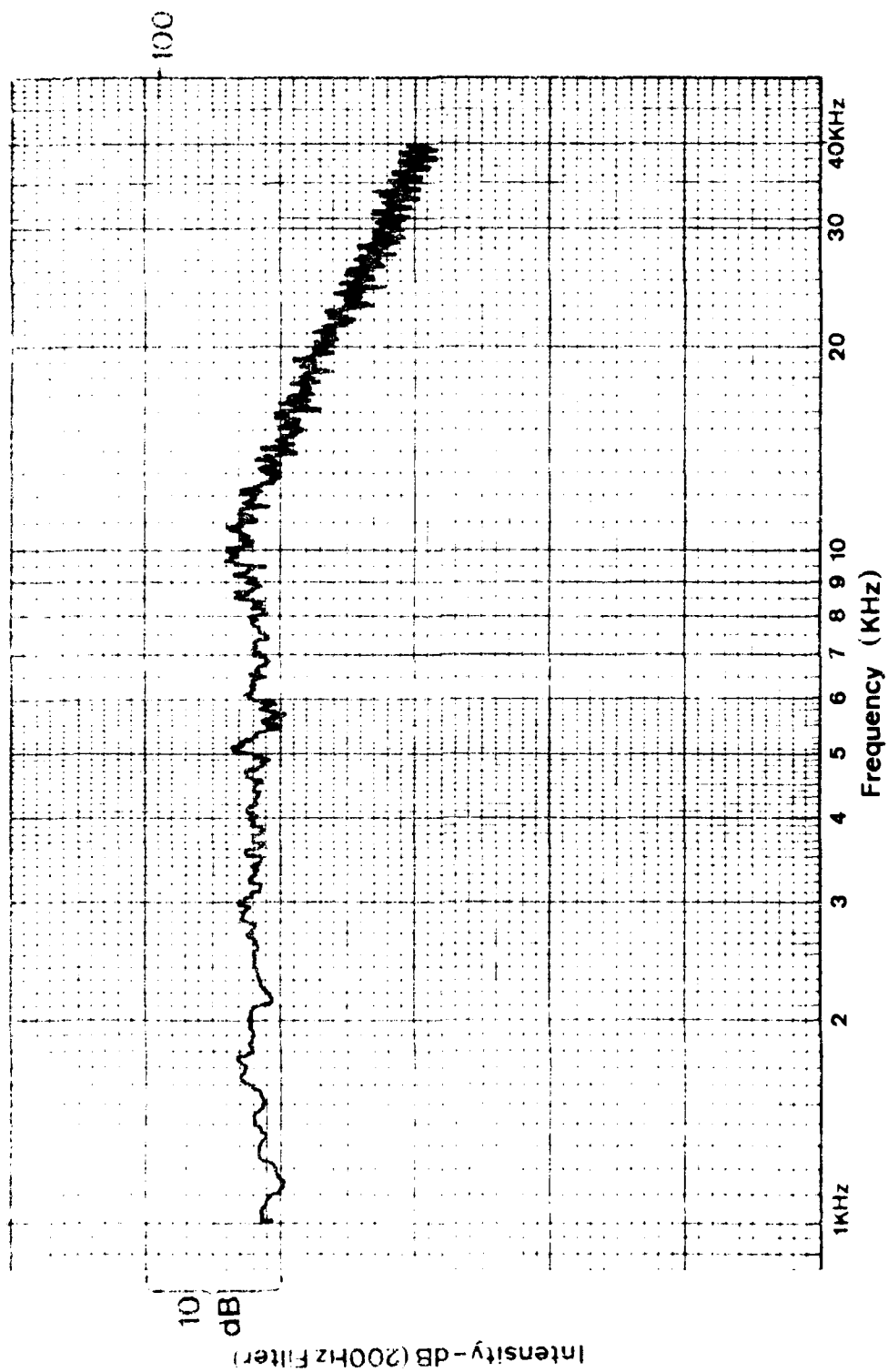
100,000 R.m.s.





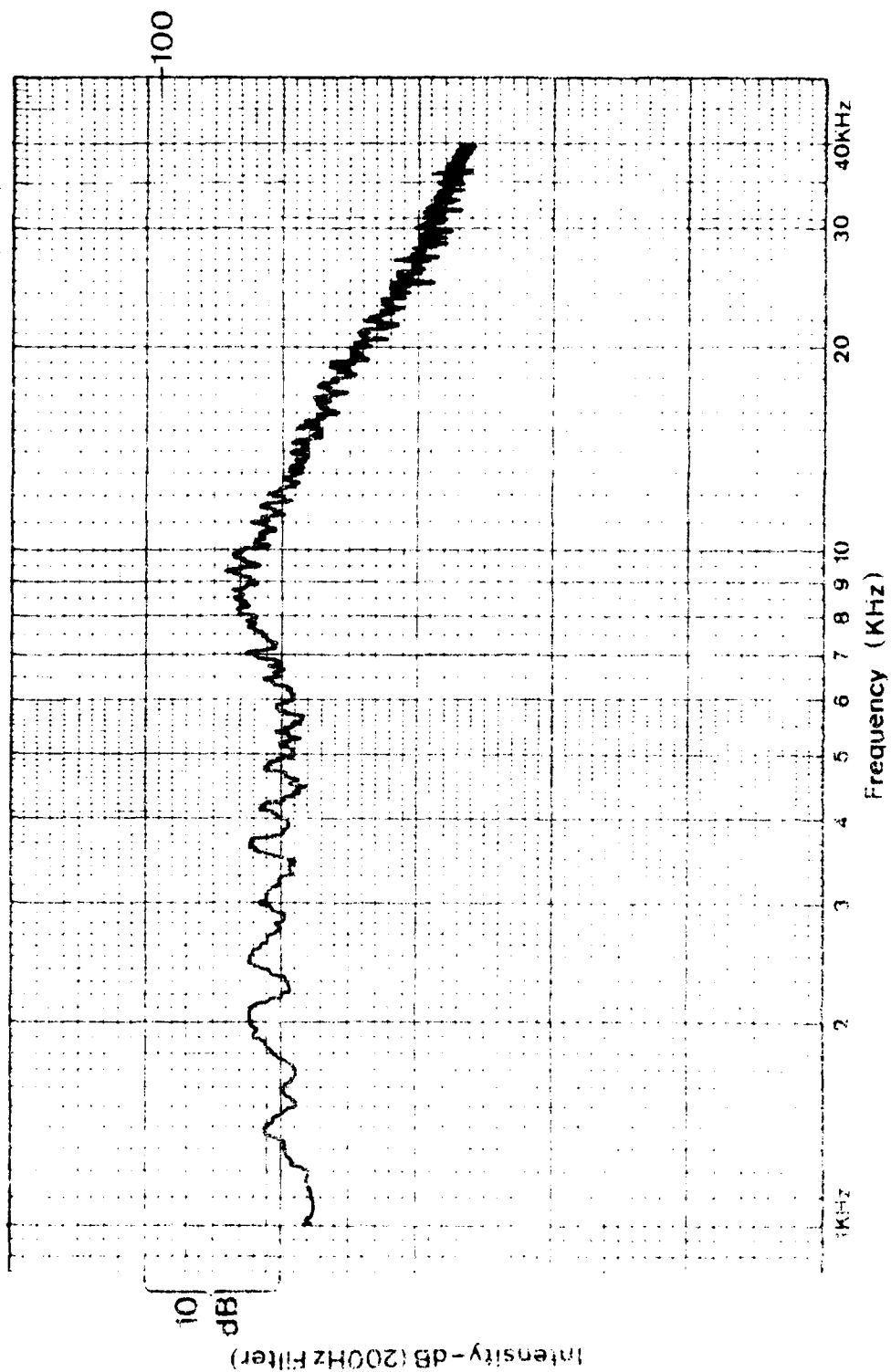


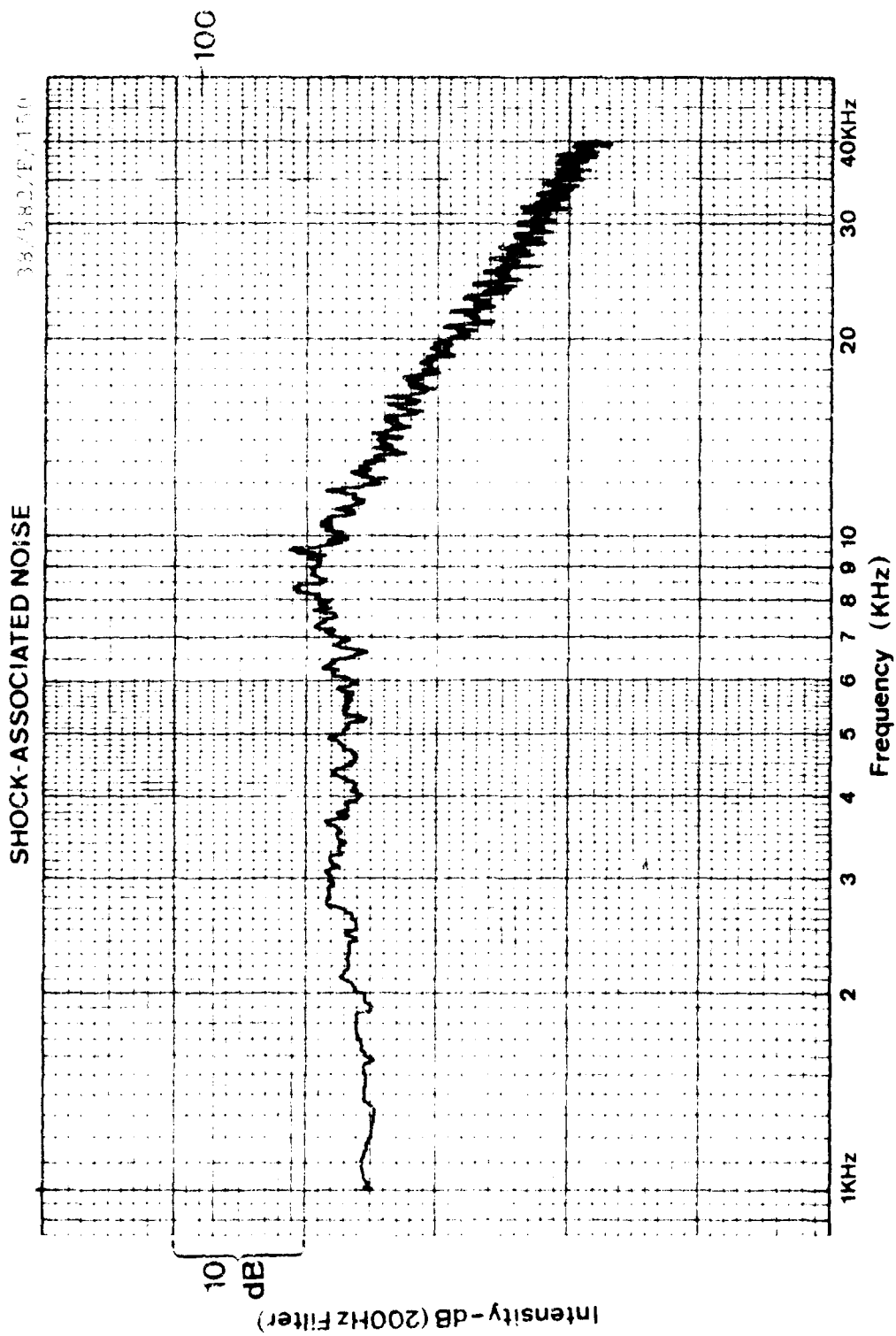
SHOCK-ASSOCIATED NOISE



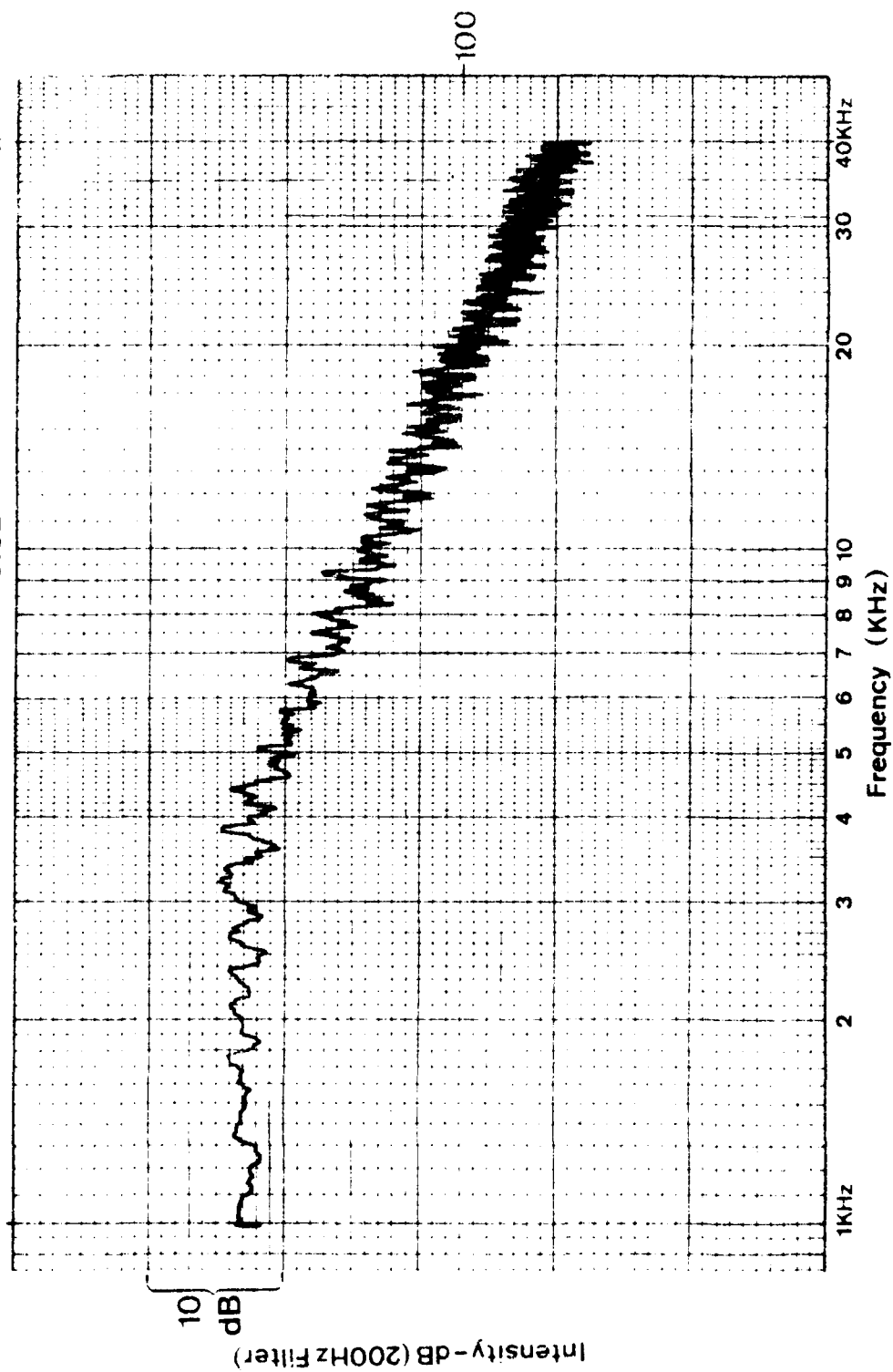
SHOCK-ASSOCIATED NOISE

38/582/F 135

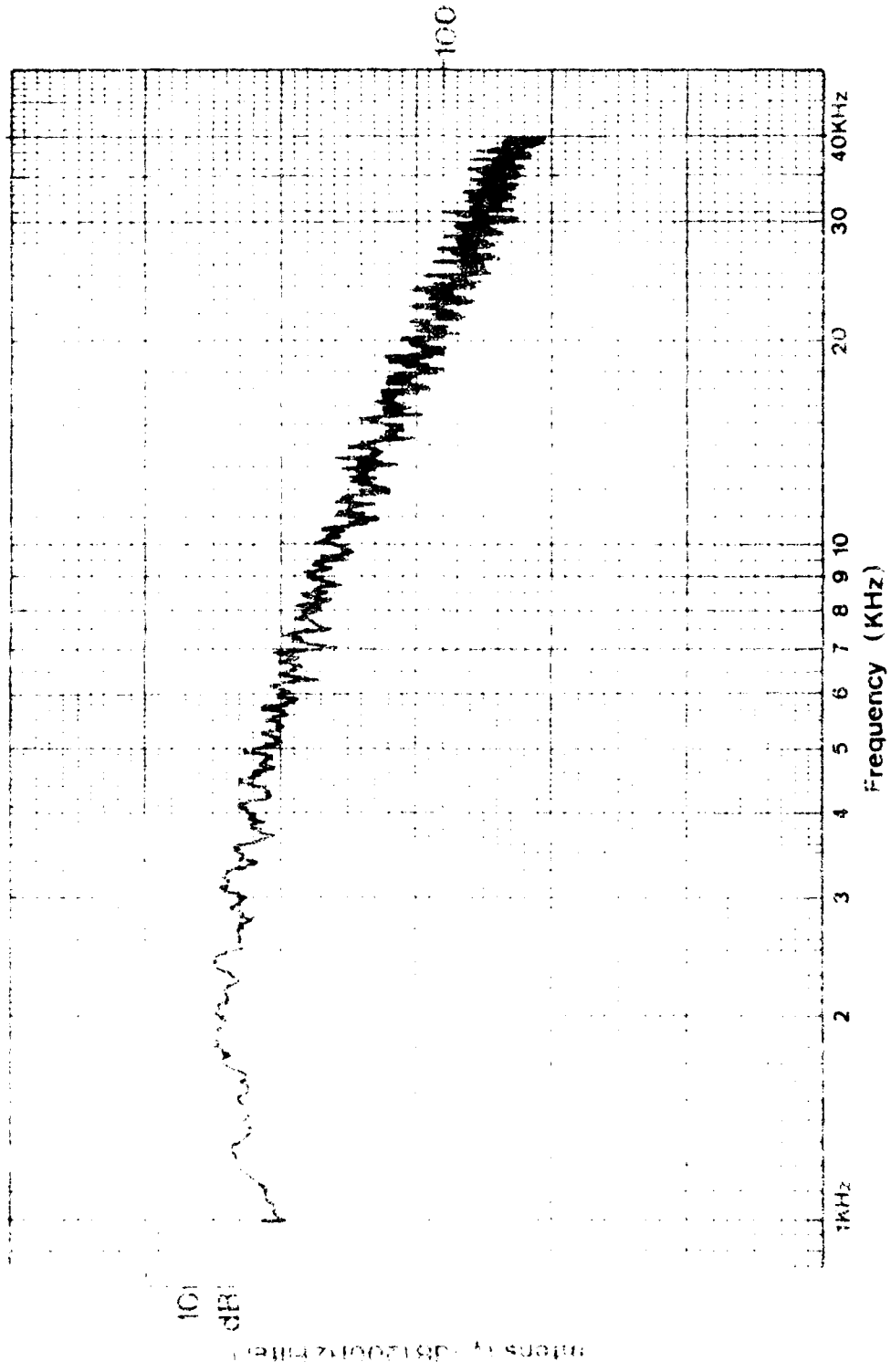




SHOCK-ASSOCIATED NOISE

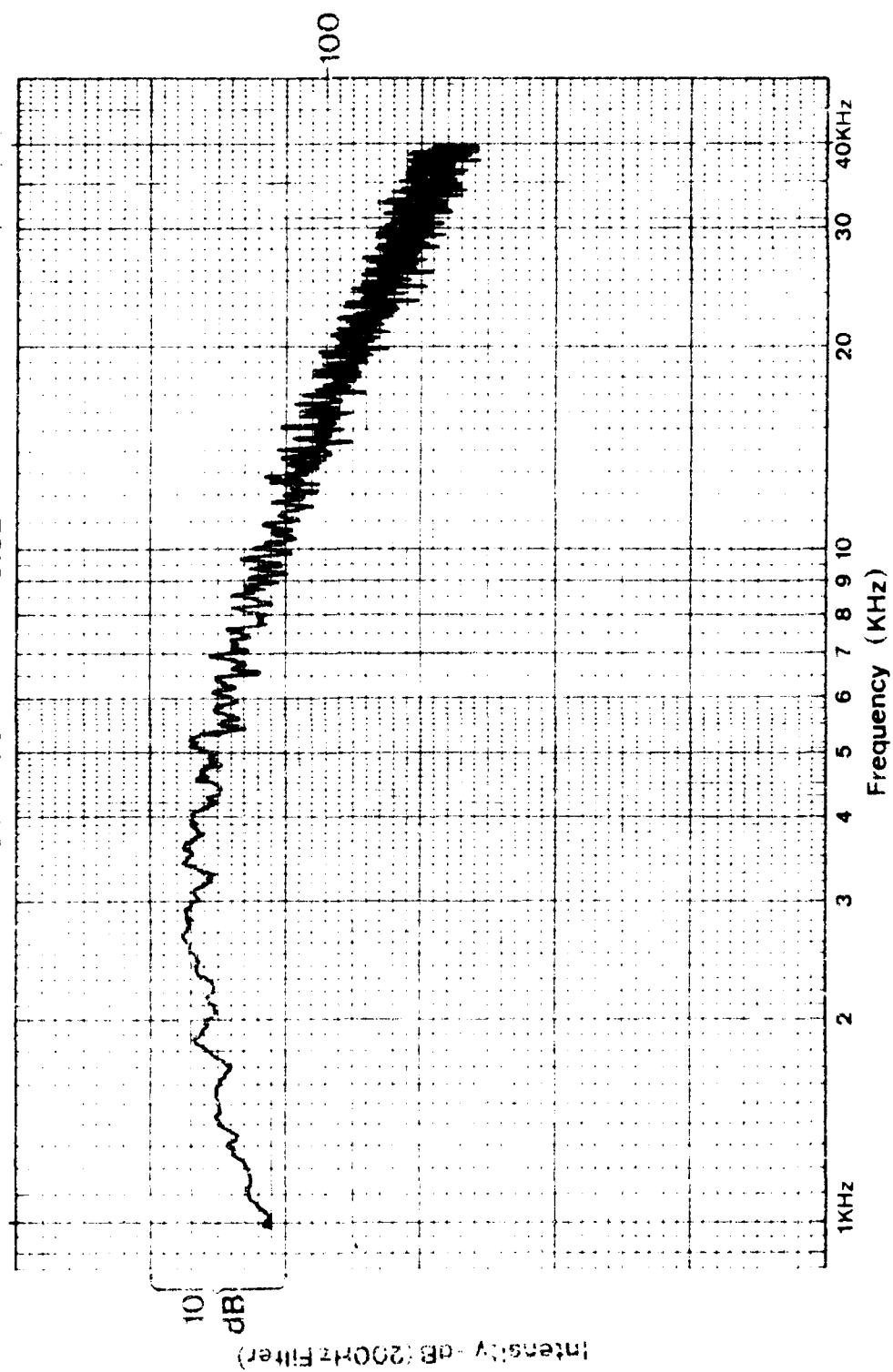


SHOCK-ASSOCIATED NOISE

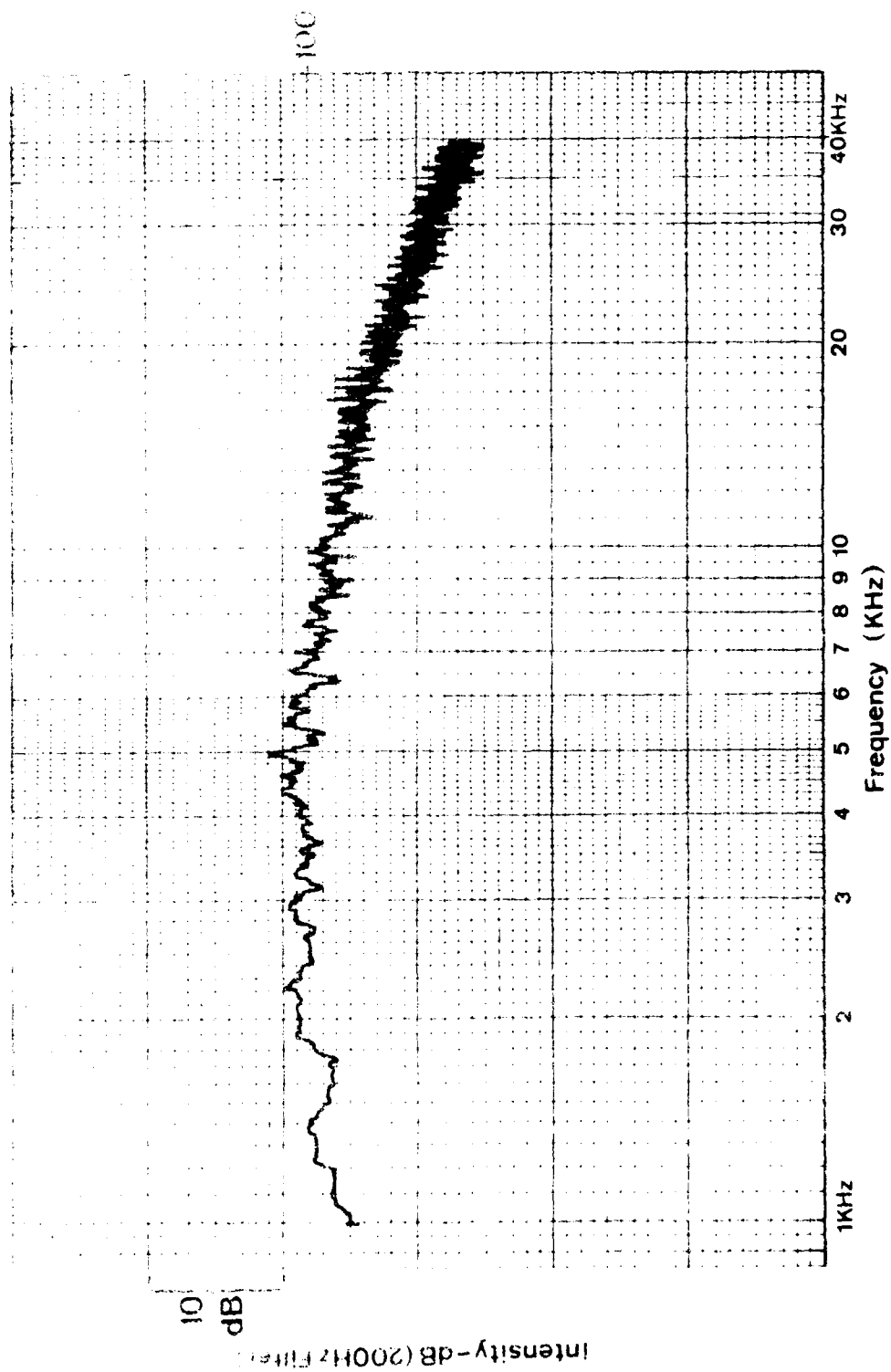


SHOCK-ASSOCIATED NOISE

39/517/R-60

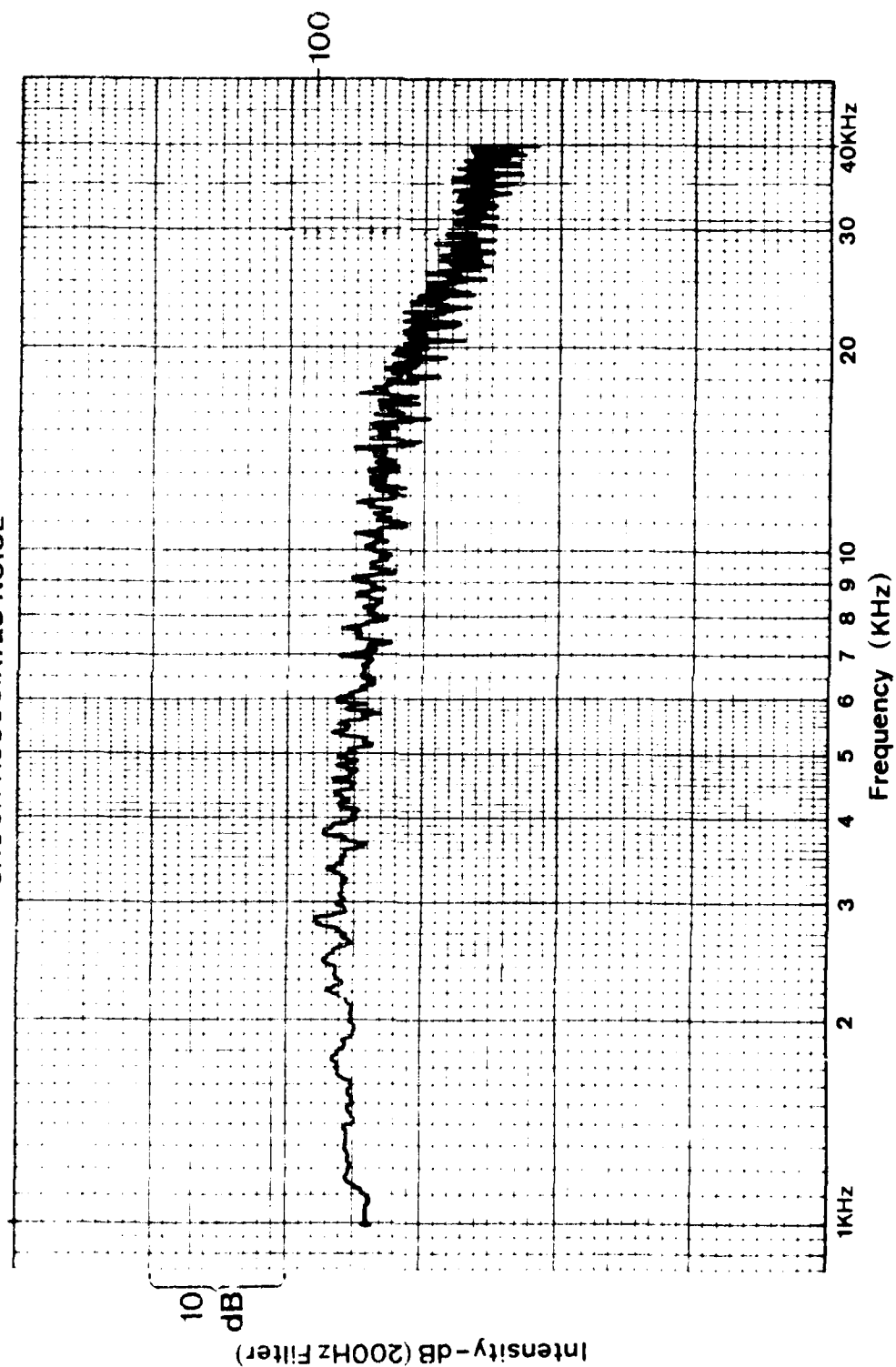


SHOCK-ASSOCIATED NOISE

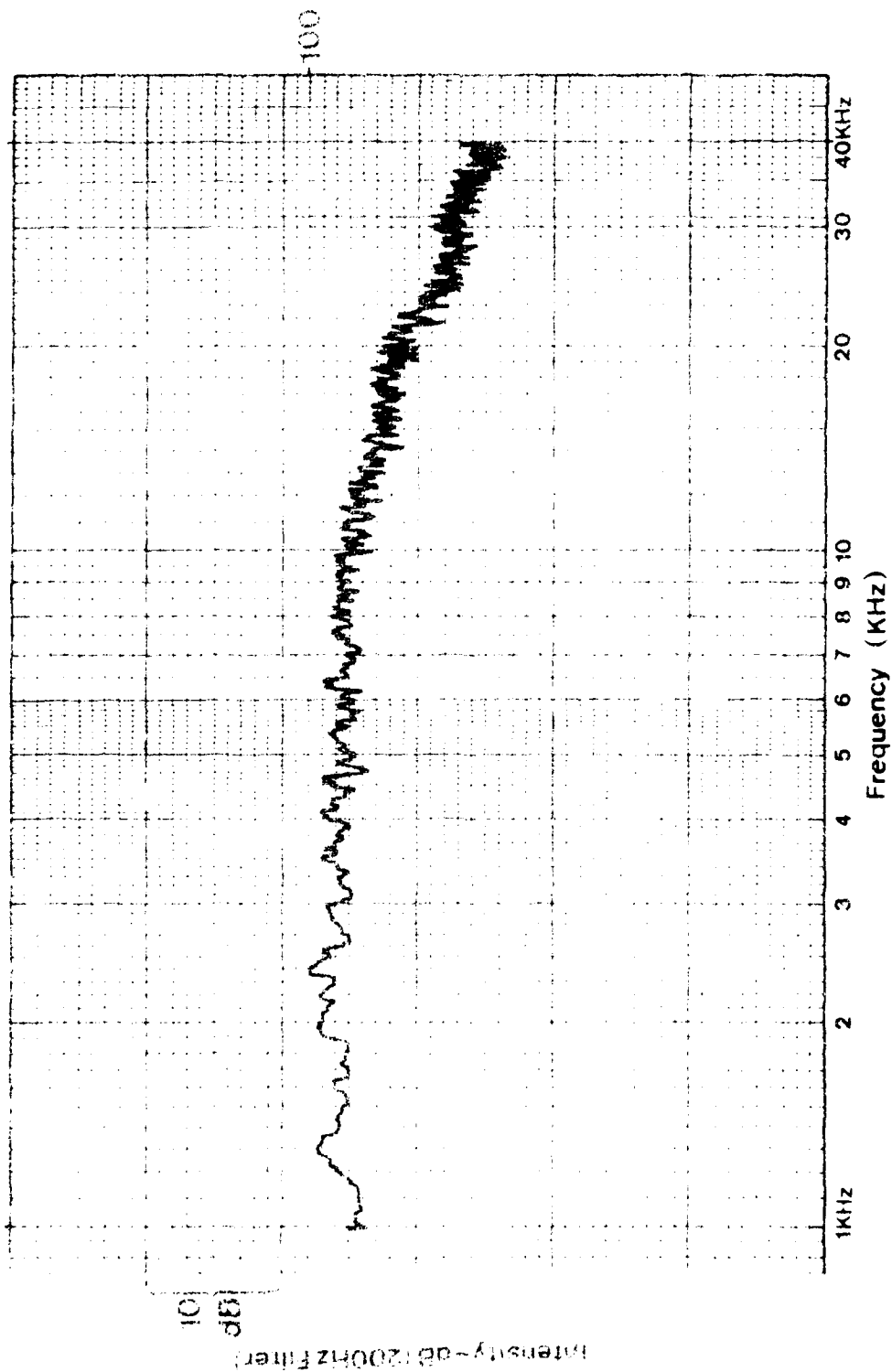


SHOCK-ASSOCIATED NOISE

39/517/R/90

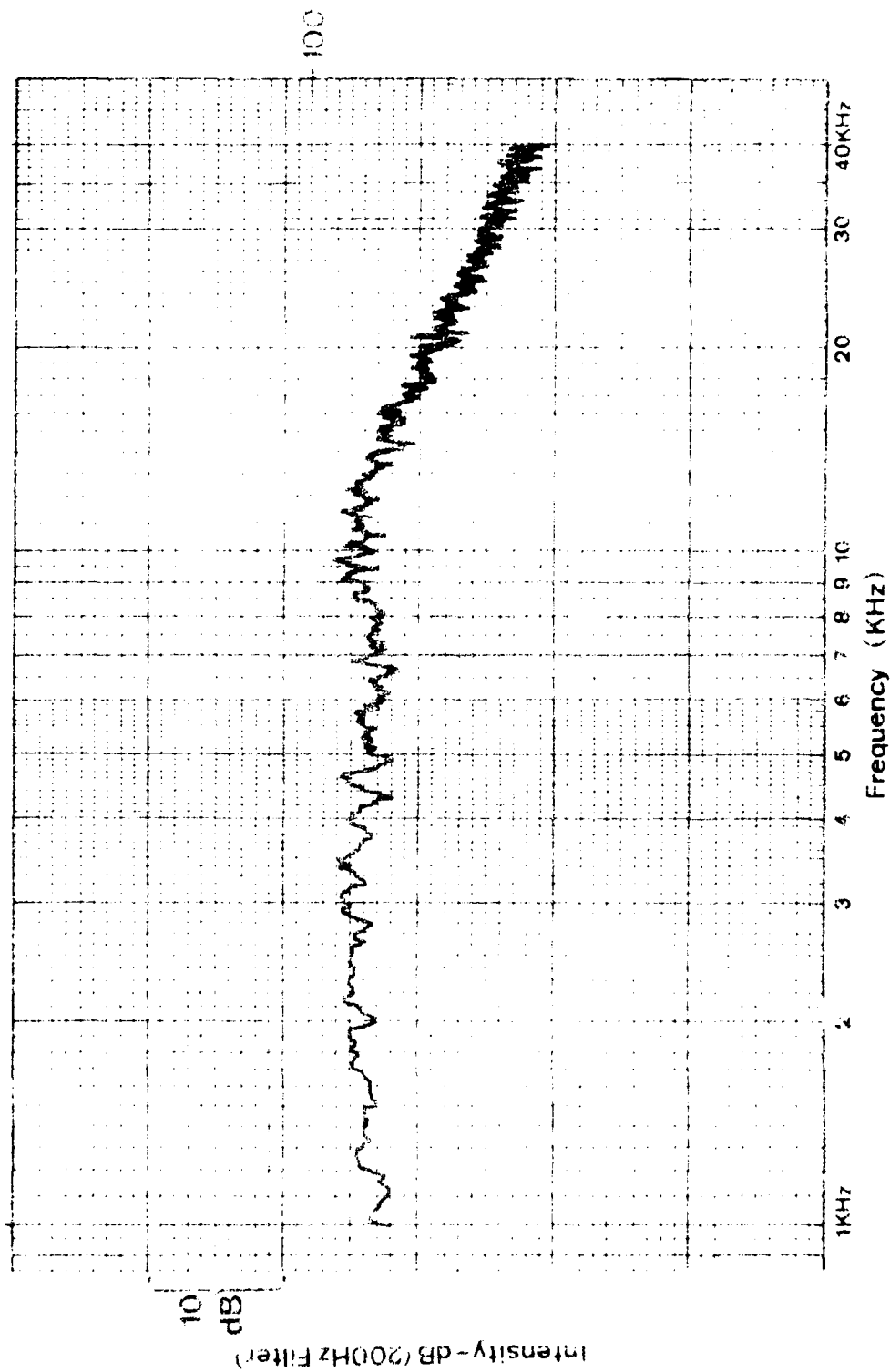


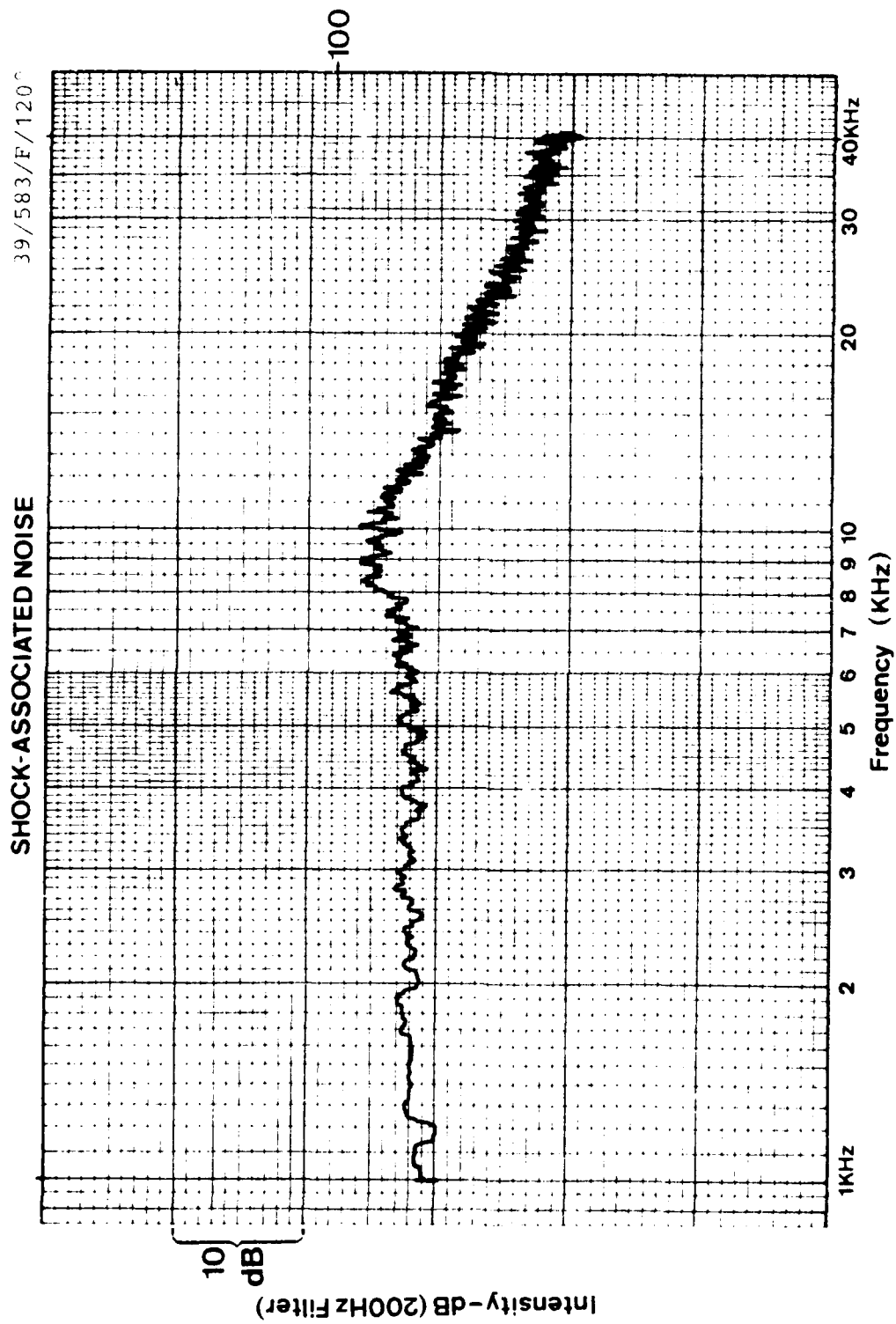
SHOCK ASSOCIATED NOISE

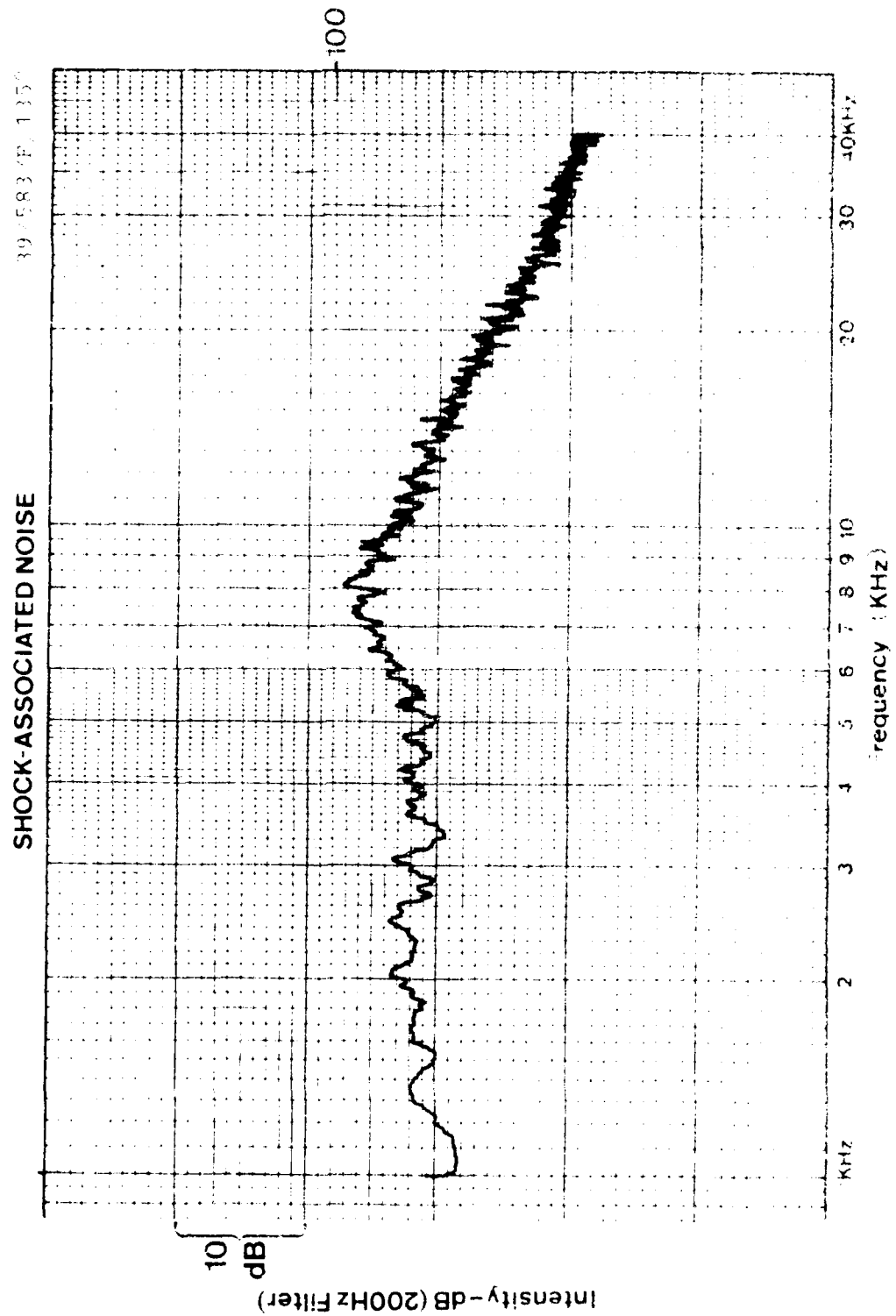


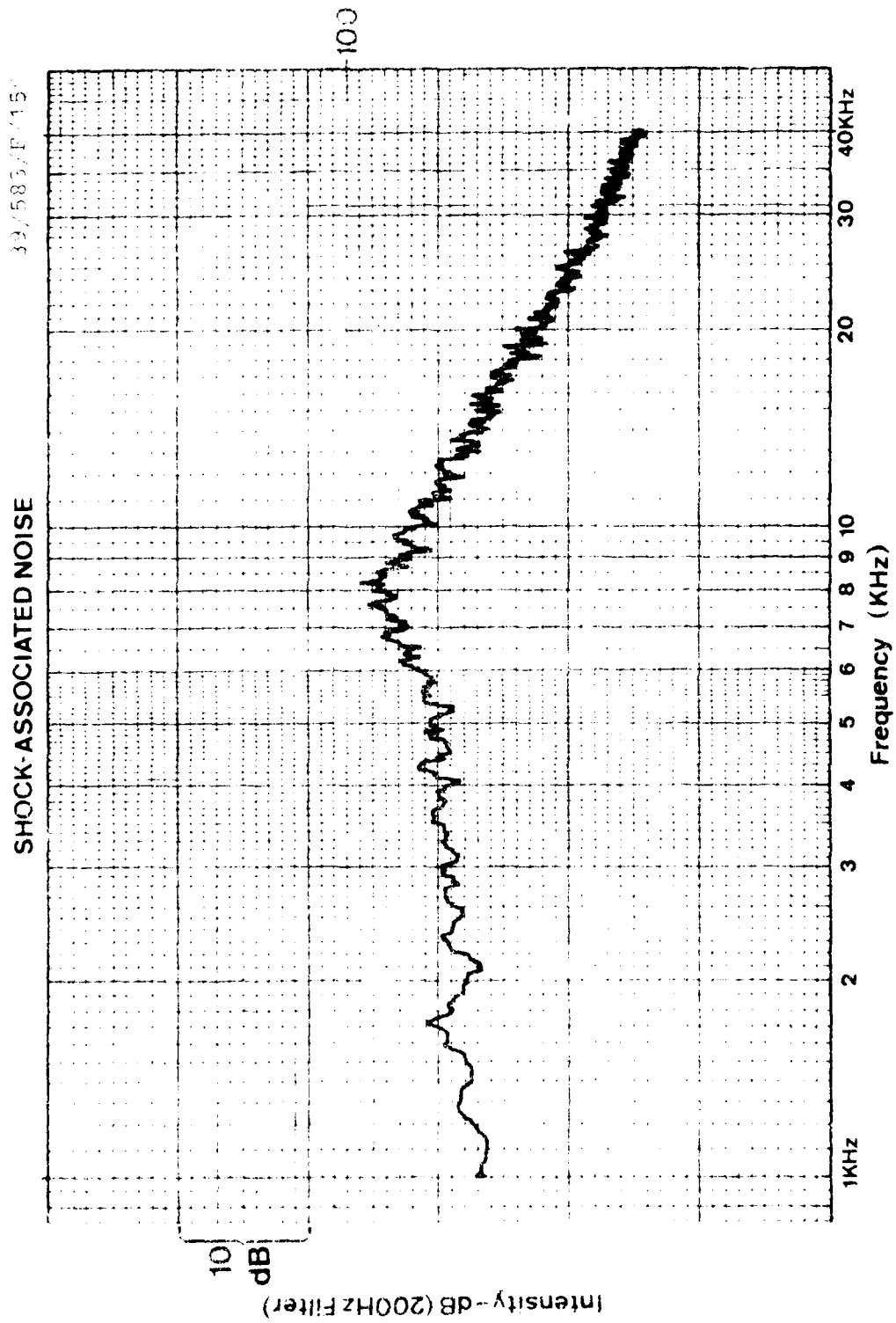
SHOCK-ASSOCIATED NOISE

39-583-9-1-1



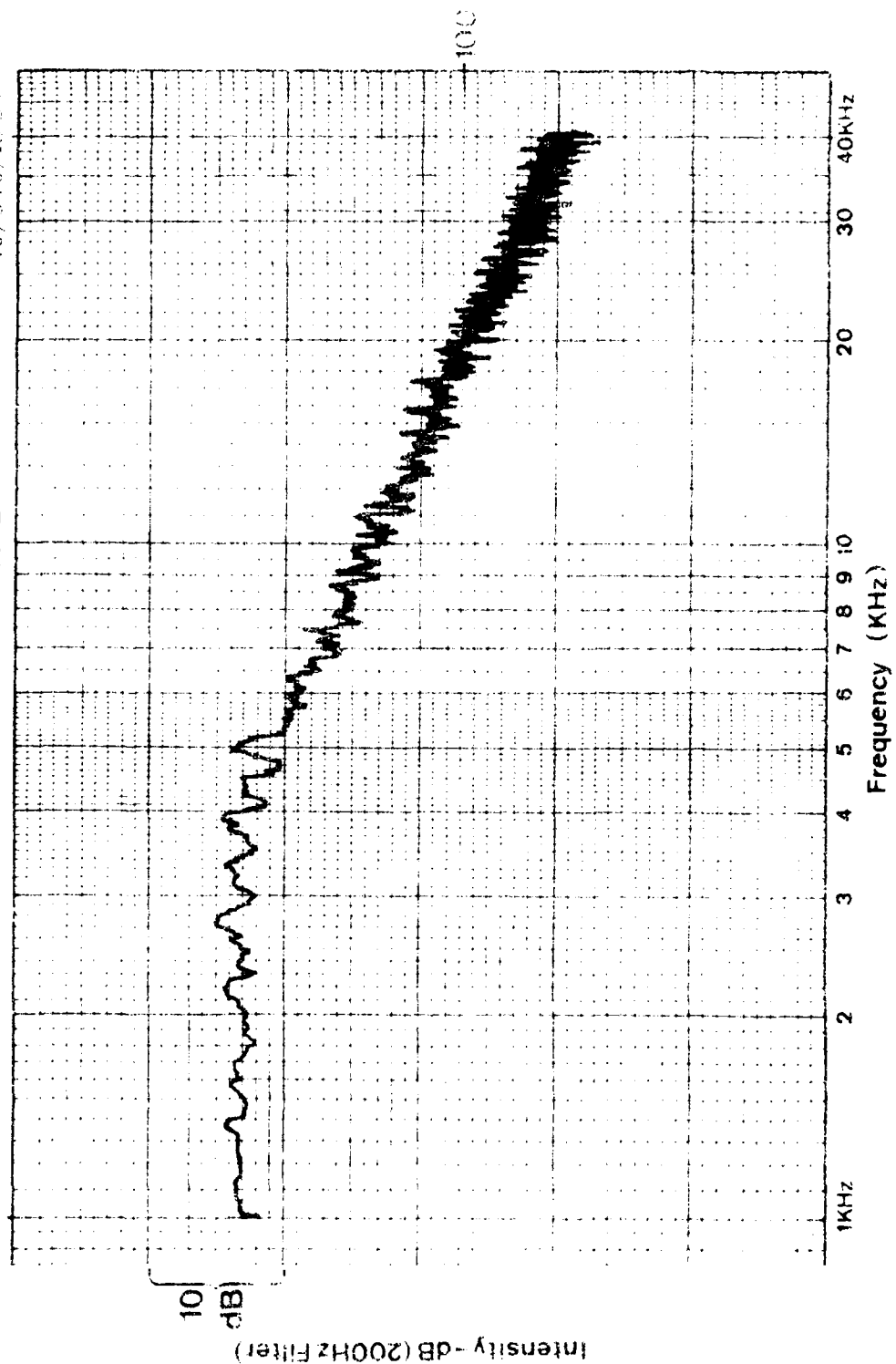


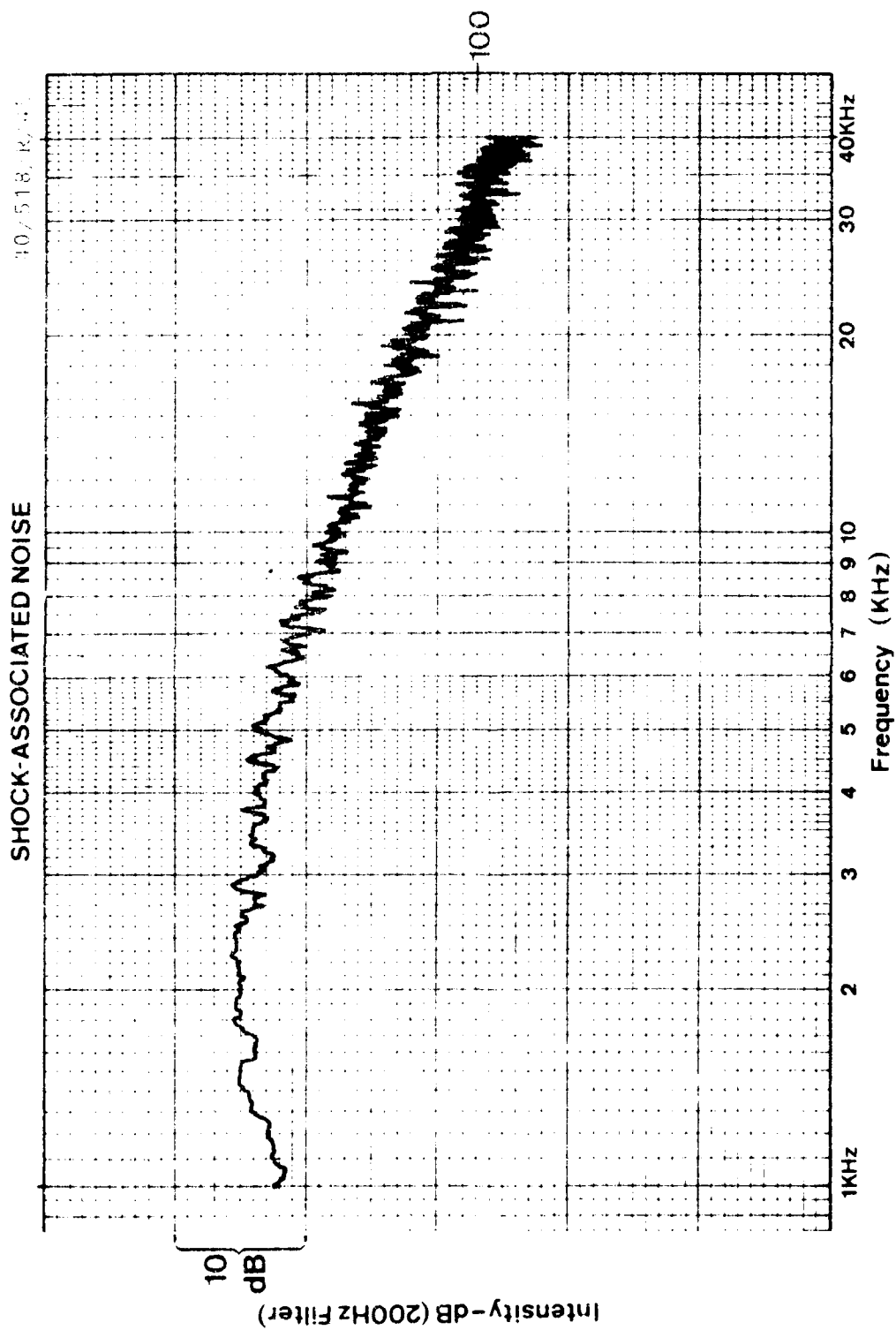


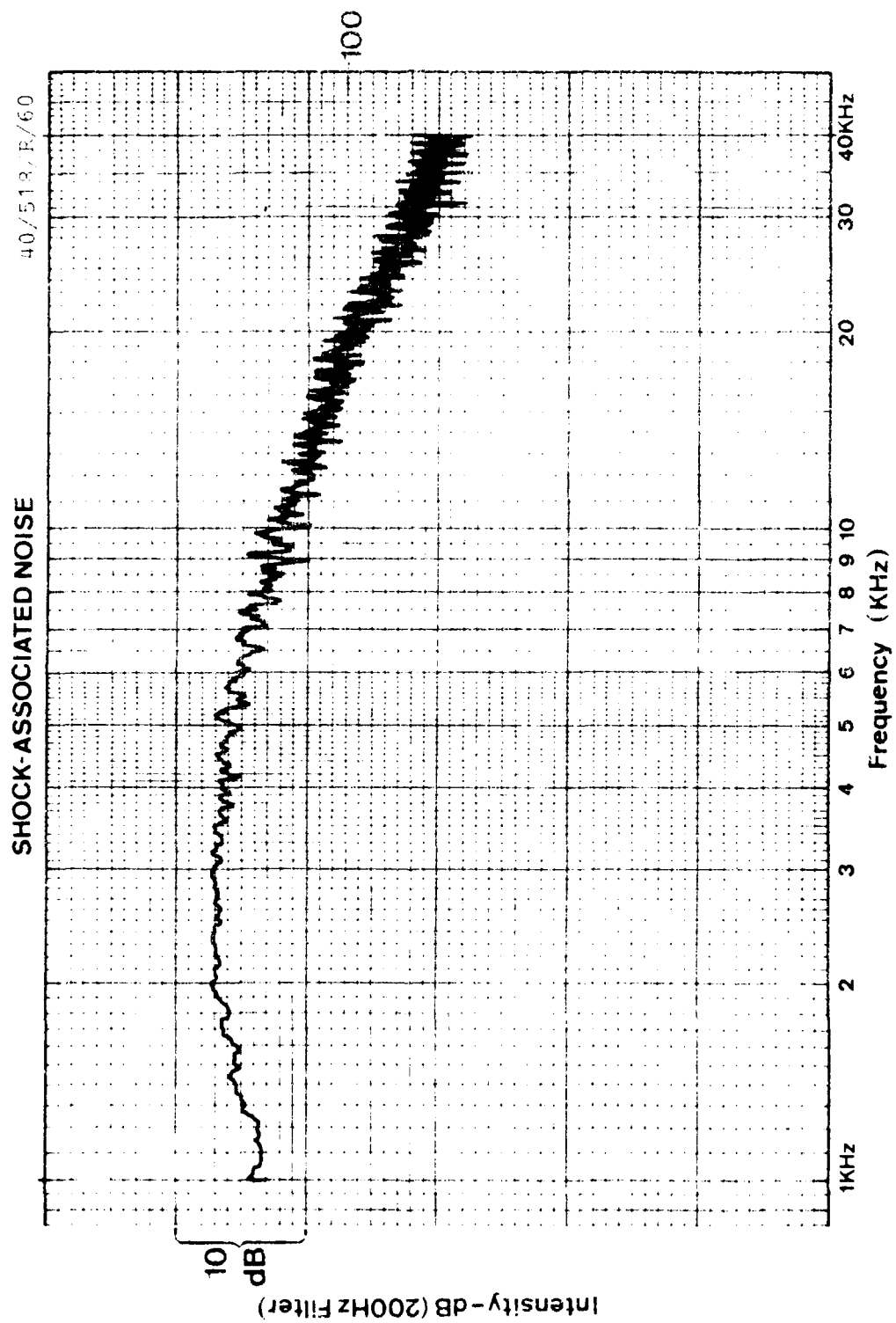


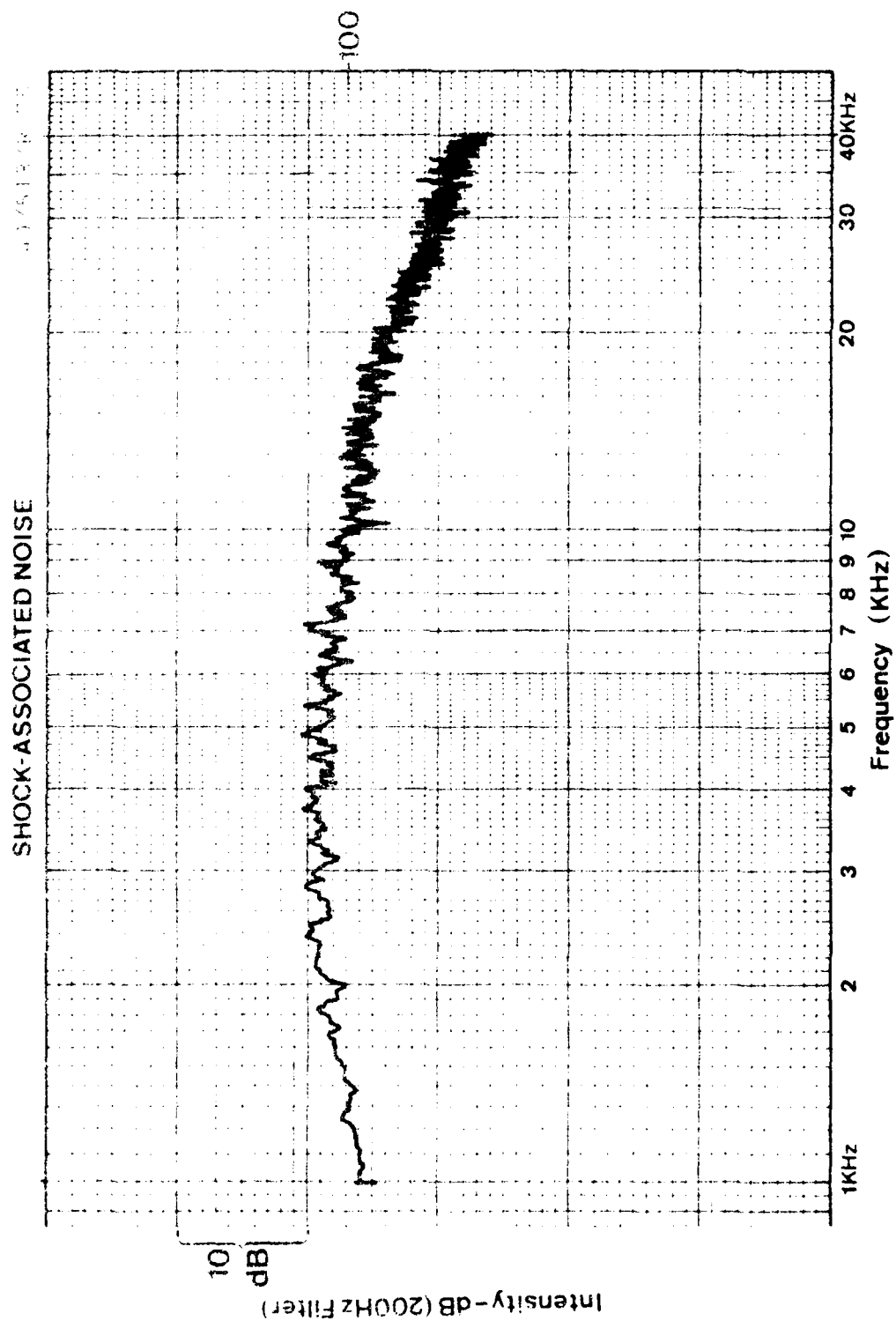
SHOCK-ASSOCIATED NOISE

40/518/R/30









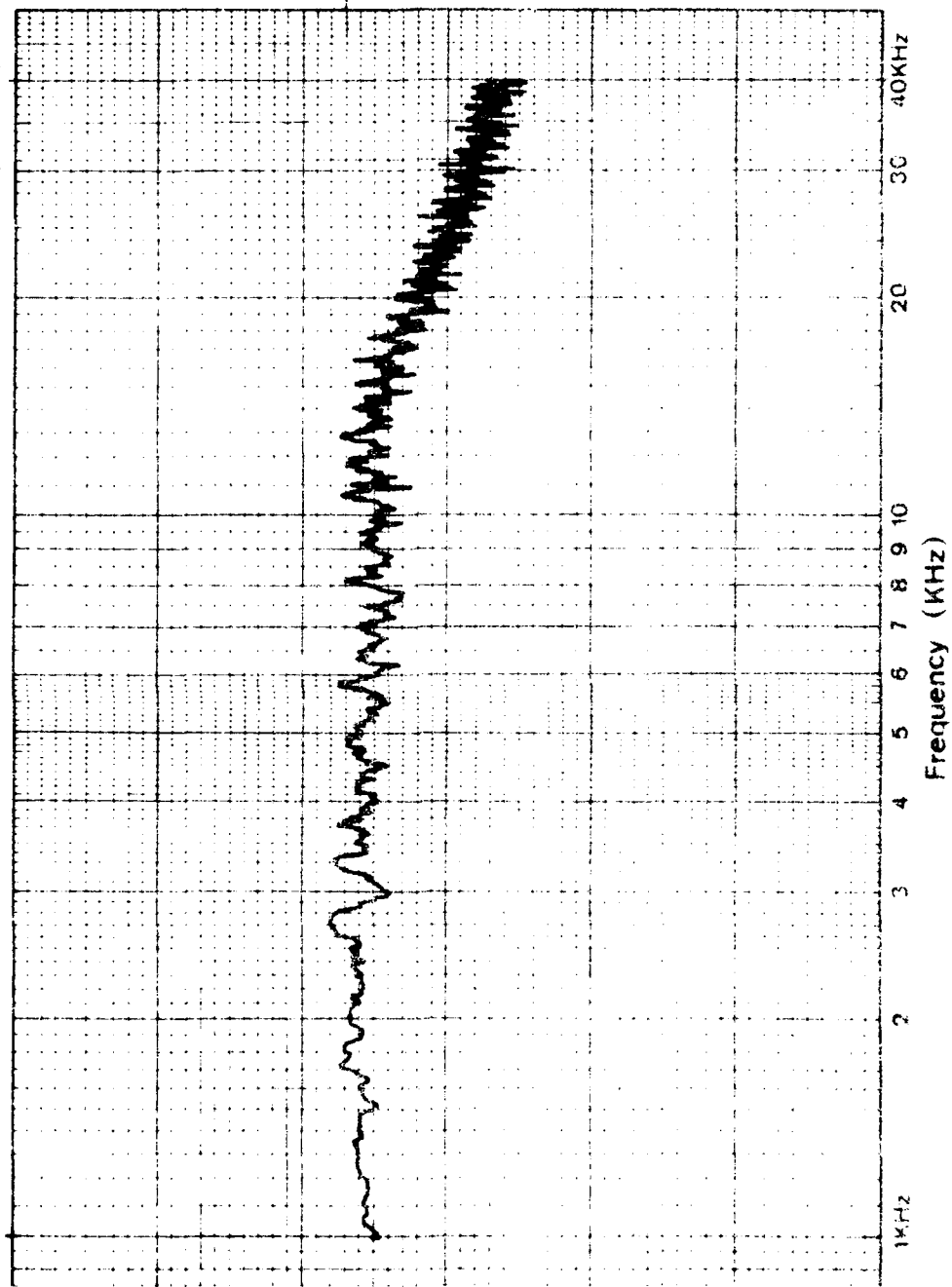
SHOCK-ASSOCIATED NOISE

40/518/R/90

Intensity - dB (200Hz Filter)

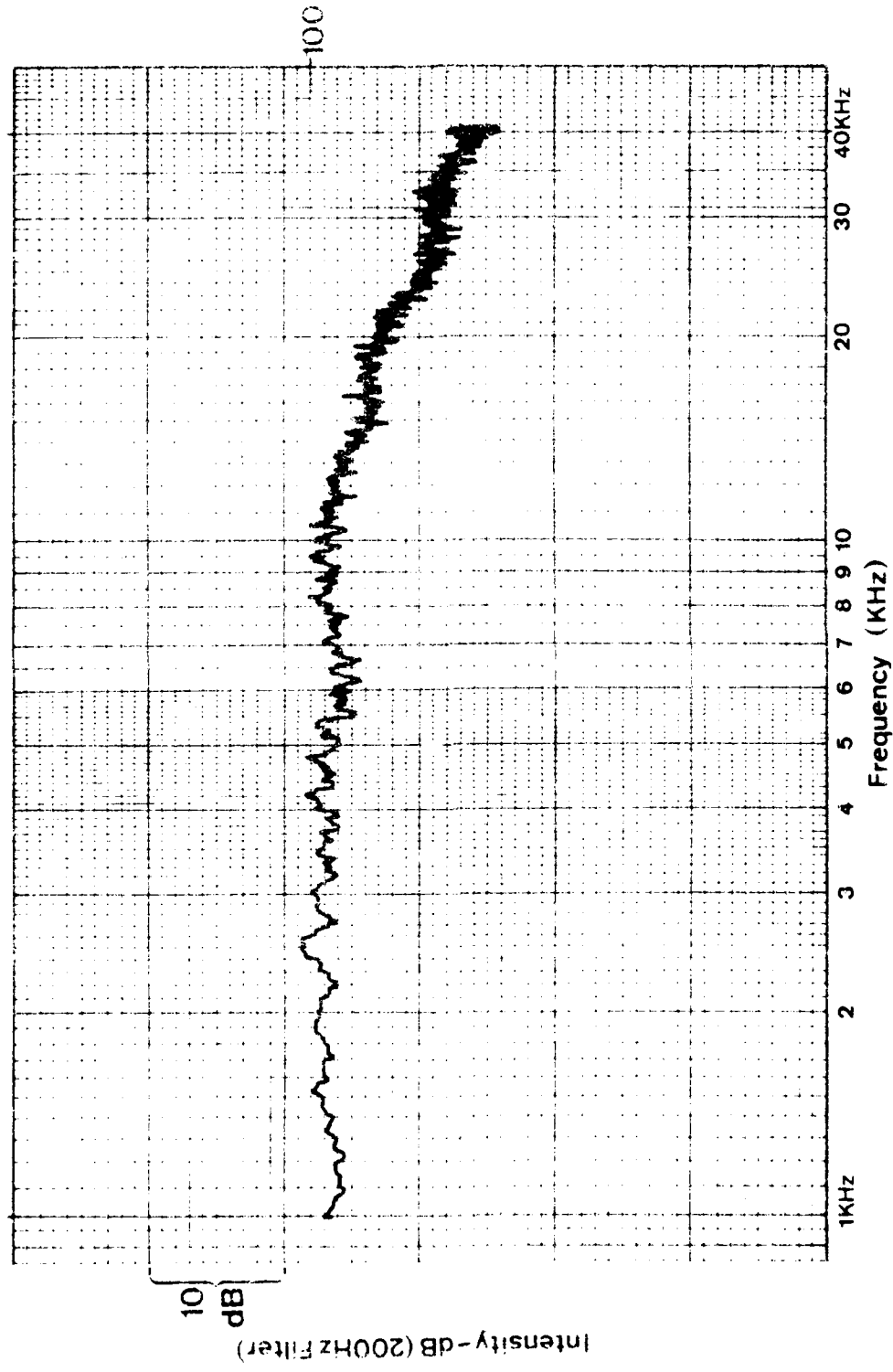
10
dB

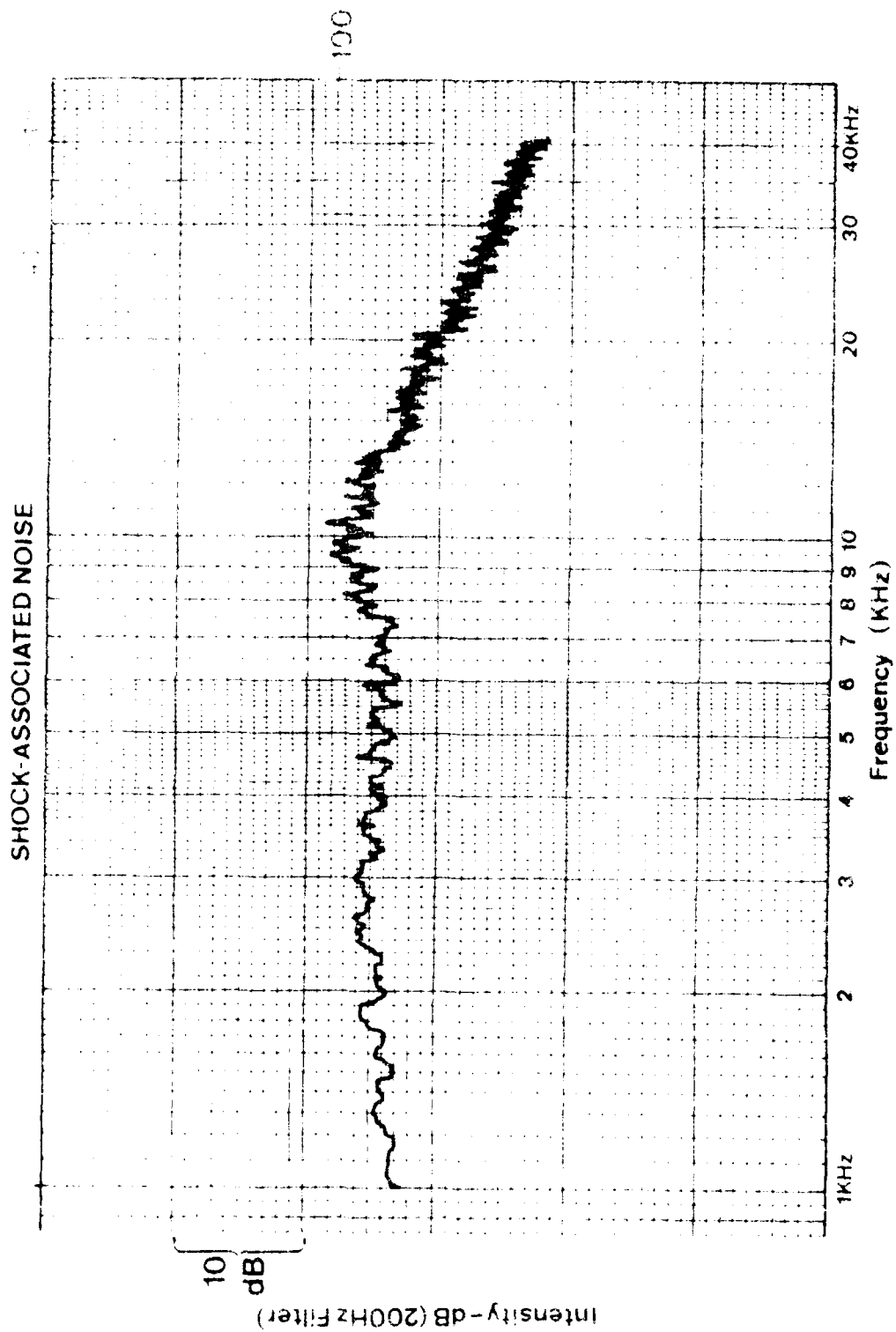
100



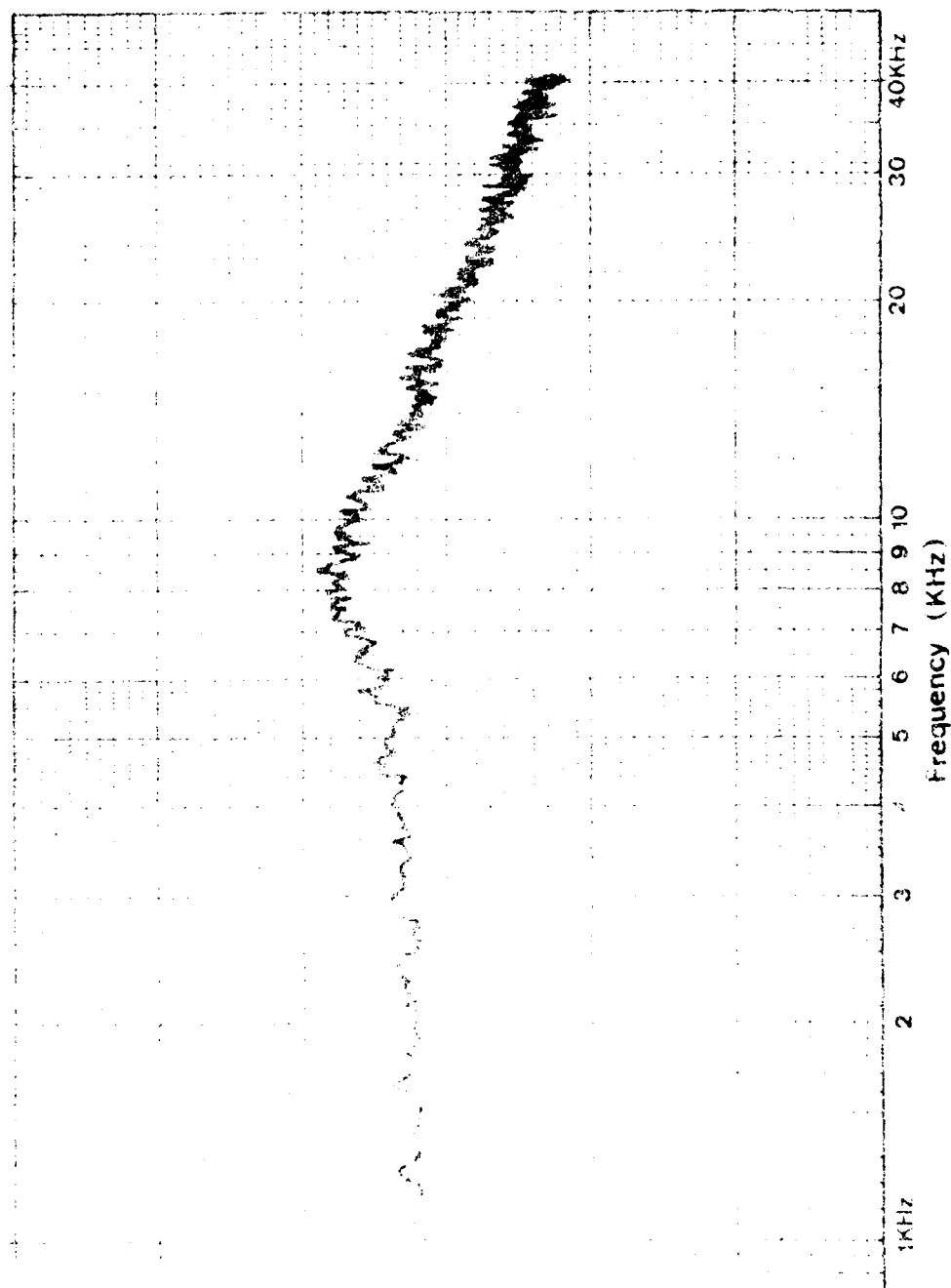
SHOCK-ASSOCIATED NOISE

40, 534, F/90





SHOCK ASSOCIATED NOISE



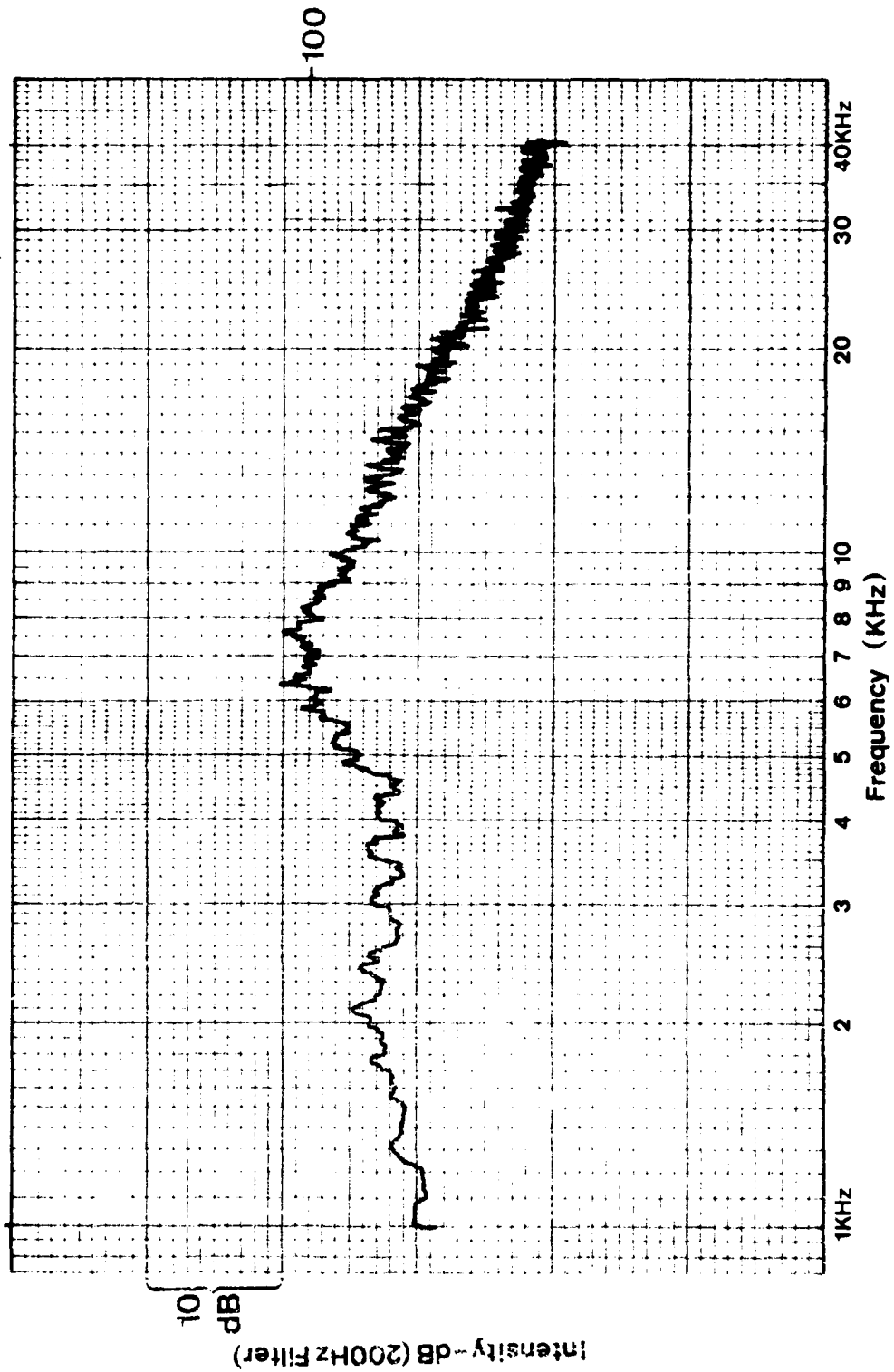
101

249

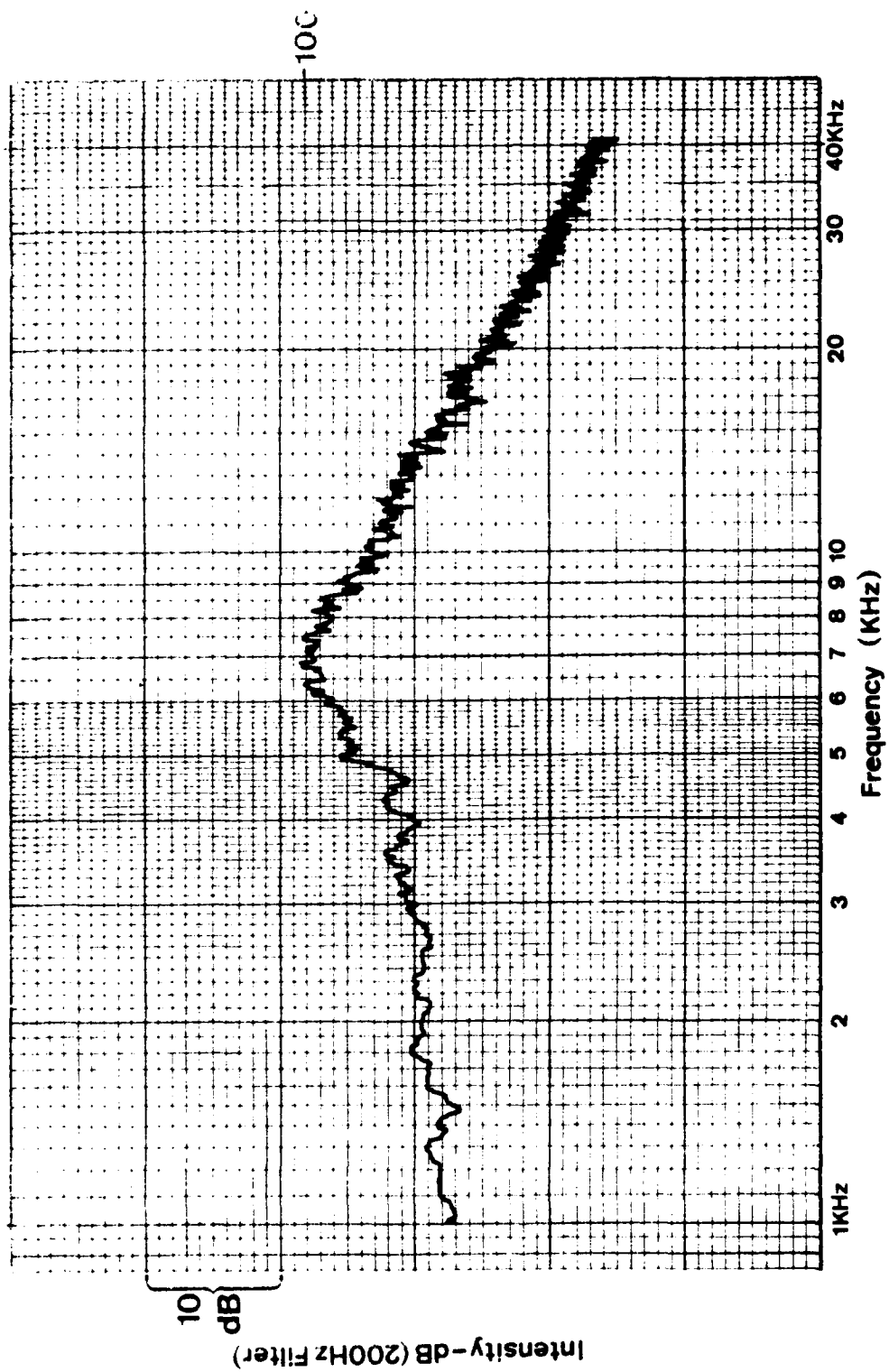
SHOCK ASSOCIATED NOISE

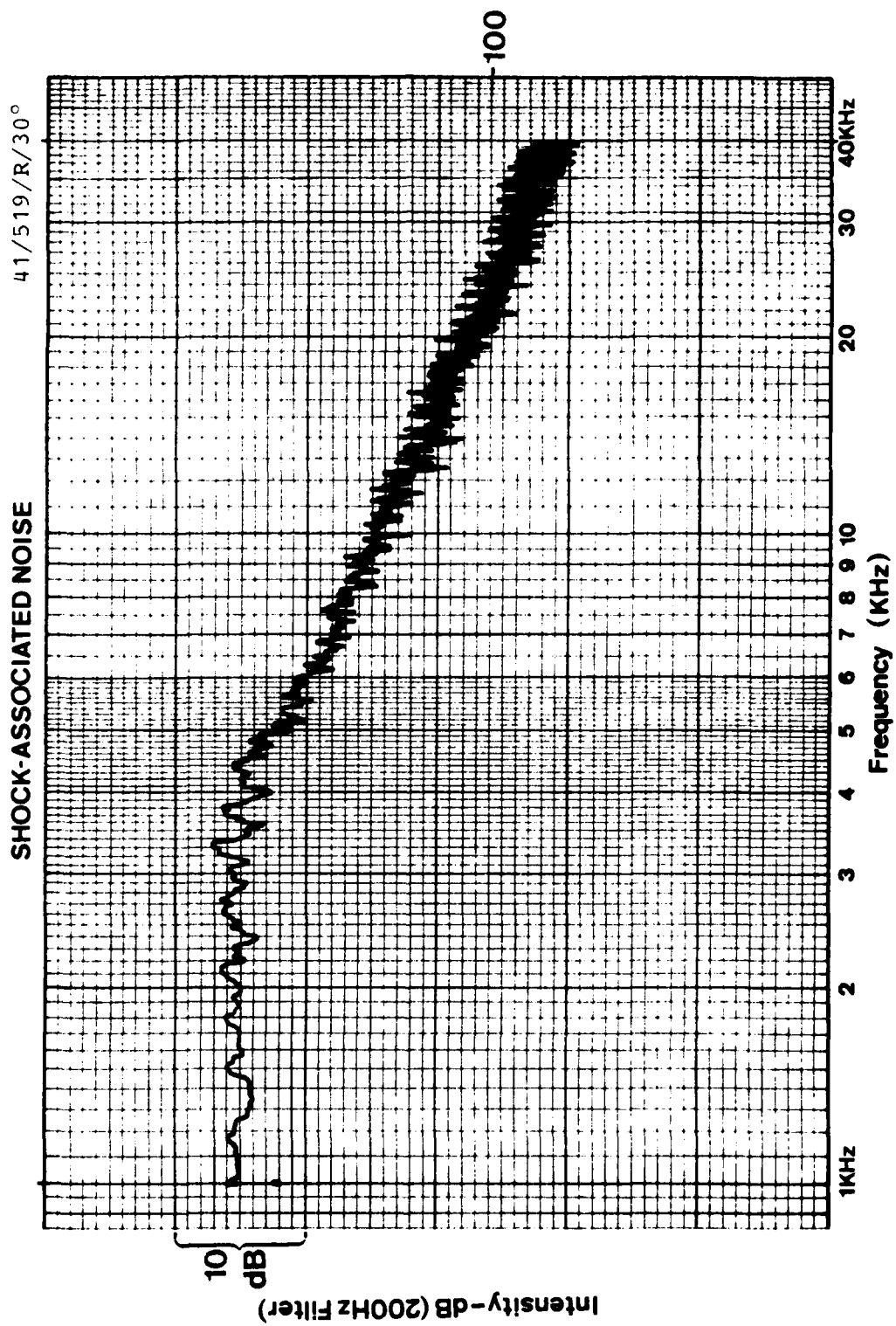
SHOCK-ASSOCIATED NOISE

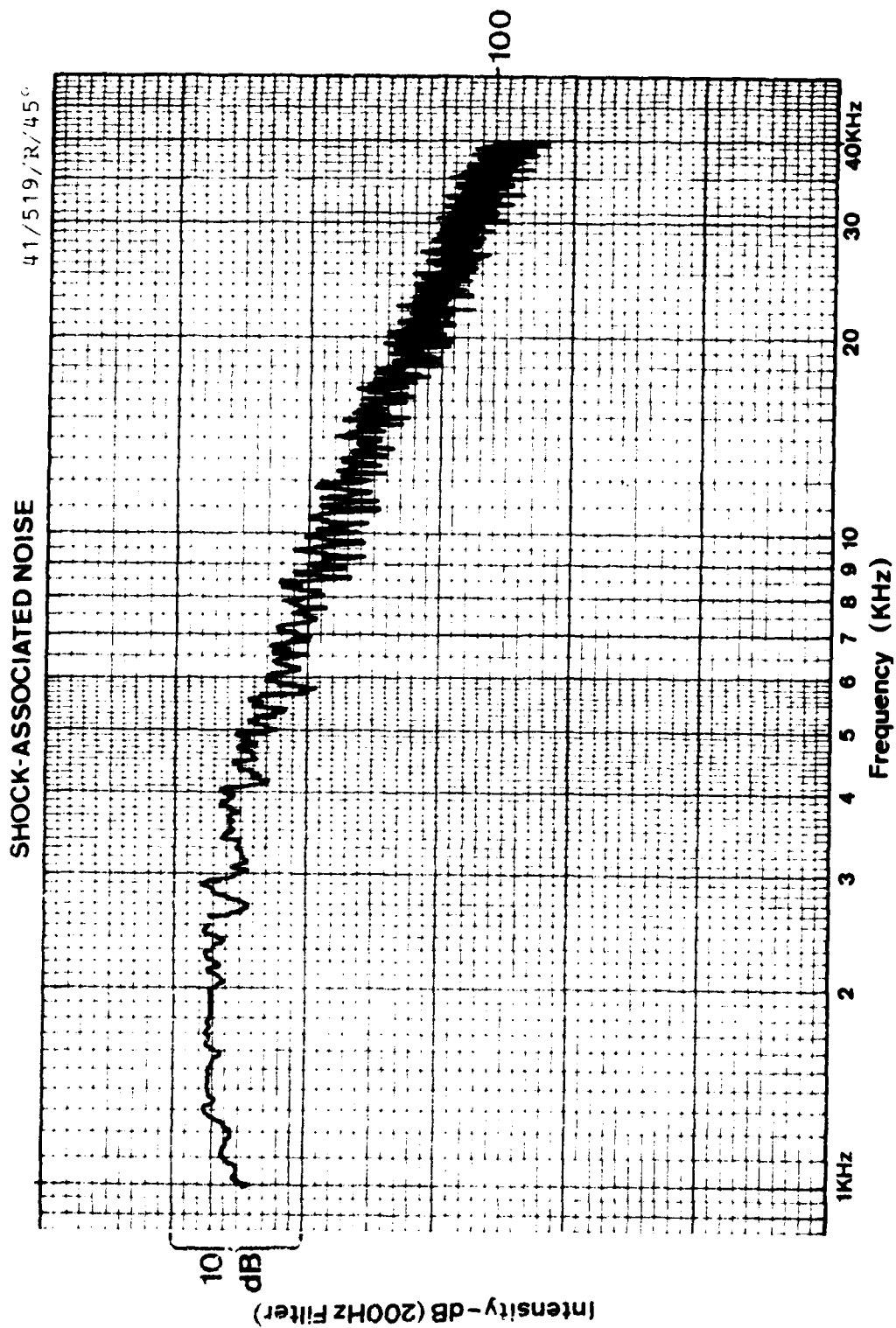
40/584/E/135



SHOCK-ASSOCIATED NOISE

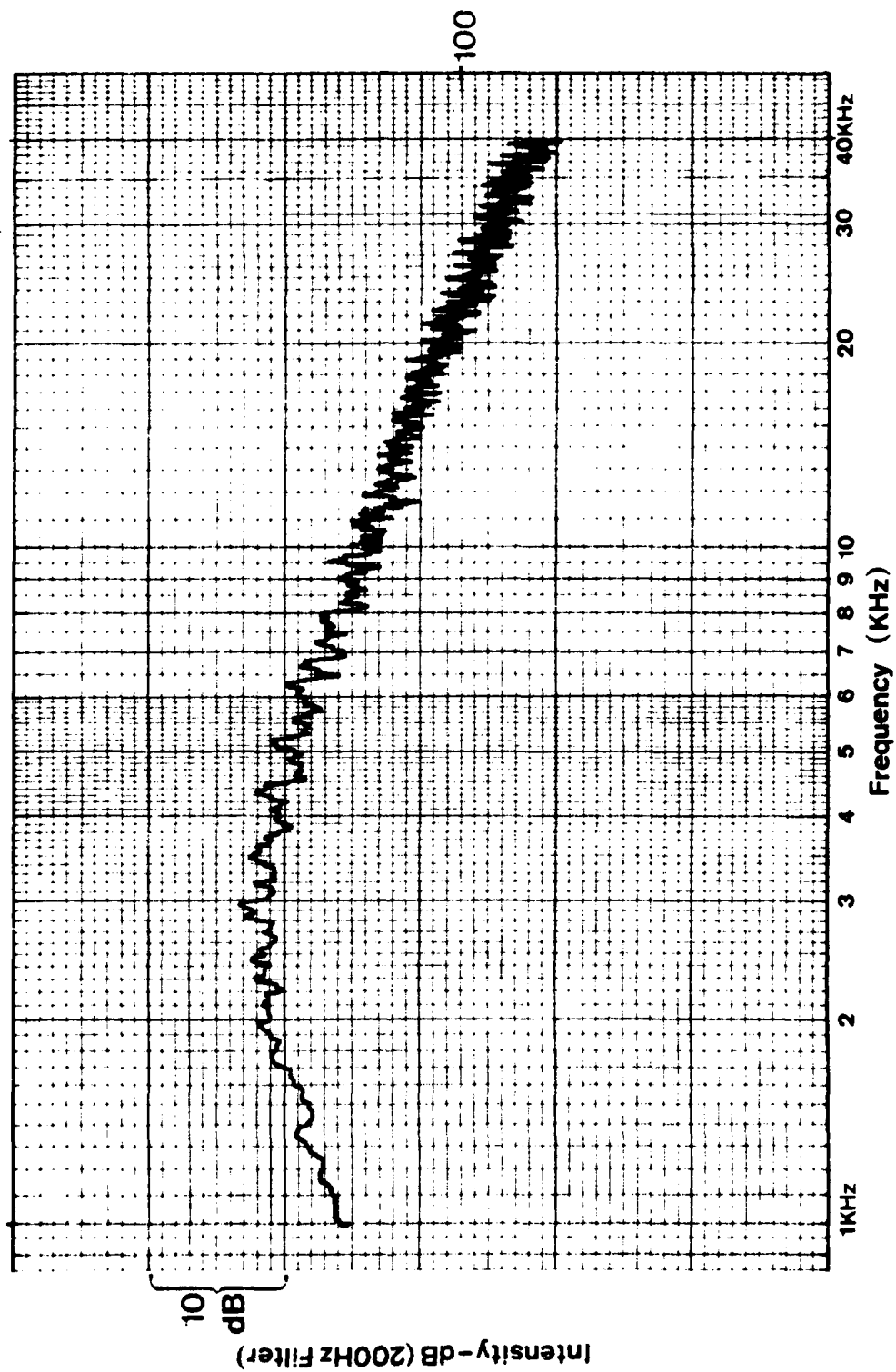


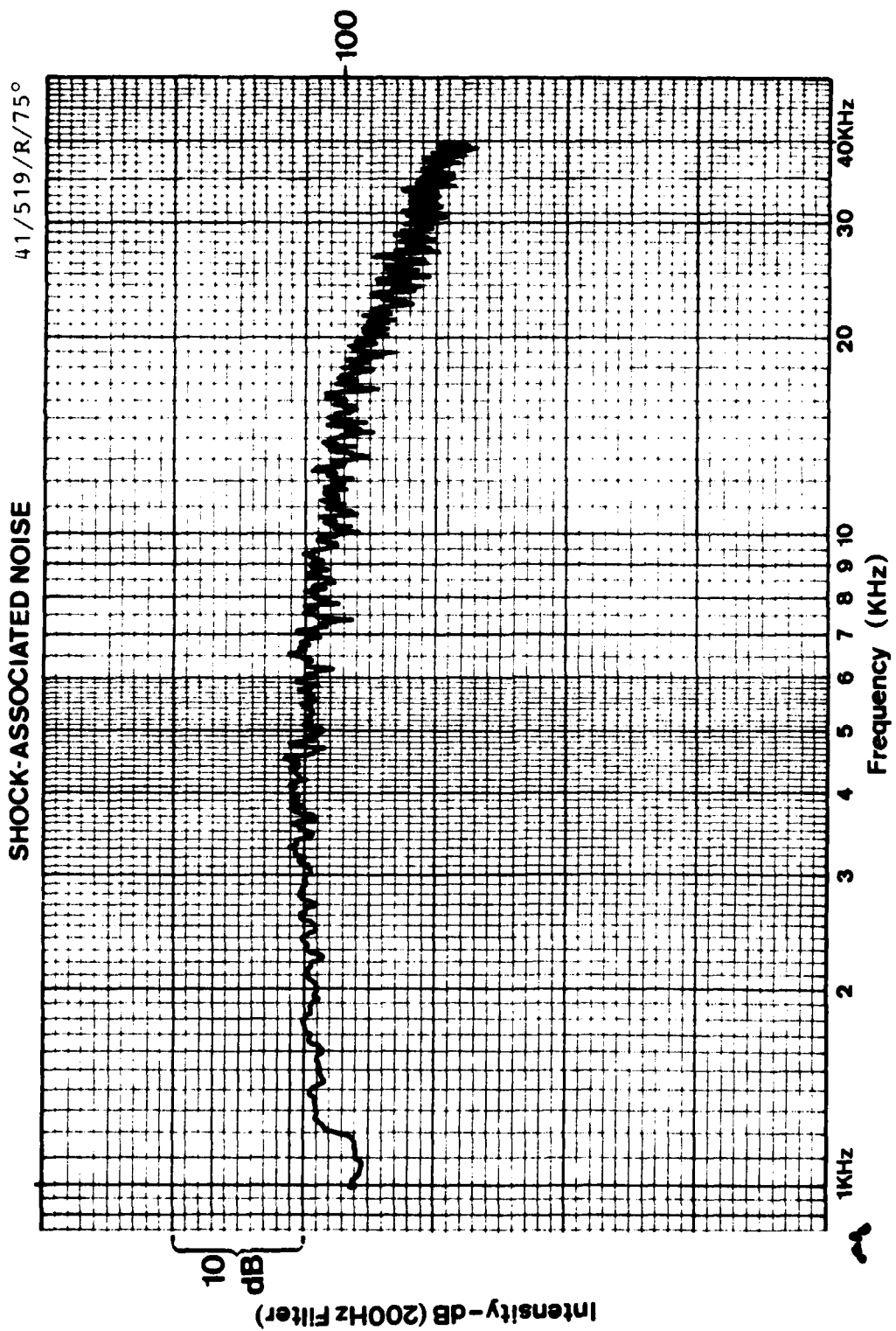


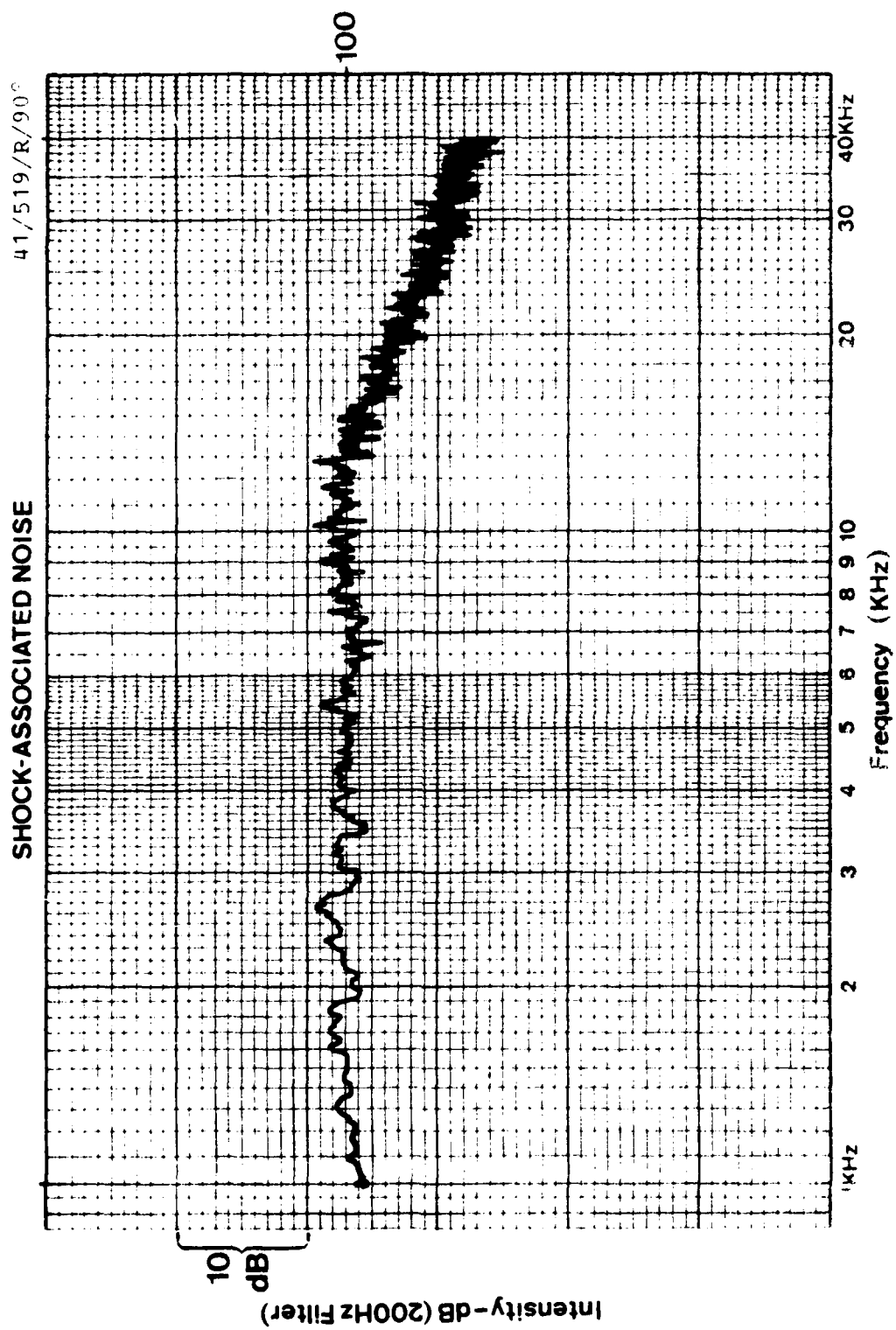


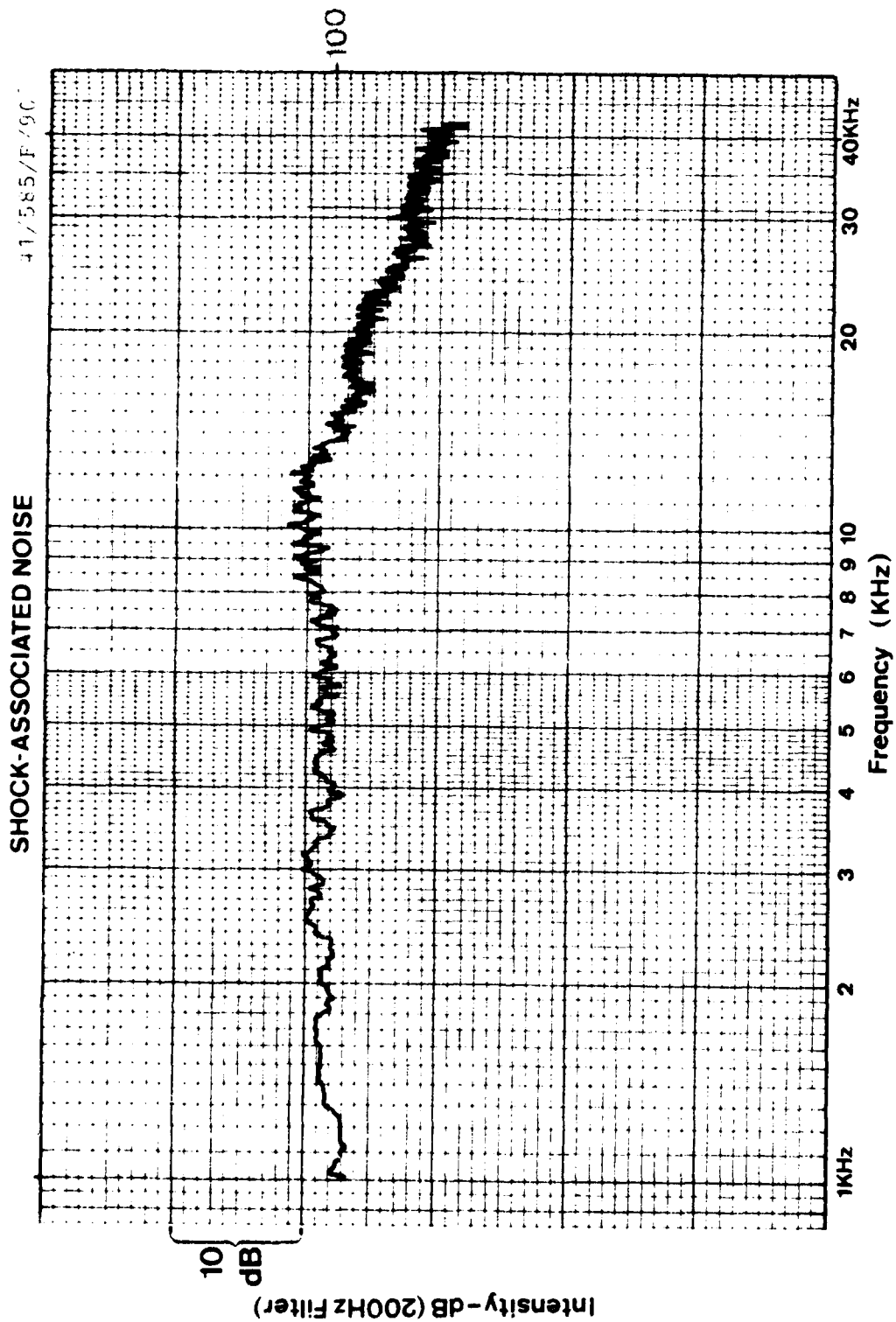
SHOCK-ASSOCIATED NOISE

41/519/R/60



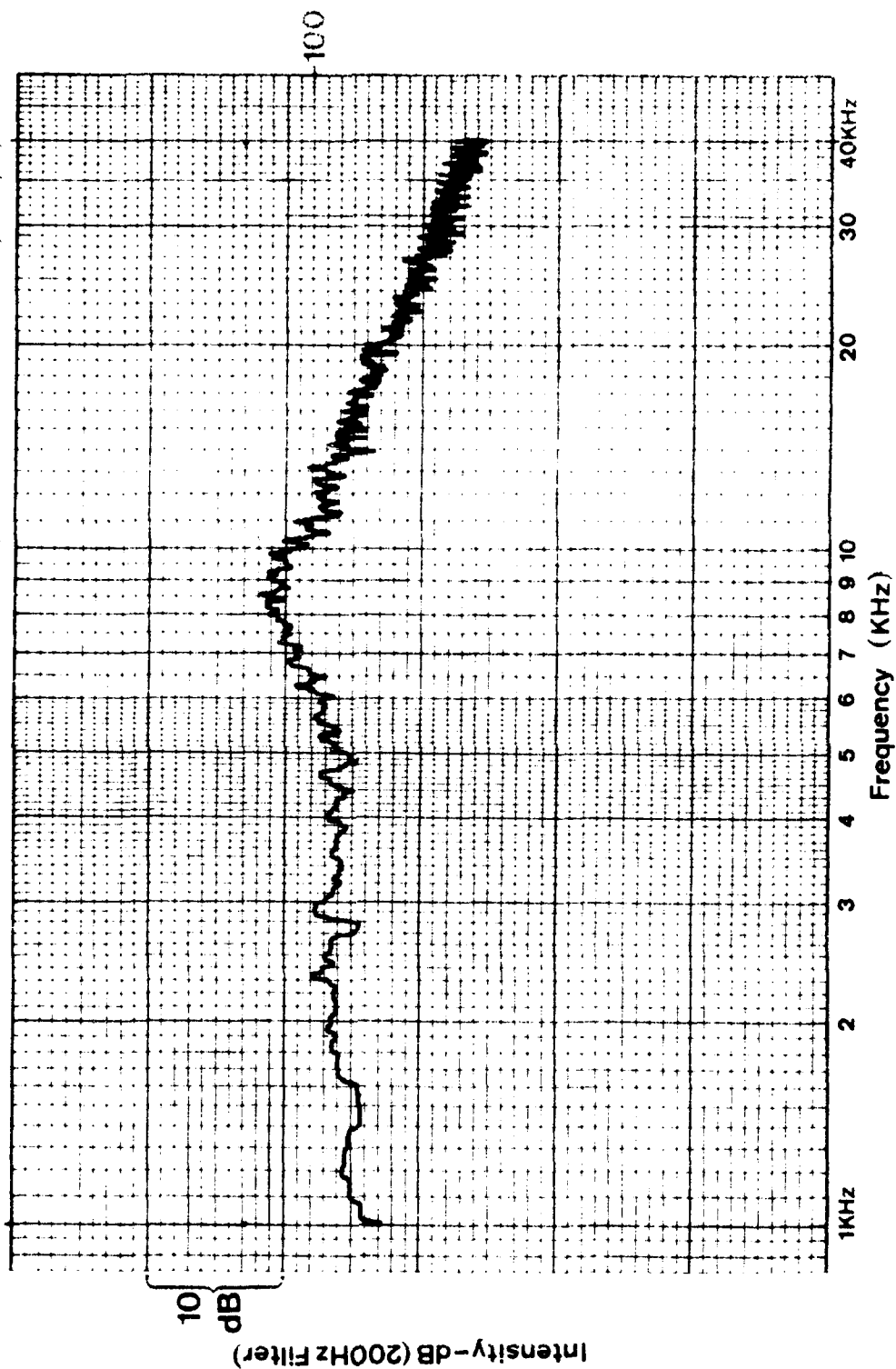






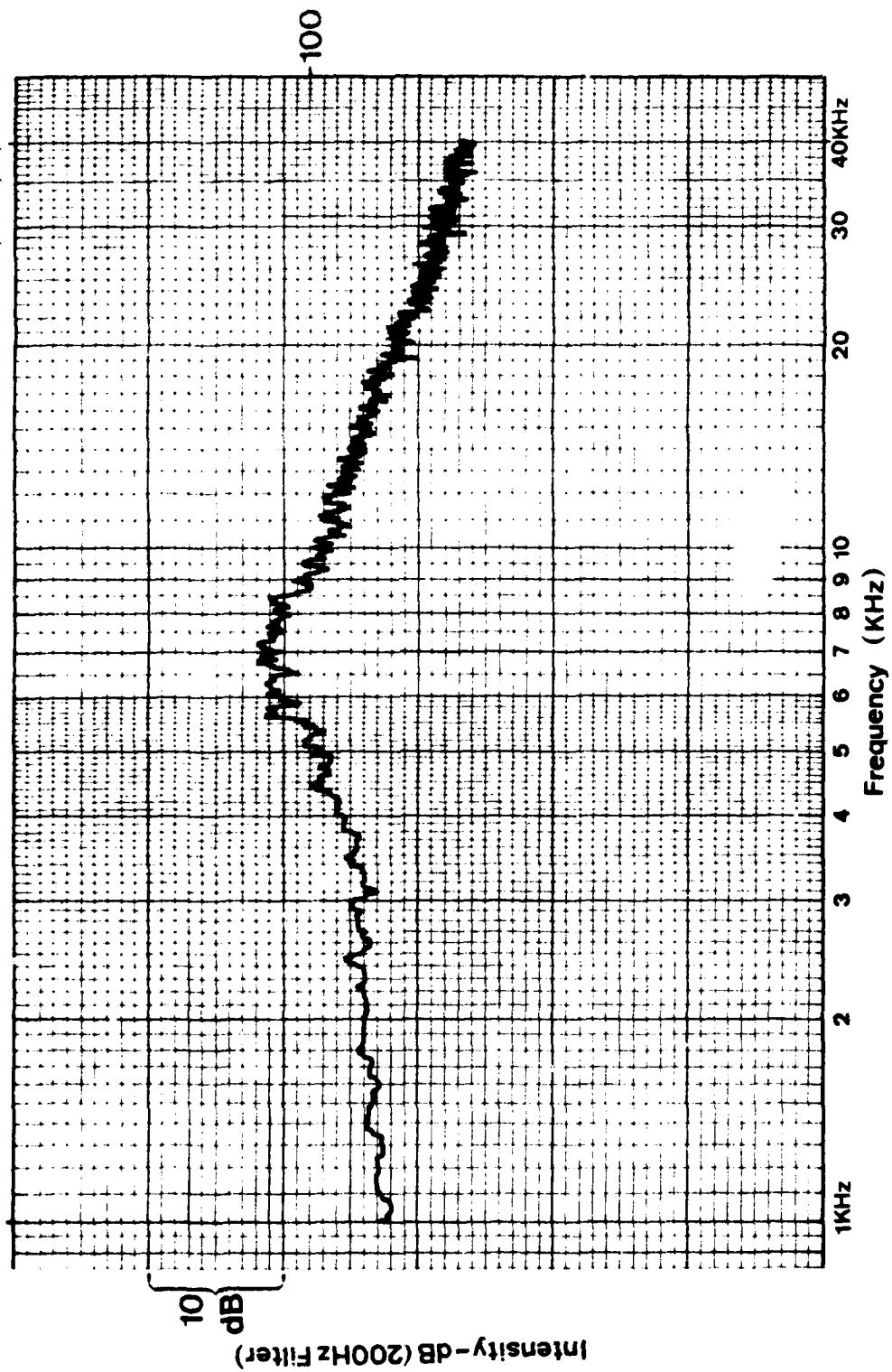
SHOCK-ASSOCIATED NOISE

41/585/F/105



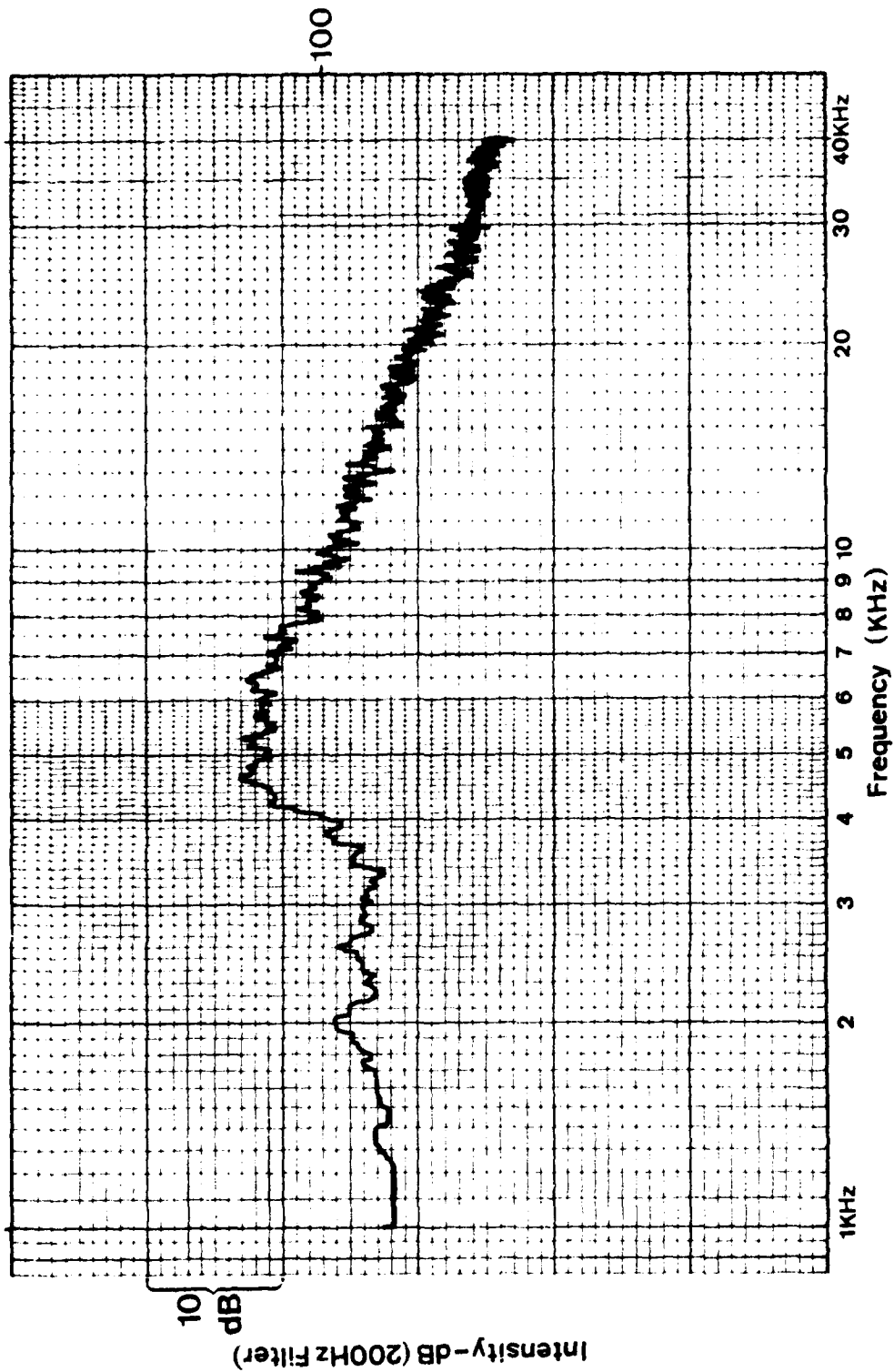
SHOCK-ASSOCIATED NOISE

41/585/F/120°

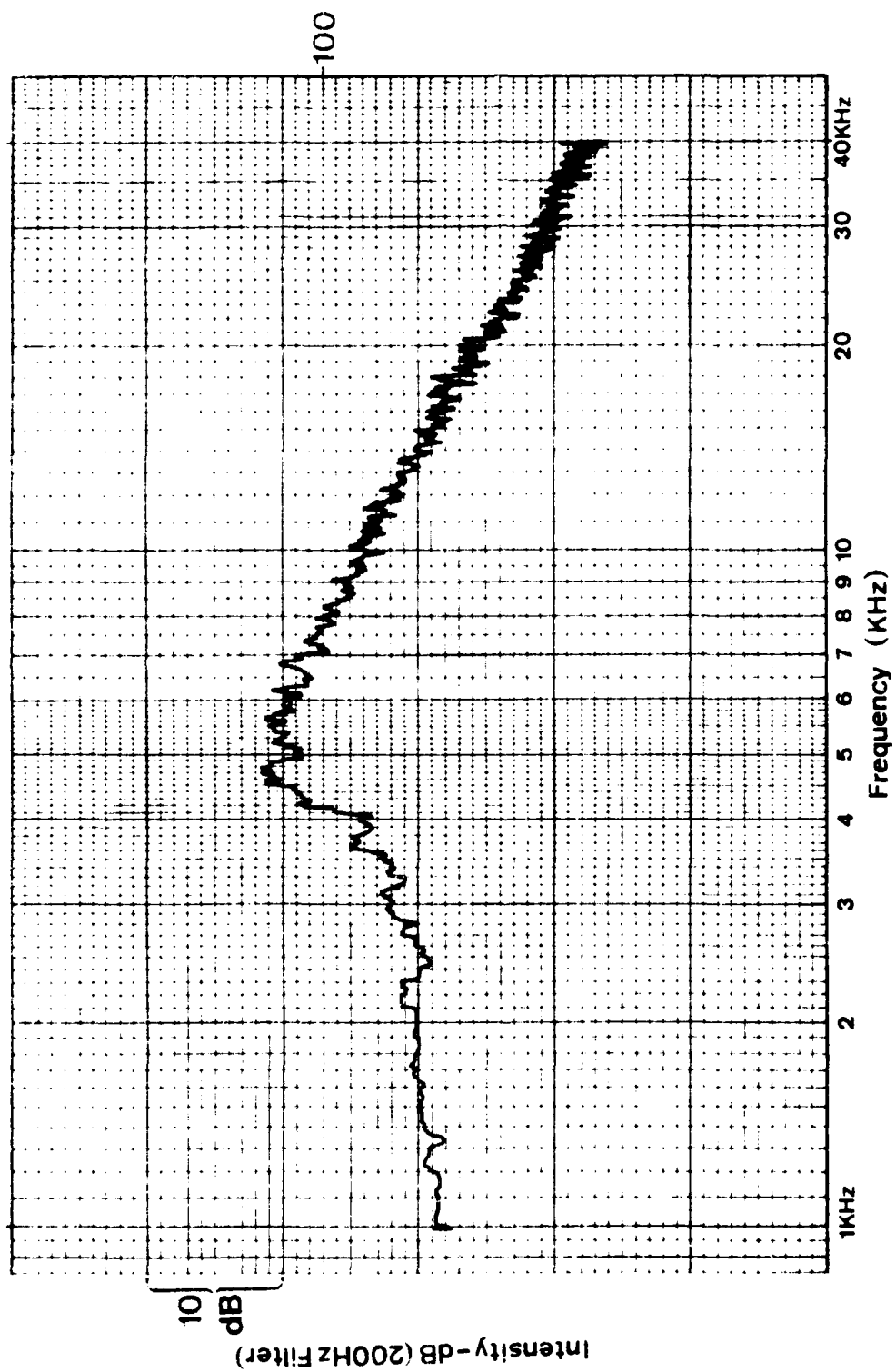


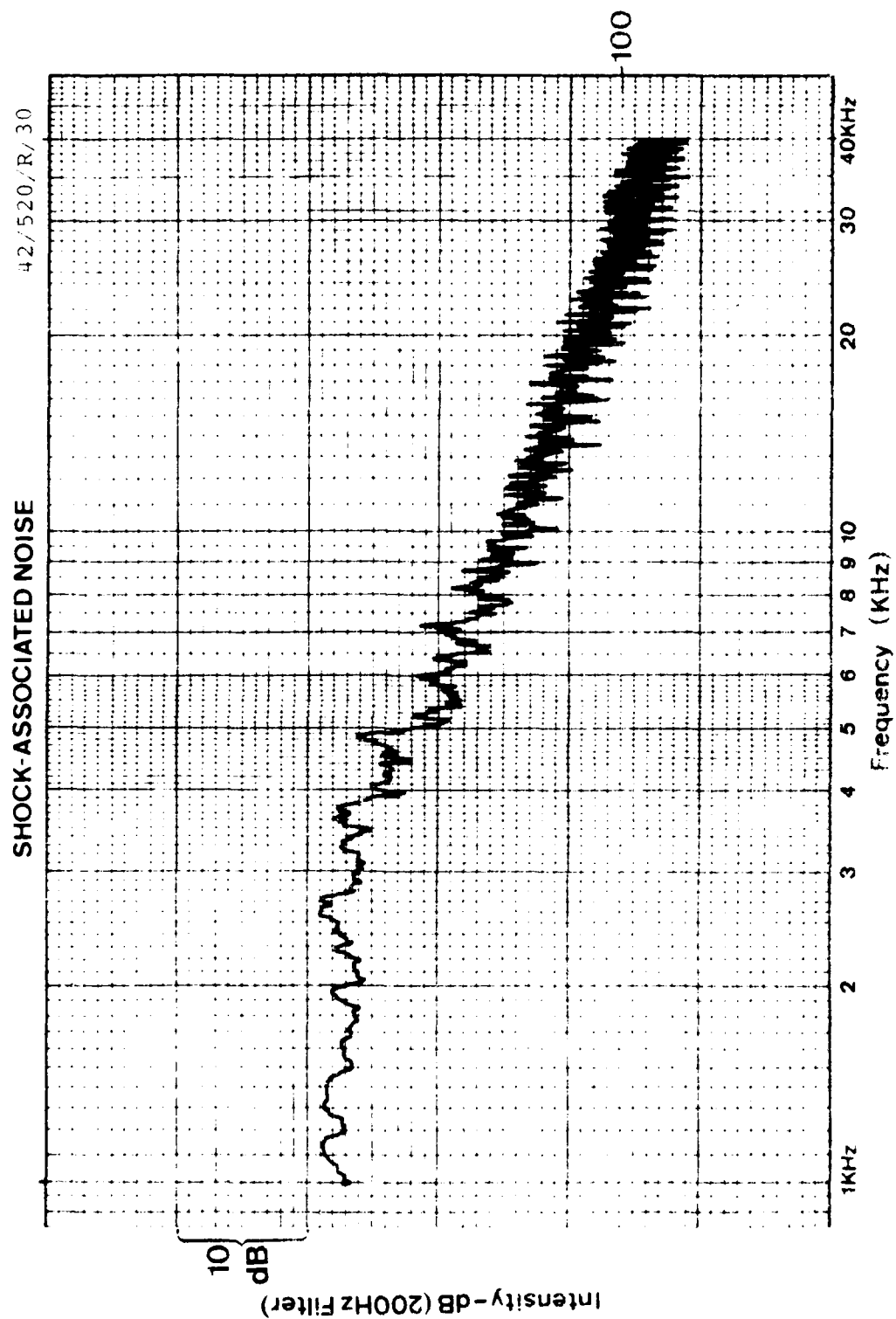
SHOCK-ASSOCIATED NOISE

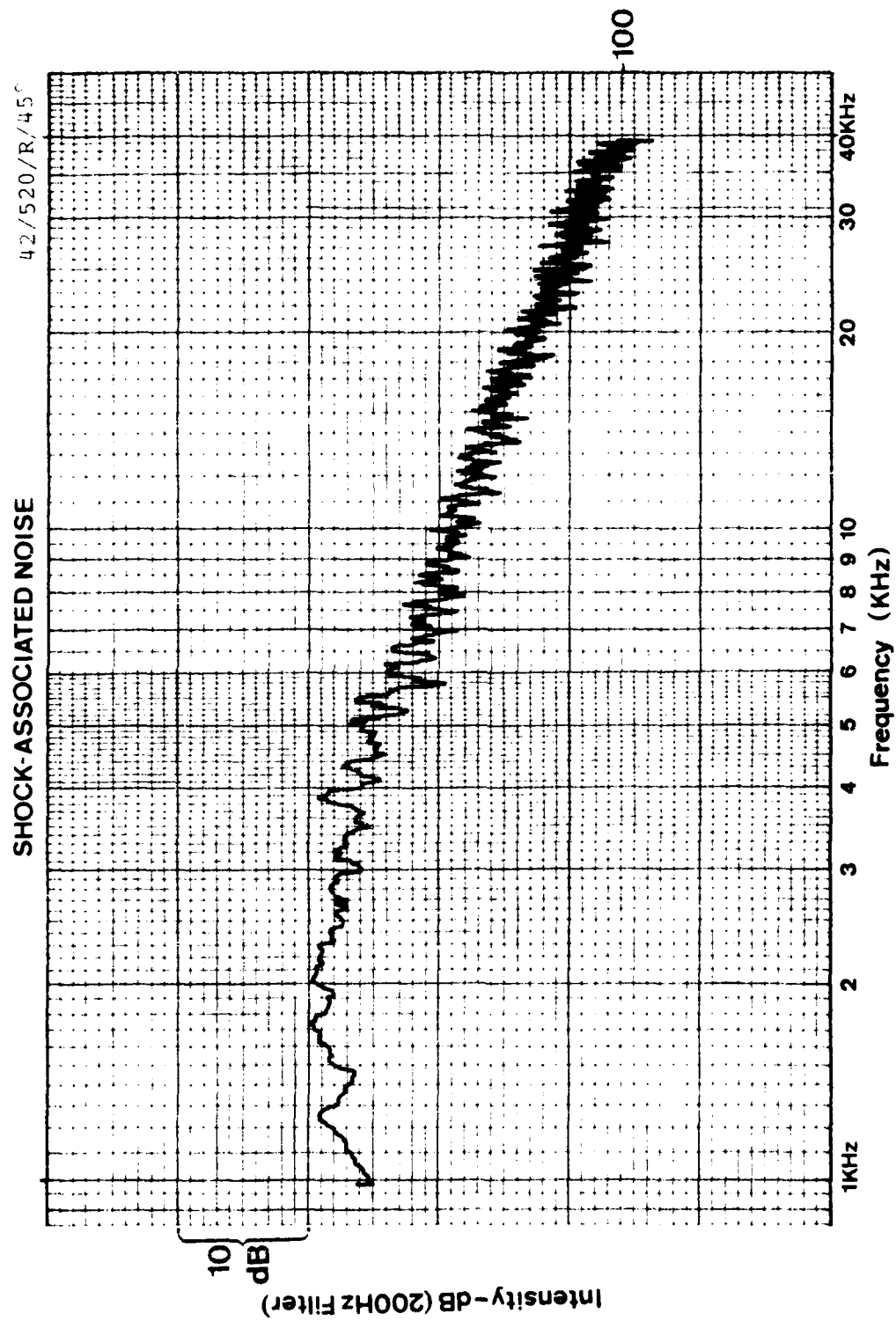
41/585/F, 135°



SHOCK-ASSOCIATED NOISE

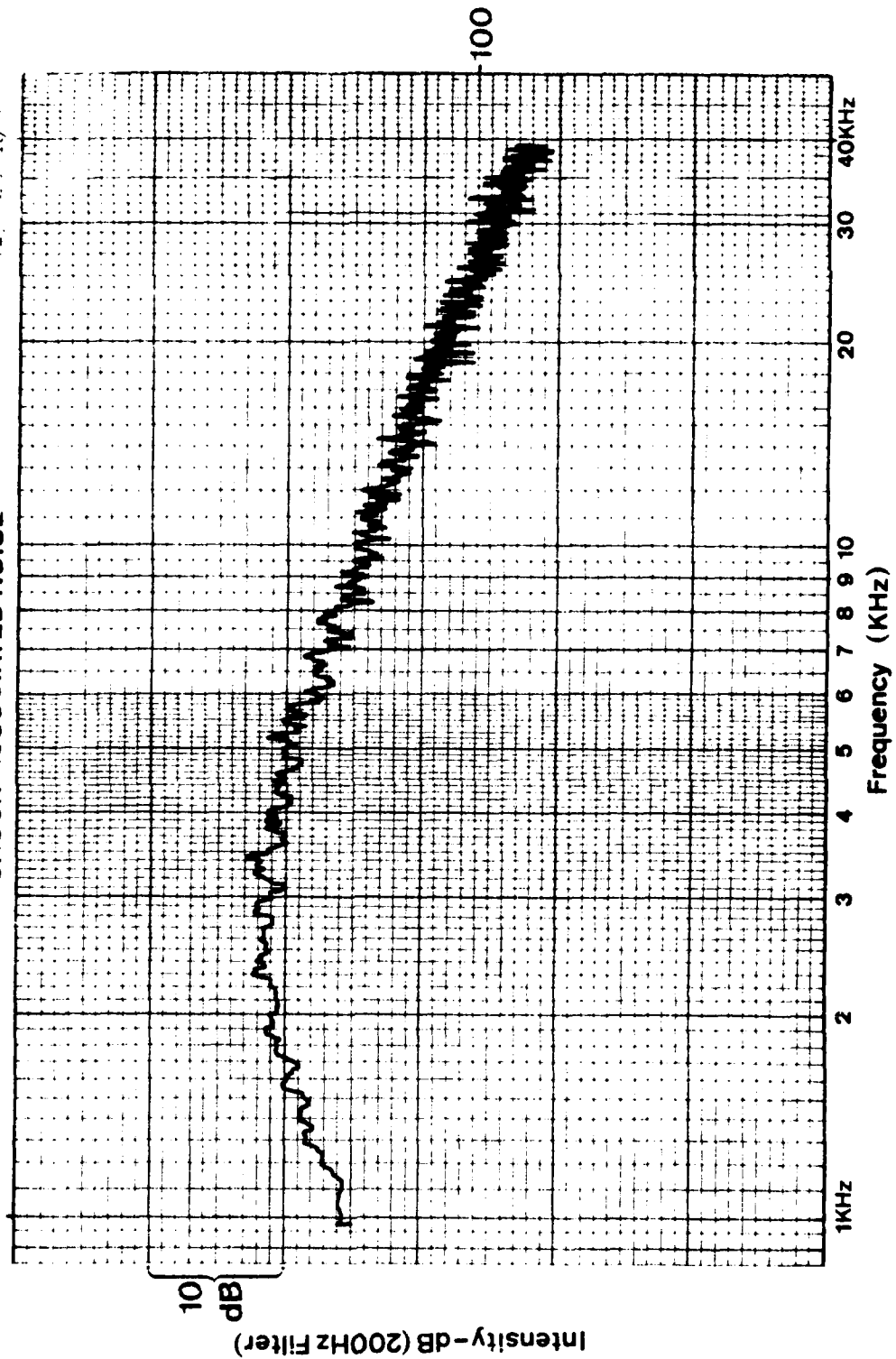






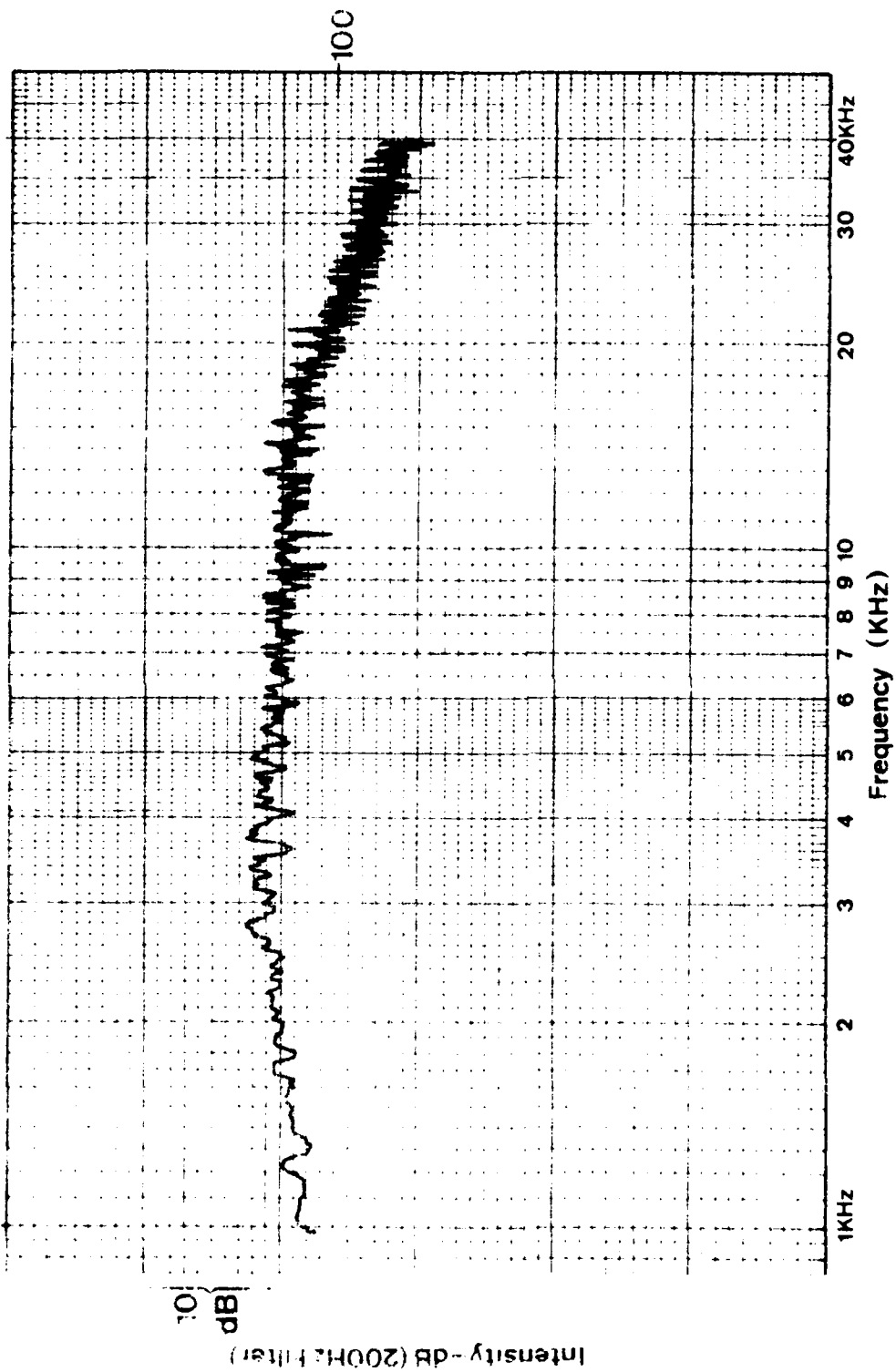
SHOCK-ASSOCIATED NOISE

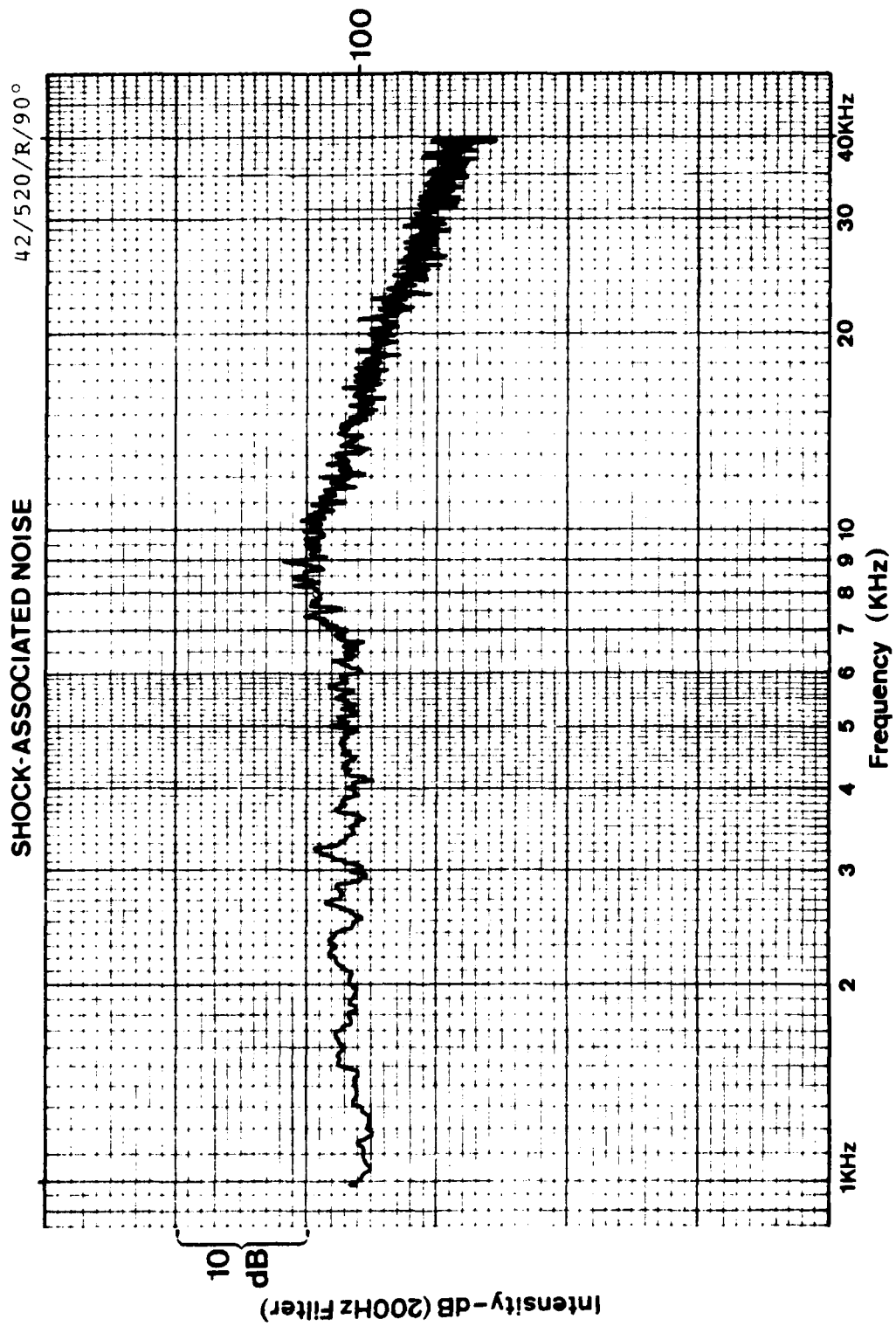
42/500/R/6



SHOCK ASSOCIATED NOISE

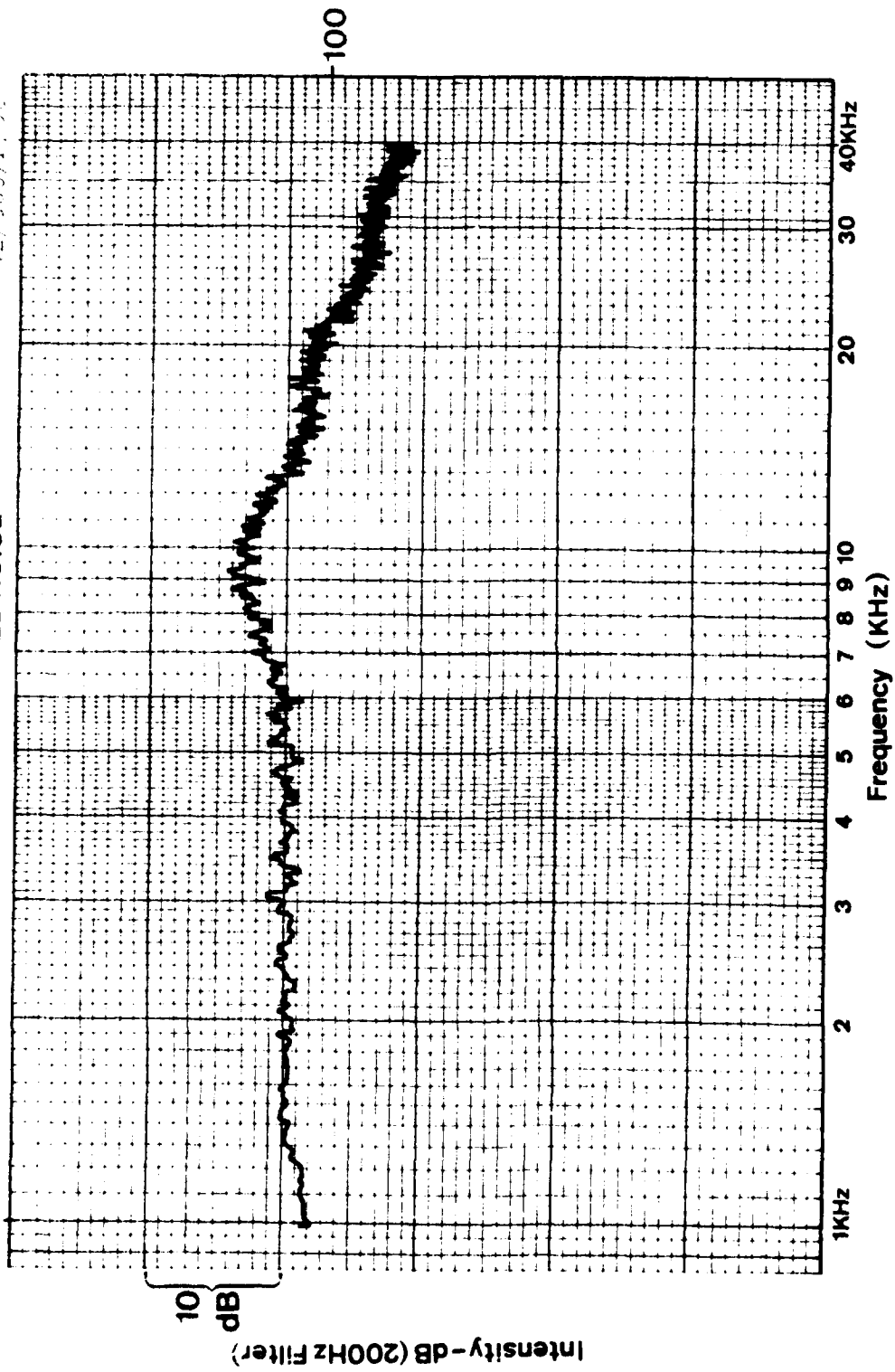
20/20/14/75

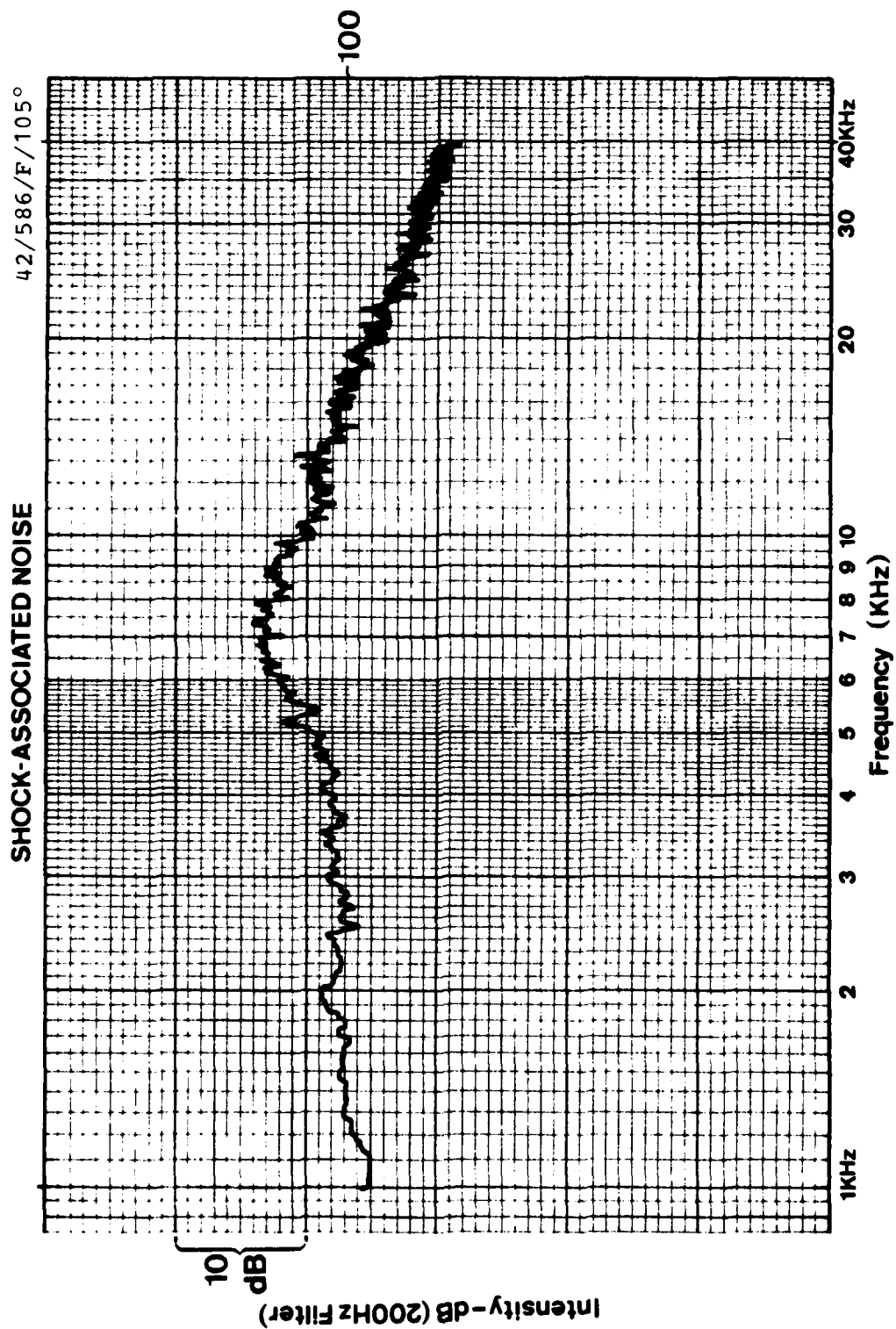


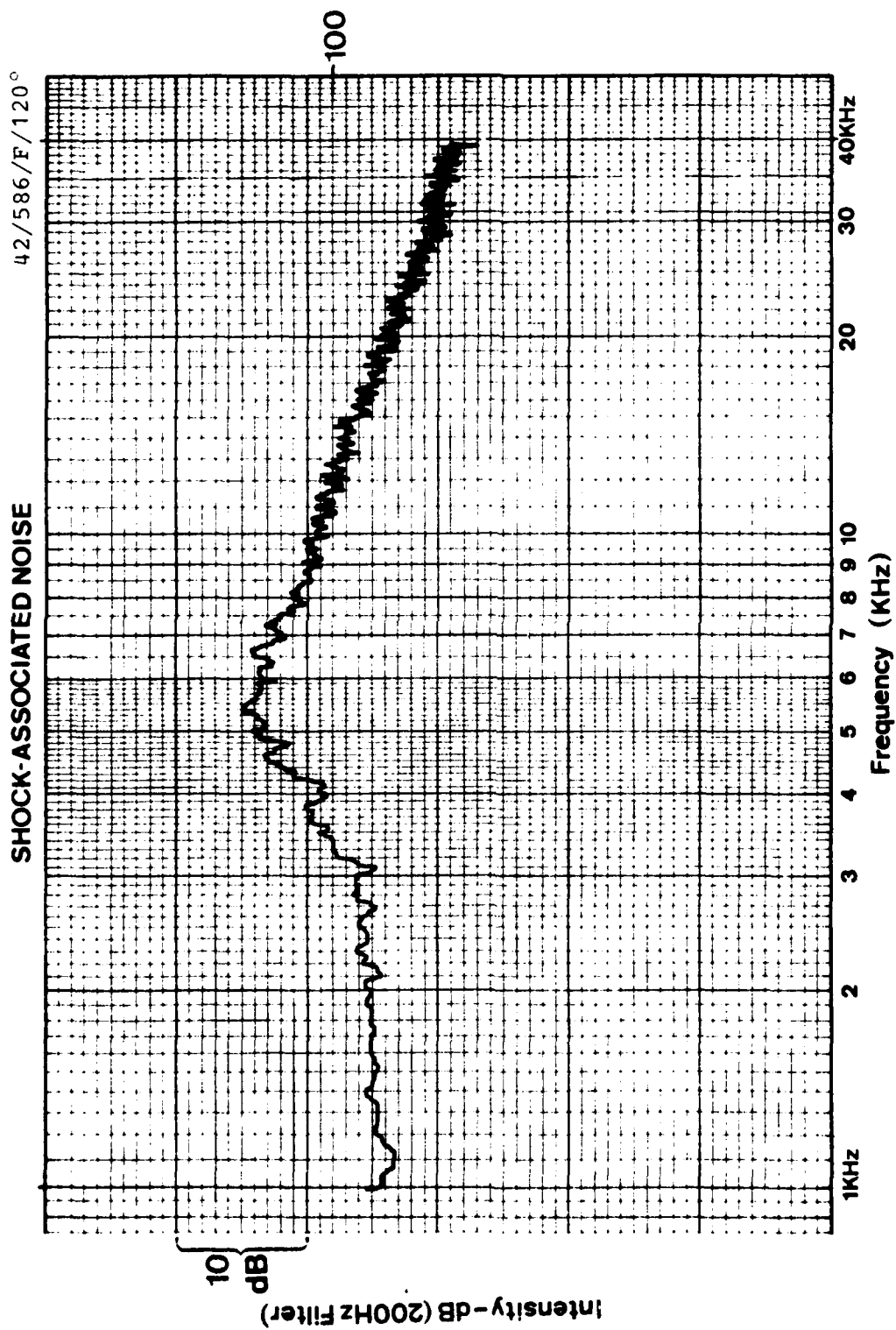


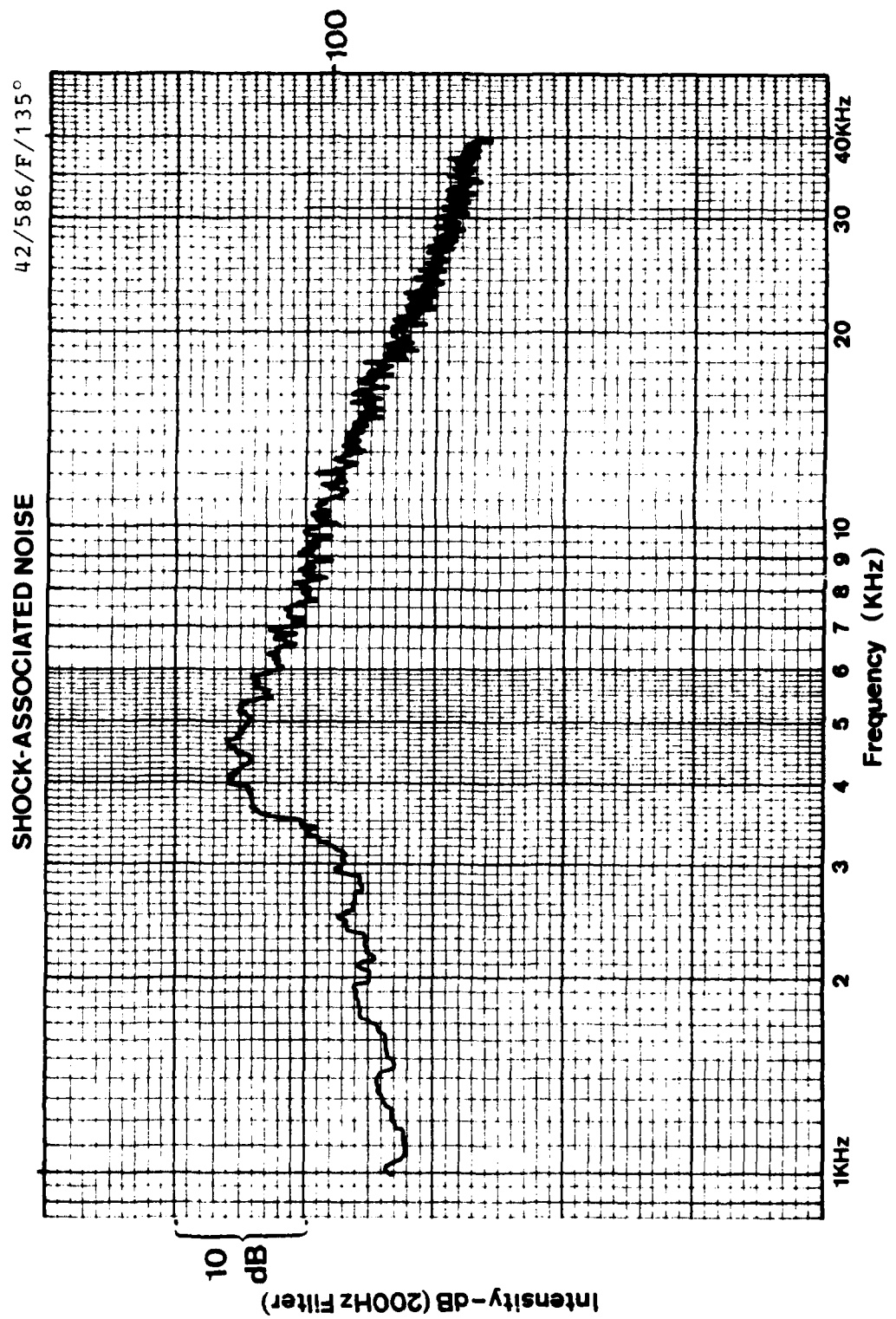
SHOCK-ASSOCIATED NOISE

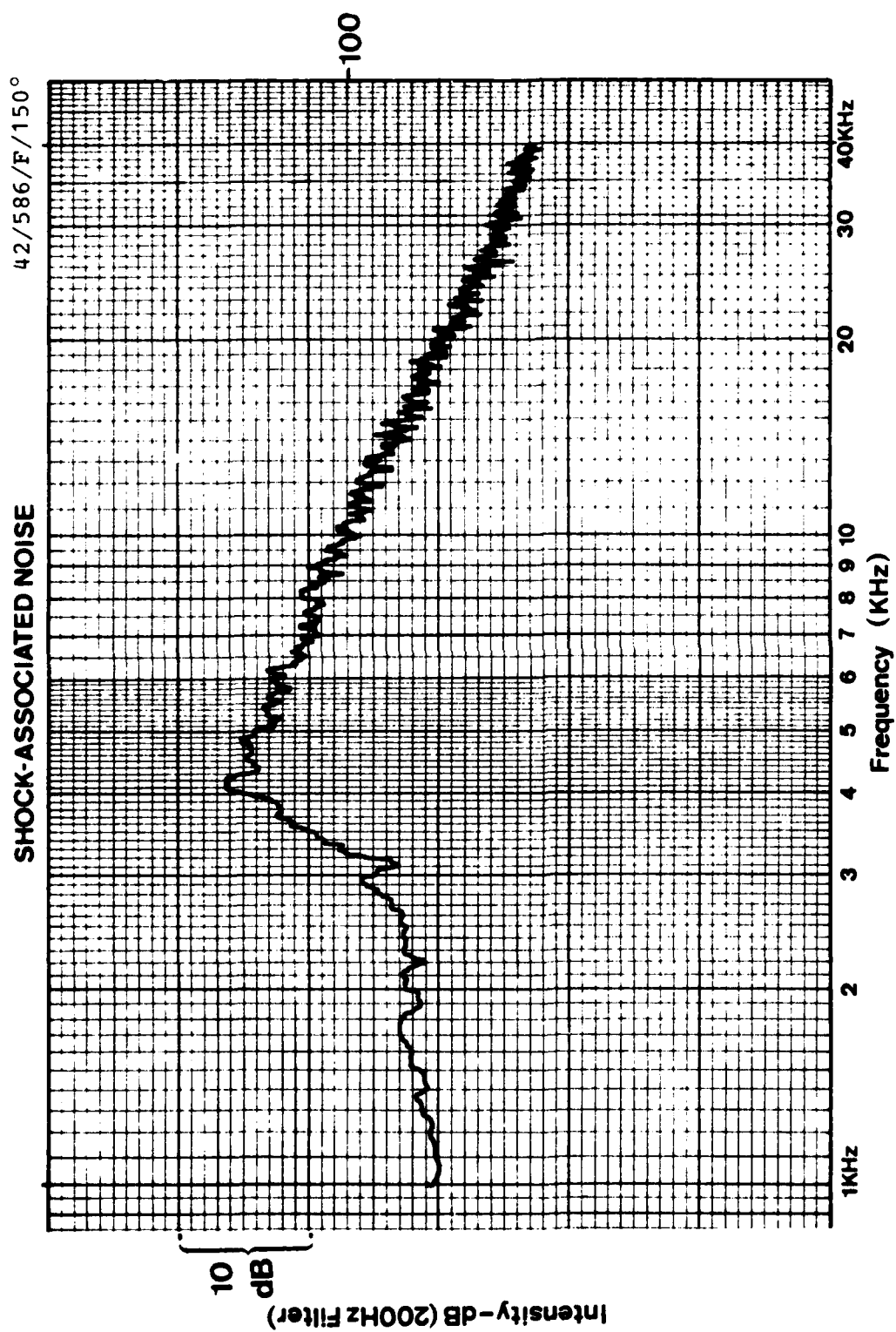
42/586/1190

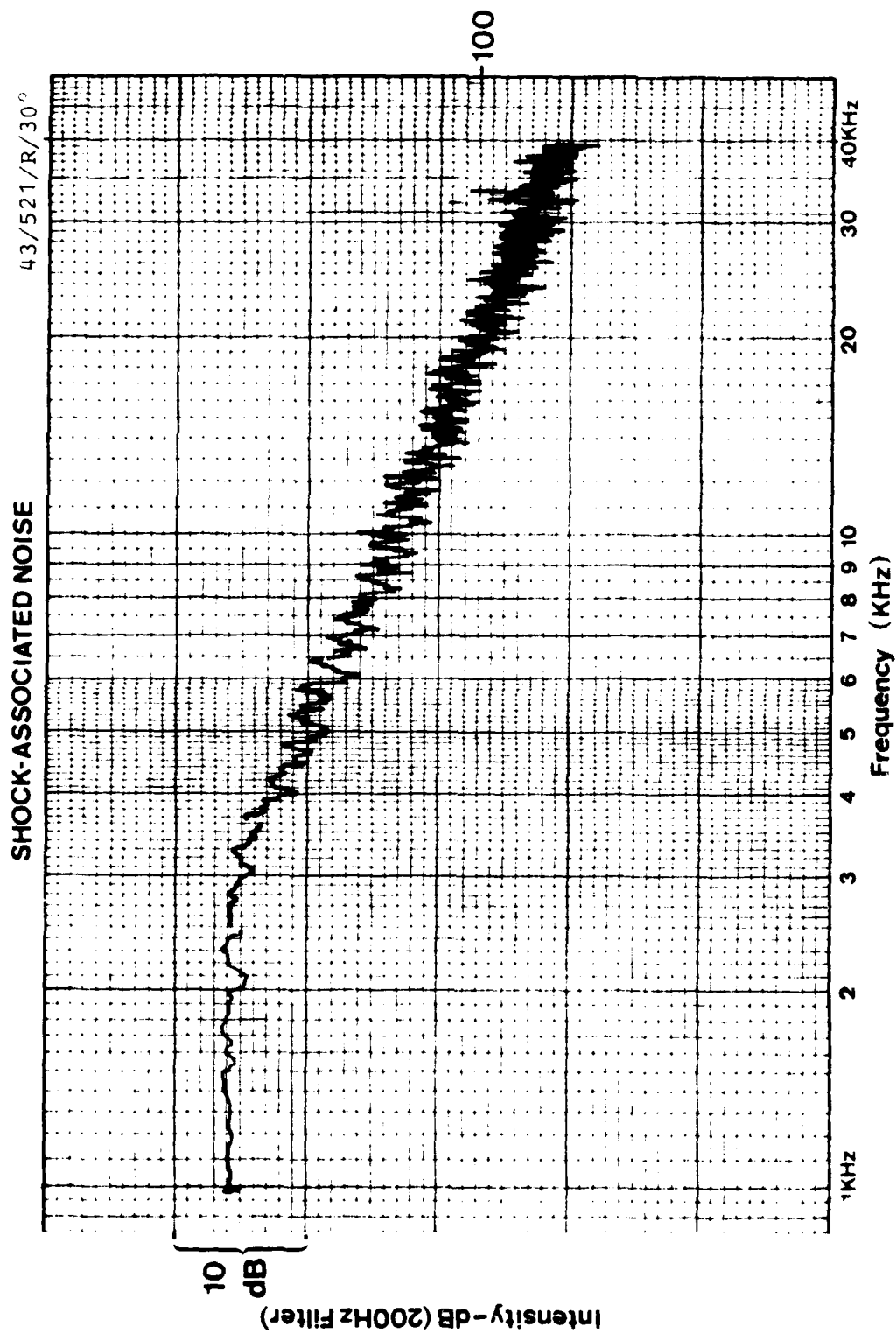


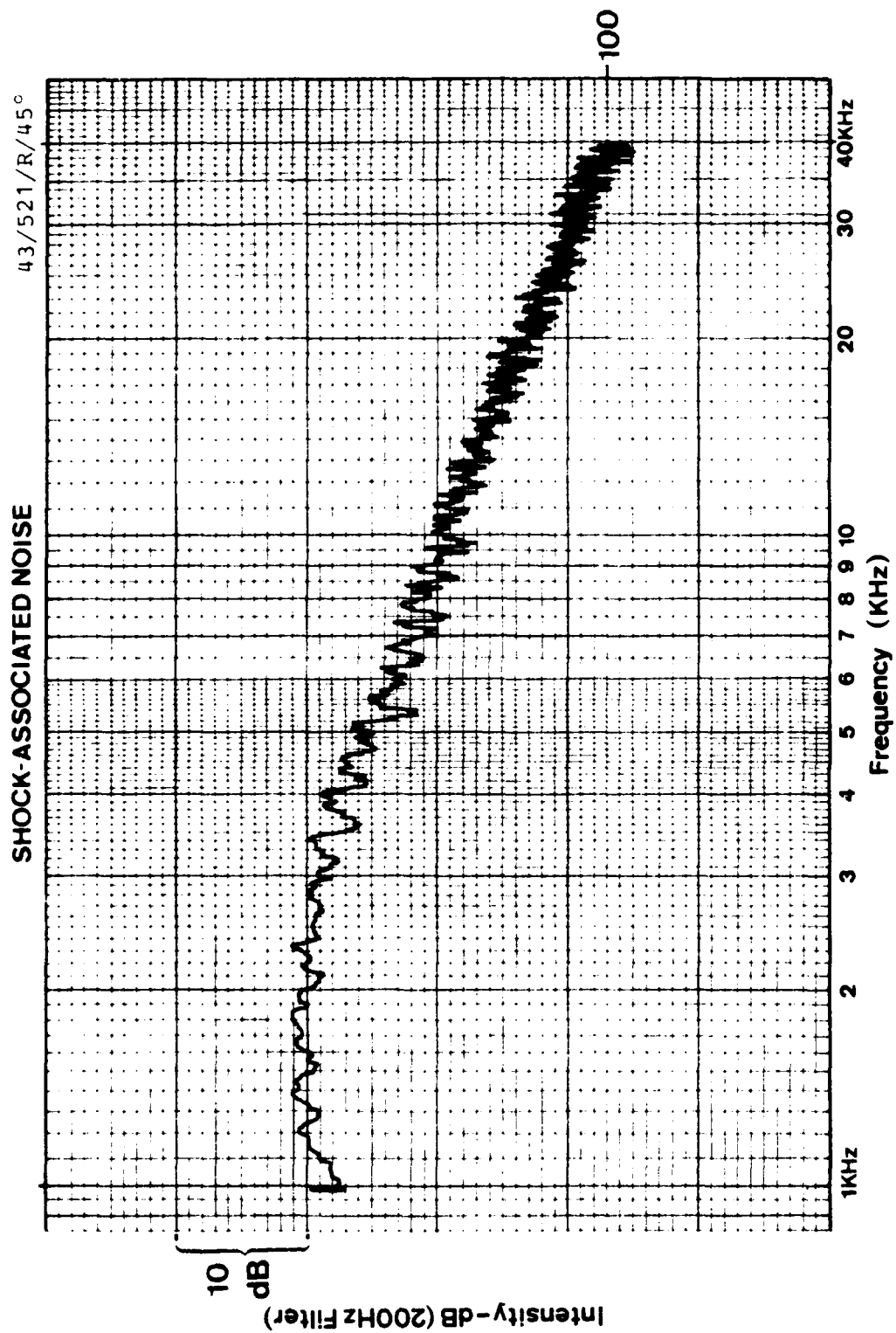


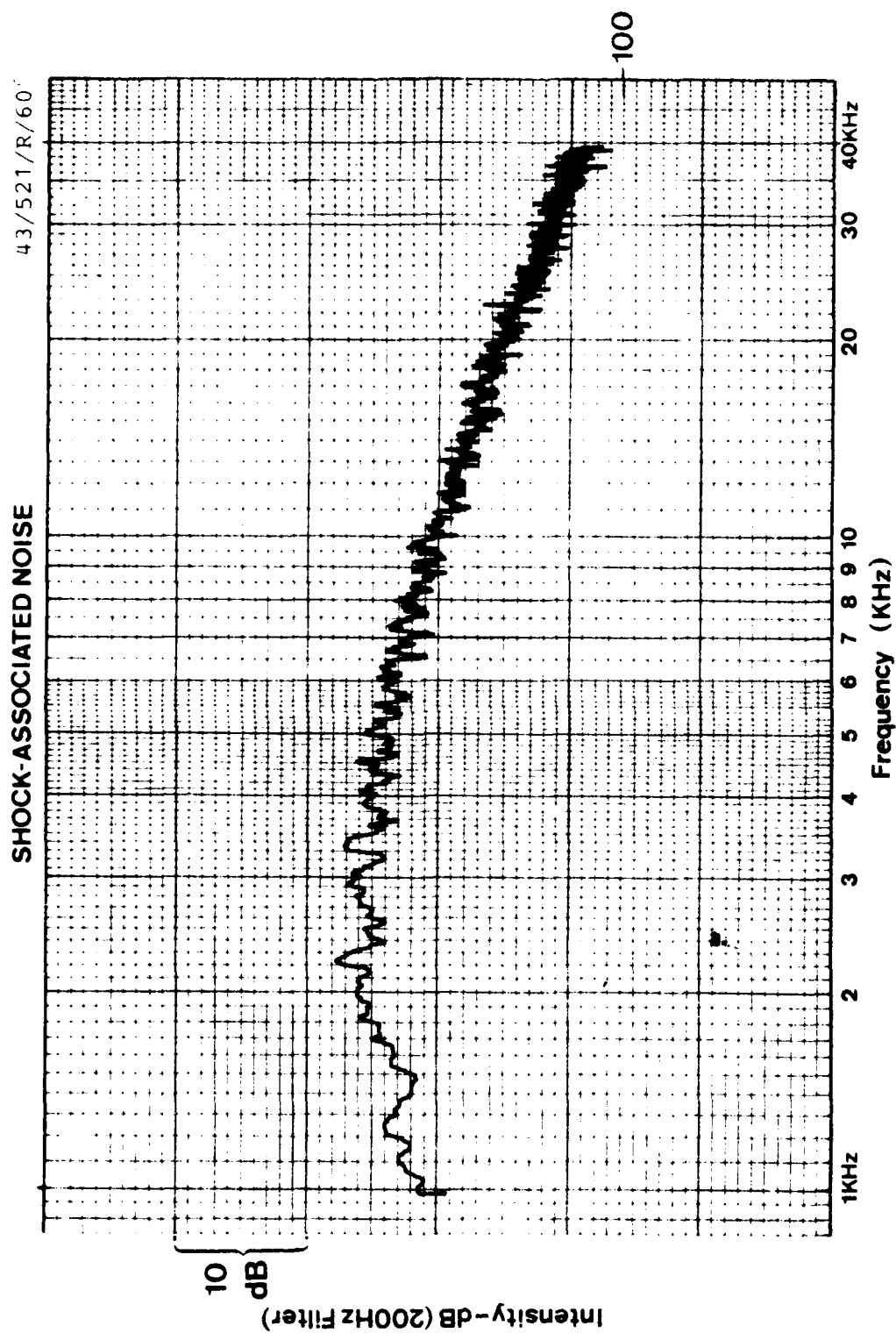


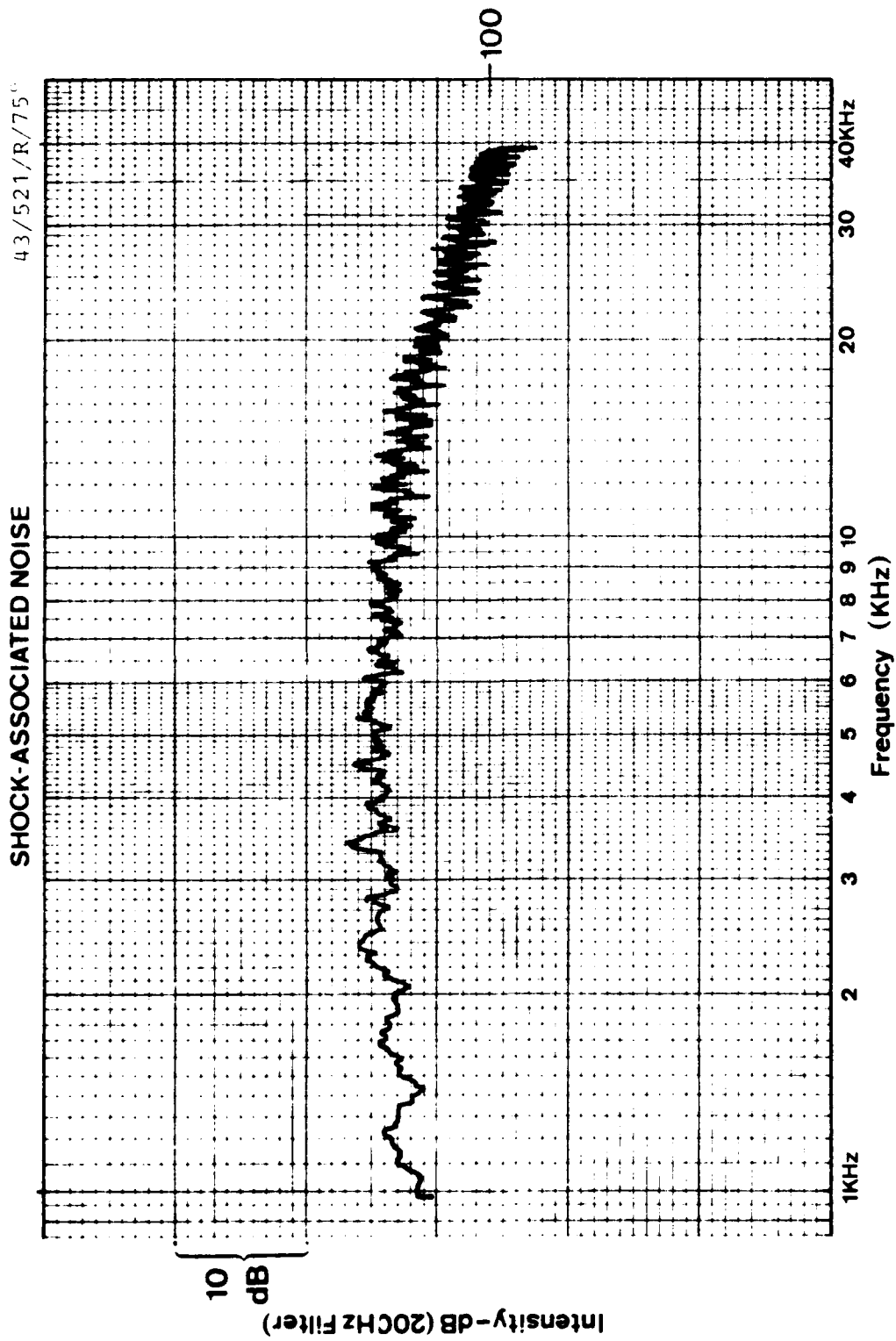


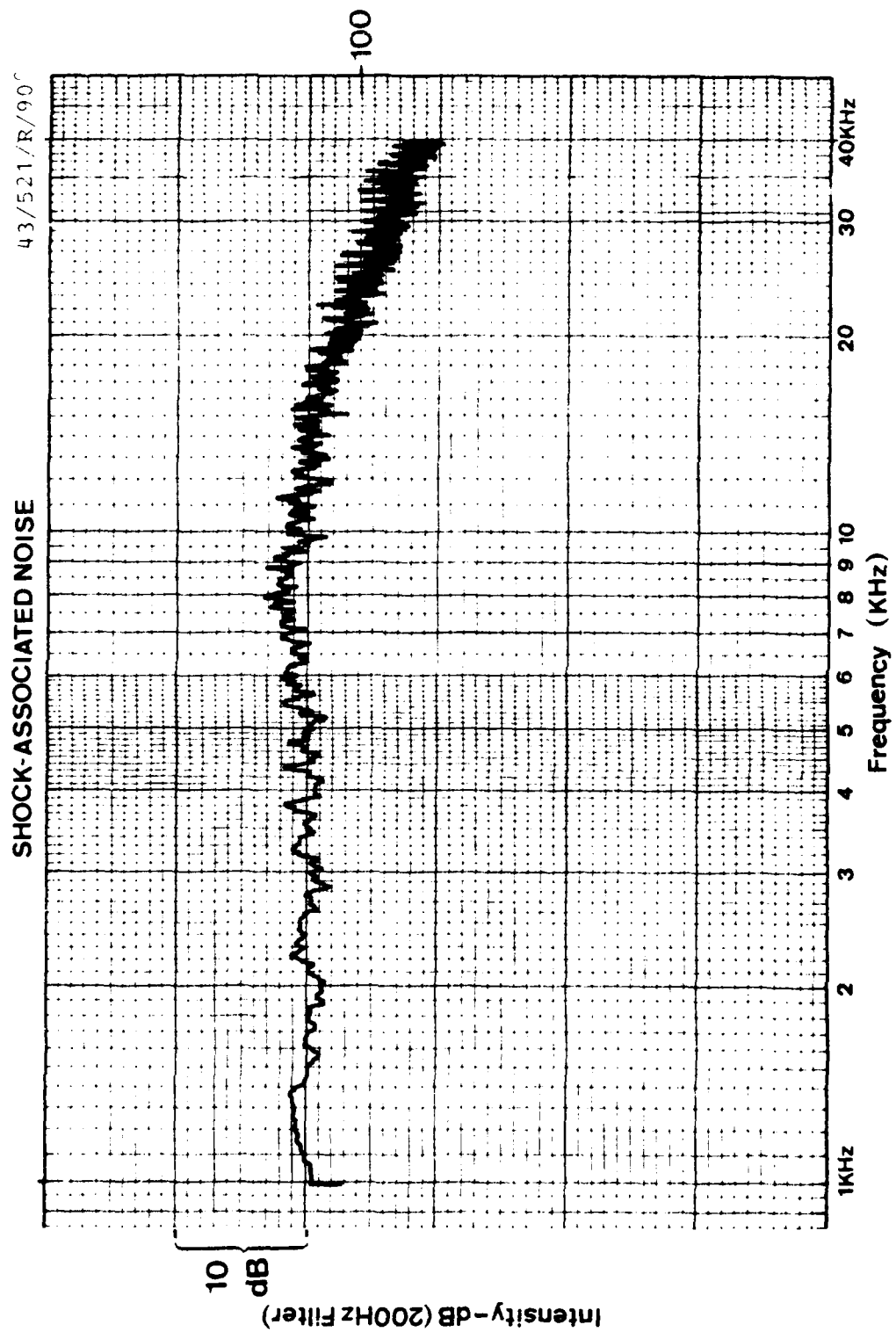












SHOCK-ASSOCIATED NOISE

43,587 P.50

